Characterisation Of Anti-Inflammatory And Pro-Inflammatory Influences On Blood-Brain Barrier Phenotype Using An *In Vitro* Human Brain Microvascular Endothelial Model

A dissertation submitted for the degree of Ph.D by

Keith D. Rochfort, B.Sc

Under the supervision of Dr. Philip M. Cummins

September 2013

Faculty of Science and Health, School of Biotechnology,

Dublin City University, Dublin 9, Ireland

Declaration

I hereby certify that this material, which I now submit for assessment on the programme of study leading to the award of Doctor of Philosophy is entirely my own work, that I have exercised reasonable care to ensure that the work is original, and does not to the best of my knowledge breach any law of copyright, and has not been taken from the work of others save and to the extent that such work has been cited and acknowledged within the text of my work.

Signed: _____

(Candidate) ID No.: _____

Date: _____

Acknowledgements

First and foremost I have to extend a large amount of gratitude to my supervisor of the last few years, Dr. Philip Cummins, who placed a lot of trust in a rookie chemist all those years ago that yielded a somewhat capable biologist. I hope I have repaid some of the faith you placed in me and I did not make it too difficult at times what with all the ambitious (and sometimes expensive) ideas I proposed and of course the edits, the oh so many edits, I provided in large and steady supply. You have had such a large part to play in this process and I could not be more grateful. I wish you and your group the best of luck in the years to come.

I also need to extend a large thanks to our collaborator; Dr. Ronan Murphy of the IBG, who has provided invaluable insight, fresh perspectives and incredible opportunities for the members of our research groups over the years. I also wish you and your group the best of luck in the years to come.

Next, I need to thank the 'old guard' of our research groups; Tony, Anthony, Paul, Mishan and Andrew. Despite being the final stages of their own projects and work they were incredibly helpful and particularly patient in bringing not only I, but a number of 'raw talents' that were introduced into the lab at once, up to speed. They were instrumental in making our first year not only productive but incredibly memorable and for that I'm grateful. I also need to thank those aforementioned 'raw talents'; Fiona, Colin, Brian, Ciarán and Shan, who I entered the lab alongside. It has been an absolute pleasure to have been a part of their projects as much as it has been to have had them as a part of mine. I take away a number of incredible memories and I look forward to making many more with you all. I also need to thank the 'future' of both of the research groups; Alisha, Laura, Rob and Hannah, who in their short time look more than capable of carrying on the good work being carried out between the groups and were incredibly understanding and accommodating in the build-up to 'viva season'.

I also need to extend my gratitude to Dr. Christine Loscher and Dr. Neal Lemon of the T3 program, who not only granted me the opportunity to pursue a PhD. but also offered some invaluable advice and support along the way. Being a part of said program has also allowed me to forge many important friendships that I hope will continue as we all go our separate ways. To have had that additional support outside of my own lab was important, and I'm grateful to have been a part of that exclusive club for the time that was on it.

Next, my girlfriend Laura, for whom there are not enough words that I can use to express how truly grateful I am. To have had your support, ideas and help over the years-you contributed so much to this journey, inside and outside of the lab, that I cannot imagine what it would have been like without you there. To have had you in a position that you could understand and relate to the trials and tribulations that accompany a PhD. meant so much. I can only hope that I can return the gesture in time.

While I have been lucky enough to have had a lot of support within DCU, I was also lucky to have had support outside of it. From those that could relate to those that tried to-my friends from home. You guys have never lost patience with the random, and at times inconvenient, 'office hours' I worked and always tried to accommodate me as such. Whether

it was a time I needed to talk about science or it was a time I needed to talk about anything but-you guys were always on hand and made a lot of hard times easier.

Last and by no means least I need to thank my family. They have been incredibly supportive of me throughout and have been a constant source of encouragement. They have been at the forefront of the many highs and lows as much as anyone and I can only hope that now it is over, I have made you proud.

Abstract

Introduction: Within the central nervous system, the cerebral endothelial cells have highly specialised structural and functional properties. Compared to the endothelium of the periphery, brain endothelial cells are phenotypically unique in that they have enhanced inter-endothelial junction complexes that provide a highly restrictive yet controlled paracellular barrier for the brain from the constituents of the circulation, effectively embodying a *blood-brain barrier*. Disruption of the proteins that form these junctional complexes (i.e. occludin, claudin-5, VE-cadherin and ZO-1) has therefore been implicated in several CNS disease states.
Endothelial functions can be modulated by both local and systemic environmental factors. The ability of the endothelium to sense its humoral and biomechanical environment and modify its functional phenotype accordingly plays a pivotal role in the maintenance of vascular homeostasis or the development of vascular pathology. However, much remains unknown about how anti- and pro-inflammatory stimuli modulate blood-brain barrier phenotype at the molecular level, thus framing the context of this thesis.
In the current study, in view of the opposing physiological and pathophysiological actions demonstrated thus far in similar yet distinctly different in vivo and in vitro endothelial models, we propose to investigate how anti-inflammatory laminar shear stress and pro-inflammatory cytokines can differentially modulate BBB phenotype, with functional consequences for endothelial homeostasis, particularly with regards to the coordination and maintenance of the BBB interendothelial junction complex.

Results: Exposure of cultured human brain microvascular endothelial cells (HBMvECs) to physiological levels of laminar shear stress (8 dynes cm^{-2}) resulted in a reduction in monolayer permeability. The transcription and translation of occludin, claudin-5, VE-cadherin and ZO-1 were all upregulated, with an enhanced localisation of said proteins at the cell-cell junctions. Moreover, our studies demonstrated laminar shear stress caused a substantial reduction in pTyr and pThr levels on each protein, with functional consequences for barrier integrity as determined using dephostatin and genistein. In addition, laminar shear stress promoted a number of anti-inflammatory mechanisms, which, in the presence of inflammatory cytokines, could partially ameliorate the injurious effects of the latter. Sophisticated co-IP techniques, coupled with mass spectrometry analysis, identified several isoforms of the 14-3-3 family of proteins as intracellular binding partners to the interendothelial junction complex. This family of proteins was implicated in contributing to the protective, barrier-stabilising effect of laminar shear, whilst inhibition of their activity exacerbated cytokine injury.
In parallel studies, exposure of cultured HBMvECs to pathophysiological levels of inflammatory cytokines, TNF-α and IL-6, resulted in an increase in monolayer permeability, an effect directly attributable to the reduction in the transcription and translation of the aforementioned tight and adherens junction proteins. Moreover, each cytokine caused a substantial increase in pTyr/Thr levels on each protein. Noteworthy, all cytokine effects were dose- and time-dependent. This increase in injury can be possibly attributed to a correlative reduction in anti-inflammatory mechanisms coupled with a correlative increase in the production and release of inflammatory mediators such as ROS and other cytokines such as IL-6 into the local environment.

Conclusions: Physiological levels of laminar shear stress and pathophysiological levels of inflammatory cytokines, TNF-α and IL-6, modulate the expression and post-translational properties of BBB tight and adherens junction proteins in an opposing manner. Inflammatory cytokines mediate their effects in part through the induced release of injury potentiating agents such as ROS and IL-6. A novel role for 14-3-3 isoforms in the modulation of interendothelial junction assembly is also implicated in these studies.

Abbreviations

ACN	Acetonitrile
ADAM	Advanced Detection and Accurate Measurement
AF	Attachment Factor
AIDS	Acquired Immunodeficiency Syndrome
AJ	Adherens Junction
ANG	Angiotensin
AP-1	Activator Protein-1
APO	Apocynin
ApoE	Apolipoprotein E
ASK-1	Apoptosis Signal-Regulating Kinase 1
Aβ	β-Amyloid
BBB	Blood-Brain Barrier
BBMvEC	Bovine Brain Microvascular Endothelial Cells
BCA	Bicinchonic Acid
bFGF	Basic Fibroblast Growth Factor
BSA	Bovine Serum Albumin
BMvEC	Brain Microvascular Endothelial Cells
cAMP	Cyclic Adenosine Monophosphate
CAT	Catalase
CI	Cell Index
CIAP-1/-2	Cellular Inhibitor of Apoptosis Proteins-1/-2
CNS	Central Nervous System
CNTF	Ciliary Neurotrophic Factor
COX-2	Cyclooxygenase-2
CSF	Cerebrospinal Fluid
CVD	Cardiovascular Disease
DAPI	4’,6-Diamidino-2-Phenylindole
DCFDA	2’, 7’-Dichlorofluorescein
DEAE	Diethylaminoethanol
DHE	Dihydroethidium
DI	Distilled
DMEM	Dulbecco’s Modified Eagle Medium
DMSO	Di methyl Sulfoxide
DNA	Deoxyribonucleic Acid
ECM	Extracellular Matrix

EDTA	Ethylenediaminetetraacetic Acid
ELISA	Enzyme-Linked Immunosorbent Assay
ERK	Extracellular Signal-Regulated Kinases
ET-1	Endothelin-1
FADD	Fas-Associated Protein with Death Domain
FAK	Focal Adhesion Kinase
FITC-Dextran	Fluorescein Isothiocyanate-Dextran
GDP	Guanosine Diphosphate
GFP	Green Fluorescent Protein
GLUT	Glucose Transporter
gp130	Glycoprotein 130
GPCR	G Protein-Coupled Receptor
GTP	Guanosine Triphosphate
HBMvEC	Human Brain Microvascular Endothelial Cells
HIV	Human Immunodeficiency Virus
HRP	Horseradish Peroxidase
ICAM	Intercellular Adhesion Molecule
IFNγ	Interferon-γ
IgG	Immunoglobulin G
IL	Interleukin
IL-6R	Interleukin-6 Receptor
IP	Immunoprecipitation
JAK	Janus Kinase
JAM	Junctional Adhesion Molecule
JNK	c-Jun N-Terminal Kinases
LB	Lysogeny Broth
LDH	Lactate Dehydrogenase
LDL	Low-Density Lipoprotein
LIF	Leukemia Inhibitory Factor
LPS	Lipopolysaccharide
LRP-1	LDL-Receptor Protein-1
MAGUK	Membrane-Associated Guanylate Kinases
MAPK	Mitogen-Activated Protein Kinase
MCAO	Middle Cerebral Artery Occlusion
MCP-1	Monocyte Chemoattractant Protein-1
M-CSF	Macrophage Colony-Stimulating Factor

MDCK	Madin-Darby Canine Kidney Cells
MIQE	Minimum Information for Publication of Quantitative Real-Time PCR Experiments
MMP	Matrix Metalloproteinase
MRP	Multidrug Resistance-Associated Protein
MTS	3-(4,5-dimethylthiazol-2-yl)-5-(3-carboxymethoxyphenyl)-2-(4-sulfophenyl)-2H-tetrazolium
MvEC	Microvascular Endothelial Cells
NAC	*N*-Acetyl-*L*-Cysteine
NADPH	Nicotinamide Adenine Dinucleotide Phosphate
NFκB	Nuclear Factor Kappa-Light-Chain-Enhancer of Activated B Cells
NO	Nitric Oxide
NOS	Nitric Oxide Synthase
NVU	Neurovascular Unit
PBS	Phosphate Buffered Saline
PCR	Polymerase Chain Reaction
PDFGB	Platelet-Derived Growth Factor B
PECAM	Platelet Endothelial Cell Adhesion Molecule
P-Glycoprotein	Permeability Glycoprotein
pH	Power of Hydrogen
PMS	Phenazine Methosulfate
pThr	Phosphothreonine
pTyr	Phosphotyrosine
PVDF	Polyvinylidene Difluoride
qPCR	Real-Time Polymerase Chain Reaction
RAGE	Receptor for Advanced Glycation End Products
RGD	Arginylglycylaspartic Acid
RIP	Receptor-Interacting Protein
RIPA	Radioimmunoprecipitation Assay
RNA	Ribonucelic Acid
RT	Reverse Transcription
SDS	Sodium Dodecyl Sulphate
SDS-PAGE	Sodium Dodecyl Sulphate-Polyacrylamide Gel Electrophoresis
SHP-2	Src Homology Phosphatase-2
sIL-6R	Soluble Interleukin-6 Receptor
siRNA	Small Interfering Ribonucleic Acid

SOC	Super Optimal Broth with Catabolite Repression
SOD	Superoxide Dismutase
SSB	Sample Solubilisation Buffer
STAT	Signal Transducer and Activator of Transcription
sTNF-α	Soluble Tumour Necrosis Factor-α
TACE	Tumour Necrosis Factor-α Converting Enzyme
TAE	Tris-Acetate-EDTA
TBI	Traumatic Brain Injury
TBS	Tris-Buffered Saline
TE	Tris-EDTA
TEER	Transendothelial Electrical Resistance
TEMED	*N,N,N',N'*-Tetramethylethylenediamine
TGF-β	Transforming Growth Factor-β
tIL-6R	Transmembrane Interleukin-6 Receptor
TJ	Tight Junction
TNFR1	Tumour Necrosis Factor Receptor 1
TNFR2	Tumour Necrosis Factor Receptor 2
TRADD	TNFR-Associated Death Domain
TRAF2	TNF-α Receptor Associated Factor 2
tTNF-α	Transmembrane Tumour Necrosis Factor-α
VCAM	Vascular Cell Adhesion Molecule
VE-Cadherin	Vascular Endothelial Cadherin
VEGF	Vascular Endothelial Growth Factor
VEGFR2	Vascular Endothelial Growth Factor Receptor
VLA-4	Very Late Antigen-4
vWF	Von Willebrand Factor
WHO	World Health Organisation
ZO-1	Zonula Occludens
γ-GTP	γ-Glutamyl Transpeptidase

Units

cm	Centimetre
cm^2	Centimetre Squared
^oC	Degree Celsius
g	Grams
hrs	Hours
kDa	Kilo Daltons
kb	Kilobase
kg	Kilogram
L	Litre
m	Metre
m^2	Metre Squared
µg	Microgram
µl	Microlitre
µm	Micrometre
µM	Micromolar
mA	Milliamps
ml	Millilitre
mm^2	Millimetre Squared
mM	Millimolar
mins	Minutes
M	Molar
ng	Nanogram
nm	Nanometre
nM	Nanomolar
Ω	Ohms
rpm	Revolution Per Minute
U	Enzyme Unit
V	Volts
v/v	Volume Per Volume
w/v	Weight Per Volume

Publications

Rochfort KD, Dowling P, Murphy RP, Cummins PM. Impact of cytokine-induced ROS production on blood-brain barrier assembly and function. *J Cell Physiol* 2013; **[In Preparation]**

Collins LE, Lynch M, Marszalowska I, Kristek M, **Rochfort KD**, O'Connell MJ, Windle H, Kelleher D, Loscher CE. *Clostridium difficile* induce clearance responses in macrophage. *Microbes Infect* 2013 **[In Preparation]**

Guinan AF, **Rochfort KD**, Fitzpatrick PA, Walsh TG, Pierotti AR, Phelan S, Murphy RP, Cummins PM. Shear stress is a positive regulator of thimet oligopeptidase (EC3.4.24.15) in vascular endothelial cells: consequences for MHC1 levels. *Cardiovasc Res* 2013

Walsh TG, Murphy RP, Fitzpatrick P, **Rochfort KD**, Guinan AF, Murphy, A, Cummins PM. Stabilization of brain microvascular endothelial barrier function by shear stress involves VE-cadherin signalling leading to modulation of pTyr-occludin levels. *J Cell Physiol* 2011

Posters/Abstracts

Rochfort KD, Martin FA, Dowling P, Murphy RP, Cummins PM. Characterisation of anti-inflammatory (shear) and pro-inflammatory (cytokine) influences on blood-brain barrier phenotype using an *in vitro* human brain microvascular endothelial cell model. *School of Biotechnology: Research Day 2013,* Dublin City University.

Rochfort KD, Martin FA, Dowling P, Murphy RP, Cummins PM. Characterisation of anti-inflammatory (shear) and pro-inflammatory (cytokine) influences on blood-brain barrier phenotype using an *in vitro* human brain microvascular endothelial cell model. *ATVB 2012,* Chicago, IL.

Davenport C, Martin FA, **Rochfort KD**, Murphy RP, Smith D, Cummins PM. The effects of inflammation, hyperglycemia and cyclic strain on osteoprotegrin production in human aortic smith muscle cells. *ATVB 2012,* Chicago, IL.

Martin FA, Davenport C, **Rochfort KD**, Murphy RP, Cummins PM. Cyclic stain-induced release of thrombomodulin from human aortic endothelial cells. *ATVB 2012,* Chicago, IL.

Rochfort KD, Martin FA, Dowling P, Murphy RP, Cummins PM. Characterisation of anti-inflammatory (shear) and pro-inflammatory (cytokine) influences on blood-brain barrier phenotype using an *in vitro* human brain microvascular endothelial cell model. *School of Biotechnology: Research Day 2012,* Dublin City University.

Martin FA, Davenport C, **Rochfort KD**, Murphy RP, Cummins PM. Cyclic stain-induced release of thrombomodulin from human aortic endothelial cells. *School of Biotechnology: Research Day 2012,* Dublin City University.

Rochfort KD, Walsh TG, Murphy RP, Cummins PM. Cytokine-induced BBB dysfunction: A human brain microvascular endothelial cell model involving TNF-α induced IL-6 release. *(Bio)pharmaceutical & Pharmacological Sciences Research Day 2011*, Dublin City University.

Martin FA, Guinan AF, **Rochfort KD**, Murphy RP, Cummins PM. Cyclic strain induced thrombomodulin release:putative role in macrovascular endothelial injury. *(Bio)pharmaceutical & Pharmacological Sciences Research Day 2011*, Dublin City University.

Rochfort KD, Walsh TG, Murphy RP, Cummins PM. Cytokine-induced BBB dysfunction: A human brain microvascular endothelial cell model involving TNF-α induced IL-6 release. *Sigma-Aldrich Functional Genomics European Seminar Tour 2011*, Dublin City University.

Oral Presentations

Martin FA, **Rochfort KD**, Davenport C, Murphy RP, Cummins PM. Cyclic-strain mediated regulation of thrombomodulin expression and release from human aortic endothelial cells. *School of Biotechnology: Research Day 2013*, Dublin City University.

Davenport C, Martin FA, **Rochfort KD**, Murphy RP, Cummins PM, Smith D. The effects of inflammation, hyperglycemia and cyclic strain on OPG production in human aortic smooth muscle cells. *Irish Endocrine Society 37th Annual Meeting*, Dublin, Ireland. *

Rochfort KD, Walsh TG, Murphy RP, Cummins PM. Cytokine-induced BBB dysfunction: A human brain microvascular endothelial cell model involving TNF-α induced IL-6 release. *School of Biotechnology: Research Day 2011*, Dublin City University. **

Rochfort KD, Walsh TG, Murphy RP, Cummins PM. Cytokine-induced BBB dysfunction: A human brain microvascular endothelial cell model involving TNF-α induced IL-6 release. *School of Health and Human Performance: School Seminar 2011*, Dublin City University.

Walsh TG, Guinan AF, **Rochfort KD**, Cummins PM. Stabilization of brain microvascular endothelial barrier function by shear stress involves a signalling pathway linking adherens and tight junctions via Rac1. *University Hospital Zurich, 13th International Symposium of the Blood Brain Barrier 2010*; Zurich, Switzerland.

* Winner of the O'Donovan Medal for Best Presentation

** Winner of Best Oral Presentation

List of Figures

Chapter 1

Chapter 2

Chapter 3

Chapter 4

Chapter 5

Chapter 6

Chapter 7

List of Tables

Table of Contents

Chapter 1:

Introduction.

1.1 Vascular Disease

Diseases of the heart and circulatory system, including the cerebrovascular system, are the main cause of death across the world accounting for over 4 million deaths annually in Europe alone (Figure 1.1). Of all the main causes of death, nearly half (47%) are attributed to cardiovascular diseases (CVD). Just under half of all deaths from CVD are from coronary heart disease with stroke accounting for nearly a third of deaths in women and a quarter of deaths in men (Nichols, Townsend et al. 2012).

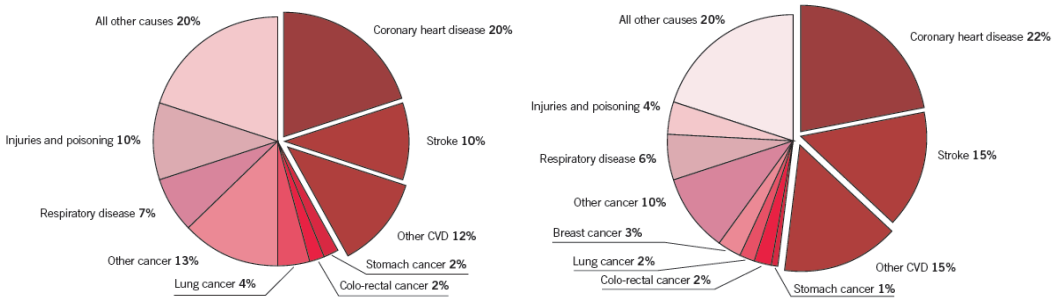

Figure 1.1: Deaths by cause, men (left) and women (right). CVD is accountable for 42% and 52% of fatalities in men and women respectively (applicable to Europe) (Nichols, Townsend et al. 2012).

CVD was often thought to be a problem of wealthy, industrialised nations. As research techniques and means of gathering and sharing information improved, CVD is now recognised as the leading cause of death worldwide, impacting equally across developed and middle to low income countries. To put this in perspective, many communicable diseases such as malaria, tuberculosis, human immunodeficiency virus/acquired immunodeficiency syndrome (HIV/AIDS) and their impact on certain societies garner much spotlight, yet CVD causes more than 3 times the annual deaths of these diseases combined (Boerma, Abou-Zahr et al. 2008). The impact CVD has had on these once low-risk regions is attributed to widespread industrialisation, urbanisation and globalisation of these regions. With these processes comes a complementary shift in the behavioural, biological and social risks which have a resounding impact on the likelihood of developing CVD (Yusuf, Reddy et al. 2001).

While some aspects of developing CVD have been attributed to hereditary processes, additional risk factors include environmental and lifestyle choices. Tobacco use, unhealthy diet, reduced physical activity, blood lipid levels and hypertension are among the factors which greatly influence the chances of developing CVD (Roger, Go et al. 2012). As a result, governments and health agencies are promoting the idea of tackling CVD in early age in the hope such ideals would be carried on throughout life. Recent statistics showed in the US that

67.3% of the adult population (≥ 20 years old) are overweight with 33.7% of the total adult population clinically obese, while the same studies reported 31.7% of children are overweight with 16.9% clinically obese (Roger, Go et al. 2012). While these statistics might not seem impressive, progress has been made. From 1998 to 2008, the rate of death attributable to CVD has decreased by 30.6% demonstrating that promotion of healthy lifestyle and raising awareness of the risk factors that can contribute to it is having a significant impact on the world's population (Roger, Go et al. 2012).

Efforts in coping with CVD are focussed on furthering the understanding of the science behind it and developing therapeutics and strategies to control it. In comparison to some of the other leading causes of mortality, CVD related diseases have shown a significant drop in their impact (Kochanek, Xu et al. 2011) (Figure 1.2). This is due to the development of better *in vitro* and *in vivo* models, techniques, instrumentation and assays, all of which have enabled the scientific community to better understand the nature of disease onset and progression.

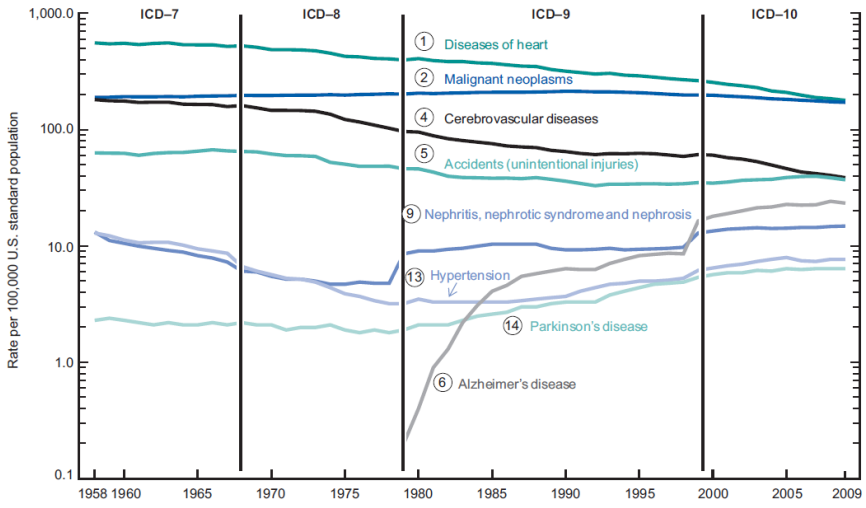

Figure 1.2: Age-adjusted death rates for selected leading causes of death in the United States, 1958-2008. Circled numbers indicate ranking of conditions as leading causes of death as of 2009 (Kochanek, Xu et al. 2011).

What follows is a brief introduction to the vascular system before focussing on the endothelium, a key cell type at the forefront of the vasculature which has been identified as playing a major role in both preventing, and in certain instances promoting, CVD onset. This thesis will focus primarily on the endothelium of the cerebrovasculature network, which forms the basis of the blood-brain barrier (BBB), a dynamic interface that separates the central nervous system from the circulation, controlling the influx and efflux of biological

materials from the blood to the brain and vice versa. The influence of physiological (shear stress) and pathophysiological (inflammatory cytokines) stimuli on endothelial phenotype will be addressed whilst highlighting the impact of said stimuli on BBB phenotype and thus, the potential role they play in the development/progression of cerebral-based pathologies.

1.1.1 Vascular system

The earliest understanding of the vasculature system originates in ancient Greece, 250BC. Then, based on the works of Erasistratus, it was believed that the heart was connected to two entirely separated sets of vessels; the arteries transported oxygen throughout the body whilst the veins transported blood. However, strict religious ideologies condemning the practise of dissection halted the progression of such studies. Regardless, evidence reports the studies evolved to the extent that the concept of 'exchange' between the purposed independent vascular systems was premised (Singer 1957, Majno 1992).

It wasn't until 1628, that William Harvey first described the 'ceaseless and circular motion' of the complete vascular system in greater detail (Fishman 1982). Since then, the understanding of blood vessels has rapidly evolved such that they are now recognised as key elements in the maintenance of tissue homeostasis, serving as conduits which facilitate the transport of nutrients and oxygen to the body's tissues and organs, whilst also removing the potentially disruptive catabolites and xenobiotics (Furchgott, Zawadzki 1980, Gimbrone, Kume et al. 1993, Gimbrone 1995, Cines, Pollak et al. 1998).

Figure 1.3 illustrates the basic composition of the blood vessels within the vasculature. The walls of arteries and veins have three layers; the tunica interna (intima), the tunica media and the tunica externa (adventitia). The outermost layer, the tunica externa is made up of fibrous connective tissue. The middle layer, the tunica media, is an 'active' layer composed of smooth muscle cells and elastic fibres. The inner most layer, the tunica interna, is comprised of the endothelium. Capillaries are tiny in size and form vast networks or capillary beds throughout the body. Their walls are typically a single layer of endothelial cells which allows for mediated exchange of materials between the blood and local tissue (Townsley 2012).

The entire vascular system is comprised of an extensive range of vessels (over 60,000 miles). While the diameter, length and degree of branching of the vessels can vary across vascular beds, one mainstay in the makeup of the vessels is the endothelium, a layer of highly metabolically active, flat squamous cells that line the entire circulatory system including the heart (Aird 2007). The following section covers a number of aspects of the endothelium discussing some of the important traits it brings to vascular homeostasis.

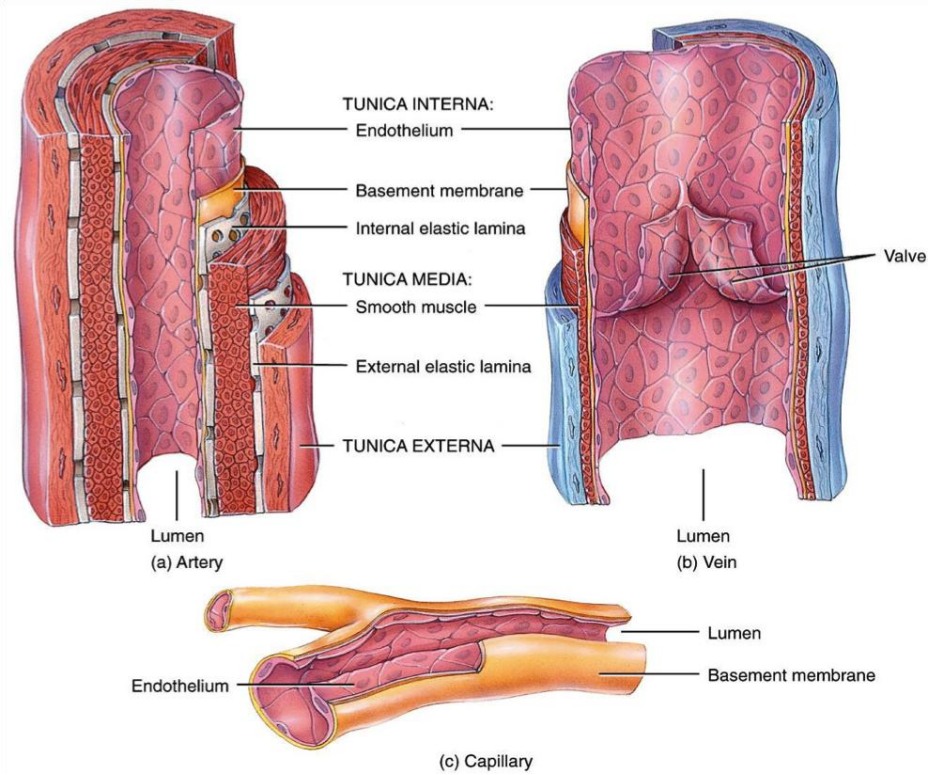

Figure 1.3: Anatomical structure of arteries, veins and capillaries. Blood vessels facilitate the transport of blood throughout the body. They are typically comprised of three main layers: tunica intima, the innermost layer comprising of endothelium monolayer; tunica media, the middle layer comprising of smooth muscle cells and elastic collagen fibres that make up the bulk of vessel wall thickness; and the tunica adventitia, the outermost layer that contains fibroblasts and elastic collagen fibres. In contrast, the capillaries are typically comprised of a single layer of endothelial cells (Tortora, Derrickson 2007).

1.1.1.1 Endothelium

During the 1880's Von Rocklinghausen described how the conduit-like vessels, lined by cells, bore deeply into the underlying tissue (von Rocklinghausen 1860). After Starling published his findings on capillary exchanges (Starling 1896), the scientific community began to recognise the inner lining of endothelial cells on the blood vessel walls as a 'selective' physical barrier.

The endothelium provides a cellular lining to all blood vessels within the circulatory tree (Aird 2007). It has been shown to form a structural barrier between the vascular space and tissue. A single endothelial cell ranges from 25-50 μm in length, 10-15 μm in width and 5 μm in height (Limaye, Vadas 2006). In an adult, as it lines the entire inner wall of all blood vessels, the collective endothelium is said to be comprised of $1.6*10^{13}$ cells on average (Limaye, Vadas 2006), collectively weighing up to 1 kg and covering a surface area of 350 m^2 (Augustin, Kozian et al. 1994, Pries, Secomb et al. 2000, Pries, Kuebler 2006). Once

thought to be inert, research conducted on the endothelium has redefined it as a dynamic organ with a myriad of important endocrine, paracrine and autocrine functions (Ryan, Ryan 1984, Hunt, Jurd 1998). In order to maintain human vascular homeostasis, the endothelium has to continuously monitor the circulatory and locally generated stimuli as well as any acute or chronic changes to its environment (Aird 2006). Given the diversity of vessels, their dimensions, the environments in which they reside and their associated stimuli, it is necessary for the endothelium to be adaptable to its microenvironment (Risau 1995). The endothelium can undergo a dynamic shift in phenotype relative to the environment in which it resides ensuring the microenvironment's complex metabolic and structural needs are met. However, any stimuli or environmental changes that may disrupt vascular homeostasis may cause a disturbance in the neighbouring vasculature beds. If substantially damaging, this in turn can alter the endothelium so that it becomes 'dysfunctional', which subsequently can lead to dysregulation of endothelium-dependent processes, e.g. antihemostatic functions, vascular tone, heightened leukocyte adhesion, reduced barrier function, increased production of cytokines and growth factors etc (Endemann, Schiffrin 2004).

1.1.1.1.1 Hemostasis

The vascular endothelium is primarily an anticoagulant surface layer. Normally platelets are unable to interact with the endothelium due to release of vaso-relaxant and platelet-inhibiting nitric oxide and prostacyclin (Gryglewski 1995, Gryglewski, Chlopicki et al. 1995, Cannon 1998, Cannon 1998). In addition, healthy endothelial cells express a number of signalling molecules which in turn can interrupt and quell the coagulation process. For example, thrombin is a primary catalyst in the coagulation process (Mann, Golden et al. 1997). Endothelial cells can nullify thrombin and use it to its own advantage in a number of ways. One pathway involves the release of heparin sulphate, which in turn increases the potency of anti-thrombin III, which in turn binds to and neutralises thrombin (Marcum, Rosenberg 1984, Marcum, Mckenney et al. 1984). Another mechanism involves the surface expression of thrombomodulin (Maruyama, Majerus 1985, Maruyama 1992), which can also bind to thrombin leading to the activation of the Protein C pathway which functionally prevents the conversion of a large number of pro-coagulant mediators, cumulatively halting a number of pathways. Endothelial cells also secrete the factors that activate the fibrinolysis pathway ensuring coagulation remains at the site of vessel injury (Levin, Santell 1987, Sawdey, Loskutoff 1991).

1.1.1.1.2 Vaso-regulation

The endothelium has also been shown to play a role in dynamically regulating its own vascular tone. A study by Furchgott and Zawadzki (1980) subjected a number of intact arteries to a regime of acetylcholine which induced vasorelaxation. In contrast, when the endothelium was removed, acetylcholine caused the arteries to undergo vasoconstriction. This led to the idea that an endothelium-derived vascular relaxation factor (EDRF) was responsible. Further studies showed that the acetylcholine caused the smooth muscle cells of the artery to undergo vasoconstriction, but in the presence of the endothelium, the free radical nitric oxide was generated in response to counteract the acetylcholine's effect clearly implicating nitric oxide in having a role in the vasoregulation. In addition to control over vessel dilation, endothelial cells also produce potent vasoconstrictors such as endothelin-1 (Levin 1996). In this way, the endothelium can dynamically regulate and adapt vessel tone by delicately balancing the release of these mediators under different conditions (e.g. hypoxia, shear stress, and ischemia).

1.1.1.1.3 Barrier Function

First and foremost, the endothelium was characterised as a compact, uniform monolayer which acts as a dynamic barrier between the circulating blood and the vessel's underlying tissue. Given the endothelium's ability to adapt to its environment, the barrier properties of the endothelium reflect the property inducing effects of the vascular beds in which they reside. As a result certain properties of the endothelium can be augmented such as the expression of certain cell surface binding proteins, the electrostatic charge of the endothelial membrane and perhaps most importantly, the effect on the proteins that comprise the intercellular junctions (Lampugnani, Dejana 1997). The effect of a particular microenvironment on the phenotype of the endothelium as well as some of the associated barrier properties that are induced will be addressed in later sections.

1.1.2 Endothelial Dysfunction/Atherosclerosis

Atherosclerosis is a progressive chronic process which is responsible for the onset of several vascular disorders. It is a condition in which an arterial wall undergoes thickening and hardening as a result of fatty material deposit and accumulation in the sub intima lining of vessel walls (Ross 1999) (Figure 1.4). Atherosclerotic lesions typically originate at the bifurcations, branching points, and curvatures of vessels (Giannoglou, Antoniadis et al. 2010). It is at these points that low or disturbed shear stress occurs, leading to endothelial 'activation'. Upon activation, the endothelium transitions to a pro-inflammatory phenotype

that contributes to vascular injury. This phenotypic change brings the release of injury markers and signalling molecules that attracts various immune cells, including monocytes and leukocytes (Hansson 2005, Charo, Ransohoff 2006). In addition to this, the endothelium increases expression levels for surface receptors P-Selectin, E-Selectin and vascular cell adhesion molecule (VCAM)-1 (Tsao, Buitrago et al. 1996, Chiu, Chen et al. 2003). This allows the localised leukocytes to attach to the monolayers surface via the very late antigen (VLA)-4 antigen present on their surface (Alon, Kassner et al. 1995). This accumulation of immune cells leads to further release of pro-inflammatory cytokines such as tumour necrosis factor-α (TNF-α), interleukin (IL)-1 and CD40L, which in turn drive up the expression of surface receptors on the endothelium such as E-Selectin, VCAM-1 and intercellular adhesion molecule (ICAM)-1 in addition to the secretion of IL-8, IL-6, monocyte chemoattractant protein (MCP)-1 and macrophage colony-stimulating factor (M-CSF) in the local microenvironment (Libby, Galis 1995, Raines, Ross 1996, Libby, Sukhova et al. 1997).

Adhered leukocytes may also transmigrate into the sub-intima tissue due compromised endothelial barrier function, a process called diapedesis, a key mechanism in atherogenesis. This in turn triggers the release of a number of chemoattractants which mediate the recruitment of more immune cells to the region of injury. Once within the intima, the invading leukocytes undergo differentiation into lipid-laden 'foam cells'. Over time, these 'foam cells' contribute to the progression of fatty lesion development via deposition of the concentrated cholesterol liquid droplets (Steinberg 1997, Libby, Ridker et al. 2011).

These fatty lesions have been shown to regress following therapeutic intervention (Pitman, Osgood et al. 1998). However as they are 'clinically silent' and asymptomatic, more often they continue to develop. Chronic inflammation over time results in the sustained recruitment of immune cells which in turn leads to the further accumulation of extracellular lipids. The resulting plaques are generally stable, and over time grow in size and subsequently narrow the vessel wall. Complicated plaques can arise when the fibrous cap ruptures or fissures and breaks away from the lipid core (van der Wal, Becker 1999). This exposes the underlying tissue and initiates the formation of a thrombus (Falk 1996). This can be dangerous in two ways: the continued growth of the thrombus can occlude the vessel or alternatively the thrombus can break away and cause an infarction in smaller vessels downstream from the site of origin (coronary artery-heart attack, cerebrovasculature-stroke).

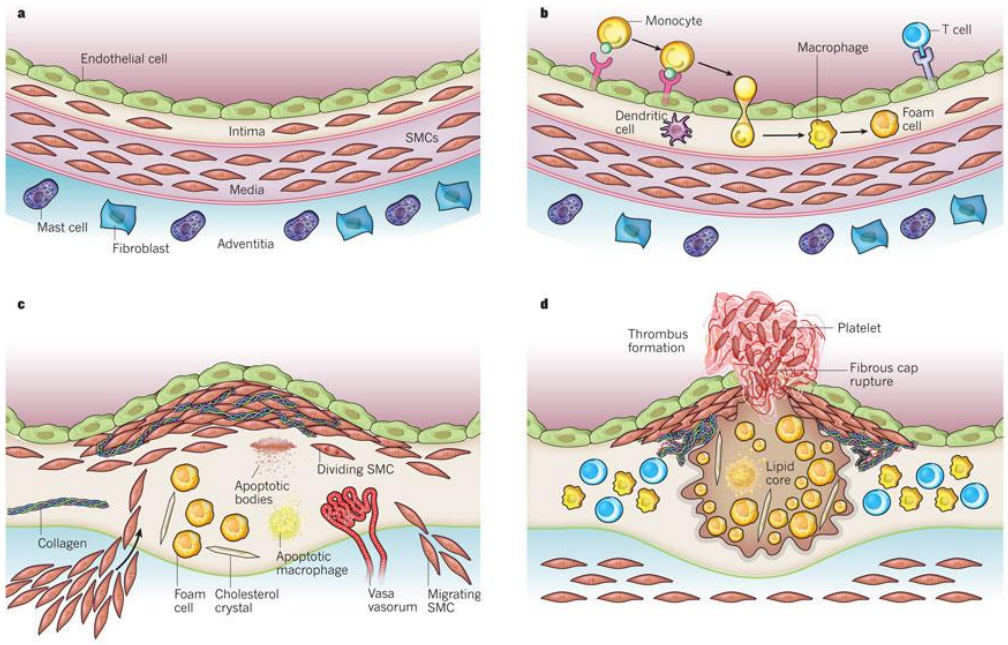

Figure 1.4: Atherosclerotic plaque progression. (a) represents a healthy, atherosclerotic resistant area of the vasculature exposed to undisturbed laminar shear stress. (b) depicts the initial steps in atherosclerosis; the recruitment, invasion and maturation into 'foam cells' of circulating immune cells by a dysfunctional endothelium. (c) lesion progression involves the dysfunctional migration and proliferation/production of smooth muscle cells and extracellular matrix molecules in the intima layer which over time (d) can result formation of an unstable plaque which upon disruption leads to thrombus formation – a potentially serious blood impeding complication of atherosclerosis (Libby, Ridker et al. 2011).

The process of atherosclerosis is important for two reasons; firstly it is the primary disease-initiating process accountable for most cardiovascular related diseases and secondly, since it is a naturally occurring mechanism associated with vascular branching it is a certainty to develop in all humans. 50% of 10-14 year olds have shown early lesion formation in the coronary artery (Hong 2010) and autopsies have even shown the presence of the same in unborn foetuses (Napoli, D'Armiento et al. 1997).

As outlined, atherosclerosis is a mechanism that results in alterations to haemodynamic forces with progression related to inflammatory mediators. These two 'stimuli' are therefore critical in studying and understanding the mechanisms that develop these diseases and will form the underlying basis for this thesis with respect to the brain microvascular endothelium.

Overall there is considerable inconsistency in determining the effect of inflammatory agents on the BBB due to a number of models lacking the inductive effect of the other cells of the neurovascular unit (NVU) and their potentially critical actions. However, improvements to

investigative models have helped to minimise this problem (Cecchelli, Berezowski et al. 2007, Ogunshola 2011). As will be seen in the next section, the NVU is comprised of a large number of cell types which contribute in their own unique way in maintaining an effective BBB and stable NVU.

1.2 The Cerebrovasculature

The brain is an incredibly complex organ with different neural tissues displaying different circulatory demands. Studies in rodents have reported that at least a ten-fold change in blood flow can be observed between the white matter of the brain (~150 capillaries/mm^2) to some of the circumventricular organs (~1500 capillaries/mm^2). Areas of the brain that require higher degrees of attention are seen to possess a higher density of capillary beds to allow a higher rate of material diffusion (Fenstermacher, Tavarekere et al. 2001).

The microcirculation of the brain is a complex network of capillary vessels. These networks are typically served by a small arteriole and drained via a number of collecting venules. The collecting venules also facilitate the exchange of materials because like capillaries they are thin walled and mostly comprised of endothelial cells (Townsley 2012). Several reports have indicated that it is these small venules that are most prone to damage and dysfunction. Taking into account that there are 3-4 times more collecting venules than there are small arterioles (Fenstermacher, Tavarekere et al. 2001), these make the venules an area of interest in identifying the underlying mechanisms associated with BBB disruption. The main area of material exchange however resides in the capillaries. Each and every capillary within the microcirculatory system is capable of branching and joining endlessly with neighbouring vessels, resulting in a vast communicative network of blood vessels in a dense area. Each capillary can vary greatly in length, width, connectivity and shape and the capillaries of the brain are said to vary from 15-400 μm in length and have a mean diameter of 3-10 μm (Kobiler, Shlomo et al. 2012).

Despite their variance in size and dimensions, all material delivered to the brain, whether carried by plasma water, plasma protein or blood cells, has to contend with the neurovascular unit and in particular the brain-specific endothelium (Persidsky, Heilman et al. 2006, Abbott, Patabendige et al. 2010). The capillaries of the brain have been shown to be 100-500 times more restrictive than those associated with muscle, skin or gut tissue owing to their specific properties (Butt, Jones et al. 1990). What follows is an introduction to the NVU before covering the structural components that comprise the BBB.

1.2.1 The Neurovascular Unit

Paul Ehrlich was the pioneer in this field who first demonstrated that following the injection of certain dyes into animal vasculature, the brain and spinal cord were the only two tissues to deny entry (Ehrlich 1885). At the time it was believed that the lack of dye uptake was due to the nervous tissue having a low affinity for the dyes (Ehrlich 1904) however numerous other studies gave credence to the idea of a blood-brain barrier (or 'Blut-Hirn-Schranke' (Lewandowsky 1900)). A defining study by Ehrlich's protégé Edwin Goldmann clearly demonstrated the presence of a blood-brain barrier, where upon direct injection of the dyes into the cerebrospinal fluid (CSF) stained all nervous tissue blue whilst the peripheral tissues remained the same (Goldmann 1913) (Figure 1.5). In the years that followed, the hypothesis was difficult to develop due to methodological limitations. However the advent of the electron microscope in the 1960's turned the concept of a blood-brain barrier into a reality. At a resolution of 100,000x, the ultrastructure of the microvessels, namely the space between the basal lamina/astrocytic endfeet and the capillary lumen could be monitored (Reese, Karnovsk 1967). It was observed how, upon administration of HRP to the vasculature, no transmission occurred beyond the vessel lumen, most likely due to the presence of epithelial-like tight junctions in the intercellular clefts (Brightman, Reese 1969).

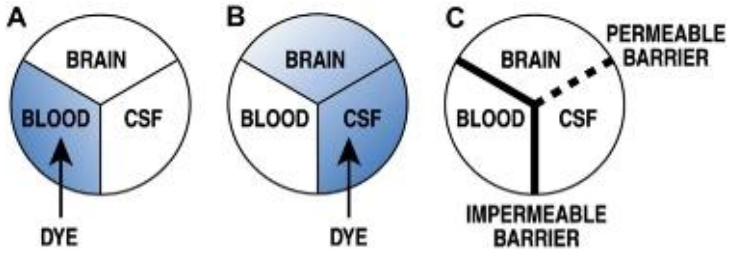

Figure 1.5: The BBB concept. (A) Intravenous injection of dyes lead to the observation that the spinal cord and brain did not permit dye uptake. (B) Direct injection into the CSF demonstrated the inverse, (C) suggesting the existence of a 'blood-brain barrier' (Zlokovic 2008).

It was discovered that there are in fact three main barrier layers in the brain and spinal cord; the epithelium of the choroid plexus, the arachnoid epithelium, and the endothelium of the microvessels (Figure 1.6) (Choi, Kim 2008, Saunders, Ek et al. 2008). While all three types of barriers express the tight junctions that significantly reduce the passage of ions and other small molecules through the intercellular clefts, it is the endothelium of the microvessels that offer a refined means of dynamically and selectively trafficking molecules across the barrier (Kimelberg 2004). A series of membrane transporters are available for the uptake and efflux of nutrients and waste products across the cellular barrier, primarily by transcytotic

pathways (Cecchelli, Berezowski et al. 2007, Herve, Ghinea et al. 2008, Candela, Gosselet et al. 2010, Tucker, Yang et al. 2012). These intricate pathways in conjunction with the enzymatic and paracellular barrier properties (Dauchy, 2008, Dutheil, 2010) the brain microvascular endothelial cells possess make capillary layer the most critical barrier in maintaining and regulating the homeostasis of the brain.

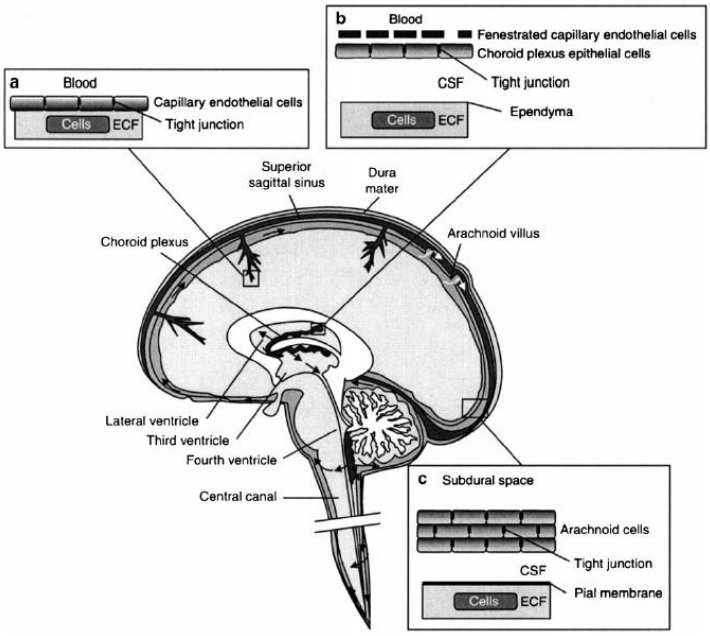

Figure 1.6: Barriers of the brain. The three principal barrier sites between the blood and brain. (a) The BBB proper, created at the level of the cerebral capillary endothelial cells by tight junction formation. (b) The blood-CSF barrier, located at the choroid plexuses in the ventricles of the brain where tight junctions are formed between plexus epithelial cells. (c) The arachnoid barrier, formed by the tight junctions of the cells of the inner layer of the arachnoid membrane which lies under the dura (Abbott 2013).

The brain and the spinal cord are the control centres of the body and make up the central nervous system (CNS). In short, the CNS is responsible for a host of integral functions such as processing sensory input, regulating motor output and coordinating many of the individual and concerted activities of tissues (Abbott, Friedman 2012). The burden of activity of the CNS is so large it is accredited for using 20% of oxygen consumption in the human body (Rolfe, Brown 1997). To carry out this array of functions, the neurons of the CNS utilise a combination of chemical (neurotransmitters and modulaters) and electrical signals (synaptic potentials, action potentials) to invoke precise ionic movements across their membranes (i.e. cell-cell communication). Proper neuronal function thus requires a highly regulated extracellular environment i.e. the concentrations of ions such as Na^+, K^+ and Ca^+ need to be tightly regulated to within a narrow range to ensure synaptic signalling is

precise, reliable and reproducible (Abbott, Patabendige et al. 2010). The ionic environment is easily subjected to imbalance via regular everyday process i.e. diet, physical activity etc. Therefore, to maintain a healthy balance the CNS has to selectively deliver the derived key nutrients, remove the subsequent waste products and restrict the entry of any foreign and potentially toxic neuroactive agents or pathogens that may be introduced via metabolic reactions. In short, to work effectively, it is critical that the environment of the CNS remains stable, an aim which is achieved through the blood-brain barrier (Abbott, Friedman 2012).

The development of the BBB in humans is regarded an evolutionary advantage. Comparisons to other vertebrates or invertebrates that have shown a negligible degree of evolution demonstrate a more primitive glial-based ultrastructure as opposed to the endothelium (Abbott, Lane et al. 1986, Abbott, Revest et al. 1992). This has led to speculation that the glial blood-brain barrier is an ancestral trait, and the development of an endothelial-based barrier arose from evolutionary selective pressure in maintaining ionic homeostasis of the CNS (Abbott, Lane et al. 1986, Banerjee, Bhat 2007). The consequent shift in cell type invoked the development of other now essential, more complex barrier functions. Thus, the BBB endothelium is the key cell type in establishing the human BBB we know today.

Whilst the phenotype of the BBB endothelium is the primary restrictive regulatory force of the NVU, attention is owed to a variety of other cell types that play key inductive and regulatory roles in creating and maintaining such a barrier. What follows is a cellular overview of the NVU.

1.2.1.1 Brain Microvascular Endothelium

A generic ‘default’ phenotype for endothelial cells is believed to exist, with heterogeneity evident between numerous different endothelial cells isolated from different vascular beds (Aird, 2012). From large vessels such as the aorta to the microvasculature, numerous traits and functions are carried over despite the location of the vascular bed (Pasqualini, 2002, Trepel, 2002). As vascularisation is seen to occur courtesy of in-growth from external vessels (Risau and Wolburg, 1990, Engelhardt and Risau, 1995), it is thought that tissues are able to induce the vasculature to generate tissue specific properties and functions.

A variety of cell culture and tissue grafting studies have clearly demonstrated that the endothelial cells of the CNS do not develop into their native BBB phenotype instinctively. The pioneer study that purported this idea involved the transplantation of avascular brain tissue from a new-born quail into the coelomic cavity of chick embryos. It was reported that

the chick endothelial cells which vascularised the quail brain grafts formed a competent BBB (Stewart and Wiley, 1981). By contrast, when the complementary study was conducted (avascular embryonic quail coelomic grafts transplanted into embryonic chick brain), the chick endothelial cells that invaded the mesenchymal tissue grafts were reported to have formed leaky blood vessels. Therefore the inductive means of the cerebral tissue is seen to be critical in inducing the BBB vascular phenotype.

The influence of the cerebral environment on the endothelium is substantive. A number of key functional aspects are greatly attenuated or amplified depending on the cerebral tissues requirements. Some of the key characteristics induced in the BBB endothelium in comparison to endothelium of the peripheral tissue include a much higher mitochondrial content (Oldendorf, Cornford et al. 1977), a lack of fenestrations (Fenstermacher, Gross et al. 1988), minimal pinocytotic activity (Sedlakova, Shivers et al. 1999), and a higher degree of transendothelial electrical resistance (TEER) and expression of tight junctions (Kniesel, Wolburg 2000) (Figure 1.7). Overall, the endothelium associated with the microvasculature of the nervous system shows the most extreme form of phenotypic differentiation compared to all other vascular beds within the body (Abbott 2005). This comes from the upregulation of features either poorly expressed or absent from the peripheral tissue and down regulation of some of the 'default' endothelial features.

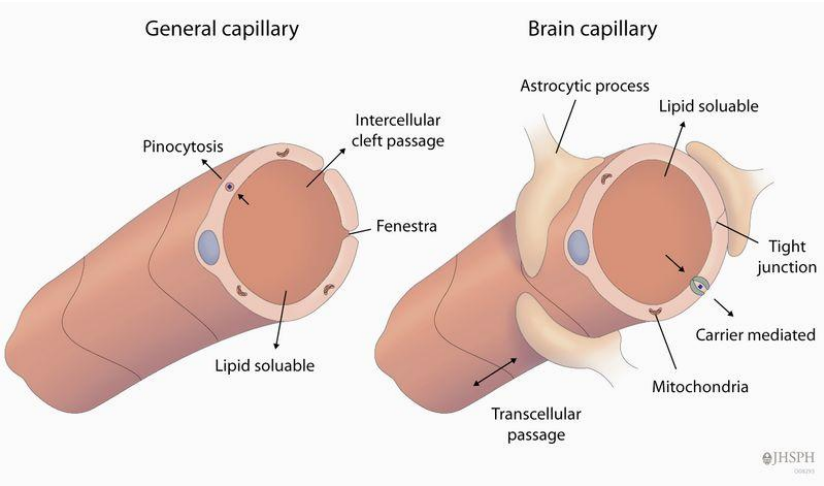

Figure 1.7: The differences between a general (non-neural) and brain capillary. BBB endothelium in comparison to endothelium of the peripheral tissue demonstrate a much higher mitochondrial content, less fenestrations, minimal pinocytotic activity and an enhanced expression of tight junction proteins (http://www.jhsph.edu/).

Whilst the basic function of the endothelial cell in the peripheral tissue has already been discussed it is necessary to address in greater detail the additional blood-brain barrier

specific properties of the endothelial cells which reside in cerebral vasculature bed. The endothelium in a (~1.3 kg) brain is estimated to cover a surface area of ~20m^2 (Pardridge 2003). The cerebrovasculature thus provides the largest surface area for blood-CNS exchange with each capillary supplying blood to neurons within proximity of 8-25 μm, identifying it as one of the key players in maintaining the homeostasis of the brain (Iadecola, Nedergaard 2007).

The brain's necessity to maintain a stable ionic environment has already been addressed. The BBB endothelial phenotype facilitates this need by not only separating but controlling the gradient of the neurotransmitters and neuroactive agents between the brain and the peripheral tissue. What follows is an overview of the distinctive barrier functions associated with the endothelium of the BBB.

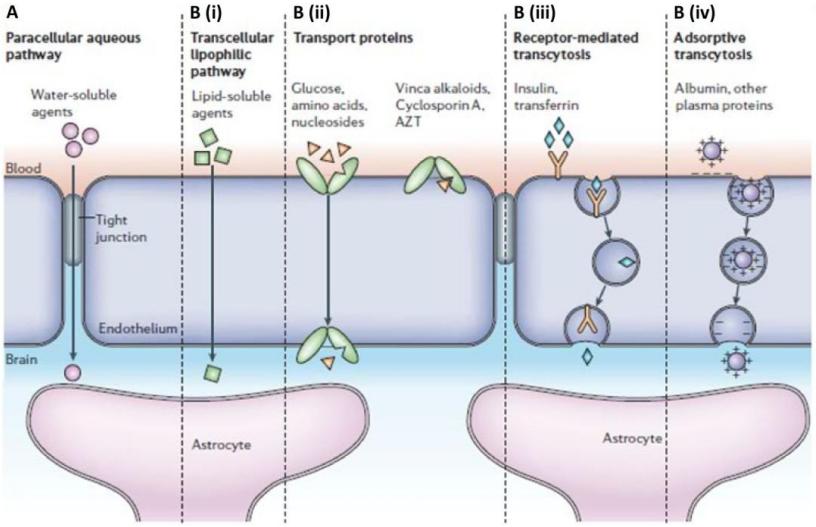

Figure 1.8: Pathways across the blood-brain barrier. A schematic representation of cerebral microvascular endothelium at the BBB and the main routes for molecular traffic across the barrier. (A) The paracellular pathway, regulated by tight junction proteins, that restrict the passage of water-soluble compounds. (B) The transcellular pathway which regulates solute flux through B (i) the cell membrane, B (ii) active transporters, B (iii) specific receptor-mediated endocytosis and B (iv) absorptive-mediated endocytosis and transcytosis (Abbott, Ronnback et al. 2006).

1.2.1.1.1 Paracellular Pathway

The flux of molecular traffic from the blood to the CNS can occur via two distinctive pathways (Figure 1.8, A). The movement of biological material via the interendothelial gaps constitutes the paracellular pathway. Here, restrictive barrier properties arise from presence of the tight junctions that allow the endothelial cells to fold over on themselves to form the vessel circumference and also seal them to neighbouring endothelial cells (Dejana, Corada et

al. 1995, Dejana, Lampugnani et al. 2000). Paracellular permeability at the BBB is maintained by the equilibrium between the adhesive forces at these cell-cell contact points and contractile forces of the endothelial cytoskeleton and (van Hinsbergh, Amerongen 2002). The dynamic interaction among these constituents of the BBB interendothelial junction complex, and the intracellular adapter proteins that link said complexes to the actin cytoskeleton, serves as a fundamental mechanism in regulating blood-brain exchange (Garcia, Davis et al. 1995). This transport means (in comparison to transcellular routes) is exclusively passive, less selective to transcellular pathways, and is driven by electrochemical, hydrostatic and osmotic gradients (Bazzoni 2006). Oxygen and carbon dioxide can freely diffuse across these intercellular regions though there is an approximate size cut-off at 5 kDa (Grieb, Forster et al. 1985). In addition to size playing a key factor in traversing this proposed route, lipid solubility is equally important. Overall, the paracellular route is incredibly restrictive and diverts the majority of molecular traffic to transcellular transport routes (Stamatovic, Keep et al. 2008).

In general, pathological increases in BBB permeability are associated with increased paracellular permeability. The dysregulation of these junctional complexes has been associated with a number of neurodegenerative diseases (Stamatovic, Keep et al. 2008) and thus, this pathway is the primary focus of this thesis. The interendothelial junction, its structure, function and role in the physiology and pathophysiology of the BBB will be covered in greater detail in later sections.

1.2.1.1.2 Transcellular Pathway

One of the obvious characteristics of brain endothelium is the lack of pinocytotic vesicles (Sedlakova, Shivers et al. 1999). The absence of these transport vesicles has been identified as one of the key factors resulting in the infamously low permeability, particularly to large macromolecules, of the BBB endothelial monolayer (Davson, Oldendorf 1967). Contrary to its restrictive nature, the BBB has been demonstrated to facilitate bi-directional travel of macromolecules across itself i.e. from blood to brain (Broadwell, Balin et al. 1988, Broadwell 1989) and vice versa (Vandeurs, Amtorp 1978), primarily by mechanisms of a transcytosis nature (Figure 1.8, B).

Whilst the intercellular junctions of the endothelial cells restrict passive transport, smaller lipid soluble molecules such as oxygen and carbon dioxide have been shown to be able to traverse not only the paracellular restrictions but also transcellular ones (Grieb, Forster et al. 1985). Therefore, the barrier presented by the cerebral endothelium appears to be only protective against the passive entry of larger, lipid insoluble compounds (Misra, Ganesh et

al. 2003). However, due to the sensitive nature of the neural environment it is essential for the cerebral endothelium to facilitate the passage of some of these larger molecules that may represent essential nutrients across its collective barrier. This comes in the form of a number of carrier-mediated transport systems that are primarily located on the abluminal side of the cerebral endothelia cells (Sanchez Del Pino, Hawkins et al. 1995). Essential amino acids and glucose enter the brain via transporters/carriers/channels present on the plasma membrane whereas non-receptor-mediated endocytosis mechanisms facilitate the influx of larger molecules (e.g. insulin, leptin, iron transferin) (Pardridge, Eisenberg et al. 1985, Zhang, Pardridge 2001, Lossinsky, Shivers 2004). Transport mechanisms are present on the luminal side of the endothelium but are more facilitative than active in their function.

1.2.1.1.3 Enzymatic/Efflux Barrier

While each transport mechanism has designated criteria to meet in order to avail of its use, a number of molecules and even computationally designed drugs which meet these criteria have been shown to traverse the BBB with difficulty (Misra, Ganesh et al. 2003). These restrictions come in the form of enzymatic and efflux mechanisms which counteract the transport of said materials. The BBB is enzymatically capable of metabolising both drugs and nutrients (Brownson, Abbruscato et al. 1994, Matter, Balda 2003, Matter, Balda 2003). The levels of enzymes such as γ-glutamyl transpeptidase (γ-GTP), alkaline phosphatase and aromatic acid decarboxylase are found to be elevated in cerebral microvessels in comparison to those of non-neuronal origin (Minn, Ghersiegea et al. 1991, Abbott, Romero 1996). These enzymes are located on both the abluminal and luminal membrane surfaces of the BBB endothelium and principally metabolise neuroactive blood-borne solutes (Betz, Firth et al. 1980). In addition, efflux transporters monitor the compounds being trafficked across the BBB and intervene should they detect anything that may be harmful or toxic. Two of the more established and understood efflux transporters are permeability (P)-Glycoprotein and Multidrug Resistance-Associated Protein (MRP). These membrane proteins are constitutively expressed by cerebral endothelium (Cordon-Cardo, O' Brien et al. 1989, Liu, Hu 2000, Demeule, Regina et al. 2002) and are understood to have arisen through evolution in order to control the passive influx of lipid-soluble compounds (Tatsuta, Naito et al. 1992). Both of these efflux transporters have a large degree of overlap in the substrates they recognise and export with non-specific interactions at the forefront of their selectivity. Whilst the development of defence mechanisms like these is to our evolutionary advantage, they have yielded a new obstacle in targeted drug delivery (Misra, Ganesh et al. 2003).

Overall, the endothelial monolayer is the single interface between the blood and extracellular fluid. The barrier mechanisms involved in limiting the flux of molecules and ions, ensuring that chemical gradients can be established, were of great importance in developing and understanding the mechanisms involved in the physiology and pathophysiology of the BBB. Early *in vitro* studies of brain endothelium had proven difficult until a greater understanding of the inductive effects which are necessary to maintain these cells (and their barrier properties) out of culture were uncovered (Abbott 2013). Culture studies have demonstrated that utilising endothelium derived from brain microvessels is more effective than attempting induction studies from other tissue derived endothelia (Dehouck, Meresse et al. 1990, Reinhardt, Gloor 1997). Primary cells cultured *in vitro* have been shown to maintain aspects of its original phenotype down to the molecular level (Li, Boado et al. 2001, Desai, Marroni et al. 2002). Steady culturing of primary derived endothelia are seen to revert back to their 'default' phenotype (Reichel, Begley et al. 2003) unless mimicking or introducing certain inductive forces into cell culture techniques has been shown to stabilise the brain phenotype and prevent differentiation. Induction is more effective if the endothelium is exposed to shear stress (Stanness, Westrum et al. 1997). Different degrees of shear stress in large versus small cerebral vessels have been thought to play a part in inducing different functional properties in the endothelium. Higher shear rates have yielded brain arterial and arteriolar endothelia which have been shown to present subsequent phenotypic properties than lower sheared capillary endothelium (Westergaard, Brightman 1973). A number of differentiating agents have also been identified (Rubin, Hall et al. 1991, ElHafny, Bourre et al. 1996, ElHafny, Chappey et al. 1997). Adrenomedullin has been shown to be an integral agent in regulating cerebral circulation and BBB functions (Kis, Abraham et al. 2003). Hydrocortisone (Hoheisel, Nitz et al. 1998) and bFGF (Sobue, Yamamoto et al. 1999) have also been utilised in culture techniques.

Now that the primary cell type of the BBB is understood it is essential to address the other cell types which comprise the NVU (Figure 1.9). As mentioned earlier, these cell types play a key role in the induction of endothelial barrier phenotype; however the overall induction process is a controversial subject owing to the fact that the different cell types of the NVU establish themselves at different times in development (Saunders, Dziegielewska et al. 1991). *In vivo* models have shown that vessels in the initial vascularisation process are discontinuous (Kniesel, Risau et al. 1996) owing to the absence of certain inductive cells at the time. During development, the barrier layers have also been shown to shift from glial/ependymal derivatives to endothelial once blood vessels start to invade the nervous system (Abbott, Revest et al. 1992). These factors have led to great debate over when a 'barrier' is in place. Alternative studies that focussed on the presence of serum proteins

reported that a protein barrier is in place during embryonic development however the ionic barrier is noted to be absent (Saunders, Dziegielewska et al. 1991) and doesn't appear until after birth stemming from studies measuring the resistance of plial vessels (1000-2000 Ω/cm^2) against peripheral vessels (10 Ω/cm^2) (Butt, Jones et al. 1990).

Studies are ongoing in understanding the factors and inductive signals which yield the overly unique BBB endothelium phenotype. Early markers of (E10.5) BBB formation have been identified (Qin, Sato 1995) though much more is expected to be uncovered. The different cell types of the NVU will be covered in the following sections and their role in the induction of the BBB and subsequent maintenance will be addressed.

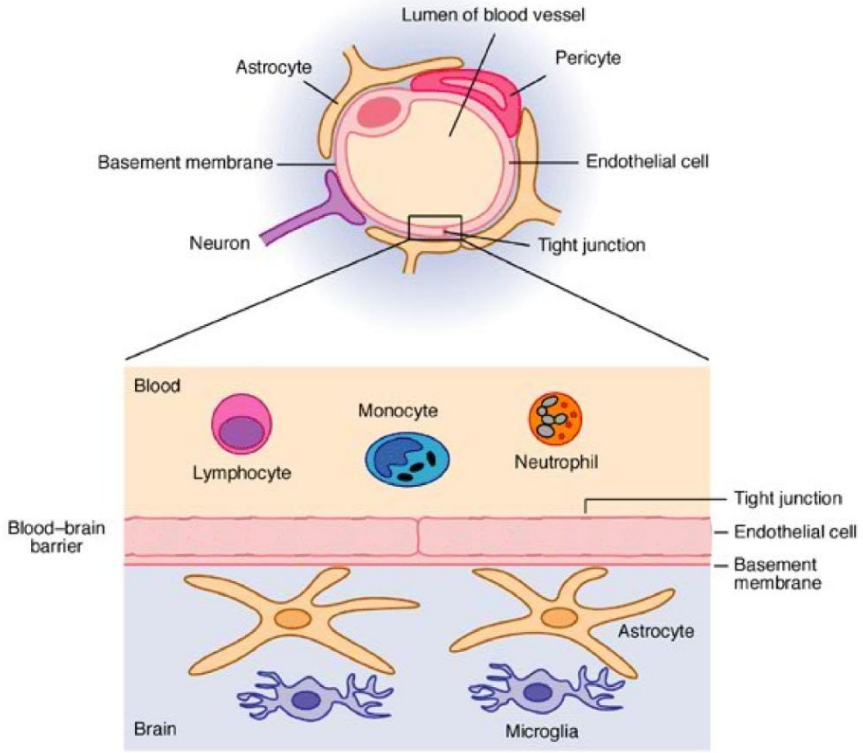

Figure 1.9: A representative cross-section of a cerebral capillary of the BBB. The BBB is composed of cerebral capillary endothelial cells that are part of an intricate network of astrocytes, pericytes, and neurons. Together, they form tight, impermeable junctions, which exclude large cells, macromolecules and excess fluid from the central nervous system (Francis, van Beek et al. 2003).

1.2.1.2 Astrocytes

Astrocytes are a major glial cell type associated with the CNS. Of the 11 distinct phenotypes, 8 have been shown to have specific interactions with blood vessels

(Reichenbach, Derouiche et al. 2004). Each cell creates a number of contact points between itself and various other cell types in the CNS via complex cellular processes (e.g. synapses, nodes of Ranvier and blood vessels) (Zhang, Barres 2010). This networking ability of the astrocytes, in addition to their close anatomical association with the BBB, identified them early on as being key players in dynamically regulating a variety of signalling events within the CNS (Davson, Oldendorf 1967). It is reported that the outer ridge of the capillary wall consists of a mesh-work of astrocytic endfeet that cover as much as 85% of the basement membrane surface. 3D visualisation of the microanatomy has given rise to the idea of 'microdomains' in which single endothelial cells associate with a single astrocyte (Kacem, Lacombe et al. 1998). These findings demonstrate just how intricate a network the astrocytes establish with the BBB endothelium and surrounding neurons.

Early studies similar to that of Stewart and Wiley (1981) that investigated this concept involved grafting purified neonatal astrocytes into the anterior chamber of the eye. Upon injection, the astrocytes were observed to have been quickly vascularised and injection of Evans blue dye to these newly formed vessels demonstrated the astrocytes excluded the dye (Janzer, Raff 1987). Further studies have shown that in endothelial-astrocyte co-culture models (Taocheng, Nagy et al. 1987, Neuhaus, Risau et al. 1991) or even astrocyte conditioned media (Maxwell, Berliner et al. 1987, Colgan, Collins et al. 2008), BBB characteristics are improved *in vitro*. However for optimal organisation of the vessel wall and BBB stability, direct contact between endothelial cells and astrocytic end-feet is necessary (Rubin, Hall et al. 1991).

It has been suggested that astrocytes work in conjunction with neurons, relaying signals to control cerebral permeability (Ballabh, Braun et al. 2004). In relation to the BBB, astrocytes have been shown to play a part in modulating blood vessel contraction and dilation, subsequently influencing region specific blood flow (Attwell, Buchan et al. 2010). In addition, astrocytes have been shown to influence junctional and transport properties of the BBB, particularly in capillary endothelial cells (Janzer, Raff 1987, Raub 1996). *In vitro* studies have shown that endothelial cultures in the presence of astrocytes or astrocyte derived factors such as angiotensin (Ang) II, have shown a decrease in permeability to tracer molecules, an increase in TEER, as well as an increase in localised P-glycoprotein (Rubin, Hall et al. 1991, Raub 1996, Rist, Romero et al. 1997, Wosik, Cayrol et al. 2007) and glucose transport (GLUT)1 (McAllister, Krizanac-Bengez et al. 2001) transporter expression. Further studies have shown with regards to barrier function, astrocytes have a direct effect on stabilising the tight junction via sonic hedgehog signalling (Alvarez, Dodelet-Devillers et al. 2011). Astrocytes have been shown to secrete a wide array of agents that can induce several different aspects of BBB phenotype in endothelial cells, among

which are transforming growth factor (TGF)-β, basic fibroblast growth factor (bFGF), and Ang II in addition to others (Abbott 2002, Haseloff, Blasig et al. 2005).

Interestingly, it should be noted that while astrocytes are seen to physically envelop the microvessels of the cerebrovasculature and also secrete a number of mediators that influence barrier function, they don't physically act as a barrier in vertebrates, the opposite of which can be said for invertebrates (Abbott 1987). It was demonstrated quite early on that upon injection of horseradish peroxidise (HRP) into intact microvessels, the agent was shown to easily migrate through the 20nm gaps between the astrocytic endfeet (Brightman, Reese 1969).

Finally, grafting studies have shown that astrocytes alone are not enough to induce a BBB phenotype in endothelial cells (Shayan, Shuler et al. 2011). Moreover, the BBB has been shown to be already under development before astrocyte generation has commenced suggesting that astroyctes are primarily involved in the maintenance of the BBB rather than development/induction (Webersinke, Bauer et al. 1992, Bauer, Bauer et al. 1993, Holash, Noden et al. 1993). *In vivo* studies have shown that in microvessels that are induced to undergo massive astrocytic loss can survive and continue to maintain a degree of barrier integrity (Krum, Kenyon et al. 1997) although other studies suggest the opposite (Willis, Nolan et al. 2004).

1.2.1.3 Pericytes

Pericytes are elongated, polymorphic cells of a mesenchymal origin that are closely associated with the vasculature system and are present in almost all tissues and organs (Diaz-Flores, Gutierrez et al. 1991). Although widespread, their density and functions can vary greatly depending on the vascular bed in which they reside (Armulik, Abramsson et al. 2005). They are commonly associated with the microvaculature, namely arterioles, venules and capillaries and are seen to be wrapped around the abluminal side of endothelial cells at irregular intervals along the vessel wall (Tagami, Nara et al. 1990), not unlike the way smooth muscle cells cradle the endothelium in larger vessels (Diaz-Flores, Gutierrez et al. 1991). Pericytes have been shown to have a particular affinity towards endothelial cells (Minakawa, Bready et al. 1991) and both cell types are known to become associated early on during embryonic development (Simionescu, Ghinea et al. 1988) with ultrastructural studies in embryonic mouse brains confirming that along with endothelial cells, pericytes are among the first cell type to invade the neural tissue as early as E10 (Bauer, Bauer et al. 1993).

Pericytes make several different types of contact with endothelial cells; namely gap junctions, adhesion plaques and peg-and-socket junctions, allowing pericytes to remain in very close proximity to the vessel wall but also to communicate with the cells that comprise it (Diaz-Flores, Gutierrez et al. 1991). Within this close proximity, and drawing on the comparison to smooth muscle cells made earlier, they have been shown to provide not only structural support to the vessel wall, and but also regulate the vasodynamics of it (Bandopadhyay, Orte et al. 2001). For example, Ang II is a vasoactive peptide present in numerous parts of the brain, often presented on the neurons and nerve terminals associated with microvessels (Healy, Wilk 1993). Pericytes have been shown to express Ang II binding sites (FerrariDileo, Davis et al. 1996) and their activity post-uptake of Ang II is well documented (Matsugi, Chen et al. 1997, Matsugi, Chen et al. 1997). Aside from Ang II, pericytes express a broad range of binding sites for other vasoactive compounds such as vasopressin (Vanzwieten, Ravid et al. 1988) and endothelin (ET)-1 (Dehouck, Vigne et al. 1997). Since ET-1 is produced primarily by endothelial cells, this gives an insight into the dynamic communication between the two cell types in regulating blood flow.

In light of this, pericytes have been shown to be both positive and negative regulators of the endothelium (Bergers, Song 2005). Aside from the already discussed dynamic control of blood flow, pericytes have been shown to play a key role in striking a balance between numerous opposing processes. For example, TGF-β release by pericytes is mediated by contact between pericytes and endothelial cells. Upon association, TGF-β becomes active and is known to inhibit endothelial cell proliferation thus stabilising developing microvessels (Crocker, Murad et al. 1970, Antonelliorlidge, Saunders et al. 1989, Yan, Sage 1998). In contrast to this, pericytes also release bFGF, which promotes cellular growth and differentiation in addition to promoting vascular tube formation.

One of the most important aspects of the endothelium is its barrier function, which pericytes have been shown to have a direct influence on. Co-culture models of pericytes and endothelium showed pericyte presence was enough to inhibit genes that increase permeability. In fact, a direct correlation between the number of pericytes in a region and the permeability of the underlying tissue exists (Daneman, Zhou et al. 2010). In pathological circumstances such as hypoxia (Gonul, Duz et al. 2002) or traumatic brain injury (TBI) (Dore-Duffy, Owen et al. 2000), symptomatic migration of pericytes away from the microvasculature coincided with an increase in microvessel permeability.

Similar to astrocytes, pericytes introduced to endothelial cultures do not appear to induce a BBB-specific endothelial phenotype from a gene expression perspective; however co-culture studies which combined pericyte, astrocytes and endothelial cells were shown to produce

stable, capillary-like structures (Ramsauer, Krause et al. 2002). Knockout mice models for pericyte recruitment agents (e.g. platelet-derived growth factor B (PDFGB)) demonstrated a poorly developed and maintained BBB (Armulik, Genove et al. 2010) in addition to microaneurysm formation (Lindahl, Johansson et al. 1997). Moreover, the concurring disruption of transcytosis pathways and an increase in the expression of leukocyte adhesion molecules resulting from PDGFB knockout underscores the importance of pericytes in microvessel homeostasis. Finally, pericytes have also shown to increase the endothelial defence against apoptotic mechanisms in tri-culture models (astrocytes, pericytes, endothelium, (Ramsauer, Krause et al. 2002)), giving rise to the argument that pericytes are directly involved in maintaining the structural integrity and inception of the BBB.

1.2.1.4 Neurons

Given the dependency of neural tissue on BBB phenotype, it is natural to assume there is a level of communication between the neurons and the microvasculature. Anatomically, direct innervations between a number of different types of neurons and the microvascular endothelium/astrocytic endfeet have been reported (Kobayashi, Magnoni et al. 1985, Vaucher, Hamel 1995, Cohen, Molinatti et al. 1997). Changes to cerebral blood flow and pressure have long been associated with BBB dysfunction and are often identified as the penultimate event that triggers the initiation of a number of different pathologies (e.g. ischemia, hemorrhage, traumatic brain injury) (Hatashita, Hoff 1990, Petty, Wettstein 2001, Petty, Lo 2002). Studies have linked this change in the microvasculature's hemodynamic forces to being a compensatory event triggered by the neurons of the NVU rather than as a symptom of anatomical disruption (Lee, Hung et al. 1999). With this in mind, a number of studies have aimed to demonstrate that while neuronal presence may not be critical in the development and induction of a BBB, they do play a key regulatory role in a number of BBB functions. Numerous cerebral diseases have shown that neuronal dysfunction often correlates with BBB dysfunction e.g. Alzheimers disease (Tong, Hamel 1999).

1.2.1.5 Basal Lamina

Pericytes and endothelial cells are ensheathed in the basal lamina, a membrane 30-40 nm thick and comprised of a myriad of growth factors and matrices such as collagen type IV, heparin sulphate, laminin and fibronectin amongst many others (Farkas, Luiten 2001). On the abluminal side, the astrocytic endfeet are contiguous with the basal lamina. The basal lamina acts as a foundation for the endothelium to anchor to via interactions with matrix proteins like laminin and integrins (Hynes 1992), while the growth factors have been shown

to have a direct influence on the expression of tight junction proteins (Tilling, Korte et al. 1998, Savettieri, Di Liegro et al. 2000). Thus, disruption of the basal lamina has been identified as a key step in certain pathological states and is linked to increased BBB permeability (Rosenberg, Estrada et al. 1993, Rascher, Fischmann et al. 2002). For example, cortical spreading depression, a mechanism associated with migraines, has been shown to upregulate matrix metalloproteases (MMP). These MMP's induce the proteolysis of the basal lamina (Sanchez-del-Rio, Reuter 2004), which has been shown to be directly linked to tight junction protein zonula occludens (ZO)-1 loss in the affected area (Gursoy-Ozdemir, Qiu et al. 2004). This identifies the proteins of the basal lamina as having a respectable role in maintaining tight junctions (TJ) and BBB homeostasis.

1.2.2 Tight Junction/Adherens Junction

What will be addressed in this section are the interendothelial transmembrane proteins comprising the tight junction complex. In addition to tight junctions, the adherens junction (AJ) complex, the gap junction and the proteins that facilitate the dynamic, reversible nature of the junctions will be discussed (Figure 1.10).

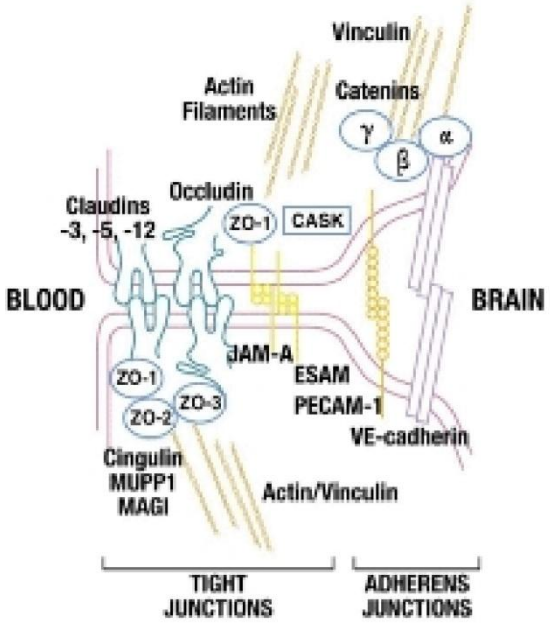

Figure 1.10: The proteins of the tight junction/adherens junction of the blood-brain barrier. Schematic figure of the proposed associations of the key proteins found at the interendothelial junctions of the BBB (Zlokovic 2008).

1.2.2.1 Occludin

Occludin was the first of the integral proteins localised at the tight junction to be identified, first in chickens (Furuse, Hirase et al. 1993) and later in mammals (Ando-Akatsuka, Saitou et al. 1996). Occludin is a 65 kDa protein whose carboxyl and amino terminals are orientated in the cytoplasm, and which displays four transmembrane domains. This orientation yields two extracellular loops which span the intercellular cleft (Furuse, Hirase et al. 1993). It was the abundance of glycine and tyrosine in the first of the extracellular loops that lead to its initial characterisation.

In comparison to non-neuronal tissues, where it is much more sparsely distributed (Hirase, Staddon et al. 1997), occludin is highly expressed in cerebral endothelial cells and cellular staining shows a continuous, uninterrupted presence along the cell membranes (Lippoldt, Kniesel et al. 2000, Hawkins, Abbruscato et al. 2004). Occludin has been shown to be directly related to the high electrical resistance demonstrated by the cerebral endothelium (McCarthy, Skare et al. 1996). The cytoplasmic C-terminus of occludin links it to the cytoskeleton via adapter proteins such as ZO-1 and ZO-2. Together with the claudins, occludin makes up the intramembranous tight junction, which despite their restrictive nature, are said to possess channels which facilitate diffusion of ions and hydrophilic molecules via paracellular transport (Matter, Balda 2003, Matter, Balda 2003). Evidence has shown that phosphorylation of occludin modulates tight junction permeability via G-protein and additional mechanisms (Hirase, Kawashima et al. 2001) and studies which utilised C-terminally truncated occludin demonstrated an increase in paracellular permeability to low molecular weight molecules (Balda, Whitney et al. 1996), suggesting its potential importance in maintaining a barrier. Despite this, knockout studies for occludin have shown that its presence is not actually necessary in facilitating the assembly of the overall tight junction. Occludin-deficient mice not only display a fully functioning BBB but other junctions that comprised of occludin in addition to other proteins (e.g. gut epithelia) remained intact (Saitou, Furuse et al. 2000). While prominent in adult brain, it is not present in fetal or newborn brain sections demonstrating it is not essential for BBB development. Animal-models have demonstrated that significant levels of occludin only appeared after the first post natal week with its appearance coinciding with the complete development of the BBB (Hirase, Staddon et al. 1997). This has lead to the belief that an alternative to occludin exists during the early developmental stages prior to occludin taking on its roles. Studies that did note an intact BBB after occludin silencing did note some anomalies such as chronic inflammation, post-natal retardation and calcification of areas of the vasculature, in particular the brain, suggesting that while occludin might not be essential in maintaining a restrictive barrier, it may be a key player in regulating other junction-associated processes

(i.e. calcium flux) across the tight junction (Saitou, Furuse et al. 2000). In spite of these studies, other evidence has shown in numerous pathologies associated with BBB dysfunction, decreased expression of occludin is at the forefront, indicating it has an integral role in maintaining tight junction stability (Bolton, Anthony et al. 1998, Huber, Hau et al. 2002, Brown, Davis 2005).

1.2.2.2 Claudins

The first claudin proteins (claudin-1 and -2) were identified in junctional fractions of chicken livers and early evidence compounded by the discovery of two isoforms at once suggested they were part of a larger family of proteins (Furuse, Fujita et al. 1998, Morita, Furuse et al. 1999, Mitic, van Itallie et al. 2000). Since their discovery, over 20 isoforms of the 24 kDa proteins have been identified in mammals (Bauer, Traweger et al. 2004). All isoforms show similar folding patterns with a very high sequence homology demonstrated in the first and fourth transmembrane domains (Heiskala, Peterson et al. 2001). Claudins also have a very similar distribution to occludin, displaying four transmembrane domains with two extracellular loops, despite almost no sequence homology (Furuse, Fujita et al. 1998). Claudins form quite long and branched intercellular strands in contrast to occludins shorter ones (Tsukita, Furuse 1999, Furuse, Sasaki et al. 1999). The extracellular loops of the claudins can interact via homo- and heterophilic interactions between adjacent cells (Furuse, Sasaki et al. 1999, Daugherty, Ward et al. 2007) giving rise to a large number of potential interactions. It should be noted that many of the claudins are tissue/cell specific and there is accumulating evidence suggesting that the composition of the the claudins directly determines the barrier function (Furuse, Hata et al. 2001). Induced expression of claudin-1 in Madin-Darby canine kidney (MDCK) cells increased transcellular resistance by four-fold with a corresponding drop in paracellular permeability (Inai, Kobayashi et al. 1999), while induction of claudin-2 into MDCK cells already expressing claudins-1 and -4 demonstrated a drop in barrier function (Furuse, Hata et al. 2001). Thus the stoichiometry of claudin species has a direct impact on cell barrier function (Tsukita, Furuse 2000, Furuse, Sasaki et al. 1999).

Within the cerebral endothelium, claudin-3 and -5 have been detected, with questionable studies regarding claudin-1 and -12 (Morcos, Hosie et al. 2001, Nitta, Hata et al. 2003, Witt, Mark et al. 2003, Wolburg, Wolburg-Buchholz et al. 2003, Hawkins, Abbruscato et al. 2004). As mentioned, the tight junction can be formed in the absence of occludin, the same of which cannot be said of the claudins. In other tight junction forming cell types, claudin-5 is ubiquitously expressed while other isoforms (-1 and -3) levels are diminished. *In vitro*

culturing of BBB endothelial cells is reported to cause certain claudin levels to decrease (Liebner, Fischmann et al. 2000, Liebner, Kniesel et al. 2000) except for claudin-5 which is sufficient to mediate tight junction formation (Wolburg, Neuhaus et al. 1994). This signifies claudin-5 as the key member of the claudins in relation to BBB homeostasis. *In vivo* mouse models, which ablate claudin-5, have shown high mortality rates at birth with dissection confirming the poor development and permeability of the BBB (Nitta, Hata et al. 2003). Moreover, occludin has been shown to only localise to the cell border in the presence of claudin (Kubota, Furuse et al. 1999). It is therefore hypothesised that the claudins form the primary seal of the tight junction with occludin providing secondary support.

1.2.2.3 JAMs

Junctional Adhesion Molecules (JAMs) are a family of 40 kDa proteins which are known to contribute via homophilic (and potentially heterophilic) interactions in the attachment of adjacent cells (Dejana, Lampugnani et al. 2000). JAM-1 (formally JAM) is expressed in a number of tight junction-forming cell types (Martin-Padura, Lostaglio et al. 1998), while JAM-2 (Aurrand-Lions, Duncan et al. 2001) and JAM-3 (Palmeri, van Zante et al. 2000) are mostly expressed in vascular endothelial cells. The JAMs are composed of a single membrane spanning chain with a large extracellular domain (Martin-Padura, Lostaglio et al. 1998). Although important in the initial contact between cells, occludin and the claudins are seen to be the primary components of the tight junction. Nevertheless, the JAM's contribute in other ways in mediating tight junction formation. In the absence of other tight junction forming proteins, the JAMs have shown to increase cellular resistance (Martin-Padura, Lostaglio et al. 1998). Over-expression of JAM-1 has also been shown to reduce permeability possibly by mediating occludin translocation to the cell membrane (Dejana, Lampugnani et al. 2000). JAM-2 and to a lesser extent JAM-3 were also shown to have a critical role in junction formation in the select tissues in which they are expressed (Palmeri, van Zante et al. 2000, Aurrand-Lions, Duncan et al. 2001).

Primarily the JAMs are seen to regulate the transendothelial migration of leukocytes and monocytes (Del Maschio, De Luigi et al. 1999, Bazzoni, Martinez-Estrada et al. 2000, Aurrand-Lions, Duncan et al. 2001), with blocking of JAM-1 seen to inhibit extravasation *in vitro* and *in vivo* (Del Maschio, De Luigi et al. 1999).

1.2.2.4 Cadherins

The adherens junctions are ubiquitous within the vasculature and play a key role in numerous endothelial processes (Lampugnani, Dejana 2007). Amongst these functions are mediating the initial adhesion and subsequent contact inhibition during vascular growth and remodelling, initiation of cell polarity, and regulation of paracellular permeability (Lampugnani, Dejana 2007, Dejana, Orsenigo et al. 2008). The regulation of cell-cell adhesion implies that the formation of the tight junction is linked to the formation of the adherens junction and mediated through a class of membrane proteins; cadherins. There are currently over 80 different types of cadherin proteins reported that range from being non-specific and expressed across a host of cell types to being wholly specific. The more commonly known cadherins such as E, P and N, are single pass transmembrane glycoproteins that form homophilic interactions (Takeichi 1995). However one of the more recent cadherins to be discovered was a unique endothelial specific cadherin that plays a major role in the adherens junction.

The primary component of the adherens junction is a Ca^{2+}-regulated protein called Vascular Endothelial (VE)-Cadherin. VE-Cadherin, like most cadherin proteins, mediates homophilic interactions between the extracellular domains of the protein expressed on adjacent cells, in this case, the endothelium (Vincent, Xiao et al. 2004). The extracellular domain however is not enough to instigate junction formation; what is crucial to forming stable junctions is the cytoplasmic tail (Gumbiner, 1996). The cytoplasmic tail binds to β- or γ-catenin and plakoglobin, which in turn bind to the actin cytoskeleton via a number of inter-skeletal proteins (α-catenin, α-actinin and vinculin), thus stabilising the adherens junction complex (Knudsen, Soler et al. 1995, Lampugnani, Corada et al. 1995, Watabe-Uchida, Uchida et al. 1998).

As mentioned, the adherens junction is primarily focused on mediating initial cell-cell adhesion (Lampugnani 2010). Therefore it is not wrong to suggest that formation of the tight junction would be improbable should the adherens junction not be formed. Whilst the tight junction resides on the apical point of the intercellular junction and is clearly separate from the adherens junction, there have been reports of inter-mixing of the strands (Schulze, Firth 1993). This sometimes close association is backed up by evidence that through the catenins that link the cadherins to the cytoskeleton and other signalling components, the adherens and tight junctions can communicate and influence one another (Staddon, Herrenknecht et al. 1995, Schulze, Firth 1993, Taddei, Giampietro et al. 2008, Walsh, Murphy et al. 2011). Accumulating evidence has suggested that maintenance of the tight junction is completely dependent on the stability of the adherens junctions. The role of VE-Cadherin in the restriction of paracellular permeability is also worth nothing. Whilst the tight junction is the

primary restrictor of paracellular passage of molecules, studies have shown that disruption of the adherens junction results in an increase in BBB permeability (Romero, Radewicz et al. 2003). Whether this is due to an indirect effect on the tight junction or VE-Cadherin itself restricting passage is to be further elucidated.

1.2.2.5 MAGUKS

Although the proteins of the tight and adherens junctions facilitate intercellular contacts, a number of cytosolic accessory proteins mediate the cellular remodelling and organisation. One of the key instigators of these processes is the membrane-associated guanylate kinase (MAGUK) family (Gonzalez-Mariscal, Betanzos et al. 2000). Three MAGUK proteins have been identified in being involved with the coordination and clustering of protein complexes at the cell membrane, namely the tight junctions; ZO-1, ZO-2, and ZO-3 (Gonzalez-Mariscal, Betanzos et al. 2000, Shin, Hsueh et al. 2000). All three contain three PDZ domains, one SH3 domain and one guanyl kinase-like domain, and can be characterised by such. Each of these domains acts as a protein-binding site, thus implicating the zonula occludens in facilitating a number of protein-protein interactions.

ZO-1, a 220 kDa protein, was the very first protein to be positively linked to the tight junction (Stevenson, Siliciano et al. 1986). ZO-1 was already an established protein, seen in many tissues that lack/contain tight junctions (Howarth, Hughes et al. 1992). As such, ZO-1 has been shown to be involved in a number of processes outside of the tight junction. Among the BBB constituents known to bind to the ZO proteins are the claudins (Itoh, Morita et al. 1999), occludin (Mitic, van Itallie et al. 2000) and JAM (Ebnet, Schulz et al. 2000). In addition, actin has been shown to bind to the carboxyl terminal of ZO-1 and ZO-2 allowing the crosslink with the transmembrane proteins of the junction. This signifies how critical ZO-1 is in mediating the formation and stability of the junctional complex, as upon dissociation, intercellular permeability is seen to increase (Abbruscato, Lopez et al. 2002, Fischer, Wobben et al. 2002, Mark, Davis 2002). ZO-1 has been shown to dissociate from the junction during proper cellular function (i.e. proliferation) but is more closely associated as a response to adverse conditions (Gottardi, Arpin et al. 1996), such as Ca^{2+} depletion (Riesen, Rothen-Rutishauser et al. 2002), and injurious stimuli such as nicotine (Hawkins, Abbruscato et al. 2004).

Less is known about ZO-2 in relation to the BBB although studies have demonstrated its ability to bind many of the BBB constituents and signalling molecules (Betanzos, Huerta et al. 2004). It also localises along the membrane in a similar fashion to ZO-1 but not in nearly as consistent a fashion (Schulze, Smales et al. 1997, Hawkins, Abbruscato et al. 2004). In

fact, initial immunoprecipitation (IP) experiments that aimed to elucidate the tight junction binding partners of ZO-1 led to the discovery of ZO-2 (Gumbiner, Lowenkopf et al. 1991), which was named based on the large degree of similarity between the two (Jesaitis, Goodenough 1994). An argument has been made that ZO-2 picks up the mantle left by ZO-1 in its absence. ZO-3 has been shown in some tight junction tissues (Inoko, Itoh et al. 2003) but not much has been explored regarding its role within the BBB.

1.3 Haemodynamics

The entire vascular tree is constantly exposed to haemodynamic forces that vary widely in magnitude, frequency and direction (Davies 1995, Chien, Li et al. 1998). The endothelium residing on the inner wall of vessels is subjected to these constant fluid-driven mechanical forces, directly resulting in the modulation of its molecular, genetic, structural and functional properties (Figure 1.11). There is overwhelming evidence that the endothelium is able to 'sense' and discriminate between these fluidic forces and to translate them into regulatory events (Gimbrone, Topper et al. 2000).

The response of the vasculature to these forces needs to be highly dynamic in order to adapt to the current situation (Beevers, Lip et al. 2001) and since the endothelium is seen to be at the forefront of these forces, an intact monolayer is essential for the processes to occur (Langille, O' Donnell 1986). Typically, undisturbed physiological haemodynamic forces are seen to promote an 'atheroprotective' phenotype, preventing undesirable remodelling of the vessel wall. They also facilitate vessel adaptation to external stimuli (Traub, Berk 1998). For example, exercise results in an increase in blood pressure. Within moments of this increase, the vessel wall of the aortic arch initiates signals to the surrounding neurons which in turn trigger the release of vasoregulators to adapt the vessel shape and signals to the kidneys to control blood volume. Upon cessation of exercise, the vasculature reverts to normal (Furchgott, Zawadzki 1980, Frangos, Eskin et al. 1985, Rubanyi, Romero et al. 1986, Vallance, Collier et al. 1989). At the cellular and molecular levels, these forces have been implicated in controlling cellular remodelling, proliferation, angiogenesis, migration, apoptosis and matrix degradation and/or synthesis (Davies, Remuzzi et al. 1986, Cho, Courtman et al. 1995, Dimmeler, Haendeler et al. 1996, Cho, Mitchell et al. 1997, Kaiser, Freyberg et al. 1997, Dimmeler, Hermann et al. 1998, White, Haidekker et al. 2001). It follows therefore that their dysregulation (e.g. during atherosclerosis and stroke) is central to disease pathogenesis.

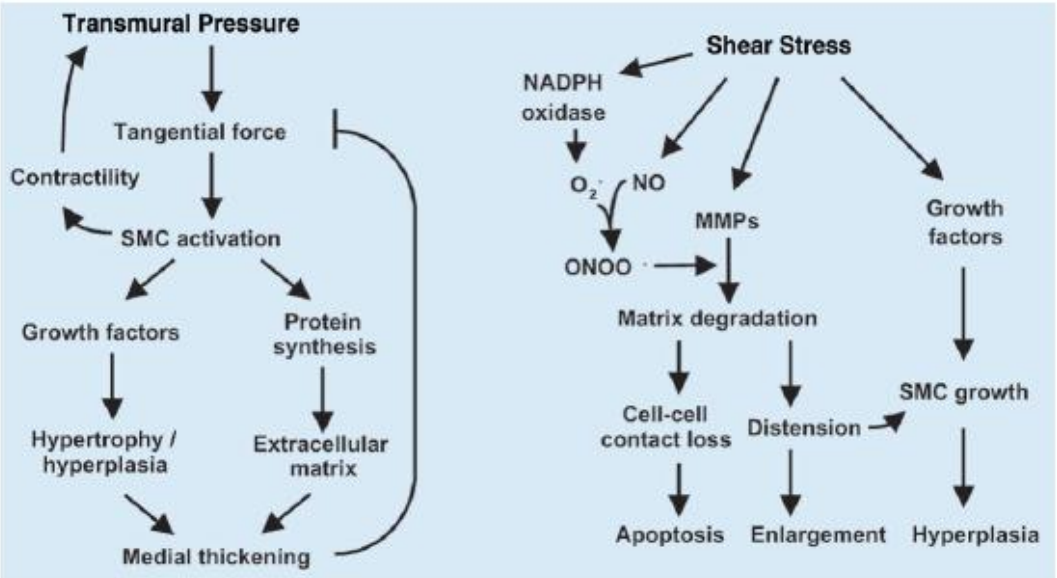

Figure 1.11: The effects of heamodynamic forces on vascular remodelling. The prototypical vascular responses stemming from changes in transmural pressure (cyclic strain, left) or shear stress (right), that lead, through sequential events, to vascular remodelling (Lehoux, Castier et al. 2006).

The following section will cover the direct effects that biomechanical forces have upon the vasculature with a focus on the endothelium and shear stress. The rapid and differential responses of the cells to the wide variety of haemodynamic forces, the factors that affect the haemodynamic forces and the subsequent transcriptional and physical changes upon the cells and their effects will also be covered.

The two major haemodynamic forces associated with blood flow consist of pressure acting perpendicular to the vessel wall (cyclic strain) and the frictional shear force acting parallel to the vessel wall acting on the surface of the endothelium (shear stress) (Figure 1.12). Both these forces have been implicated in inducing biochemical and biological responses that act as accelerators or decelerators to overall disease progression (Patrick, McIntire 1995, Hahn, Schwartz 2009). Before looking at their individual effects some basic aspects of the vasculature need to be addressed.

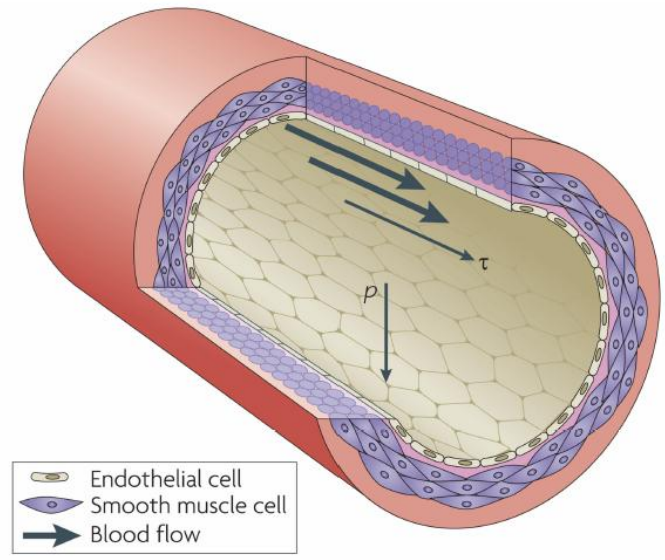

Figure 1.12: Mechanical forces on the vessel wall. A section of a blood vessel experiencing haemodynamic forces associated with the vasculature: pressure or 'cyclic strain' (*p)*, resulting in circumferential stretch of the vessel wall; and shear stress (τ), a force acting parallel to the vessel wall and exerted longitudinally in the direction of blood flow (Hahn, Schwartz 2009).

1.3.1 Haemodynamic Forces

1.3.1.1 Shear Stress

It is well established that shear stress; the frictional drag from blood flow has a potent regulatory effect on vascular physiology and pathology (Davies 1995). *In vitro* modelling systems backed up by *in vivo* measurements have calculated that shear stress can range from 10-70 dynes/cm^2 in large arteries (Thorin, Thorin-Trescases 2009). Typically the flow pattern of the blood in straight vessels is described as laminar. Laminar flow is associated with being 'healthy' and is characterised as streamlined flow which is undisturbed. In areas of unique geometry such as the points of curvature, branching or bifurcations, vessel irregularities cause the steady laminar flow of blood observed in the linear vessel regions to become disrupted. Turbulent flow is characterised as 'unhealthy' and the flow pattern is seen to vary continuously over time despite the rate of flow being stable. Commonly, laminar flow can become 'disturbed' (typically in areas of bifurcation) which results in flow separation, recirculation and reattachment to the forward flow creating a gradient of flow profile in that particular area (Feldman, Ilegbusi et al. 2002, Nichols 2005). These regions of separated flow can register shear stress readings of 0 dynes/cm^2 due to the genesis of recirculation sites (Benson, Nerem et al. 1980, Langille, O' Donnell 1986, Davies 1995, Malek, Alper et al. 1999) (Figure 1.13).

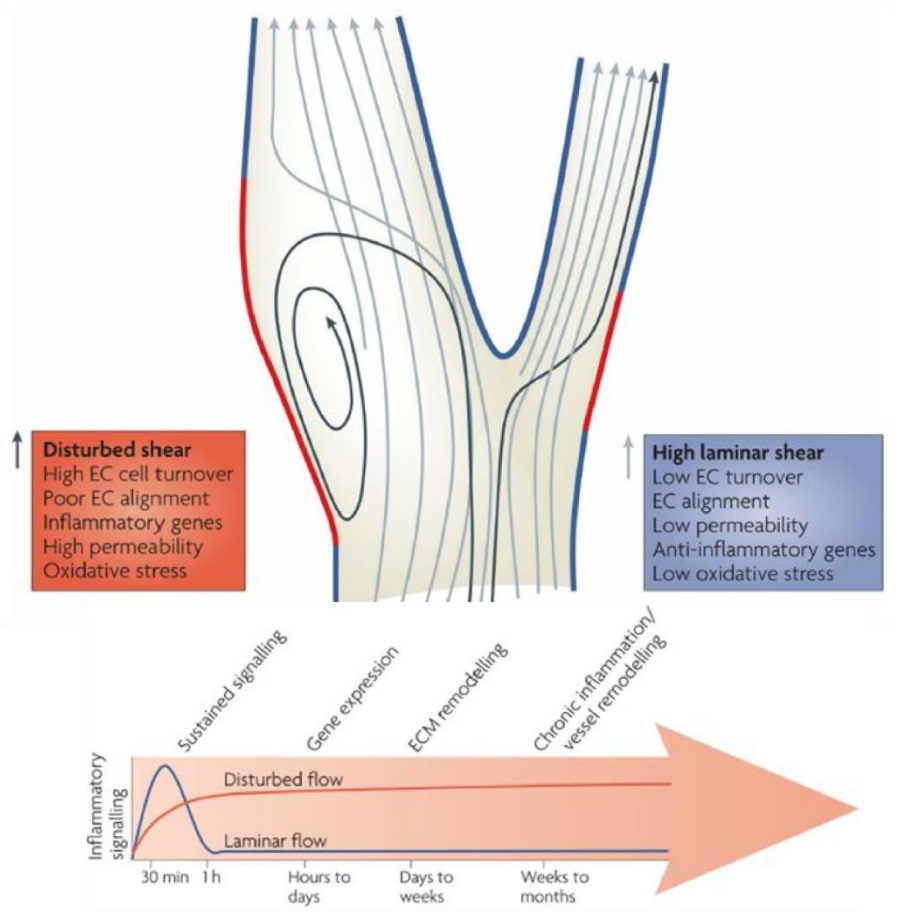

Figure 1.13: Vascular bifurcation and flow patterns. In linear regions of blood vessels the rate, direction and patterns of blood flow are 'laminar' (Blue). In regions that that curve sharply (i.e. branching points or 'bifurcations'), complex flow patterns develop (Red). Flow in these regions is reduced or become oscillatory in nature, and is often described as 'disturbed flow'. Areas of disturbed flow are known to sustain inflammatory signalling pathways and are common sites for atherosclerotic plaque development. Consequential endothelial cell fates at the specific sites in the vessel wall are presented in the colour coded boxes (Hahn, Schwartz 2009).

As Virchow noted endothelial cells under the influence of shear stress change from a raised polygonal to a flattened elongated morphology (del Zoppo 2008). The degree of elongation correlates with respect to the magnitude of shear stress applied (Reneman, Arts et al. 2006) and orientate to the direction of local blood flow (Malek, Alper et al. 1999). This alignment of endothelial cells with the direction of blood flow is seen to reduce the maximum shear stress experienced by the vessel wall by up to 50% (Barbee, Davies et al. 1994).

The composition of the vessel wall is directly controlled by shear-induced mechanotransduction with *in vivo* models demonstrating a reduction in the diameter of developing vessels coinciding with a reduction in applied blood flow (Langille, Bendeck et

al. 1989). This control over vessel size is demonstrated in physiological conditions, where the mean shear stress to which the vascular endothelium is exposed to is dynamically controlled to remain constant. The best example of this phenomenon is seen in the arteriovenous fistula model. In this model increasing the flow rate by up to a factor of 8 is seen to trigger a compensatory increase in vessel diameter accordingly (Tronc, Wassef et al. 1996).

Several studies have also shown that shear stress activation of the endothelium is directly involved in the modulation of expression of a wide array of genes. Initial studies identified over 40 genes that were regulated by LSS, either via increased or decreased expression in response to flow (Tardy, Resnick et al. 1997, Chien, Li et al. 1998, Chiu, Wang et al. 1998, Malek, Alper et al. 1999, Lelkes 1999, Nagel, Resnick et al. 1999, Gimbrone, Topper et al. 2000, Resnick, Yahav et al. 2000). As techniques developed and gene arrays became readily available, more in-depth studies were conducted, examining the endothelial response to acute and chronic, laminar and turbulent regimes of shear (Chen, Li et al. 2001, Garcia-Cardena, Comander et al. 2001, McCormick, Eskin et al. 2001, Brooks, Lelkes et al. 2002). While the methodologies and post-experimental analysis between studies varied greatly, the principal findings of these studies found that hundreds of endothelial genes are regulated by physiological levels of shear stress. A large degree of overlap was found between the studies with several gene trends observed to be identical, namely under chronic regimes where more genes were suppressed than induced and under acute regimes where the response in gene expression directly correlated with the degree of endothelial activation that was induced. Chronic regimes were also shown to activate a number of genes associated with inhibiting proliferation and inflammatory mechanisms. These studies confirmed that of classical thinking that high shear stress is considered atheroprotective (Carlier, van Damme et al. 2003) while low shear stress is associated with atherogenesis (Caro, Fitzgerald et al. 1971) (Figure 1.14). Areas of the vasculature that are subjected to a steady laminar shear, such as large arteries, have become associated with inducing low proliferation of endothelial cells and the surrounding cell cultures, increasing cell survival times, reorganisation of the cellular cytoskeleton, improved cell adhesion and production of anti-thrombotic and vasoactive agents (Levesque, Nerem et al. 1990, Korenaga, Ando et al. 1994, Ando, Tsuboi et al. 1994, Yoshida, Okano et al. 1995). If you compare this phenotype to that of the aortic arch which is prone to atherosclerosis, these regions are absent of lipid deposits and mechanisms associated with atherogenesis.

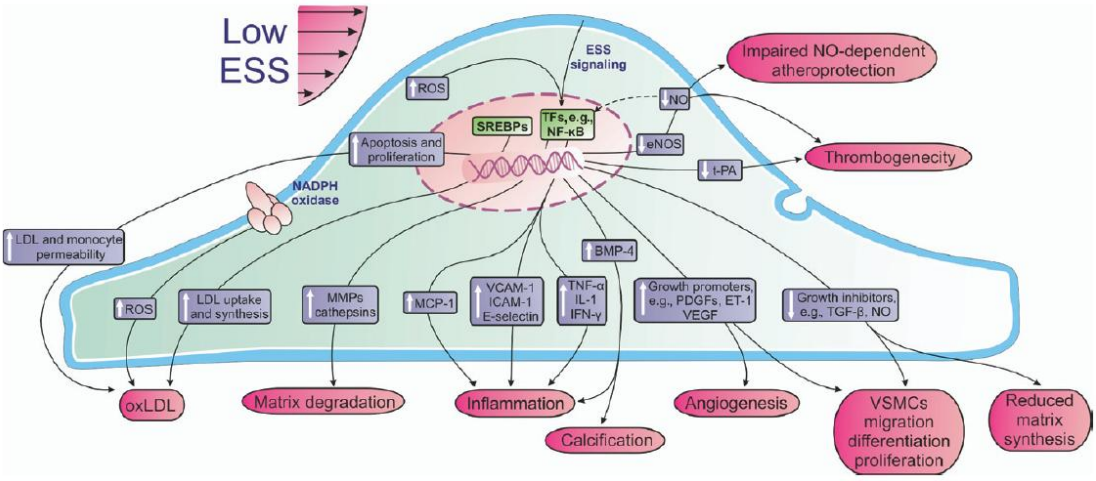

Figure 1.14: The role of shear stress in endothelial dysfunction. In areas of disturbed flow, reduced levels of shear stress shift the endothelial function and structure towards an atheroprogressive phenotype (Chatzizisis, Coskun et al. 2007).

1.3.1.2 Cyclic Strain

Blood vessels are constantly subjected to the mechanical stretching force of blood due to its pulsatile nature. The major factor determining applied stretching force upon the vessel wall is blood pressure. Blood pressure creates a radial and tangential force which counteracts the effect of intraluminal pressure. While shear stress predominantly affects the endothelium, cyclic strain affects all layers of the vessel wall.

Based on observations made in chick embryos, Thoma (1893) first hypothesized that the thickness of the vessel walls depends on the magnitude of the tensional force applied to it by the pressure exerted by the blood. Comparing the development of the pulmonary artery and aorta from birth demonstrates this; the thickness of the two vessels are identical pre-natal yet a drop in blood pressure in the pulmonary artery following birth leads to atrophy and a decrease in vessel wall thickness. Conversely, the increase in pressure in the aorta leads to an increase in the vessel wall thickness (Leung, Glagov et al. 1977). This is due to a close relationship between blood pressure and the smooth muscle cells that surround the vessel wall that ensures (via dynamic remodelling of the vessel wall) that the circumferential stress applied to the vessel wall remains constant throughout the vascular tree.

Aside from mechanisms of vascular remodelling, cyclic strain has also been identified in the release of signalling molecules. MMPs are known to be released in response to stretch forces (Jackson 2002, Asanuma, Magid et al. 2003, Grote, Flach et al. 2003) and have been identified in mediating further remodelling processes. For example, MMP-9 activation

correlated with increased vessel size, a process which could be attenuated in MMP-9 knockout animal models that were subjected to similar cyclic strain regimes (Lehoux, Lemarie et al. 2004). Acute pressure changes induced by elevated cyclic strain forces are also seen to trigger calcium signalling events in the vessels subjected to the force (Davis, Wu et al. 2001). The elevated pressure opens non-specific cation channels which results in membrane depolarisation.

Overall, cyclic strain is seen to be a key force in inducing vascular remodelling and is seen to do so via initiation of primarily pro-inflammatory mechanisms. However, like shear stress, these mechanisms are subject to dysfunction and are often implicated in the pathogenesis of disease states. Sustained hypertension has been shown in a variety of models to have a negative impact on the overall blood vessel shape leading to increased vessel thickness due to SMC hypertrophy which under chronic conditions leads to hyperplasia and in turn proportional changes in contractile and matrix proteins often resulting in dysfunctional tissue (Integan, Schiffrin 2000), a precursor to the atherogenesis process (Chobanian, Alexander 1996). The resulting increase in blood pressure in the carotid artery along with the intima thickness offers an index of potential atheroma size (O'Leary, Polak et al. 1999). In apolipoprotein E $(ApoE)^{-/-}$ mice models, induction of vessel coarctations is seen to facilitate the formation of plaques in vascular segments upstream of the surgically modified area (Wu, Hagaman et al. 2002). Increased levels of cyclic strain have also resulted in increased expression of adhesion molecules (Wang, Nawata et al. 2004) and production of pro-atherogenic factors such as ROS and pro-inflammatory cytokines (Chobanian, Alexander 1996).

1.3.2 Mechanotransduction

The ability of the endothelium to detect and transduce mechanical forces deriving from blood flow is due to a collaborative effort by numerous cell receptors (Figure 1.15) (Davies 1995). Typically the activation of biomechanical receptors and the cellular signalling that they invoke are transient effects. As noted in gene studies earlier, a number of genes whose expression is acutely induced by either onset of changes in the haemodynamic forces soon become quiescent or down regulated under chronic time periods (Hahn, Schwartz 2009). This ‘adaptation’ to the fluid microenvironment normally starts with the rapid onset of a number of signalling cascades (tyrosine kinases, Rho family guanosine triphosphate (GTP)ases, extracellular signal-regulated kinases (ERK), c-Jun N-terminal kinases (JNK) etc) (Davies 1995, Takahashi, Ishida et al. 1997) before culminating in the reorganisation of the cellular cytoskeleton and yield a new cellular phenotype. Ultimately, the aim of this

adaptation to shear stress or cyclic strain is to transform the structure of the vessel to accommodate the new conditions and restore the experienced forces back to basal levels (Tronc, Wassef et al. 1996). A brief overview of known mechanotransduction systems (some of which will be addressed in this thesis) is outlined below.

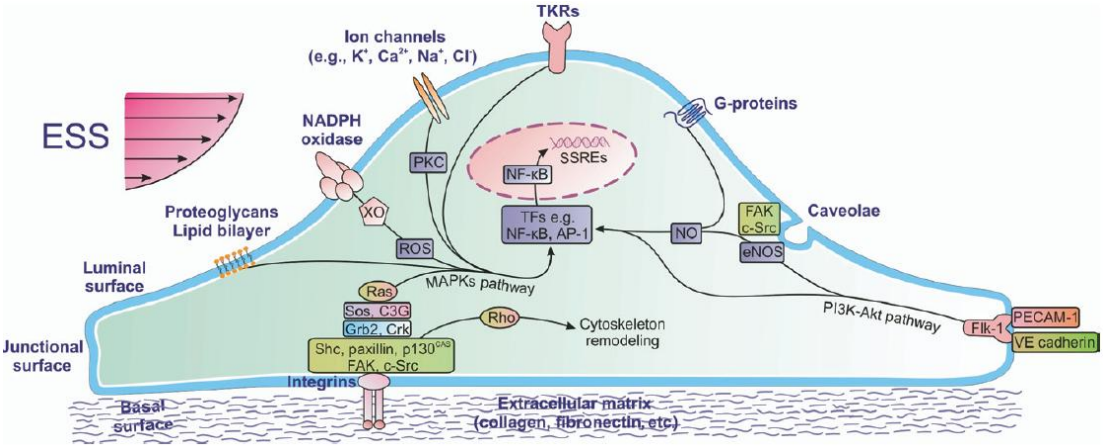

Figure 1.15: Endothelial mechanotransduction by shear stress. A schematic of the luminal endothelial mechanoreceptors such as ion channels, G-proteins, caveolae, tyrosine kinase receptors and NAPDH oxidase, and how they transmit their mechano-induced signals through the actin cytoskeleton. These signals can transmit to the basal or junctional endothelial surfaces, where additional mechano-sensitive receptors such as integrins or PECAM-1 can further initiate downstream signalling (Chatzizisis, Coskun et al. 2007).

1.3.2.1 Cytoskeleton

The number of molecules and structural elements implicated in biomechanical signalling and transduction is ever growing. The fact that a number of these elements are localised within endothelial compartments and are not directly acted upon by the haemodynamic forces suggests there is a common structural framework that can tie all the receptors and mediators together (Ali, Schumacker 2002). The requirements of such a structure would be to sense the mechanical force as it acts upon the cell and relay the signal to the different cellular compartments. The endothelial cytoskeleton meets all these criteria. It is capable of binding directly or indirectly to a number of known biomechanical receptors (Barbee, Davies et al. 1994, Barbee, Davies et al. 1994, Barbee, Mundel et al. 1995, Helmke, Goldman et al. 2000, Helmke, Thakker et al. 2001, Helmke, Davies 2002) and has also been shown to relay the transduced signal from the apical cell surface to several points of attachment within the endothelium that can resist the force and anchor the cell in place (Davies 1995, Maniotis, Chen et al. 1997, Ingber 1998, Pourati, Maniotis et al. 1998). The endothelial cytoskeleton undergoes rapid morphological and orientation changes of its cortical actin cytoskeletal stress fibres and associated vimentin and tubulin filaments in response to flow (Helmke,

Goldman et al. 2000, Helmke, Thakker et al. 2001, Helmke, Davies 2002) allowing it to dynamically change with respect to the forces acting upon it. It is the associated microfilaments of actin that are bound to the large number of intracellular proteins that keep the entire actin cytoskeleton in continuous dynamic communication with nearly all cellular structures. Collectively, these scaffold proteins localise to the cellular periphery and give the cell its shape, typically orientating it in the direction of blood flow and disruption of the actin cytoskeleton has been demonstrated to inhibit shear stress mediated signalling (Knudsen, Frangos 1997, Imberti, Morigi et al. 2000). As mentioned, evidence has suggested the cytoskeleton mediates the signal relay to a number of endothelial compartments in order to facilitate adaptation. What follows are just a few of the structures that are linked to the cytoskeleton and are known to receive signals from it.

1.3.2.2 Integrins

Integrins are heterodimeric α/β chains that are involved in the interaction of the cell and extracellular matrix. A number of studies have positively identified integrins as signal transducers, typically translating mechanical stimuli into biochemical signals capable of modulating transcriptional regulation (Ingber 1998, Schwartz, Ginsberg 2002). Formation of new integrin-ligand complexes is a dynamic process and correlates with respect to stretch- or shear-based mechanotransduction. Blocking of unbound extracellular matrix (ECM) ligand sites with antibodies or arginylglycylaspartic (RGD) peptides inhibits any integrin-specific intracellular signalling that may be induced by mechanical forces. In the case of shear stress, flow mediated release of nitric oxide (NO) in coronary arteries could be attenuated using integrin-extracellular matrix inhibitors (Muller, Endlich et al. 1997, Muller, Endlich et al. 1998). Other flow-related studies have demonstrated how integrins relay signal transduction from the actin cytoskeleton to integral membrane proteins such as platelet endothelial cell adhesion molecule (PECAM)-1 and VE-Cadherin (Osawa, Masuda et al. 2002, Jin, Ueba et al. 2003, Tzima, Irani-Tehrani et al. 2005) as well as increase integrin binding to the subendothelial ECM. In the case of cyclic strain, integrins allow for the endothelial cells to cope with both acute and chronic remodelling that may occur. The mechanical stretch induces structural reinforcement of integrin adhesions and also stimulates integrin-associated signalling (focal adhesion kinases (FAK) and mitogen-activated protein kinases (MAPK)). As well as being involved in signalling pathways, integrins also have a physical role to play and assist in any cytoskeletal remodellings that are required, particularly in relation to the cell binding to the extracellular matrix (Jalali, del Pozo et al. 2001, Tzima, Del Pozo et al. 2002, Tzima, Reader et al. 2003, Tzima, Kiosses et al. 2003). These studies amongst others

(Bhullar, Li et al. 1998, Chen, Li et al. 1999, Shyy, Chien 2002) support the hypothesis that these molecules are involved in mechanotransduction of endothelial cells.

1.3.2.3 Interendothelial Junctions

Several molecular interactions implicate a role for the interendothelial junctions in mediating mechanotransduction. Both the adhererns and tight junction are seen to adapt their structure concurrently with the actin cytoskeleton, with many proteins involved in the cell-cell junction complex undergoing changes in response to haemodynamic forces (Davies 1995).

Exposure to acute laminar shear stress causes a redistribution of VE-Cadherin, and its associated intracellular proteins (α-catenin, β-catenin and plakoglobin). Chronic exposure causes the expression patterns of the aforementioned proteins to change from punctuated complexes to continuous structures located along the cell-cell border and associate with the concurrent redistribed F-actin stress fibres (Noria, Cowan et al. 1999). Temporary translocation of the catenins following onset of shear stress has been observed to activate a number of signalling pathways (Noria, Cowan et al. 1999). Vascular endothelial growth factor (VEGF) plays an important role in mediating adherens junction formation, inducing tyrosine phosphorylation of VE-Cadherin, β-catenin, pakoglobin and p-120 via vascular endothelial growth factor receptor (VEGFR)2 (Esser, Lampugnani et al. 1998). This complex forms within minutes of laminar shear stress onset and deletion or truncation of VE-Cadherin was shown to abolish the formation of this complex with the endothelial cytoskeleton and other mechanosensitive signalling pathways (Carmeliet, Ng et al. 1999, Carmeliet, Lampugnani et al. 1999, Shay-Salit, Shushy et al. 2002, Walsh, Murphy et al. 2011).

PECAM-1, another protein involved in endothelial cell-cell adhesion has also been implicated in mechanosensing. Upon application of shear stress, PECAM-1 undergoes tyrosine phosphorylation within 30 seconds which in turn mediates the binding of Src homology phosphatase (SHP)-2 to PECAM-1's cytoplasmic tail (Osawa, Masuda et al. 1997, Osawa, Masuda et al. 2002). Knockout of PECAM-1 or SHP-2 was seen to disrupt the activation of signalling pathways by shear stress such as ERK1/2 (Kano, Katoh et al. 2000, Fujiwara, Masuda et al. 2001).

These observations suggest that many of the membrane bound proteins that primarily form junctions may also serve as mechanoreceptors or sensors to haemodynamic forces. The impact of shear (and cytokines) on the expression and assembly of junctions will form an important aspect of this thesis.

1.3.2.4 Heterotrimeric G proteins and GTPase family members (Rho/Rac)

The ability to bind to guanine nucleotides, guanosine diphosphate (GDP) and guanosine triphosphate (GTP) conferred G proteins their name. Structurally, G proteins are heterotrimers consisting of α-, β-, and γ-subunits. G proteins located within the cell are activated by G protein-coupled receptors (GPCR). GPCRs span the cell membrane and are comprised of extracellular loops that mediate ligand binding and a cytoplasmic tail which interacts with the heterotrimeric G-proteins. Upon successful ligand-binding, the α-subunit undergoes a conformational change that facilitates the exchange of GTP for GDP. This exchange initiates the dissociation of the α-subunit, bound to GTP, from the βγ complex and GPCR. The GPCR continues the cycle with each consequent subunit activating a wide range of metabolic pathways resulting in the activation of secondary messengers, enzymes and ion channels (Taylor 1990, Wieland, Mittmann 2003) until hydrolysation of GTP to GDP by GTPases occurs. There are over 150 small GTPases encoded by the human genome. The various subclasses of this protein superfamily (Ras, Rab, Arf, Ran and Rho) have been implicated in almost every aspect of cell biology. The members of the GTPase family act as binary 'molecular switches', whose cycling between active and inactive forms is regulated by a number of cellular factors.

The G-proteins located on the apical surface of BBB have been identified as direct transducers of haemodynamic forces (Walsh, Murphy et al. 2011). G-protein activation occurs within 1 second of flow onset, characteristic of direct mechanotransduction (Gudi, Clark et al. 1996, Frangos, Gahtan et al. 1999, Gudi, Huvar et al. 2003). Gudi (1996) reported treatment of endothelial cells with anti-sense oligonucleotides to Gαq inhibited shear-induced Ras-GTPase activity (shear stress activation of the Ras superfamily of GTPases, the Rho subfamily in particular, has been identified as a critical mediator of endothelial signalling pathways associated with cytoskeletal remodelling, barrier function and immune cell trafficking (Adamson, Wilbourn et al. 2002, Walsh, Murphy et al. 2011). Gudi (1998) further demonstrated that G proteins reconstituted in liposomes in the absence of proteins receptors showed an increase in activity in response to shear stress. This increase in activity was attenuated following reinforcement of the lipid bi-layer by the addition of cholesterol, a finding which potentially links G protein activity to that of the caveolae.

The application of shear stress is also seen to increase lateral diffusion in the upstream portion of the apical membrane, an event which occurred almost immediately in response to flow (Butler, Norwich et al. 2001). Whole cell measurements demonstrated increased fluidity (Haidekker, L'Heureux et al. 2000) which coincided with G-protein activation

(Frangos, Gahtan et al. 1999). Artificially decreasing whole cell fluidity subsequently blocked activation of G-proteins.

1.3.2.5 Caveolae

Caveolae are rigid, cholesterol-rich membrane domains which have been shown to contain a myriad of signalling molecules including serine and tyrosine kinases and NO (Kurzchalia, Parton 1999). The plasma membrane phospholipid bilayer and its constituents have often been implicated as a transducer of force and caveolae given their location have been hypothesized to mediate flow-dependent responses (Rizzo, McIntosh et al. 1998, Park, Go et al. 2000). Upon subjection to shear stress, NO was seen to be rapidly released including from one of its binding partners, caveolin within the caveolae, into the cytoplasm where it binds to calmodulin (Rizzo, McIntosh et al. 1998). Blockade of caveolin has been shown to allow eNOS activation and subsequently the unregulated production of NO suggesting the caveolae are required to suppress this event (Bernatchez, Bauer et al. 2005). Caveolae are also seen to mediate shear-dependent cholesterol signalling within the endothelium. Treatment of endothelial cell cultures with cholesterol inhibiting antibiotics such as filipin and digitonin prior to shearing disrupted the shear-mediated activation of ERK1/2 (Park, Go et al. 1998).

1.3.2.6 Glycocalyx

The luminal surface of the endothelium is covered by a ~300-500 nm membrane bound macromolecular coating that forms a barrier layer (Weinbaum, Tarbell et al. 2007) such that the mechanical forces at the apical plasma membrane are zero (Vink, Duling 2000, Smith, Long et al. 2003). It is reported that mechanical forces applied to the glycocalyx are transmitted through glycosaminoglycan chains to the transmembrane anchors, relaying the mechanotransduction signals (Weinbaum, Zhang et al. 2003). Studies have shown that digestion of the glycosaminoglycan chains interfered with established flow-mediated NO production (Florian, Kosky et al. 2003, Mochizuki, Vink et al. 2003), however it is also possible the digestion enzymes employed disrupted signalling mediators at the basal cell surface. It is believed that the glycocalyx is the primary mechano-transducer of shear stress to the cytoskeleton and plays an integral part in dynamic response of the vessel wall (Pahakis, Kosky et al. 2007).

As mentioned, biomechanical forces are necessary in maintaining normal vascular homeostasis and atheroprotection. In certain areas these forces are disturbed and a number of

regulatory processes are seen to become disrupted, typically leading to an inflammatory response. These two processes are seen to coincide with onset of endothelial dysfunction, barrier disruption and lesion formation (Malek, Alper et al. 1999, Gimbrone, Topper et al. 2000, Stone, Coskun et al. 2003, Stone, Coskun et al. 2003, Cunningham, Gotlieb 2005). A good example of this is nuclear factor kappa-light-chain-enhancer of activated B cells (NFκB), a transcription factor shown to be involved in the expression of a number of key molecules implicated in the early stages of endothelial dysfunction (Nagel, Resnick et al. 1999, Orr, Sanders et al. 2005). Seen to be activated in regions of disturbed flow among others, this is just one of many pathways closely associating haemodynamic and inflammatory forces with endothelial activation. As will be discussed in the next section, inflammation plays a critical a role in the onset of endothelial dysfunction and vascular diseases.

1.4 Inflammation

In vivo, areas predisposed to develop atherosclerotic plaques (e.g. bifurcations) are seen to have their endothelium in an elevated activated state (Hahn, Schwartz 2009). In this state, the expression and release of inflammatory mediators is widely reported. The effect of a number of these agents on the development of atherosclerosis has already been covered. In this section, the mechanisms by which these inflammatory mediators are induced/released and their subsequent effects, primarily in the brain and the cerebrovascualture, will be examined.

The vascular beds in which the endothelial cells reside can have an influential inductive role on the endothelium and its function (Hawkins, Davis 2005). In comparison to the peripheral endothelium for example, the cerebrovascular endothelium is remarkably resistant to inflammatory mediators (Hickey 2001). This has primarily been attributed to the brain endothelium restricting the passage of potentially damaging leukocytes across the vessel wall and protecting the brain from any disruption of neural networks. *In vivo* experiments have shown that systemic injections of the bacterial endotoxins (e.g. lipopolysaccharide (LPS)) known to induce severe illness in rodents had no obvious impact on the BBB integrity (Perry, Anthony et al. 1997). Other studies however which extended this premise found simultaneous injection with another inflammatory mediator (Arsenijevic, Girardier et al. 1998) or a course of LPS injections (Xaio, Banks et al. 2001) did have a pronounced effect on the BBB. Other *in vitro* and *in vivo* studies have also confirmed the negative impact of inflammatory mediators on BBB endothelium, in particular the ability to induce an increase in the monolayers permeability (Kim, Wass et al. 1992, Megyeri, Abraham et al.

1992, Deli, Joo 1996, DeVries, BlomRoosemalen et al. 1996, DeVries, BlomRoosemalen et al. 1996, DeVries, Kuiper et al. 1997). This would suggest that the cerebrovascular endothelial cells are more resistant to circulating cytokines whose origin may be in the peripheral vasculature however when in situ damage is caused and multiple factors commonly seen to trigger CNS pathologies are present and in high concentration, injury, primarily to the barrier, will be induced (it should be noted however that the injury inflicted upon the cerebrovasculature is not uniform across all cell types of the brain).

Inflammation of the cerebral endothelium can originate from a diverse range of insults (Abbott 2000). Alteration or imbalance of the local levels of cytokines, viral infection, the formation and action of free radicals to name but a few have all been shown to induce endothelial activation in the cerebral tissue and subsequently alter or disrupt cellular function. The key source for these inflammatory agents comes from the surrounding cells within the NVU (Minagar, Alexander 2003) though evidence has shown that these inflammatory mediators do not necessarily have to originate within the cerebral tissue to induce injury. *In vivo* studies have demonstrated that injection of inflammatory mediators into the hind paw of rodents increased BBB susceptibility to sucrose uptake (Huber, Witt et al. 2001). Further studies demonstrated a corresponding decrease in occludin and ZO-1 expression at the cell membrane and a decrease in association with the actin cytoskeleton (Huber, Hau et al. 2002). This, and similar observations, demonstrate that upon initiation of inflammatory injury, the integrity of the BBB is seen to go into decline with an overall loss of barrier function (Megyeri, Abraham et al. 1992). This presents a window of opportunity for leukocytes and other potentially harmful substances to enter the brain and trigger a variety of signal transduction pathways leading to further damage (Kim, Wass et al. 1992). A number of reasons have been presented for the onset of this inflamed barrier state including natural barrier disruption due to atherogenesis, to blood flow disruption and ischemia, to onset of neurological conditions including HIV-associated dementia, multiple sclerosis and Alzheimer's disease to name but a few (Petty, Lo 2002).

Numerous transport systems have been identified in assisting the passage of cytokines across the BBB (Banks 2005). Generally, the BBB offers cytokine binding sites that serve a dual function; namely they can alter intracellular functions or facilitate the passage of the cytokine across the BBB. In some unique cases, the transporter binding site is a product of the same gene which encodes for the cytokine receptor involved in triggering an intracellular response. These concepts will be discussed below with respect to TNF-α, IL-6 and reactive oxygen species (ROS), pro-inflammatory mediators prevalent in the disruption of neurovascular barrier integrity during diseases of the cerebrovasculature and which form central aspects of investigation in this thesis.

1.4.1 TNF-α

The potent pro-inflammatory cytokine, TNF-α, is a member of the TNF superfamily of ligands, which are heavily involved in promoting inflammatory signalling (Wallach, Varfolomeev et al. 1999, Wajant, Pfizenmaier et al. 2003, Shen, Pervaiz 2006). Isolated from mouse serum, TNF-α was initially discovered via its effects on tumour viability *in vivo* (Carswell, Old et al. 1975). Initially described as a 'necrotic factor of peripheral inflammation', TNF-α has lived up to its original description and is one of the best characterised pro-inflammatory cytokines to date.

TNF-α is constitutively expressed in its 26 kDa transmembrane form (tTNF-α) where it resides in an inactive state. In a process called ectodomain shedding (Black, Rauch et al. 1997), transmembrane TNF-α is cleaved at its extracellular domain to yield a newly-active 17kDa form (sTNF-α). Therefore the synthesis and release of soluble TNF-α is regulated by the matrix metalloproteinase which facilitates the cleavage of TNF-α from the membrane surface; TNF-α converting enzyme (TACE). The newly active form is then free to exert its effects in both an autocrine and/or paracrine manner. *In vivo* models which abolish the actions of TACE have demonstrated an ablation in automimmune pathology suggesting soluble TNF-α is the primary mediator of the inflammatory response.

TNF-α has been reported in a number of varied functions, such as cell proliferation, cell differentiation (Jelinek, Lipsky 1987, Murphy, Perussia et al. 1988) and gene transcription (Collins, Lapierre et al. 1986, Grilli, Chentran et al. 1993). It is TNF-α's ability to induce selective function of some cells whilst sparing others that has led researchers to discover its role in multiple signalling cascades.

The pleiotropic actions of TNF-α are mediated through two distinct transmembrane glycoprotein receptors; tumour necrosis factor receptor-1 and -2 (TNFR1 and TNFR2) (Figure 1.16). Whilst a degree of overlap exists between the receptors with regard to the signalling pathways they can elicit, both receptors differ greatly in their expression profiles, cytoplasmic tail structure and downstream signalling pathway activation (Aggarwal, Eessalu et al. 1985, Aggarwal 2003), which presents the opportunity for each to activate their own unique signalling events (Hsu, Xiong et al. 1995, Hsu, Shu et al. 1996, Declercq, Denecker et al. 1998, Quintana, Giralt et al. 2005).

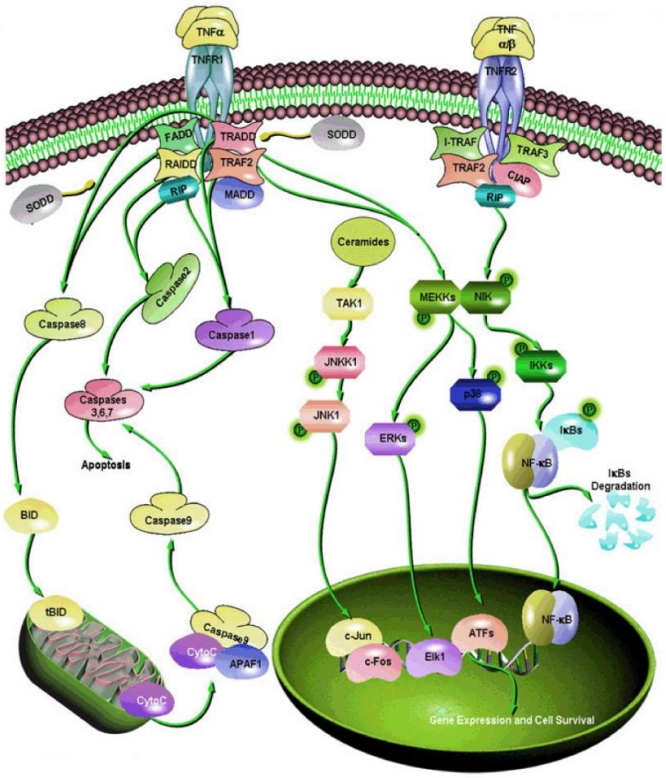

Figure 1.16: TNF-α signalling through TNFR1 and TNFR2
(http://www.sabiosciences.com)**.**

TNFR1 is expressed in most cell types and can be activated via binding of tTNF-α and sTNF-α with a partial preference to the soluble form. Overall, TNFR1 is capable of binding more adaptor proteins via its intracellular domain and thus presents a greater choice of signalling pathways which can be activated as compared to TNFR2. Upon binding of sTNF-α to TNFR1, a biphasic reaction occurs in which the silencer of death domains (SODD) dissociates from the TNFR1 signalling complex while TNFR-Associated Death Domain (TRADD) binds in its place (Tartaglia, Ayres et al. 1993, Tartaglia, Pennica et al. 1993, Tartaglia, Rothe et al. 1993, Ware, VanArsdale et al. 1996). TRADD then actively recruits additional adaptor proteins; Fas-Associated Death Domain (FADD), Receptor-Interacting Protein (RIP) and TNF-α Receptor Associated Factor 2 (TRAF2) (Hsu, Xiong et al. 1995, Hsu, Shu et al. 1996, Hsu, Shu et al. 1996, Jiang, Woronicz et al. 1999) which can activate very distinct pathways. The complex leads to the RIP-dependent activation of NFκB to trigger pro-survival signalling, cellular proliferation and cytokine production. The cumulative effect of TRADD, TRAF2 and RIP also activates cellular inhibitor of apoptosis proteins-1 and -2 (cIAP-1 and -2) which themselves can activate ERK, JNK, p38 MAP kinase and ceramide/sphinomyelinase pathways (Winston, Langecarter et al. 1995, Shu,

Takeuchi et al. 1996, Schievella, Chen et al. 1997). The kinetics of JNK activation is of particular importance in the resulting effect of TNF-α binding. Transient levels of TNF-α induce JNK activation which is pro-survival. If JNK activation is sustained this can lead to apoptosis signal-regulating kinase 1 (ASK1) phosphorylating JNK, which can then promote apoptosis via caspase dependent pathways (Tobiume, Matsuzawa et al. 2001). Finally, binding of TRADD and FADD can lead to the recruitment and activation of Caspase 8. Activation of Caspase 8 subsequently leads to the recruitment of fellow caspases and cleavage of BH3 Interacting Death Domain ultimately resulting in a proteolytic cascade ending in cellular apoptosis.

TNFR2 is restricted to endothelial, hematopoietic and neural cells in addition to some immune cell types. TNFR2 shares a number of pro-survival and inflammatory responses as TNFR1, with signalling occurring through the recruitment of the TRAF1 and TRAF2 proteins and subsequent activation of cIAPs and NFκB (Rothe, Wong et al. 1994, Rothe, Sarma et al. 1995). TNFR2 also lacks a DD and unlike TNFR1, induction of caspase-driven apoptosis is absent. Overall, TNRF2 activation is believed to be pro-survival. However it should be noted that TNFR2 has preferential binding to the transmembrane form of TNF-α, which in conjunction with its limited expression, results in a far more muted biological impact as compared to TNFR1 (Grell, Douni et al. 1995). In fact, TNFR2 has been demonstrated to enhance TNFR1 signalling via a 'ligand-passing' mechanism. It is thought this enhancement of TNFR1 is the primary contribution of TNFR2 in TNF-α mediated signalling as compared to signalling events which occur through the intracellular domain of TNFR2 (Tartaglia, Pennica et al. 1993, Tartaglia, Rothe et al. 1993, Tartaglia, Ayres et al. 1993).

There are a number of critical factors which determine whether TNF-α will have a protective or injurious role; the differential patterns of localisation of TNFR1 and TNFR2 and their expression, in conjunction with the activation state of the cells, all play a cumulative role in the resulting beneficial or harmful effect (Dopp, MackenzieGraham et al. 1997, Sairanen, Lindsberg et al. 2001, Sairanen, Carpen et al. 2001, Fontaine, Mohand-Said et al. 2002, Akassoglou, Douni et al. 2003). NFκB, p38, JNK are just some of the pathways activated by TNF-α which have been reported in influencing a number of key physiological process; inflammation, proliferation, cell migration, apoptosis and necrosis (Tartaglia, Ayres et al. 1993, Tartaglia, Pennica et al. 1993, Tartaglia, Rothe et al. 1993, Eissner, Kirchner et al. 2000, Harashima, Horiuchi et al. 2001, Eissner, Kolch et al. 2004, Ware 2005).

1.4.1.1 TNF-α in the CNS

The biological function of TNF-α in the CNS was not considered until 1987 when microglia were the first cell type found to produce the cytokine in that region (Frei, Siepl et al. 1987). Since then, other cell populations of the CNS have been shown to synthesise and secrete high levels of sTNF-α and tTNF-α including astrocytes (Lieberman, Pitha et al. 1989) and some distinct populations of neurons (Tchelingerian, LeSaux et al. 1996, Kogo, Takeba et al. 2006). When regulated, TNF-α signalling has been indentified as having several important functions within the CNS (Tansey, Wyss-Coray 2008). This can include activation of microglial and astrocyte populations, regulation of blood brain barrier permeability, febrile responses, glutamatergic transmission and synaptic plasticity (Selmaj, Farooq et al. 1990, Merrill 1991, Merrill, Chen 1991, Sedgwick, Riminton et al. 2000, Leon 2002, Beattie, Stellwagen et al. 2002, Pickering, Cumiskey et al. 2005). However, like most inflammatory agents, imbalances in the microenvironments levels can result in local cellular dysfunction. A rapid increase in TNF-α expression is reported in response to both acute and chronic injuries (Allan, Rothwell 2001, Viviani, Bartesaghi et al. 2004). As a result, sustained expression of TNF-α and its receptors have been linked in the pathogenesis of a number of neurodegenerative disorders such as Parkinson's (Nagatsu, Mogi et al. 2000) and Alzheimer's disease (Perry, Dewhurst et al. 2002), Multiple Sclerosis (Hofman, Schulte et al. 1989, Rieckmann, Albrecht et al. 1995), prion diseases (Veerhuis, Hoozemans et al. 2002), neurotrauma and stroke (Barone, Parsons 2000).

As has been detailed, TNF-α can contribute to the pathophysiology of disease in a variety of means. For example, TNF-α is seen to play a critical role in ischemic brain injury with high levels reported in ischemic stroke models (Tarkowski, Blennow et al. 1999, Vila, Castillo et al. 2000). Increased levels (3-fold) of TNF-α have been observed in the serum and CSF of patients having incurred an ischemic event with the elevated levels persisting for up to ninety days post-ischemia (Ferrarese, Mascarucci et al. 1999). Real time PCR analysis conducted on tissue isolated from rats subjected to middle cerebral artery occlusion (MCAO) also showed an increase in TNF-α transcription levels within 3 hours of ischemia onset. This change was closely followed by changes in the messenger ribonucleic acid (mRNA) for IL-1β, IL-6, E-Selectin and ICAM-1, and an increase in NFκB activity and infiltration of inflammatory cells (Berti, Williams et al. 2002). The sites at which TNF-α propagates also changes with increases seen not only in neurons but in astrocytes, microglia, choroid plexus, endothelial cells and leukocytes (Buttini, Appel et al. 1996, Meistrell, Botchkina et al. 1997). In addition, separate studies utilising MCAO reported that the induction of TNF-α coincided with exacerbation of neurological deficits and infarct size (Barone, Arvin et al. 1997). Complementary studies demonstrated that inhibition of TNF-α

activity was seen to reduce the infarct volume and to suppress any neurological deficits in BALB/c mice which underwent similar MCAO procedures (Nawashiro, Martin et al. 1997, Nawashiro, Martin et al. 1997, Nawashiro, Tasaki et al. 1997, Meistrell, Botchkina et al. 1997).

While there is much evidence identifying TNF-α as a neurotoxic agent in the CNS, scientists are now questioning whether TNF-α actively contributes to neuronal injury or attempts to limit the affliction. Several studies have demonstrated its role in promoting not only neural survival but differentiation, proliferation and growth. TNF-α has been shown to assist in the survival of oligodendroglia which in turn negate the effect of demyelation by reparative means (Plant, Arnett et al. 2005). Studies have reported an acquired means of neuroprotection in rat ischemia models post-administration of excitotoxic stimuli (Hurtado, Cardenas et al. 2001, Hurtado, Lizasoain et al. 2002). The suppression of cerebral damage coincided with an increase in the level of TACE. It is hypothesised this results in an elevated level of freely available TNF-α which is predicted to play a critical role in mounting the cerebral defence. Complimentary studies showed in TNFR1- and TNFR2-deficient mice, post-ischemic and excitotoxic brain injury, that neural populations in the CNS were more susceptible to and incurred more damage than their normal counterparts (Bruce, Boling et al. 1996, Gary, Bruce-Keller et al. 1998). In another study, TNF-α was shown to protect against cell death in the presence of β-amyloid peptide via activation of NFκB and antioxidant pathways (Barger, Horster et al. 1995, Goodman, Mattson 1996).

The dual role of TNF-α is therefore evident. However, despite its protective function TNF-α is recognised solely as a pro-inflammatory cytokine which is more heavily involved in the progression of disease than preventing it.

1.4.2 IL-6

IL-6 is a 20-30 kDa glycoprotein which has been shown to have pleiotropic properties and play a critical role in host defence (Akira, Taga et al. 1993). Initially discovered in the secretory profile of lymphocytes, IL-6, amongst other agents, was reported to drive the differentiation of naive B-cells into an antibody-producing mature state (Hirano, Taga et al. 1985). Since then IL-6 has not only been investigated within the immune system, but in monocytes, macrophage, fibroblasts, keratinocytes, mesangial cells, chondrocytes, osteoblasts, smooth muscle cells, T cells, B cells, mast cells and endothelial cells to name a few (Akira, Taga et al. 1993) (Figure 1.17). IL-6 has since been studied within a number of systems; nervous, endocrine and cardiovascular, and has been reported to play an integral role within numerous signalling pathways (Kishimoto, Akira et al. 1995).

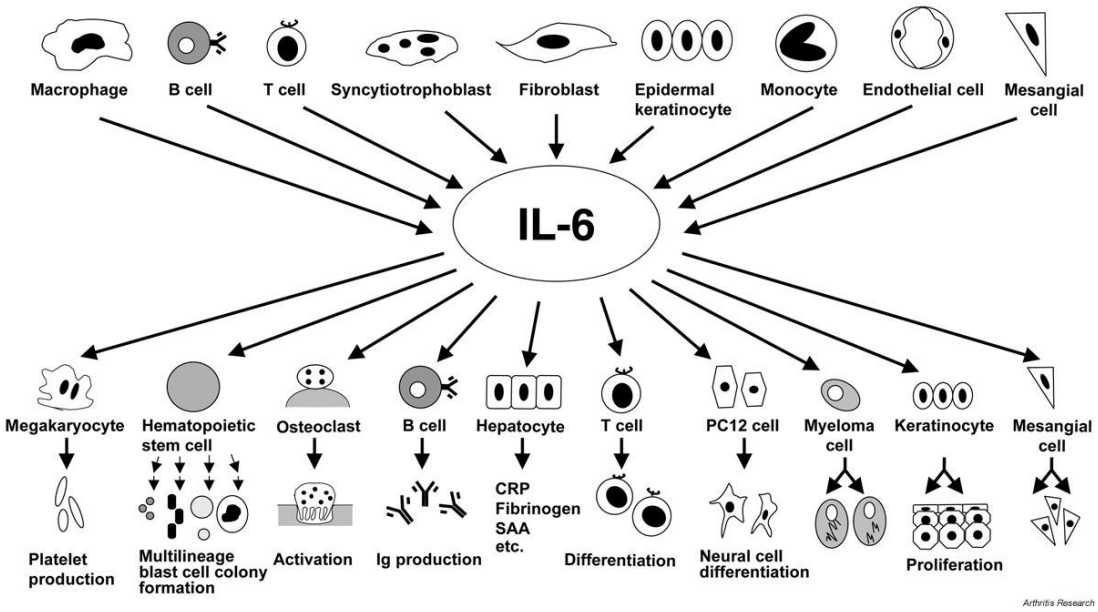

Figure 1.17: IL-6 producing cells and subsequent biological activities. IL-6 is produced by a wide range of lymphoid and non-lymphoid cells and is linked to a wide range of biological activities on various target cells (Naka, Nishimoto et al. 2002).

IL-6 is the prototypical member within its cytokine family. Whilst the members of this family share little homology in their amino acid sequences, they all share a similar tertiary structure; four α-helices in an up up down down topology (Bazan 1990, Bazan 1990). Molecules sharing this structure can be further subclassified into short- and long-chain α-helix bundle cytokines (Nicola 1994) with the latter subgroup comprised of IL-6, IL-11, leukemia-inducing factor (LIF), oncostatin M, ciliary neurotrophic factor (CNTF) and cardiotropin-1 amongst others. Given the homology of their structures, each of the preceding molecules can signal via a common receptor; glycoprotein (gp)130 (Heinrich, Behrmann et al. 2003)-explaining the name of the IL-6 family of cytokines; the gp130 family.

The nature of gp130 signalling is complicated (Figure 1.18). Signal transduction through the receptor is modular and requires each member of the gp130 complex to bind with ligand-specific receptors prior to binding with the surface receptor (Heinrich, Behrmann et al. 2003). In the case of IL-6, it must first bind to the IL-6 receptor, (IL-6R), of which there are two forms, a transmembrane 80 kDa form with a short cytoplasmic domain (tIL-6R) and a soluble form (sIL-6R) (Yamasaki, Taga et al. 1988, Kishimoto, Akira et al. 1992). The resulting IL-6/tIL-6R/sIL-6R complex can then associate with gp130 (Hibi, Murakami et al. 1990, Kishimoto, Akira et al. 1992), which upon binding, assists in the homodimerization of gp130 forming an overall hexameric structure (Boulanger, Chow et al. 2003).

The existence of a soluble form of the IL-6R represents a unique feature in IL-6 signalling. The gp130 surface receptor has been shown to be ubiquitously expressed throughout in contrast to tIL-6R whose expression is quite limited (Saito, Yoshida et al. 1992). Early studies confirmed not only could sIL-6 in the presence of IL-6 could elicit a response from gp130 presenting cells but it was also naturally occurring being detected in urine (Novick, Engelmann et al. 1989) and serum (Honda, Yamamoto et al. 1992). The origin of sIL-6R is thought to be a product of alternative splicing of tIL-6R mRNA (Lust, Donovan et al. 1992) and/or proteolytic shedding of the surface expressed extracellular domain of tIL-6R by metalloproteases (Mullberg, Schooltink et al. 1993). Either way, sIL-6R presents an untypical feature of soluble forms of cytokines receptors in that it appears to act in a agonistic fashion, enabling cells lacking tIL-6R to undergo a 'trans-signalling' means of IL-6 signal transduction provided gp130 is present (Rose-John, Scheller et al. 2006, Jones, Scheller et al. 2011). To complicate matters further, a soluble form of gp130 exists which can act in an antagonistic fashion to trans-signalling mechanisms, competing with tgp130 to complex with available IL-6-sIL-6R (Narazaki, Yasukawa et al. 1993).

The Janus kinase/signal transducer and activator of transcription (JAK/STAT) pathway has been identified as the primary pathway initiated by IL-6 binding to gp130. Upon binding, tyrosine kinases of the JAK family (JAK1, JAK2, Tyk2) become activated and induce the phosphorylation of the cytoplasmic tail of gp130. Several of the newly phosphorylated phosphotyrosine (pTyr) sites on the cytoplasmic tail can now act as docking points for STAT factors which present similar SH2 domains. STAT1, and in particular, STAT3 (Cattaneo, Conti et al. 1999), are most commonly associated with IL-6 signalling (Stahl, Farruggella et al. 1995) and upon interaction with the cytoplasmic tail become themselves phosphorylated, form dimers, then translocate to the nucleus where they regulate the transcription of target genes (Lutticken, Wegenka et al. 1994, Stahl, Boulton et al. 1994, Darnell, Kerr et al. 1994). While the JAK/STAT pathway remains the key signalling pathway of IL-6, this cytokine has also been identified in activating other signalling pathways to a lesser degree i.e. MAPK, PI3/Akt, MEK/ERK1/2, NFκB (Stahl, Farruggella et al. 1995, Heinrich, Behrmann et al. 2003).

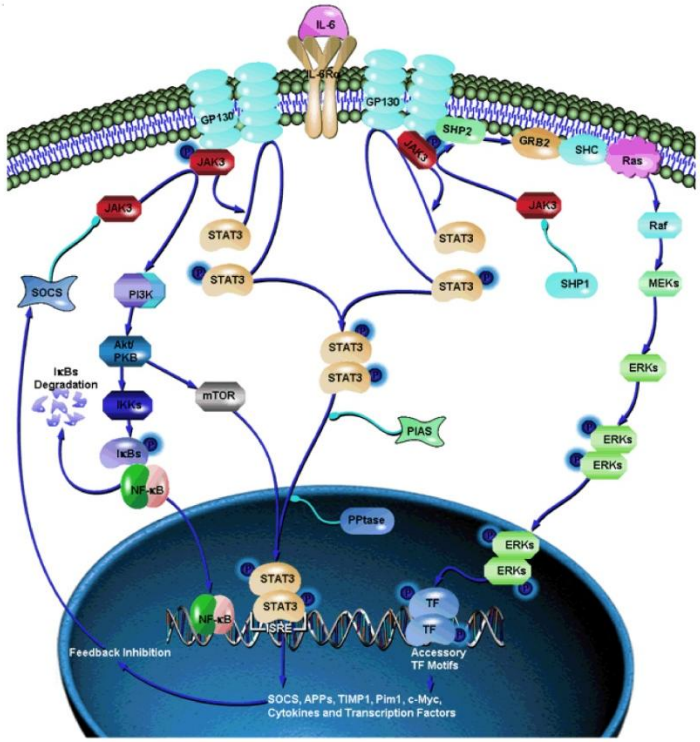

Figure 1.18: IL-6 signalling through the gp130 receptor, (http://www.sabiosciences.com)**.**

1.4.2.1 IL-6 in the CNS

Given the breadth of cells from which IL-6 can originate, IL-6 is seen to have a prominent presence in the CNS. Early studies classified IL-6 as a pro-inflammatory cytokine with subsequent studies focussed on elucidating its role in the development and progression of various CNS disorders. As a result, much work on IL-6 identifies it as an injury mediator involved in numerous inflammatory, automimmune and degenerative disorders (Van Wagoner, Benveniste 1999). Neural, glial and endothelial cells are all capable of constitutively producing IL-6 (Loddick, Turnbull et al. 1998, Suzuki, Tanaka et al. 1999, Orzylowska, Oderfeld-Nowak et al. 1999, Suzuki, Tanaka et al. 2009). Of these cells types, various agents have been shown to provoke IL-6 stimulation; from neurotransmitters to inflammatory cytokines activating various transcription pathways such as NFκB, activator protein (AP)-1 and cyclic adenosine monophosphate (cAMP) response element binding protein, a substantive increase in IL-6 production is observed within the CNS (Dendorfer, Oettgen et al. 1994, Van Wagoner, Benveniste 1999). An increase in IL-6 in the serum levels of acute ischemic stroke patients has been reported to occur within 24 hours of the ischemic event with the elevated levels peaking by day 4 but persisting for 90 days thereafter. The elevated levels coincided with other inflammatory biomarkers such as CRP, fibrinogen, IL-1 receptor antagonist and TNF-α (Fassbender, Rossol et al. 1994). In addition,

as the responsiveness of a given cell type to IL-6 correlates with the local levels of the respective receptor ligands, the elevation of sIL-6R has also been noted in a number of cerebrovascular injuries also implicating it in several pathophysiological process. This is of particular relevance to endothelial cells which lack tIL-6R (Schobitz, Pezeshki et al. 1995, Marz, Otten et al. 1999).

With regards to cerebral endothelial cells, IL-6 has been reported to have a negative impact, promoting injury through different inflammatory responses. IL-6 has been shown to increase permeability and induce angiogenesis via direct release of VEGF (Nakahara, Song et al. 2003), in addition to inducing the production of adhesion molecules and chemokines (Prudhomme, Sherman et al. 1996, Penkowa, Moos et al. 1999), all of which are key factors in facilitating leukocyte infiltration and promoting cerebral inflammation (Huang, Upadhyay et al. 2006).

The ease and volume at which IL-6 can be produced within the CNS made it of particular focus in delineating CNS disease. However as injury models for CNS diseases were refined and improved, secondary data to the initial findings yielded interesting fresh perspectives. Particularly in models for cerebral ischemia, while IL-6 was shown to elicit its typical inflammatory response, it also demonstrated positive neurotrophic effects. For the first time, researchers started to question whether IL-6 was a driving force in the progression of inflammatory damage or whether it was attempting to adopt a neuroprotective role. As a result IL-6 has since been reclassified as also being an anti-inflammatory cytokine and has been shown to inhibit the actions of typical cytokines within the CNS (Ulich, Yin et al. 1991, Xing, Gauldie et al. 1998) amongst other protective actions. However, this new perspective presents a new outlook on a number of diseases in which over-production of IL-6 in its attempt to be protective force can elicit autoimmune damage. This ‘over-protective’ effect of IL-6 has been implicated in the onset and development of Crohn’s disease, rheumatoid arthritis and multiple sclerosis as well as other disease states such as atherosclerosis (Hirano, Akira et al. 1990). Concentrated levels of IL-6 have been detected in areas afflicted with atherosclerotic plaques (Schieffer, Schieffer et al. 2000) and as a result, IL-6 serum levels are now being looked upon as early prognostic markers for myocardial necrosis, ischemia reperfusion damage and severe coronary atherosclerosis (Ridker, Rifai et al. 2000, Libby 2002). In addition, elevated serum levels of IL-6 are now a tool utilised in identifying unstable plaques and assist in the early detection of potential cerebral infarction events (Yamagami, Kitagawa et al. 2004).

1.4.3 Reactive Oxygen Species

Reactive oxygen species are a key signalling component involved in both vascular homeostasis (Griendling, Harrison 1999) and in disease progressing pathways (Zalba, Beaumont et al. 2000). Free radicals are a natural by-product of normal metabolism with oxygen being the most influential free radical utilised in a variety of processes (Miller, Buettner et al. 1990). Free radicals and ROS can be produced via a number of cellular sources; nicotinamide adenine dinucleotide phosphate (NAPDH) oxidases (Mohazzab-H, Kaminski et al. 1994), nitric oxide synthases (NOS) (Pritchard, Groszek et al. 1995, Wang, Pagano et al. 1998), xanthine oxidoreductase (Phan, Gannon et al. 1989) and to a lesser extent lipooxygenases, cyclooxygenases and mitochondrial oxidases (Figure 1.19). These enzyme complexes facilitate the reduction of molecular oxygen to its superoxde anion form; O_2^- (Miller, Buettner et al. 1990). Superoxide while harmful in itself also acts as a source for other detrimental oxygen-centred radicals such as hydrogen peroxide and hydroxide anion (Nickenig, Harrison 2002). Normally in times of ROS or free radical production, local antioxidant defence mechanisms counteract the production of these dangerous molecules. However, whether due to dysfunction of the defence mechanisms or stimulated increased production of the harmful ROS species, oxidative stress can occur. As a consequence ROS can be initiators or secondary players in endothelial dysfunction leading to the onset and development of a number of cardiovascular related diseases (Harrison 1997).

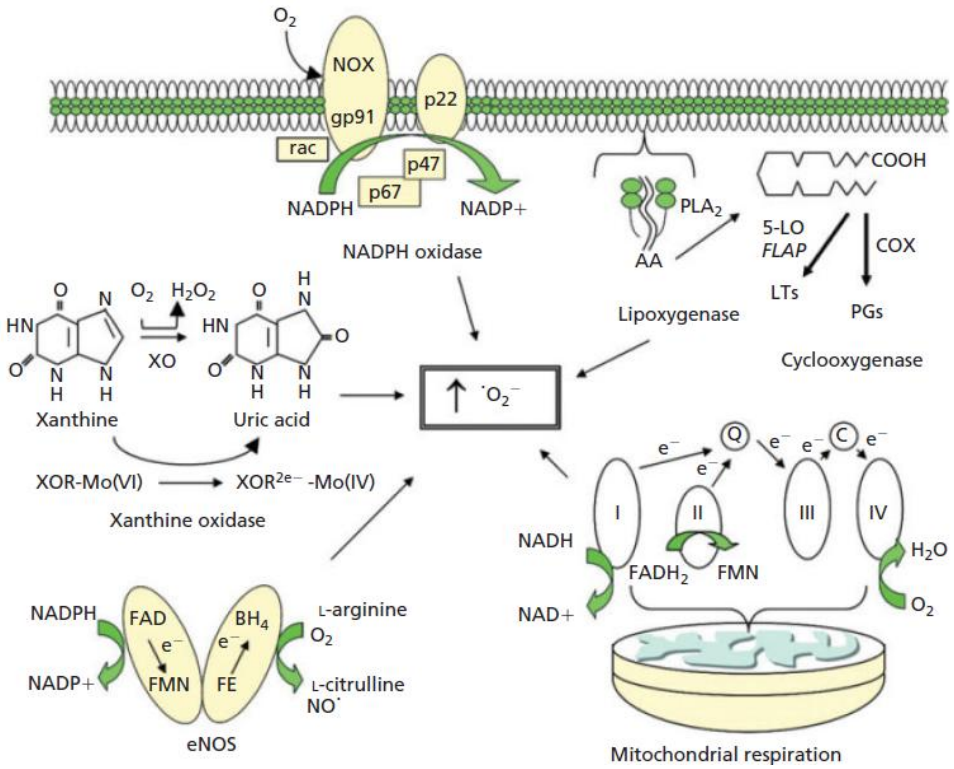

Figure 1.19: Sources of superoxide in the vasculature, (Leopold, Loscalzo 2005).

Two of the primary transcription factors affected by oxidative stress are AP-1 and NFκB (Collins 1993, Luft, Mervaala et al. 1999). These pathways have been shown to modulate the expression of some of the key genes in early onset atherogenesis such as MCP-1, VCAM-1 and ICAM-1 along with a host of pro-inflammatory cytokines (Luft, Mervaala et al. 1999, Pueyo, Gonzalez et al. 2000, Usui, Egashira et al. 2000).

NO's role in vasoregulation of blood vessels walls has already been described. In a highly oxidative environment, ROS not only plays a role in activating the endothelium and disrupting its production of NO (Harrison 1997), but it also targets and destroys any bioavailable NO to generate the highly destructive peroxynitrite species, a potent damaging oxidant (Babior 2000).

ROS species are a typical mediator of the atherosclerosis process and have been shown to modify low-density lipoprotein (LDL) particles at the site of endothelial injury (Podrez, Abu-Soud et al. 2000). Superoxide acts as both reactive oxygen radical for the mediated oxidation of LDL or can also act as a substrate or cofactor in the reaction. The conversion of the LDL assists in the generation of 'foam cells', and therefore directly ties ROS formation to atheromas in prone areas. In addition, arteries afflicted with atherosclerotic plaques have been shown to display elevated levels of p22phox and subsequent elevation in NADPH activity (Azumi, Inoue et al. 1999). This surge in superoxide production coincides with a reduced bioavailability of NO in that area (Gryglewski, Palmer et al. 1986, Rubanyi, Vanhoutte 1986). Evidence has shown that increased production of ROS coincides with endothelial activation and through the induction of redox-sensitive genes, ROS may activate inflammatory cascades that lead to the production of numerous pro-inflammatory mediators (e.g. TNF-α, IL-1β and interferon (IFN)γ) (Collins 1993, Wung, Cheng et al. 1997, Pun, Lu et al. 2009). These agents in turn can have a direct effect on NADPH oxidase and other ROS producers which results in further saturation of the environment by superoxide species (Behrendt, Ganz 2007). This vicious feedback loop of inflammatory and oxidative processes contributes greatly to atherosclerotic progression (Figure 1.20) (Marumo, Schini-Kerth et al. 1997, De Keulenaer, Alexander et al. 1998, Behrendt, Ganz 2007, Pun, Lu et al. 2009).

As previously mentioned, there are a number of in-built defence mechanisms available to the vasculature which scavenge for superoxide and its counterparts (Valko, Leibfritz et al. 2007). Under physiological conditions, endogenous anti-oxidant defense mechanisms include superoxide dismutase (SOD), catalase and glutathione. The former is a major antioxidant enzyme that assists in the release of NO from the endothelium and also accelerates the removal of O_2^-. However as outlined, patients suffering from coronary artery

disorder have been shown to display a diminished SOD activity similar to that of the other ROS defences (Landmesser, Merten et al. 2000).

Uniform laminar shear stress has been shown to upregulate the genes associated with endothelial NOS, cyclooxygenase (COX)-2 and Mn-SOD, which collectively have a vaso-protective effect on the associated vessel. Oscillatory shear, often seen in regions of vasculature branching has been shown to significantly increase the levels of p22phox and subsequently drive up superoxide expression via increased NADPH oxidase activity (Behrendt, Ganz 2007).

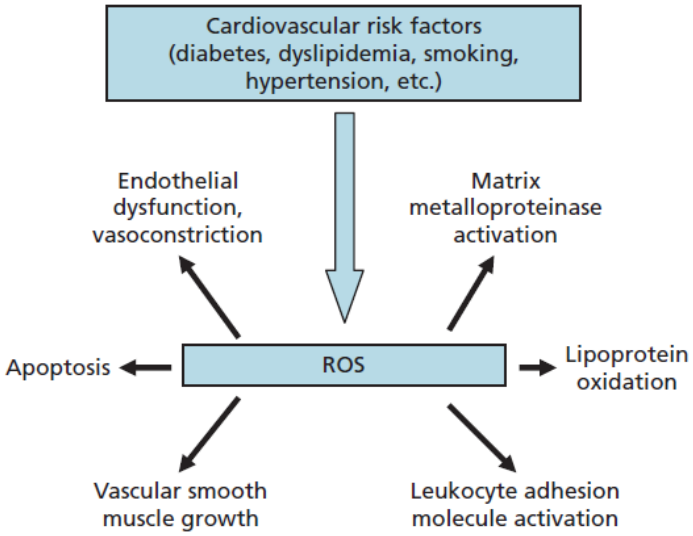

Figure 1.20: Cardiovascular risk factors that augment ROS and activate pro-atherogenic pathways, (Harrison, Griendling et al. 2003).

1.5 Signalling in the BBB

There are two key signal transduction pathways necessary to maintain a competent BBB; (i) signals sent from the junction complex to the cell interior i.e. gene expression, cell proliferation and differentiation and; (ii) signals sent from the cell interior to the junctional complex to mediate its assembly and regulate paracellular permeability (Matter, Balda 2003, Matter, Balda 2003). Given the nature of the NVU, a multitude of signalling pathways are involved. The following section focuses on a couple of the classic signalling mechanisms involved in NVU signalling, in addition to one of the more novel proteins involved in BBB signalling; 14-3-3, a primary focus of this thesis.

1.5.1 Calcium

It has long been known that calcium signalling plays an integral role in modulating BBB permeability. Calcium has been shown to act both intracellularly and extracellularly with respect to influencing the tight junction. *In vitro* models demonstrated that upon switch over to Ca^{2+}-deficient media, the tight junction demonstrated a significant loss of ZO-1, ZO-2 and occludin from the cell membrane in conjunction with a subsequent increase in paracellular permeability (Klingler, Kniesel et al. 2000). Complementing this effect, other studies showed that increasing extracellular levels of calcium induced the translocation of ZO-1 from the nucleus to the membrane and an increase in membrane resistance and decrease in permeability (Stevenson, Begg 1994). Numerous other studies exist demonstrating the sensitive nature of the tight junction to environmental Ca^{2+} levels (Nagy, Goehlert et al. 1985, Abbott, Revest 1991). This accumulating evidence quickly led to the belief that the environmental calcium levels were critical in maintaining a stable signalling environment, whilst inducing abnormally high (Stuart, Sun et al. 1996) or abnormally low (Ye, Tsukamoto et al. 1999) levels of available calcium was seen to disrupt a number of key properties other than the tight junction. Later studies confirmed that a number of known BBB permeability modulators were seen to be exacting the effect on the barrier via indirect targeting of intracellular calcium.

Since Ca^{2+} can influence cells in a number of ways, different signalling pathways are activated/deactivated as a result. In the same study which utilised Ca^{2+}-deficient media to disrupt the tight junction, the effects could be reversed upon addition of Protein Kinase A inhibitors (Klingler, Kniesel et al. 2000). In a separate study, activation of Protein Kinase C could also overcome the negative impact of extracellular calcium deficiency (Balda, Gonzalez-Mariscal et al. 1993). These studies amongst others heavily implicates Ca^{2+} in using kinase signalling cascades leading to the activation of a number of transcription factors (e.g. NFκB, cAMP) that have significant impact on the tight junction and consequently, the BBB (Brown, Davis 2002).

1.5.2 Phosphorylation

Phosphorylation is a major regulatory mechanism involved in the modulation of both the transmembrane junction and cytosolic accessory proteins (Staddon, Herrenknecht et al. 1995, Sakakibara, Furuse et al. 1997) of the BBB. Given the number of proteins involved in forming the intercellular junctions and the multiple sites on these proteins that can undergo modification of their phosphorylation state, it is highly unlikely that any one clear mechanism exists between phosphorylation and intercellular junction formation and

function. It is more likely the change and combinatorial effect of the phosphorylation states of distinct serine, threonine and tyrosine residues that produce distinct and functional effects (Sakakibara, Furuse et al. 1997).

Occludin and ZO-1 were targeted in early studies to link post-translational modifications to junction modulation (Sakakibara, Furuse et al. 1997). Early studies suggested that the phosphate content of ZO-1 was the determinant of junction permeability (Stevenson, Anderson et al. 1989), although further studies have expanded on this idea and indicated that phosphorylation of ZO-1 is critical to its membrane targeting during tight junction formation (Kurihara, Anderson et al. 1995). Similar studies have identified a number of phosphorylation changes in occludin with serine phosphorylation playing a large part in regulating the subcellular localisation of occludin (Andreeva, Krause et al. 2001) and both phosphorylation of serine and threonine residues on occludin highly correlate with tight junction reassembly post-disruption (Farshori, Kachar 1999, Tsukamoto, Nigam 1999).

Whilst much can be said about serine and threonine residues and their subsequent effects post-phosphorylation on protein function, tyrosine phosphorylation however has been identified as the key event in regulating cell-cell junctions. Tyrosine phosphorylation levels of tight junction proteins are seen to be diminished during development suggesting that this event coincides with acquisition of barrier function (Maher, Pasquale 1988). Studies also show that inhibition of protein tyrosine phosphatases leads to the significant increase in tyrosine phosphorylation state of the intercellular junction proteins which is seen to lead to an increase in permeability (Staddon, Herrenknecht et al. 1995). Tyrosine kinases have also been reported to localise at the adherens junctions (Tsukita, Oishi et al. 1991) and the susceptibility of components such as β-catenin and ZO-1 to undergo phosphorylation at this junction suggests all junctions within the intercellular complex were targets for tyrosine kinases. Complementary studies have suggested that tyrosine phosphorylation of junctional proteins decreases following cell-cell contact and maturation of junctions (Lampugnani, Corada et al. 1997).

1.5.3 14-3-3

The 14-3-3 family of proteins were first discovered during a routine characterisation of bovine brain proteins. The name was given to the protein owing to its particular elution (14^{th} fraction of bovine brain homogenate) and migration pattern (fraction 3.3) demonstrated on 2D diethylaminoethyl (DEAE) cellulose chromatography and subsequent starch gel electrophoresis (Moore, Perez 1967).

The highest tissue concentration of 14-3-3 proteins is found in the brain, estimated to comprise 1% of total soluble protein (Boston, Jackson et al. 1982, Boston, Jackson et al. 1982, Pawson, Scott 1997, Baxter, Fraser et al. 2002, Baxter, Liu et al. 2002) though it has been found to be ubiquitously expressed in almost every other tissue in the human body including testes, liver and heart (Celis, Gesser et al. 1990). Within a eukaryotic cell, 14-3-3 is predominantly found in the cytoplasm however it has also be shown at the plasma membrane and within intracellular organelles such as the nucleus and Golgi apparatus (Celis, Gesser et al. 1990, Freed, Symons et al. 1994, Tang, Suen et al. 1998, Fanger, Widmann et al. 1998, Garcia-Guzman, Dolfi et al. 1999).

In humans there are seven known isoforms categorised by Greek letters (β, γ, ε, η, σ, τ and ζ) after their elution profile on reversed phase high performance liquid chromatography (Ichimura, Isobe et al. 1988, Martin, Patel et al. 1993). The species initially designated α and δ were later found to be the phosphorylated forms of β and ζ respectively (Aitken, Howell et al. 1995). They are a highly homologous family of proteins with a very high degree of sequence conservation between species (Wang, Shakes 1996) (Figure 1.21).

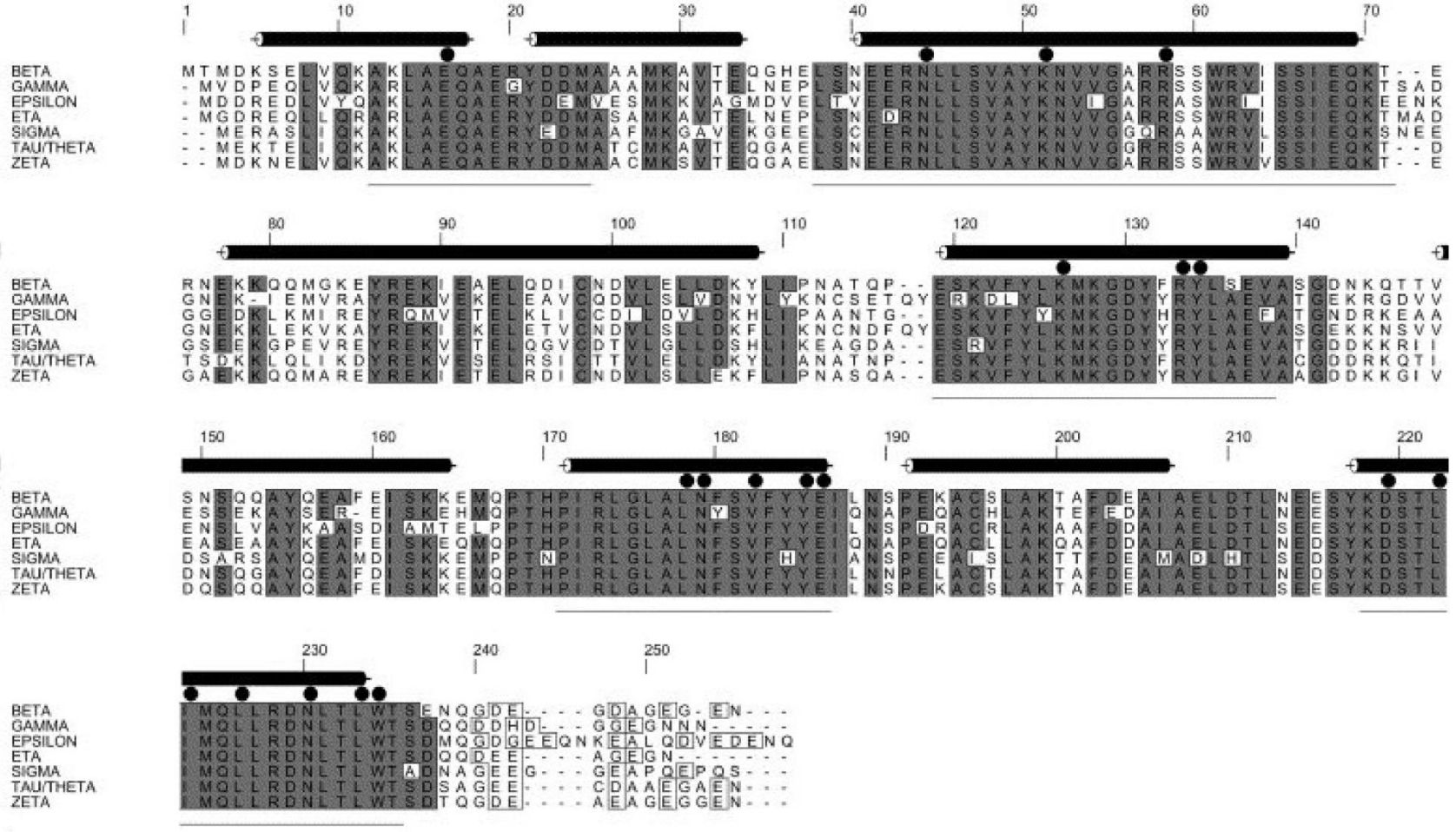

Figure 1.21: Sequence alignment of human 14-3-3 isotypes. Residues conserved in six of the seven isoforms are shaded gray. The structure of 14-3-3 is indicated by helices above the sequence alignment (Yaffe 2002).

Initially described as activators of neurotransmitter synthesis, 14-3-3 has since been shown to bind to protein kinases, enzymes, receptor proteins, cytoskeletal and other structural proteins. Over 200 proteins have been shown to interact with members of the 14-3-3 family with the list continuing to expand (Pozuelo Rubio, Geraghty et al. 2004, Jin, Smith et al. 2004, Meek, Lane et al. 2004, Benzinger, Popowicz et al. 2005). This broad array of binding partners has identified 14-3-3 in mediating various physiological cellular processes such as cell signalling, cell growth, adhesion, division, differentiation, apoptosis and ion channel regulation. Whilst extensive research has been conducted on the 14-3-3 family, they are still not completely understood in terms of their overall role however certain functional properties of the family have been established. These functions include regulating enzyme activity, acting as localisation anchors which dictate the subcellular localisation of proteins and acting as adapter molecules thus facilitating protein-protein interactions.

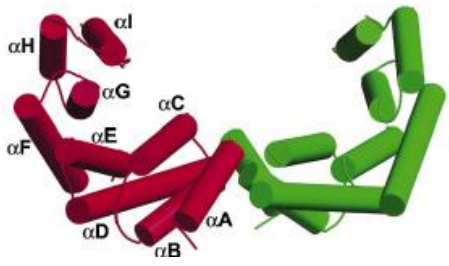

Figure 1.22: The structure of 14-3-3. Helices αA-αI are represented by cylinders (Yaffe 2002).

X-ray diffraction studies of 14-3-3 ζ and τ led to a greater understanding of how 14-3-3 facilitates the binding of so many ligands (Liu, Bienkowska et al. 1995, Xiao, Smerdon et al. 1995). These studies identified the 14-3-3 members as existing as dimers and being highly helical. Each 14-3-3 monomer consists of nine anti-parallel alpha helices (αA-αI) organised into an N terminal and C terminal domains (Figure 1.22). The nine α-helices form an 'L' shaped structure which forms walls around a negatively charged channel. The helices within this channel (αC, E, G, I) are highly conserved throughout the 14-3-3 family while the surface layer of each isoform is highly variable (Xiao, Smerdon et al. 1995, Liu, Bienkowska et al. 1995, Petosa, Masters et al. 1998, Yaffe 2002). This highly conserved interior channel suggests that the specific isoform binding to diverse targets rests on the interaction on the outside of the protein.

The N termini on 14-3-3 proteins, where dimer formation occurs, is highly variable and it is the residues present here that limit the number of possible homo- and heterodimer combinations which may confer some specificity to 14-3-3 function (Jones, Ley et al. 1995, Chaudhri, Scarabel et al. 2003). αA on one monomer binds with αC and αD on a

complimentary 14-3-3 protein forming a 'U' shaped dimer. This dimerisation process is an important functional characteristic of the 14-3-3 family as it facilitates the binding of two different regions on proteins. In the case of two interacting motifs with a weak affinity for one another, a more stable interaction can be facilitated, whereas in the case of two motifs with a strong affinity towards one another, unique conformation of the protein might be facilitated (Fu, Subramanian et al. 2000). Alternatively the dimer can bind two identical or different target proteins thereby acting as an adapter bringing disparate target ligands together, which in turn may modulate the activity of one another for better or for worse (Vincenz, Dixit 1996, Fu, Subramanian et al. 2000, Sehnke, DeLille et al. 2002). In almost every known organism, multiple (at least two) isoforms of 14-3-3 have been observed to allow for the formation of these variable dimer conformations (Aitken, Baxter et al. 2002). The reason why organisms require more than one isoform is unknown. Certain isoform expression is stress regulated of cell-type specific. It is thought this regulated expression of the 14-3-3 isoforms allows the organism improved control over the levels of the 14-3-3 proteins. While much has been muted about how the family share many biochemical properties, subtle differences have been reported suggesting potential unique roles for certain isoforms.

It should be noted that aside from the various characteristics that define what can bind with 14-3-3, the state of the 14-3-3 proteins themselves plays a critical determinant in their function within particular pathways. Regulatory mechanisms placed upon 14-3-3 include isoform specificity, post-translational modification and expression levels in cells.

One of the key problems with delineating the complete function of the 14-3-3 proteins is the sheer complexity of potential interactions they can be involved in. Their basic mechanisms in regulating enzyme activity, subcellular localisation of binding partners, and stimulation of protein-protein interactions occur on many, many levels and thus make them a complex family to study (van Hemert, de Steensma et al. 2001, Yaffe 2002). Given the abundance of the 14-3-3 family in brain tissue and the substantial amount of signalling that occurs within the organ, this makes them an attractive molecule to examine in relation to modulation of the BBB.

1.6 BBB Pathophysiology

1.6.1 BBB Models

Until the 1970's, studies on the barriers of the CNS were conducted primarily in *in vivo* models and in situ tissue preparations (Bradbury 1979). These studies mostly focussed on

monitoring dyes or tracer extravasation from parenchymal vessels or examining permeability changes in vessels in real time (Butt, Jones et al. 1990, BUTT 1995, Abraham, Deli et al. 1996). The introduction of methods which allowed the isolation of cerebral capillaries (Joo, Karnushi 1973) sparked a new generation of studies *in vitro* which have enabled the scientific community to examine the mechanisms responsible for barrier function in greater detail, on both a cellular and molecular level (Kramer, Abbott et al. 2001). In using primary cell cultures (Revest, Abbott et al. 1991) it became apparent quite quickly that cell culture of these isolated fractions perturbed the cells from their quiescent *in vivo* states (0.1% replications per day) to an activated phenotype (1 to 10% replications per day) with a severe loss of specialised functions associated with diverse vessels and organ systems. This not only led to improved culture conditions (e.g. co-culture models (Deli, Abraham et al. 2005)) but also opened up a search for alternative models which have granted a greater understanding overall of the mechanics of these cell cultures. Immortalised cell lines that lack the entire *in vivo* phenotype have proved useful in examining specific signal transduction pathways and their interactions (Nobles, Revest et al. 1995, Nobles, Abbott 1998). Similarly, the overlap of properties between epithelial and endothelial cell types has led to the utilisation of epithelial models (e.g. MDCK and Caco2) in establishing numerous generic regulatory mechanisms (Balda, Whitney et al. 1996, Balda, Matter 2000, Balda, Matter 2000, Balda, Flores-Maldonado et al. 2000). More intricate cell models exist (e.g. ECV304 cell line-brain endothelial phenotype with epithelial features) and have also proved useful in furthering our understanding of the BBB (Hurst, Fritz 1996, Easton, Abbott 2002) (Figure 1.23).

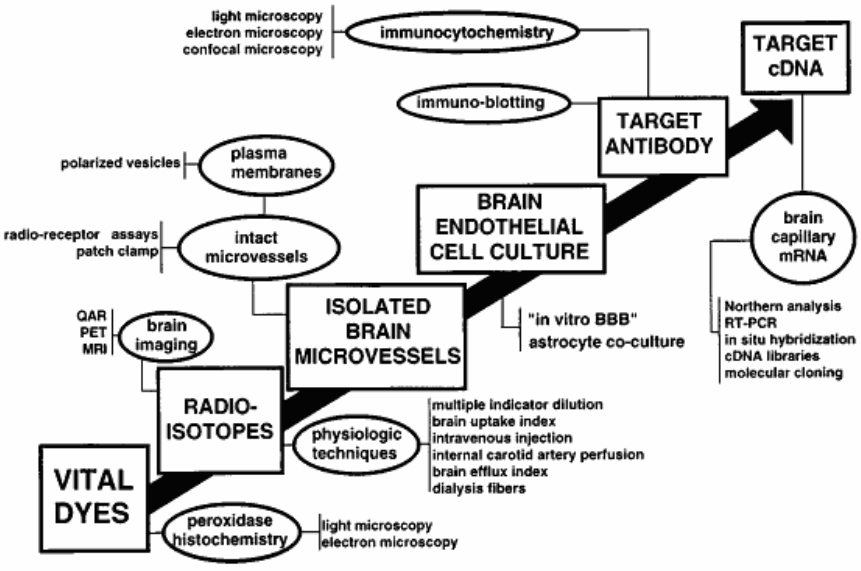

Figure 1.23: Linear evolution of blood-brain barrier methodologies from vital dyes to molecular biology, (Pardridge 2003).

1.6.2 BBB Disruption

Physiologically sound BBB models are essential to understanding CNS pathologies and developing therapeutic strategies. As already mentioned, most of the work conducted on understanding the NVU and the mechanisms related to vascular permeability has been carried out using animal models or isolated-perfused organ preparations (Takasato, Rapoport et al. 1984), making the understanding of certain CNS based diseases difficult to interpret. In time, it became possible to isolate intact, functional and morphologically correct cerebral microvessels (Joo, Karnushi.i 1973). Upon development of this method (Panula, Joo et al. 1978), CNS-based BBB diseases were much easier to dissect and understand. What follows is an outline of some of the key CNS-based diseases manifesting BBB disruption that afflict the population and the difficulties that are associated in treating them.

1.6.2.1 Stroke

Stroke is a transient or permanent reduction to the cerebral blood flow, originating from ischemia or haemorrhage based injury. Stroke, and its subsequent damaging after-effects, is one of the major contributors to global disease (Lopez, Mathers 2006). It is the third most leading cause of death and the most frequent cause of permanent disability in the world (Donnan, Fisher et al. 2008). In the acute phase of stroke, neurological complications such as cerebral edema and hemorrhagic transformation are a major contributor to stroke-based fatalities (Balami, Chen et al. 2011), however the majority of deaths arise from the medical complications in the aftermath of the event (Slot, Berge et al. 2009, Kumar, Selim et al. 2010) (Figure 1.24).

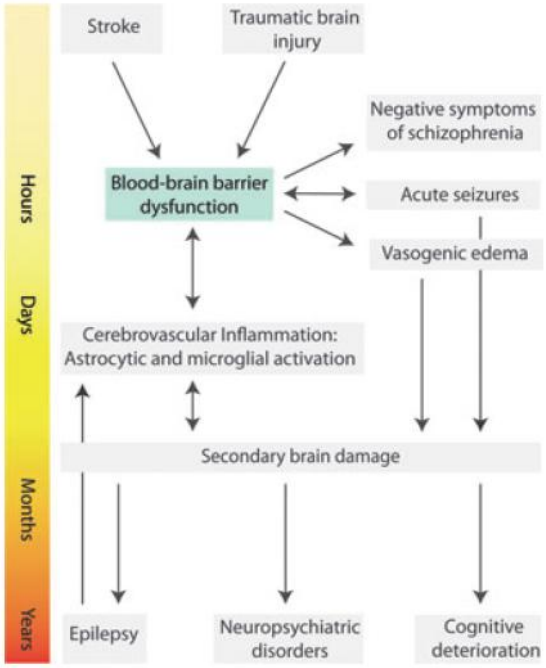

Figure 1.24: The relationship between BBB dysfunction and different neurological disorders. BBB dysfunction typically occurs as an acute consequence of stroke and traumatic brain injury resulting in an inflammatory response, the consequence of which may lead to development of other neurological disorders (Schoknecht, Shalev 2012).

Since the events resulting in stroke are acute and time is critical, a greater understanding of time-dependent recruitment of immune cells and their contribution to ischemic brain injury is essential for developing effective therapeutics. As already detailed, local cerebral ischemia results in a time-dependent recruitment and activation of wide variety of inflammatory cells including T cells, monocytes, macrophage and neutrophils results in the onset of a number of inflammatory processes. These inflammatory responses are geared towards repairing the damaged tissue but in fact can often result in the development of other neuronal diseases. In early stages, ROS and proinflammatory cytokines and chemokines are released from injured tissue. These agents assist in the expression of adhesion molecules. In the latter stages (days later) infiltrating leukocytes release further amount of cytokines and induce the excessive release of MMPs and ROS which amplify the brain's inflammatory response further causing extensive activation of resident immune cells. This can frequently lead to further disruption of the BBB resulting in brain edema, neuronal death and hemorrhagic transformation. However some of the inflammatory mediators have been shown to have dual roles. For example while MMP-9 has been shown to greatly pronounce brain injury in the early stages it has been shown to play a role in brain regeneration and neurovascular remodelling in the latter stages. Each individual's systemic inflammatory processes vary greatly and it's these

collective mechanisms that potentially reveal the susceptibility and outcome of an individual to stroke and its aftermath.

BBB dysfunction has been identified as a critical step in the acute phase of stroke, although the means by which in contributes to the anomalies listed above is diverse. Release and action of ROS, MMP's, pro-inflammatory cytokines and chemokines are among the mechanisms shown to influence the BBB following cerebral ischemia. As mentioned the aftermath of stroke is often the more complicated aspect of the injury. Long term consequences of stroke include delayed cognitive deterioration, dementia, depression and epilepsy, with stroke being identified as the most common cause of epilepsy in the elderly (Herman 2002). As a result, stroke has now being examined from the perspective that it acts as a key initiator of cerebrovascular inflammation (Balami, Chen et al. 2011, Gorelick, Scuteri et al. 2011).

1.6.2.2 Traumatic Brain Injury

Traumatic Brain Injury is shown to be the biggest cause of disability and death in adults younger than 45 in developed countries (Bruns, Hauser 2003). Similar to stroke, TBI is often an initiator of BBB dysfunction which can have an acute effect or with a delay of several days (Lenzlinger, Marx et al. 2002, Rodriguez-Baeza, La Torre et al. 2003, Shlosberg, Benifla et al. 2010, Chodobski, Zink et al. 2011). TBI damage often results in the formation of edema at the site of injury which in turn triggers a rise in intracellular pressure with consequences for cerebral blood flow and ischemic lesion development. The cells of the NVU can also be affected by this surge in intracranial pressure often leading to disruption of the NVU structure. The mechanisms involved in TBI in relation to BBB dysfunction do not differ excessively from stroke in that the subsequent aftermath is often the most damaging in the long term. In addition to the onset of ischemia, there is an increase in the production of free radicals, pro-inflammatory cytokines and MMPs, all of which have been detailed in causing BBB dysfunction and resulting in an increase in permeability.

1.6.2.3 Epilepsy

Epilepsy is one of the more common neurological disorders with a prevalence of 0.5-1% on a global scale and a cumulative incidence of 3% by the age of 74. As already mentioned, stroke is the primary cause of epilepsy development (20%) (Herman 2002, Sander 2003). Stroke-dependent epilepsy onset is accredited to the generation of brain lesions associated with ischemia in the months to years after stroke occurrence. Like most CNS injuries,

epilepsy can be accredited to inflammatory-based damage and subsequent dysfunction of the BBB. Healthy animal models that utilise BBB-disrupting techniques have shown onset of epileptic activity (Seiffert, Dreier et al. 2004, van Vliet, Araujo et al. 2007).

Numerous studies have already targeted the signalling cascades associated with BBB dysfunction in preventing seizures and onset of epilepsy. TGF-β and its signalling pathways pertaining to albumin extravasation have emerged as a potential candidate for nullifying epileptogenesis (Ivens, Kaufer et al. 2007, Kim, Buckwalter et al. 2012) as well as neutralising inflammatory mediators such as TNF-α, IL-6 and IL-1β which have been shown to promote seizures (Vezzani, Balosso et al. 2008). Patients have responded to anti-inflammatory treatments which were shown to reduce seizure frequency (Sotgiu, Murrighile et al. 2010, Marchi, Granata et al. 2011).

1.6.2.4 Multiple Sclerosis

Sophisticated MRI studies have shown that BBB disruption is one of the early symptoms of multiple sclerosis development, preceding the onset of any well known clinical symptoms. Most investigators believe MS to be an autoimmune disease with experimental models attempting to replicate the environment for MS development identifying the actions of T Cells (Seeldrayers, Syha et al. 1993) and monocytes (Morrissey, Stodal et al. 1996) as the primary instigators for BBB disruption. These cells have been known to release pro-inflammatory mediators such as MCP-1 (Song, Pachter 2004), TNF-α, IL-1β and IFNγ amongst others (Minagar, Alexander 2003).

Studies into these immune responses have uncovered antigen-specific receptors on particular T-cell lines in MS patients that recognise peptides presented on microglia (Lang, Jacobsen et al. 2002). This targeting mechanism to the site of the BBB in conjunction with the release of pro-inflammatory mediators noted earlier results in the interference of the myelination processes that occur in the nervous tissue (Merrill, Ignarro et al. 1993, Chao, Hu et al. 1995). As a result, the myelin sheath undergoes serious damage, exposing the underlying axons to further injury (Wekerle, Hohlfeld 2003).

Further investigations into areas suffering from MS lesions have subsequently shown a loss of occludin and ZO-1 in the underlying tissues of the microvasculature (Bolton, Anthony et al. 1998, Plumb, McQuaid et al. 2002, Kirk, Plumb et al. 2003). Similar observations have been noted in post-mortem studies of brain tissue originating from sufferers of HIV-encephalitis (Dallasta, Pisarov et al. 1999) and Alzheimers disase (Fiala, Liu et al. 2002).

1.6.2.5 Alzheimer's Disease

A key factor in the development of Alzeimer's disease is the effect of β-amyloid (Aβ) on the NVU's astrocytes and microglia (Braak, Braak 1991). Once considered the result of Aβ overproduction that subsequently lead to the generation of plaques (Blennow, de Leon et al. 2006), recent hypothesis suggest that a toxic oligomeric form of Aβ is the main cause of Alzheimer's disease (Selkoe 2000) (though this hypothesis, amongst many others relating to Alzheimer's disease, remain unproven and greatly disputed (Van Broeck, Van Broeckhoven et al. 2007, Huang, Potter et al. 2012)). Regardless of form, deficient clearance of Aβ from the CNS to the peripheral circulation for degradation and systematic removal exacerbates any potential for Aβ-driven damage to be incurred (Hardy, Selkoe 2002, Mawuenyega, Sigurdson et al. 2010). Recent studies claim that Alzheimer's disease is directly linked to the dysfunction of the specific transport systems of the BBB (P, glycoprotein, LDL-receptor protein (LRP)-1 and the receptor for advanced glycation end products (RAGE) (Zlokovic, Yamada et al. 2000, Zlokovic, Deane et al. 2005, Deane, Zlokovic 2007, van Assema, Lubberink et al. 2012) that maintain CNS Aβ concentrations. In addition, development of Alzheimer's disease has itself been linked to inducing BBB-disruption, facilitating the entry of Aβ from the systemic circulation into the brain creating a vicious circle (Kalaria 1992). Conversely, Aβ directly (and indirectly via production of toxic metabolites) induces a number of signalling events in the brain, (such as NFκB), resulting in the release of inflammatory mediators such as IL-1β, TNF-α, IL-6, MCP-1, NO and ROS (Rubio-Perez, Morillas-Ruiz 2012) that are known to not only cause the neuronal damage and synaptic dysfunction associated with Alzheimer's disease, but also potentiate BBB-disruption (Giulian 1995, Giulian, Haverkamp et al. 1995, Klegeris, McGeer 1997, Klegeris, Walker et al. 1997). Clinical evidence demonstrates immunotherapy with monocolonal antibodies reduces amyloid burden in the cerebral microvessels. Such amyloid-lowering strategies have been hypothesised to rescue BBB function (Zlokovic, Deane et al. 2005, Dickstein, Biron et al. 2006) with successful clinical trials hinging on such.

1.7 Summary and study rationale

CVD begins in childhood, progressing silently through a long preclinical stage before manifesting clinically from middle age. The initiation, progression, and eventually activation, of CVD depends on profound dynamic changes in vascular biology. The endothelium has emerged as the key regulator of vascular homeostasis. Once assumed an inert barrier, the endothelium has been shown to participate in a number of important endocrine, paracrine and autocrine vascular functions. However it can also act as an active signal transducer for environmental influences that can induce a change in its overall

phenotype (Figure. 1.25). Alteration in endothelial function precedes the development of phenotypic changes that can contribute to clinical complications. For example, systemic factors such as growth factors, hormones, bacterial and viral products, and in particular, cytokines, can activate the endothelial monolayer, resulting in the establishment of a procoagulant surface, the active recruitment of immune cells, the release of inflammatory cytokines and perhaps most importantly, the disruption of the selective permeability barrier. Concurrently, local stimuli such as haemodynamic forces exerted by pulsatile nature of blood flow, can adapt endothelial function resulting in both short-term vasoactive responses and long-term remodelling of the vessel wall. The ability of the endothelium to sense its biochemical and biomechanical environment, and generate an integrative response to these stimuli, results in the alteration of cellular structure and function. This adaptation plays a defining role in the maintenance of vascular homeostasis or the development of vascular pathologies.

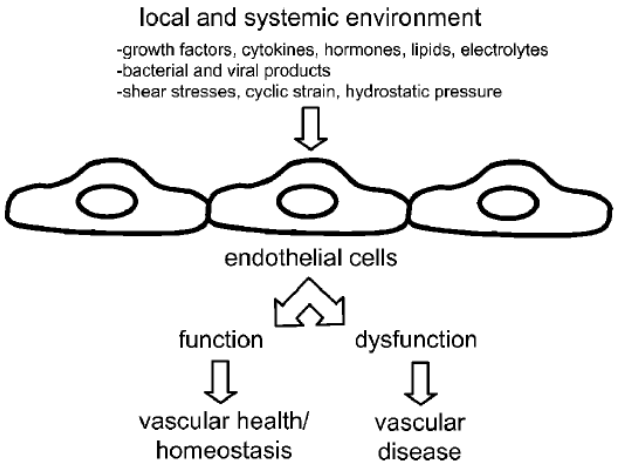

Figure 1.25: The effect of the endothelial environment on vascular health and disease. Local and systemic environmental factors impact endothelial phenotype. The integrative response of the endothelium to these stimuli results in the alteration of cellular structure and function that can lead to vascular health or disease. Inflammatory cytokine and shear stress were aspects that were integrated into our experimental paradigm (Wasserman, Topper 2004).

The endothelium of the cerebral microvasculature constitutes the BBB, a physical and metabolic barrier that controls the flux of blood-borne neurotransmitters and neuroactive agents between the brain and the peripheral tissue and vice versa. This barrier plays an important role in the homeostatic regulation of the brain microenvironment that is necessary for proper neuronal and glial function. The majority of molecular traffic proceeds via transcellular routes due to the presence of tight and adherens junctions, a series of

transmembrane and cytoplasmic proteins located between adjacent cells that effectively seal the paracellular pathway from passive diffusion of solutes. These proteins, like many others, are subject to change in response to local and systemic environmental influences. Pathological levels of these influences are associated with the dysfunction of the processes involved in coordinating the formation, maintenance and sustainment of BBB junctions. In the cerebral vasculature, disruption of these processes and others, particularly those pertaining to proper barrier function, are poorly understood and have been strongly implicated in the initiation, progression and activation of several disease states of the CNS (e.g. stroke, multiple sclerosis, Alzheimer's disease).

The purpose of this study is to build on previous published findings from our laboratory in which the effects of a physiological stimulus, laminar shear stress, on BBB phenotype were examined. Our previous studies employed a bovine culture model so in part we were assessing the translation of our previous findings into a newly established human culture model. In parallel, the effects of pathophysiological stimuli, inflammatory cytokines, on BBB phenotype were also examined. This thesis will primarily focus on the effect each stimulus has on the modulation of barrier function within an *in vitro*, monoculture model of the BBB. Peripheral objectives entail the examination of some of the mechanisms and processes that mediate such modulation, whilst the effects of each stimulus on the anti-inflammatory response of the BBB are also explored. Elucidation of how the BBB responds to these physiological and pathophysiological stimuli will not only provide a greater understanding of the mechanisms involved in mediating diseases of the CNS, but also those that can be potentially manipulated and implemented in the development of novel therapeutic strategies that involve controlled modulation of barrier function, impacting on drug delivery strategies to the brain and thus the treatment of several neurological diseases.

1.8 Thesis Overview

The research data presented herein describes the effects of a physiological (shear stress) and pathophysiological (inflammatory cytokines) stimuli on a human brain microvascular endothelial cell blood-brain barrier model. The data focuses on the effect of each stimulus on blood-brain barrier phenotypic properties, in particular barrier function, before investigating whether shear stress could ameliorate the effects of cytokine injury *in vitro*, and if so, by which anti-inflammatory mechanism/s. The effects of cytokine-induced released inflammatory mediators; ROS and IL-6, from HBMvECs on overall cytokine-induced injury were also investigated. Finally, the identification and delineation of the role of a potentially novel binding partner of the brain interendothelial junction; 14-3-3, is explored with respect to our physiological and pathophysiological stimuli. The findings are presented in the following manner.

Chapter 3: The effects of laminar shear stress on HBMvEC blood-brain barrier properties.

Chapter 4: The effects of inflammatory cytokines; TNF-α and IL-6, on HBMvEC blood-brain barrier properties.

Chapter 5: The independent contribution of reactive oxygen species, and IL-6 to cytokine-induced modulation of HBMvEC blood-brain barrier properties.

Chapter 6: The role of 14-3-3 in shear- and cytokine-induced modulation of HBMvEC junction assembly and barrier function.

See Figure 1.26 below for a schematic depiction of the experimental approaches used in this thesis.

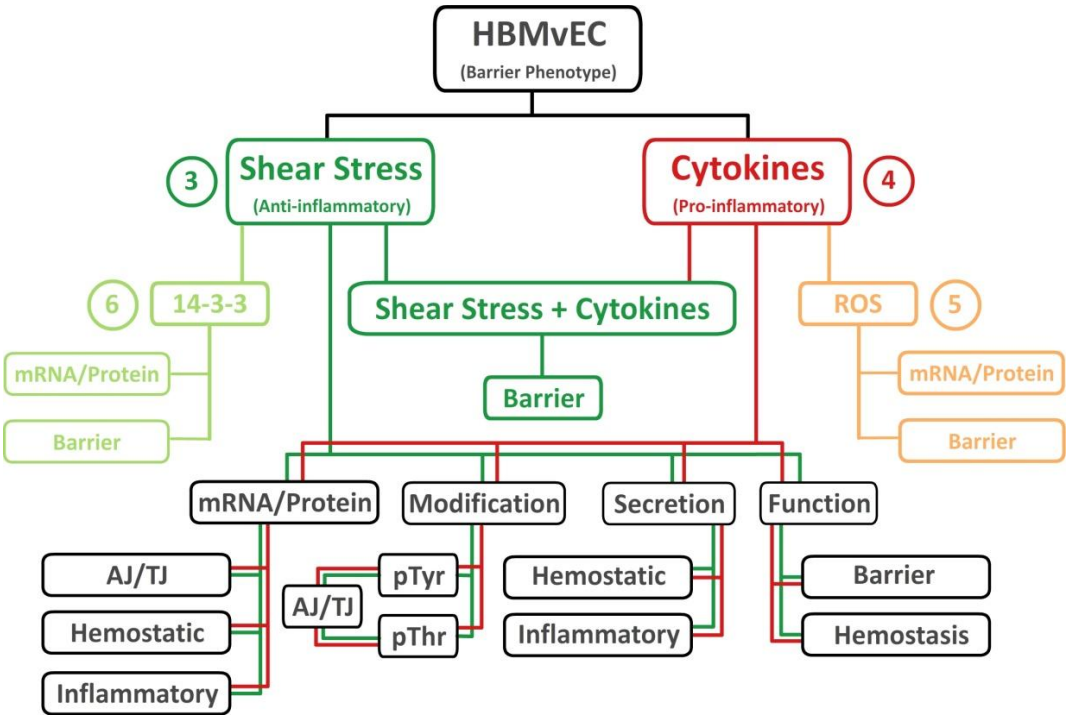

Figure 1.26: Schematic depiction of experimental approach. Primary human brain microvascular endothelial cells (HBMvECs) were subjected to different experimental paradigms; physiological shear conditions (dark green, chapter 3) and pathophysiological inflammatory cytokines (red, chapter 4) and monitored for genetic, molecular, structural and functional changes in BBB phenotype, particularly pertaining to the interendothelial junction. The effect of co-exposing the HBMvECs to both stimuli was then investigated on barrier function, in parallel with further mechanistic studies related to each stimulus's experimental outcomes; the influence of ROS of cytokine-induced damage (orange, chapter 5) and the role of 14-3-3 in shear-mediated barrier enhanced (light green, chapter 6).

Chapter 2:

Materials and Methods.

2.1 Materials

2.1.1 Reagents and Chemicals

Abcam (MA, USA)	Catalogue No.
Mouse anti-thrombomodulin IgG antibody	AB6980
Mouse anti-VE-cadherin monoclonal IgG2a antibody	AB7047
Rabbit anti-14-3-3 polyclonal IgG antibody	AB9063
Rabbit anti-vWF polyclonal IgG antibody	AB6994

Aktiengeselischaft and Company (Numbrecht, Germany)	Catalogue No.
1.5 ml micro tube with safety cap	72.706.200
10 µl pipette tips	70.1130
200 µl pipette tips	70.760.002
1000 µl pipette tips	70.762
15 ml reagent and centrifuge tubes	62.554.502
50 ml reagent and centrifuge tubes	62.559.001
2 ml serological pipettes	86.1252.001
10 ml serological pipettes	86.1254.001
25 ml serological pipettes	86.1685.001
6-well tissue culture plates	83.1839
24-well tissue culture plates	83.1836
96-well tissue culture plates	83.1835
58 cm^2 tissue culture dishes	83.1802
T-25 tissue culture flasks	83.1810.002
T-75 tissue culture flasks	83.1813.002
Cell scrapers	83.1830
Cryopure tubes	72.380.992
Filtopur 0.2 µm syringe filters	83.1826.001
Multiply® PCR Cup, 200ul	72.737.002

Multiply® PCR Cup, 500ul	72.735.002
Reagent and centrifuge tube	62.515.006
Weigh boats	71.9923.212

Ambion (TX, USA)	Catalogue No.
CDH5 Silencer Select small interfering RNA (siRNA)	4392420
RNase AWAY Spray Solution	10328-011

Applied Biosystems (CA, USA)	Catalogue No.
Fast Optical 96-well reaction plates	4346906
Fast Optical 384-well reaction plates	4309849
High Capacity cDNA Reverse Transcription Kit	4368814
Microamp Optical Adhesive Film	4311971
CLDN5 Stealth siRNA	1299001

Becton Dickinson (NJ, USA)	Catalogue No.
FACS Rinse Solution	340346
FACSFlow™ Sheath Fluid	342003
Microlance Hypodermic Needle 19G	BD301750
Round-bottomed FACS tubes	352054

Cell Applications (CA, USA)	Catalogue No.
Bovine Brain Microvascular Endothelial Cells (BBMvEC)	B840-05

Cell Signalling (MA, USA)	Catalogue No.
Anti-mouse IgG, HRP-linked antibody	7076S
Anti-rabbit IgG, HRP-linked antibody	7074S

Cell Systems Inc., (WA, USA)	Catalogue No.
Attachment Factor™	4Z0-210
Human Brain Microvascular Endothelial Cells (HBMvEC)	ACBRI 376

Clontech Laboratories Inc. (CA, USA)	Catalogue No.
pEGFP-N1	pEGFP-N1

DAKO (CA, USA)	Catalogue No.
Fluorescent Mounting Media	53023

Davidson and Hardy (Belfast, Northern Ireland)	Catalogue No.
Carl Zeiss High Performance Coverslips	474030-9000

eBioscience (CA, USA)	Catalogue No.
Human IL-6 ELISA Ready-SET-Go!®	88-7066

Eurofins MWG Operon (Edersberg, Germany)

Claudin 5 Primers (Human and Bovine)

GAPDH Primers (Human and Bovine)

Occludin Primers (Human and Bovine)

VE-Cadherin Primers (Human and Bovine)

ZO-1 Primers (Human and Bovine)

vWF Primers (Human)

IL-6 Primers (Human)

TNF-α Primers (Human)

TNFR1 Primers (Human)

TNFR2 Primers (Human)

gp130 Primers (Human)

sIL-6R Primers (Human)

14-3-3β Primers (Human)

14-3-3ζ Primers (Human)

14-3-3ε Primers (Human)

14-3-3γ Primers (Human)

14-3-3θ Primers (Human)

GE Healthcare (Buckinghamshire, UK)	Catalogue No.
Bovine Brain Microvascular Endothelial Cells (BBMvEC)	B840-05
Donkey anti-rabbit HRP-linked IgG antibody	NA9340
Sheep anti-mouse HRP-linked IgG antibody	NA931V

Gibco (Scotland, UK)	Catalogue No.
Fetal Calf Serum	10106169

ibidi (Martinsried, Germany)	Catalogue No.
Fluorescent Mounting Medium	50001
Olaf Humidifying Chamber	80008
µ-slide $I^{0.6}$ Leur	80186
µ-slide y-shaped	80126

Invitrogen (Groningen, Netherlands)	Catalogue No.
Alexa Fluor® 488 Donkey Anti-Goat IgG (H+L)	A11055
Alexa Fluor® 488 Donkey Anti-Mouse IgG (H+L)	A21202
Alexa Fluor® 488 Donkey Anti-Rabbit IgG (H+L)	A21206
Alexa Fluor® 546 Donkey Anti-Mouse IgG	A10036
Alexa Fluor® 546 Donkey Anti-Rabbit IgG	A10040
Alexa Fluor® 488 Phalloidin	A12379

Alexa Fluor® 546 Phalloidin	A22283
Dead Cell Apoptosis Cytometry Kit	V13241
Claudin-5 Monoclonal Antibody, Mouse (4C3C2)	35-2500
Occludin Monoclonal Antibody, Mouse (OC-3F10)	33-1500
Phosphothreonine (pTyr) Mouse Monoclonal Antibody	13-9200
Phosphotyrosine (pThr) Mouse Monoclonal Antibody Cocktail	13-6600
ZO-1 Monoclonal Antibody, Mouse (ZO1-1A12)	33-9100
Neon™ Transfection System 100 µl Kit	MPK10096
SYBR®Safe DNA Gel Stain	S33102
TRIzol®	15596-018

Lonza (Basel, Switzerland)	Catalogue No.
Mycozap™ Antibiotics	VZA-2022

Meso Scale Discovery (MD, USA)	Catalogue No.
Human ProInflammatory-4 1 Ultra-Sensitive Kit	K15009C-1
Human Vascular Injury 1 Kit	K15135C-1

Millipore (MA, USA)	Catalogue No.
Amicon Ultra-2 Centrifugal Filter Unit with Ultracel-30 membrane	UFC203024
Apocynin (APO)	178385
EndoGRO-MV Complete Culture Media Kit	SCME004
GAPDH, Polyclonal Antibody, Rabbit	ABS16
Immobilin-P polyvinylidene fluoride (PVDF) 0.45 µm Membrane	IPVH00010
Luminata Forte Western HRP substrate	WBLUF0100
Millicell Hanging Cell Culture Transwell Inserts	PIHT30R48
Recombinant Human Basic Fibroblast Growth Factor (bFGF)	GF003
Recombinant Human IL-6	IL006

Recombinant Human Monocyte Chemotactic Protein-1 (MCP-1)	GF012
Recombinant Human Tumour Necrosis Factor-Alpha (TNF-α)	GF023

Miltenyl Biotec (Cologne, Germany)	Catalogue No.
Propidium Iodide (PI) Solution	130-093-233

NanoEntek (Seoul, South Korea)	Catalogue No.
ADAM Accuhip^{4x} Kit	AD4K-200

Pall (Portsmouth, UK)	Catalogue No.
Biotrace^{TM} NT Nitrocellulose Transfer Membrane	66485

Pierce Chemicals (Cheshire, UK)	Catalogue No.
BCA Protein Assay Reagent	23225
Co-Immunoprecipitation Kit	26149

Promega (WI, USA)	Catalogue No.
CellTiter 96® AQ_{ueous} One Solution Cell Proliferation Assay	G3580
Sequencing Grade Modified Trypsin	V5111

PromoCell (Heidelberg, Germany)	Catalogue No.
Freezing Medium	C-29912

Qiagen (West Sussex, UK)	Catalogue No.
HiSpeed Midi-Prep Kit	12643

R&D Systems (MN, USA)	Catalogue No.
Goat anti-IL-6 polyclonal IgG antibody	AF-206-NA

Human Thrombomodulin DuoSet ELISA	DY3947

Roche Diagnostics (Basal, Switzerland)	Catalogue No.
Complete EDTA-free Protease Inhibitor Cocktail Tablets	04693132001
E-Plate xCELLigence™ plates	05469830001
FastStart Universal SYBR Green Master Mix	04673492001

Sigma-Aldrich (Dorset, UK)	Catalogue No.
2-Mercaptoethanol	M6250
2',7'-Dichlorofluorescin diacetate	D6883
4',6-Diamidino-2-Phenylindole Dihydrochloride (DAPI)	32670
Acetone	34850
Acetonitrile (ACN)	271004
Acrylamide/Bis-acrylamide Solution	A3574
Agarose	A5093
Albumin from bovine serum	A2153
Ammonium Bicarbonate	A6141
Ammonium Chloride	A9434
Ammonium Persulfate	A9164
Ampicillin sodium salt	A9518
Brilliant Blue R	B0149
Brilliant Blue G Colloidal Concentrate	B2025
Bromophenol Blue Sodium Salt	B8026
Catalase from bovine liver (CAT)	C-9322
Chloroform	C2432
Crystal Violet	C3886
Dihydroethidium	37291
Dimethyl Sulfoxide (DMSO)	D8418

DNase 1 Kit	AMPD1
Dulbecco's Modified Eagle's Medium-High Glucose (DMEM)	D5796
Ethylenediaminetetraacetic Acid Disodium Salt Dihydrate (EDTA)	E5134
Fluorescein Isothiocyanate-Dextran-40kDa (FITC-Dextran)	FD40S
Formaldehyde Solution	F8775
Formic Acid	F0507
Gelatin from cold water fish skin	G7765
Glycerol	G6279
Glycine	G8898
Heparin Sodium Salt	H3149
HEPES	H4034
Hydrogen Peroxide Solution	H1009
Kanamycin sulphate from *Streptomyces kanamyceticus*	K4000
Lysogeny broth (LB) Agar EZMix™ Powder	L7533
LB Broth EXMix™ Powder	L7658
Magnesium Chloride	M8266
Magnesium Sulfate	M7506
Methanol	34860
Methyl-3,4-dephostatin	M9440
N-Acetyl-L-Cysteine (NAC)	A9165
N,N,N',N'-Tetramethylethylenediamine (TEMED)	T9281
PAP Pen, 2 mm	Z672548
PAP Pen, 5 mm	Z377821
Paraformaldehyde	P6148
Penicillin-Streptomycin	P0781
Phosphate Buffered Saline (PBS) Tablets	P4417
Ponceau S solution	P7170
Potassium Chloride	P9541

R18 trifluoroacetate	SML0108
RNA Sample Loading Buffer without Ethidium Bromide	R1386
Saponin from quillaja bark	S7900
Sodium Azide	13412
Sodium Chloride	S3014
Sodium Deoxycholate	D6750
Sodium Dodecyl Sulfate (SDS)	L3771
Sodium Fluoride	S7920
Sodium Orthovanadate	S6508
Sodium Phosphate Dibasic	S3264
Sucrose	S0389
Superoxide Dimutase from bovine erythrocytes (SOD)	S5395
Thrombin from bovine plasma	T9549
Tris Acetate-EDTA Buffer	T9650
Triton™X-100	X-100
Trizma Base	T6066
Trypsin-EDTA Solution	T4174
Tryptone	T7293
Water	W4502
Yeast Extract	Y1625

Terumo Medical (NJ, USA)	Catalogue No.
10cc Syringes	SS-10ES

Thermo Fisher Scientific (Leicestershire, UK)	Catalogue No.
6x DNA Loading Dye	R0611
10x Phosphate Buffered Saline Solution	BP399-20
Acetic Acid Glacial	A35-500

Buffer Solution pH4 (phthalate)	J/2825/15
Buffer Solution pH7 (phosphate)	J/2855/15
Buffer Solution pH10 (borate)	J/2885/15
DreamTaq DNA Polymerase Kit	EP0702
GeneRuler™ 100 bp DNA Ladder Plus	SM0321
PageRuler Plus Prestained Protein Ladder	26619
Parafilm Wrap	PM-992
Propan-2-ol	P/7490/15
Spectra Multicolor High Range Protein Ladder	26625
Tris Base	T1503
Western Blot Stripping Reagent	10057103
White Microtitre Plates	611F96WT

vWR International Ltd. (Maidstone, UK)	Catalogue No.
Cover slips 24*24 mm	631-0127
L-Shaped Spreaders	612-1561
Microscopy Slides	631-0103
Tween®20	66368

2.1.2 Apparatus

Applied Biosystems 7900HT Fast Real Time PCR	Applied Biosystems (CA, USA)
FACSAria	Becton Dickinson (NJ, USA)
Mini PROTEAN® Trans Blot Module	Bio-Rad (CA, USA)
MJ Mini Thermal Cycler	Bio-Rad (CA, USA)
ELx800 Microplate Reader	Biotek (VT, USA)
Centrifuge	Eppendorf, (Cambridge, UK)
ibidi pump and flow system	ibidi (Martinsried, Germany)
SECTOR® Imager 6000	Meso Scale Discovery (MD, USA)
Cryo-freezing container	Nalgene, (NY, USA)
ADAM-MC	NanoEntek (Seoul, South Korea)
Microporator Mini MP-100	NanoEntek (Seoul, South Korea)
Nikon Eclipse Ti	Nikon (Tokyo, Japan)
Nikon Eclipse TS100 phase-contrast microscope	Nikon (Tokyo, Japan)
Olympus Fluoview FV10i Confocal Microscope	Olympus (Tokyo, Japan)
xCELLigence Real Time Cell Analyzer (RTCA) DP	Roche (Basal, Switzerland)
Vortex, Orbital Shaker	Stuart Scientific (UK)
See-Saw Rocker	Stuart Scientific (UK)
Block Heater	Stuart Scientific (UK)
Rotator	Stuart Scientific (UK)
G-Box chemi-luminescence analysis system	Syngene (Cambridge, UK)
TECAN Safire 2 Fluorospectrometer	Tecan, (Männedorf, Switzerland)
Nanodrop 1000 Spectrophotometer	Thermo Fisher (UK)
Zeiss 710 Confocal Microscope	Carl Zeiss (Oberkochen, Germany)

2.1.3 Preparation of stock solutions and buffers

2.1.3.1 Molecular Biology

Super Optimal Broth with Catabolite Repression (SOC) Media

Tryptone	2% (w/v)
Yeast Extract	0.5% (w/v)
Sodium Chloride	10 mM
Potassium Chloride	2.5 mM
Magnesium Chloride	10 mM
Magnesium Sulfate	10 mM
Glucose	20 mM

Tris-EDTA (TE) Buffer

Tris	10 mM
EDTA	1 mM

2.1.3.2 SDS-PAGE and Immunoblotting

RIPA Cell Lysis Buffer Stock (1.28x)

HEPES, pH7.5	64 mM
Sodium Chloride	192 mM
Triton X-100	1.28% (v/v)
Sodium Deoxycholate	0.64% (v/v)
SDS	0.128% (w/v)

RIPA Cell Lysis Buffer (1x)

1.28x RIPA Stock	1x
Sodium Fluoride	10 mM
EDTA, pH8.0	5 mM
Sodium Phosphate	10 mM
Sodium Orthovanadate	1 mM

Protease Inhibitors	1x

Running Buffer (1x)

Tris	25 mM
Glycine	192 mM
SDS	0.1% (w/v)

Sample Solubilisation Buffer (4x)

Tris-HCl, pH6.8	250 mM
SDS	8% (w/v)
Glycerol	40% (v/v)
2-Mercaptoethanol	4% (v/v)
Bromophenol Blue	0.008% (w/v)

Filter the Sample Solubilisation Buffer using a 0.25 µm filter

Tris Buffered Saline (10x)

Tris-HCl, pH6.8	152 mM
Tris Base	46 mM
Sodium Chloride	1.5 M

Transfer Buffer (1x)

Tris-HCl, pH6.8	25 mM
Glycine	192 mM
SDS	0.1% (w/v)
Methanol	20% (v/v)

Tris Buffered Saline (10x)

Tris	2.4% (w/v)

Sodium Chloride	8.8% (w/v)

Coomassie R-250 Stain

Coomassie Brilliant Blue R250	1% (w/v)
Glacial Acetic Acid	10% (v/v)
Methanol	40% (v/v)
Distilled (DI) Water	50% (v/v)

Filter the Coomassie stain using a 0.25 µm filter

Coomassie R-250 Destain

Methanol	20% (v/v)
Glacial Acetic Acid	10% (v/v)
DI Water	70% (v/v)

2.1.3.3 Immunoprecipitation

SDS-PAGE Gel Fixative

Methanol	40% (v/v)
DI Water	53% (v/v)
Glacial Acetic Acid	7% (v/v)

Coomassie G-250 Stain

DI Water	64% (v/v)
Brilliant Blue G Colloidal Concentrate	16% (v/v)
Methanol	20% (v/v)

Coomassie G-250 Destain

Methanol	25% (v/v)
Glacial Acetic Acid	10% (v/v)
DI Water	65% (v/v)

2.1.3.4 Mass Spectrometry

Coomassie G-250 Destain

100 mM Ammonium Bicarbonate	50% (v/v)
Acetonitrile	50% (v/v)

Digestion Buffer

Trypsin, sequencing grade	12.5 ng/µl
Ammonium Bicarbonate	10 mM
Acetonitrile	10% (v/v)

Extraction Buffer

5% Formic Acid	33% (v/v)
Acetonitrile	66% (v/v)

2.1.3.5 Agarose Gel Loading Buffer (6x)

Sucrose	40% (w/v)
Bromophenol Blue	0.25% (w/v)

2.1.3.6 FACS Buffer

Fetal Calf Serum	2% (v/v)
Sodium Azide	0.1% (w/v)
PBS	98% (v/v)

Filter the FACS Buffer using a 0.25 µm filter

2.1.3.7 Microscopy

Paraformaldehyde

Paraformaldehyde	3% (w/v)
0.1M NaOH	500 ml

Place in a 70^{o}C water bath until dissolved. Cool to room temperature and pH with HCl to 7.2

Permablock Solution

Saponin	0.1% (v/v)
Fish gelatine	0.25% (v/v)
Sodium Azide	0.02% (w/v)
PBS	10 ml

2.2 Methods

2.2.1 Cell Culture Techniques

All cell culturing techniques were undertaken in a clean and sterile environment using a Holten Lamin Air laminar flow cabinet. Cells were visualised using a Nikon Eclipse TS100 phase-contrast microscope.

2.2.1.1 Human Brain Microvascular Endothelial Cell (HBMvEC) Culture

HBMvEC's are a strongly adherent cell line which over time form a confluent, contact-inhibited monolayer with distinct cobblestone morphology. HBMvEC's (Cell Systems Inc.) were initiated by isolation of dispase-dissociated normal human brain cortex tissue and subsequent culturing in the presence of serum free medium and a naturally derived human astrocyte extracellular matrix. Cells were reported to test negative for the presence of *Mycoplasma spp*. and characterised via the cytoplasmic uptake of Di-l-Ac-LDL and expression of vWF/Factor VIII. Cells at <9 cumulative population doublings *in vitro* (Passage 2) were cryopreserved serum-free in aliquots of ~$1*10^6$ cells per millilitre prior to shipping. Cells were cultured onto Attachment Factor™ (AF) coated tissue culture grade plastic-ware containing ENDO-Gro MV Basal Medium and Supplement Kit and Mycozap™ antibiotic. To summarise, the final constituents and their concentrations in each bottle of medium were Foetal Bovine Serum (FBS) (5%), L-Glutamine (10 mM), Ascorbic Acid (50 µg/ml), Heparin Sulfate (0.75 U/ml), Hydrocortisone Hemisuccinate (1 µg/ml), recombinant human Epidermal Growth Factor (rhEGF) (5ng/ml), EndoGRO-LS Supplement (0.2%) and Mycozap (100 µg/ml). Cells were cultured onto T25 and T75 flasks for early passage/freeze-stock generation, whilst 58 cm^2 dishes were routinely used for experimental work alongside 6-, 24- and 96-well plates. For experimental purposes, cells were used between passages 5-12. Cells were maintained in 5% CO_2/95% humidity at 37^{o}C.

2.2.1.2 Bovine Brain Microvascular Endothelial Cell (BBMvEC) Culture

BBMvEC's are the bovine equivalent of HBMvEC's. BBMvEC's (Cell Applications Inc.) were isolated directly from microvessels located in the bovine brain and cultured using Bovine Brain Endothelial Cell Culture Medium. Cells were reported to test negative for bacterial, mycoplasma and fungal contaminants and characterised via cytoplasmic uptake of Dil-l-Ac-LDL prior to cryopreservation and shipping. Cells at <9 cumulative population doublings *in vitro* (Passage 2) were cryopreserved in Bovine Brain Endothelial Cell Basal Medium containing 10% FBS and 10% Dimethyl Sulfoxide (DMSO) in aliquots of >$5*10^5$

cells per millilitre prior to shipping. Cells were cultured onto tissue culture grade plastic-ware containing high glucose DMEM supplemented with FBS (10%), Heparin (3 µg/ml), human recombinant basic fibroblast growth factor (bFGF) (3 ng/ml), penicillin (100 U/ml) and streptomycin (100 µg/ml). Cells were cultured onto T25 and T75 flasks for early passage/freeze-stock generation whilst 58 cm^2 dishes were routinely used for experimental work alongside 6-well plates. For experimental purposes, cells were used between passages 5-12. Cells were maintained in 5% CO_2/95% humidity at 37^oC.

2.2.1.3 Trypsinisation of cells

As both HBMvECs and BBMvECs are an adherent cell type, trypsinisation was required to perform sub-culture. Cells were typically passaged at approximately 70-90% confluency confirmed via light microscopy. In preparation, all solutions used for sub-culturing; Sterile Phosphate Buffered Saline (PBS), Growth Medium, Trypsin/EDTA and AF (HBMvEC's only), were pre-warmed to 37^oC in the water bath. In the laminar hood, culture medium was added to the prospective dishes and placed in an incubator to equilibrate the medium to 37^oC with 5% CO_2. In the case of HBMvEC's the plastic-ware required a coating to facilitate attachment prior to the addition of the medium. Briefly, an appropriate amount of attachment factor relative to the surface area onto which the cells were to be seeded was added (~20-70 µl). A sterile cell spreader was then used to coat the well with any residual AF removed using a sterile aspirator before growth medium was added.

For trypsinisation, first the growth medium was removed using a sterile aspirator. Following this the culture dish was washed briefly 2-3 times using sterile PBS to ensure the removal of any residual α_1-antitrypsin (Trypsin inhibitor found in serum). An appropriate volume of Trypsin-EDTA, enough to cover the cell population, was then added to the dishes and then the dishes were placed into the incubator for 5-10 minutes. Cells were routinely observed over this time course until they had displayed a rounded morphology but had not yet fully detached. Following a gentle tap to facilitate detachment, an equal volume of growth medium to Trypsin-EDTA was added to the dish and the cell suspension then pooled into a 15 ml tube. Following centrifugation at 700 rpm for 5 minutes, the Trypsin-EDTA/growth medium was aspirated and the resulting cell pellet was gently resuspended via pipetting in 1 ml of fresh growth medium. This cell suspension was then counted and either seeded to an appropriate density for experimental purposes or split 3,000 cells/cm^2 of a cell dish for sub-culturing.

2.2.1.4 Cell Counting

In order to ensure accurate reproducibility of experiments and assess cell densities and viability for experiments, sub-culturing and cryopreservation, cell counts were routinely performed via two platforms; a Neubauer haemocytometer and the Advanced Measurement and Accurate Detection (ADAM™) Counter.

2.2.1.4.1 Haemocytometer

In order to perform a cell count, a square glass coverslip was mounted onto the centre chamber of the haemocytometer (Figure 2.1) and adjusted until Newton rings were visible. To assess cell viability, 100 µl of cell suspension was mixed with 20 µl of trypan blue and the mixture was set aside for 2 minutes. 10 µl of the mixture was then added to the haemocytometer chamber via capillary action and the cells were visualised under a 4x magnification via phase-contrast microscopy. Typically each corner square of the grid had their contents counted, noting the numbers of viable vs. non-viable cells (dead cells take up the trypan dye due to their compromised membrane and appear blue, whilst live cells with an intact membrane exclude it). Viable cells which fell on the top and/or within the left hand margin of the grids were included in the counts whilst those that fell on the bottom and right hand side of the grid were excluded. The total number of cells in each of the four corner quadrants were added then divided by four to obtain an average count per 1 mm^2. The number of viable cells was calculated utilizing the following equation:

$$Avg.Cell\ No.\ \times 1.2\ (Dilution\ Factor)\ \times 1 \times 10^4\ (Conversion\ Factor)\ = Viable\ Cells/ml$$

In order to assess cell viability, the total average cell count (live cells PLUS dead cells) was substituted into the above equation and using the two values, cell viability could be expressed as a percentage of the total population.

$$\left(\frac{Avg.Live\ Cell\ No.\ \times 1.2\ (Dilution\ Factor)\ \times 1 \times 10^4\ (Conversion\ Factor)}{Avg.Total\ Cell\ No.\ \times 1.2\ (Dilution\ Factor)\ \times 1 \times 10^4\ (Conversion\ Factor)}\right) \times 100 = \%\ Viability$$

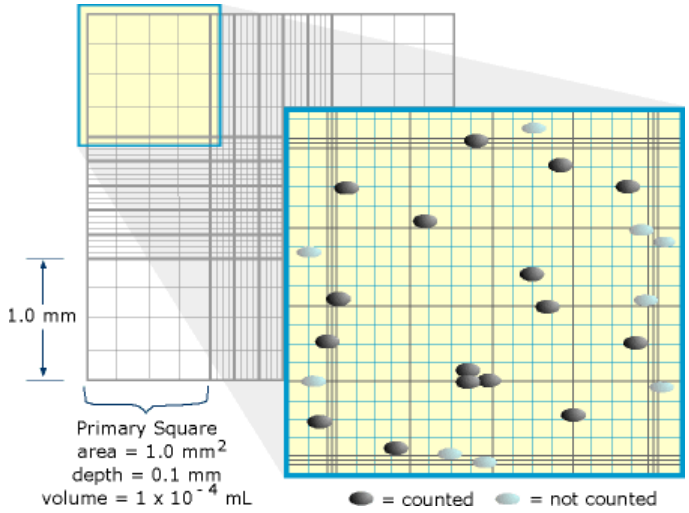

Figure 2.1: The Haemocytometer.

2.2.1.4.2 ADAM™ Counter

The ADAM™ counter is based on the concept of using fluorescent microscopy to detect and count cells. Combining sensitive fluorescence dye staining, LED optics and CCD detection technologies, the ADAM™ counter eliminates often encountered problems associated with using a haemocytometer; false positives, limitation of the human eye, limited sample volume and cell aggregation. To count, 2x 15 µl aliquots of cell suspension were put aside in sterile micro tubes. One micro tube had 15 µl of N Accustain Solution added to it whilst the other micro tube had 15 µl of T Accustain Solution added. Both were mixed gently before 20 µl of each micro tube was added to the respective channel on a fresh ADAM Accuchip. The ADAM™ Accuchip is then processed by the counter and 40-60 images are taken of preset coordinates along the Accuchip channels. Any fluorescent signal detected is recorded via a sensitive CCD array and the average cell number and viability are computed by integrated image analysis software.

Solution N contains Propidium Iodide (PI), a stain which has the ability to intercalate with DNA and stains cell nuclei a distinctive red colour. When in contact with a cell suspension, only the cells with ruptured membranes will allow the dye to permeate giving all ‘injured’ or non-viable cells a distinct fluorescent tag with which the ADAM counter can detect. Solution T on the other hand contains both PI and a detergent, the detergent acting to destroy every cell in the suspension and the PI acting as earlier described allowing the ADAM counter to assess a total cell count. As both suspensions are from the same source, an accurate and fast total viable cell count can be obtained (Figure 2.2).

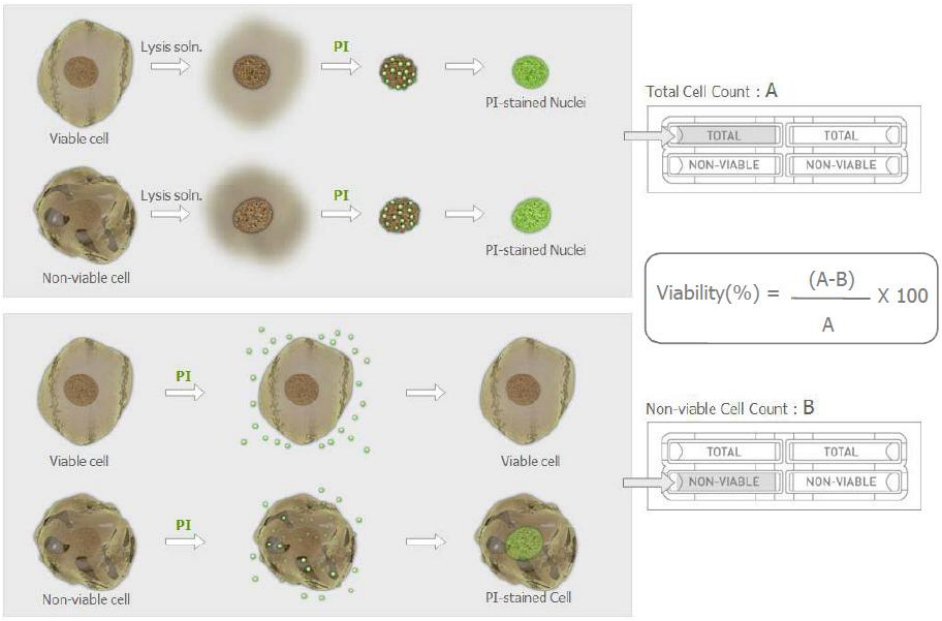

Figure 2.2: The principle of the ADAM™ Counter, (http://www.nanoentek.com/).

2.2.1.5 Cryogenic preservation and recovery of cells

For long term storage, HBMvEC's and BBMvEC's were preserved in a liquid nitrogen cryo-freezer unit. Following trypsinisation, cells were centrifuged at 700 rpm for 5 minutes and the supernatant removed. The resulting pellet as resuspended in the appropriate freeze-down medium; for HBMvEC's PromoCell Cell Freezing Medium was used, for BBMvEC's; high glucose DMEM supplemented with 20% v/v FBS, DMSO (20% v/v), Heparin (3 ug/ml), bFGF (3 ng/ml), Penicillin (3 U/ml), Streptomycin (100 µg/ml). Cell suspensions were typically in the range of $0.5\text{-}1.0*10^6$ cells/ml. 1 ml aliquots were placed in sterile CryoPure cryovials and stored in a Mr. Freeze® cryo-freezing container before being placed in a -80°C freezer. The Mr. Freeze® ensured the cryovials were cooled at a rate of -1°C/min. Following this, the cryovials were transferred to a liquid nitrogen cryo-freezing container until further required.

For the recovery of cells, cryovials were heated rapidly to 37°C in a waterbath. Upon entering a full liquid phase the contents were quickly transferred to 58 cm^2 dishes containing pre-warmed growth medium and AF if necessary (HBMvECs). After 24 hours the plates were inspected via phase-contrast microscopy to inspect the adherence and morphology of the cells before all growth medium was aspirated and the dishes washed with sterile PBS to remove any residual DMSO. This was replaced by fresh pre-warmed growth medium.

2.2.2 Cell Treatments

2.2.2.1 Cytokine Injury

For cytokine injury studies, cells were seeded onto 58 cm^2 dishes, 6-well dishes or 96-well dishes. The cell number seeded depended entirely on the experiment setup though the aim was typically to have a confluent monolayer to achieve a more physiologically relevant model (for proliferation assays, cells were seeded to sub-confluent levels to monitor the rate of proliferation over a time course, Section 2.2.8.2 and 2.2.8.3).

Cytokines used in the early investigation of the induction of endothelial injury included Tumour Necrosis Factor-Alpha (TNF-α), Interleukin-6 (IL-6), Monocyte Chemotactic Protein-1 (MCP-1) and Interleukin-1 Beta (IL-1β) with a subsequent shift in focus onto the effects of TNF-α and IL-6 for the majority of the thesis. For all experiments involving cytokine injury, four concentrations were employed; 0, 1, 10 and 100 ng/ml and two incubation times; 6 and 18 hours. Following cytokine stimulation, the cells were either: (i) harvested for mRNA to conduct Real-Time PCR measurement of particular gene expression levels; (ii) harvested for protein to examine protein expression levels via Western Blotting; (iii) fixed *in situ* for immunocytochemical staining; or (iv) transplanted into Millicell hanging cell culture inserts for transendothelial permeability assays.

2.2.2.2 Shear Stress Experiments

2.2.2.2.1 Orbital Shear

For laminar shear stress studies, orbital rotation was applied as in previous publications (Fitzpatrick, Guinan et al. 2009, Walsh, Murphy et al. 2011). HBMvEC's and BBMvEC's were seeded at 0.5-1.0*10^5 cells/well of a sterile, cell culture grade 6-well plate and allowed to adhere for 24 hrs. Fresh growth medium was added the following day and the cells were cultured to >90% confluency (typically 4-7 days). Culture medium was then removed and replaced with 4 ml of fresh pre-warmed culture medium. Cells were then exposed to laminar shear stress (0-10 dynes/cm^2, 0-48 hrs) using an orbital rotator (Stuart Scientific Mini Orbital Rotator) set to 0-230 rpm depending on the required shear level (Figure 2.3). The calibration of the rotator was determined by the following equation (Hendrickson et al., 1999).

$$\boldsymbol{Shear\ Stress} = \boldsymbol{\alpha}\sqrt{\boldsymbol{\rho n}(\boldsymbol{2\pi f})^{\boldsymbol{3}}}$$

Where: α = radius of orbital rotator circumrotation (cm)

ρ = density of liquid (g/L)

n = 7.5 * 10^{-3} (dynes/cm^2 at 37^{o}C)

f = rotation per second

The ‘dyne’ or ‘dyne/cm^2’ us one of the smallest units of pressure for measuring force and is defined as ‘the force required to accelerate a mass of one gram at a rate of one centimetre per second squared’. It is one of the most commonly used units in fluid mechanics and is often associated with surface tension (dyne/cm) and thus shear stress (dynes/cm^2).

Control plates containing un-sheared ‘static’ cells were also routinely cultured in the same incubator but on a different shelf to avoid any vibrations that may be caused by the presence of the orbital rotator. Studies were carried out over different periods of time (0-48 hrs) and shear rates (0-10 dynes/cm^2) in the absence and presence of inflammatory cytokines (TNF-α or IL-6) at varying concentrations (0, 1, 10 and 100 ng/ml) and exposure times (6 and 18 hrs). Following shearing experiments, the cells were harvested for analysis as described in Section 2.2.2.1.

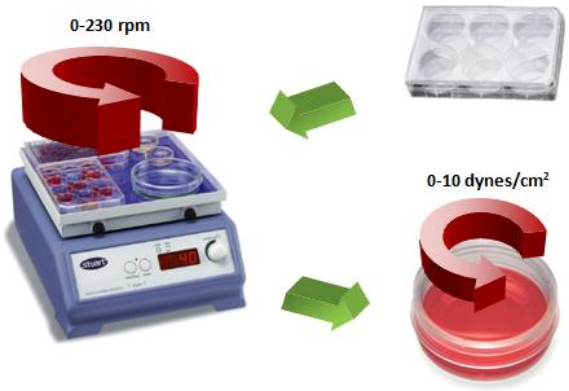

Figure 2.3: Orbital rotation model used in laminar shear stress studies.

2.2.2.2.2 ibidi® Flow System

The ibidi® pump system is a novel perfused flow system. It is a refined means of replicating vascular shear profiles in that it: (i) allows for the culture, simultaneous perfusion and observation to occur on the same platform; (ii) delivers a range of uni-directional shear stress profiles (oscillatory and laminar) and µ-slides dimensions that simulate the physiological spectrum of veins and arteries; (iii) allows for long term studies with its cost-effective requirement of cell culture reagents, the modest volumes required also allowing for the effective examination of secreted soluble factors by cells (Figure 2.4).

This method was applied as in previous publications (Kowalsky, Byfield et al. 2008, Walsh, Murphy et al. 2011). Prior to cell seeding, all removable tubing and medium reservoirs were

autoclaved and kept in a sterile environment until required. The slides, tubing and cell culture medium were then equilibrated overnight at 37°C in a tissue culture incubator. The following day, BBMvEC's or HBMvEC's were trypsinised and counted as previously described. The cells were then seeded onto µ-slides (HBMvEC slides were AF pre-treated) 200 µl at a time at a density of $1*10^6$ cells/ml taking care not to introduce any air bubbles. The µ-slides were filled until the reservoirs on each end of the slide were full before being covered with the provided reservoir caps. The µ-slides were incubated within the confines of a humidity chamber at 37°C and observed over the next 24-48 hrs, with the medium changed at least twice a day until a confluent and healthy morphology was observed. The µ-slides were then connected to the pump system via the luer connectors in accordance with the manufacturer's instructions and previous publications (Walsh, Murphy et al. 2011), taking the utmost care not to introduce air bubbles. The cells were then exposed to laminar shear stress for the required time before the immunocytochemistry protocol was carried out as described in Section 2.2.10.

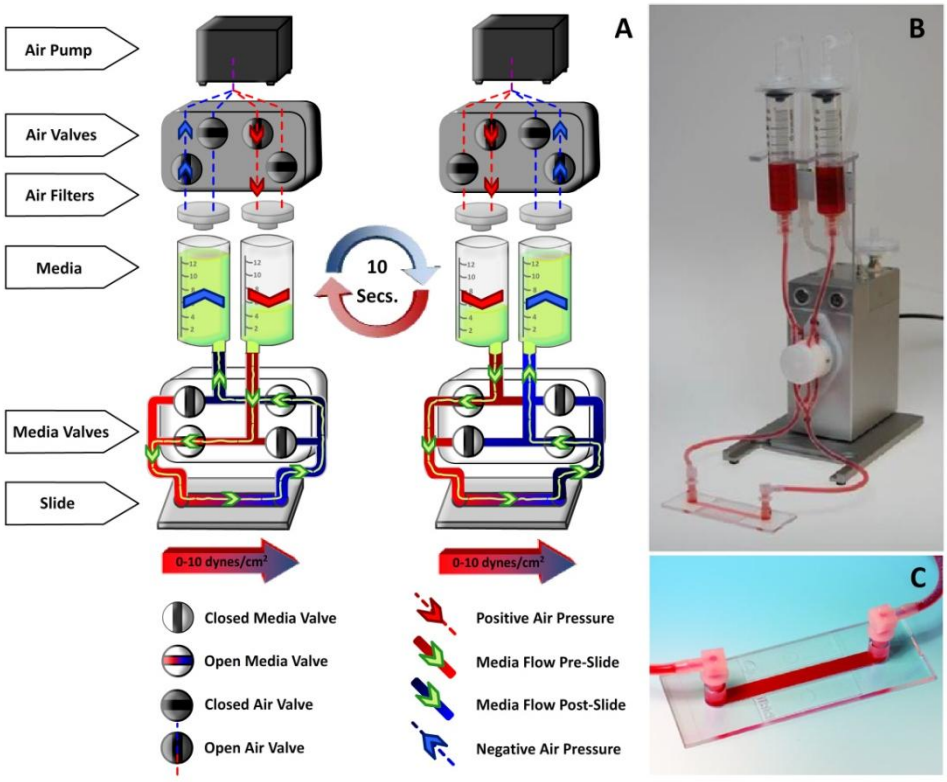

Figure 2.4: The ibidi® flow system. (A) The principle of the ibidi® system which allows for a continuous unidirectional shear to be applied to the cultured cells in the µ-slide. (B) The ibidi® setup. (C) A close-up of a µ-slide.

2.2.2.3 Treatment with Pharmacological Inhibitors

Prior to treatment with anti-oxidants or pharmacological inhibitors, HBMvECs or BBMvECs were grown to their experimentally required degree of confluency before having their growth medium removed and the cells washed twice using PBS. Inhibitors and anti-oxidants were reconstituted in a suitable solvent. Working concentrations were then made up in EndoGRO-MV Growth Medium or DMEM containing antibiotics. For DMSO-soluble compounds, a suitable stock concentration was prepared so that the final concentration of DMSO in the working solutions was less than 0.5%.

Inhibitor concentrations used in experiments were taken from current literature (Sweeney, Morrow et al. 2004, Du, Khuri et al. 2008, Fitzpatrick, Guinan et al. 2009, Walsh, Murphy et al. 2011, Guinan, Rochfort et al. 2013) and based on manufacturers recommendations in tandem with an inhibitor concentration gradient.

Inhibitor	Effective Dosage
Apocynin	10 mM
Catalase	250 U
Dephostatin	20 µM
Genistein	50 µM
N-Acetyl-L-Cysteine	5 mM
R18	100-1000 nM
Superoxide Dismutase	100 U

Table 2.1: The effective doses of inhibitors used.

2.2.2.4 Treatment with Pre-Conditioned Medium

Prior to treatment with pre-conditioned medium, HBMvECs or BBMvECs were grown to their experimentally required degree of confluency before having their growth medium removed and the cells washed twice using PBS. For conditioned medium experiments, serum-free medium was employed. Conditioned medium from stimulated cultures were harvested and 2 ml volumes were aliquoted into Amicon Ultra-2 centrifugal filter devices. The filters were spun at 4,000 g for 15 mins before device was reassembled as per the manufacturer's instructions and centrifuged once more at 1000 g for 2 mins. The collected concentrate was then used immediately or stored at -80^{o}C for further use.

2.2.3 Molecular Biology

2.2.3.1 Reconstituting Plasmid cDNA

Plasmid deoxyribonucleic acid (DNA) constructs were received as small amounts of DNA air-dried onto filter paper, which were stored at 4^{o}C until required. To reconstitute the DNA, a region of the filter paper containing the air-dried plasmid (~1 cm^{2}) was sectioned from the filter paper and handled using a flame sterilised set of scissors and forceps. The section was added to a 1.5 ml micro-centrifuge tube before 100 µl of sterile, endotoxin-free, TE buffer was added also. The tubes contents were then vortexed gently for 5-10 seconds, incubated at room temperature for 5 mins and subsequently vortexed again. The tube was then centrifuged for 15 sec at 1000 rpm. Approximately 1-10 µl of the supernatant was used for subsequent bacterial transformations.

2.2.3.2 Transformation of competent cells

Approximately 1-10 µl of reconstituted plasmid DNA (10-50 ng) or 10 µg of purified DNA construct was gently added to 25-50 µl of competent DH5α *Escherichia. Coli* bacterial cells. The DNA-bacterial mixture was then incubated on ice for 30 min. The tube was 'heat-shocked' at 42^{o}C for 30 sec before a further incubation on ice was carried out for 2 min. Following this step, 500 µl of room temperature SOC medium was added to the tube and the mixture was incubated for a further 30 min at 37^{o}C on a bacterial culture shaker at 150 rpm. The resulting transformed cells were spread on two LB agar plates containing the appropriate selective antibiotics (Table 2.2) in volumes of 50 µl and 500 µl. Approximately 5 µl of competent cells (without plasmid DNA) were spread on selective agar plates to serve as negative controls for bacterial growth. The spread plates were inverted and incubated at 37^{o}C overnight to facilitate optimal bacterial growth. Transformed colonies were isolated the following day for broth cultures and subsequent DNA midi-preparations.

Antibiotic	Solvent	Final Concentration (µg/ml)
Ampicillin	dH_2O	50 µg/ml
Kanamycin	dH_2O	50 µg/ml

Table 2.2: Antibiotic Concentrations.

2.2.3.3 Purification of plasmid DNA

Following bacterial transformation, successfully transformed colonies were isolated from the selective agar plates using a flame-sterilized inoculating loop. The transformed colony was used to inoculate 150 ml of LB broth supplemented with the appropriate antibiotics in

sterilised baffled flasks. The flasks were incubated overnight at 37^{o}C on a bacterial shaker at 150 rpm.

The next day the plasmid DNA was purified from the culture using a Qiagen plasmid midi-prep kit as per the manufacturer's instructions. Briefly, the cultured bacteria were centrifuged at 4000 rpm for 15 min at 4^{o}C. The supernatant was carefully decanted by tube inversion and the resultant pellet was dissolved via the addition of 6 ml of chilled P1 buffer and subsequent vortexing. 6 ml of P2 lysing buffer was then added to the tube and the mixture was vortexed vigorously for 30 sec before being left to rest at room temperature for a further 5 mins. The P2 lysing buffer was then neutralised by the addition of 6 ml of chilled P3 buffer and a thorough vortexing for 30 sec. The resulting cell lysate mixture was transferred into the barrel of a Qia Midi-cartridge and incubated at room temperature for 10 minutes to settle any debris. Following this, a Qia Midi-filter was attached to the Midi-cartridge and the cell lysate was filtered into a previously equilibrated Hi-speed Midi-prep tip containing a resin column to which DNA binds. The column was then washed with 20 ml of QC buffer to eliminate any bacterial cell proteins which might be present. The DNA was then eluted from the column with the addition of 5 mls of QF buffer into a sterile 15 ml tube. 3.5 mls of isopropanol was then added to the tube and the contents were mixed via gentle inversion before being left to incubate for 5 mins at room temperature. This was to precipitate the DNA before the mixture was filtered through a Qia-precipitator. The bound plasmid DNA was then washed with 2 ml of 70% v/v ethanol before air was flushed through the filter to air dry the contents. 700 µl of TE buffer was then added to the Qia-precipitator and the contents were eluted into a sterile 1.5 ml centrifuge tube. Finally the eluate was then passed through the Qia-precipitator once more to remove any unbound DNA. The purified plasmid was ready for quantification via spectrophotometric analysis (Section x).

2.2.3.4 Preparation of glycerol stocks

Glycerol enables the long term storage of bacteria by the prevention of water in the bacterial culture producing ice crystals which can subsequently damage the frozen samples. Glycerol stocks were prepared by mixing 0.5 ml of a 50% (v/v) glycerol solution with 0.5 ml of the bacterial culture of interest and storing at -80^{o}C for future use.

2.2.3.5 Microporation

Microporation is a unique transfection technique that utilises a gold-plated pipette tip as an electroporation device (Kim, Cho et al. 2008) (Figure 2.5). This allows for a more uniform

electric field to be generated with minimal heat generation, metal ion dissolution, pH variation and oxide formation- consistent difficulties in conventional electroporation protocols. Microporation was carried out using a microporation solution kit in accordance with the manufacturer's instructions.

This method was applied as in previous publications (Walsh, Murphy et al. 2011, Guinan, Rochfort et al. 2013). Cells were trypsinised and centrifuged at 700 rpm for 5 minutes at room temperature as outlined in Section 2.2.1.2. The growth medium was aspirated off so that 1 ml remained and a cell count was performed. Once the cells were counted the required number of cells to carry out each transfection study aliquoted into individual tubes, centrifuged at 700 rpm for 5 minutes and washed gently in sterile PBS before being pelleted again at the same conditions. The PBS was carefully aspirated off and the cell pellet was resuspended in R Buffer at a typical concentration of $5*10^5$ cells/100 µl. 120 µl of the cell suspension was then aliquoted into sterile 1.5 ml micro tubes and 1-100 nM siRNA/$5*10^5$ cells was added. Upon addition of 3 ml of Buffer E, a microporation tube was inserted into the Microporation Pipette Dock. The microporation pipette was then fitted with a 100 µl gold-tip and the cell/siRNA suspensions were reverse pipetted taking extra care to avoid introducing air bubbles into the tip. After insertion of the pipette/gold-tip into the docking station, the cells were subjected to the programmed transfection procedure (for HBMvEC's and BBMvEC's the Microporator's optimal settings were determined to be 1000 V, a pulse width of 30 ms, and pulse number of 3) and the cells were quickly ejected from the tip into a pre-equilibrated 6-well dish; in parallel with the transfection protocol, for every transfection to be conducted, one well of a 6-well dish was prepared by coating with AF (for HBMvEC's only) and adding 2 ml of pre-warmed culture medium containing serum and supplements but omitting antibiotics. The plate was left to equilibrate at $37^oC/5\%$ CO_2 in a tissue culture incubator until further required. Cells were allowed to adhere overnight and the culture medium was changed the next day.

Figure 2.5: The Microporation System. (A) The Microporation unit that generates the electrical parameters necessary for electroporation which is transmitted to (B) the Microporation pipette dock consisting of a microporation tube containing electroporation buffer and the microporation pipette used to deliver electroporation to the cells through a gold plated pipette tip. (C) Microporation kit with all the necessary solutions, (http://www.invitrogen.com/).

For the optimisation of transfection, GFP protein was routinely used as means of determining transfection efficiency. GFP can be detected using a FITC laser and thus can be detected via microscopy and flow cytometry (Section 2.2.9.2).

2.2.4 Quantitative Polymerase Chain Reaction (qPCR)

2.2.4.1 RNase-free Environment

As RNA is easily degraded by ubiquitous RNases, standard procedures were employed in an effort to avoid this potential hazard. Prior to any RNA work, any surface, instrument or apparatus which was to be used was treated with RNaseAWAY™ Spray and/or wiped down with RNase wipes to remove any potential residing RNases. Latex gloves were worn throughout the procedures.

2.2.4.2 RNA Isolation

TRIzol® Reagent is a ready-to-use reagent for the isolation of high-quality total ribonucleic acid (RNA), (or the simultaneous isolation of RNA, DNA, and protein) from a wide range of biological samples and sources. An improvement on the method developed by Chomcynski and Sacchi (Chomczynski, Sacchi 1987, Chomczynski, Sacchi 2006), this monophasic solution of phenol and guanidine isothiocyanate, as well as other proprietary components, facilitates the disruption and digestion of cells and their contents, as well as effective inhibition of all present RNAses whilst maintaining the integrity of all present RNA.

Following experimental procedures, cells were lysed *in situ* with typically 1 ml of TRIzol® per sample. Cells were then scraped with a sterile cell scraper to assist in the lysing process, and then incubated for 5 minutes at room temperature to allow the complete dissociation of nucleoprotein complexes. The solution was then transferred to an RNAse-free micro tube and 0.2 ml of chloroform was added per ml of TRIzol®. The contents of the micro tube were then shaken vigorously for 15 seconds and then left at room temperature for 10 minutes. The micro tubes were then centrifuged at 13,000 rpm for 20 minutes on a balanced, refrigerated centrifuge (preset to 4^{o}C). The resulting mixture consisted of three distinct phases: the lower red phenol-chloroform phase (~45-50% of total volume), a white viscous layer (>5% of total volume), and a clear upper aqueous phase (45-50% of total volume) (Figure 2.6). As RNA is retained in the aqueous phase, this was carefully removed and placed into another RNAse-free micro tube taking extra precaution not to introduce any of the other layers with the extraction. Next, the RNA was precipitated following the addition of 0.5 ml of 100% Propan-2-ol to each tube containing the extracted aqueous phase. Samples were inverted 5-8 times before being stored at -20^{o}C overnight.

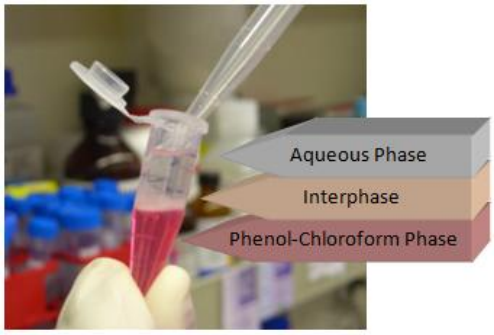

Figure 2.6: The three distinct phases of TRIzol extractions.

The following day, samples were removed from the freezer and left to reach ambient room temperature for 10-15 minutes. Samples were then transferred to a balanced, refrigerated centrifuge (4^{o}C) and spun at 13,000 rpm for 15 minutes. Following centrifugation, careful examination yielded a gel-like pellet on the wall of the micro tube; this is the pelleted RNA. The supernatant was carefully removed and the gel-like pellet was gently washed off the wall of the tube using 1 ml of 75% ethanol, taking care not to resuspend it. The micro tubes were once again centrifuged at 13,000 rpm for 10 minutes at 4^{o}C before the supernatant was once again removed and the resultant pellets left to air dry in the fume hood for ~ 5 – 10 min. The pellet was then resuspended in 50 µl of RNAse-free water and then heated to 60^{o}C in a water bath for 10 min to homogenise the sample prior to quantification. The concentration of total RNA was determined by means of a Nanodrop, outlined in Section 2.2.4.3. The samples were stored at -80^{o}C until further required.

2.2.4.3 Nanodrop®

In the analysis of nucleic acid samples, the Nanodrop® (Figure 2.7) examines the sample at absorbances at 230 nm, 260 nm and at 280 nm with the ratios (ABS_{260}/ABS_{280} and ABS_{260}/ABS_{230}) acting as means of assessing the purity of the nucleic acids present. Pure DNA which is free of protein impurities has a ratio of 1.8 whereas pure RNA has a ratio of 2.0 (due to the spectophotometric reading of uracil compared to thymidine). Lower ratios indicate the presence of proteins and carbohydrates or organic solvents such as phenol, guanidine or any other organic solvent commonly used in nucleic acid extraction. Further purification of RNA samples was achieved by means of a DNAse 1 treatment kit (Section 2.2.4.5).

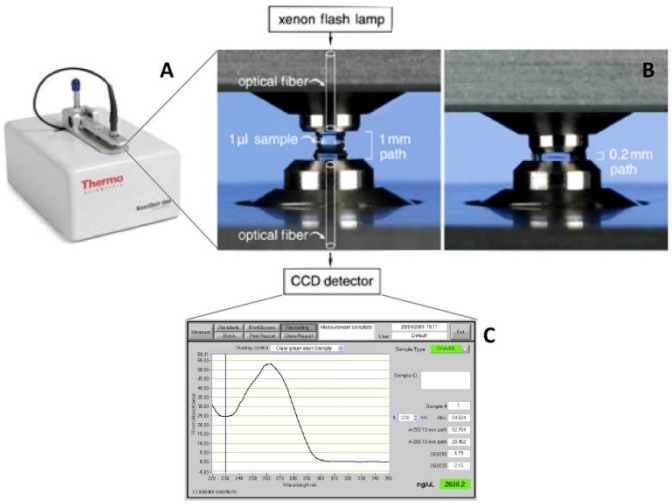

Figure 2.7: The Nanodrop® System. (A) The Nanodrop®. (B) The principle of spectrophotometrically reading biological samples. (C) A sample's typical data readout, (http://www.nanodrop.com/).

2.2.4.4 RNA Integrity Gel

RNA samples were routinely run on agarose gels to assess their quality and check for genomic DNA contamination. RNA samples were diluted using RNA Sample Loading Buffer in a ratio of 3:1, ensuring at least 1 µg of RNA was being loaded (Section 2.2.4.3). Prior to loading, the samples were heated at 65^{o}C for 10 minutes using a heating block and then chilled on ice. The samples were then loaded onto an agarose gel (as described in Section 2.2.4.11) and run at 100 V for 60-120 minutes or until sufficiently resolved. RNA was then visualised using a G-BOX fluorescence gel documentation and analysis system and the images saved for densitometric analysis (Figure 2.8).

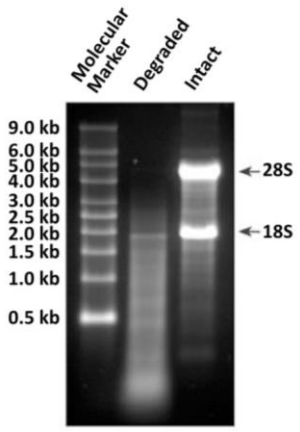

Figure 2.8: Assessing RNA integrity. Intact RNA displays two distinct bands at 4.5 kb (28S) and 1.9 kb (18S) in a ratio of 2:1 respectively. Partially degraded RNA will lack the sharp band definition and have a smeared appearance, whilst completely degraded RNA will appear as a very low molecular weight smear

2.2.4.5 DNase 1 Treatment

Deoxyribonuclease 1 (DNase 1) is an endonuclease isolated from bovine pancrease. It has the ability to digest any present double- and single-stranded DNA it comes in contact with into oligo- and mono-nucleotides. 1000 ng of RNA sample was diluted down to a final volume of 8 µl in RNase-free water. 1 µl of 10 x DNase Buffer and 1 µl of RNase-free DNase 1 was added to each prospective tube and left for 15 minutes at room temperature. 1 µl of DNase Stop Solution was added then to each tube and the tubes were further incubated for 10 minutes in a water bath at 70^{o}C to denature the DNase enzyme. The samples were then chilled on ice and typically processed immediately into cDNA.

2.2.4.6 cDNA Synthesis

In this process, genomic DNA-free mRNA was transcribed into cDNA by the enzyme Reverse Transcriptase (RT). A High Capacity cDNA Reverse Transcription Kit was used according to the manufacturer's specifications.

10x RT Buffer	2 µl
10x Random Primers	2 µl
Multiscribe Reverse Transcriptase, 50 U/µl	1 µl
25x dNTP Mix, 100mM	0.8 µl
Nuclease-free Water	3.2 µl
Total volume	9 µl

Table 2.3: cDNA Transcription Mixture.

This was added to a 0.2 ml Rnase-free polymerase chain reaction (PCR) tube containing 1000 ng of genomic DNA-free RNA diluted in nuclease-free water to 11 µl. Samples were mixed gently before being centrifuged briefly to ensure complete mixing. All tubes were then placed into a MJ Mini Thermal Cycler and run at 25^{o}C for 10 minutes, 37^{o}C for 120 minutes and finally 85^{o}C for 5 minutes, before being held at 4^{o}C until retrieved. cDNA products were then quantified on the Nanodrop® (Section 2.2.4.3) to assess final working concentrations and purities of the samples.

2.2.4.7 Primer Design

For PCR, DNA primers were designed using the online website http://frodo.wi.mit.edu/ with the parameters changed to fall into accordance with standard rules of primer design in addition to some additional parameters implemented in our lab. Using the website http://www.basic.northwestern.edu/biotools/OligoCalc.html, the potential primer candidates were then verified by BLAST (to check their sequence homology and specificity) and mFold (to check for any hairpin formations).

2.2.4.8 Benchtop PCR

Benchtop PCR was routinely undertaken to optimise primer amplification conditions and ensure a single product at the pre-determined location, as well as the absence of secondary products and primer dimers. A number of parameters such as primer concentration and annealing temperatures could be optimised here before Quantitative Real Time PCR was conducted.

Before starting, cDNA samples were analysed by means of the Nanodrop® and appropriately diluted using RNase-free water to a final concentration of 500 ng/µl. Each reaction mixture was made up in a 0.2 ml RNase-free PCR tube and was comprised of the following:

Forward Primer (10 µM)	1 µl
Reverse Primer (10 µM)	1 µl
cDNA Sample (500 ng/µl)	2 µl
10x Reaction Buffer	2.5 µl
dNTP (10 mM)	2 µl
$MgCl_2$ (25mM)	1.5 µl
DreamTaq Polymerase (5 U/µl)	0.2 µl
Rnase Free Water	14.8 µl
Total Volume	25 µl

Table 2.4: Standard PCR Reaction Mixture.

Each tube was then placed into an MJ Mini Thermal Cycler and samples were subjected to the following reaction cycle:

Denature		95°C	5 minutes	
Cycling	Denature	95°C	15 seconds	40 cycles
	Annealing	55-63°C	30 seconds	
	Extension	72°C	15 seconds	
Extension		72°C	5 minutes	
Hold		4°C	Forever	

Table 2.5: Standard PCR Method.

Annealing temperatures varied depending on the primer in question:

Target	**Sequence**	**Product Size**	**Annealing Temp. °C**
Human GAPDH F	5’ gag tca acg gat ttg gtc gt 3’	238 bp	59.97 °C
Human GAPDH R	5’ ttg att ttg gag gga tct cg 3’		60.01 °C
Human Occludin F	5’ cct tca ccc cca tct gac ta 3’	224 bp	59.92 °C
Human Occludin R	5’ gca ggt gct ctt ttt gaa gg 3’		59.99 °C
Human Claudin 5 F	5’ gag gcg tgc tct acc tgt tt 3’	240 bp	59.50 °C
Human Claudin 5 R	5’ agt act tca cgg gga agc tg 3’		59.35 °C
Human VE-Cad F	5’ cag ccc aaa gtg tgt gag aa 3’	185 bp	59.87 °C
Human VE-Cad R	5’ cgg tca aac tgc cca 106act t 3’		59.99 °C
Human ZO-1 F	5’ gaa cga ggc atc atc cct aa 3’	218 bp	60.04 °C
Human ZO-1 R	5’ cca gct tct cga aga acc ac 3’		59.99 °C
Human vWF F	5’ cca gat ttg cca ctg tga tg 3’	232 bp	60.11 °C

Human vWF R	5’ aaa ggc ctt cag cac ttc aa 3’		59.99 °C
Human TNF-α F	5’ ccc acg gct cca ccc tct ctc 3’	220 bp	60.11 °C
Human TNF-α R	5’ ttc cct ctg ggg gcc gat ca 3’		60.02 °C
Human IL-6 F	5’ aaa gag gca ctg gca gaa aa 3’	183 bp	59.99 °C
Human IL-6 R	5’ agc tct ggc ttg ttc ctc ac 3’		59.60 °C
Human TNFR1 F	5’ gtg cct acc cca gat tga ga 3’	175 bp	60.07 °C
Human TNFR1 R	5’ tgt cga ttt ccc aca aac aa 3’		59.94 °C
Human TNFR2 F	5’ gga aac tca agc ctg cac tc 3’	224 bp	60.00 °C
Human TNFR2 R	5’ tgc aaa tat ccg tgg atg aa 3’		59.89 °C
Human GP130 F	5’ tca act tgg agc cag att cc 3’	159 bp	60.20 °C
Human GP130 R	5’ ccc act tgc ttc ttc act cc 3’		59.84 °C
Human sIL-6R F	5’ tgc cag tat tcc cag gag tc 3’	227 bp	60.07 °C
Human sIL-6R R	5’ tct tgc cag gtg aca ctg ag 3’		60.02 °C
Human 14-3-3β F	5’ acc caa ttc gtc ttg gtc tg 3’	249 bp	59.99 °C
Human 14-3-3β R	5’ tcc gat gtc cac aga gtg ag 3’		60.01 °C
Human 14-3-3γ F	5’ ctg aat gag cca ctg tcg aa 3’	155 bp	59.98 °C
Human 14-3-3γ R	5’ gca cgg acc atc tca atc tt 3’		60.08 °C
Human 14-3-3ζ F	5’ ttc ttg atc ccc aat gct tc 3’	211 bp	60.01 °C
Human 14-3-3ζ R	5’ agt taa ggg cca gac cca gt 3’		59.99 °C
Human 14-3-3θ F	5’ gag cag aag acc gac acc tc 3’	206 bp	59.99 °C
Human 14-3-3θ R	5’ cac gca act tca gca agg ta 3’		60.05 °C
Human 14-3-3ε F	5’ aat ttg cca cag gaa acg ac 3’	171 bp	59.98 °C
Human 14-3-3ε R	5’ cac ggt cag ggg aat taa ga 3’		59.93 °C
Bovine GAPDH F	5’ agg tca tcc atg acc act tt 3’	337 bp	59.97 °C
Bovine GAPDH R	5’ ttg aag tcg cag gag aca a 3’		59.98 °C
Bovine Occludin F	5’ tgg aac ctt aat ggg agc tg 3’	186 bp	60.07 °C
Bovine Occludin R	5’ atc acc aat gca gca atg aa 3’		60.08 °C
Bovine Claudin 5 F	5’ aga ttc tcg gct tgg tgc t 3’	167 bp	59.97°C
Bovine Claudin 5 R	5’ cat gtg ccc tgt gct ctg 3’		59.97 °C
Bovine VE-Cad F	5’ gac atc cgt ggt tct gga ct 3’	172 bp	59.97 °C
Bovine VE-Cad R	5’ aga tgg gga agt tgt cgt tg 3’		59.97 °C
Bovine ZO-1 F	5’ gaa cga ggc atc atc cct aa 3’	218 bp	60.04 °C
Bovine ZO-1 R	5’ cca gct tct cga aga acc ac 3’		59.99 °C

Table 2.6: Primer Information. The primers utilised over the course of this study, their sequences, their expected product size and their annealing temperatures.

2.2.4.9 Quantitative Real-Time PCR

After the primers had been optimised the conditions yielded were then carried over for use in qPCR. qPCR allows for real time monitoring of gene amplification as it accumulates in the reaction well. This quantification is facilitated by means of SYBR Green, a nucleic acid stain which has the ability to bind to double-stranded DNA. Upon exposure to blue light (~497 nm), SYBR Green produces a detectable green signal (~520 nm), that is recorded at the end of each PCR cycle allowing the amount of amplified cDNA product to be quantified and graphed in real time (Figure 2.9). To normalise the SYBR Green signal, ROX, a passive dye, is incorporated into the SYBR mastermix. The signal generated by the reporter dye (SYBR Green) is measured against the signal generated by the passive reference dye (ROX) and the non-PCR-related fluorescence anomalies occurring based on well-to-well variation is removed via normalisation algorithms. The threshold cycle represents the refraction cycle number at which a positive amplification reaction was measured and was set at 10 times the standard deviation of the mean baseline emission calculated for PCR cycles 3 to 15. The results were then analysed according to the Comparative C_T method ($\Delta\Delta C_T$) as described by (Livak and Schmittgen, 2001).

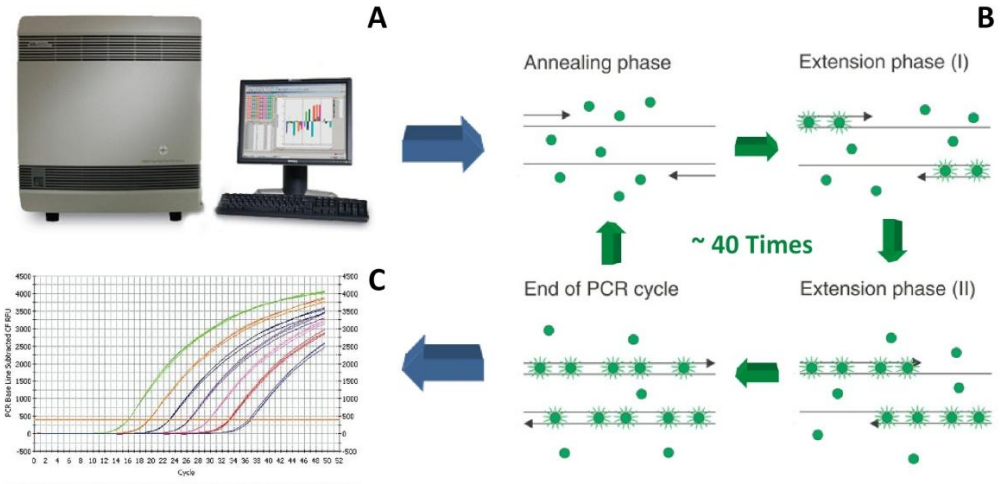

Figure 2.9: The qPCR system. (A) The Applied Biosystems 7900HT Fast Real Time PCR system, (B) the principle of how SYBR Green quantifies gene amplification products and (C) Real Time PCR data readout, (http://www.lifetechnologies.com/).

qPCR was carried out using an Applied Biosystems 7900HT Fast Real-Time PCR machine. This method was applied as in previous publications (Guinan, Rochfort et al. 2013). Each reaction was set up in triplicate as follows:

Forward Primer (10 µM)	3.2 µl
Reverse Primer (10 µM)	3.2 µl
cDNA (500 ng/µl)	6.5 µl
SYBR Green	39.1 µl
RNase Free Water	29.4 µl
Total Volume	81.5 µl

Table 2.7: qPCR Reaction Mixture.

In addition, for every sample which was being analysed a 'Non-RT Control' was included. This is essentially a sample which had the Reverse Transcriptase omitted from the reaction mixture when cDNA was being generated (Section 2.2.4.6). If a product is seen in the Non-RT Control wells contaminating genomic DNA can be said to be present.

Samples were placed in 25 µl aliquots in 96-well Fast Optical PCR plates and sealed with an adhesive optical film. After a short centrifugation to pool the samples and remove bubbles, the plate was loaded onto the ABI 7900HT and subjected to the following procedure:

Denature		95°C	10 minutes	
Cycling	Denature	95°C	15 seconds	50 cycles
	Annealing	58-60°C	60 seconds	
	Extension	72°C	15 seconds	
Extension		72°C	5 minutes	
Hold		4°C	Forever	

Table 2.8: qPCR Method

Quantification of cDNA targets was normalised for differences across experiments/samples using an endogenous control; GAPDH.

Routinely, melt curve analysis was conducted to ensure single product formation and to rule out possible contamination by non-specific binding and primer dimerisation. Samples from both standard PCR and qPCR were then visualised on 1% agarose gels as described in Section 2.2.4.11.

2.2.4.10 Primer Efficiency Curves

Primer efficiencies for each primer pair were calculated by means of a standard curve analysis (Figure 2.10). To conduct primer efficiency curves the same reaction mixture used for qPCR is utilised with the exception that the template cDNA is omitted. Instead, a dilution

of a PCR product which had been run previously using the same primer set is substituted. Briefly, the PCR product was excised from the reaction plate and a 1/1000 dilution was made in RNase-free water. From here a 7-fold 1/10 serial dilution of this 1/1000 dilution was made with 6.5 µl of each dilution substituting for the raw cDNA in each reaction mixture. An additional reaction mixture was made substituting the PCR product for RNase-free water. This acted as a non-template control.

The temperature profile run for standard qPCR was utilised and the software was programmed to recognise the serial dilutions and plot their Threshold Cycle (C_T Value) versus the immunofluorescent signal (number of copies of the target gene). To calculate primer efficiency:

$$PCR\ Efficiency = 10^{-1/Slope} - 1$$

The Minimum Information for publication of Quantitative real-time PCR Experiments (MIQE) guidelines has set a standard that all qPCR results considered for publication must fall under (Bustin, Benes et al. 2009). Ideally primer sets should have an efficiency of between 90 and 105%, (Section A.27).

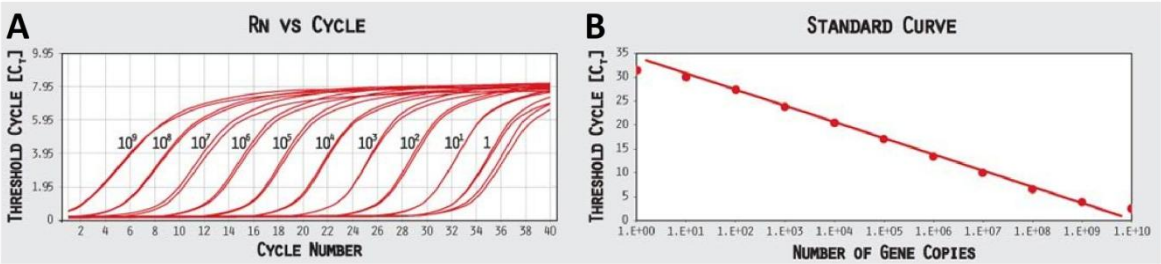

Figure 2.10: Principal of primer validation. (A) An amplification plot of a serial dilution of cDNA and (B) the interpreted standard curve, (http://www.sabiosciences.com/).

2.2.4.11 Agarose Gel Analysis

Agarose gel electrophoresis was often used as a quality control to visualise and assess PCR product sizes (standard and qPCR) as well as mRNA (Section 2.2.4.2), cDNA and oligonucleotide primer sets (quality and purity). A 1% agarose gel was typically used by adding 1 g of ultra-pure agarose to a conical flask and adding 100ml of 1 x Tris acetate-EDTA (TAE) buffer (40 mM Tris-Acetate pH 8.2, 1 mM EDTA). The mixture was brought to a boil until the solution had turned clear and the agarose had fully dissolved. Once cooled (~50-60^{o}C), 10 µl of (1 x) SYBR® Safe was added to the solution and swirled to ensure a thorough mixing. The mixture was then poured into a casting plate which had been pre-sealed using masking tape. A gel comb was then inserted and the presence of any bubbles

was eliminated. The gel casket was then covered with tin foil to protect the light sensitive SYBR® Safe and left for ~20 minutes as the gel polymerised. The masking tape was then removed and the solid agarose gel was placed within a suitable gel rig and filled to the specified mark with 1 x TAE buffer ensuring the gel was completely submerged. For standard PCR product analysis, the reaction mixture already contains a dye for tracking the product as it migrates electrophoretically through the gel. This allows for direct loading into the wells. qPCR samples however require 4 x Loading Buffer (Section 2.1.3.4) to be added for tracking purposes before being loaded onto the gel (this also applied to any primer dilutions and primer stocks that were to be examined). After sample loading, approximately 6 µl of GeneRuler™ 100 bp DNA Ladder Plus was added to the lanes flanking the samples loaded onto the gel for relative band size comparison. The gel was resolved for ~90 minutes at 100 V or until the tracking dye had been deemed to have resolved sufficiently. DNA was visualised using a G-BOX fluorescence gel documentation and analysis system and the images saved for densitometric analysis.

2.2.5 Protein Isolation and Quantification

2.2.5.1 Protein Extraction

This method was applied as in previous publications (Harhaj, Felinski et al. 2006). For the purposes of Western Blotting and Immuno-precipitation pulldown assays, cells were harvested in the following manner. The culture dishes were placed on ice and had the growth medium removed. The dishes were washed three times with PBS before radioimmunoprecipitation assay (RIPA) Buffer (Section 2.1.3.1) was added (20 µl per well of a 6-well or 100 µl per 58cm^2 dish). A sterile cell scraper was taken and the cells were harvested. The cell/RIPA Buffer suspension was relocated to sterile 1.5 ml micro tubes and the mixture was rotated at 4^{o}C in a cold room for 1 hour. The micro tubes were subsequently centrifuged at 10,000 rpm for 20 minutes at 4^{o}C to pellet any present triton-insoluble material. After the supernatant was removed into a fresh tube, the cell lysate samples were aliquoted and stored at -80^{o}C until further required with one aliquot used to establish the concentration immediately by BCA Assay (Section 2.2.5.2).

2.2.5.2 Bicinchoninic Acid (BCA) Assays

This method was applied as in previous publications (Smith, Krohn et al. 1985). The BCA or Smith Assay is an accurate means of determining protein concentration in whole cell lysates and affinity-column fractions. The assay is based upon two key reactions, the first of which

is the ability of peptide bonds to reduce Cu^{2+} to Cu^{1+}. The degree of reduction depends entirely on the amount of peptide bonds present i.e. a direct correlation to the amount of protein present. The second reaction is the ability of bicinchonic acid, (a green reactant), to bind to each Cu^{1+} ion forming a distinctive purple complex, which can strongly absorb light at 562 nm.

To carry out the assay first a sterile 96-well plate was used to plate out 10 µl aliquots of 11 BSA standards (concentration range of 0 – 2 mg/ml) in triplicate along with the RIPA lysis buffer used to extract the protein and all protein samples to be analysed. Next, the commercially available BCA kit provides two solutions; Reagent (A); an alkaline bicarbonate solution and Reagent (B); a copper sulphate solution. Reagents (A) and (B) were mixed in a ratio of 50:1 respectively so that 200 µl of reaction solution could be added to each test well. Once added, the plate was covered in tin foil and incubated at 37^{o}C for 30 minutes. The absorbance was then read at 562 nm on an ELx800 Microplate Reader and the unknown concentrations calculated using standard curve analysis.

2.2.6 Immunoprecipitation and Mass Spectrometric Analysis

2.2.6.1 Immunoprecipitation

2.2.6.1.1 Column Preparation

Immunoprecipitation to investigate the putative binding partners of occludin and other tight junctions under static and shear conditions was performed using a Pierce Co-Immunoprecipitation Kit. All reagents were prepared and pre-equilibrated as per the manufacturer's instructions beforehand. All centrifuge steps for this section were performed at 1000 g for 1 minute.

50 µl of AminoLink Plus Coupling Resin was added to a Pierce Spin Column. The column was placed in a collection tube, centrifuged and the flow-through discarded. The resin was then washed twice with 200 µl aliquots of 1 x Coupling Buffer with the tube centrifuged and the flow-through discarded each time. The column was then dried for excess liquid before 10 µg of capture antibody was diluted down to a final volume of 200 µl using 1 x Coupling Buffer. The mixture was then added to the column once a plug was added to the column to retain the liquid. 3 µl of Sodium Cyanoborohydride Solution was added to the column within the confines of a fume hood before the column was capped and the mixture turned over on a rotator for 120 minutes at room temperature.

Following incubation, the bottom plug was removed and the tube was placed in a fresh micro tube before being centrifuged. The flow-through was retained to later verify if the antibody coupling had been successful. 200 µl of 1 x Coupling Buffer was added to the column which was then centrifuged before the flow-through was discarded. This step was repeated once more before 200 µl of Quenching Buffer was added to the column, which was then centrifuged and the flow-through discarded. The column was dried of any excess liquid before the bottom plug was inserted again and 200 µl of Quenching Buffer was added to the column. In a fume hood, 3 µl of Sodium Cyanoborohydride Solution was added and the column sealed before being incubated for 15 minutes with gentle rotation. The plug was removed and the column centrifuged in a fresh collection tube before being centrifuged and the flow-through discarded. The column was then washed twice with 200 µl of 1 x Coupling Buffer followed by centrifugation. The column was then washed six times with 150 µl of Wash Solution followed by centrifugation. The column was then either used immediately or stored by first washing the column twice with 200 µl of 1 x Coupling Buffer followed by centrifugation before inserting the bottom plug, adding a further 200 µl of 1 x Coupling Buffer supplemented with 0.02% (w/v) sodium azide and stored at 4^{o}C.

In order to carry out the co-immunoprecipitation experiments, a number of controls had to be implemented. In addition to the column containing the capture antibody, two additional control columns were made; one which replaces the AminoLink Plus Coupling Resin with a Control Resin composed of the same support material as the co-IP resin but is not activated, and another which replaces the capture antibody/1 x Coupling Buffer mixture with 200 µl of Quenching Buffer.

2.2.6.1.2 Co-Immunoprecipitation

All reagents were prepared and pre-equilibrated as per the manufacturer's instructions beforehand. All centrifuge steps for this section were performed at 1000 g for 1 minute.

Prior to preparing the columns, protein lysate from cells cultured under static and shear conditions (Section 2.2.2.2.1) were prepared and lysed as outlined in Section 2.2.5.1. The protein lysate was diluted down to a final volume of 300 µl using IP Lysis/Wash Buffer and placed on ice. Meanwhile, the column along with the additional two control columns were washed twice using 200 µl of IP Lysis/Wash Buffer followed by centrifugation and the flow-through discarded. The column was dried of any excess liquid before the bottom plug was inserted. The protein lysate/IP Lysis/Wash Buffer mixture was added to the three columns and the columns sealed before being rotated for 4 hours at 4^{o}C in a cold room.

Following incubation, the columns had the bottom plug removed and were placed in fresh collection tubes. The columns were then centrifuged and the flow-through stored for future analysis. The columns were placed into fresh collection tubes and then washed with 200 µl of IP Lysis/Wash Buffer before being centrifuged and the flow-through stored for future analysis. This was repeated twice more before the columns were transferred to fresh collection tubes and 10 µl of Elution Buffer added. The tubes were then centrifuged and an additional 50 µl of Elution Buffer added. The columns were incubated for five minutes at room temperature before being centrifuged once more and the flow-through stored for future analysis. This was repeated twice more with each elution stored for future analysis (Figure 2.11). To preserve the columns, they were then washed with 100 µl of 1 x Coupling Buffer and centrifuged twice before being prepped for long term storage as described at the end of Section 2.2.6.1.1.

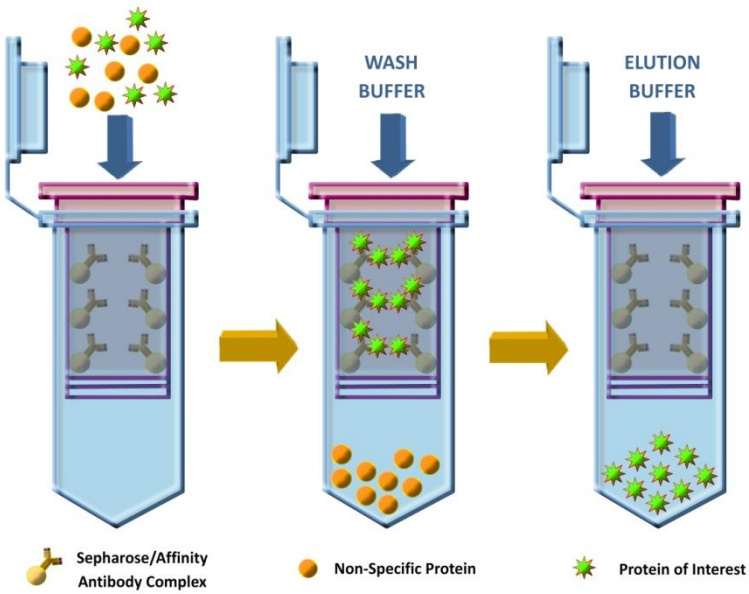

Figure 2.11: An overview of the immunoprecipitation procedure

2.2.6.1.3 Co-Immunoprecipitation Sample Analysis

Samples which had been eluted from the columns were ready for analysis via Mass Spectrometry (Section 2.2.6.2.2). Occasionally samples had to undergo electrophoretic separation in order to confirm that occludin had been successfully immunoprecipitated. Samples which were run out on SDS-PAGE gels could be analysed for target verification and then directly digested for analysis as outlined in the following sections.

2.2.6.1.4 Coomassie Blue G-250

Similar to the Coomassie Blue R-250 (Section 2.2.7.3) in principal, Coomassie Blue G-250 is a colloidal suspension of coomassie suspended in a trichloroacetic acid solution eliminating the presence of methanol. The result is a stain which specifically visualises only the protein bands within the gel. This results in the elimination of non-specific background and the accompanying wash steps and it allows the samples to be analysed via Mass Spectrometry analysis.

Briefly, the gel was washed with two lots of DI water. The gel was then fixed (Section 2.1.3.2) for ~10 minutes. Next the gel was stained using the prepared colloidal coomassie solution (Section 2.1.3.2) for 90 minutes on a gentle setting with a 3D orbital rotator. The gel was briefly destained with colloidal coomassie destain (Section 2.1.3.2) for 1 minute and then a further rinse with 25% Methanol in DI Water. The gel was then imaged using a G-BOX fluorescence gel documentation and analysis system and the images saved for densitometric analysis. For long term storage, the gel was kept hydrated in DI Water until all samples were procured for band excision and digestion.

2.2.6.2 Mass Spectrometry

2.2.6.2.1 Band Extraction and Digestion

SDS-PAGE gel bands were excised from Coomassie Blue G-250 stained protein gels and placed in a 1.5 ml micro tube. The bands were then destained (Section 2.1.3.3) for 30 minutes with occasional vortexing. Samples were then dehydrated with the addition of neat ACN then swelled to rehydration in digestion buffer (Section 2.1.3.3) before being incubated at 37^{o}C overnight.

The next day, the peptides were extracted using extraction buffer (Section 2.1.3.3) and incubated at 37^{o}C in a shaker for 15 minutes. Samples were then dried down in a vacuum centrifuge. Tryptic peptides were re-dissolved in 15 µl of 0.1% formic acid containing 2% ACN. Samples were then ready for analysis via Mass Spectrometry.

2.2.6.2.2 Mass Spectrometry

Liquid Chromatography-Tandem Mass Spectrometry (LC-MS/MS) was performed on an Ultimate 3000 NanoLC System (Dionex) interfaced to a Linear Trap Quadrupole Orbitrap XL (Thermo Fisher Scientific). 5 µl of sample was loaded onto a trapping column packed with C18 PepMAP100 (Dionex) at a flow rate of 20 µl/minute in 0.1% formic acid. After 5

minutes of washing, peptides were eluted into a C18 PepMAP100 nanocolumn (15 cm * 75 µm ID, 3 µm particles) (Dionex) at a flow rate of 350 nl/min. Peptides were separated using the mobile phase gradient : from 5% to 50% of Solvent B in 30 minutes, and from 50% to 90% of Solvent B in 5 minutes. Solvent A was comprised of Water and #acn (v/v) (98:2) containing 0.1% formic acid. Solvent B was Water:ACN (v/v) (2:98) containing 0.08% formic acid.

LC-MS/MS data was acquired in data-dependent acquisition (DDA) mode controlled by Xcalibur 2.0.7 software (Thermo Fisher Scientific). A typical DDA cycle consisted of an MS scan within m/z 300-1800 performed under the target mass resolution of 60,000 (full width at half maximum) followed by MS/MS fragmentation of the six most intense precursor ions under normalised collision energy of 35% in the linear trap. Database searches were performed using TurboQUEST software (Bioqorks Browser v. 3.3.1) (Thermo Fisher Scientific) using the SWISSPROT database. The following filters were applied: for charge state 1, X_{Corr}>2.0; for charge state 2, X_{Corr}>2.2; for charge state 3, X_{Corr}>2.5. Artificial modifications of peptides (carbamidomethylation of cysteines and partial oxidation of methionines) were considered. Searches were also carried out allowing for one missed cleavage. Protein identifications were accepted if they had at least two matched identified peptides and passed relevant statistical criteria.

2.2.7 Western Blotting

2.2.7.1 Polyacrylamide Gel Electrophoresis

Sodium Dodecylsulphate-Polyacrylamide Electrophoresis (SDS-PAGE) resolution of protein lysates was carried out according to the protocol of Laemmli (Laemmli 1970). In brief, a pair of 10 * 100mm glass plates (one short and one long with a 1.0 mm spacing) were washed with 70% (v/v) IMS and then rinsed with water before being dried completely. The componenets of the Mini-PROTEAN electrophoresis system were assembled according to the manufacturer's instructions. Accordingly, the short plate was placed over the long plate so that the spacers created an interstitial space between them. Both plates were then clamped together using the casting frame and the unit was sealed tight when docked onto the casting stand. To test the assembly, DI water was poured between the plates and the level monitored throughout the mixing of the gel solutions. Any drop in level suggested the assembly was compromised and in such an event the plates were taken apart and reassembled examining for cracks or chips in the glass that may be causing such problems.

Meanwhile the resolving gel was setup. Depending on the protein of interest, different percentage gels could be utilised in order to better resolve the area of interest relative to protein size. The components for polyacrylamide gels and their respective percentages and resolutions are listed in order in the table below. The TEMED was added only once the casting plate assembly had been tested for leaks and dried afterwards by pouring the majority of the water out and placing a folded piece of Whatman paper between the plates to remove any trace of water that might remain.

	6%	**8%**	**10%**	**12%**	**14%**
Gel Resolution (kDa)	60-300	40-250	30-200	20-150	10-80
Distilled Water	5.2 ml	4.6 ml	4.0 ml	3.4 ml	2.7 ml
1.5M Tris-HCl pH 8.8	2.5 ml	2.5 ml	2.5 ml	2.5 ml	2.5 ml
Acrylamide/Bis-Acrylamide 30%	2.0 ml	2.6 ml	3.3 ml	4.0 ml	4.6 ml
10% SDS	100 µl	100 µl	100 µl	100 µl	100 µl
10% Ammonium Persulfate	50 µl	50 µl	50 µl	50 µl	50 µl
TEMED	5 µl	5 µl	5 µl	5 µl	5 µl
Total Volume			10 ml		

Table 2.9: SDS-PAGE resolving gel compositions.

Approximately 6-8 ml of the mixture was gently poured between the glass plates taking care to avoid bubbles. Next, ~2-3 ml of DI water was added gently to the top of the gel between the plates. This was to remove any bubbles that might be present on the top of the gel and also give an even surface to the cusp of the gel. The gel was then left to set for ~30-45 minutes.

A 4% (v/v) polyacrylamide stacking gel was used throughout all experiments. Its components were assembled in the order listed.

	4%
Distilled Water	6.0 ml
0.5M Tris-HCl, pH 6.8	2.5 ml
Acrylamide/Bis-Acrylamide 30%	1.3 ml
10% SDS	100 µl
10% Ammonium Persulfate	100 µl
TEMED	10 µl
Total Volume	10 ml

Table 2.10: SDS-PAGE stacking gel composition.

Following the pouring of the stacking gel on top of the polymerised resolving gel, the gel comb was inserted. Any spill-over was carefully removed with tissue and the stacking gel was then left to set for 15-20 minutes.

Upon polymerisation, the glass plates were removed from the docking station and the casting frame removed. The glass plates were then assembled, using a buffer dam if necessary, into the electrophoresis rig and placed into the tank. The inner chamber of the electrophoresis rig was filled to the brim and the tank to the designated marker using ~700 ml of Running Buffer (Section 2.1.3.1) in total. The unit was left in this manner until the protein samples were ready to load.

Based on the results obtained from the BCA Assay (Section 2.2.5.2), all protein samples were equally loaded (10-50 µg) and had 6.25 µl of 4x Sample Solubilisation Buffer (SSB) (Section 2.1.3.1) added then made up to a 25 µl volume with DI water. Samples were then heated on a heating block at 95^{o}C for 5 minutes before being centrifuged briefly to collect any sample that may have condensed onto the walls and lid of the tube, and then chilled on ice.

The samples were then loaded into the gel wells (~25 µl). 6 µl of molecular weight marker (PageRuler Plus Prestained Protein Ladder and/or Spectra Multicolor High Range Protein Ladder) were added individually to the lanes flanking either side of those containing samples. The electrophoresis tank was then sealed and underwent electrophoresis at a constant voltage of 80 V for 20 minutes (until the samples migrated from the stacking gel into the resolving gel) and then an increase to 100 V for approximately 90-180 minutes (until the gel had resolved sufficiently which in turn depended on the percentage acrylamide used in the resolving gel) (Figure 2.12).

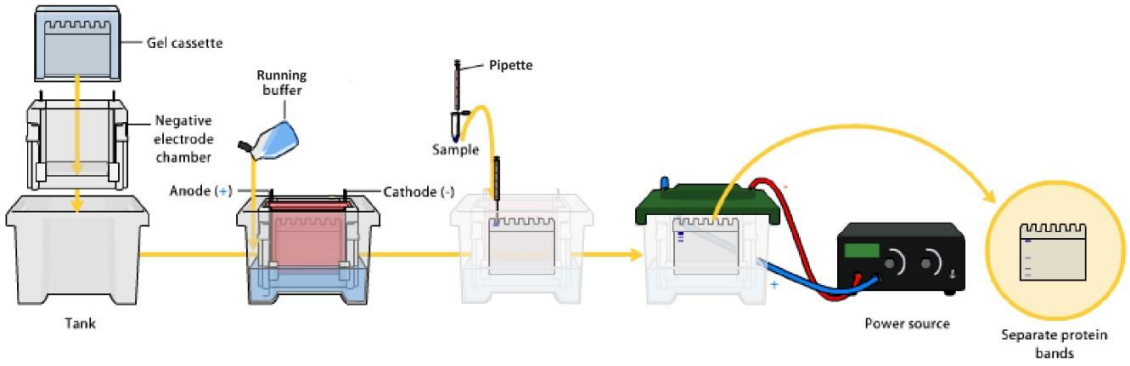

Figure 2.12: A workflow of running an SDS-PAGE gel, (http://www.bio-rad.com/).

2.2.7.2 Electrophoretic Transfer

Electrophoretic transfer is the transfer of proteins from a gel to a membrane whilst maintaining their relative position and resolution. The wet transfer technique (Towbin, Staehelin et al. 1979) was the method of choice for all Western Blot experiments. Upon completion of the SDS-PAGE procedure, gels were removed from the glass plates encasing it and the stacking gel was removed. The gel was then left to soak in pre-chilled transfer buffer (Section 2.1.3.1) for ~10 minutes to remove any residual SDS that may be bound to the gel and have an inhibitory effect on protein transfer. Meanwhile, Polyvinylidene Difluoride (PVDF) membrane was trimmed to the size of the gel and soaked in methanol for 5-10 minutes. The transfer cassette was then assembled as indicated below.

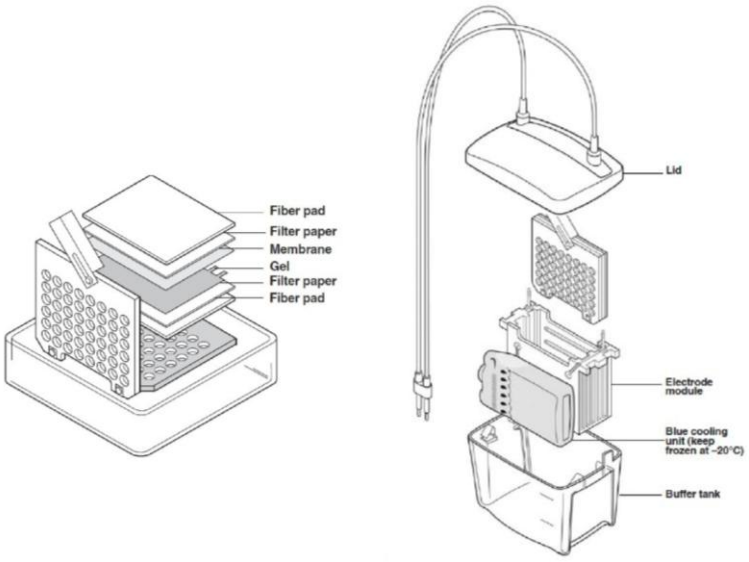

Figure 2.13: The assembly of the electrophoretic transfer system, (http://www.bio-rad.com/).

Prior to inserting the transfer cassette into the electrophoresis system, the cassette was rolled using a 15 ml tube to remove any potential air bubbles that may hinder the transfer process. The cassette was then placed into the electrophoresis system along with an ice pack and a stirring bar and sealed shut. The tank, along with a power pack and stirring plate, were transferred to a cold room (4^{o}C) and the tank placed on a stirring plate on a low setting. The power pack was then attached and set to run at a constant voltage of 50 V overnight (Figure 2.13).

2.2.7.3 Coomassie Blue R-250

CoomassieBlue R-250 is a general gel stain used to visualise protein bands on an SDS-PAGE gel. This was used as a quality control in order to assess the efficiency of the transfer method. Briefly, following transfer, the SDS-PAGE gel was washed gently in DI water before pre-filtered (0.25 µm) coomassie blue solution was overlaid. The gel was left on a 3D rotator overnight swirling gently.

The next day the gel was destained using coomassie destain solution (Section 2.1.3.1). The destain solution was left to act on the gel for 10-15 minutes before being replaced with fresh destain solution. This process was repeated until distinct protein bands were left on the gel with little to no background. The gels were imaged by a G-BOX fluorescence gel documentation and analysis system and the images saved for densitometric analysis.

2.2.7.4 Ponceau S

Ponceau S staining of the nitrocellulose or PVDF membrane is a rapid and reversible stain used for Western Blots that allows for the visualisation of the proteins that did complete the transfer from the SDS-PAGE gel to the membrane allowing for the estimation of efficiency of both electrophoretic transfer and protein loading. Briefly, Ponceau S stain was applied to the membrane for ~3 minutes under gentle agitation. Transferred bands were represented as pink bands against the white membrane. Following confirmation, the membrane was washed in DI water until the Ponceau stain was removed entirely. Once removed the membrane was used for immuno-blotting.

2.2.7.5 Immunoblotting

Following transfer, the PVDF membrane was blocked for 1 hour at room temperature in a 5% Bovine Serum Albumin (BSA) + 0.1% Tween-Tris Buffered Saline solution with gentle rocking. After an hour, the membrane was cut into manageable sections for the protein of

interest and incubated overnight in a cold room (4°C) with gentle rocking with the appropriate primary antibody (made up in 1% BSA-0.1% Tween-TBS). The appropriate dilutions are summarised in the table below.

1° Antibody	1° Antibody Stock	1° Antibody Dilution	2° Antibody	2° Antibody Dilution
Occludin (Invitrogen)	0.5 mg/ml	1/1000	Anti-Rabbit	1/2000
Claudin 5 (Invitrogen)	0.5 mg/ml	1/1000	Anti-Mouse	1/2000
VE-Cadherin (Invitrogen)	0.5 mg/ml	1/500	Anti-Rabbit	1/1000
ZO-1 (Invitrogen)	0.5 mg/ml	1/1000	Anti-Mouse	1/2000
Thrombomodulin (Abcam)	1 mg/ml	1/1000	Anti-Mouse	1/2000
vWF (Abcam)	8 mg/ml	1/1000	Anti-Rabbit	1/2000
IL-6 (R&D)	0.2 mg/ml	1/500	Anti-Goat	1/1000
14-3-3 (Abcam)	Whole Sera	1/1000	Anti-Rabbit	1/2000
P-Tyrosine (Invitrogen)	0.5 mg/ml	1/500	Anti-Mouse	1/1000
P-Serine (Millipore)	0.5 mg/ml	1/500	Anti-Mouse	1/1000
P-Thymine (Invitrogen)	0.5 mg/ml	1/500	Anti-Mouse	1/1000
GAPDH (Santa Cruz)	0.2 mg/ml	1/1000	Anti-Rabbit	1/2000

Table 2.11: Antibody concentrations used for immunoblotting.

The next day, the blots were left for 1 hour to return to room temperature before being washed three times for 5 minutes in 1% Tween-TBS using vigourous agitation. The blots were then incubated with the appropriate Horse Radish Peroxidase (HRP)-conjugated secondary antibody in 1% BSA-1% Tween-TBS solution for 2 hours at room temperature with gentle rocking (refer to Table X for corresponding secondary antibody concentrations). Membranes were then washed three times for 5 minutes using 1% Tween-TBS with vigourous agitation and then stored in TBS until used for detection of targets via chemi-luminescence.

Luminata chemi-luminescent substrate was used to detect HRP-conjugated secondary antibody binding. The blots were dried carefully removing all residual PBS before applying the substrate. Immediately the blot was transferred to the G-BOX fluorescence gel documentation and analysis system and the blots were exposed for different times. Images

were saved for densitometric analysis using NIH Image J software (http://rsbweb.nih.gov/ij/) to obtain a relative comparison between protein bands.

2.2.7.6 Immunoblot Stripping

For phosphorylation work, immunoblots were commonly subjected to two different primary antibodies targeting the same protein. To facilitate this, immunoblots had to be initially probed with one antibody (phosphorylation antibody) and analysed, before being stripped of that antibody and probed with the second (target protein antibody). To do this, Restore Western Blot Stripping Buffer was used. Briefly, post analysis of the first antibody, the immunoblot was washed in TBS-Tween to remove the substrate before being immersed in stripping buffer under agitation for 10 mins. The blot was then washed in 1% Tween-TBS wash buffer for 5 mins before being checked for complete removal of the first antibody. The membrane was once again coated in Luminata chemi-luminescent substrate and exposed using the G-BOX fluorescence documentation and analysis software. If no signal was present, the blot was successfully stripped of secondary antibody. The blot was once again washed with 1% Tween-TBS wash buffer and incubated with the same secondary antibody regime as before prior to analysis using the G-BOX. Once again, if no signal was present, successful removal of the primary antibody was achieved. After another wash with 1% Tween-TBS the blot was blocked with 5% Bovine Serum Albumin (BSA) + 0.1% Tween-Tris Buffered Saline for 1 hr before the standard Immunoblotting procedure (Section X) for the second antibody was carried out.

2.2.8 Physiological Assays

2.2.8.1 Trans-Endothelial Cell Permeability Assay

This method was applied as in previous publications (Collins, Cummins et al. 2006, Walsh, Murphy et al. 2011). Following cell treatments (e.g. exposure to cytokines, shear stress etc), HBMvEC's and BBMvEC's were trypsinised and counted as previously described. Sterile transwell inserts were placed into a sterile 6-well dish and fresh pre-warmed culture medium was added to the upper (apical) and lower (baso-lateral) chambers of the Millicell hanging cell culture insert (6-well format, 0.4 µm pore size, 24 mm filter diameter) within the 6-well dish (1 ml – Upper Compartment, 4 ml – Lower Compartment). The cells were replated at a high density ($4*10^5$ cells/insert) within the Millicell inserts. After the cells had adhered overnight, transendothelial permeability was assessed as previously described (Walsh et al., 2011, Collins et al., 2006). Briefly, a FITC-labelled dextran (40 kDa) was added to fresh

pre-warmed growth medium at a pre-determined concentration. All medium in the apical and baso-lateral chambers of the transwell apparatus were replaced, with the apical medium containing 250 µg/ml of FITC-Dextran. At time (t) = 0, 28 µl was collected from the baso-lateral chambers, and diluted to 400 µl with 372 µl fresh medium. As the FITC-Dextran was left to diffuse across the monolayer, medium samples were taken in a similar fashion every 30 minutes (for up to 3 hours) from the baso-lateral chamber with each diluted aliquot plated in triplicate on a white 96-well microplate (3*100 µl volumes). Using a TECAN Safire 2 fluorospectrometer (Tecan Group, Switzerland), excitation and emission wavelengths of 490 and 520 nm respectively were selected. % Transendothelial Exchange (%TEE) of FITC-Dextran 40 kDa was expressed as the total baso-lateral fluorescence at a given time point (from 0 – 180 minutes) expressed as a percentage of total apical fluorescence at (t) = 0 min (Figure 2.14).

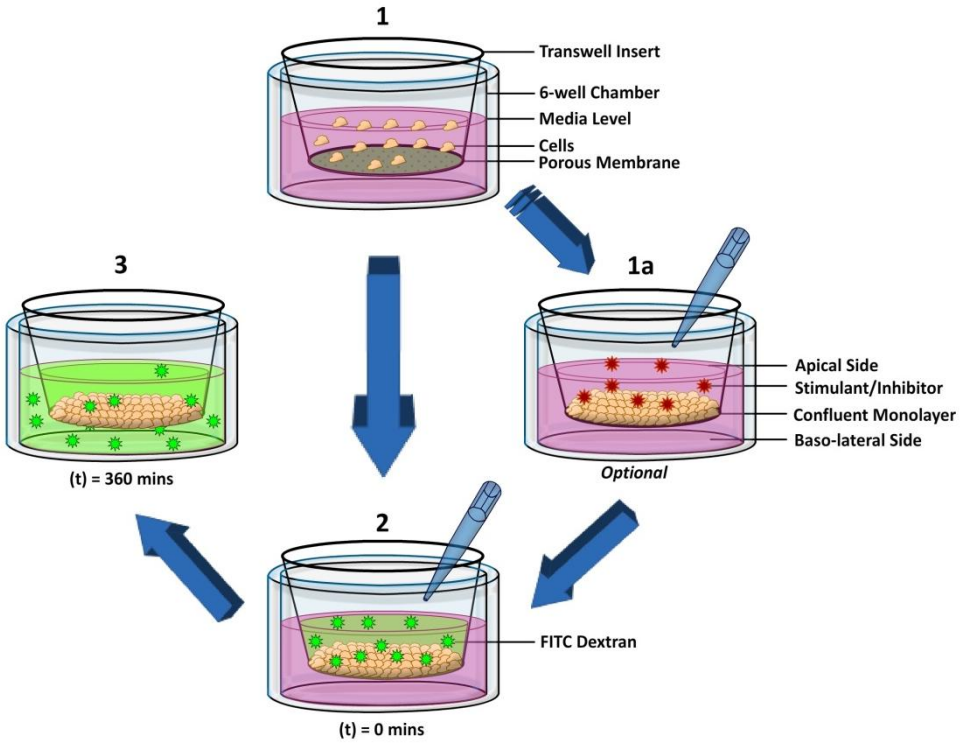

Figure 2.14: Trans-Endothelial Cell Permeability Assay. (1) Cells are counted and seeded equally across transwell inserts and left to adhere. (1a) 24hrs later, treatments such as adding inflammatory cytokines or pharmacological inhibitors may be added if required. (2) FITC-Dextran supplemented medium replaces the medium in the apical chamber and (t)=0 is recorded. (3) Samples are collected over 30 minute timepoints from the baso-lateral chamber and the samples are prepared to be read by a flourimeter.

2.2.8.2 Adhesion Assay

96-well plates were coated with Attachment Factor (~10 µl) before 50 µl of pre-warmed medium was added to each well. The plate was stored was placed in an incubator until further required. Meanwhile cells were trypsinised, pelleted and counted before being resuspended at a concentration of $2.5*10^5$ cells/ml and 100 µl of the suspension was added via a multichannel pipette in triplicate to the pre-prepared 96-well plate. All wells were brought to a final volume of 200 µl before the plate was returned to the incubator and left there overnight. The experimental procedure was performed in replicate as required for a pre-determined number of time points.

The next day the cell culture medium was aspirated and replaced with 200 µl of fresh medium. If required, peptide inhibitors were added to the medium before addition to the necessary wells. Upon return to the incubator, (t)=0 min was established. Upon completion of each time point, the plate corresponding to said timepoint was removed from the incubator and the medium was aspirated from the wells. The wells were washed briefly with PBS before 100 µl of 3.75% formaldehyde was added to each well and left to incubate for 15 mins at room temperature. The wells were then briefly washed with PBS before 100 µl of a 5 mg/ml crystal violet solution was added to each well. The plate was left to incubate at room temperature for 5 mins before being washed briefly with water. The plates were turned upside down and left to air dry for 10 mins. Once completely dry, 50 µl of a 2% SDS solution was added to each well and the plate was left to incubate for 30 mins at room temperature. The absorbance was then read at 562 nm on an ELx800 Microplate Reader and treated samples were compared against the control cells.

2.2.8.3 xCELLigence™

The xCELLigence™ system monitors cellular events in real time without the incorporation of labels. The system measures electrical impedence across micro-electrodes integrated on the bottom of tissue culture E-Plates. The presence of the cells on top of the electrodes affects the local ionic environment at the electrode/solution interface leading to an increase in the electrode impedance. The more cells attached on the electrodes, the larger the increases in electrode impedance and vice versa. In addition, the impedance depends on the quality of the cell interaction with the electrodes so increased cell adhesion or spreading will lead to a larger change in electrode impedance. Thus electrode impedance, represented as cell index (CI) values, can be used to monitor cell viability, number, morphology, monolayer integrity and adhesion in a number of cell-based assays (Figure 2.15). This system was used

to monitor the effect of inflammatory cytokines and peptide inhibitors on viability and proliferation on HBMvEC's.

This method was applied as in previous publications (Luissint, Federici et al. 2012, Kobayashi, Tsubosaka et al. 2013). Cells were trypsinised and a cell count performed (Section 2.2.1.3). For proliferation studies, 2,500 cells were added to each AF coated well on a 16-well E-plate in duplicate whereas for viability studies 25,000 cells per well was employed. Initial adhesion of the cell was measured every 15 minutes for 24 hours. After this, measurements were extended to every 25 minutes for up to 4 days afterwards. Normally after the initial 24 hour adhesion phase, conditions could be inflicted on the cells *in situ*. Typically this would entail spiking the fresh growth medium intended for the cells with inflammatory cytokines of varying concentrations or inhibitors to block specific protein-protein interactions. The cells were fed with fresh growth medium every 24 hours directly after a measurement had been taken in order to have as minimal an effect on the results. This was achieved by removing 100 µl of growth medium from each well and replacing it with 100 µl of fresh medium. Water levels were also maintained in reservoirs surrounding the wells to ensure the cells were kept humidified at all times.

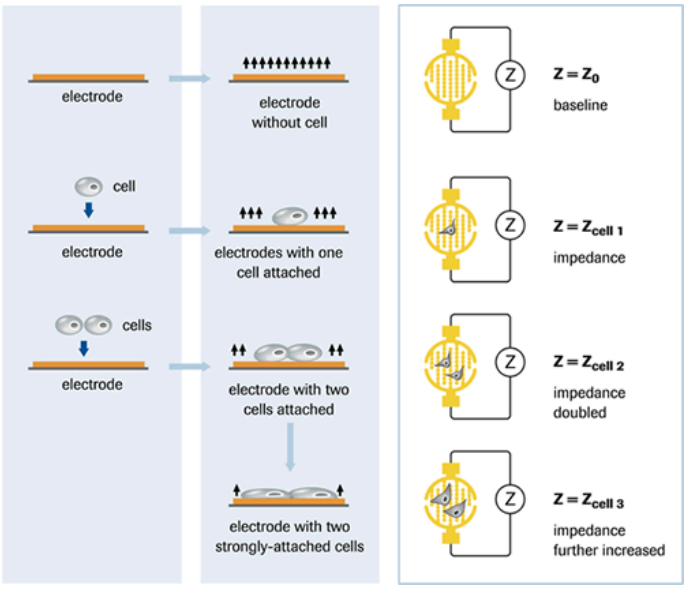

Figure 2.15: The principle of the xCELLigence system, (http://www.roche-applied-science.com)**.**

2.2.8.4 MTS Assays

MTS assays are a colorimetric method for determining the number of viable cells in a proliferative or chemosensitive manner. The CellTiter 96 AQ_{ueous} Assay is composed of

solutions containing a novel tetrazolium compound (3-(4,5-dimethylthiazol-2-yl)-5-(3-carboxymethoxyphenyl)-2-(4-sulfophenyl)-2H-tetrazolium (MTS)) and an electron coupling reagent (phenazine methosulfate, PMS). MTS is reduced by cells into a formazan product that is soluble in tissue culture medium (Figure 2.16). The conversion of MTS into formazan is accomplished by dehydrogenase enzymes found in metabolically active cells. The absorbance of the produced formazan can be measured at 490 nm by means of a plate reader and the signal acquired correlates directly to the cell number present.

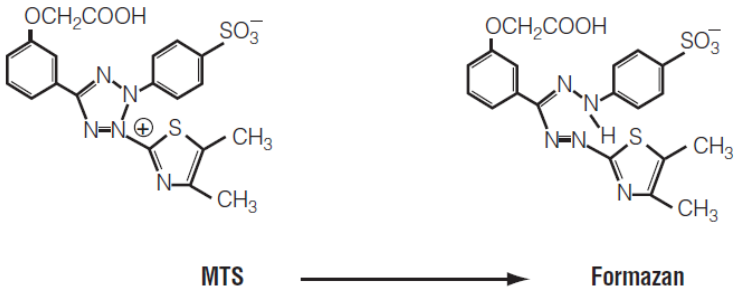

Figure 2.16: MTS assay principle. The reduction of MTS by metabolically active cells results in formazan, a product which is detectable at 490 nm and correlates to the number of live cells present.

The MTS reagent was used as both a means of measuring proliferation and viability. The key difference between the two was the starting number of cells in each well; proliferation used 1,000 cells/well and viability used 25,000 cells/well.

Following trypsinisation of the cells, the cells were counted and resuspended at the required cell number/100 µl of cell culture medium. The cells were then plated in triplicate onto AF-coated 96-well plates and left to adhere overnight. The following day the cells were stimulated accordingly (Section 2.2.2.1) and left to incubate for the required time. Following the experimental design, 20 µl of MTS/PMS solution was added to each well on the assay plate containing 100 µl of culture medium. The plate was then incubated for 4 hours at 37^{o}C in a humidified 5% CO_2 tissue culture incubator. The absorbance was then read at 490 nm on an ELx800 Microplate Reader.

2.2.8.5 Lactate Dehydrogenase Assays

Another means of assessing viability was the measurement of cellular lactate dehydrogenase (LDH) release, a trait of cells which have undergone damage or are under stress. Lactate dehydrogenase is released rapidly into the culture medium from damaged cells. This excess of LDH facilitates the conversion of lactate to pyruvate. This is turn facilitates the reduction

of NAD^+ to $NADH/H^+$. Concurrently, the catalyst diaphorase transfers the H/H^+ from the $NADH/H^+$ to the tetrazolium salt INT (pale yellow) which is reduced to formazan (red) (Figure 2.17). An increase in the amount of dead or membrane-damaged cells results in an increase in LDH activity in the cell culture supernatant. This increase correlates directly to the amount of formazan formed over a controlled time period. Therefore the farther the supernatant colour is pushed into the red end of the spectrum the greater the amount of LDH released which is inversely proportional to the cell viability.

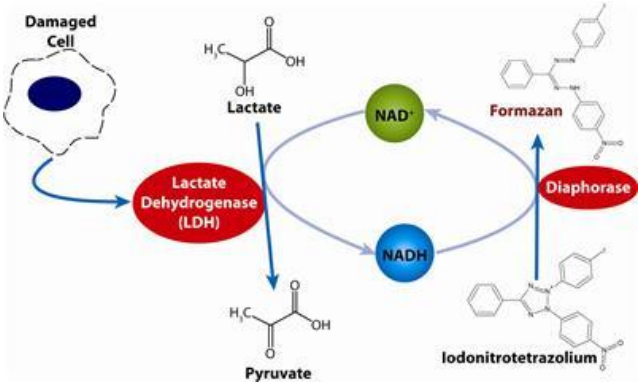

Figure 2.17: LDH assay principle. The release of LDH from damaged cells creates a cascade effect initiating a number of reactions. The end result is the production of formazan, a detectable product which correlates directly to the number of damaged cells present, (http://flipper.diff.org/)

Following cell treatments, culture medium was harvested for LDH analysis. Untreated cells and lysed cells served as 'Low' and 'High' LDH Controls respectively. 100 µl of the medium samples were plated in triplicate on a sterile 96-well plate. 100 µl of Reaction Mixture was added to each well and the plate was incubated for 30 minutes at room temperature protected from light. 50 µl of Stop Solution was then added to each well and the plate was shaken gently for 10 seconds. The plate was then read at 490 nm on an ELx800 Microplate Reader. The percentage cytotoxicity was calculated as follows:

$$Cytotoxicity\ (\%) = \frac{(Experimental\ Value - Low\ Control)}{(High\ Control - Low\ control)} \times 100$$

2.2.8.6 ELISA

2.2.8.6.1 Multiplex ELISA

Compared to regular ELISAs (Section 2.2.8.5.2), Multiplex ELISA allows for the simultaneous screening of up to 10 targets of interest in each well. The principal revolves

around the capture antibodies of interest being coated onto distinct spots in each well. Samples are added to the wells along with a solution containing the detection antibodies labelled with an electrochemiluminescent compound. Following an incubation period in which the samples bind to the capture antibodies immobilised on the working electrode surface, which in turn bind the detection antibody completing the sandwich. Finally, the addition of the Read Buffer provides the appropriate chemical environment for electrochemiluminescence and the MSD® SECTOR instrument applies a voltage to the electrodes causing the bound labels in the well to emit a quantitative measure of light proportional to the amount of captured analyte which can be measured and interpreted by the instrument (Figure 2.18).

2.2.8.6.1.1 Human ProInflammatory 1 4-Plex Ultra-Sensitive Kit

This plate could detect levels of Interferon Gamma (IFN-γ), Interleukin 1-Beta (IL-1β), Interleukin 6 (IL-6) and Tumour Necrosis Factor Alpha (TNF-α) in a biological sample. All reagents were previously made up as per the manufacturer's instructions. 25 µl of Diluent 2 was added per well and the plate sealed and shaken vigorously (300-1000 rpm) for 30 minutes. 25 µl of sample or calibrator was then added per well with the plate sealed and shaken vigorously (300-1000 rpm) overnight. The following day the plate was washed three times using PBS-Tween (0.05%) before 150 µl of 2 x Read Buffer T was added per well taking care not to introduce bubbles. The plate was then analysed on the SECTOR Imager Instrument.

2.2.8.6.1.2 MULTI-SPOT Vascular Injury Panel 1 Assay

This plate could detect levels of Thrombomodulin, Intercellular Adhesion Molecule 3 (ICAM-3), P-Selectin and E-Selectin in a biological sample. All reagents were made up prior as per the manufacturer's instructions. 150 µl of Blocker A Solution was added to each well and the plate was sealed and shaken overnight at 4^{o}C. The following day the plate was washed with 200 µl per well of PBS-Tween (0.05%) three times. 40 µl of Diluent 10 was added to each well followed by 10 µl of sample or calibrator before the plate was sealed and incubated overnight at 4^{o}C. The following day the plate was washed with 200 µl per well of PBS-Tween (0.05%) three times. 25 µl of 1 x Detection Antibody Solution was added to each well and the plate sealed and incubated at room temperature for 1 hour with shaking. The plate was washed a further three times. 150 µl of 1 x Read Buffer T was added to each well taking care not to introduce bubbles and the plate was read on the SECTOR Imager instrument.

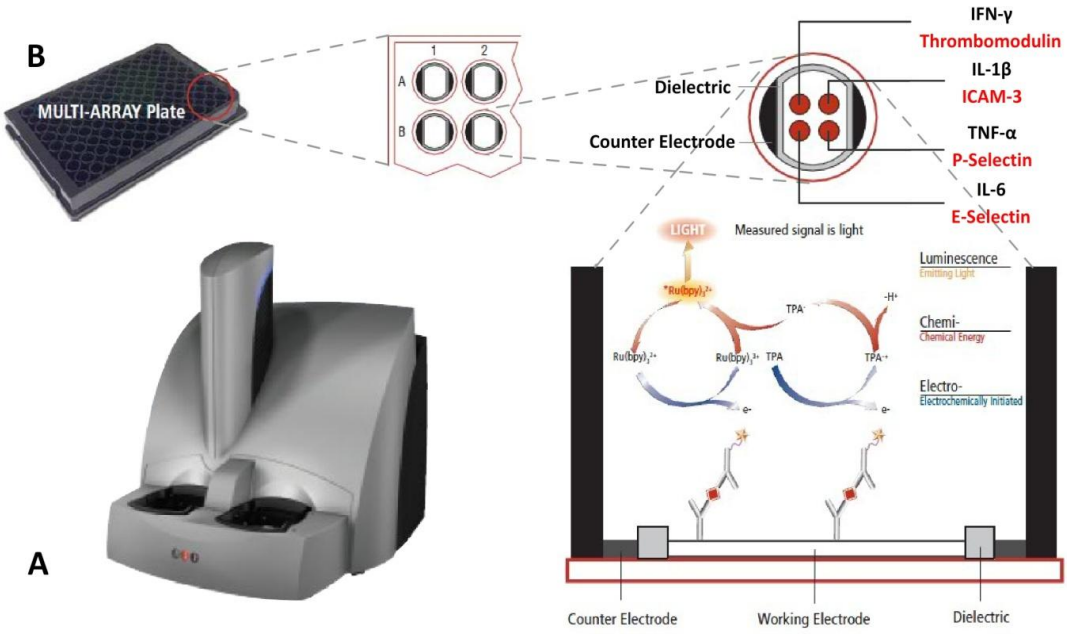

Figure 2.18: Multiplex ELISA system and principle. (A) The SECTOR® Imager 6000 Multiplex ELISA Reader and (B) the experimental setup and principal behind the spotwells on the Multiplex ELISA plate, (http://www.meso-scale.com/).

2.2.8.6.2 Standard ELISA

96-well plates were coated with 100 µl/well of capture antibody in coating buffer. The plate was then sealed and incubated overnight at 4^{o}C.

The following day the wells were aspirated and washed five times with >250 µl of wash buffer per well. 1 x Assay Diluent was prepared (5 x Assay Diluent and DI water, 1:4) and the wells were blocked using 200 µl/well. The plate was incubated for 1 hour at room temperature. The 1 x Assay Diluent was removed from the wells and the plate was washed five times as before. Using 1 x Assay Diluent, the provided standards were diluted according to the manufacturer's instructions and 100 µl was added to the appropriate wells. A two-fold serial dilution was performed across the plate using the top standard to create a standard curve. In addition, all samples to be analysed were added to the plate and the plate then sealed and incubated overnight at 4^{o}C.

The following day the wells were aspirated and washed five times as before. 100 µl/well of detection antibody (diluted in 1 x Assay Diluent as per the manufacturer's instructions) was added to each well and the plate was sealed and incubated at room temperature for 1 hour. The plate was aspirated and washed five times as before. 100 µl/well of Avidin-HRP (diluted in 1 x Assay Diluent as per the manufacturer's instructions) was added to each well and the plate sealed and incubated at room temperature for 30 minutes. The plate was

aspirated and washed seven times. 100 µl/well of Substrate Solution was added to each well and the plate sealed and incubated at room temperature for 15 minutes. 50 µl of Stop Solution was then added to each well and the plate read at 450 nm on an ELx800 Microplate Reader (Figure 2.19).

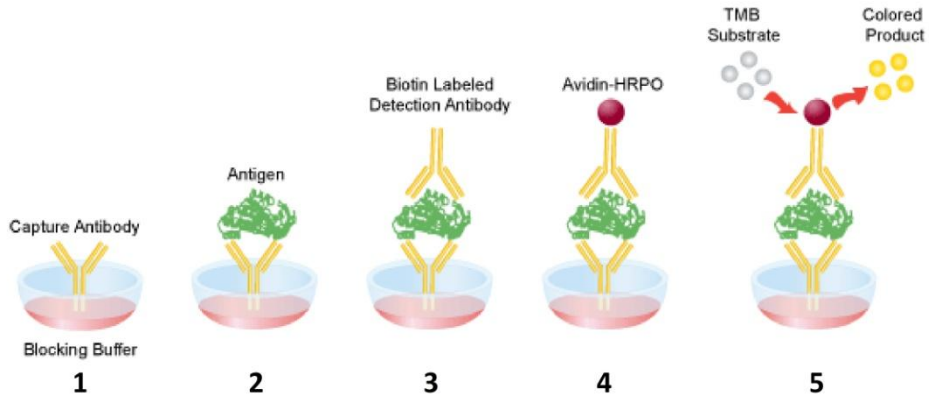

Figure 2.19: The principle steps in an ELISA. (1) Coating of the wells of a 96-well plate with a capture antibody and blocking the non-specific sites in the well with a blocking buffer; (2) incubation of samples and standards on the plate; (3) incubation with a suitable detection antibody for the antigen of interest; (4) the addition of Avidin-HRP that binds to any biotin-labelled detection antibody present and; (5) addition of TMB substrate to generate a detectable product that correlates to the amount of antigen of interest present, (http://www.abcam.com/).

2.2.9 Flow Cytometry Analysis

Flow cytometry is a technology that allows a cell suspension to be counted and have each individual cell measured for a variety of characteristics, determined by examining how they flow in a liquid. Each cell suspension under investigation is entered into a hydrodynamically-focused stream of liquid which has a beam of laser light of a single wavelength directed on it. A number of detectors are aimed at the point where the stream passes through the light beam; one in-line with the light beam (Forward Scatter-overall cell size) and several perpendicular to it (Side Scatter-cell granularity) in addition to multiple fluorescent detectors (fluorescent labelling). Each suspended particle that passes through the beam scatters the ray, and any fluorescent chemicals found on the surface of the particle can become excited into emitting light at a longer wavelength than the light source. The strategically placed detectors pick up all these signals and interpret the fluctuations in brightness detected to build a profile on the physical and chemical structure of each individual particle and thus the overall cell suspension. All flow cytometry experiments were performed on the FACSAria

2.2.9.1 Viability

In order to assess cell health following exposure to different concentrations of cytokine over different incubation times, or to assess the effect of different inhibitors, an Alexa Fluor 488 Annexin V/Dead Cell Apoptosis Kit was utilised. The advantage to using this kit is the ability to distinguish the degree of cell health rather than labelling a cell live or necrotic. To do this, fluorescent labelling of characteristic morphological and biochemical changes in the cell is employed highlighting key changes in the cell which act as a detectable readout for assessing overall health of a cell population. In normal live cells, phosphatidylserine (PS) is located on the cytoplasmic surface of the cell membrane. In apoptotic cells, PS is translocated from the inner to the outer leaflet of the plasma membrane thus exposing PS to the extra cellular environment. The human anticoagulant, Annexin V, is a phospholipid-binding protein that has a high affinity for PS, which when tagged with a fluorophore makes the identification of apoptotic cells achievable. The other dye utilised in the kit is propidium iodide (PI), a red fluorescent nucleic-binding dye. PI is impermeant to live cells and apoptotic cells but stains dead cells with red fluorescence. By utilising the two dyes, distinct populations of dead cells (red and green), apoptotic cells (green) and live cells (neglible fluorescence) can be easily distinguished from one another using the FACS Aria with the 488 nm line of an argon-ion laser for excitation.

Briefly, cells were exposed to experimental treatments as required. An untreated culture of cells was employed as a control. Cells were trypsinised and pelleted before being washed in warmed PBS. 1 x Annexin-binding buffer was prepared (5 x Annexin binding Buffer and DI Water, 1:4) and a 100 µg/ml aliquot of PI was prepared by diluting 5 µl of PI stock solution in 45 µl of 1 x Annexin-binding buffer. The cells were re-centrifuged and the pellet was resuspended in 100 µl of 1 x Annexin-binding buffer. The cell suspensions were transferred to sterile FACs tubes and 5 µl of Alexa Fluor 488 Annexin V and 1 µl of the PI 100 µg/ml aliquot were then added to the cell suspension. The cells were then incubated for 15 minutes at room temperature in the dark. Following incubation, 400 µl of Annexin-binding buffer was added to each tube and the samples were mixed gently. The cells were kept on ice and protected from light until read as soon as was possible by flow cytometry.

Note: This kit could also be used for microscopy work. See Section 2.2.10.

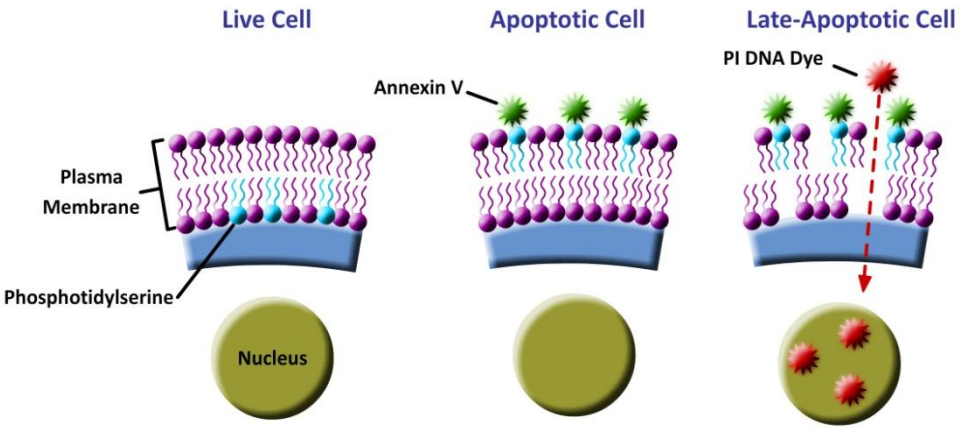

2.20: Annexin V/PI Viability Principle. Distinguishing between 'live' (no label), 'apoptotic' (Annexin V - green label) and late-apoptotic (Propidium Iodide - red label) cells.

2.2.9.2 Transfection Efficiency

Post-transfection with green fluorescent protein (GFP), cells were trypsinised and pelleted (Section 2.2.1.2). The resultant pellet was washed in PBS before being centrifuged once more. Following aspiration of the growth medium, the pellet was resuspended in 100 µl of FACS Buffer (Section 2.1.3.4). 6 µl of PI stain was added to the tubes and the tubes were left to incubate for 15 minutes at room temperature in the dark. The tubes were then brought to a final volume of 500 µl with the addition of 400 µl of FACS Buffer. The tubes were then kept on ice and protected from light until read as soon as was possible by flow cytometry.

2.2.9.3 Oxidative Stress

This method was applied as in previous publications (Gertzberg, Neumann et al. 2004, Mozo, Ferry et al. 2006, Lee, Lee et al. 2010). 2',7'-dichlorofluorescein diacetate (DCFDA) is a fluorogenic dye that measures hydroxyl, peroxyl and other ROS activity within a cell culture. Once taken up by the cell, cellular esterases cause DCFDA to become deacetylated. This non-fluorescent compound can then become oxidized upon interaction with ROS to yield the highly fluorescent 2', 7' – dichlorofluorescin (Figure 2.21). For the DCFDA assay, cells were treated with the compound at a final concentration of 5 µM at (t) = 0, with the compound present for the entire incubation period of the treatment.

Dihydroethidium (DHE) is a superoxide indicator. It stains the cytoplasm of living cells blue until it becomes oxidised by ROS yielding ethidium which is free to intercalate with DNA. (Figure 2.21). For the DHE assay, cells were treated with the compound at a concentration of 3 µM for 30 mins prior to completion of the treatment incubation period.

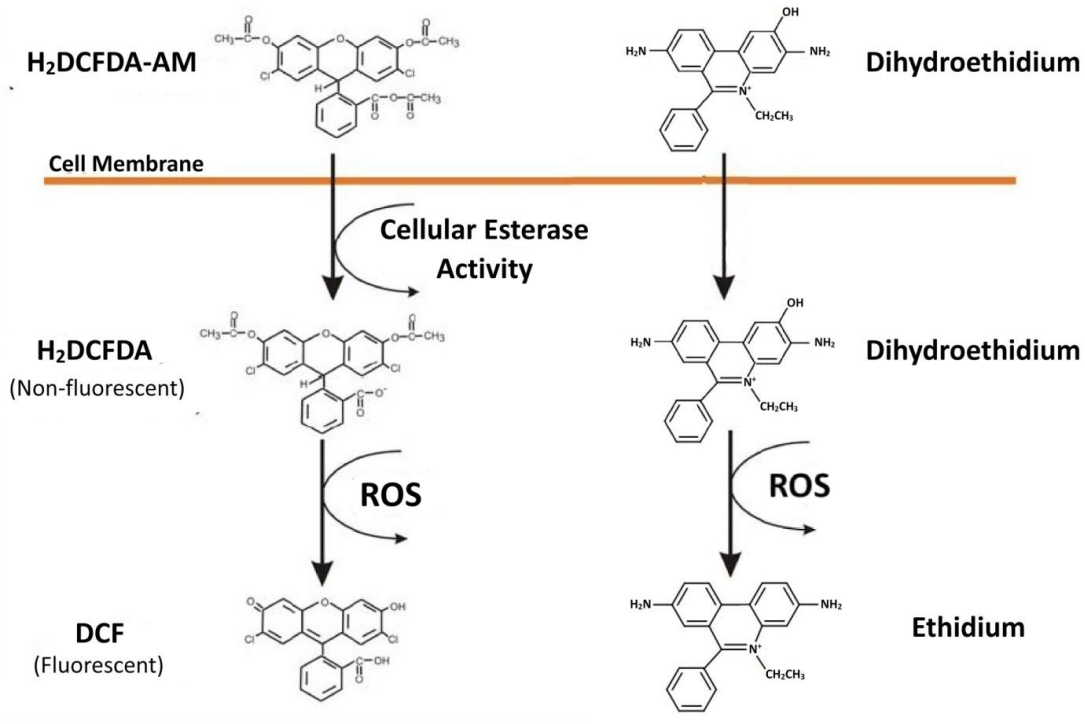

Figure 2.21: CFDA and DHE Principle, (http://www.biotek.com/).

The cells were exposed to experimental treatments as required. An additional culture of untreated cells was employed as an unstained control. Cells were trypsinised and pelleted before being washed in warmed PBS. The cells were re-centrifuged and the pellet was resuspended in 500 µl of FACS buffer before being transferred to sterile FACs tubes. The cells were then kept on ice and protected from light until read as soon as was possible by flow cytometry.

Note: These stains could also be used for microscopy work. See Section 2.2.10.

2.2.10 Immunofluorescent Microscopy

In order to monitor the expression and/or subcellular localisation of proteins, BBMvEC's and HBMvEC's were prepared for immunofluorecent analysis according to the method of previous publications (Walsh, Murphy et al. 2011, Guinan, Rochfort et al. 2013) with minor modifications. Immunofluorescent staining was carried out on cells seeded onto ibidi® slides (Section 2.2.2.2.2) or glass coverslips. This section will refer to the more common practice of using coverslips (but the procedure is the same for ibidi® slides). Briefly, coverslips were immersed in 100% IMS and flame sterilised before being placed in a well of a sterile 6-well dish. The six-well dish was then exposed to UV exposure for 1 hr in the laminar flow cabinet.

The coverslips had ~20 µl of AF added and gently smeared over their surface using a sterile cell scraper. 1 ml of growth medium was then added to each well and the plate was incubated at 37^{o}C/5% CO_2 in a tissue culture incubator until further required. Cells were then trypsinised, pelleted and resuspended (as outlined in Section 2.2.1.2) at a density of $1.0*10^6$ cells/ml. 1 ml of the cell suspension was added onto coverslips and the cells left to adhere overnight.

The next day prior to carrying out the immunofluorescence protocol, the adhered cells could be subjected to a set of conditions depending on the experimental setup if necessary. Post-treatment, the following steps were done as quickly as possible. All growth medium was removed and the cells washed with pre-warmed (37^{o}C) PBS. Cells were then fixed *in situ* with 3.7% (v/v) para-formaldehyde on ice for 10 minutes. Coverslips were then washed twice with PBS and briefly dried before having the perimeter marked with a PAP pen. 100 ul of ammonium chloride was added to each coverslip before being left to incubate for 10 minutes. Following incubation, the ammonium chloride was aspirated and 100 ul of permablock solution was then added to the coverslip. After 30 minutes incubation, cells were then incubated with 100 µl of primary antibody in a fresh aliquot of permablock solution (1^{o} and 2^{o} antibody dilutions and Incubation times are listed in the table below) overnight at 4^{o}C. Following incubation, if the primary antibody was unconjugated (i.e. lacking a fluorescent probe) the coverslips were washed twice with permablock before the specific secondary antibody was made up in permablock and 100 µl added. The coverslips were incubated in the dark. They were then washed twice with permablock before carrying out the optional incubation step of F-Actin antibody made up in permablock. Alternatively, post-secondary antibody incubation, the cells had their nuclei stained as a positive control with either DAPI or PI. Coverslips were then washed twice more before being inverted and mounted onto 100% IMS washed microscope slides using DAKO fluorescent mounting medium. The slides were kept in a slide box for 1-2 hours to allow the DAKO medium to set before being sealed using nail varnish. The slides were stored at 4^{o}C until visualised by standard fluorescent microscopy or confocal microscopy.

1° Antibody/Stain	1° Antibody Concentration	Incubation Time	2° Antibody Concentration	Incubation Time
14-3-3 (Abcam)	1:50	Overnight	1:500	2 hours
Claudin 5 (Invitrogen)	1:50	Overnight	1:500	2 hours
VE-Cadherin (Abcam)	1:50	Overnight	1:500	2 hours
vWF (Abcam)	1:50	Overnight	1:500	2 hours
ZO-1 (Invitrogen)	1:50	Overnight	1:500	2 hours
DAPI (Sigma)	1:2000	3 mins		
F-Actin (Invitrogen)	1:50	30 mins		
Annexin V (Invitrogen)	1:5	15 mins		
Propidium Iodide (Invitrogen)	1:100	15 mins		
DCFDA (Sigma)	1:6000	0-24 hrs		
DHE (Sigma)	1:3000	30 mins		

Table 2.12: Antibody/stain concentrations for immunofluorescence.

2.2.11 Statistical Analysis

Results are expressed as mean ± SD. Experimental points were performed in triplicate with a minimum of three independent experiments (n=3). Statistical comparison between control and experimental groups were by ANOVA in conjunction with a Dunnett's *post-hoc* test for multiple comparisons. A Student's *t*-test was also employed for pairwise comparisons. A value of $P \leq 0.05$ was considered significant.

Chapter 3:

The effects of laminar shear stress on HBMvEC blood-brain barrier properties.

3.1 Introduction

The concept of the BBB has been recognised for more than 100 years, following the demonstration that most organs could be stained by dye injected intravenously, with the exception of the brain and spinal cord (Ehrlich 1885, Goldmann 1913). Since then, the BBB is now recognised as the key regulator of the molecular and cellular traffic between blood and brain, providing a natural defence against circulating toxic and infectious agents. Several groundbreaking anatomical studies (Reese, Karnovsk 1967, Brightman, Reese 1969) provided a reasonable knowledge of the functions and capabilities of the BBB; however after decades of research the responsible factors or induction signals are still not characterised in detail. Over the years, several cellular and molecular studies have been conducted in an effort to elucidate the underlying biology of the BBB (Stewart, Wiley 1981); however discrepancies tarnish many founding bodies of work as a result of the restrictions and limitations at the time. Perhaps the greatest obstacle at the time, and one which remains today, albeit to a much smaller degree, is the procurement of a fully representative model of the BBB.

To date, the majority of studies have focussed on the effects of local and systemic influences that drive the induction of the highly specialised brain endothelial cells that comprise the BBB. Of these studies, the vast majority have focussed on the inductive effects of systemic factors such as growth factors, hormones and cytokines (Abbott 2002). Historically, the BBB was considered to encompass the structural, physiological and biochemical processes of the endothelial cells of the cerebral microvasculature. However, recent studies have demonstrated the interaction of the endothelium with cell types of the vessel wall and CNS such as neurons and glial cells, thus constitutes a functional unit termed the neurovascular unit (NVU). There is an ever-growing recognition directed towards the secreted agents and physical contact of the cell types that comprise the NVU, in contributing to the formation of a fully functional BBB. ***However, local influences such as haemodynamic forces play perhaps as great a part as that played by the neighbouring cell types in the induction of these specialised endothelial cells*** (Krizanac-Bengez, Mayberg et al. 2004, Krizanac-Bengez, Hossain et al. 2006, Krizanac-Bengez, Mayberg et al. 2006, Cucullo, Hossain et al. 2011). Several studies in other vascular beds have demonstrated the mechanotransductive effect of haemodynamic forces on endothelial phenotype from a genetic through to molecular, functional and morphological levels (Davies 1995, del Zoppo 2008, Hahn, Schwartz 2009). These adaptive responses have been identified in promoting vascular homeostasis, and are said to exert a protective effect against the pathophysiology of several vascular disorders. With regards to the cerebrovasculature, studies pertaining to the effect of haemodynamic forces are limited. Difficulties attributed to recreating the cerebral

microenvironment resulted in several earlier studies being conducted in macrovessels from which a larger cell number could be obtained and with greater ease (Rubin, Staddon 1999). At present, far superior models exist (Joo, Karnushi.i 1973), and only now are the true effects of haemodynamic forces on the cerebral microvasculature being uncovered. Several robust human models are readily available and with this in mind, we re=revisited in chapter 3 the works of Walsh (2011) and Colgan (2007) ***with the objective of clarifying the translative effects of previously examined shear-induced upregulation of BBB barrier function, and further expand on this with specific relevance to tight junction assembly and anti-inflammatory mechanisms.***

3.1.1 Study Aims

In this chapter we examined the effects of physiological levels of laminar shear stress on HBMvEC blood-brain barrier phenotypic properties. Therefore, the overall aims of this chapter include:

- To conduct basic characterisation studies on HBMvECs
- To investigate the effect of physiological levels of laminar shear stress on TJ/AJ protein (occludin, claudin-5, VE-Cadherin, ZO-1) transcriptional and translational expression.
- To investigate the effect of physiological levels of laminar shear stress on TJ/AJ protein phosphorylation.
- To investigate the effect of physiological levels of laminar shear stress on HBMvEC barrier function.
- To investigate the effect of inflammatory cytokines; TNF-α and IL-6, on HBMvEC barrier function following pre-conditioning by physiological levels of laminar shear stress.
- To determine if physiological levels of laminar shear stress influence HBMvEC anti-inflammatory properties.

3.2 Results

3.2.1 The positive characterisation of commercially obtained HBMvECs

HBMvECs were characterised for a number of specific markers to confirm effective culturing of the cerebral endothelial phenotype (Figure 3.1). Endothelial cells present a number of biomarkers that are easily characterised to ensure the validity of commercially-sourced cell lines. von Willebrand Factor; a key glycoprotein involved in hemostasis, is a common biomarker of endothelial cells. Confluent HBMvEC cultures were harvested for whole cell protein lysate and mRNA, following which vWF presence was demonstrated at both a translational (i) and transcriptional (ii) level by western blotting and qPCR techniques, respectively. Furthermore, vWF presence was further confirmed by immunofluorescence microscopy (iii-vi). Confluent HBMvECs were fixed in situ and stained for vWF which was evident by the characteristic shape of the Wiebel-Palade bodies which are known to store the protein in its native form. To ensure the HBMvECs were effectively maintaining their BBB properties and that the culture regime adopted had not driven the cultures into reverting to a 'default' endothelial phenotype, a number of proteins located at the intercellular junctions that are involved in the unique barrier expressed by CNS endothelial cells were examined. Confluent HBMvECs were fixed in situ and stained for immunofluorescence examination of ZO-1 (vii), Claudin-5 (viii) and VE-Cadherin (ix). Each protein was highly expressed and localised at the cell-cell borders.

3.2.2 Exposure of HBMvECs to laminar shear stress induces morphological and cytoskeletal realignment in the direction of the flow vector

The effect of laminar shear stress on morphological and cytoskeletal organisation was examined (Figure 3.2). Confluent cultures were maintained in static environments (left hand side; LHS) or subjected to laminar shear stress (8 dynes cm^{-2}) (right hand side; RHS) for 24 hrs. Under brightfield microscopic conditions, static cultures demonstrated the characteristic endothelial growth patterns; a 'cobblestone' morphology (i). Under shear conditions HBMvECs realigned in the direction of the flow vector (ii). When fixed in situ and stained for filamentous F-actin, a similar trend was observed; in static cultures the actin filaments lacked any organisation (iii) versus sheared cultures where the actin filaments had realigned in the direction of the flow vector (iv).

3.2.3 Exposure of HBMvECs to laminar shear stress enhances the cell-cell border localisation of intercellular junction proteins, ZO-1, claudin-5 and VE-Cadherin

The effect of laminar shear stress on the expression and localisation patterns of proteins involved forming the intercellular junctions of HBMvECs was examined (Figure 3.3). Confluent HBMvECs were maintained in static environments (LHS) or subjected to laminar shear stress (8 dynes cm^{-2}) (RHS) for 24 hrs before being fixed in situ for immunofluorescence microscopy. Cultures were stained for ZO-1 (i, ii), claudin-5 (iii, iv) and VE-Cadherin (v, vi) to assess the subcellular localisation of the intercellular junction proteins in the absence and presence of laminar shear stress. In unsheared cultures, the staining pattern for each protein displayed an irregular and discontinuous presence at the cell-cell border. In contrast, the staining pattern of cultures exposed to shear stress displayed enhanced immunoreactivity and a more consistent and stable localisation pattern at the cell-cell borders for each of the proteins.

3.2.4 Exposure of HBMvECs to laminar shear stress induces an upregulation of interendothelial junction proteins; occludin, claudin-5, VE-Cadherin and ZO-1

The effect of laminar shear stress on the expression of proteins involved in forming the intercellular junctions of the BBB was examined on both a transcriptional level in HBMvECs and BBMvECs and on the translational level in HBMvECs (Figure 3.4). Confluent BBMvECs and HBMvECs were maintained in static environments or subjected to laminar shear stress (8 dynes cm^{-2}) for 24 hrs before being harvested for whole cell mRNA or protein lysate. The transcriptional levels of occludin, claudin-5, VE-Cadherin and ZO-1 were examined by qPCR. In both species, each gene demonstrated a moderate increase in their transcription levels following exposure to laminar shear stress (i, ii). The translational levels of each protein in response to shear were then examined in HBMvECs by western blot (iii). A similar trend was observed in which each protein experienced a significant increase in protein levels in response to laminar shear stress (iv). The importance of these intercellular junction proteins; claudin-5 and VE-Cadherin, in barrier formation was further examined utilising siRNA technology. Briefly, transfection parameters were optimised using recombinant GFP protein and GFP expressing plasmid (Figure A.1) before optimisation of siRNAs specifically targeting claudin-5 (Figure 3.5) and VE-Cadherin (Figure 3.6) were carried out. The silencing of claudin-5 and VE-Cadherin was demonstrated to induce a significant increase in paracellular flux of 40kDa FITC-Dextran (%TEE of FD40) across the cell monolayer. (Note: Figures A.1-A.3 are located in Appendix)

3.2.5 Exposure of HBMvECs to laminar shear stress reduces phosphotyrosine and phosphothreonine levels of occludin, claudin-5 and VE-Cadherin

The effect of laminar shear stress on the phosphorylation levels of tyrosine and threonine residues of intercellular junction proteins occludin, claudin-5 and VE-Cadherin was examined (Figure 3.5). Confluent HBMvECs were maintained in static environments or subjected to laminar shear stress (8 dynes cm^{-2}) for 24 hrs before being harvested for whole cell protein lysate. Samples were then subjected to immunoprecipitation and western blot analysis for phosphotyrosine (pTyr)- (LHS) and phosphothreonine (pThr)-levels (RHS). pTyr- and pThr-levels for occludin, claudin-5 and VE-Cadherin were seen to be very significantly reduced following exposure to laminar shear stress.

3.2.6 Exposure of HBMvECs to laminar shear stress induces an upregulation of barrier function in-part via tyrosine phosphatase activity

The effect of laminar shear stress on the barrier function of HBMvECs was examined with a focus on the role to tyrosine phosphatases in mediating such activity (Figure 3.6). Confluent HBMvECs were maintained in static environments or subjected to laminar shear stress (8 dynes cm^{-2}) for 24 hrs before being assessed for transendothelial permeability. Exposure of HBMvECs to laminar shear stress results in a significant drop in FITC-Dextran paracellular flux across the cell monolayer (i, ii). In comparison to static cultures, the significant reduction in permeability reflects a significant increase in barrier function. To investigate the role of tyrosine phosphatases in modulating barrier function, confluent HBMvECs were maintained in static environments or subjected to laminar shear stress (8 dynes cm^{-2}) for 24 hrs in the absence or presence of the phosphatase inhibitor dephostatin, before being assessed for transendothelial permeability. The shear-induced reduction of permeability in HBMvECs was significantly attenuated when dephostatin was present during exposure of the cultures to laminar shear stress (iii, iv).

3.2.7 Cytokine-mediated injury is reduced by shear in HBMvECs

The concurrent effect of laminar shear stress and inflammatory cytokines on the barrier function of HBMvECs was examined (Figure 3.7; LHS). Confluent HBMvECs were maintained in a static unsheared condition or pre-conditioned with laminar shear stress (8 dynes cm^{-2}) for 24 hrs (i). TNF-α (0-100ng/ml) was then added to the cultures. The cultures were then either maintained in static environments or subjected to further laminar shear stress (8 dynes cm^{-2}) for a further 6 or 18 hrs (ii). Post-treatment the cultures were trypsinised and seeded at a known density into transwell inserts and left to adhere overnight

(iii) prior to assessment for transendothelial permeability (iv). Exposure of static HBMvECs to TNF-α resulted in a significant increase in FITC-Dextran paracellular flux (%TEE of FD40) across the cell monolayer in a dose- and time-dependent manner. Moreover, exposure of HBMvECs to laminar shear stress demonstrated a significant drop in FITC-Dextran paracellular flux (%TEE of FD40) across the cell monolayer. In the presence of shearing, TNF-α induced significantly lower absolute increases in paracellular flux of FITC-Dextran label (Figure 3.8; i, ii). A similar observation was made in cultures treated with IL-6 in place of TNF-α (Figure 3.9; i, ii).

An alternative means of examining the concurrent effect of laminar shear and inflammatory cytokines on the barrier function of HBMvECs was performed (Figure 3.7; RHS). Confluent HBMvECs were maintained in static environments or pre-conditioned with laminar shear stress (8 dynes cm^{-2}) for 24 hrs (i). Cultures were then seeded at a known density into transwell inserts and left to adhere overnight (ii). TNF-α or IL-6 (0-100 ng/ml) were then added to the cultures for 6 or 18 hrs (iii) prior to assessment for transendothelial permeability (iv). Results obtained were identical to those reported above for TNF-α (Figure A.4) and IL-6 (Figure A.5).

3.2.8 Laminar shear stress induces changes in transcriptional levels of cytokines and their signal-transducing receptors in HBMvECs

The effect of laminar shear stress on cytokines and their signal-transducing receptors over time was examined on a transcriptional level (Figure 3.10). Confluent HBMvECs were maintained in static environments or subjected to laminar shear stress (8 dynes cm^{-2}) for 0-24 hrs before being harvested for whole cell mRNA. The transcriptional levels of TNF-α receptors TNFR1 (i) and TNFR2 (ii) and IL-6 receptor GP130 (iii) were examined from 0-24 hrs by qPCR. A significant change was observed for all three receptors in response to acute shear exposure (0-2 hrs); TNFR1 and GP130 transcription levels were significantly increased in response to acute laminar shear stress before returning to baseline levels within 8 hrs of shear onset. Unlike TNFR1, GP130 levels continued to decrease in response to laminar shear stress, resulting in a significant overall decrease in levels at 24 hrs. Conversely, TNFR2 demonstrated an initial decrease followed by an increase in levels in response to laminar shear stress resulting in significantly higher mRNA levels after 24 hrs. IL-6 mRNA levels followed a pattern similar to that of its GP130 receptor, with a net reduction in IL-6 mRNA levels after 24 hrs laminar shear (iv). Conversely, a slight increase in IL-6 protein expression was observed in response to laminar shear stress after 24 hrs in comparison to static cultures. Interestingly, an initial increase in IL-6 release levels was

observed in the acute onset of laminar shear stress (0-8 hrs), yet this surge plateaued thereafter with static IL-6 release levels comparable by 24 hrs (Figure A.6).

3.2.9 Laminar shear stress induces an increase in the expression and secretion of thrombomodulin from HBMvECs

The effect of laminar shear stress on HBMvEC levels of thrombomodulin over time was examined on a translational level (Figure 3.11). Confluent HBMvECs were maintained in static environments or subjected to laminar shear stress (8 dynes cm^{-2}) for 0-24 hrs before being harvested for whole cell protein lysate and spent medium. The translational levels of thrombomodulin were examined by western blot, in which a significant increase in thrombomodulin expression was observed in response to laminar shear stress after 24 hrs in comparison to static cultures (i, ii). Conditioned medium harvested at different timepoints during the static and shear conditions were analysed for thrombomodulin levels by ELISA. In response to laminar shear stress, a significant increase in thrombomodulin release into medium was observed after 4 hrs with levels climbing sharply up to 24 hrs. Static cultures in contrast released considerably smaller amounts of thrombomodulin across all timepoints up to 24 hrs (iii).

The thrombin-binding activity of the released thrombomodulin in response to laminar shear stress was also examined. Confluent HBMvECs were subjected to laminar shear stress (8 dynes cm^{-2}) for 24 hrs before being harvested for spent medium. The collected medium was then concentrated using centrifugal filtration. In parallel, confluent HBMvECs were seeded at a known density into transwell inserts and left to adhere overnight. The following day the cell monolayers were stimulated with 2U of thrombin in the absence and presence of different volumes of concentrated conditioned medium for 30 mins. Post-stimulation, the cultures were assessed for transendothelial permeability. Exposure of static HBMvECs to thrombin resulted in a significant increase in FITC-Dextran paracellular flux across the cell monolayer. This thrombin-induced increase in permeability in HBMvECs was significantly attenuated when conditioned medium was present during exposure of the cultures to thrombin (iv).

Complimentary studies on another factor involved in hemostasis; vWF were conducted (Figure A.7). A significant increase in vWF protein expression was observed in response to laminar shear stress after 24 hrs in comparison to static cultures. By contrast, an initial increase in vWF transcriptional levels was observed in the acute onset of laminar shear stress (0-2 hrs), yet a significant decrease in mRNA expression was observed by 24 hrs.

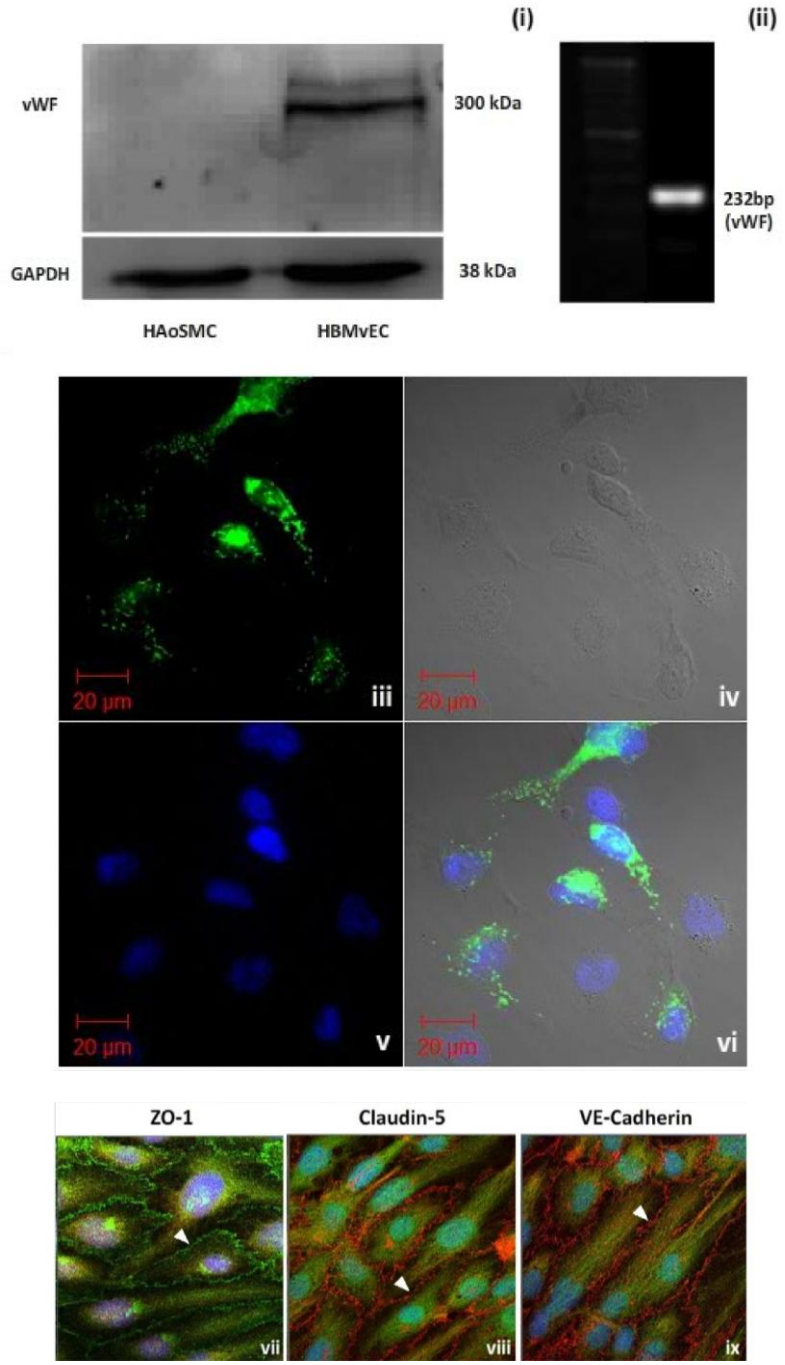

Figure 3.1: Characterisation of HBMvEC's. HBMvECs were initially grown to confluency for characterisation studies. The presence of the endothelial cell marker vWF as detected by Western blot (i), qPCR (ii) and fluorescence microscopy (green) (iii), (vi). In all fluorescence imaging studies, brightfield images of the cultures were obtained (iv) and cultures were typically counterstained for the nuclei (blue) as a control parameter (v). The resulting overlaid image series thus facilitated localisation studies (vi). Additional cell markers in the intercellular junction regions were examined in the form of ZO-1 (green) (vii), Claudin-5 (red) (viii) and VE-Cadherin (red) (ix). Images are representative.

Note: Human Aortic Smooth Muscle Cells (HAoSMCs) were used as a control in vWF protein studies (i).

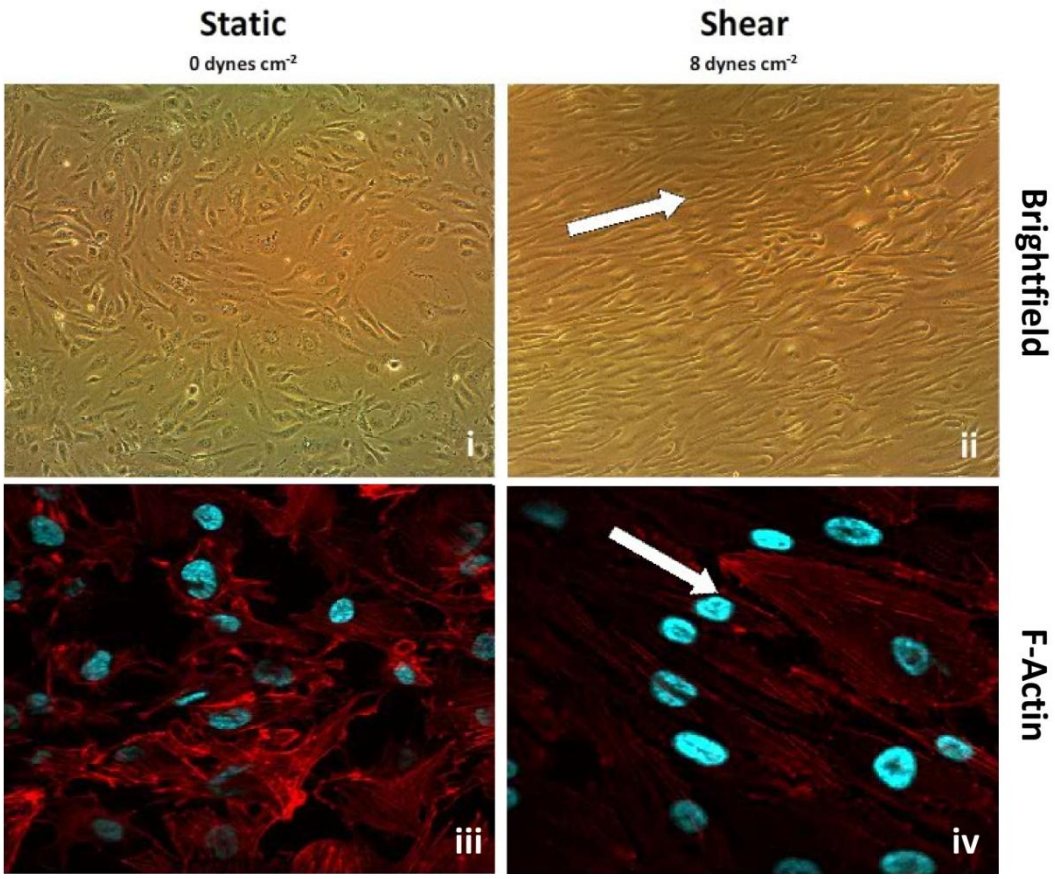

Figure 3.2: The effect of laminar shear stress on HBMvEC morphology and F-actin alignment. Confluent HBMvECs were exposed to laminar shear stress (8 dynes cm^{-2}, 24 hr) and examined for morphological realignment by brightfield microscopy (i-ii) and fluorescent microscopy (rhodamine phalloidin staining of F-Actin) (iii-iv). The white arrows represent the direction of the flow vector. DAPI was used to counterstain the nuclei of the cells (iii-iv). Images are representative.

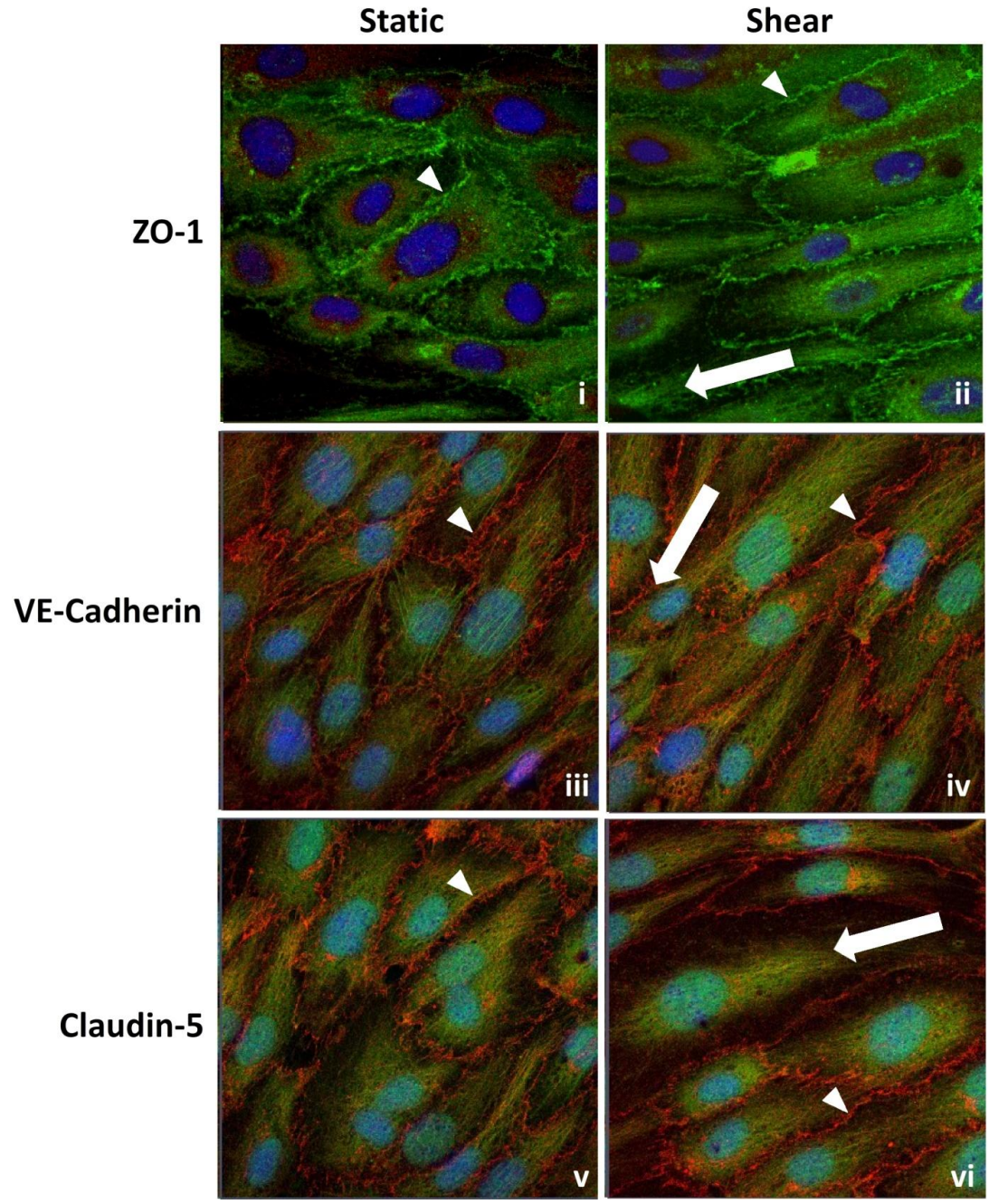

Figure 3.3: The effect of laminar shear stress on HBMvEC intercellar junctional protein localisation. Confluent HBMvECs were exposed to laminar shear stress (8 dynes cm^{-2}, 24 hr) and examined for changes in the expression and localisation patterns of intercellular junction proteins. Static cultures (LHS) were compared to that of sheared (RHS) for ZO-1 (green) (i, ii), VE-Cadherin (red) (iii, iv) and Claudin-5 (red) (v, vi). Membrane localisation is indicated by the small white arrow. The larger white arrow indicates the direction of the flow vector. All cultures were counterstained for F-actin (red – i, ii, green – iii, iv, v, vi) and the nuclei (blue). Images are representative.

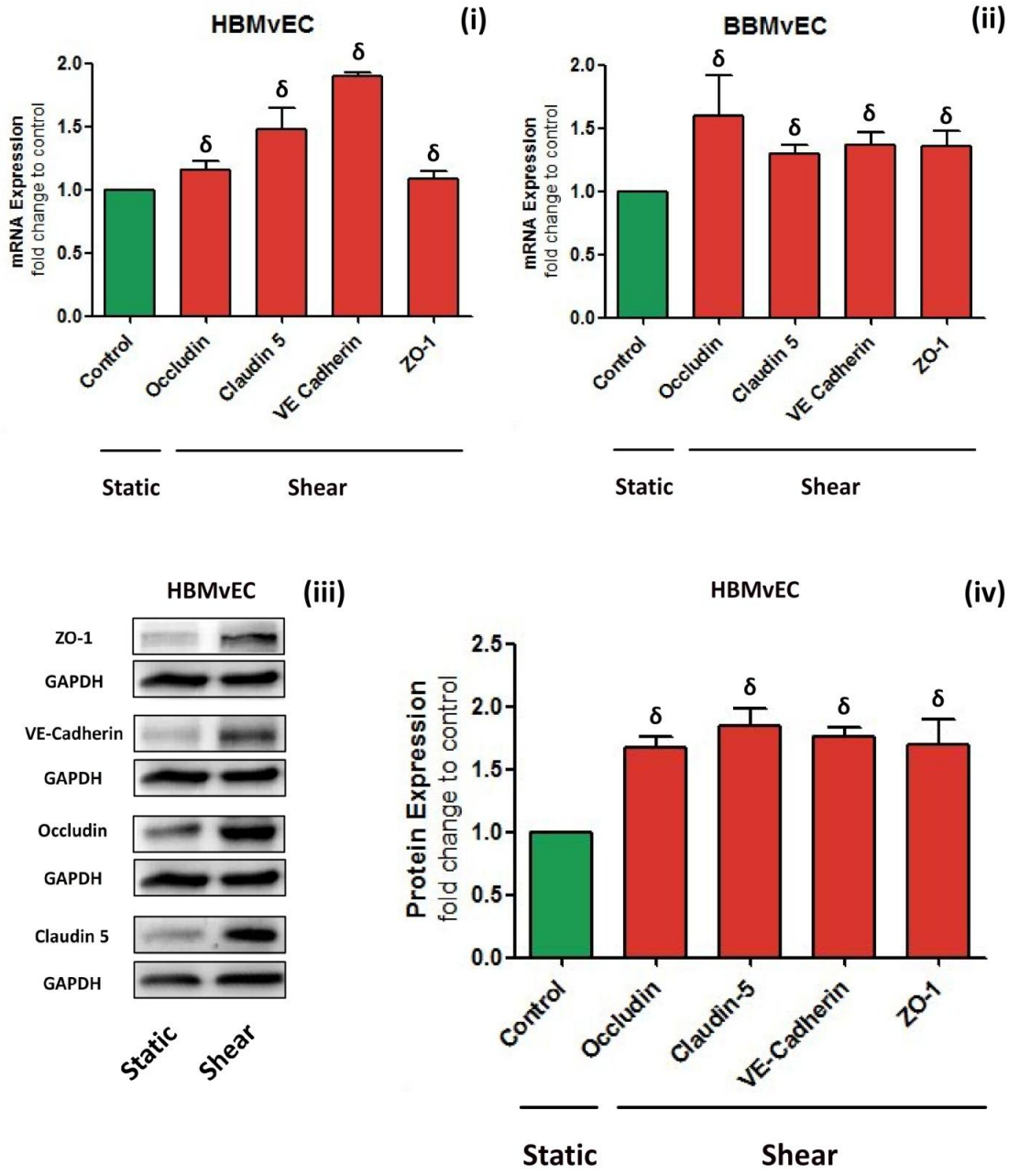

Figure 3.4: The effect of laminar shear stress on interendothelial junction protein expression. Confluent BBMvECs and HBMvECs were exposed to laminar shear stress (8 dynes cm^{-2}, 24 hr), following which they were harvested for whole cell mRNA and protein lysate. The histograms represent the mRNA expression changes in selected interendothelial junction proteins in BBMvECs (i) and HBMvECs (ii). The translational effect on these proteins was also investigated by western blot in HBMvECs (iii, iv). Results are averaged from three independent experiments ± SD; $\delta P \leq 0.05$ vs. Unsheared Control. Blots are representative.

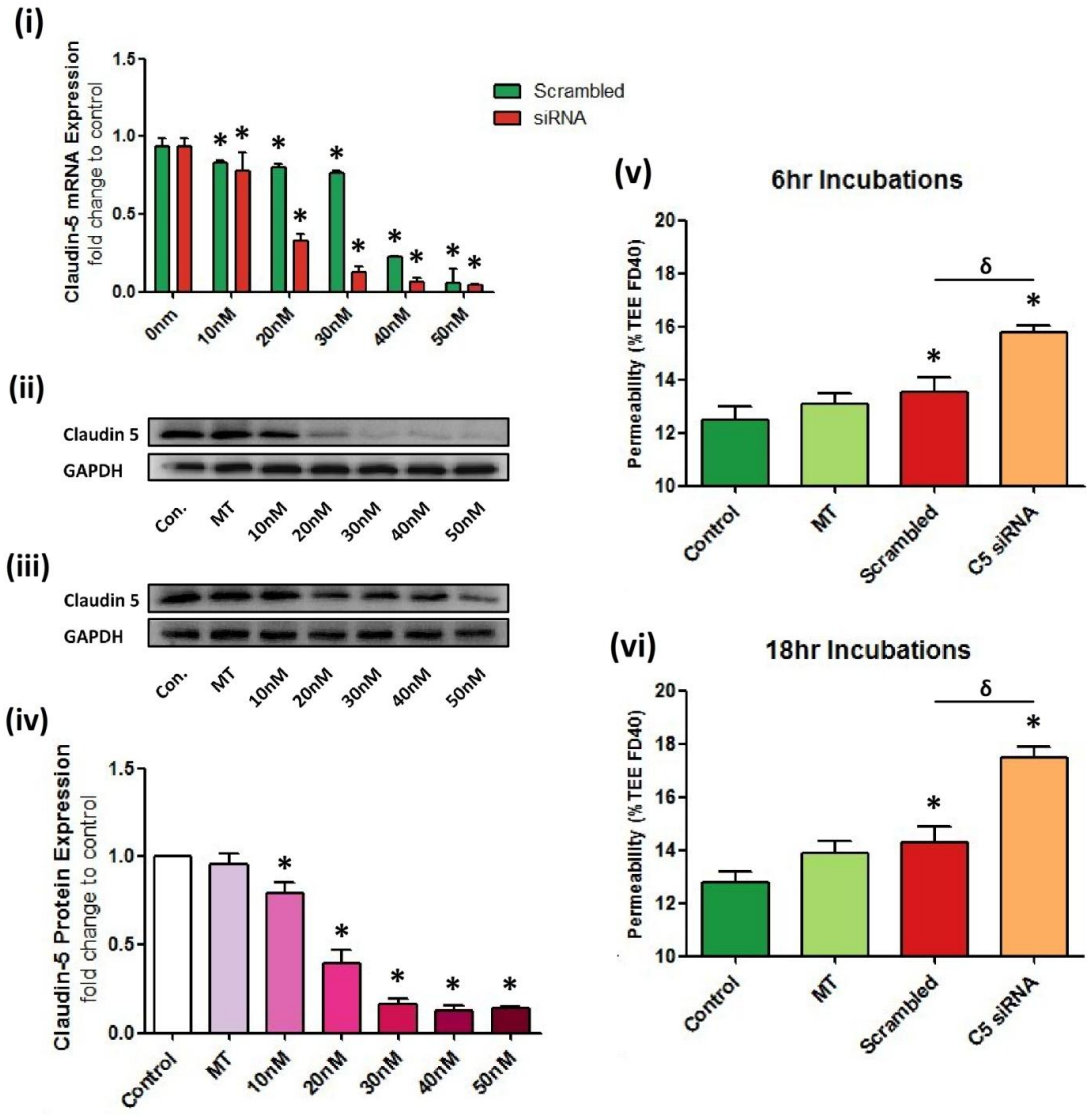

Figure 3.5: The optimisation and subsequent effect of claudin-5 knockout on HBMvEC barrier function. HBMvECs were grown to 70-80% confluency and transfected with claudin-5 siRNA (0-50 nM) as described in section 2.2.3.5. The following day, cells were harvested for mRNA and protein lysate. The samples were analysed by qPCR for the transcriptional levels (i) and by western blot for the translational levels (ii, iii, iv) of claudin-5 with respect to siRNA concentration. The transfection of a scrambled siRNA at concentrations equal to the claudin-5 siRNA was employed as a control. HBMvECs were thus transfected with the optimised concentration of claudin-5 siRNA, plated into transwell inserts and left to adhere overnight. The following day, the cultures were examined by transendothelial permeability assay. The histograms (v, vi) reflect the change in permeability (% TEE FD40) at a given time point(s) (t) = 180 mins. Results are averaged from three independent experiments ± SD; *P≤0.05 vs. 0 nM (i) or Untransfected Control (iv, v, vi) respectively. δP≤0.05. Blots are representative.

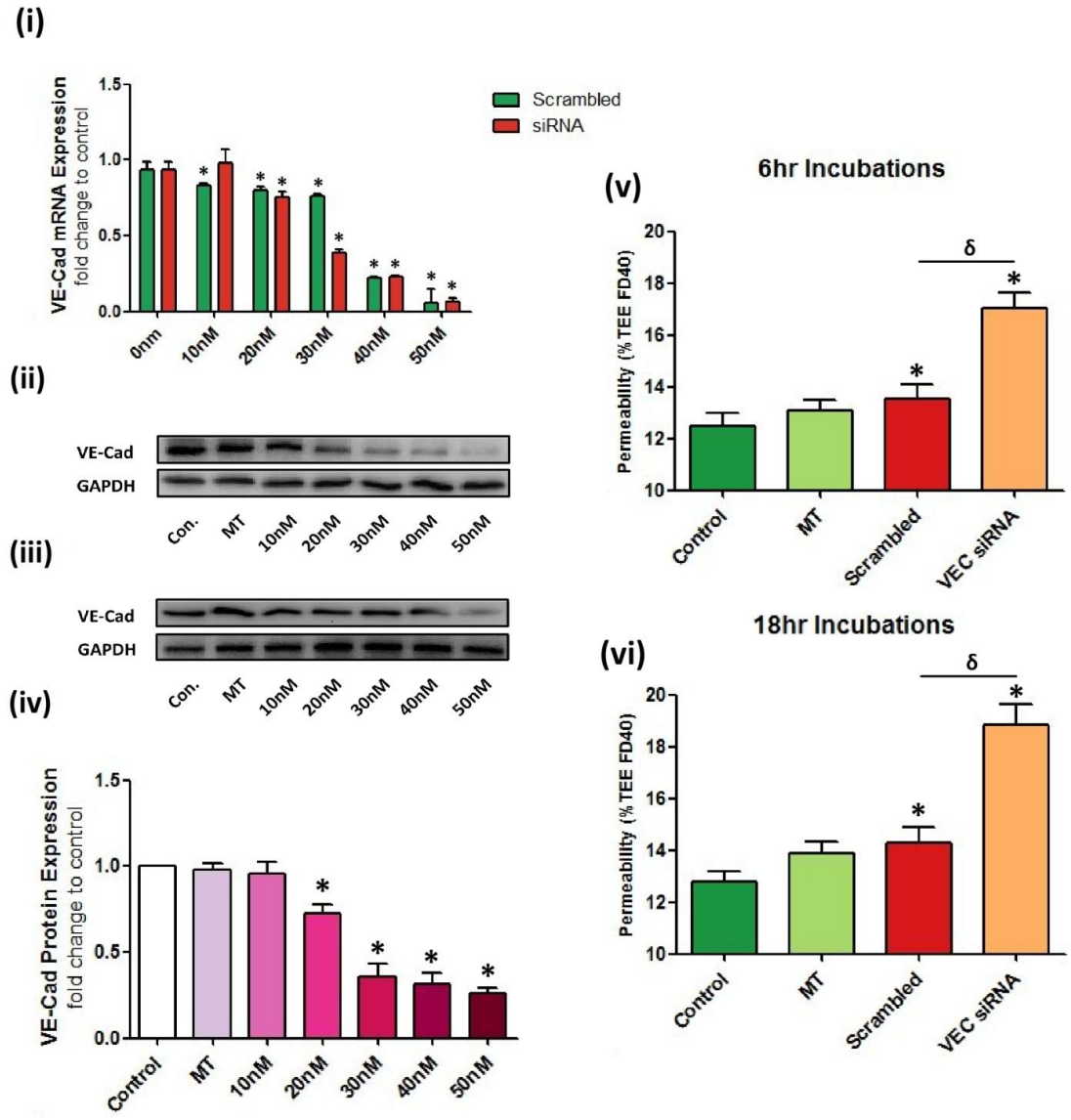

Figure 3.6: The optimisation and subsequent effect of VE-Cad knockout on HBMvEC barrier function. HBMvECs were grown to 70-80% confluency and transfected with VE-Cadherin siRNA (0-50 nM) as described in section 2.2.3.5. The following day, cells were harvested for mRNA and protein lysate. The samples were analysed by qPCR for the transcriptional levels (i) and by western blot for the translational levels (ii, iii, iv) of VE-Cadherin with respect to siRNA concentration. The transfection of a scrambled siRNA at concentrations equal to the VE-Cadherin siRNA was employed as a control. HBMvECs were thus transfected with the optimised concentration of VE-Cadherin siRNA, plated into transwell inserts and left to adhere overnight. The following day, the cultures were examined by transendothelial permeability assay. The histograms (v, vi) reflect the change in permeability (% TEE FD40) at a given time point(s) (t) = 180 mins. Results are averaged from three independent experiments ± SD; *P≤0.05 vs. 0 nM (i) or Untransfected Control (iv, v, vi) respectively. δP≤0.05. Blots are representative.

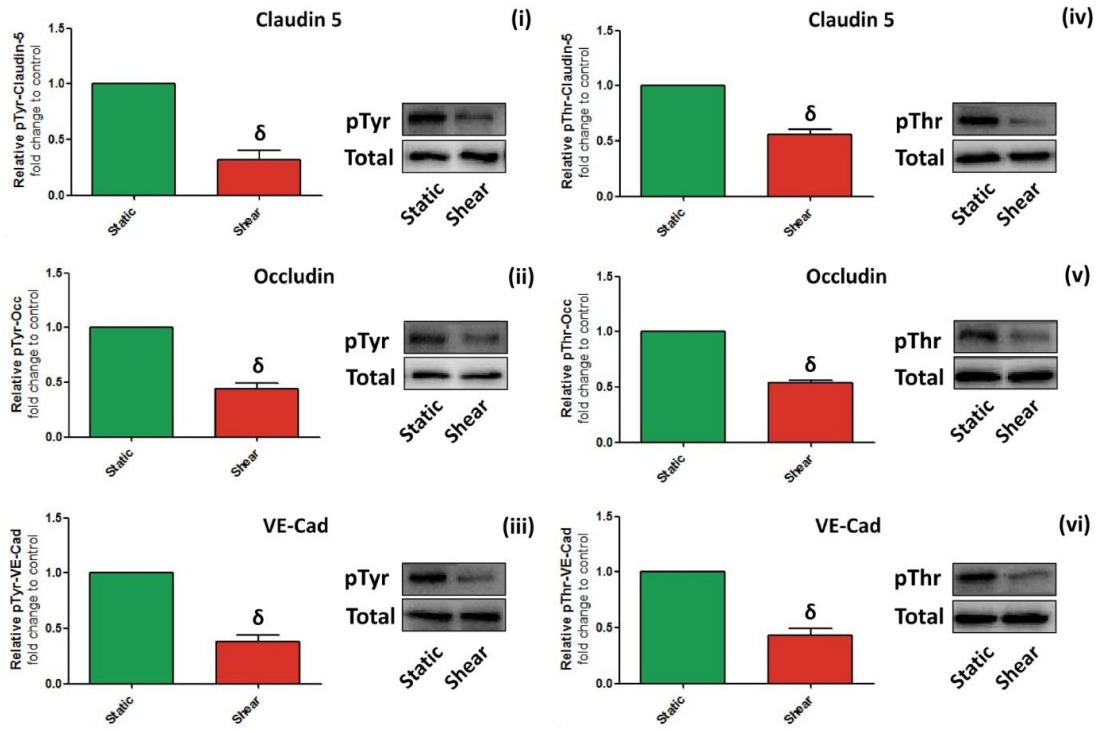

Figure 3.7: The effect of laminar shear stress on interendothelial junction protein tyrosine and threonine phosphorylation. Confluent HBMvECs were exposed to laminar shear stress (8 dynes cm^{-2}, 24 hr), following which they were harvested for whole cell protein lysate. The lysates were subjected to IP/IB analysis for relative pTyr and pThr levels of the target protein against total target protein levels. The histograms represent the relative pTyr (LHS) and pThr (RHS) levels for Claudin-5 (i, iv), Occludin (ii, v) and VE-Cadherin (iii, vi) derived by scanning densitometry from western blots. Results are averaged from three independent experiments ± SD; $\delta P \leq 0.05$ vs. Unsheared Control. Blots are representative.

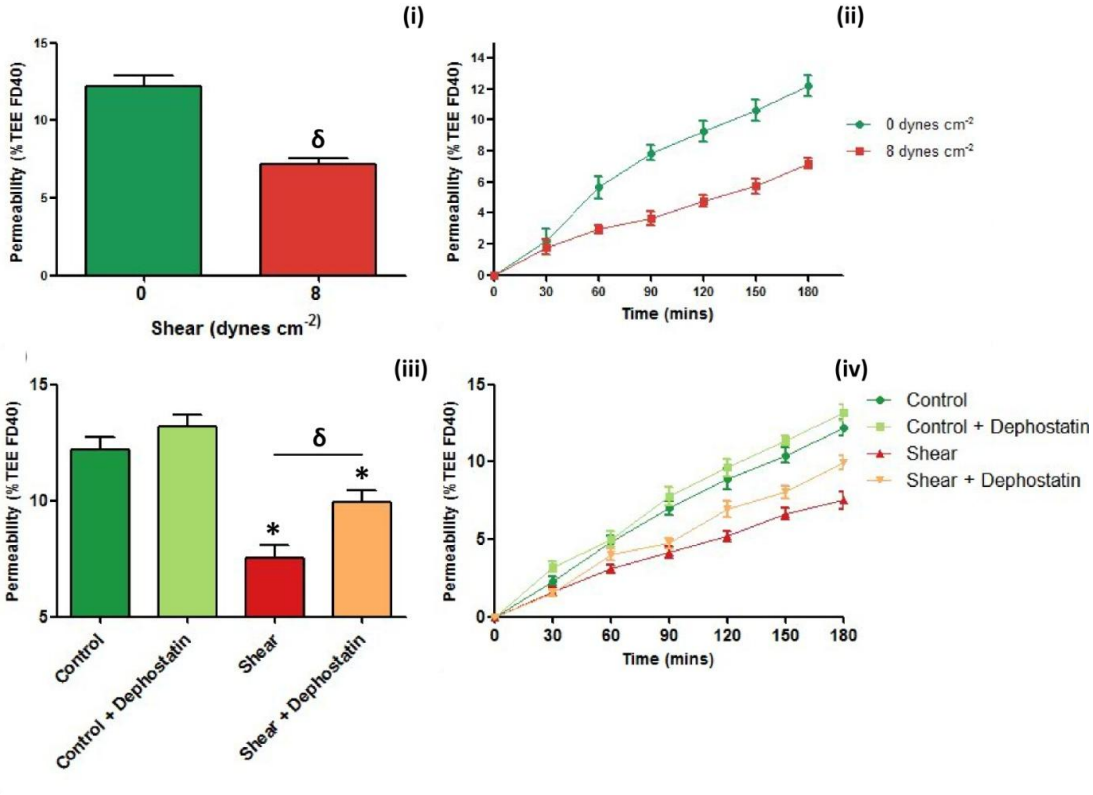

Figure 3.8: The effect of laminar shear stress on HBMvEC barrier function – effect of dephostatin. Confluent HBMvECs were exposed to laminar shear stress (8 dynes cm^{-2}, 24 hr) following which they were examined by transendothelial permeability. The histogram (i) and line graph (ii) show the change in permeability (% TEE FD40) at a given time point(s) (t) = 180 mins and 0-180 mins, respectively. In an independent study, HBMvECs were either maintained under static conditions or exposed to laminar shear stress (8 dynes cm^{-2}, 24 hr) in the absence and presence of the protein tyrosine phosphatase inhibitor, dephostatin and examined for transendothelial permeability. The histogram (i) and line graph (ii) show the change in permeability (% TEE FD40) at a given time point(s) (t) = 180 mins and 0-180 mins respectively. Results are averaged from three independent experiments ± SD; *P≤0.05 vs. Control, δP≤0.05 vs. Unsheared Control (i) and Shear (ii), respectively.

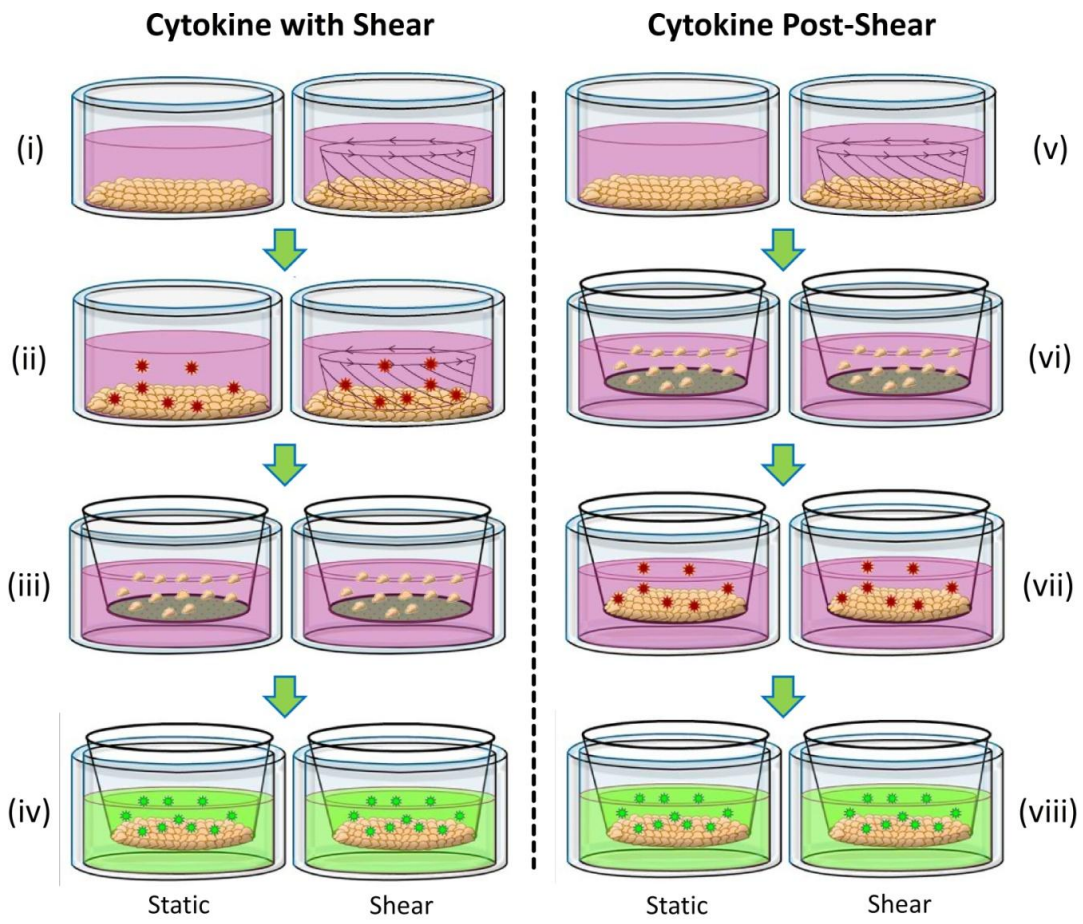

Figure 3.9: The experimental paradigms to investigate the protective effect of laminar shear stress on cytokine-induced injury of HBMvECs. Two approaches were taken to investigate this effect; exposing confluent pre-sheared HBMvECs to laminar shear stress and cytokines in tandem (LHS), and exposing confluent pre-sheared HBMvECs to cytokines without further shear (RHS). In both setups, confluent HBMvECs were exposed to laminar shear stress (8 dynes cm^{-2}, 24 hr) (i, v). In the first setup (LHS), the HBMvEC cultures were exposed to TNF-α or IL-6 (0-100 ng/ml) for 6 to 18 hr *whilst* the laminar shear stress was applied (ii). Following this the cultures were replated into transwell inserts and left to adhere overnight (iii) before being examined by transendothelial permeability assay (iv). In the second setup (RHS), HBMvECs were exposed to laminar shear stress and then replated into transwell inserts and left to adhere overnight (vi), following which they were exposed to TNF-α or IL-6 (0-100 ng/ml) for 6 to 18 hr (vii). The cultures were then examined by transendothelial permeability assay (viii).

Legend: Red Stars-Cytokines (TNF-α/IL-6), Green Stars-FITC dextran

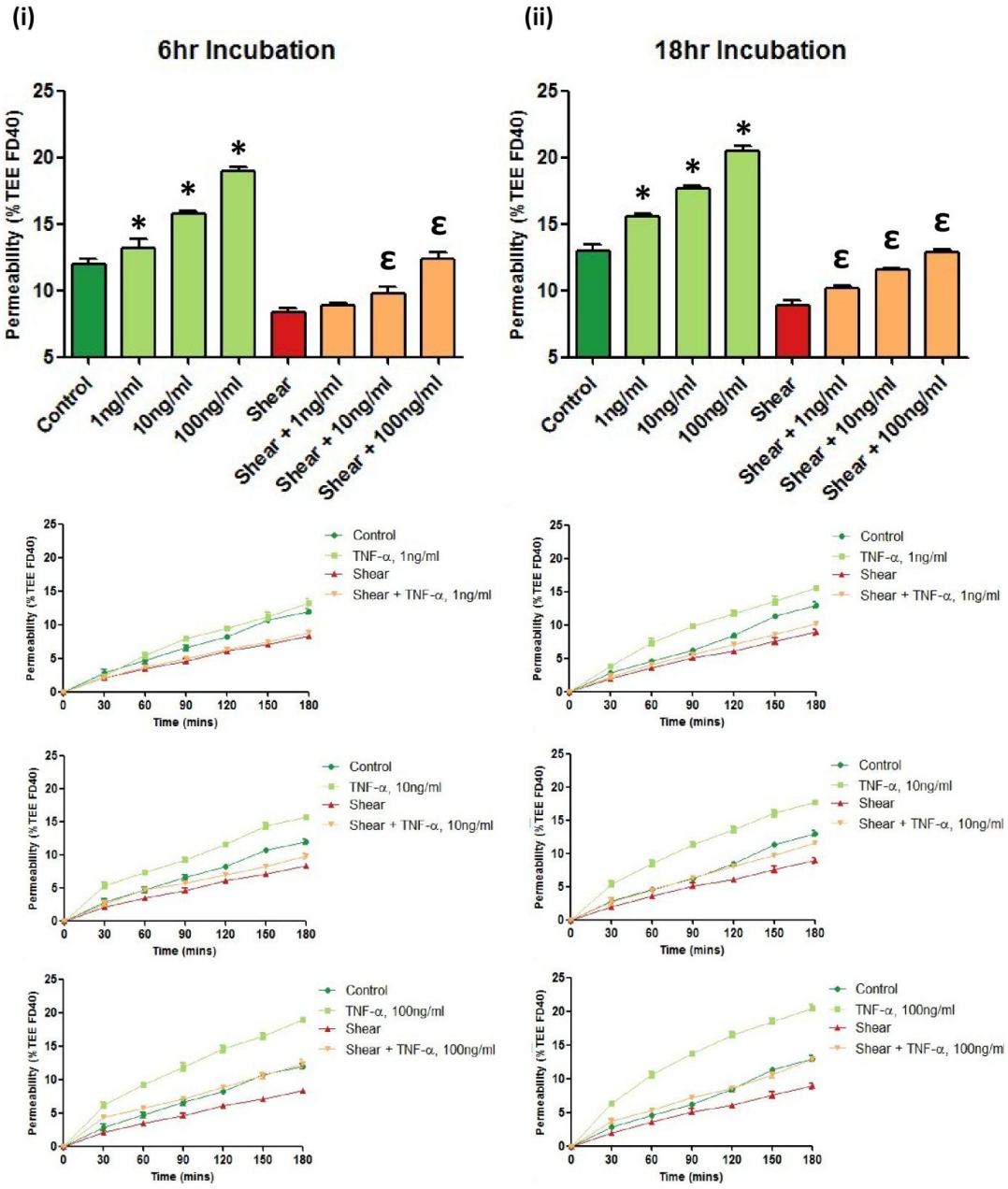

Figure 3.10: The effect of laminar shear stress on TNF-α-induced injury of HBMvECs. Confluent HBMvECs were pre-conditioned by laminar shear stress (8 dynes cm^{-2}, 24 hr), following which TNF-α (0-100 ng/ml) was added to the cultures. The laminar shear stress was continued for an additional 6 or 18 hr. Post-treatment, the cultures were replated into transwell inserts and left to adhere overnight before being examined by transendothelial permeability. The histograms and line graphs show the change in permeability (%TEE FD40) at a given time point(s) (t) = 180 mins and 0-180 mins after 6 hr (i) and 18 hr (ii) exposure to TNF-α (0-100 ng/ml). Results are averaged from three independent experiments ± SD; *P≤0.05 vs. Unsheared Control. εP≤0.05 vs. Sheared Control.

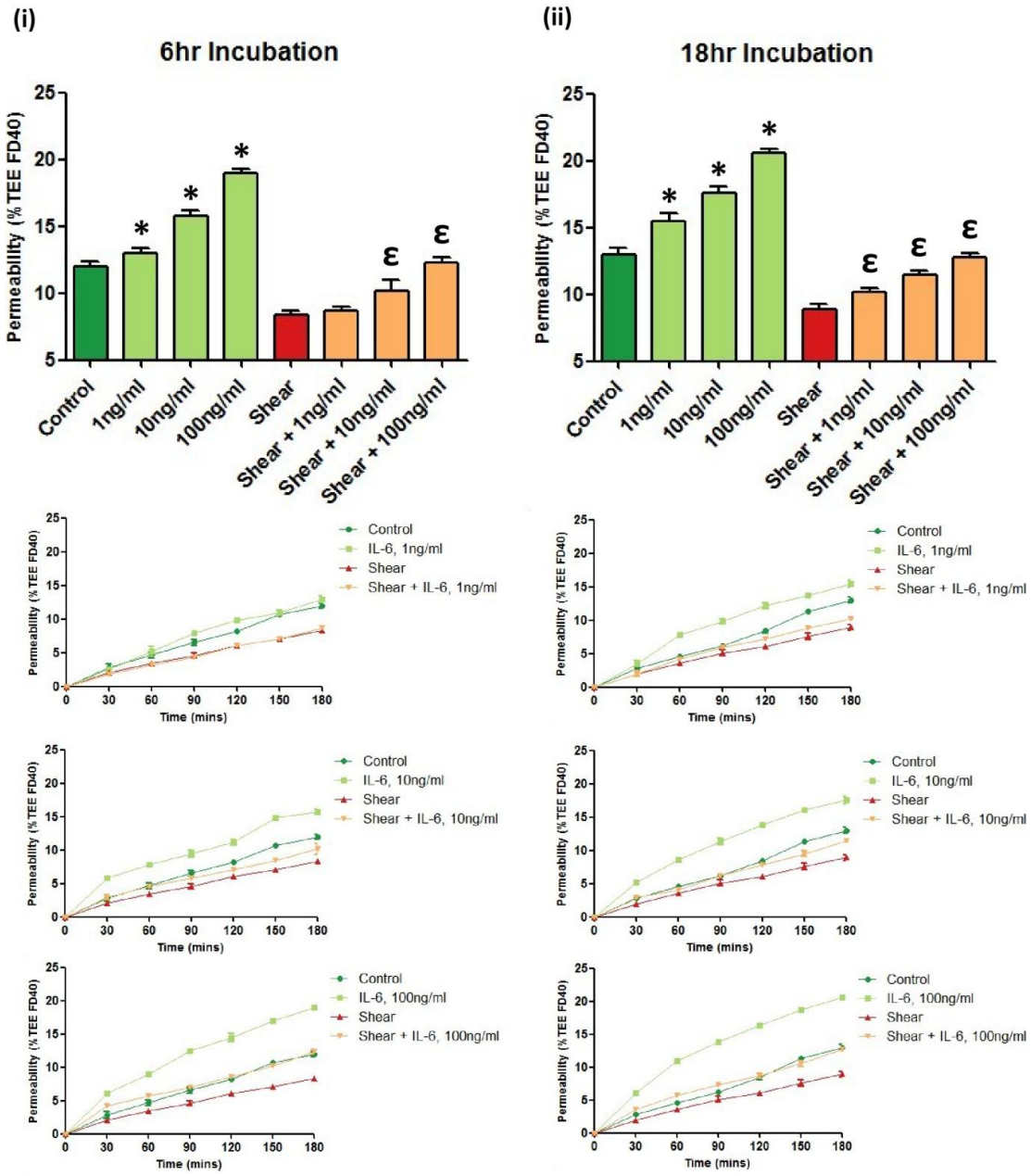

Figure 3.11: The effect of laminar shear stress on IL-6-induced injury of HBMvECs. Confluent HBMvECs were pre-conditioned by laminar shear stress (8 dynes cm^{-2}, 24 hr), following which IL-6 (0-100 ng/ml) was added to the cultures. The laminar shear stress was continued for an additional 6 or 18 hr. Post-treatment, the cultures were replated into transwell inserts and left to adhere overnight before being examined by transendothelial permeability. The histograms and line graphs show the change in permeability (%TEE FD40) at a given time point(s) (t) = 180 mins and 0-180 mins after 6 hr (i) and 18 hr (ii) exposure to TNF-α (0-100 ng/ml). Results are averaged from three independent experiments ± SD; *P≤0.05 vs. Unsheared Control. εP≤0.05 vs. Sheared Control.

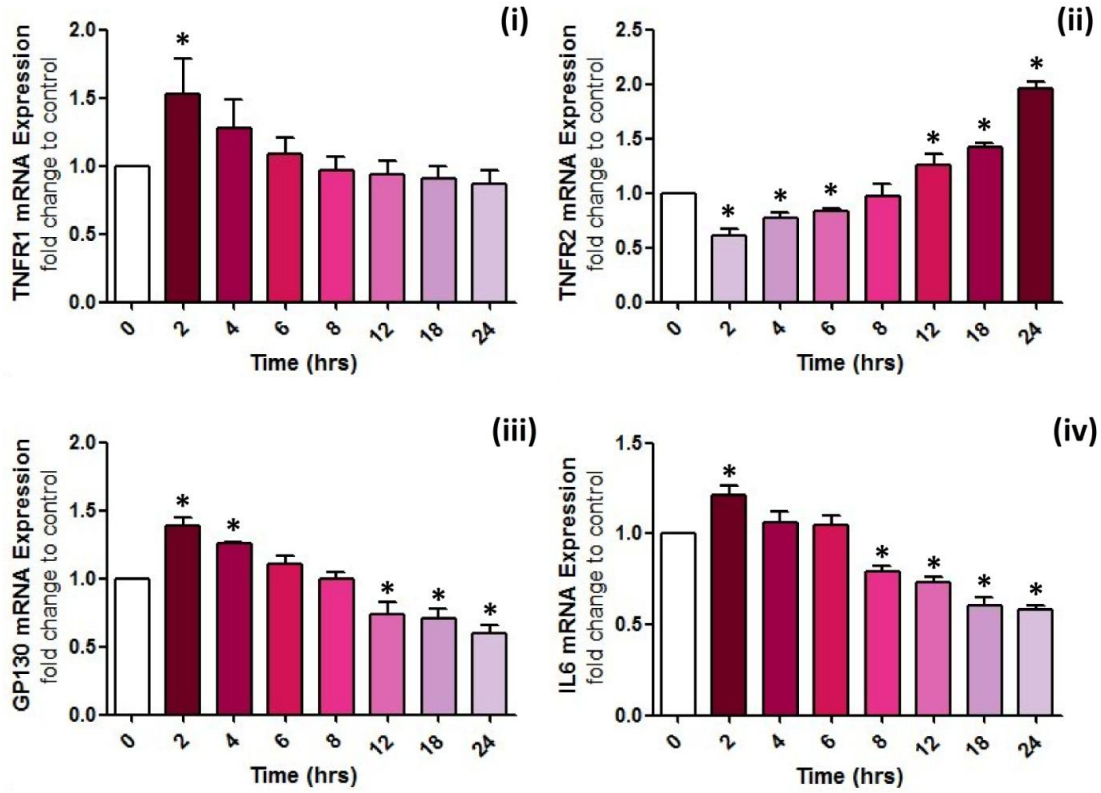

Figure 3.12: The effect of laminar shear stress on cytokines and their signal-transducing receptors. Confluent HBMvECs were exposed to laminar shear stress (8 dynes cm^{-2}, 0-24 hr) following which they were harvested for whole cell mRNA. The samples were analysed by qPCR for the transcriptional levels TNFR1 (i), TNFR2 (ii), GP130 (iii) and IL-6 (iv). Results are averaged from three independent experiments ± SD; *P≤0.05 vs. 0 hrs

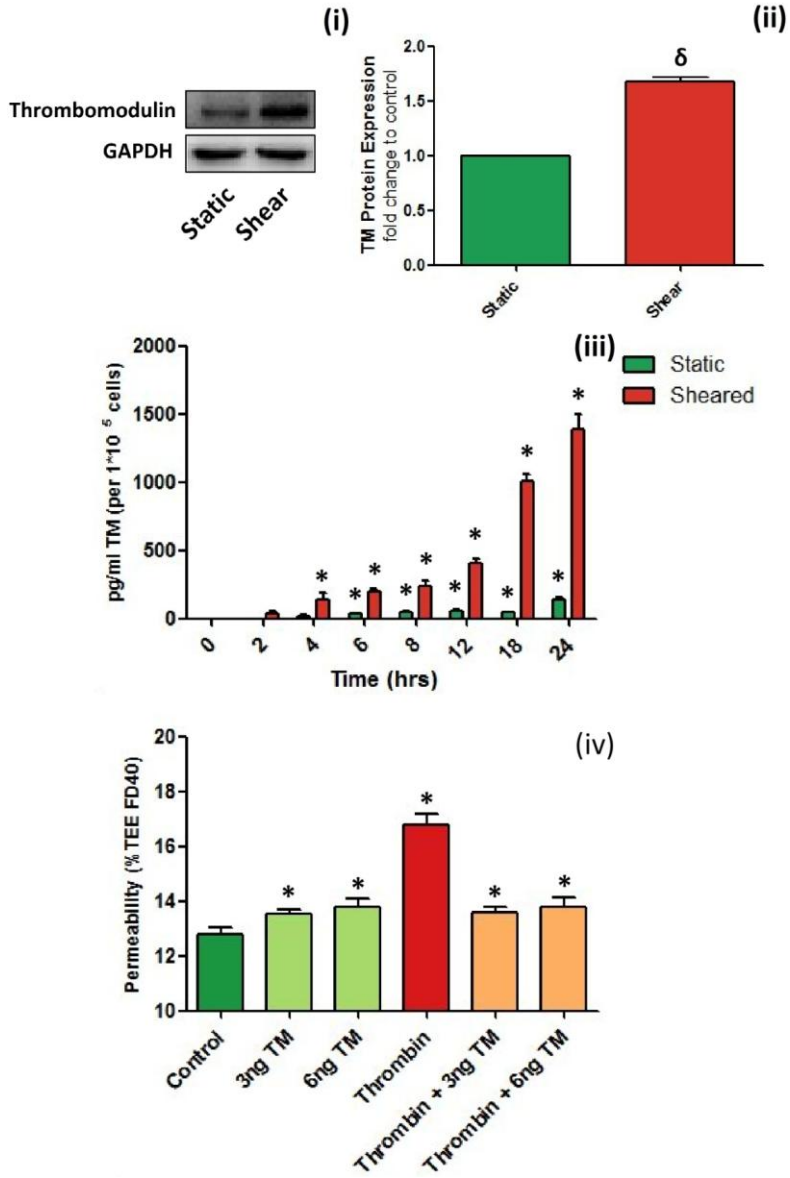

Figure 3.13: The effect of laminar shear stress on thrombomodulin expression, secretion and activity. Confluent HBMvECs were maintained under static conditions or exposed to laminar shear stress (8 dynes cm^{-2}, 0-24 hr) following which they were harvested for whole cell protein and conditioned medium. Whole cell protein lysate was examined by western blot to investigate the translational change in thrombomodulin expression (i, ii). The conditioned medium was examined by ELISA to monitor the effect on thrombomodulin release in the absence or presence of shear forces (iii). The activity of released thrombomodulin in conditioned medium was also examined by implementing barrier-permeabilising thrombin into a permeability assay. Conditioned medium was concentrated to a specific concentration of thrombomodulin as monitored by the ELISA (3 ng and 6 ng of TM) and added in tandem with 2U of thrombin to confluent HBMvEC cultures in transwell inserts for 30 mins. Post treatment, the confluent monolayers were examined for transendothelial permeability. The histograms shows the change in permeability (%TEE FD40) at (t) = 180 mins. Results are averaged from three independent experiments ± SD; *P≤0.05 vs. 0 hrs, *P≤0.05 vs. Unsheared Control, δP≤0.05 vs. Static

3.3 Discussion

Given the functional diversity and broad metabolic requirements of the brain, sustainment of homeostasis is of utmost importance. *In vivo*, the BBB is physiologically regulated by a number of signalling mediators that includes both humoral and hemodynamic stimuli. Together, these stimuli promote a BBB phenotype functionally capable of protecting the CNS from the fluctuations in concentrations of ions, neurotransmitters, blood-borne factors and particularly toxins/pathogens in the microenvironment that may disrupt neuronal/glial function. The majority of experimental data to date has focussed on co-culturing models that aim to recreate the BBB-inducing microenvironment, and whilst these models have proven invaluable in broadening our understanding of BBB, many lack the fundamental hemodynamic aspect. Shear stress plays a crucial role in neural homeostasis and pathophysiology of the cerebral microvasculature (Krizanac-Bengez, Kapural et al. 2003, Krizanac-Bengez, Mayberg et al. 2004, Krizanac-Bengez, Hossain et al. 2006, Krizanac-Bengez, Mayberg et al. 2006). In this chapter the aim was to investigate the effect of physiological levels of laminar shear stress on HBMvECs and to assess what impact (if any) was imparted on some of the key functional parameters associated with the BBB phenotype.

Our initial objective was to establish a culture regime in which HBMvEC phenotype could be sustained and thus characterised. Our HBMvECs were commercially bought and were primary-derived, thus expressing the phenotypic properties associated with BBB. However, differentiation to a 'default' endothelial phenotype is problem commonly associated with primary-derived endothelial cultures. Culture techniques absent of the requisite inductive forces necessary to stabilise phenotypic properties are the primary cause of such (Ballermann, Ott 1995, Ott, Ballermann 1995, Reichel, Begley et al. 2003). A number of molecular cell markers were selected for examination by qPCR, western blot and immunofluorescence. Once an effective culturing regime was established based on typical cell doubling time and morphological characteristics, the HBMvECs were harvested and prepared for analysis. vWF is a typical marker of endothelial cells (Jaffe, Nachman et al. 1973, Jaffe, Hoyer et al. 1973) and, according to the cell datasheet, is a routinely examined marker for confirming successful isolation of the cerebral endothelial tissue. We examined the expression of vWF and successfully verified its presence in the cell population in response to our culture conditions. An additional marker utilised by both the company from whom we procured the cells was ZO-1, an important physiological mediator of tight junction assembly (Lee, Zeng et al. 2006). As a primary focus of this thesis was to monitor the effect of different stimuli on HBMvEC barrier function, the sustained expression of intercellular junction proteins was of utmost importance. We examined the expression of ZO-1, claudin-5, VE-Cadherin and occludin and successfully verified their presence in the cell population

in response to our culture conditions, thus confirming we could effectively culture and maintain BBB properties in our primary-derived cultures, (Weksler, Subileau et al. 2005).

We next shifted our focus onto examining the effect of laminar shear stress on HBMvECs. In the absence of haemodynamic forces, confluent cultures of endothelial cells present a 'cobblestone'-like morphology. When we examined structural components of the cells, such as the actin cytoskeleton, we observed a lack of orientation, with the cell alignment random and multidirectional. Following exposure of the cell cultures to physiological levels of laminar shear stress (8 dynes cm^{-2}) (Desai, Marroni et al. 2002), the cell population became elongated with the primary axis orientated to the direction of the haemodynamic force (Goode, Davies et al. 1977, Nerem, Levesque et al. 1981). Subsequent examination of the actin cytoskeleton showed that the actin fibres had also become orientated in the direction of the flow vector, presenting a much more organised structure (Wechezak, Wight et al. 1989, Kim, Gotlieb et al. 1989, Kim, Langille et al. 1989, Galbraith, Sheetz 1998, Galbraith, Skalak et al. 1998). As one of our primary objectives was to examine the effect of laminar shear on barrier function and we had optimised a number of immunofluorescence labels for some of the intercellular junction proteins, we subsequently conducted some preliminary work on the localisation and expression of each protein following exposure to our shear stress regime. Cultures maintained in a static environment demonstrated consistent expression of each of the examined intercellular junction proteins of interest, with predominant localisation at the cell-cell border (Weksler, Subileau et al. 2005). In comparison, following exposure to laminar shear stress, a sharper, more well-defined localisation of each protein along the cell border was observed. Expression of each protein was enhanced with distribution more constant in comparison to static cultures. Previous work in our group demonstrated a similar response in ZO-1, claudin-5 and occludin in BBMvECs (Colgan, Ferguson et al. 2007, Walsh, Murphy et al. 2011).

In the early stages of model development, BBMvECs were often employed as a control given our groups experience with that particular cell line in the past (Colgan, Ferguson et al. 2007, Colgan, Collins et al. 2008, Walsh, Murphy et al. 2011). Previous work in our group using BBMvECs had demonstrated an increase in the expression of intercellular junction proteins following exposure to laminar shear stress by immunofluorescence techniques (Colgan, Ferguson et al. 2007, Walsh, Murphy et al. 2011). We decided to explore this increase in expression on a molecular level in both HBMvECs and BBMvECs. Following 24 hrs exposure to laminar shear stress the transcription levels for occludin, claudin-5, VE-Cadherin and ZO-1 displayed a significant increase in comparison to control static cultures. We carried this paradigm forward with HBMvECs to examine the effect of this increase on a translational level with a similarly significant increase in protein levels observed. Colgan

(Colgan, Ferguson et al. 2007) noted a similar increase in transcription and translation levels of both occludin and ZO-1 in BBMvECs following exposure to laminar shear stress. A number of other studies have reported similar trends with regards to the transcription and translation for both occludin and ZO-1 in addition to VE-Cadherin and claudin-5 in response to shear stress (Schnittler 1998, Cucullo, Hossain et al. 2011).

Following the shear-dependent trends observed with the intercellular junction proteins, we then decided to investigate whether any post-translational modifications were taking place following exposure to laminar shear stress. We found with regards to claudin-5, occludin and VE-Cadherin, that a significant reduction in the phosphorylation of tyrosine and threonine residues took place following 24 hrs exposure to laminar shear stress. This objective expanded on work previously done within our group; Walsh (2011) demonstrated a shear-induced reduction in pTyr levels of occludin in BBMvECs following exposure to laminar shear stress. A number of studies based in other vascular beds have also implicated tyrosine (Demaio, Chang et al. 2001, Young, Sui et al. 2003) and threonine (Soma, Chiba et al. 2004) in modulating endothelial barrier function. Additionally, this study primarily focussed one (i.e. the phosphorylation state) of many potential post-translational modifications of a number of key proteins examined can undergo. Protein turnover, trafficking and ubiquitination to name a few are critical aspects presently unexplored with respect to our body of work and are expected to play potentially as large a role of the phosphorylation state in HBMvEC barrier dynamics.

To summarise at this point, we could successfully maintain the HBMvEC phenotype and demonstrated that upon exposure to laminar shear stress, an upregulation in the key intercellular junction proteins was observed, in parallel with changes in their phosphorylation state (likely affecting tight junction assembly). We also decided to examine the impact of these expressional changes on HBMvEC barrier function. Induced expression of occludin and ZO-1 has previously been correlated to improved barrier function in BBMvECs (Colgan, Ferguson et al. 2007, Siddharthan, Kim et al. 2007, Colgan, Collins et al. 2008). Collins (Collins, Cummins et al. 2006) demonstrated that physiological cyclic strain of BAECs caused an increase in occludin expression in parallel with a reduction in phosphorylation of tyrosine and threoine residues, the cumulative effect of which coincided with an increase in barrier function. Using our established transwell permeability assay, we found that cultures pre-exposed to laminar shear stress demonstrated a significant reduction in permeability (ergo, a significant increase in barrier function) in comparison to control static cultures. Logically, the reduction in permeability could be attributed to the increase in intercellular junction protein levels (Colgan, Ferguson et al. 2007, Siddharthan, Kim et al. 2007, Colgan, Collins et al. 2008). In a parallel study, we utilised siRNA techniques to

ablate the presence of claudin-5 and VE-Cadherin independent of one another to investigate the impact of each protein's expression on barrier integrity. We found that independent knockout of claudin-5 and VE-Cadherin induced a significant increase in monolayer permeability. This reduction in barrier was consistent with similar studies in which interference with/knockout of VE-Cadherin (Xu, Waters et al. 2007) and claudin-5 (Nitta, Hata et al. 2003, Argaw, Gurfein et al. 2009, Morrow, Tyagi et al. 2009) lead to disruption of the cellular barrier properties. Thus, if knockout of their expression induces a significant reduction in barrier function, an increase in their expression should (as was demonstrated) result in a subsequent increase in barrier function.

The effect of interfering with phosphorylation events on shear-induced barrier enhancement was also investigated. Interestingly, cultures pre-exposed to laminar shear stress in the presence of a tyrosine phosphatase inhibitor, dephostatin, demonstrated a significant blockade in the shear-mediated reduction of permeability, strongly implicating tyrosine dephosphorylation as a key mechanism in the protective effect of laminar shear stress on HBMvEC cultures. Walsh (2011) demonstrated a similar effect in BBMvECs based on the blockade of shear-induced occludin pTyr dephosphorylation using dephostatin. A study by Takenaga (2009) adds weight to this notion by showing that inhibition of tyrosine phosphorylation of occludin reduced BBB leakage in isolated brain capillaries. Whilst much has been reported on the phosphorylation of TJ/AJ proteins with respect to barrier modulation, data specific to the human brain microvasculature is limited. Whilst studies have demonstrated that injury-induced elevation of pTyr and pThr levels on the interendothelial junction proteins correlated with increased BBB dysregulation (Soma, Chiba et al. 2004, Haorah, Knipe et al. 2005, Haorah, Heilman et al. 2005, Stamatovic, Dimitrijevic et al. 2006, Yamamoto, Ramirez et al. 2008, Willis, Meske et al. 2010), very little focus has been placed upon the relationship between protective forces (i.e. shear stress) and phosphorylation (and in particular on pThr phosphorylation events). In one of the few studies pertaining to this area, Walsh (2011) demonstrated silencing of VE-Cadherin in BBMvECs had a significant impact on the shear-induced dephosphorylation of occludin which in turn had a negative impact on monolayer barrier function. This identified a novel cross-talk between VE-Cadherin and occludin suggesting occludin's functional capacity would reduce in the absence of VE-Cadherin underlying the importance of VE-Cadherin in BBB formation and sustainment. Our studies represent the first comprehensive approach to examining these events within the human BBB.

Having confirmed that laminar shear stress can induce barrier 'strengthening' in confluent HBMvEC cultures, we decided to test the degree of barrier protection exerted by shear in the presence of an injurious stimulus. A number of inflammatory cytokines have been shown to

exert a destabilising effect on endothelial barriers (the effect of TNF-α and IL-6 is covered in more detail in Chapter 4). We aimed to investigate the co-exposure of HBMvECs to laminar shear stress and inflammatory cytokines to determine if the protective influence of shear extends to a pro-inflammatory injury. We found that exposure of HBMvECs to laminar shear stress in the presence of either TNF-α or IL-6 (1-100 ng/ml) gave lower absolute increases in FITC-Dextran flux when compared to treatment of static cultures with cytokines alone. We concluded from this that shear stress can protect barrier phenotype within the cerebral endothelium from other pro-inflammatory stimuli. Consistent with this, Yoshizumi (2003) demonstrated in HUVECs that steady laminar flow inhibited cytokine-activation of MAPK pathways. A number of other studies corroborate the protective influence shear stress has in tissue simultaneously exposed to inflammatory stimuli (Surapisitchat, Hoefen et al. 2001, Berk, Abe et al. 2001, Berk, Min et al. 2002, Yamawaki, Lehoux et al. 2003, Ni, Hsieh et al. 2004).

Overall, the reduction in cytokine induced damage could be possibly accredited to the increase in the expression of intercellular junction proteins and/or the shear-dependent tyrosine and threonine dephosphorylation of interendothelial junction proteins. Other mechanisms cannot be excluded. For example, nitric oxide is a key component in the regulation of vascular tone, and has been shown to induce a number of protective properties within the vascular walls (Harrison, Widder et al. 2006). Physiological laminar shear stress represents the most potent stimulus for continuous production of NO by the endothelium, an effect mediated at both the transcriptional level (via upregulation of eNOS (Lam, Peterson et al. 2006)) or at the translational level (via eNOS protein phosphorylation and activation (Go, Boo et al. 2001)). Thus, disturbance or removal of shear stress drastically reduces the bioavailability of NO in the afflicted area exposing the endothelium to the dysfunctional effect of local and systemic risk factors (Ziegler, Bouzourene et al. 1998, Ziegler, Silacci et al. 1998, Qiu, Tarbell 2000, Cheng, van Haperen et al. 2005, Harrison, Widder et al. 2006, Gambillara, Chambaz et al. 2006). Reduction or removal of shear forces has also been seen to promote damaging effects such as ROS (Mohan, Koyoma et al. 2007) (examined in greater detail in Chapter 5). Enhancement of the transcription and post transcriptional activity of major oxidative enzymes such as (NADPH) oxidase and xanthine oxidase has been reported in endothelium in the absence of non-physiological levels of shear stress (McNally, Davis et al. 2003, Hwang, Saha et al. 2003, Hwang, Ing et al. 2003, Harrison, Widder et al. 2006). Parallel to this, a reduction in ROS scavengers such as manganese superoxide dismutase and glutathione may further augment ROS damage (Mueller, Widder et al. 2005). Importantly, our work also demonstrated the influence of shear on cytokine signal-transducing receptors; TNFR1, TNFR2 and gp130. We found that within 2 hrs of

exposure to laminar shear stress, each cytokine receptor demonstrated a significant change in mRNA levels; TNFR1 and gp130 both increased while TNFR2 was decreased. Within 8 hrs, transcription levels for all three returned to baseline levels and in the case of TNFR1, this level was sustained up to 24 hrs. In contrast, TNFR2 transcription levels continued to rise with a significant increase observed after 24 hrs. Several experimental paradigms have investigated the independent effects of cytokine-receptor expression and hemodynamic forces on mediating cytokine-receptor signalling, however studies are scarce in relation to the effect of said hemodynamic forces on cytokine-receptor expression, particularly in the microvasculature of the brain. Whilst we have yet to examine the effect of shear stress on cytokine-receptor protein level, similar studies in other cell models have noted a similar 'protective' effect imparted by hemodynamic forces in relation to the expression, and mostly cleavage, of cytokine receptors. Wang (Wang, Lv et al. 2011) observed a reduction in TNF-α-induced apoptosis via shear stress-induced reduction of TNFR1 cell-surface expression.

We expanded this study to include some of the factors known to be released by HBMvECs and in some cases transduce their signal through these surface receptors. For instance, we found in the case of IL-6, mRNA levels spiked within 2 hrs of shear exposure. However, within 24 hrs an overall decrease in IL-6 levels was observed. Given the parallel reduction in gp130 receptor expression in conjunction with IL-6 ligand, this relationship may represent an additional reason for the shear-induced reduction in cytokine afflicted damage to HBMvEC barrier integrity. Interestingly, a significant increase in IL-6 protein expression was observed following shear, in contrast to our mRNA studies. We also examined the effect of laminar shear stress on IL-6 release. Interestingly, laminar shear stress drove up the release of IL-6 within 2 hrs as compared to static control cells. However, this spike in IL-6 release plateaued from 8 hrs onward in contrast to control static cultures. It is plausible that laminar shear stress, despite causing a surge in the acute phase of exposure, downregulates cytokine production and release over chronic time frames (i.e. beyond the experimental 24 hrs). This is consistent with a study by Passerini (Passerini, Polacek et al. 2004) that demonstrated a reduction in the transcription levels *in vivo* for a number of pro-inflammatory cytokines (IL-6 included) in areas pre-disposed to uniform laminar shear stress as compared to areas of disturbed flow. Conversely, *in vitro*, shear stress has been shown to stimulate the release of IL-6 from endothelial cells (Sterpetti, Cucina et al. 1993, Krizanac-Bengez, Kapural et al. 2003) though studies examining this relationship in the microvasculature, much like that of the cytokine-receptors, are scarce.

Laminar shear stress appeared to be a positive influence on our HBMvEC cultures, inducing a 'protected' phenotype via augmentation of integral proteins (i.e. the intercellular junctions) and repression of pro-inflammatory mediators and their receptors (e.g. IL-6 and gp130).

Tian (2013) previously demonstrated how exposure of rat BMvEC to laminar shear stress reduced ischemia-induced apoptosis. Song (2001) demonstrated how chronic exposure of BMvECs to laminar shear stress reduced the expression of adhesion molecules implicated in the recruitment of immune cells which accelerate inflammatory responses (i.e. ICAM-1). Aside from driving down the release of pro-inflammatory mediators, we investigated whether laminar shear stress could induce the release of any anti-inflammatory mediators. Since a pivotal function of the endothelium is to regulate the coagulation cascade by maintaining anticoagulant activity and an anti-thrombotic surface, we investigated this hypothesis via thrombomodulin, an endothelial surface molecule capable of converting pro-inflammatory/pro-coagulant thrombin to an anti-coagulant molecule upon binding (Dittman, Majerus 1990). Following exposure to laminar shear stress, thrombomodulin protein expression and release was significantly increased in comparison to control static cultures. This was consistent with results obtained in other microvascular endothelial cell models (Takada, Shinkai et al. 1994, Kawai, Matsumoto et al. 1997, Ishibazawa, Nagaoka et al. 2011). We decided to further expand this concept by attempting to test the potency/activity of the shear-released thrombomodulin. HBMvEcs were prepared for assessment of barrier function in response to pro-inflammatory thrombin by our transwell permeability assays. Binding of thrombin to its receptor PAR-1 has been proven to cause a number of pro-inflammatory gene expressional changes in ECs that induces an increase in paracellular permeability (Bogatcheva, Garcia et al. 2002, Guan, Sun et al. 2004), in addition to promoting coagulation via platelet activation and several pro-coagulant factors. We observed that shear-conditioned medium (containing released thrombomodulin) could neutralise the ability of thrombin to induce HBMvEC barrier dysfunction. This not only confirmed our hypothesis that laminar shear stress also induced the release of barrier-protective agents, but also confirmed a role for laminar shear stress in mediating the anti-coagulative phenotype associated with a healthy endothelium. The concept that increased endothelial release of thrombomodulin acts as a protective agent within the vasculature has been explored *in vivo* and is consistent with our data (Giwa, Williams et al. 2012).

In parallel studies, the effect of laminar shear stress on vWF; a co-factor for a number of molecules involved in the coagulation cascade, was investigated. Although vWF release in has yet to be explored in our model, its transcription levels displayed a significant decrease after 24 hrs exposure to laminar shear. In contrast, a significant increase in translational levels was observed in whole cell protein lysate. Galbusera (1997) observed an increase in endothelial release of vWF following exposure to shear stress. Having observed a negligible change in the transcription levels of the protein, they accredited the consequent increase in vWF release to shear-mediated enhancement of secretory pathways. However, their

exposure times were within the confines in which we also saw very little change. Similar to the trends seen with IL-6, it is possible that laminar shear stress may downregulate vWF production and release over chronic time frames. *In vivo* studies have shown areas predisposed to disturbed shear demonstrate elevated vWF expression and release, highlighting the potential role of laminar shear stress on regulating vWF pro-coagulant activity (Rand, Badimon et al. 1987, Wu, Drouet et al. 1987, Badimon, Badimon et al. 1993).

In conclusion, we have comprehensively demonstrated how laminar shear stress plays a pivotal role in the maintenance of vascular homeostasis and BBB phenotype through modulation of interendothelial protein expression and post-translational modification, as well as modulation of endothelial anti-inflammatory mechanisms and responsiveness to cytokine injury.

Chapter 4:

The effects of inflammatory cytokines; TNF-α and IL-6, on HBMvEC blood-brain barrier properties.

4.1 Introduction

In chapter 3, the effects of physiological levels of blood flow-associated laminar shear stress on HBMvEC cultures were investigated. Following exposure, several aspects of the BBB phenotype were seen to be enhanced. Transcription and translation of most of the key proteins that comprise the tight and adherens junctions were seen to be upregulated. Parallel immunofluorescence studies demonstrated this increase coincided with an enhancement in said protein localisation at the cell-cell borders. In addition, each protein was seen to undergo post-translational modification, with tyrosine and threonine residues dephosphorylated; a process that upon inhibition partially reduced the shear-mediated increase in HBMvEC barrier function implicating phosphorylation as a key regulatory event in HBMvEC barrier regualtion. Moreover, laminar shear stress also appeared to exert a 'protective' effect on the endothelium by promoting a number of anti-inflammatory mechanisms as seen by the simultaneous release of anti-inflammatory molecules, and reduction in pro-inflammatory mediators and their signal-transducing receptors. Taken together, laminar shear stress was seen to promote a protected BBB phenotype, so much so that in the presence of inflammatory cytokines, laminar shear stress exerted a protective effect, partially ameliorating their well characterised BBB-destabilising effects.

Overall, the inductive and protective effect of laminar shear stress on BBB phenotype was comprehensively investigated in chapter 3. Several studies have demonstrated the inductive effect of haemodynamics forces on the endothelium across several vascular beds, with abrogation of these forces promoting entirely different endothelial phenotypes (Davies 1995). Several points within the vasculature (i.e. bifurcations, branching points and curvatures) experience low or disturbed shear stress profiles. Several mechanoreceptors detect these changes and generate an integrative response which typically results in changes in the profiles of nitric oxide and reactive oxygen species, while several classical signalling pathways involving kinases and GTPases are altered in parallel to multiple transcription factors. Chronic attenuation of shear stress activates several pro-inflammatory pathways, resulting in a drastic remodelling of the endothelium that coincides with altered functions; causing a pro-coagulant surface, increased expression of adhesion receptors, the active recruitment of immune cells and an overall reduction in barrier function (Hahn, Schwartz 2009). With regards to the NVU, said dysfunction of the cerebral endothelium that comprises the BBB is associated with the pathophysiology of several neurological disorders (e.g. stroke, multiple sclerosis, Alzheimer's disease). Therefore, understanding the mechanisms that underlie BBB dysfunction may lead to the identification of new therapeutic targets.

Aside from haemodynamic forces, several other local and systemic environmental factors can mediate inflammatory events in the brain, leading to BBB dysfunction. Growth factors, cytokines, hormones, lipids, electrolytes, bacterial and viral products are just some of the many factors present in the circulation or secreted by cell-types in the microenvironment that can impact greatly on endothelial phenotype and thus function (Charo, Ransohoff 2006). ***For chapter 4, we decided to focus the parallel pathophysiological aspect of our study on a selection of inflammatory cytokines known to be present in the cerebromicrovasculature; TNF-α, IL-6 and MCP-1.*** Cytokines can activate a myriad of signalling pathways that at times can be beneficial, although increased levels are more commonly associated with the initiation, progression and activation of several neurological diseases, mediated in part via dysfunctional endothelium and BBB disruption (Abbott 2000, Hawkins, Davis 2005). Unlike laminar shear stress, a wealth of data is available directly linking the effects of cytokines to numerous cerebral processes, be they beneficial or harmful. However, the direct and indirect effect of these cytokines on interendothelial TJ/AJ properties, particularly on primary human brain microvascular endothelial cultures, is limited.

4.1.1 Study Aims

In this chapter we examine the individual impact of inflammatory cytokines; TNF-α and IL-6, on HBMvEC blood-brain barrier phenotypic properties. Therefore, the overall aims of this chapter include:

- To conduct basic characterisation studies of TNF-α and IL-6 on HBMvECs.
- To investigate the effect of TNF-α and IL-6 on TJ/AJ protein (occludin, claudin-5, VE-Cadherin, ZO-1) transcriptional and translational expression.
- To investigate the effect of TNF-α and IL-6 on TJ/AJ protein phosphorylation.
- To investigate the effect of TNF-α and IL-6 on HBMvEC barrier function.
- To determine if TNF-α and IL-6 influence HBMvEC anti-inflammatory properties.

4.2.1 Exposure of HBMvECs to TNF-α or IL-6 has no significant impact on cell viability

The effect of TNF-α and IL-6 on HBMvEC viability was examined (Figure 4.1-4.5). Confluent HBMvECs were stimulated with TNF-α or IL-6 (0-100 ng/ml) for 6 or 18 hrs. Post-treatment, cells were harvested and prepared for analysis by flow cytometry. Annexin V and PI stains were employed to assess the stage and respective degree of cytokine-induced damage. Using parameters deduced from positively stained cells (Figure 4.1), there were no significant changes in cell viability, membrane disruption or necrosis induced by TNF-α or IL-6 with respect to either dose or time (Figure 4.2-4.4). Complimentary studies examined the effect of TNF-α and IL-6 on other aspects pertaining to endothelial homeostasis (Figure 4.5). Confluent HBMvECs of a known density were stimulated with TNF-α or IL-6 (0-100 ng/ml) for 6 or 18 hrs. Post-treatment the conditioned medium was harvested and replated into fresh cultures dishes. The metabolic activity of treated cells was examined using MTS reagent. A significant decrease in metabolic activity with respect to time and dose was observed in response to TNF-α and IL-6 treatment (i, iv). In parallel, the replated harvested medium was examined for LDH release. No significant changes in LDH levels were observed after 6 hrs treatment with TNF-α or IL-6 across all doses; although slight-to-moderate increases after 18 hrs treatments were observed with both cytokines (ii, v). Finally the cellular morphology and adhesion profile of HBMvECs in response to TNF-α and IL-6 was examined using the xCelligence® system. HBMvECs were seeded to a known density on E-Plates and allowed to adhere overnight. The following day the cultures were treated with TNF-α or IL-6 (0-100 ng/ml) and monitored for 24 hrs. The xCelligence® data showed a slight non-significant decrease in HBMvEC Cell Index (%) in response to TNF-α and IL-6 with respect to dose and time indicating that the cellular monolayer remained intact throughout the treatment (iii, vi). This data was backed up by bright field microscope observations.

4.2.2 Exposure of HBMvECs to either TNF-α, IL-6 or MCP-1 initiates the expression and release of inflammatory mediators

The effect of TNF-α, IL-6 and MCP-1 on the secretory profile of HBMvECs was examined (Figure 4.6). Confluent HBMvECs were stimulated with TNF-α, IL-6 or MCP-1 (0-100 ng/ml) for 6 or 18 hrs. Post-treatment, cells were harvested for whole cell protein lysate and conditioned medium for analysis by multiplex ELISA. The multiplex ELISA facilitated the concurrent examination of four well known inflammatory mediators; IFNγ, IL-1β, IL-6 and TNF-α (i, ii). Post-analysis, interesting trends such as the release of IL-6 were repeated on standard single-plex ELISAs to verify multiplex results. TNF-α, IL-6 and MCP-1 all induced

a significant increase in IL-6 release from HBMvECs in both a time- and dose-dependent manner in comparison to control cultures (iii).

The effect of TNF-α and IL-6 on the release of other injury markers, namely thrombomodulin (Figure A.8) and vWF (Figure A.9) was also investigated. These cytokines had contrasting effects on each marker. A significant decrease in thrombomodulin protein expression was observed in HBMvECs in response to TNF-α with respect to dose and time (Figure A.8; i, iii). However, a significant increase was observed in secreted thrombomodulin in conditioned medium (v, vii). In contrast a significant increase in vWF protein and mRNA expression was observed in response to TNF-α with respect to dose and time (Figure A.9; i, iii, v, vii). A similar trend is observed in parallel experiments utilising IL-6 in place of TNF-α (Figure A.8 and A.9; ii, iv, vi, viii).

4.2.3 Exposure of HBMvECs to TNF-α and IL-6 induces a downregulation of barrier function

The effect of TNF-α and IL-6 on the barrier function of HBMvECs was examined (Figure 4.7). HBMvECs were seeded at a known density into transwell inserts and left to adhere overnight. The following day the confluent HBMvECs were stimulated with TNF-α or IL-6 (0-100 ng/ml) for 6 or 18 hrs. Post-stimulation, the cellular monolayers were assessed for transendothelial permeability. Exposure of HBMvECs to either cytokine results in a significant increase in FITC-Dextran paracellular flux (%TEE of FD40) across the cell monolayer with respect to dose and time (i-viii).

4.2.4 Exposure of HBMvECs to TNF-α and IL-6 induces a downregulation of the transcriptional levels of interendothelial junction proteins; occludin, claudin-5, VE-Cadherin and ZO-1

The effect of TNF-α and IL-6 on the expression of proteins involved in forming the intercellular junctions of the BBB was examined on the transcriptional level (Figure 4.8). Confluent HBMvECs were stimulated with TNF-α or IL-6 (0-100 ng/ml) for 6 or 18 hrs before being harvested for whole cell mRNA. The mRNA levels of occludin, claudin-5, VE-Cadherin and ZO-1 were examined by qPCR. Each protein demonstrated a significant decrease in their mRNA levels following exposure to either TNF-α or IL-6 in both a time- and dose-dependent manner in comparison to control cultures (i-viii).

The effect of TNF-α and IL-6 on cytokine signal-transducing receptors over time was also examined on a transcriptional level (Figure A.10). Confluent HBMvECs were stimulated with TNF-α or IL-6 (0-100 ng/ml) for 0-24 hrs before being harvested for whole cell mRNA. The mRNA levels of TNF-α receptors TNFR1 and TNFR2 and IL-6 receptor GP130 were examined from 0-24 hrs by qPCR. A significant increase was observed for all three receptors in response to acute cytokine treatment (0-4 hrs). TNFR1 and GP130 transcription levels continued to increase in response to either cytokine up to 24 hrs. Conversely, TNFR2 returned to baseline levels within 8 hrs of TNF-α or IL-6 stimulation and continued to decrease thereafter.

4.2.5 Exposure of HBMvECs to TNF-α and IL-6 induces a downregulation of the translational levels of interendothelial junction proteins; occludin, claudin-5, VE-Cadherin and ZO-1

The effect of TNF-α and IL-6 on the expression of proteins involved in forming the intercellular junctions of the BBB was examined on the translational level (Figure 4.9). Confluent HBMvECs were stimulated with TNF-α or IL-6 (0-100 ng/ml) for 6 or 18 hrs before being harvested for whole cell protein lysate. The protein levels of occludin, claudin-5, VE-Cadherin and ZO-1 were examined by western blot (i, ii). Each protein demonstrated a significant decrease in their transcription levels following exposure to TNF-α or IL-6 in both a time and dose-dependent manner in comparison to control cultures (iii-x).

4.2.6 Exposure of HBMvECs to TNF-α and IL-6 increases phosphotyrosine and phosphothreonine levels of occludin, claudin-5 and VE-Cadherin

The effect of TNF-α and IL-6 on the phosphorylation levels of tyrosine and threonine residues of interendothelial junction proteins occludin, claudin-5 and VE-Cadherin was examined (Figure 4.10, 4.11). Confluent HBMvECs were stimulated with TNF-α or IL-6 (0-100 ng/ml) for 6 or 18 hrs before being harvested for whole cell protein lysate. Samples were then subjected to immunoprecipitation and western blot analysis for phosphotyrosine (pTyr)- and phosphothreonine (pThr)-levels. pTyr- and pThr-levels for occludin, claudin-5 and VE-Cadherin were seen to be significantly increased in both a time- and dose-dependent manner following exposure to TNF-α (Figure 4.10) or IL-6 (Figure 4.11) in comparison to control cultures.

4.2.7 Exposure of HBMvECs to TNF-α and IL-6 induces a downregulation of barrier function via tyrosine kinase activity

The effect of TNF-α and IL-6 on the barrier function of HBMvECs was examined with a focus on the role to tyrosine kinases (Figure 4.12). HBMvECs were seeded at a known density into transwell inserts and left to adhere overnight. The following day the confluent HBMvECs were pre-treated with genistein 1 hr prior to stimulation with either TNF-α or IL-6 (0-100 ng/ml) for 6 or 18 hrs. Post-stimulation, the cellular monolayers were assessed for transendothelial permeability. Exposure of HBMvECs to TNF-α (i-iv) and IL-6 (v-viii) results in a significant increase in FITC-Dextran paracellular flux (%TEE of FD40) across the cell monolayer with respect to dose and time. The cytokine-induced increase of permeability in HBMvECs was significantly attenuated when genistein was present during exposure of the cultures to TNF-α or IL-6.

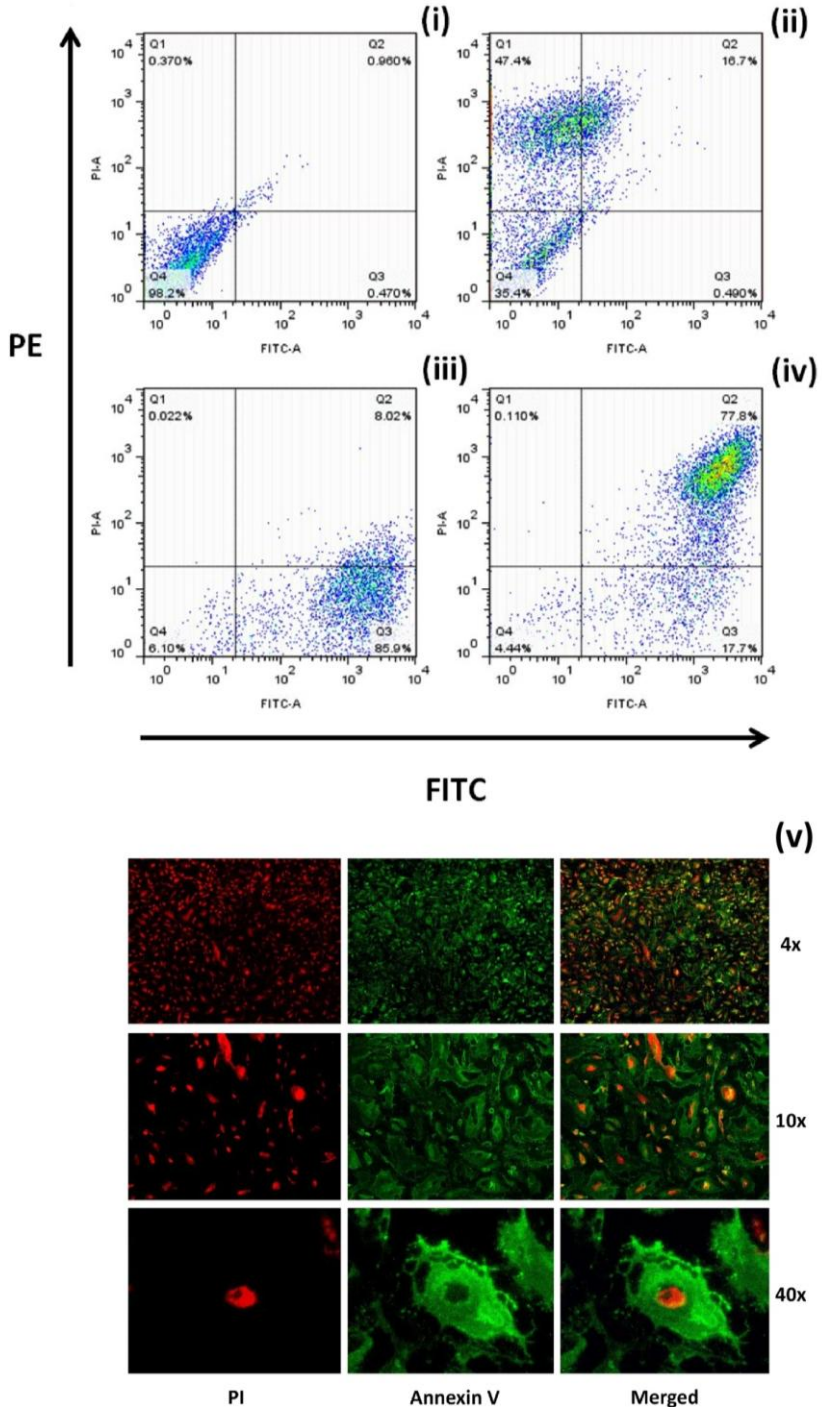

Figure 4.1: The effect of H_2O_2 on HBMvEC Viability-Flow Cytometry, Positive Controls. In order to effectively gate cell viability by means of flow cytometry, positively stained cells were required. Confluent HBMvECs were stimulated with 1 mM H_2O_2 overnight. The following day the entire cell population was harvested and prepared for flow cytometry analysis accordingly. The dot plots represent unstained control (i), injured cells single stained with PI (ii), injured cells single stained with Annexin V (iii) and injured cells double stained with PI and Annexin V (iv). The efficacy of the flow cytometry stains was also examined by immunofluorescence. HBMvECs were seeded onto coverslips and grown to confluency before being treated with 1mM H_2O_2 overnight. The following day the coverslips were stained with Annexin V and PI and examined by immunofluorescence microscopy (v). Images are representative.

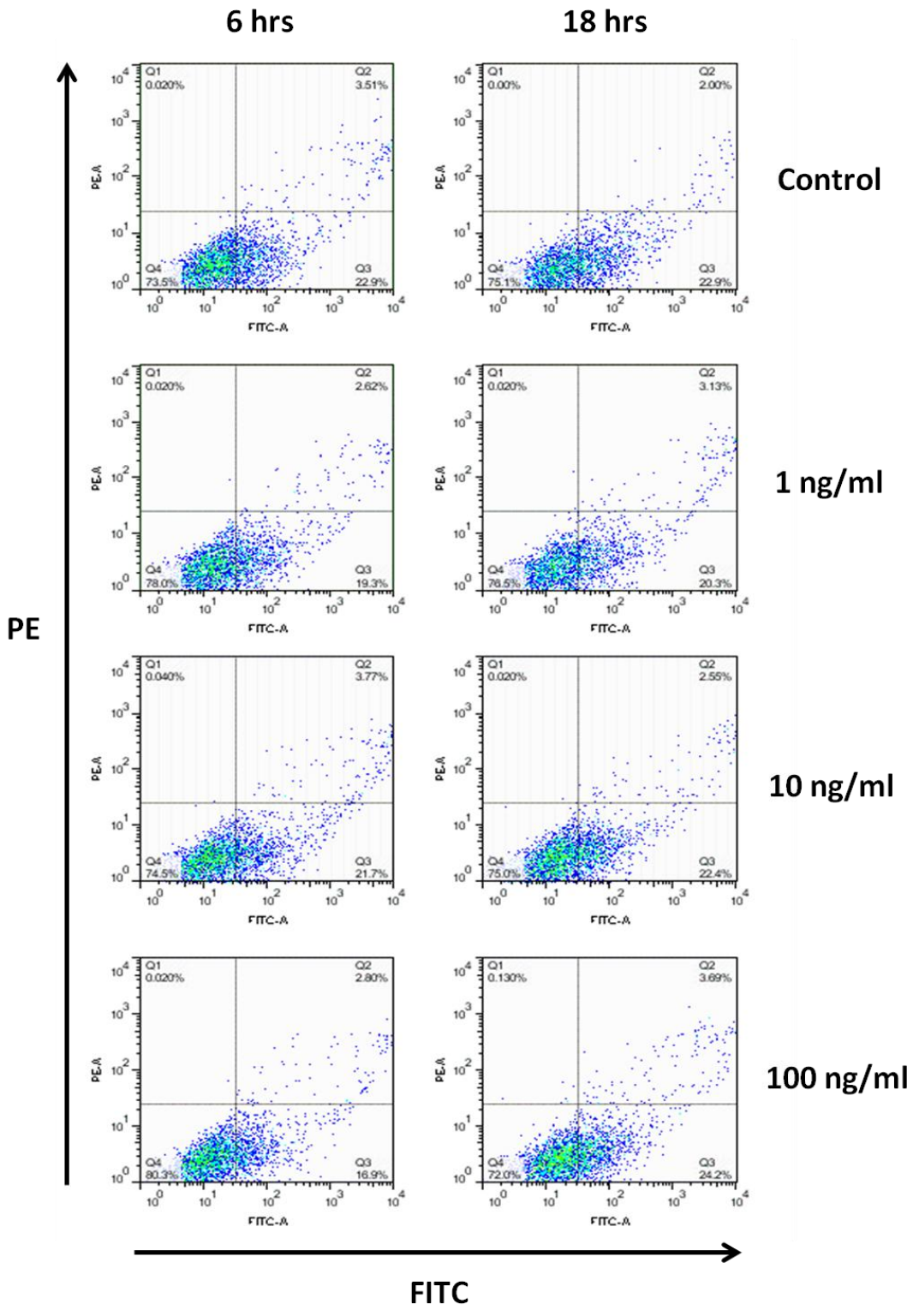

Figure 4.2: The effect of TNF-α on HBMvEC viability-Flow Cytometry. Confluent HBMvECs were stimulated with TNF-α (0-100 ng/ml) for 6 and 18 hr, respectively. Post-treatment the entire cell population was harvested and subsequently prepared for flow cytometry analysis using Annexin V and PI stains. The dot plots represent the spread of the cell populations as a result of the flow cytometry stains, which reflect the degree of injury inflicted by TNF-α. Dot plots are representative of three independent experiments.

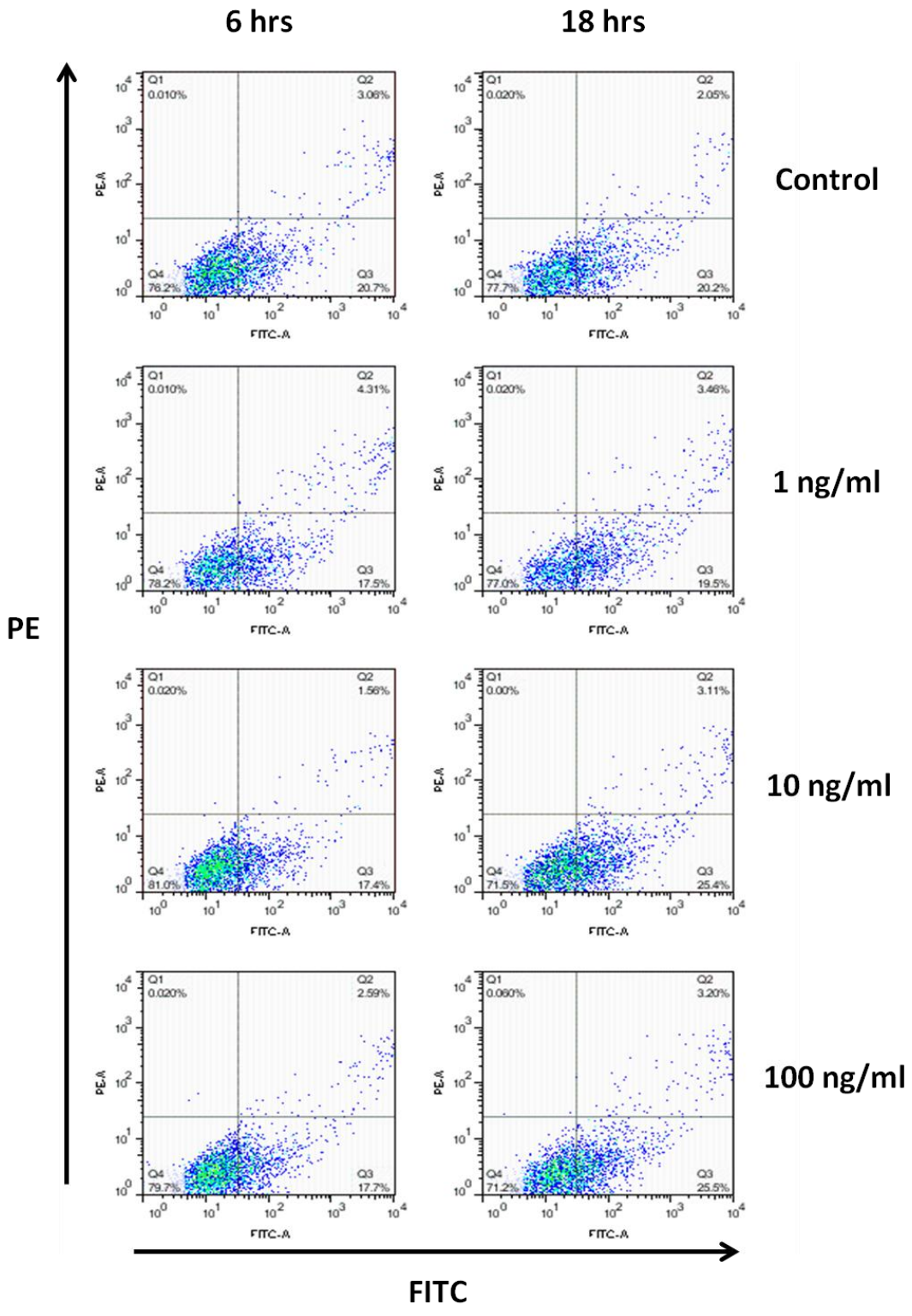

Figure 4.3: The effect of IL-6 on HBMvEC viability-Flow Cytometry. Confluent HBMvECs were stimulated with IL-6 (0-100 ng/ml) for 6 and 18 hr, respectively. Post-treatment the entire cell population was harvested and subsequently prepared for flow cytometry analysis using Annexin V and PI stains. The dot plots represent the spread of the cell populations as a result of the flow cytometry stains which, reflect the degree of injury inflicted by IL-6. Dot plots are representative of three independent experiments.

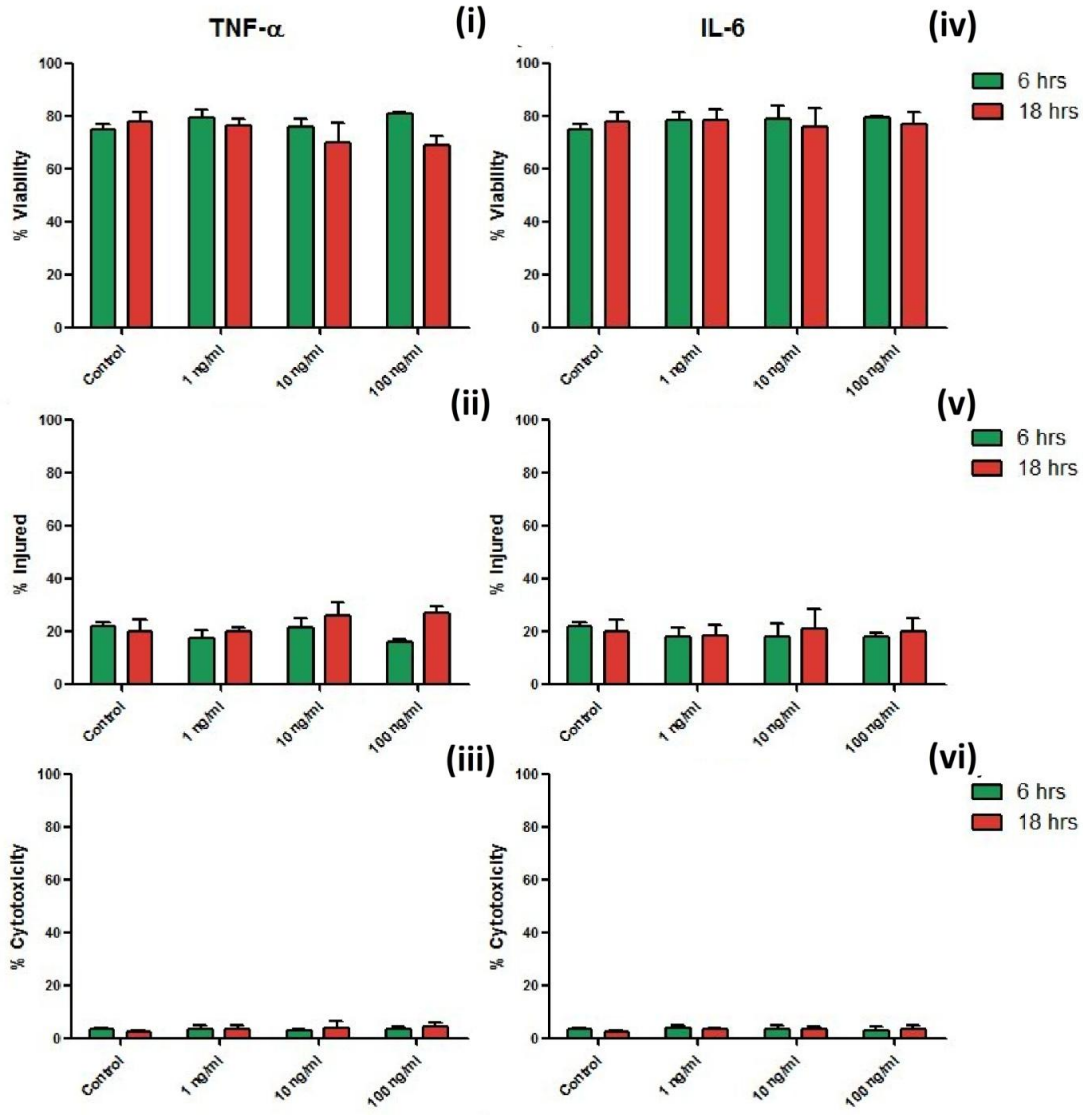

Figure 4.4: The effect of TNF-α and IL-6 on HBMvEC viability-Flow Cytometry Analysis. Confluent HBMvECs were stimulated with TNF-α or IL-6 (0-100 ng/ml) for 6 and 18 hr. Post-treatment, cells were harvested and subsequently prepared for flow cytometry analysis using Annexin V and PI stains. The dot-plots for each cytokine-treated sample (Fig. 4.2 and 4.3) were analysed using FlowJo Flow Cytometry Analysis Software to identify the viable (i, iv), injured (ii, v) and cytotoxic (iii, vi) cell populations in response to TNF-α (LHS) and IL-6 (RHS). Results are averaged from three independent experiments ± SD.

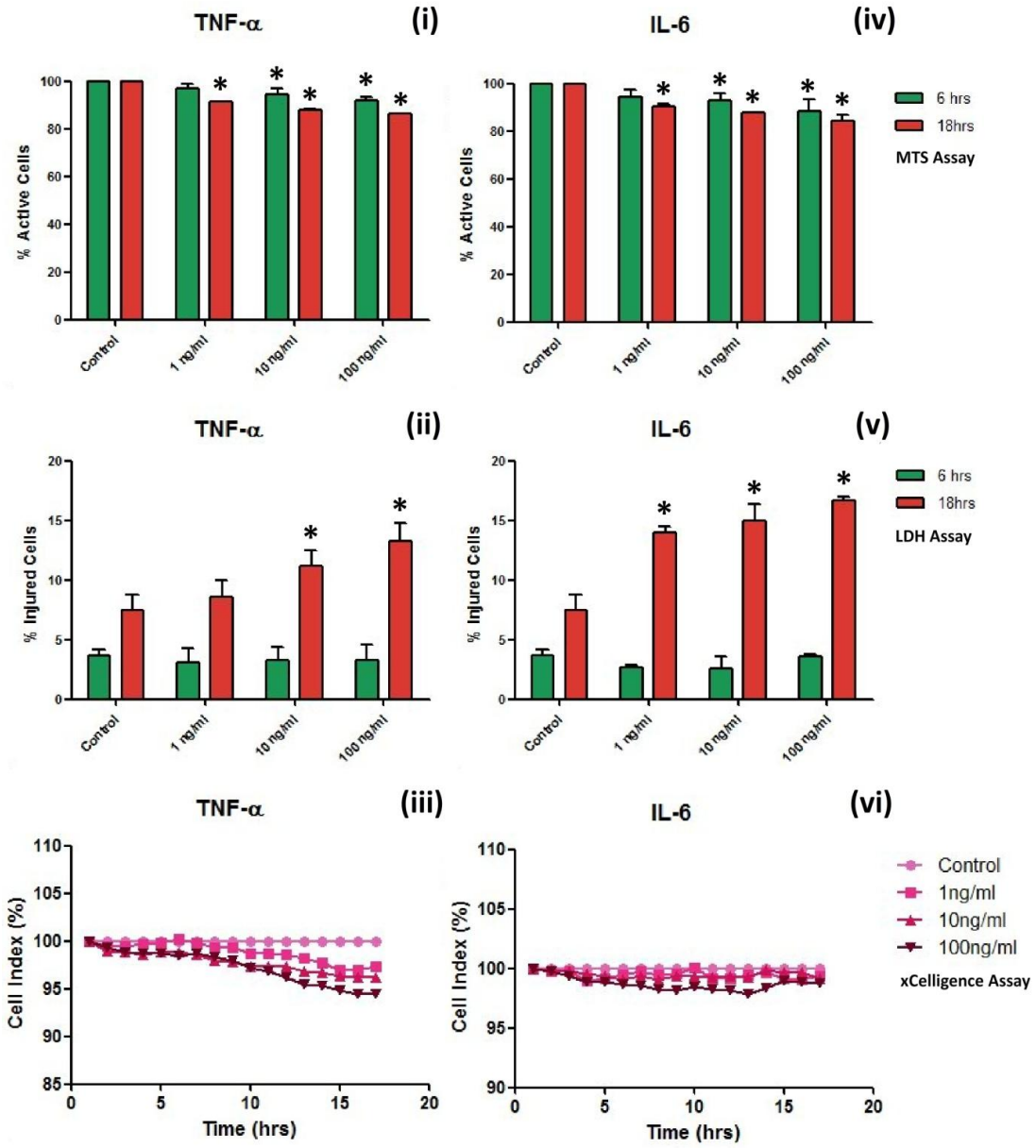

Figure 4.5: The effect of TNF-α and IL-6 on HBMvEC metabolism, LDH release and adherence. HBMvECs were seeded at a known density then stimulated with TNF-α or IL-6 (0-100 ng/ml) for 6 and 18 hr, respectively, following which the conditioned medium was harvested. Fresh medium was applied to the cell cultures with MTS reagent added to quantify the % of metabolically active cells post-treatment with TNF-α (i) or IL-6 (iv). The conditioned medium was transferred to an empty plate and examined for LDH release from the cell cultures following treatment with TNF-α (ii) or IL-6 (v). HBMvECs were also seeded at a known density on xCelligence plates and had their Cell Index (%) monitored over 18 hrs in real-time in response to TNF-α (iii) or IL-6 (vi). Results are averaged from three independent experiments ± SD; *P≤0.05 vs. Untreated Control.

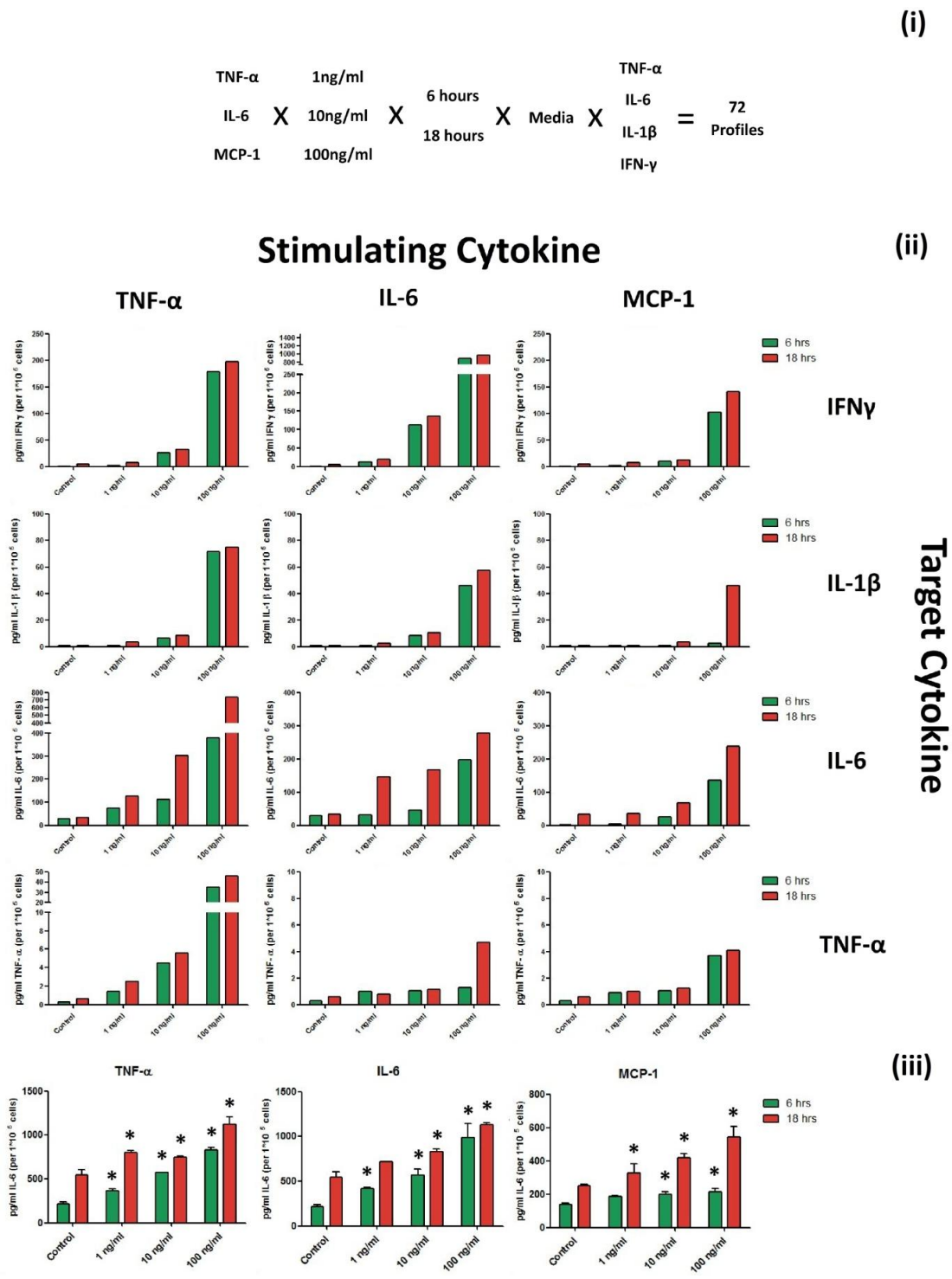

Figure 4.6: The effect of TNF-α, IL-6 and MCP-1 on HBMvEC's secretory profile. Confluent HBMvECs were stimulated with TNF-α, IL-6 or MCP-1 (0-100ng/ml) for 6 and 18 hr respectively, after which the whole cell protein lysates and conditioned medium were harvested. Samples and controls were loaded onto multiplex ELISAs which facilitate the simultaneous analysis of a number of cell injury markers at once. Data from the harvested conditioned medium is presented here (i, ii). Several findings (e.g. IL-6 release) were confirmed by standard single-plex ELISAs (iii). *P≤0.05 vs. Untreated Control.

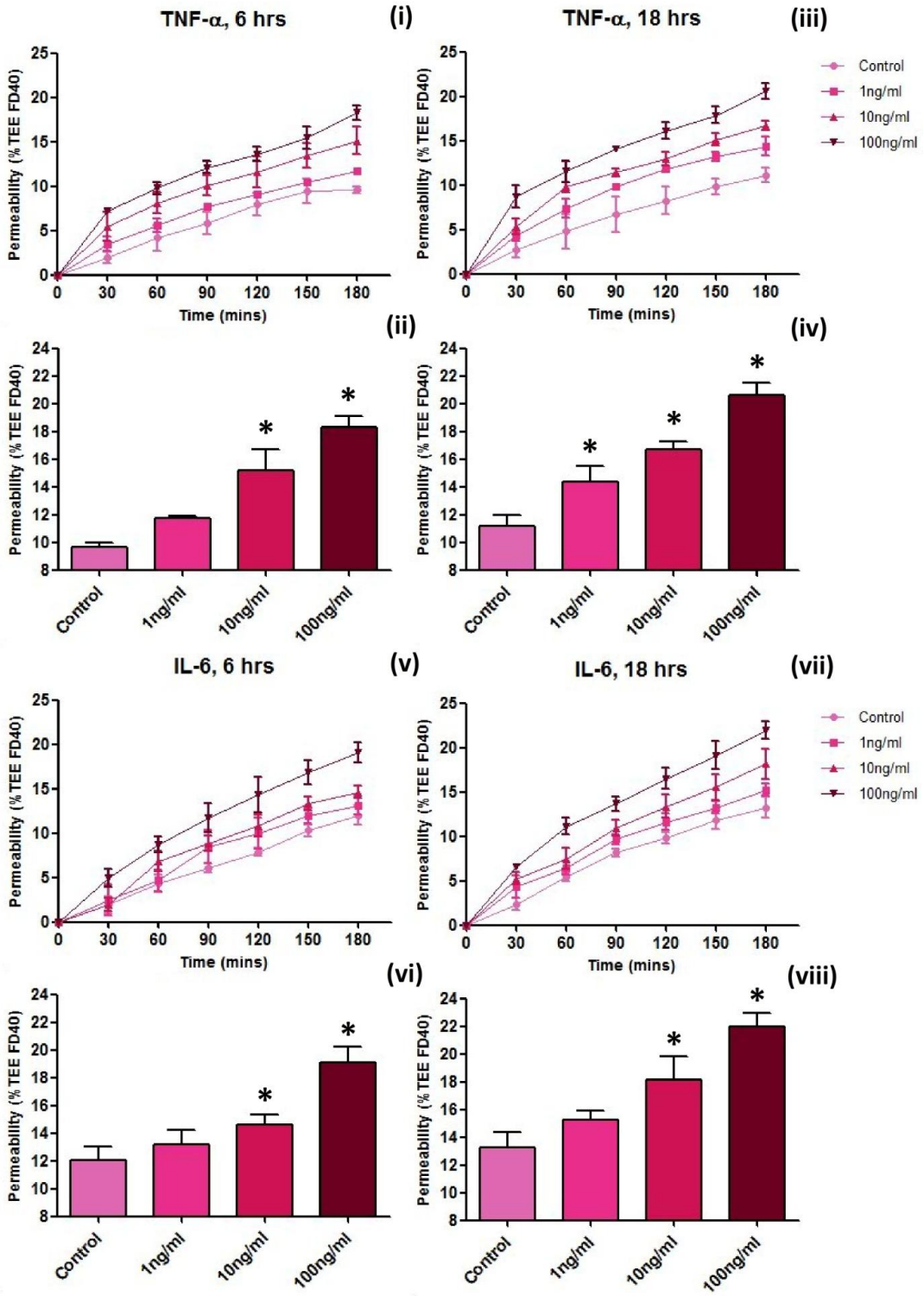

Figure 4.7: The effect of TNF-α and IL-6 on HBMvEC Barrier Function. HBMvECs were seeded at a known density and allowed to adhere prior to stimulation with TNF-α or IL-6 (0-100 ng/ml) for 6 and 18 hr, respectively. Following this they were examined by transendothelial permeability. The line graphs (i, iii, v, vii) and histograms (ii, iv, vi, viii) show the change in permeability (% TEE FD40) at a given time point(s) (t) = 0-180 mins or 180 mins, respectively, in response to TNF-α (i-iv) or IL-6 (v-viii). Results are averaged from three independent experiments ± SD; *P≤0.05 vs. Untreated Control.

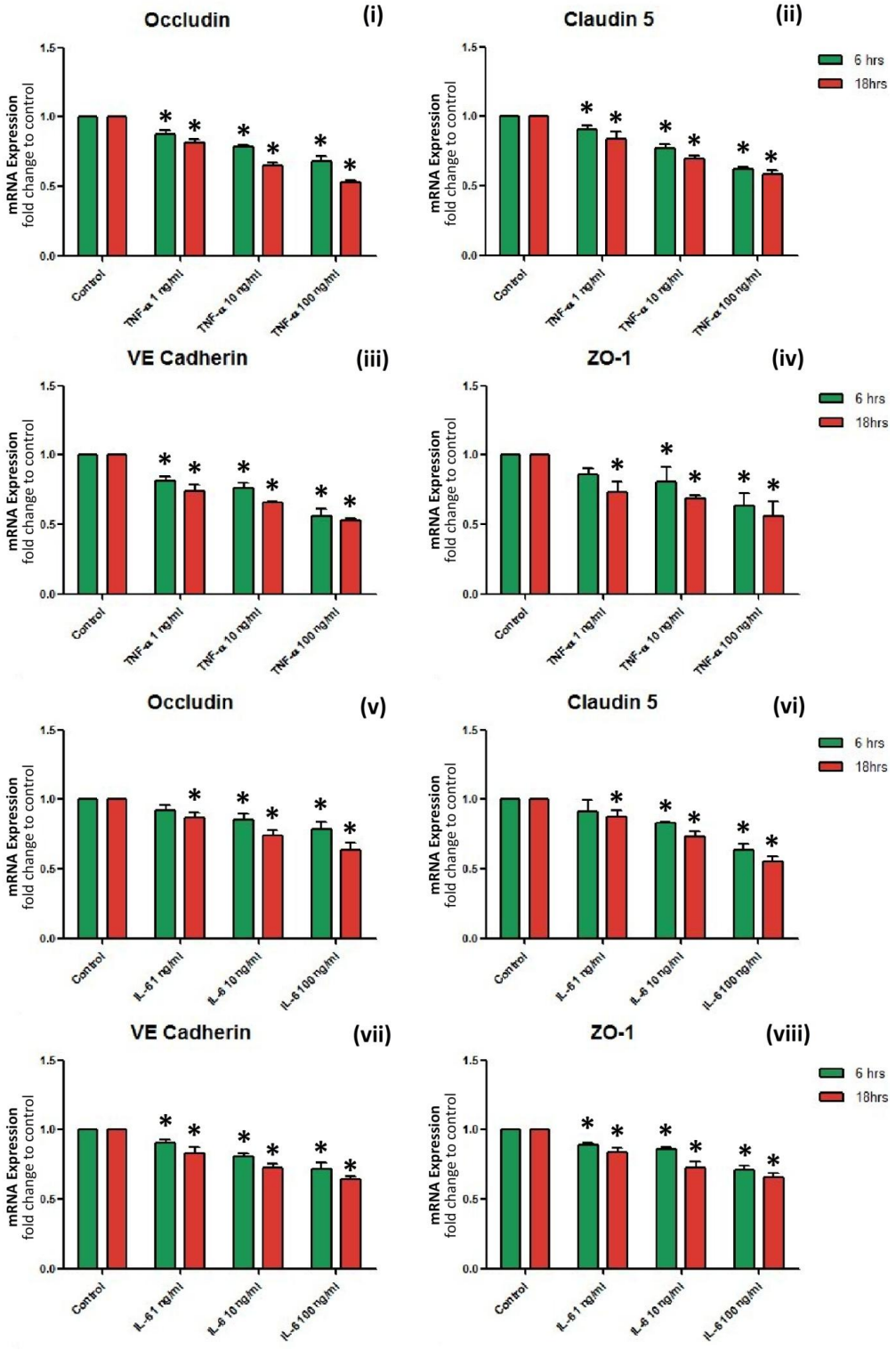

Figure 4.8: The effect of TNF-α and IL-6 on interendothelial junction protein transcription. Confluent HBMvECs were stimulated with TNF-α or IL-6 (0-100 ng/ml) for 6 and 18 hr, following which they were harvested for whole cell mRNA. The samples were analysed by qPCR. The histograms represent the changes in occludin, claudin-5, VE-Cadherin and ZO-1 on a transcriptional level in response to TNF-α (i-iv) or IL-6 (v-viii). Results are averaged from three independent experiments ± SD; *P≤0.05 vs. Untreated Control.

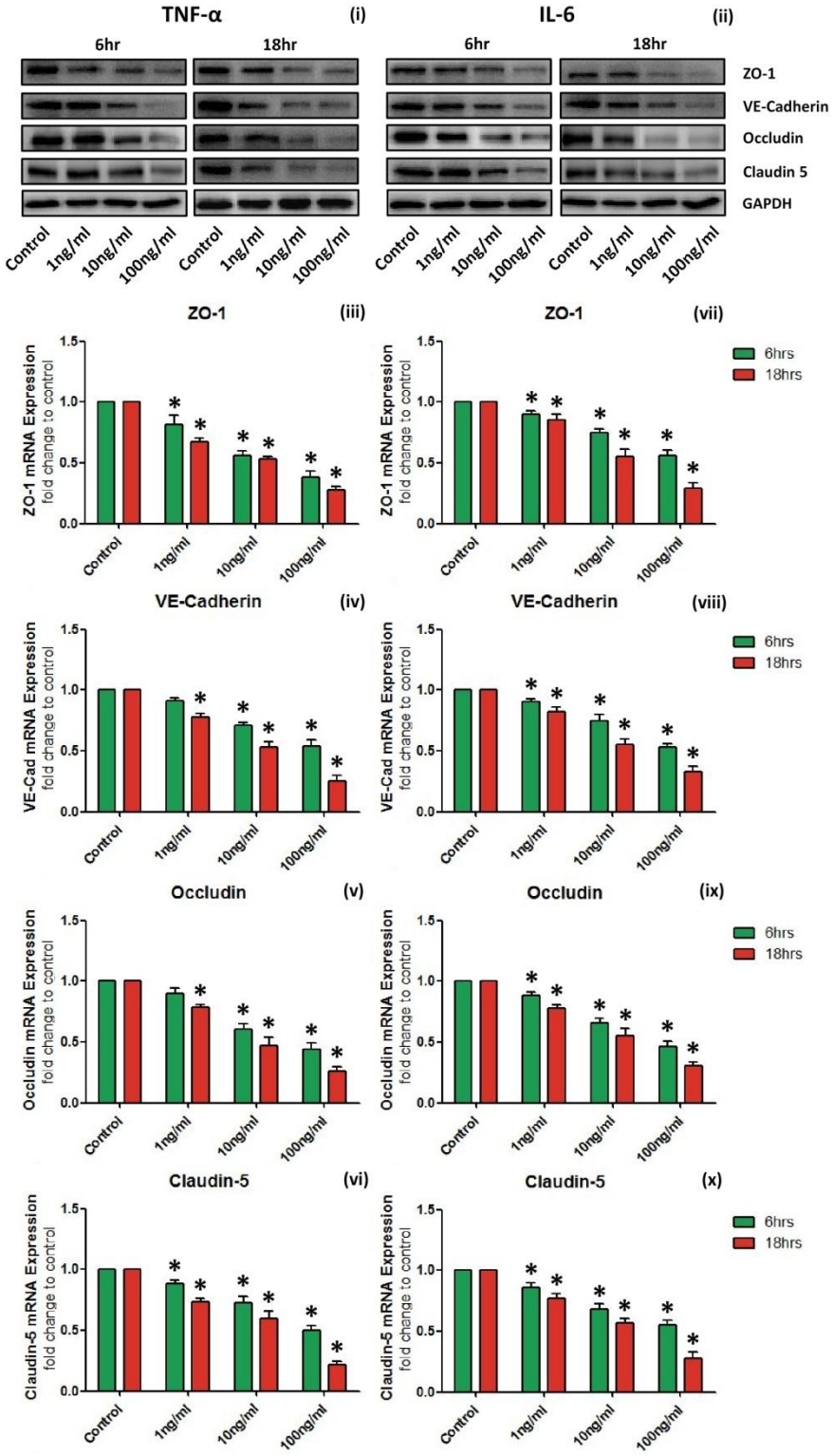

Figure 4.9: The effect of TNF-α and IL-6 on interendothelial junction protein expression. Confluent HBMvECs were stimulated with TNF-α or IL-6 (0-100ng/ml) for 6 and 18 hr, following which they were harvested for whole cell protein lysate. The translational effect on these proteins was investigated by western blot (i, ii). The histograms represent the changes in ZO-1, VE-Cadherin, occludin and claudin-5 expression in response to TNF-α (LHS) or IL-6 (RHS). Results are averaged from three independent experiments ± SD; *P≤0.05 vs. Untreated Control. Blots are representative.

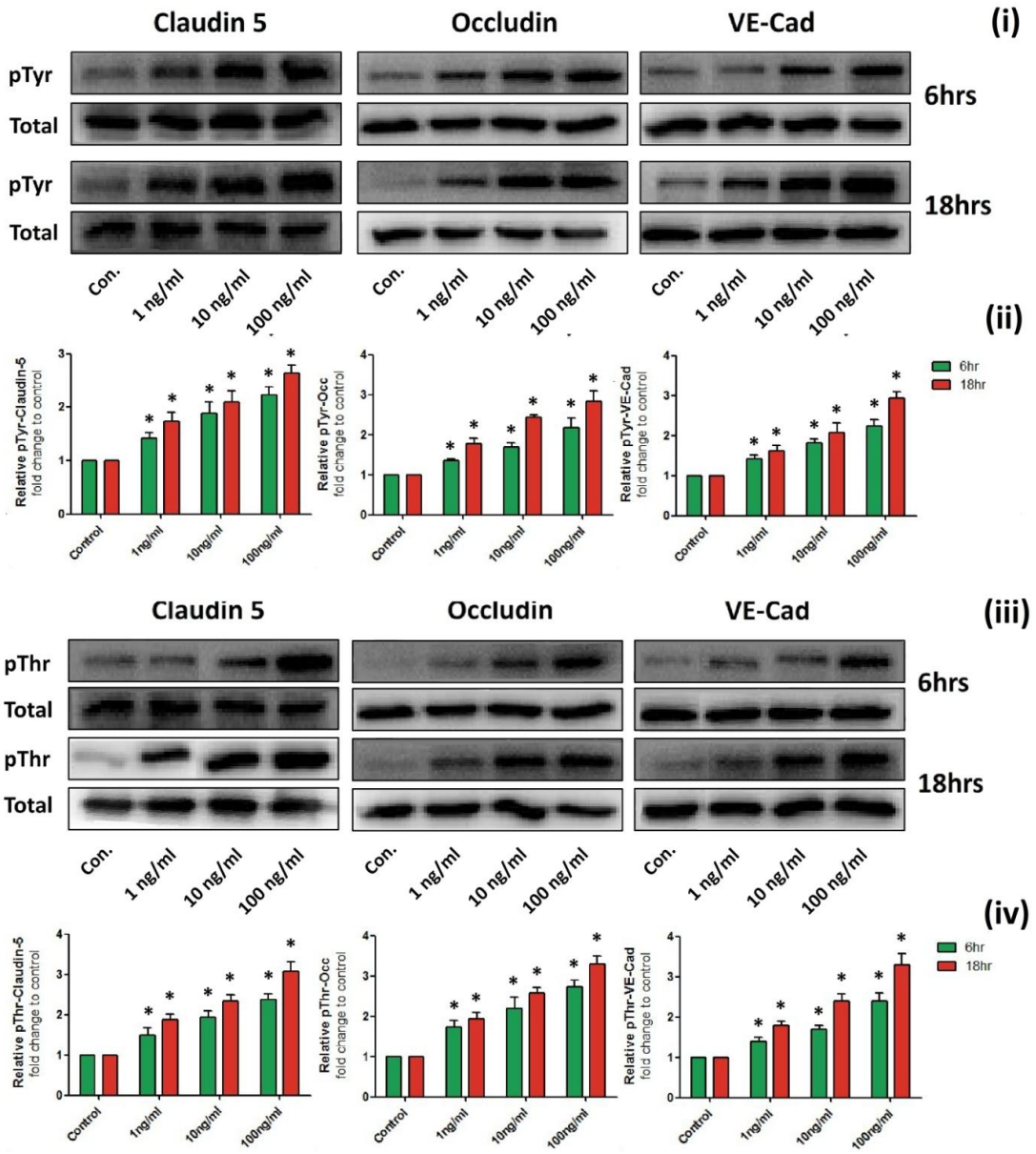

Figure 4.10: The effect of TNF-α on interendothelial junction protein tyrosine and threonine phosphorylation. Confluent HBMvECs were stimulated with TNF-α (0-100 ng/ml) for 6 and 18 hr following which they were harvested for whole cell protein lysate. The lysates were subjected to IP/IB analysis for relative pTyr (i) and pThr (iii) levels of the target protein against total target protein levels. The histograms represent the relative pTyr (ii) and pThr (iv) levels for claudin-5, occludin and VE-Cadherin as derived by scanning densitometry from western blots. Results are averaged from three independent experiments ± SD; *P≤0.05 vs. Untreated Control. Blots are representative.

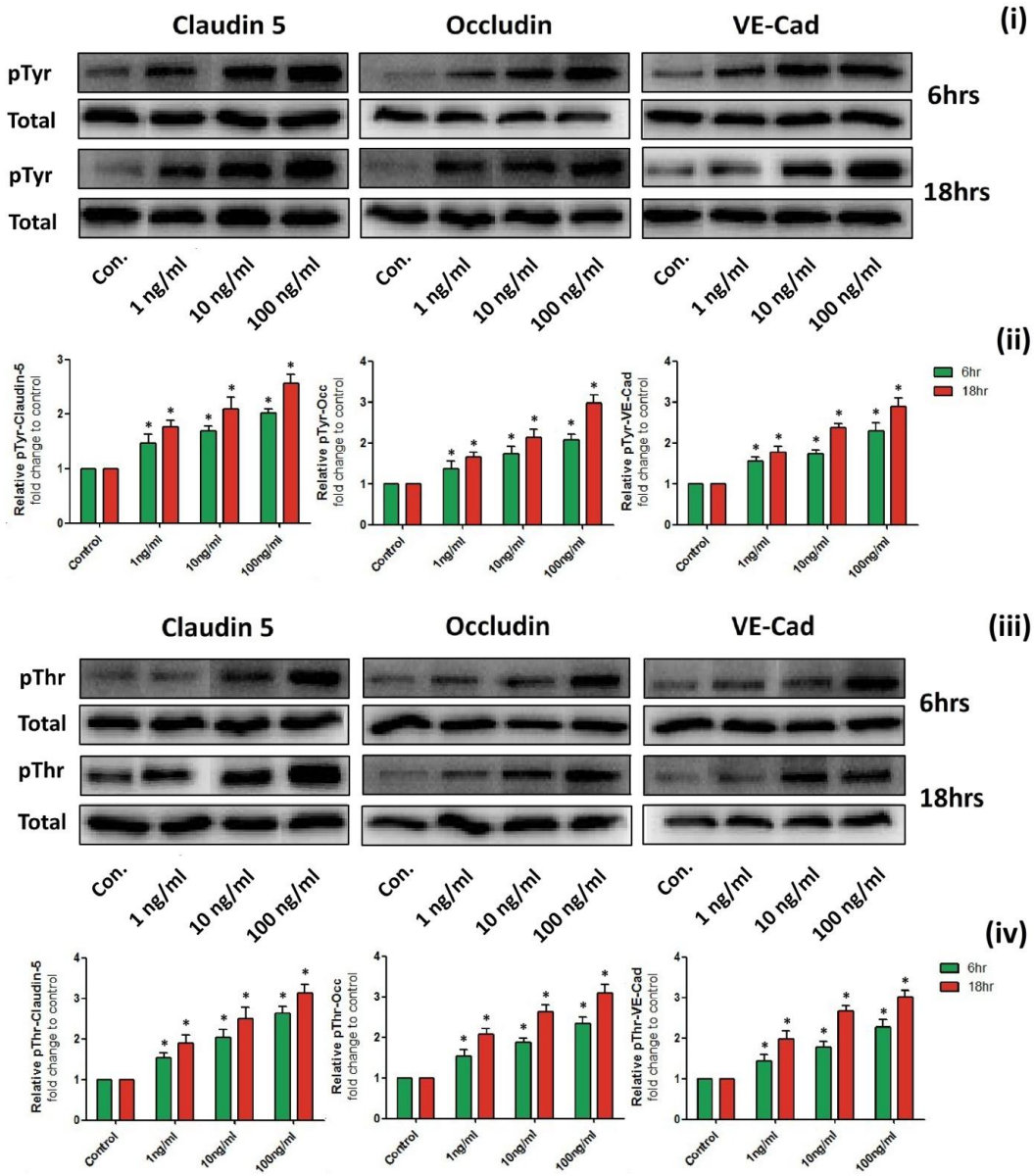

Figure 4.11: The effect of IL-6 on interendothelial junction protein tyrosine and threonine phosphorylation. Confluent HBMvECs were stimulated with IL-6 (0-100 ng/ml) for 6 and 18 hr, following which they were harvested for whole cell protein lysate. The lysates were subjected to IP/IB analysis for relative pTyr (i) and pThr (iii) levels of the target protein against total target protein levels. The histograms represent the relative pTyr (ii) and pThr (iv) levels for claudin-5, occludin and VE-Cadherin as derived by scanning densitometry from western blots. Results are averaged from three independent experiments ± SD; *P≤0.05 vs. Untreated Control. Blots are representative.

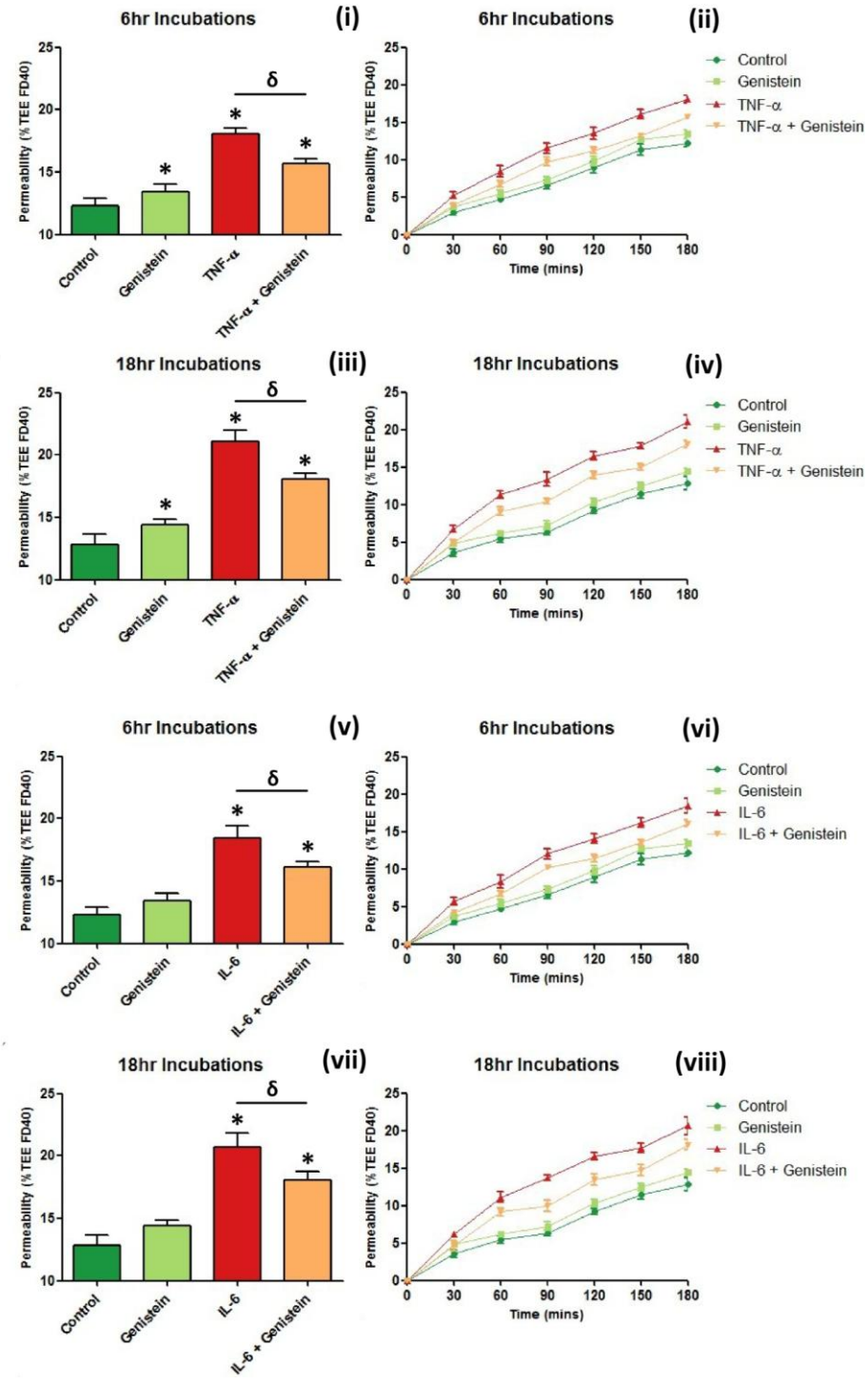

Figure 4.12: The effect of genistein on cytokine-induced HBMvEC barrier modulation. HBMvECs were seeded at a known density and allowed to adhere prior to examination by transendothelial permeability. HBMvECs were then maintained in the presence of TNF-α or IL-6 (0-100 ng/ml) for 6 or 18 hrs in the absence or presence of the protein tyrosine kinase inhibitor, genistein, prior to examination by transendothelial permeability assay. The histograms and line graphs show the change in permeability (% TEE FD40) at a given time point(s) (t) = 0-180 mins or 180 mins, respectively, in response to TNF-α (i-iv) or IL-6 (v-viii). Results are averaged from three independent experiments ± SD; *P≤0.05 vs. Untreated Control.

4.3 Discussion

While the endothelium is primarily recognised as a restrictive interface between tissue and the circulation, it also plays a key role in active endocrine, paracrine and autocrine functions, indispensable in the maintenance of vascular homeostasis. In order to maintain this stance, the endothelium must continuously monitor all blood-borne and locally produced stimuli and adapt accordingly to cope with the immediate or long-term imbalance in its environment. Disruption of haemostasis by a particular stimulus can in certain instances cause 'endothelial dysfunction'. In Chapter 3 we examined the effect of a positive stimulus (i.e. laminar shear stress) on HBMvECs and the positive influence imparted on barrier phenotype. In one study, we demonstrated the protective effects of laminar shear stress towards inflammatory cytokine injury. Inflammatory cytokines are one of the key agents implicated in triggering, sustaining and exacerbating endothelial dysfunction (DeVries, Kuiper et al. 1997, Zhang 2008). In this section, we characterise the effect of two prominent inflammatory cytokines of the cerebrovasculature; TNF-α and IL-6, on HBMvEC homeostasis and barrier phenotype.

A number of inflammatory mediators have been identified and characterised in the cerebral tissue. In selecting a panel of agents known to elicit and/or mediate inflammatory processes within the NVU, certain criteria needed to be fulfilled; of significant importance was the source of the inflammatory agents. Peripheral injury is known to facilitate inflammation via the transport of agents from the site of injury to the cerebrovasculature, where they have been reported to have an effect (Huber, Hau et al. 2002, Huber, Hau et al. 2002, Semmler, Okulla et al. 2005, Xanthos, Puengel et al. 2012). We wanted to select our agents solely from the perspective that they were known to be produced from the cell types that comprise the NVU, including the microvascular endothelium. For example, a significant increase in TNF-α level is observed within 1 hr of cerebral injury implicating it in the acute mechanisms of early injury (Shohami, Novikov et al. 1994, Fassbender, Rossol et al. 1994, Hallenbeck 2002). Conversely, IL-6 serum levels are also seen to increase significantly within the first hours of disease/injury onset (Shohami, Novikov et al. 1994, Fassbender, Rossol et al. 1994). In addition to cytokine release, a number of chemokines such as MCP-1 are released in the acute injury phase of CNS inflammation. Whilst a number of these chemokines mediate leukocyte influx across the BBB, they are also implicated in directly promoting aspects of endothelial dysfunction (Losy, Zaremba 2001, Weber, Blumenthal et al. 2003, Stamatovic, Shakui et al. 2005). In addition, all three have been shown to be a secretory by-product of BMvEC injury (Fabry, Fitzsimmons et al. 1993, Simpson, Newcombe et al. 1998, Reyes, Fabry et al. 1999, Lee, Hennig et al. 2001, Lee, Hennig et al. 2001, Verma, Nakaoke et al. 2006). For these reasons we chose to examine TNF-α, IL-6 and MCP-1.

Our primary aim was to ultimately examine endothelium barrier function following induction of an inflammatory response; therefore we wanted to ensure that the cell monolayer was not significantly compromised throughout our treatment regimes. Cells which undergo apoptosis may compromise monolayer integrity and release further apoptotic factors resulting in an ever-escalating injury process (Woywodt, Bahlmann et al. 2002). Thus, our first objective was to establish a working concentration range for each cytokine in which injury could be potentially pronounced with respect to the cytokine's concentration while firmly maintaining cell viability. Cellular viability was initially assessed by flow cytometry using a dual-stain protocol; Annexin V and PI. The employment of dual stains not only allowed for accurate measurement of cytotoxicity (PI), but also an assessment of membrane integrity (Annexin V). Several studies have previously implemented this protocol for assessing the effect of TNF-α and IL-6 on cell viability (Barnes, Spiller et al. 2011, Alejandro Lopez-Ramirez, Fischer et al. 2012).

Flow cytometry gates were established using cultures subjected to critical levels of oxidative stress (H_2O_2) after which HBMvEC cultures exposed to different concentrations (0-100 ng/ml) of TNF-α, IL-6 and MCP-1 over different exposure times were assessed. In comparison to control cultures, no significant change in cell viability was observed in cultures exposed to either TNF-α, IL-6 or MCP-1 (1-100 ng/ml) over acute (6 hrs) and chronic (18 hrs) timeframes. Similarly, no significant change in membrane integrity or cytotoxicity levels was observed. NOTE: MCP-1 data not presented.

We also examined other markers of injury. A significant reduction in the cellular reduction of MTS salt to formazan was observed in HBMvECs in response to TNF-α and IL-6. This reduction in metabolic activity was exacerbated with respect to both cytokine concentration (0-100 ng/ml) and exposure time (6 or 18 hrs). Concurrently, a moderate increase in the release of the cytoplasmic enzyme LDH into culture medium was observed only in response to 18 hr TNF-α and IL-6 treatments. A possible reason for the reduction in metabolic activity and slight increase in LDH release was induction of apoptotic mechanisms and subsequent loss of some cells. Microscopy evaluations of the cultures in response to TNF-α and IL-6 in conjunction with screenings of culture medium for cellular debris by flow cytometry suggested otherwise. However, such estimations are subjective, and so we investigated the impact of the working concentrations of our cytokines on membrane integrity by way of the xCelligence® system; a real-time recording of membrane integrity, to further delineate our viability study. Following exposure of HBMvECs to TNF-α and IL-6 (0-100 ng/ml) a slight reduction (≤5%) in Cell Index (%) was observed over 24 hrs of recording implying no significant disruption in membrane integrity had occurred. The xCelligence® system has been previously utilised in monitoring barrier function of endothelial cells (Schubert-

Unkmeir, Konrad et al. 2010, Chen, Nam et al. 2012, Luissint, Federici et al. 2012) and such reductions are characteristic of cell contractility as opposed to cell loss in the monolayer. This allowed us to interpret the MTS data as a reduction in metabolic activity rather than cell apoptosis. LDH release is typically a marker of plasma membrane compromisation, however we observed via flow cytometry that the cytokine parameters did not induce a significant change in membrane integrity. Therefore we interpreted the minor increase in LDH levels in culture medium (~7%) to a dose- and time-dependent increase in cellular activity, as opposed to apoptotic-driven membrane disruption which would be represented by a much larger percentage (Woywodt, Bahlmann et al. 2002).

Following confirmation that our working concentrations were having no significant impact on the viability and integrity of the HBMvEC monolayer, we next aimed to assess whether or not our concentrations were inducing an inflammatory response and to what degree. A key response of ECs during the inflammatory process is the release of inflammatory mediators (Verma, Nakaoke et al. 2006). Therefore we assessed the release of some of the best characterised inflammatory mediators of CVD (IFNγ, IL-1β, IL-6, TNF-α) simultaneously using a multiplex ELISA system. HBMvECs were stimulated with TNF-α, IL-6 and MCP-1 (0-100 ng/ml) at acute (6 hrs) and chronic (18 hrs) exposure times and the culture medium containing the released (if any) mediators was harvested and assayed. Each of the targeted inflammatory mediators was released from HBMvECs, the levels of which increased with respect to both dose and time. The more robust and significant events were repeated on standard single-plex ELISAs for verification. One of the key responses observed in HBMvECs was the substantial release of IL-6 in response to our inflammatory cytokines, in particular; TNF-α. We therefore decided to primarily focus on the effects of TNF-α treatment on HBMvEC barrier phenotype. In addition, we also decided to examine the effects of IL-6 on HBMvEC barrier in view of its significant release levels in response to other inflammatory stimuli. It can be noted that a potent event in the early stages of tissue injury or infection is the stimulated release of IL-6 from local immune cells such as monocytes, macrophage and toll-like receptors (Janeway, Medzhitov 2002, Matzinger 2002). This acute surge in IL-6 levels has thus implicated it in a host of early phase mechanisms with IL-6 demonstrated to actively promote (Clark, Rinker et al. 2000) and prevent (Swartz, Liu et al. 2001) damage depending on the area of interest. Regarding the cerebral tissue, the exact role of IL-6 is subject to much debate, yet it can originate from a number of cell types in response to cerebral injury; neurons, glial cells and as we have shown, the endothelium (Loddick, Turnbull et al. 1998, Suzuki, Tanaka et al. 1999, Orzylowska, Oderfeld-Nowak et al. 1999, Suzuki, Tanaka et al. 2009). Stroke patients have been shown to display a significant increase of IL-6 in both the CSF and serum, the level of

which correlates to infarct size (Beamer, Coull et al. 1995, Tarkowski, Rosengren et al. 1995). In addition, genomic studies have identified clear links between IL-6 and its related pathways in advancing aspects of CVD (Sarwar, Butterworth et al. 2012).

Having confirmed that our working concentrations of TNF-α induced an inflammatory response in HBMvEC we shifted our focus on examining the effect of the induced inflammation on HBMvEC barrier function. We assessed barrier function following exposure to TNF-α (1-100 ng/ml) and found barrier function suffered a significant dose-dependent reduction. A strong reduction in barrier function was also observed with respect to time, with a significant increase in monolayer permeability observed when comparing acute (6 hrs) and chronic (18 hrs) treatments. Mark (1999) noted a similar relationship between TNF-α concentration and endothelial barrier function, which they monitored using different size fluorescein tracers. This injurious trend is consistent with several cerebral injury models (Kim, Wass et al. 1992, Deli, Descamps et al. 1995, Anda, Yamashita et al. 1997, Yang, Gong et al. 1999, Tsao, Hsu et al. 2001, Lv, Song et al. 2010). Our parallel studies showed IL-6 elicited a similar response to TNF-α over similar concentrations (1-100 ng/ml) and exposure times (6 and 18 hrs). A study by Bamforth (1996) using an *in vivo* retinal endothelial cell model clearly demonstrated a similar response in endothelial barrier function to TNF-α yet noted no change in response to IL-6. A number of other studies noted similar or conflicting effects and implicated endothelial IL-6 release as a regulator of barrier function (Maruo, Morita et al. 1992, Ali, Schlidt et al. 1999, Krizanac-Bengez, Kapural et al. 2003). Nakahura (Nakahara, Song et al. 2003) reported increases in vessel wall permeability and enhanced angiogenesis in regions of lesion formation in patients suffering with rheumatoid arthritis. He accredited these changes in the inflammatory state to IL-6-induced release of VEGF. Similar injury models noted a link between IL-6 and increased permeability at the BBB (Brett, Mizisin et al. 1995, Saija, Princi et al. 1995) yet note such a relationship is complex (Paul, Koedel et al. 2003). It is entirely likely, based on the wealth of data available, that IL-6 release exerts different actions depending on the environment in which it has the opportunity to induce a response. The release of these IL-6 induced factors then have the potential to invoke barrier deterioration, suggesting a possible transignaling means for IL-6 in exacerbating endothelial permeability. Regardless, our model only utilises a lone cell type and IL-6 has been shown to activate numerous pathways implicated in inducing an inflammatory response in ECs (i.e. p38 MAP kinase, NFκB, (Birukova, Tian et al. 2012) protein kinase C (Desai, Leeper et al. 2002)). This evidence, in conjunction with the effect on endothelial barrier function and the secretory profile obtained by the multiplex and standard ELISAs effectively confirmed IL-6 was capable of inducing a pro-inflammatory response in HBMvECs.

Several studies have linked dysregulation of the BBB to down regulation or degradation of the interendothelial junction proteins (Mark, Davis 2002, Fischer, Wiesnet et al. 2004, Andras, Pu et al. 2005, Koto, Takubo et al. 2007, Afonso, Ozden et al. 2007, Schreibelt, Kooij et al. 2007, Argaw, Gurfein et al. 2009, Stamatovic, Keep et al. 2009, Tai, Holloway et al. 2010, Jiao, Wang et al. 2011). The significant reductions in barrier function in response to TNF-α and IL-6 led us to examine the effect of these cytokines at the interendothelial junction on a molecular level. Hoffman (2009) demonstrated in cerebral tissue of subjects suffering from severe diabetic ketoacidosis, a neuroinflammation-induced reduction in BBB function coincided with a marked reduction in occludin, claudin-5 and ZO-1. Focussing on occludin, claudin-5, VE-Cadherin and ZO-1, a significant decrease in the mRNA levels was observed in response to TNF-α and IL-6. The reduction in transcription levels was exacerbated with increasing concentration (1-100 ng/ml) and exposure times (6 and 18 hrs). Aveleira (2010) demonstrated a reduction in endothelial barrier function in response to TNF-α, noting a decrease in transcription and translation of claudin-5 and ZO-1. This study was further developed, noting TNF-α caused repression of claudin-5 through NFκB signalling. Hofmann (Hofmann, Grasberger et al. 2002) demonstrated a similar effect in relation to VE-Cadherin. We saw a similarly significant decrease in the protein levels of TJ/AJ proteins in response to TNF-α and IL-6, again with respect to both dose and time. Duchini (Duchini, Govindarajan et al. 1996) previously demonstrated a similar effect in that TNF-α and IL-6 had a direct impact on endothelial paracellular diffusion via a decrease in the tight junction. This is consistent with similar trends observed at the tight junction in other injury models (Lv, Song et al. 2010, Wang, Lv et al. 2011, Valeria Perez, Marcelo Sobarzo et al. 2012).

While we have yet to examine the effect of TNF-α and IL-6 on the distribution of the aforementioned proteins at the cell-cell junction, Desai (2002) demonstrated IL-6 induced disruption of ZO-1 expression patterns at the cell-cell borders that coincided with a decrease in barrier function. Similarly, Lopez-Ramirez (Alejandro Lopez-Ramirez, Fischer et al. 2012) demonstrated the redistribution of ZO-1 and VE-Cadherin in response to TNF-α. This is consistent with observations made in similar tight junction injury models (Zeissig, Buergel et al. 2007, Aveleira, Lin et al. 2010) however information pertaining to the microvasculature of the brain is limited, particularly with respect to IL-6. We plan to investigate the localisation patterns of occludin, claudin-5, VE-Cadherin and ZO-1, to not only verify whether a reduction in expression (as seen by western blot) is observed at the cell-cell junction but also to investigate the effect if any on translocation of the proteins in question.

We next hypothesized that cytokines may have the inverse effect on junctional protein phosphorylation at tyrosine and threonine residues as that exhibited by shear stress. Shen

(2011) demonstrated an increase in the tyrosine levels of claudin-5 and VE-Cadherin in response to TGF-β1, an effect which coincided with an increase in paracellular permeability. This trend of increased tyrosine phosphorylation levels coinciding with a reduction in barrier function has been observed independently with occludin, VE-Cadherin and claudin-5 in a number of other endothelium-injury models (Andriopoulou, Navarro et al. 1999, Antonetti, Barber et al. 1999, Lohmann, Krischke et al. 2004, Persidsky, Heilman et al. 2006, Yukitatsu, Hata et al. 2013). In contrast, little has been explored by way of the effect of phosphorylation of threonine residues pertaining to barrier function, though some isolated studies possibly indicate a similar trend as seen with pTyr (Soma, Chiba et al. 2004, Haorah, Knipe et al. 2005, Stamatovic, Dimitrijevic et al. 2006, Yamamoto, Ramirez et al. 2008, Willis, Meske et al. 2010). We observed following exposure of HBMvECs to TNF-α, that pTyr and pThr levels of occludin, claudin-5 and VE-Cadherin were significantly increased with respect to both dose (0-100 ng/ml) and time (6 and 18 hrs). This contrasts with the decrease in protein expression for these junctional proteins observed following cytokine treatments. We subsequently decided to test the effect of blocking tyrosine phosphorylation on the cytokine-induced elevation of HBMvEC permeability. Genistein, a tyrosine kinase inhibitor, was used to pretreat HBMvECs grown in transwell inserts for barrier function assays. Following exposure of the HBMvEC cultures to TNF-α and IL-6, barrier function was assessed and we observed that inhibition of tyrosine kinase activity reduced in-part the impact TNF-α and IL-6 on HBMvEC barrier function. This data, in conjunction with the relationship demonstrated between the phosphotyrosine levels of the interendothelial junction proteins in response to laminar shear stress in Chapter 3 (as tested with dephostatin), suggests that phosphorylation, particularly of pTyr, plays an integral part in modulating HBMvEC barrier integrity. Several BBB studies add credence to these observations with regards to occludin (Andras, Pu et al. 2005, Takenaga, Takagi et al. 2009), claudin-5 and VE-Cadherin (Shen, Li et al. 2011) and even ZO-1 which was omitted from our studies (Staddon, Herrenknecht et al. 1995). The impact of phosphothreonine changes, which displayed parallel trends to phosphotyrosine changes, has yet to be explored in greater detail by our group. However, several other studies have established similar links between increased pThr of claudin-5, occludin and ZO-1 and BBB dysregulation (Soma, Chiba et al. 2004, Haorah, Knipe et al. 2005, Haorah, Heilman et al. 2005, Stamatovic, Dimitrijevic et al. 2006, Yamamoto, Ramirez et al. 2008, Willis, Meske et al. 2010). It should be noted, as stated in the discussion of Chapter 3, that the impact of other post-translational modifications are recognised as potentially playing as critical a role as phosphorylation in HBMvEC barrier dynamics. These aspects, amongst others, are currently being considered in furthering this body of work and furthering our understanding of HBMvEC barrier mechanics.

To summarise at this point our working concentrations of TNF-α and IL-6 were shown to elicit an inflammatory response in conjunction with negative impacts upon HBMvEC barrier function. We also expanded our cytokine studies to explore other aspects of endothelial biology and their impact (if any) on other functional roles the endothelium encompasses. We decided to examine the effect of inflammation on some of the regulatory molecules the endothelium provides in maintaining hemostasis. In normal physiological conditions, the endothelium acts as an antiplatelet, anticoagulant and fibrinolytic surface (Stern, Esposito et al. 1991). In contrast, during inflammation this phenotype is compromised and the resulting dysfunctional EC provides a prothrombotic, antifibrinolytic surface. In Chapter 3, we examined two key factors involved in the coagulation cascade which are associated with injury and wound repair in the vasculature; vWF and thrombomodulin. We demonstrated that laminar shear stress promoted anti-coagulant activity with respect to these two proteins. In contrast, exposure of HBMvECs to our working range of inflammatory cytokines appears to manipulate these mechanisms to promote a pro-coagulation environment. We observed a significant decrease in thrombomodulin protein levels in response to TNF-α and IL-6 in both a dose- and time-dependent manner. This is consistent with other endothelial injury models (Lentz, Tsiang et al. 1991, Lin, Hsieh et al. 2009). Concurrently, a significant increase in the release of soluble thrombomodulin levels into culture medium was observed. This is consistent with other studies (Nawroth, Stern 1986, Bauer, Rosenberg 1987). Boehme (Boehme, Deng et al. 1996) observed a concurrent increase in endothelial release of thrombomodulin and decrease in intracellular levels following exposure to TNF-α. Together these observations may suggest a natural acute defensive response by the endothelium, attempting to nullify any inflammatory, pro-coagulant mechanisms encountered in the local environment (Takahashi, Ito et al. 1992). Interestingly, our data in Chapter 3 demonstrated a substantial and sustained increase in thrombomodulin expression and release following exposure of HBMvECs to laminar shear stress. This increase in endothelial release of thrombomodulin is consistent with observations made in similar cerebral injury models *in vivo* (Macko, Killewich et al. 1999, Giwa, Williams et al. 2012). In parallel studies, vWF mRNA and protein expression is significantly increased in response to inflammatory cytokines, an increase which is augmented with respect to increasing cytokine concentration and exposure times. While vWF release was not examined, the increase in its expression was observed by confocal microscopy. Increases in vWF expression and release have long been considered a marker of vascular injury (Boneu, Abbal et al. 1975). Indeed, elevated levels of vWF have been observed in several vascular pathologies (Kahaleh, Osborn et al. 1981, Pedrinelli, Giampietro et al. 1994), including those of the cerebrovasculature (Mettinger 1982). Lip (Lip, Blann et al. 2002) observed an increase in serum levels of a number of pro-coagulant (vWF included) molecules in acute stroke patients. This inverse relationship; the

reduction in expression of anti-coagulant thrombomodulin and increase in expression of pro-coagulant vWF leads us to conclude that exposure of HBMvECs to our working cytokine concentrations is likely inducing whole cell endothelial dysfunction. This data is consistent with observations made in similar cerebral injury models (Tsuchida, Salem et al. 1992, Zarifis, Blann et al. 1996, Wang, Tran et al. 1997, Faust, Levin et al. 2001, Isermann, Hendrickson et al. 2001).

Finally, the effect of inflammatory cytokines on the expression of their signal-transducing receptors was investigated. The expression profiles and localisation of the receptors in conjunction with local levels of the necessary adapter proteins are what determines which potential pathways become activated and exert physiological changes in the cell population. We found that both TNF-α and IL-6 drove up the transcriptional levels of TNFR1 and gp130 in a time- and dose-dependent manner, likely culminating in elevated inflammatory signalling. Interestingly, Cook, (2008) noted the increase in TNFR1 levels coincided with an increase in TACE activity. They concluded that targeting TNFR1 expression as opposed to the cytokine itself may be a more effective strategy in the regulation of TNF-α-mediated events. Similarly, Pradillo (2005) demonstrated that ischemic pre-conditioning led to an upregulation of TNFR1 and TACE activity that in turn promoted ischemic tolerance. Whilst there is little evidence of a similar adaptive mechanism involving soluble gp130 in the microvasculature, studies suggest it is plausible (Hirota, Izumi et al. 2004, Inta, Weber et al. 2009). In contrast, a number of cerebral diseases have reported a correlation between elevated levels of cytokine receptors and the onset of such diseases. The IL-6 transignalling molecule; sIL-6R, which transduces IL-6 signals through gp130, has been reported to have a significant impact on endothelial cells, mediating the recruitment and assisted invasion of leukocytes via induction of leukocyte adhesion molecules; E-Selectin, ICAM-1 and VCAM-1, in addition to stimulating the release of a number of cytokines known to provoke an inflammatory response in endothelial cells; IL-6, IL-8 and MCP-1 (Modur, Li et al. 1997). It is worth noting that endothelial cells characteristically do not express IL-6R, the precursor to sIL-6R, so for the purposes of our studies, transignalling via IL-6 likely occurred through naturally occurring sIL-6R that may be present in the culture medium supplements. Whilst the effects of elevated levels of sIL-6R were not investigated, the elevated levels of gp130 would work in a comparative way to facilitate/modulate the binding and signal transduction of gp130 ligands. Yu (2007) demonstrated TNF-α caused an increase in the transcription and translation of gp130 via NFκB.

TNFR2, by contrast, showed a significant increase in transcription levels within 4 hrs of cytokine exposure. This increase was normalised within 8 hrs with levels returning to baseline levels with further reductions incurred giving an overall significant decrease in

transcription levels after 24 hrs of exposure. TNFR1 is the predominantly expressed TNF receptor in endothelial cells (Nadeau, Rivest 1999) and any increase in its expression results in increased NFκB signalling and an increased inflammatory state (Wosik, Biernacki et al. 2007). TNFR2 is also capable of mediating an inflammatory response in the CNS, similar to TNFR1 albeit with a reduced functional capacity (Akassoglou, Douni et al. 2003). Ferrero (2001) demonstrated via agonists and antagonists for both receptors, that endothelial permeability is primarily mediated via signalling through TNFR1, though barrier degree was observed to be regulated to a small extent through TNFR2 signalling. Further studies exploring endothelial dysfunction reached a similar conclusion (Slowik, Deluca et al. 1993). TNFR2 has also been implicated in initiating pro-survival signalling (Zhang 2008). Thus the differential expression patterns of each of the TNFRs play a significant role in shaping the TNF-α-induced inflammatory response in HBMvECs (e.g. malaria (Lucas, Juillard et al. 1997a, Lucas, Lou et al. 1997, Lucas, Lou et al. 1997b)).

In conclusion, we have comprehensively demonstrated how inflammatory cytokines, such as TNF-α and IL-6, play a pivotal role in the disruption of vascular homeostasis and BBB phenotype. Aside from inducing the release of pro-inflammatory mediators, both cytokines are capable of promoting an injured BBB phenotype through the modulation of interendothelial protein expression and post-translational modification, as well as modulation of endothelial anti-inflammatory mechanisms.

Chapter 5:

The independent contribution of reactive oxygen species, and IL-6, to cytokine-induced modulation of HBMvEC blood-brain barrier properties.

5.1 Introduction

In chapter 4, the effects of a pathophysiological stimulus in the form of well-known inflammatory cytokines, TNF-α and IL-6, on HBMvEC cultures were investigated. Following exposure, several aspects of the BBB phenotype previously demonstrated to be enhanced by laminar shear stress were seen to regress. Exposure of HBMvEC monolayers to each cytokine was seen to cause a reduction in barrier integrity. This was likely due to an observed cytokine-induced reduction in the transcription and translation of the key proteins of interest at the tight and adherens junctions. Similar to laminar shear stress, each protein was seen to undergo post-translational modification, however the inverse was observed in that tyrosine and threonine residues become increasingly phosphorylated with direct consequences for barrier function. In addition, several anti-inflammatory mechanisms were modulated such that the resulting HBMvEC phenotype was susceptible to further inflammatory injury. Of note, all observed effects were seen to be potentiated with increasing cytokine concentration or exposure time.

Several pathways have been identified in initiating BBB dysfunction. The kinin system, excitotoxicity, neutrophil recruitment, mitochondrial alterations and macrophage/microglial activation are just some of the events affiliated with BBB disruption and interestingly they all share a common characteristic, namely reactive oxygen species (ROS) (Pun, Lu et al. 2009). Several cerebral pathologies have accredited their initiation and progression to the oxidative stress imparted by ROS wherein the oxidant-antioxidant ratio of the microenvironment becomes imbalanced, resulting in a surge in the local levels of free radicals. Increased levels of ROS are now a hallmark of numerous cerebral pathologies (e.g. multiple sclerosis, stroke) and several studies have associated ROS with direct influence on BBB dysfunction, specifically barrier function (Collins-Underwood, Zhao et al. 2008). This has resulted in several clinical trials aiming to develop antioxidant therapies; however translation from animal models into an efficient therapeutic remains evasive (Steinhubl 2008). The lack of success to date is attributed to a lack of underlying knowledge of the biology of ROS in the microvasculature. It has been suggested that the time of administration of antioxidant therapies is crucial to the success, with several studies indicating the therapeutic window is limited (within 1-2 hrs of injury). ***For these reasons, in chapter 5 we focussed our attention on whether the release and effects of ROS were attributable to the cytokine-induced injury of HBMvECs.***

In addition, chapter 4 focussed in large part on the secretory profile of HBMvECs in response to inflammatory cytokines. In parallel with our ROS studies therefore, we decided to investigate the impact of any mediator we felt had a substantial presence in the culture microenvironment post-treatment. In chapter 4, the secretory profile of our HBMvEC model

in response to TNF-α and IL-6 was examined. The release of several well-known influential promoters of CVD was investigated in response to a number of experimental paradigms, and for chapter 5 we focussed on one of the more robust trends in the acute increase in IL-6 levels following exposure to TNF-α. As a result of this, in chapter 4 we afforded IL-6 the same level of characterisation as the well known mediator of inflammatory responses; TNF-α. ***For chapter 5, we focussed on the effects of IL-6 release following TNF-α, investigating whether the subsequent injury could be attributable in part to the production and release of IL-6.*** Several stimuli, from neurotransmitters to inflammatory cytokines as we have seen can induce IL-6 release in several cell types within the CNS (including those that comprise the NVU (Akira, Taga et al. 1993)), with several of the aforementioned also expressing the appropriate receptor for IL-6 signal transduction. Thus, IL-6 was implicated in potentially having several roles within the CNS. Since its discovery, a wealth of data has been generated demonstrating the role of IL-6 in development and normal physiology as well as injury and disease (Erta, Quintana et al. 2012). However, its ever-growing list of responsibilities and functions, of which there is much contradictory data, has lead to it being routinely re-characterised (Paul, Koedel et al. 2003). Having already extensively characterised the effects IL-6 had on HBMvECs in chapter 4, we decided to revisit it but focus our efforts on evaluating its role from the context of TNF-α inducing its release. Together with ROS, we were tackling both an unverified and verified mediator of inflammatory injury in HBMvECs, allowing us to further delineate the means by which both our inflammatory cytokines, TNF-α and IL-6, impart their injury on the BBB endothelium.

5.1.1 Study Aims

In this chapter we examine the potential roles of reactive oxygen species, and IL-6, in the cytokine-induced disruption of HBMvEC blood-brain barrier properties. Therefore, the overall aims of this chapter include:

- To investigate the effect of TNF-α and IL-6 on ROS production in HBMvECs.
- To determine whether TNF-α- and IL-6-induced levels of ROS contribute to the cytokine-induced disruption of TJ/AJ protein (occludin, claudin-5, VE-Cadherin, ZO-1) translational expression.
- To determine whether TNF-α- and IL-6-induced levels of ROS production contribute to the cytokine-induced disruption of HBMvEC barrier function.
- To further investigate the effect of TNF-α on IL-6 production in HBMvECs.

- To determine whether TNF-α-induced levels of IL-6 contribute to the TNF-α-induced dysfunction of HBMvECs with respect to the aforementioned injury indices (ROS, TJ/AJ, barrier function).

5.2.1 Exposure of HBMvECs to TNF-α and IL-6 increases cellular production of ROS over time

The effect of TNF-α and IL-6 on cellular ROS production with respect to time was examined (Figure 5.1). Confluent HBMvECs were stimulated with TNF-α or IL-6 (100 ng/ml) for 0-24 hrs in the presence of ROS detecting dyes; CFDA or DHE. Post-treatment, the entire cell population was harvested and prepared for analysis by flow cytometry. A significant increase in ROS in response to TNF-α (i-iv) and IL-6 (v-viii) treatment was observed with respect to time using both CFDA and DHE.

The effect of TNF-α and IL-6 on cellular ROS production with respect to time was also examined by immunofluorescence microscopy (Figure A.13). HBMvECs were seeded onto coverslips and grown to confluency prior to stimulation with TNF-α or IL-6 (100 ng/ml) for 0-24 hrs in the presence of ROS-detecting dyes; CFDA or DHE. Post-treatment, the cells were fixed and prepared for examination by immunofluorescence microscopy. A similar trend was observed in comparison to the flow cytometry results with significant increases in CFDA and DHE signals in response to TNF-α and IL-6 observed with respect to time.

5.2.2 Exposure of HBMvECs to TNF- α and IL-6 increases cellular production of ROS in a dose-dependent manner

The effect of TNF-α and IL-6 on cellular ROS production with respect to cytokine dose was examined (Figure 5.2). Confluent HBMvECs were stimulated with TNF-α or IL-6 (0-100 ng/ml) for either 6 or 18 hrs in the presence of ROS-detecting dyes; CFDA or DHE. Post-treatment, the entire cell population was harvested and prepared for analysis by flow cytometry. A significant increase in ROS in response to TNF-α (i, ii) and IL-6 (iii, iv) was observed with respect to dose using both CFDA and DHE.

5.2.3 Pre-treatment with antioxidants can reduce the cytokine-stimulated increase in ROS production

The effect of different antioxidants on TNF-α-induced increase in ROS production was examined Figure 5.3). Confluent HBMvECs were independently pre-treated with different antioxidants; Apocynin, N-Acetylcysteine, Superoxide Dismutase and Catalase for 1 hr. Post-treatment, the cultures were stimulated with TNF-α (100 ng/ml) for 6 or 18 hrs in the presence of ROS-detecting dye; CFDA. Post-treatment, the entire cell population was harvested and prepared for analysis by flow cytometry. A significant increase in ROS in response to TNF-α was observed in comparison to control cultures for both 6 and 18 hr

treatments. A significant increase in CFDA signals in response to TNF-α in the presence of each of the antioxidant treatments were also observed in comparison to untreated control cultures. Following antioxidant treatments, a very significant reduction in TNF-α-induced ROS production was observed (LHS). A similar trend was observed in parallel experiments utilising IL-6 in place of TNF-α (RHS), and indeed utilising DHE instead of CFDA (Figure A.14). The effect of the antioxidant concentration on HBMvEC viability was also examined by flow cytometry to determine the effective dose (Figure A.15).

5.2.4 Pre-treatment with antioxidants can reduce the cytokine-driven downregulation of intercellular junction proteins; occludin, claudin-5 and VE-Cadherin

The effect of antioxidants on TNF-α-induced downregulation of intercellular junction proteins; occludin, claudin-5 and VE-Cadherin were examined (Figure 5.4). Confluent HBMvECs were independently pre-treated with different antioxidants; Apocynin, N-Acetylcysteine, Superoxide Dismutase and Catalase for 1 hr. Post-treatment, the cultures were stimulated with TNF-α (100 ng/ml) for 18 hrs before being harvested for whole cell protein lysate. The translational levels of each protein in response to TNF-α in the absence and presence of each antioxidant were then examined by western blot (i, v, ix, xiii). Each protein demonstrated a significant decrease in their expression following cytokine exposure in comparison to untreated control cultures. Following antioxidant treatments, the cytokine-induced reduction in protein expression was partially attenuated (ii-iv, vi-viii, x-xii, xiv-xvi). A similar trend was observed in parallel experiments utilising IL-6 in place of TNF-α (Figure 5.5) and also following the earlier 6 hr cytokine treatment time for either cytokine (Figure A.16, A.17).

5.2.5 Pre-treatment with antioxidants can reduce the cytokine-driven downregulation of barrier function

The effect of antioxidants on TNF-α-induced downregulation of HBMvEC barrier function was examined (Figure 5.6). HBMvECs were seeded at a known density into transwell inserts and left to adhere overnight. The following day the confluent HBMvECs were pre-treated with antioxidants; Apocynin, N-Acetylcysteine, Superoxide Dismutase and Catalase, 1 hr prior to cytokine treatment (100 ng/ml) for 18 hrs. Post-treatment, the cellular monolayers were assessed for transendothelial permeability. Exposure of HBMvECs to TNF-α resulted in a significant increase in FITC-Dextran paracellular flux (%TEE of FD40) across the cell monolayer. Following antioxidant treatment, the cytokine-induced permeabilisation of

HBMvECs was significantly attenuated (i-viii). A similar trend is observed in parallel experiments utilising IL-6 in place of TNF-α (Figure 5.7; i-viii) and also following the earlier 6 hr treatment time for either cytokine (Figure A.18, A.19).

5.2.6 Exposure of HBMvECs to TNF-α induces an upregulation in IL-6 expression

The effect of TNF-α on the expression in HBMvECs of IL-6 in HBMvECs was examined (Figure 5.8). Confluent HBMvECs were stimulated with TNF-α (0-100 ng/ml) for 0-24 hrs before being harvested for whole cell mRNA or protein lysate. The transcriptional level of IL-6 mRNA was examined by qPCR. IL-6 mRNA levels significantly increased following exposure to TNF-α in both a time- and dose-dependent manner in comparison to untreated control cultures (i, ii). The translational levels of IL-6 protein in response to TNF-α were then examined in HBMvECs by western blot (iii). A similar trend was observed in that IL-6 experienced a significant increase in protein levels following TNF-α treatment in both a time- and dose-dependent manner in comparison to untreated control cultures (iv). A similar trend was observed in parallel experiments utilising IL-6 in place of TNF-α (Figure A.20).

5.2.7 Treatment with an IL-6 neutralising antibody (NtAb) can partially reduce TNF-α-induced damage of HBMvECs

The effect of an IL-6 NtAb on TNF-α induced damage of HBMvEC barrier properties was examined (Figure 5.9, 5.10). Confluent HBMvECs were stimulated with TNF-α (100 ng/ml) in the absence and presence of 250 ng of IL-6 NtAb for 18 hrs in the additional presence of ROS detecting dyes; CFDA or DHE (Figure 5.9). Post-treatment, cells were harvested and prepared for analysis by flow cytometry. A significant increase in ROS levels in response to TNF-α was observed and indeed was partially attenuated by IL-6 NtAb treatment (i-iv). The effect of the IL-6 NtAb on TNF-α induced downregulation of HBMvEC barrier function was also examined. HBMvECs were seeded at a known density into transwell inserts and left to adhere overnight. The following day the confluent HBMvECs were treated with TNF-α (100 ng/ml) in the absence and presence of 250 ng of IL-6 NtAb for 18 hrs. Post-treatment, the HBMvEC monolayers were assessed for transendothelial permeability. Exposure of HBMvECs to TNF-α resulted in a significant increase in FITC-Dextran paracellular flux (%TEE of FD40) across the cell monolayer, an effect that was partially attenuated by IL-6 NtAb treatment (v, vi). Similar results were also observed for the earlier 6 hr treatment with TNF-α (Figure A.22).

Further studies focused on the effect of IL-6 NtAb on TNF-α-induced downregulation of intercellular junction proteins; occludin, claudin-5 and VE-Cadherin (Figure 5.10). Confluent HBMvECs were stimulated with TNF-α (100 ng/ml) in the absence and presence of 250 ng of IL-6 NtAb for either 6 or 18 hrs before being harvested for whole cell protein lysate. The translational levels of each protein in response to TNF-α in the absence and presence of the IL-6 NtAb were then examined by western blot (i, ii). Each protein demonstrated a significant decrease in expression following treatment with TNF-α in comparison to untreated control cultures. Moreover, this decrease was partially attenuated by treatment with IL-6 NtAb (iii-viii).

Finally, the specificity of the IL-6 NtAb against recombinant forms of both IL-6 and TNF-α was also investigated by western blot (Figure A.21, i). The working concentration of the IL-6 NtAb was also determined based on efficacy in ablating IL-6-driven barrier disruption as monitored by transwell permeability assay (ii-v).

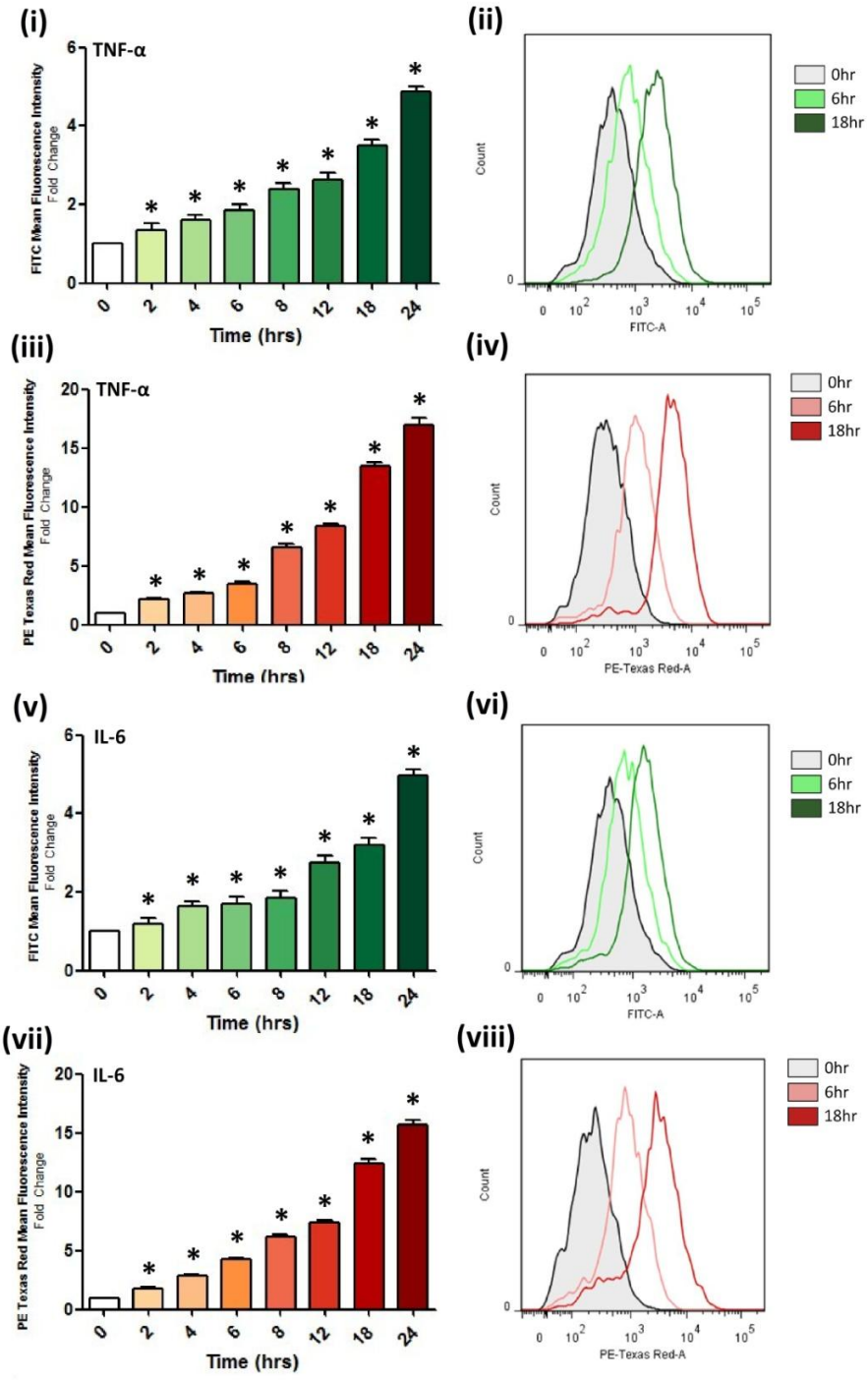

Figure 5.1: The effect of TNF-α and IL-6 on ROS production-Time Response. Confluent HBMvECs were stimulated with TNF-α or IL-6 (100 ng/ml, 0-24 hrs) in the presence of either CFDA or DHE. Post-treatment, cells were harvested and subsequently prepared for flow cytometry. The histograms (LHS) represent the intensity of ROS-detecting dyes prepared from the representative FACS scans (RHS). The cytokine-treated samples were analysed using FlowJo Flow Cytometry Analysis Software to quantify the respective signal from CFDA- (i, ii, v, vi) and DHE- (iii, iv, vii, viii) stained cell populations in response to TNF-α and IL-6 from 0-24 hrs. Results are averaged from three independent experiments ± SD. *P≤0.05 vs. 0hr Control.

Legend: FITC-A = CFDA; PE-Texas Red-A = DHE

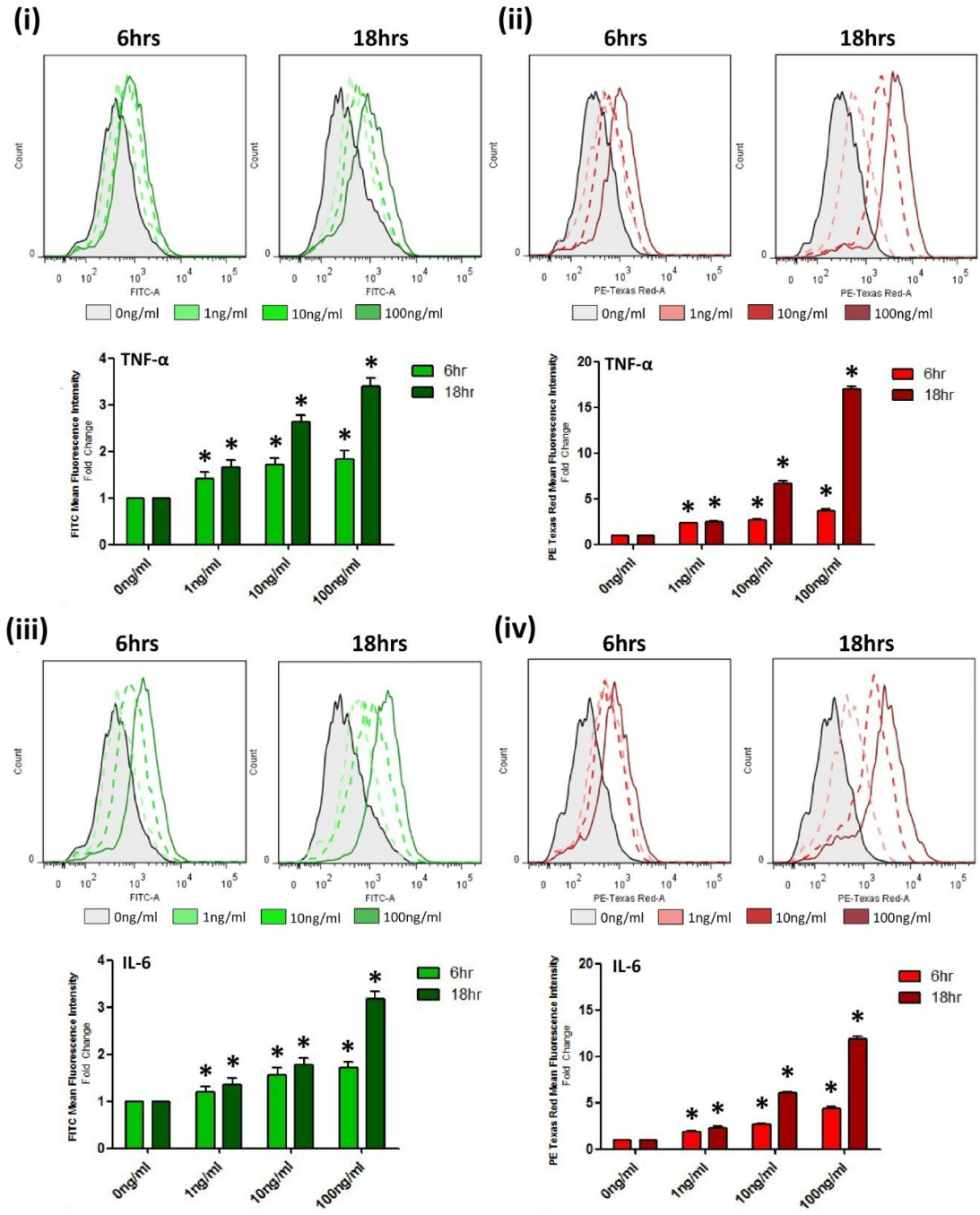

Figure 5.2: The effect of TNF-α and IL-6 on ROS production-Dose Response. Confluent HBMvECs were stimulated with TNF-α or IL-6 (0-100 ng/ml) for 6 or 18 hrs in the presence of either CFDA or DHE. Post-treatment cells were harvested and subsequently prepared for flow cytometry. The histograms represent the intensity of ROS-detecting dyes prepared from the representative FACS scans. The cytokine-treated samples were analysed using FlowJo Flow Cytometry Analysis Software to quantify the respective signal from CFDA- (i, iii) or DHE- (ii, iv) stained cell populations in response to TNF-α and IL-6 at 6 and 18 hrs. Results are averaged from three independent experiments ± SD. *P≤0.05 vs. 0 ng/ml Control.

Legend: FITC-A = CFDA; PE-Texas Red-A = DHE

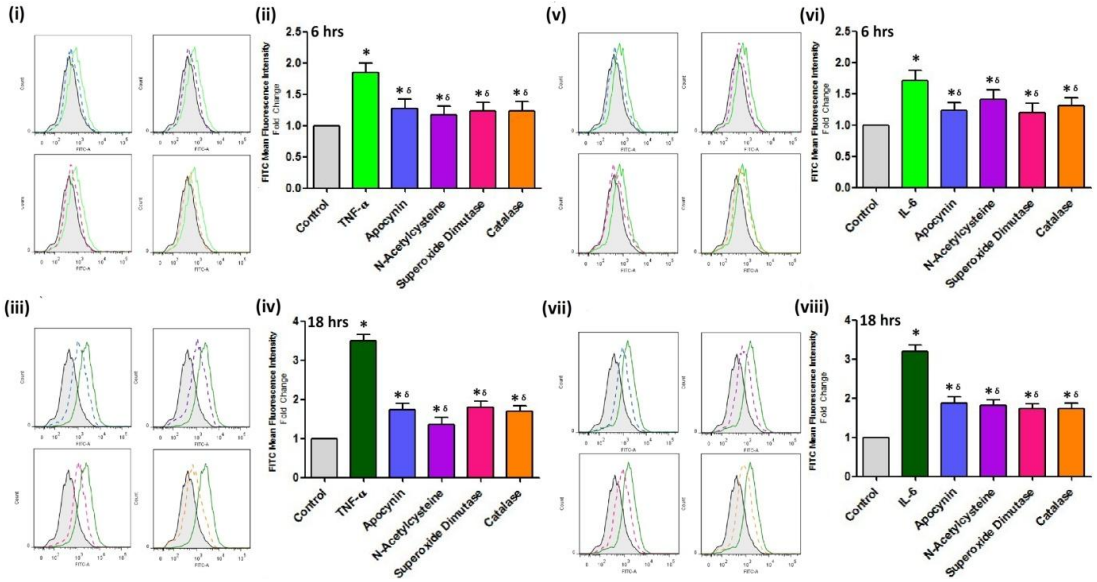

Figure 5.3: The effect of antioxidants on TNF-α- and IL-6-induced ROS production-CFDA. Confluent HBMvECs were stimulated with TNF-α or IL-6 (100ng/ml) for 6 or 18 hrs in the presence of CFDA and a range of antioxidant compounds. Post-treatment, cells were harvested and subsequently prepared for flow cytometry. The histograms represent the intensity of the CFDA dye prepared from the corresponding representative FACS scans. The cytokine-treated samples were analysed using FlowJo Flow Cytometry Analysis Software to quantify the respective signal from CFDA-stained cell populations in response to TNF-α (ii, iv) and IL-6 (v, vii) at 6 (upper) and 18 (lower) hrs. Results are averaged from three independent experiments ± SD. *P≤0.05 vs. Untreated Control. δP≤0.05 vs. TNF-α or IL-6 treatment.

Legend: FITC-A = CFDA

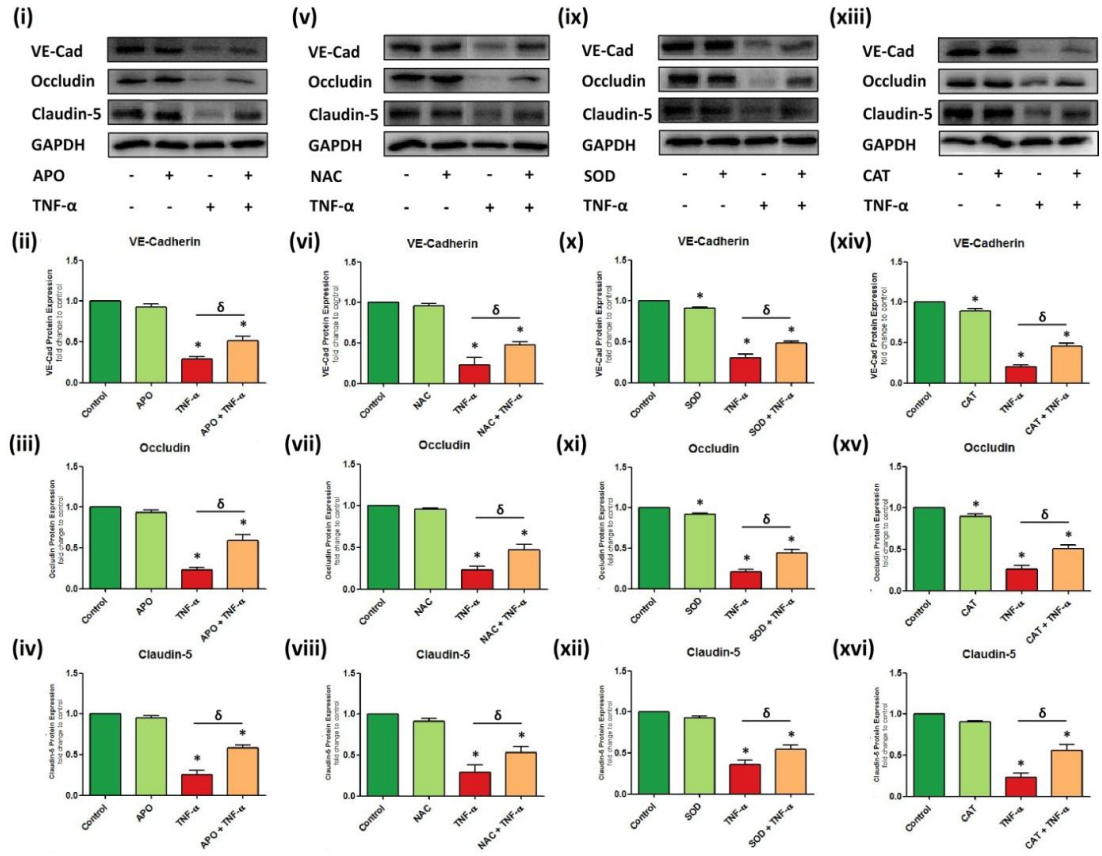

Figure 5.4: The effect of antioxidants on TNF-α-induced downregulation of TJ/AJ proteins. Confluent HBMvECs were treated with TNF-α (100 ng/ml) for 18 hrs in the presence of a number of antioxidant compounds. Post-treatment, cells were harvested for whole cell protein lysate. The translational effect on particular intercellular junction proteins was investigated by western blot. The histograms represent the changes in relative protein expression for VE-Cadherin (ii, vi, x, xiv), occludin (iii, vii, xi, xv) and claudin-5 (iv, viii, xii, xvi). Results are averaged from three independent experiments ± SD; *P≤0.05 vs. Untreated Control, δP≤0.05. Blots are representative.

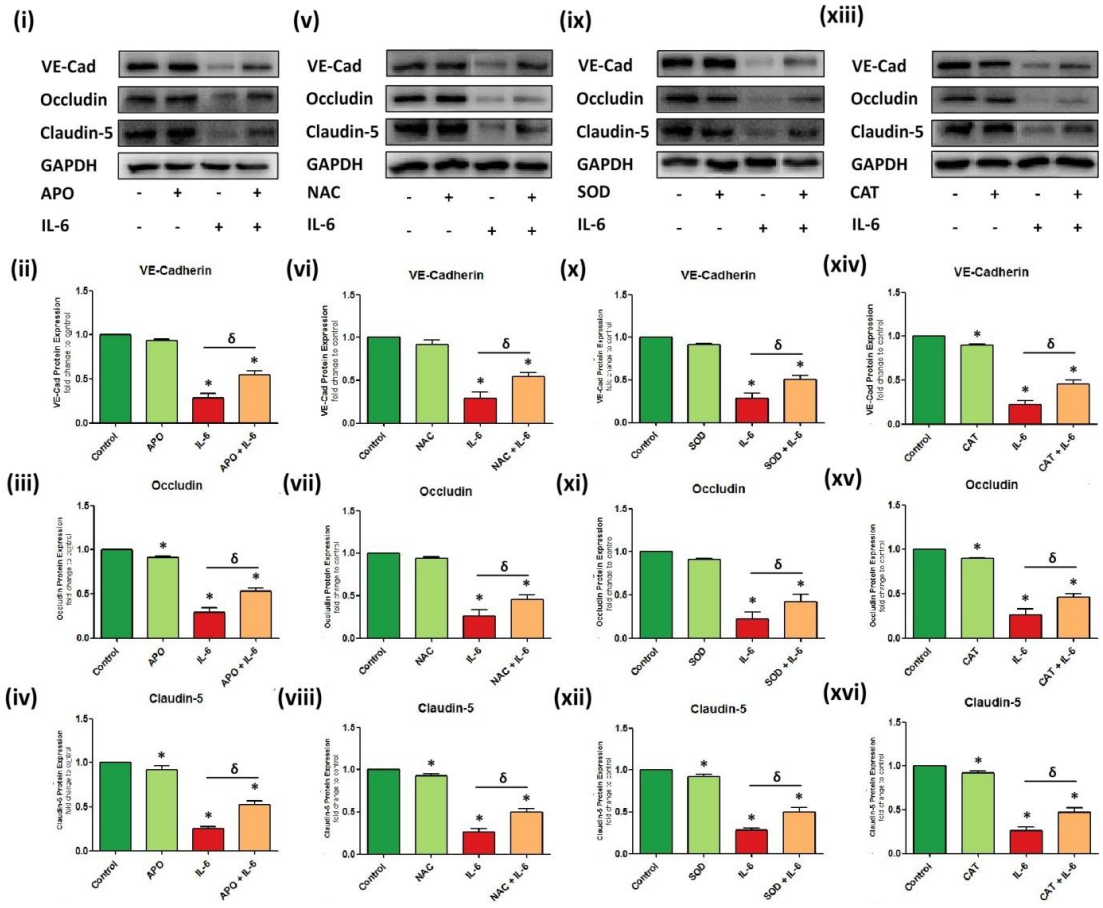

Figure 5.5: The effect of antioxidants on IL-6-induced downregulation of TJ/AJ proteins. Confluent HBMvECs were treated with IL-6 (100 ng/ml) for 18 hrs in the presence of a number of antioxidant compounds. Post-treatment, cells were harvested for whole cell protein lysate. The translational effect on particular intercellular junction proteins was investigated by western blot. The histograms represent the changes in relative protein expression for VE-Cadherin (ii, vi, x, xiv), occludin (iii, vii, xi, xv) and claudin-5 (iv, viii, xii, xvi). Results are averaged from three independent experiments ± SD; *P≤0.05 vs. Untreated Control, δP≤0.05. Blots are representative.

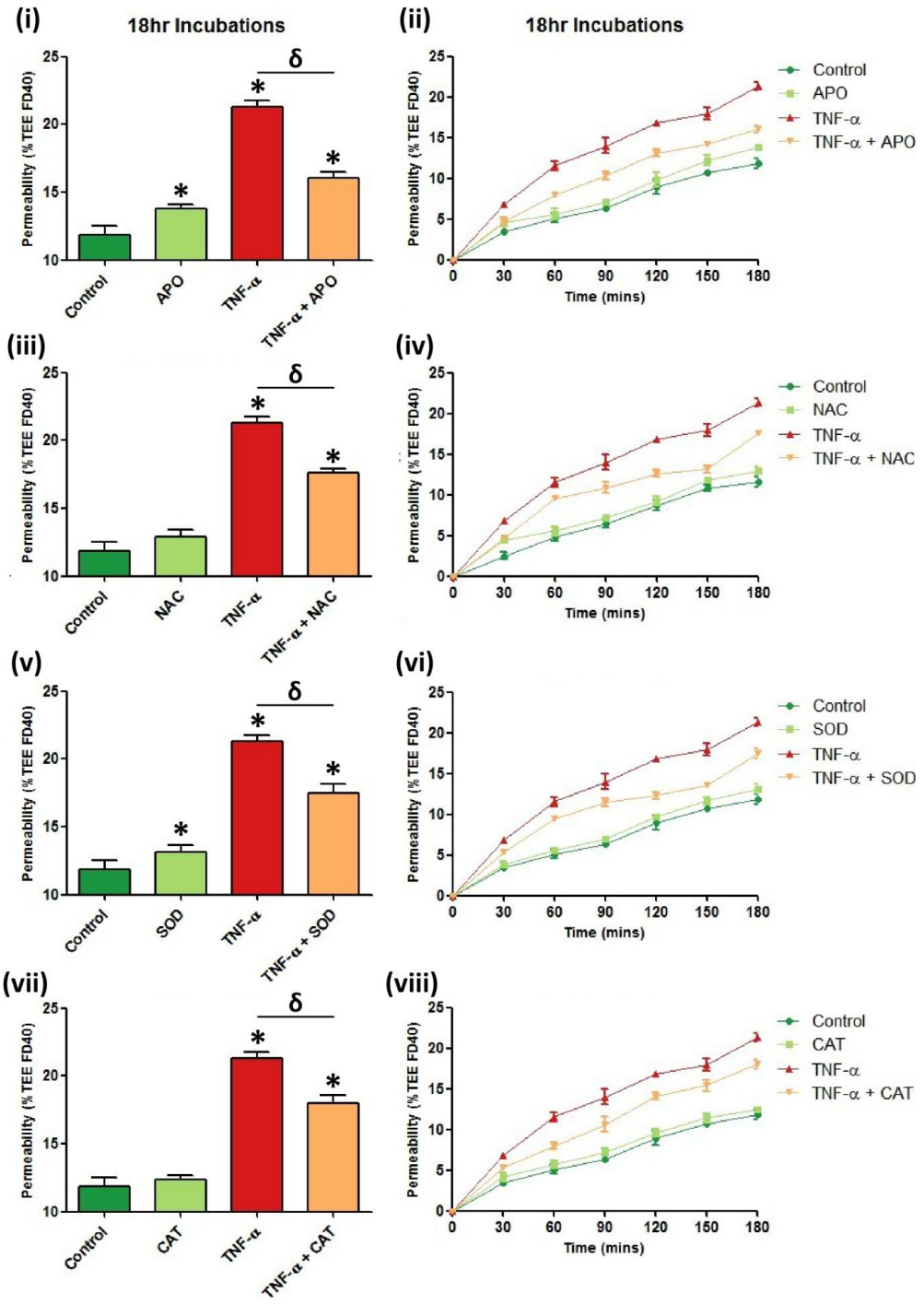

Figure 5.6: The effect of antioxidants on TNF-α-induced disruption of HBMvEC barrier function. HBMvECs were seeded at a known density and allowed to adhere prior to examination by transendothelial permeability. HBMvECs were then pre-treated with TNF-α (100 ng/ml) for 18 hrs in the presence of a number of antioxidant compounds. Post-treatment, monolayers were examined by transendothelial permeability assay. The histograms (LHS) and line graphs (RHS) show the change in permeability (% TEE FD40) at a given time point(s) (t) = 180 mins or 0-180 mins, respectively. Results are averaged from three independent experiments ± SD; *P≤0.05 vs. Untreated Control, δP≤0.05.

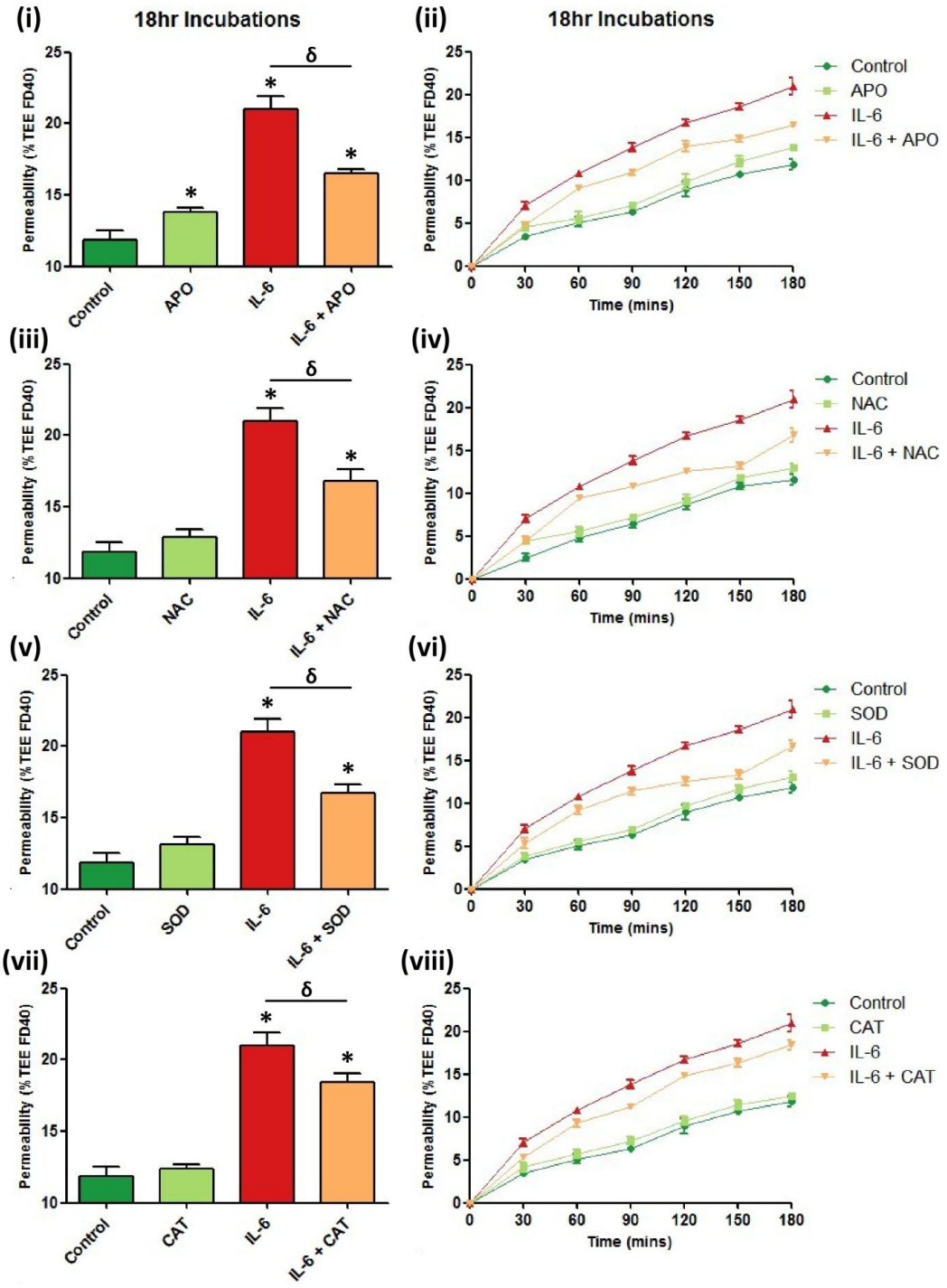

Figure 5.7: The effect of antioxidants on IL-6-induced disruption of HBMvEC barrier function. HBMvECs were seeded at a known density and allowed to adhere prior to examination by transendothelial permeability. HBMvECs were then pre-treated with IL-6 (100 ng/ml) for 18 hrs in the presence of a number of antioxidant compounds. Post-treatment, monolayers were examined by transendothelial permeability assay. The histograms (LHS) and line graphs (RHS) show the change in permeability (% TEE FD40) at a given time point(s) (t) = 180 mins or 0-180 mins, respectively. Results are averaged from three independent experiments ± SD; *P≤0.05 vs. Untreated Control, δP≤0.05.

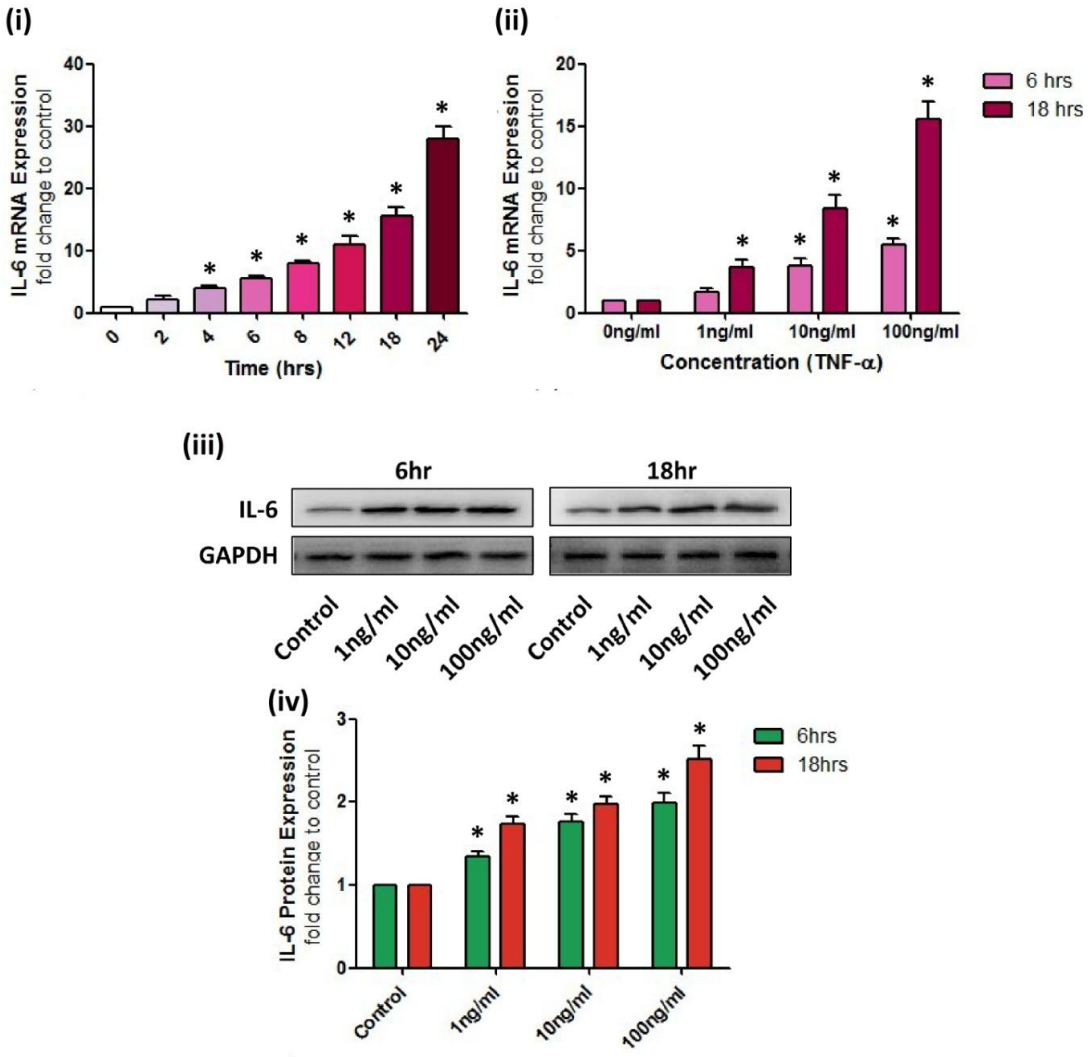

Figure 5.8: The effect of TNF-α on IL-6 expression. Confluent HBMvECs were stimulated with TNF-α (0-100 ng/ml) for 0-24 hrs following which they were harvested for whole cell mRNA and protein lysate. The histograms represent the changes in IL-6 mRNA over time (i) and with respect to dose at 6 and 18 hrs (ii). The translational effect of TNF-α on IL-6 protein was investigated by western blot (iii, iv). Results are averaged from three independent experiments ± SD; *P≤0.05 vs. 0 hrs (i), 0 ng/ml (ii) and Untreated Control (iv). Blots are representative.

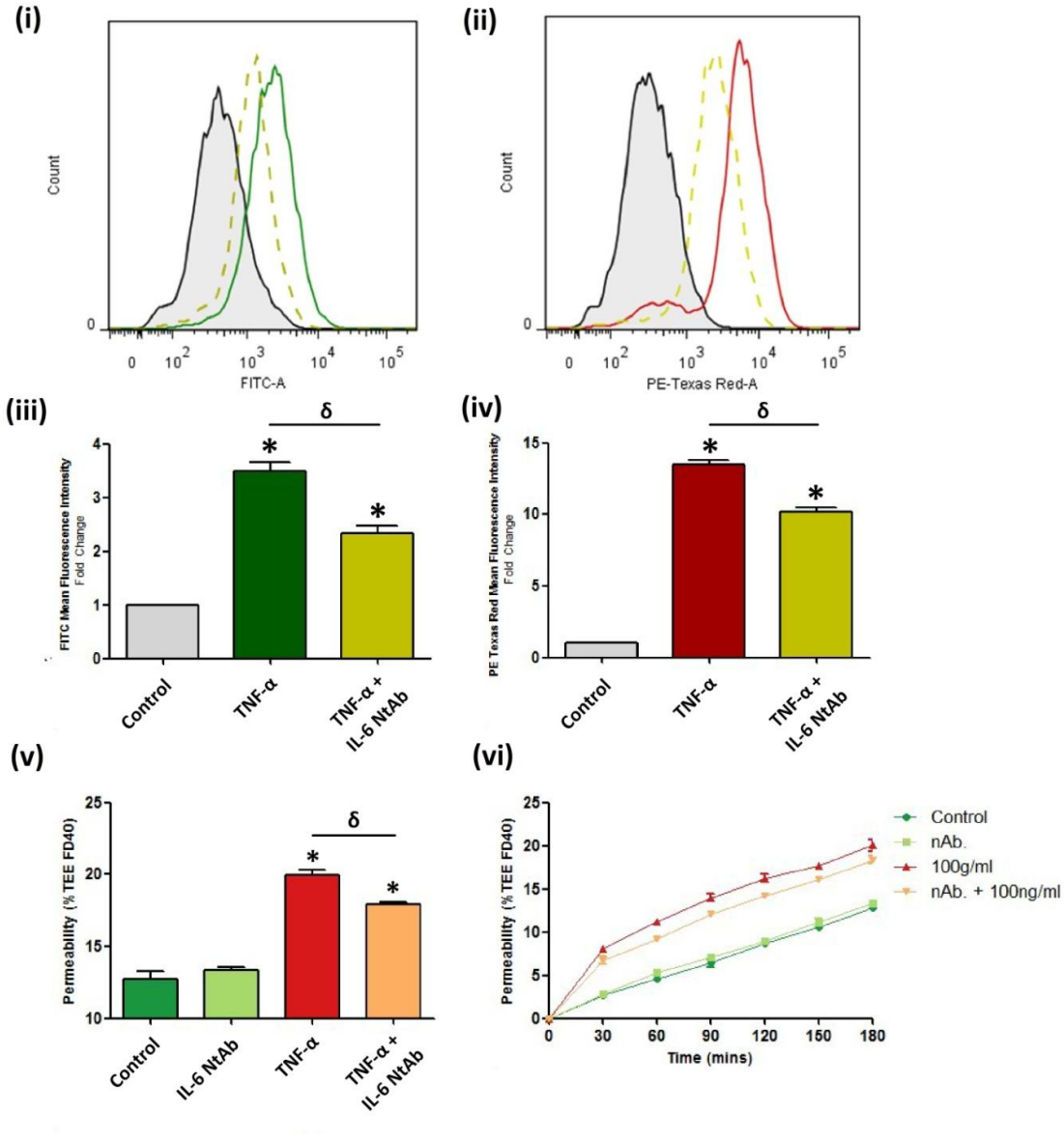

Figure 5.9: The effects of an IL-6 NtAb on TNF-α-induced disruption of HBMvEC barrier properties. Confluent HBMvECs were stimulated with TNF-α (100 ng/ml) for 18 hrs in the presence of CFDA or DHE, and in the absence and presence of an IL-6 NtAb Post-treatment, cells were harvested and subsequently prepared for flow cytometry. The histograms represent the intensity of the CFDA (iii) and DHE (iv) ROS signals prepared from the corresponding FACS scans (i, ii). The TNF-α-treated samples were analysed using FlowJo Flow Cytometry Analysis Software. Results are averaged from three independent experiments ± SD. *P≤0.05 vs. Untreated Control. In a parallel study, HBMvECs were seeded into transwell inserts at a known density and allowed to adhere prior to examination by transendothelial permeability assay. HBMvECs were then treated with TNF-α (100 ng/ml) for 18 hrs in the presence of the IL-6 NtAb. The histogram (v) and line graph (vi) show the change in permeability (% TEE FD40) at a given time point(s) (t) = 180 mins or 0-180, respectively. Results are averaged from three independent experiments ± SD; *P≤0.05 vs. Untreated Control, δP≤0.05.

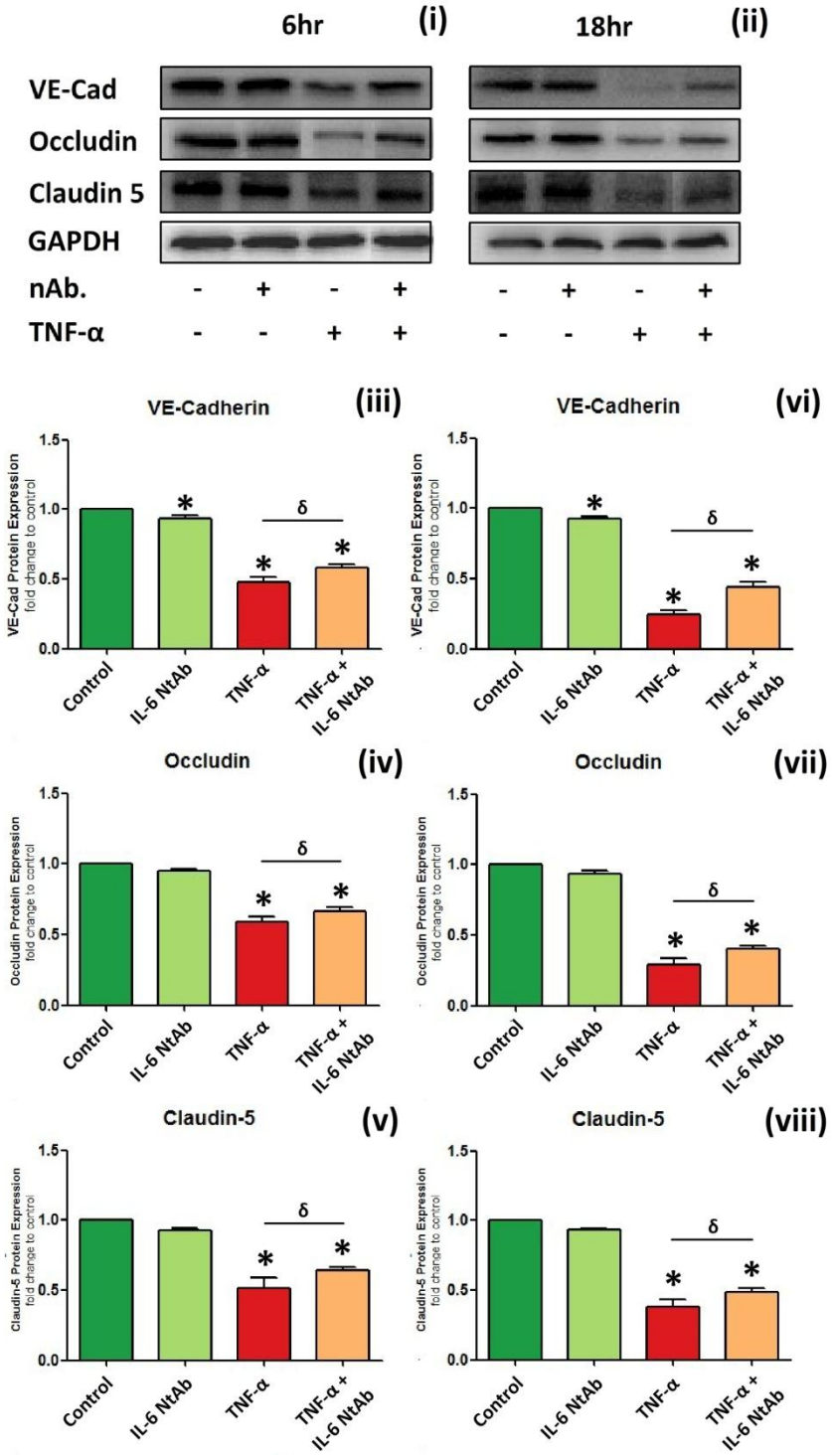

Figure 5.10: The effect of an IL-6 NtAb on TNF-α-induced disruption of HBMvEC barrier properties. Confluent HBMvECs were stimulated with TNF-α (100 ng/ml) for 6 and 18 hrs in the absence and presence of an IL-6 NtAb. Post-treatment, cells were harvested for whole cell protein lysate. The translational effect on particular intercellular junction proteins was investigated by western blot (i, ii). The histograms represent the changes in relative protein expression for VE-Cadherin (iii, vi), occludin (iv, vii) and claudin-5 (v, viii) on a expressional level in response to TNF-α (100ng/ml) for 18 hrs in the presence of an IL-6 NtAb. Results are averaged from three independent experiments ± SD; *P≤0.05 vs. Untreated Control, δP≤0.05. Blots are representative.

5.3 Discussion

Having characterised how the brain microvascular endothelium responds to both protective (Chapter 3) and injurious stimuli (Chapter 4), we next decided to examine those mechanisms mediating inflammatory damage to the endothelium. The mechanisms that mediate this inflammatory response during the early stages of endothelial dysfunction are often sustained and become exacerbated as damage to barrier phenotype continues. The increased production of ROS is a well established mechanism coinciding with inflammatory-based activation and sustained dysfunction of the endothelium (see Chapter 1). During the inflammatory initiation of CVD, cytokines and growth factors such as TNF-α, IL-1β and IFNγ have been shown to trigger ROS-producing molecules such as NADPH oxidase resulting in a surge of ROS in the area of injury. ROS can regulate a number of redox-sensitive genes to produce inflammatory mediators and activate several signalling pathways that promote vascular inflammation (Sun, Oberley 1996, Winyard, Blake 1997, Kunsch, Medford 1999). For example, peroxynitrite and superoxide have been shown to directly activate pro-inflammatory transcription factors such as NFκB and AP-1, which regulate the genes for most cytokines and is regularly implicated in endothelial dysfunction and vascular inflammation (Collins 1993). In addition to inducing the production and release of pro-inflammatory cytokines, increased ROS production has also been demonstrated to directly induce the upregulation of adhesion molecules (e.g. ICAM-1) and chemoattractants (i.e. MCP-1) (Marui, Offermann et al. 1993, Satriano, Shuldiner et al. 1993, Weber, Erl et al. 1994). The induction, release and actions of these factors in addition to those pertaining to local levels of ROS can in turn cause the exacerbation of vascular oxidative stress, creating a vicious circle of oxidative and inflammatory processes which are fundamental in the development and manifestation of CVD in both peripheral and cerebrovascular beds. It was therefore felt the influence of ROS was likely to be central to our inflammatory studies and so we decided to investigate the degree of impact, if any, it had on our HBMvEC/cytokine injury model. Whilst much data is available on the general ROS mechanisms associated with the endothelium, published mechanistic studies involving ROS in the microvasculature, and particularly in the human cerebral microvasculature, are limited. Thus, the effect of inflammatory cytokines (TNF-α and IL-6) on the ROS formation leading to consequences for BBB phenotype were investigated *in vitro*.

Two means of tracking and quantifying ROS production were employed; DCFDA, a probe which following cellular deacetylation is free to be oxidised by available ROS into a highly fluorescent compound, and DHE; which in the presence of superoxide becomes reduced to form the highly fluorescent DNA binding ethidium. Using these dyes, a fluorimetric signal proportionate to the intracellular levels of ROS could be easily measured by flow cytometry

(Carter, Narayanan et al. 1994). In response to TNF-α treatment we saw significant dose- and time-dependent increases in DCFDA and DHE signal. This increase in signal was sustained and propagated to a 4-fold change in DCFDA signal and a 15+ fold change in DHE signal by 24 hrs. A similar trend was observed in response to IL-6 treatment over 24 hrs. TNF-α is a well-documented initiator of ROS production in endothelial cells (Busik, Mohr et al. 2008, Montiel-Davalos, de Jesus Ibarra-Sanchez et al. 2010) although little data is available on the ROS-inducing effect of IL-6 in endothelial cells (Christov, Ottman et al. 2004). Based on these findings, we hypothesized that ROS production may play an integral part in cytokine induced-endothelial injury.

ROS have been identified as secondary messengers in a number of signalling pathways, having been shown to participate in a number of physiological functions such as regulation of blood flow, coagulation, inflammation and cellular growth (Griendling, Sorescu et al. 2000, Griendling, Sorescu et al. 2000). Whilst ROS surges have been characteristically looked upon as risk factors, a controlled increase may have beneficial effects. Zahler (2000) demonstrated acute pre-conditioning of endothelial cells to oxidative stress attenuated subsequent cytokine-induced damage. In order to examine this concept, a number of agents that are capable of scavenging for and/or disrupting the mechanisms that produce ROS were employed to elucidate whether ablation of the induced ROS production may attenuate (or exacerbate) the damage inflicted on HBMvEC barrier phenotype. A broad range of antioxidants compounds were employed; Apocynin; an inhibitor of the superoxide producing enzyme NAPDH oxidase, N- Acetyl-L-cysteine; a broad spectrum antioxidant that increases cellular levels of the major detoxification enzyme gluthathione, Superoxide dismutase; which catabolises superoxide anion to yield oxygen and water, and catalase; which catalyses the breakdown of hydrogen peroxide into oxygen and water. In the case of each compound, we found a significant decrease in DCFDA and DHE ROS signal following either acute (6 hrs) or chronic (18 hrs) exposure to TNF-α and IL-6 (100 ng/ml). The main source of cytokine-induced ROS within the microvasculature therefore appears to originate from NADPH oxidase. A number of earlier studies have implicated it in contributing to the development of a host of microvascular dysfunctions (Ishikawa, Stokes et al. 2004, Wood, Hebbel et al. 2005, Collins-Underwood, Zhao et al. 2008). Consistent with our study, Basuroy (2009) also demonstrated that porcine microvascular endothelial cells treated with TNF-α underwent oxidative damage, which could be ameliorated via direct inhibition of NADPH oxidase using either apocynin or diphenylene iodonium.

We next looked at whether cytokine-induced ROS production had any influence on the expression of proteins located at the intercellular junctions. Previous studies in BBMvECs reported that direct induction of oxidative stress by H_2O_2 treatment significantly increased

occludin and actin expression but was seen to disrupt their (and ZO-1's) localisation at the tight junctions (Lee, Namkoong et al. 2004). In contrast, models utilising Aβ to induce ROS production in cortical capillaries reported a dramatic loss of occludin, claudin-5 and ZO-1 expression at the tight junction (Carrano, Hoozemans et al. 2011). Synonymous with this, Schreibelt (2007) observed both an overall reduction in occludin and claudin-5 protein expression and localisation at rat BMvEC cell-cell junctions following induced increase in the microenvironment's ROS levels. We found for each antioxidant treatment that a partial, but significant, recovery in the cytokine-induced reduction in expression of VE-Cadherin, occludin and claudin-5 was achieved thus implicating the fold change in intracellular ROS levels to be damage-inducing. This effect was shown in both acute (6 hrs) and chronic (18 hrs) treatment with TNF-α and IL-6 in the presence of the different antioxidant compounds.

Based on the partial recovery of intercellular junction protein levels, the antioxidant strategies were next implemented to assess whether the recovery in protein was enough to attenuate TNF-α- and IL-6-induced loss of barrier function in HBMvECs. Studies examining the mechanism of IL-17A-induced ROS release on BBB disruption reported loss of barrier function due to cell contractility and loss of occludin at the tight junction, a pathway which could be prevented by inhibition of IL-17A activation of NADPH oxidase and xanthine oxidase production of ROS (Huppert, Closhen et al. 2010). Similar reversible effects on the tight junction and BBB permeability were observed using oxidised low-density lipoprotein to induce ROS-production in mouse BMvECs (Wang, Sun et al. 2012). Schreibelt (2007) also noted a reduction in BMvEC barrier integrity via ROS-induced reductions in claudin-5 and occludin. We found for each antioxidant treatment of HBMvECs exposed to TNF-α and IL-6 (100 ng/ml), a very significant recovery in barrier function was achieved, once again highlighting the negative impact of cytokine-induced ROS production on cerebrovascular homeostasis. We observed this once again for both acute (6 hrs) and chronic (18 hrs) treatments with TNF-α and IL-6. Whilst studies examining the direct effect of cytokine-induced ROS production on BBB barrier function are scarce, the majority of existing work focuses on ischemia/reperfusion experimental paradigms that corroborate our observations regarding the influence of oxidative stress on BBB barrier modulation (Witt, Mark et al. 2003, Witt, Mark et al. 2008).

Based on these collective findings, pharmacological intervention of cytokine-induced ROS using antioxidant compounds was shown to partially restore intercellular junction expression and BBB phenotype. While exploration into the actions of ROS within the cerebral microvasculature has been scarce, some mechanisms have been elucidated. Nagyoszi (2010) demonstrated how increased concentrations of ROS can induce the upregulation of certain TLRs in cerebral endothelial cells, which upon activation were shown to mediate the

ablation of tight junction proteins; claudin-5 and occludin. Haorah (2007) also reported increased permeability in HBMvECs in response to induced oxidative stress. Interestingly, a dual mechanism involving the enhanced activity of MMPs and protein tyrosine kinases on proteins of the tight junction was demonstrated. The effects observed in this paper, and others by Haorah (2005, 2005, 2007), regarding tyrosine and threonine phosphorylation of tight junction proteins, provides an interesting link between the effects of ROS on barrier function and our own earlier findings on tyrosine levels in response to shear (Chapter 3) and cytokine injury (Chapter 4). These mechanisms may apply in the actions of cytokines on HBMvEC and may be worth exploring. A number of related articles also make similar claims regarding ROS induction in the cerebrovascualture and disruption of vascular homeostasis yet the focus lies squarely on unnatural means of inducing oxidative stress (Haorah, Ramirez et al. 2007) or agents of abuse (i.e. alcohol (Haorah, Knipe et al. 2005, Haorah, Heilman et al. 2005) and methamphetamines (Zhang, Banerjee et al. 2009)).

Based on our results, and the wealth of existing data on this subject, the impact of oxidative stress in the disruption of vascular homeostasis and barrier phenotype makes it an ideal candidate for therapeutic intervention. A number of studies have yielded strategies that restore the balance of ROS within the vascular system. One pioneering study involved the administration of a polyethyleneglycol-superoxide dismutase conjugate to atheroprone animal models that restored impaired endothelial function (Mugge, Elwell et al. 1991). Despite the consistency and successes achieved using *in vitro* and *in vivo* (Mugge, Elwell et al. 1991) models in negating and reversing the effect of oxidative stress, the translation of findings into clinical trials has been disappointing thus far with very few drug candidates achieving significant impact (Steinhubl 2008) (lipid-lowering drugs such as simvastatin and pravastatin have been shown to demonstrate secondary pleiotropic anti-oxidant effects; increasing local SOD, eNOS and gluthione peroxidise activity (Tandon, Bano et al. 2005)). With regards to the cerebrovasculature, the prevention of oxidative stress is of utmost importance as many of the debilitating diseases of the cerebral tissues derive from oxidative stress in their progression and disruption (e.g. Parkinson's disease, Alzheimer's disease etc (Ali, Barnham et al. 2004)). Delivery of potential compounds to the afflicted areas remains difficult due to the problems typically associated with traversing the BBB, however great progress has been made in the field of nanotechnology with breakthroughs such as 'nanozymes' at the forefront of solving this problem (Manickam, Brynskikh et al. 2012, Klyachko, Manickam et al. 2012). In the meantime, antioxidant treatment is now looked upon as a risk reducer more so than a damage repairer, and dietary studies involving vitamin supplementation has transferred relatively well into human models with clinical studies demonstrating increases in vitamin C and E in the diet can drastically improve negative

aspects imparted by oxidative damage caused by chronic smoking, type 1 and 2 diabetes mellitus, hypercholesterolemia and chronic heart failure amongst others (Frei, England et al. 1989, Packer, Valacchi 2002, Zaidi, Banu 2004), although there are conflicting reports regarding the efficacy (Behrendt, Krawinkel 2007, Behrendt, Ganz 2007).

To summarise at this point, we find we have clearly demonstrated that TNF-α and IL-6 are capable of elevating ROS production of HBMvECs in both a time- and dose-dependent manner. Having demonstrated a controlled means of significantly reducing ROS presence using antioxidant compounds, we verified the elevated levels induced by TNF-α and IL-6 were enough to sufficiently cause a reduction in tight junction protein levels; occludin, claudin-5 and VE-Cadherin, and subsequently cause a reduction in barrier function. We feel this data presents a comprehensive outlook on the cytokine-induced mechanisms in the acute and chronic stages of microvascular injury and underlines the importance of developing antioxidant treatments which are capable of effectively treating oxidative stress in the cerebral tissue.

In addition to the release of ROS, we extensively examined the secretory profile of HBMvECs in response to a range of different cytokines (TNF-α, IL-6, MCP-1) over different exposure times (6 and 18 hrs). A relationship that we found interesting, and relatively unexplored, was the TNF-α-induced release of IL-6 (Chapter 4). To expand on this concept, further studies on this pathway were conducted. The transcription of IL-6 in response to TNF-α was examined first; IL-6 mRNA levels were significantly increased in a dose- and time-dependent manner following treatment with TNF-α (100 ng/ml) with an overall fold change of over 25 achieved by 24 hrs. Earlier studies in HUVECs reported similar fold changes in IL-6 transcription levels in response to TNF-α (Yamagishi, Inagaki et al. 2004). IL-6 protein expression in response to TNF-α was also investigated with a dose-dependent increase observed following both acute and chronic treatment of HBMvECs. This is consistent with earlier studies (Modur, Zimmerman et al. 1996, van den Berghe, Vermeulen et al. 2000). Earlier studies in HAECs have demonstrated the ability of IL-4 to upregulate IL-6 levels and induce its release (Lee, Lee et al. 2010). The same study also demonstrated the ability of IL-4 to drive up ROS production, whilst treatment with antioxidants, particularly those targeting NADPH oxidase, attenuated HAEC IL-6 release. It is possible therefore that TNF-α-mediated IL-6 production in our HBMvEC model may proceed in part via ROS production (examined later).

TNF-α is a potent cytokine within the acute phase of cerebrovascular injury with elevated levels recorded within the first hour in the area of inflicted injury (Shohami, Novikov et al. 1994, Fassbender, Rossol et al. 1994, Hallenbeck 2002). Our observation of TNF-α inducing

the production of IL-6 in HBMvECs is of great interest therefore. Between the IL-6 expression data in this chapter and the HBMvEC secretory profile reported in Chapter 4, we have demonstrated that HBMvECs are a reliable source for IL-6 in response to inflammatory cytokines such as TNF-α. We have also demonstrated that IL-6 within certain concentration and incubation ranges (1-100ng/ml, 6 and 18 hrs) has a damaging effect on HBMvEC cultures at both molecular and functional levels. Therefore it is imperative to investigate the response of the TNF-α-induced level of IL-6 on the homeostasis of HBMvECs to understand the potential mechanisms within the NVU. This pertains to the complex biology of IL-6 with much conflicting data describing it as having both protective and damaging effects within the NVU (Barkhudaryan, Dunn 1999, Erta, Quintana et al. 2012).

Given the role of IL-6 in the pathogenesis of several disease states, targeted inhibition of IL-6 activity is an attractive prospective therapeutic strategy (Kishimoto 2005, Tanaka, Narazaki et al. 2011, Tanaka, Narazaki et al. 2012). Due to the complex signalling nature of IL-6, a number of potential molecules (i.e. gp130, sIL-6R, tIL-6R, IL-6) were readily targetable for developing novel interventions in the blockade of IL-6 signalling (Ataie-Kachoie, Pourgholami et al. 2013). To date, the most famous of the IL-6 therapeutics comes in the forms of tocilizumab, a humanised anti-human IL-6R monoclonal antibody which competes with freely available tIL-6R and sIL-6R. Tocilizumab is readily available in over 90 countries and its efficacy is such that it is the first line biologic in Japan, India, USA and the EU for treating various forms of arthritis (Tanaka, Narazaki et al. 2012).

Initially, clinical trials involving IL-6 therapeutics, in particular tocilizumab, targeted automimmune diseases such as rheumatoid arthritis (Nakahara, Song et al. 2003, Nishimoto, Miyasaka et al. 2009, Nishimoto, Miyasaka et al. 2009) and systemic juvenile arthritis (Yokota, Miyamae et al. 2005). Data accumulated from these trials reported interesting secondary effects opening the door for additional treatment of other IL-6-based diseases. Improvements in the levels of HbA1c (Ogata, Morishima et al. 2011) and reactive oxygen metabolites (Hirao, Nampei et al. 2011) have sparked a number of new trials investigating the potential of targeted IL-6 therapy in halting atheroprogressive mechanisms subsequently decreasing the chances of developing a form of CVD (Boekholdt, Stroes 2012). The efficacy of these therapies in combating CVD has been so successful that a number of other cytokine-targeting therapies developed for autommunity-based diseases have been considered and trialled for similar purposes (i.e. TNF-α inhibitor, etanercept).

On the basis of the proven pathological role of IL-6 in conjunction with the proven beneficial effect of anti-IL-6 therapies such as tocilizumab, IL-6 targeting is now considered a rational strategy in the treatment of various diseases with a number of IL-6 inhibitors being

developed (Jones, Scheller et al. 2011). As part of our study, an IL-6 NtAb was employed to investigate the impact of TNF-α-induced injury when IL-6 activity was ablated. We began by identifying an effective concentration of IL-6 NtAb whilst ensuring specificity to IL-6 was maintained (and direct interference in the activity of TNF-α was ruled out). We confirmed the specificity of the NtAb by western blot in which HBMvEC lysate and recombinant IL-6 (1 ng/ml) were run out on a SDS-PAGE gel along with our working concentrations of TNF-α (1-100 ng/ml) and subjected to immunblot analysis. Only the HBMvEC lysate and recombinant IL-6 displayed a band in the correct size region confirming our NtAb would not interfere with TNF-α activity. We then optimised our working antibody concentration based on its ability to prevent IL-6-mediated barrier disruption and permeabilisation. Different doses of NtAb were tested against a fixed concentration (20 ng/ml) of IL-6 with the concentration of NtAB chosen on the basis of effective barrier restoration and insignificant impact of the NtAb on the HBMvEC cultures themselves.

The IL-6 NtAb was first utilised in examining the effect of TNF-α on ROS production. Cultures exposed to TNF-α (100 ng/ml) in the presence of the IL-6 NtAb demonstrated a reduction in ROS levels in both acute (6hrs) and chronic (18 hrs) experimental paradigms. Our earlier data obtained for IL-6 over the working concentration range (1-100 ng/ml) clearly demonstrated IL-6 could induce an increase in ROS production. With the employment of the NtAb therefore, TNF-α-mediated induction of IL-6 could now be partially attributed to the elevation in ROS production by TNF-α. The effect of TNF-α-induced reduction in HBMvEC barrier function in the presence of the IL-6 NtAb was next explored. Cultures incubated with the IL-6 NtAb in the presence of TNF-α clearly demonstrated a significant restoration in barrier function following exposure to TNF-α alone in both acute and chronic treatments. This experimental paradigm was further explored to investigate the impact of TNF-α on the proteins involved at the intercellular junctions. Attenuating IL-6 activity with the NtAb during TNF-α treatment demonstrated a partial recovery in occludin, claudin-5 and particularly VE-Cadherin levels. As mentioned in chapter 4, the biology of IL-6 is complex, with several studies outlining both its beneficial and harmful inductive properties. An *in vivo* study by Paul (Paul, Koedel et al. 2003) addresses this utilising a similar strategy to ours in which the BBB is injured in the absence of IL-6 activity and subsequently characterised. Whilst certain inflammatory aspects (such as cytokine release) were exacerbated, a concurrent reduction in BBB disruption was observed. Therefore, whilst we have categorically identified IL-6 as having a disruptive role in HBMvEC homeostasis, there are several arguments that can be made indicating its beneficial effects (Woodroofe, Sarna et al. 1991, Taupin, Toulmond et al. 1993, Klein,

Moller et al. 1997, Penkowa, Moos et al. 1999, Hans, Kossmann et al. 1999, Penkowa, Giralt et al. 2000, Swartz, Liu et al. 2001, Galiano, Liu et al. 2001).

In conclusion, we found the impact of TNF-α-induced IL-6 release on HBMvECs significant across a number of molecular and functional aspects. The levels of IL-6 released in response to inflammatory mediators such as TNF-α may therefore contribute to the overall damage inflicted by TNF-α on HBMvEC barrier phenotype.

Chapter 6:

The role of 14-3-3 in shear- and cytokine-induced modulation of HBMvEC junction assembly and barrier function.

6.1 Introduction

As evidenced from the works of chapters 3, 4, and 5, the junctions of the BBB are dynamic structures. Following exposure to our local (shear stress) and systemic (TNF-α, IL-6, ROS) factors of interest, the proteins that comprise these junctions were demonstrated to become subject to molecular changes in expression, subcellular localisation, and post-translational modification, under both physiological (shear) and pathophysiological (cytokine) conditions. A number of intracellular signalling pathways regulate these processes with the BBB endothelium.

The regulation of paracellular permeability is indeed subject to the complex interactions between several agonist-activated signalling pathways and key structural components of the endothelial cells. Phosphorylation is one such regulatory mechanism. Many of the proteins located in the interendothelial junctions of the BBB are classified as phosphoproteins, and possess several phosphorylation sites which can be affected during these complex signalling cascades. Several studies have identified the phosphorylation state of both the transmembrane and adapter proteins located at the interendothelial junction in several important functional events, from mediating subcellular localisation of tight junction proteins to overall junction assembly (Staddon, Herrenknecht et al. 1995). Given the multiple sites for phosphorylation on these proteins, it is likely that the cumulative phosphorylation levels of distinct tyrosine, threonine and serine residues on each protein have distinct functional consequences for BBB phenotype (Sakakibara, Furuse et al. 1997). Shifts in the equilibrium of phosphorylation state of certain proteins can lead to significant cellular dysfunction and ultimately cell death. These imbalances in phosphorylation state have been identified as a driving force in the development of several neurodegenrative diseases. A common trait in such disorders, hyperphosphorylation of fundamental proteins are indicative of disease and is generally believed to lead to their misfolding and aggregation. Several cerebral pathologies have identified hyperphosphorylation of BBB proteins as a hallmark in their development (e.g. stroke, MS, Alzheimer's disease) and as a result are at the forefront of the rationale for modulating phosphorylation for therapeutic benefit. Together, all these events can contribute to abnormal phosphorylation states that can either cause or exacerbate disease. Therefore, homeostatic control of phosphorylation is vital in maintaining the physiological functions of the BBB and the associated wide range of cellular signalling processes it partakes in (Luissint, Artus et al. 2012).

To date, the majority of CNS molecular studies pertaining to tyrosine, threonine and serine phosphorylation events have focussed on their role in the initiation and progression of cerebral pathologies, with ample evidence pertaining to their effect on BBB dysfunction. In contrast, there is very little information on the effects of protective influences, such as

laminar shear stress, on mediating these phosphorylation events (Walsh, Murphy et al. 2011). These post-translational modifications are invariably mediated by a multitude of binding partners; kinases, phosphatases and facilitative adapter proteins that can mediate these phosphorylative events. Within our model of shear-induced enhancement of HBMvEC barrier function, ***our attention for chapter 6 turned to identifying the potentially novel binding partners that mediate the shear-mediated dephosphorylation of junction proteins, resulting in enhanced barrier function.*** Sophisticated co-immunoprecipitation techniques coupled with advanced liquid chromatography-mass spectrometry analysis identified the 14-3-3 family of proteins as having a substantial presence at the interendothelial junction complex during shear-mediated events. The nature of 14-3-3 binding, coupled with its extensively documented relationship with regards to phosphorylation events, made it an ideal candidate for further investigation as a potential mediator of phosphorylation-driven events at the interendotheial junction of the BBB (Yaffe 2002).

6.1.1 Study Aims

In this chapter we examine the potential role of the 14-3-3 family in the shear- and cytokine-induced modulation of HBMvEC interendothelial junction assembly and barrier function. Therefore, the overall aims of this chapter include:

- To identify novel binding partners of TJ/AJ proteins following pre-conditioning by physiological levels of laminar shear stress.
- To clarify the relationship between the identified potential binding partners (14-3-3) and the TJ/AJ protein (occludin, claudin-5, VE-Cadherin, ZO-1).
- To investigate the effect of physiological levels of laminar shear stress, and TNF-α and IL-6, on 14-3-3 family isoforms transcriptional expression.
- To investigate the effect of the inhibition of 14-3-3 binding by R18 peptide on HBMvEC barrier function during exposure to physiological levels of laminar shear stress or TNF-α and IL-6.

6.2.1 The 14-3-3 family of proteins interact with a number of interendothelial junction proteins in response to shear

The identification of novel binding partners to a number of the interendothelial junction proteins was carried out (Figure 6.1, 6.2). Confluent HBMvECs were maintained in static cultures or subjected to laminar shear stress (8 dynes cm^{-2}) for 24 hrs before being harvested for whole cell protein lysate. Samples were then subjected to immunoprecipitation for each protein of interest; occludin, claudin-5, VE-Cadherin and ZO-1 with successful pulldown confirmed by SDS-PAGE and subsequent staining with coomassie reagent (Figure 6.1, i, ii). Protein bands of interest were excised from the SDS-PAGE gels and sent with IP elutions for analysis by LC-MS/MS (iii-v). Peptide libraries for each sample set were cross-referenced to identify a novel binding partner (vi). The 14-3-3 family of proteins appeared in the peptide libraries for each junction protein with an elevated peptide frequency routinely observed in samples exposed to laminar shear stress (Fig. 6.2, i). The co-association of 14-3-3 with the intercellular junction proteins was confirmed by western blot using the IP eluates (ii).

6.2.2 Exposure of HBMvECs to laminar shear stress increases the association between 14-3-3 and the intercellular junction proteins-an effect which can be blocked by R18 peptide

The effect of laminar shear stress on 14-3-3 association with the intercellular junction proteins was examined (Figure 6.3, 6.4). Confluent HBMvECs were maintained in static environments or subjected to laminar shear stress (8 dynes cm^{-2}) for 24 hrs before being harvested for whole cell protein lysate. Samples were then subjected to immunoprecipitation for each protein of interest; occludin, claudin-5, VE-Cadherin and ZO-1. The 14-3-3 levels were then examined by western blot. 14-3-3 showed a significant increase in protein levels (and thus association) in response to laminar shear stress for each of the interendothelial junction proteins (Figure 6.3, i-iv). A complimentary reverse study in which samples were immunoprecipitated for 14-3-3 showed a similar trend, whereby interendothelial junction protein association with 14-3-3 underwent a significant increase in response to laminar shear stress (Figure 6.4, i-iv).

In order to explore the impact of 14-3-3 association with junctions, inhibition of its binding was necessary. R18 peptide is a commercially available inhibitor which effectively binds to 14-3-3 to inhibit its association with other ligands. Confluent HBMvECs were maintained in static environments or subjected to laminar shear stress (8 dynes cm^{-2}) for 24 hrs in the absence or presence of 100 nM R18 peptide before being harvested for whole cell protein

lysate. Samples were then subjected to immunoprecipitation for each protein of interest; occludin, claudin-5, VE-Cadherin and ZO-1. The 14-3-3 levels were then examined by western blot. Exposure of HBMvECs to laminar shear stress resulted in a significant increase in 14-3-3 association with each of the interendothelial junction proteins of interest, an association that was completely blocked by R18 peptide (Figure 6.3, 6.4, i-iv).

6.2.3 Pro-longed exposure of HBMvECs to laminar shear stress induces the downregulation of transcriptional levels of 14-3-3 family isoforms

The effect of laminar shear stress on 14-3-3 family isoforms over time was examined on a transcriptional level (Figure 6.5). Confluent HBMvECs were maintained in static environments or subjected to laminar shear stress (8 dynes cm^{-2}) for 0-24 hrs before being harvested for whole cell mRNA. The mRNA levels of five members of the 14-3-3 family; ζ, γ, ε, β and θ were examined from 0-24 hrs by qPCR. A significant change was observed for all five receptors in response to acute shear exposure (0-4 hrs); levels initially increased in response to acute laminar shear stress. All levels returned to baseline levels within 8 hrs of shear stress onset with a continued reduction in mRNA levels resulting in a moderate decrease in levels at 24 hrs in comparison to static cultures (i-v).

6.2.4 R18-inhibition of 14-3-3 causes a downregulation in barrier function

The effect of R18 inhibition of 14-3-3 in relation to barrier function was examined (Figure 6.6). HBMvECs were seeded at a known density onto transwell inserts and left to adhere overnight. The following day the cultures were treated with R18 peptide (0-1000 nM) for 6 hrs before being assessed for transendothelial permeability. Exposure of HBMvECs to R18 results in a significant increase in FITC-Dextran paracellular flux (%TEE of FD40) across the cell monolayer (i, ii).

The effect of laminar shear stress on the barrier function of HBMvECs in the presence of R18 was then examined. Confluent HBMvECs were maintained in static environments or subjected to laminar shear stress (8 dynes cm^{-2}) for 24 hrs in the absence or presence of R18 peptide (0-1000 nM) before being assessed for transendothelial permeability. Exposure of HBMvECs to R18 results in a significant increase in FITC-Dextran paracellular flux (%TEE of FD40) across the cell monolayer. Exposure of HBMvECs to laminar shear stress decreases permeability as expected, an effect that is completely blocked by R18 peptide in a dose-dependent manner (iii-vi). Complimentary studies conducted after 18 hrs incubation with R18 peptide show a similar trend which corroborates this data (Figure A.23).

Moreover, the effect of the R18 peptide concentration on HBMvEC viability was also examined by flow cytometry to determine the effective dose (Figure A.24).

6.2.5 Exposure of HBMvECs to TNF-α induces the upregulation of transcriptional levels of 14-3-3 family isoforms

The effect of TNF-α on members of the 14-3-3 family over time was examined on a transcriptional level (Figure 6.7). Confluent HBMvECs were stimulated with TNF-α (0-100 ng/ml) for 0-24 hrs before being harvested for whole cell mRNA. The transcriptional levels of five members of the 14-3-3 family; ζ, γ, ε, β and θ were examined from 0-24 hrs by qPCR. An initial increase was observed for all five members in response to acute shear exposure (0-4 hrs). Transcription levels across all five members continued to increase robustly with respect to time and dose (i-x). A similar trend was observed in parallel experiments utilising IL-6 in place of TNF-α (Figure A.25).

6.2.6 R18-inhibition of 14-3-3 can potentiate the injury caused by TNF-α and IL-6

The effect of R18 inhibition of 14-3-3 in relation to TNF-α and IL-6 induced barrier dysfunction was examined (Figure 6.8). HBMvECs were seeded at a known density onto transwell inserts and left to adhere overnight. The following day the cultures were stimulated with TNF-α or IL-6 (100ng/ml) in the absence or presence of R18 peptide (0-1000 nM) for 6 hrs before being assessed for transendothelial permeability. Exposure of HBMvECs to cytokines also results in a significant increase in FITC-Dextran paracellular flux (%TEE of FD40) across the cell monolayer. Furthermore, exposure of HBMvECs to cytokines in the presence of R18 resulted in a further moderate increase in permeability (i-iv). Complimentary studies conducted after 18 hrs incubation with TNF-α and IL-6 show a similar trend which corroborates this data (Figure A.26).

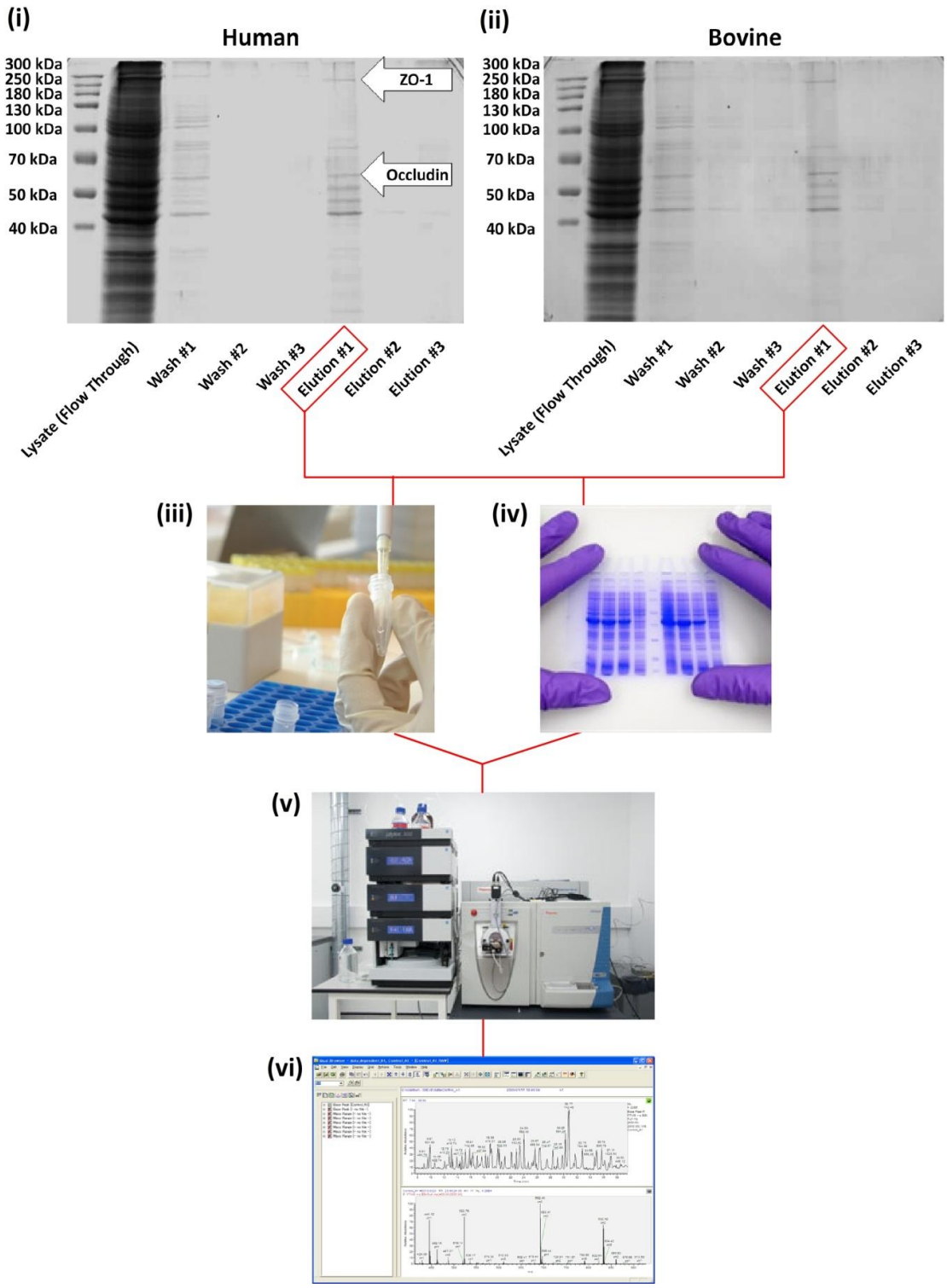

Figure 6.1: The experimental paradigm for identifying novel binding partners of interendothelial junction proteins. Confluent BBMvECs and HBMvECs were maintained in static conditions or exposed to laminar shear stress (8 dynes cm^{-2}, 24 hr) following which they were harvested for whole cell protein lysate. The lysates were subjected to IP with successful pulldown confirmed by coomassie staining of SDS-PAGE gels (i, ii). IP eluates (iii) and isolated bands of interest on the coomassie stained gels (iv) were prepared and analysed by LC-MS/MS (v) with the resulting spectrum cross referenced with peptide databases (vi). Note: Gels above shown for occludin IP.

(i)

Target	Static	Shear
Occludin	-	14-3-3ζ 14-3-3γ 14-3-3ε
Claudin-5	14-3-3ε 14-3-3ζ 14-3-3θ	14-3-3ε 14-3-3ζ 14-3-3θ 14-3-3γ
VE-Cadherin	-	14-3-3ε 14-3-3ζ
ZO-1	-	14-3-3ζ 14-3-3γ

(ii)

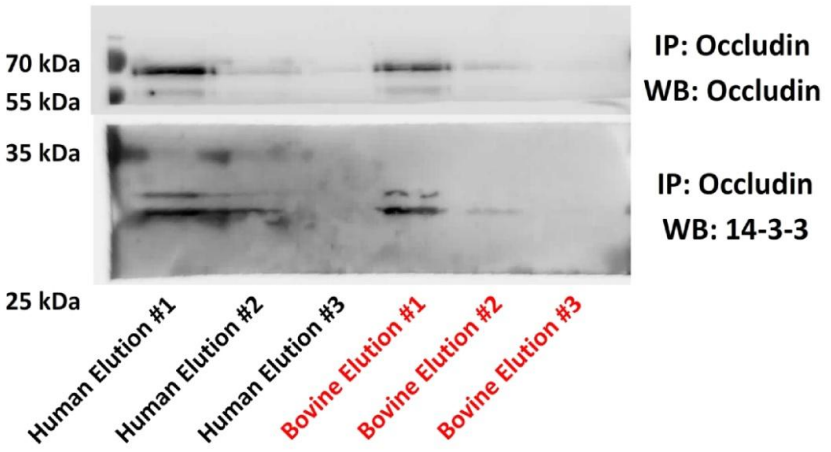

Figure 6.2: The identification and verification of novel binding partner interaction with interendothelial junction proteins. The resulting peptide libraries for each interendothelial junction protein were cross-referenced between one another and in the absence and presence of shear stress. The 14-3-3 family of proteins were identified as having a greater presence in the interendothelial junction plaque following the application of shear stress (i). The interaction of 14-3-3 with interendothelial junction proteins was confirmed by western blot (ii). Note: Gels above are shown for occludin IP.

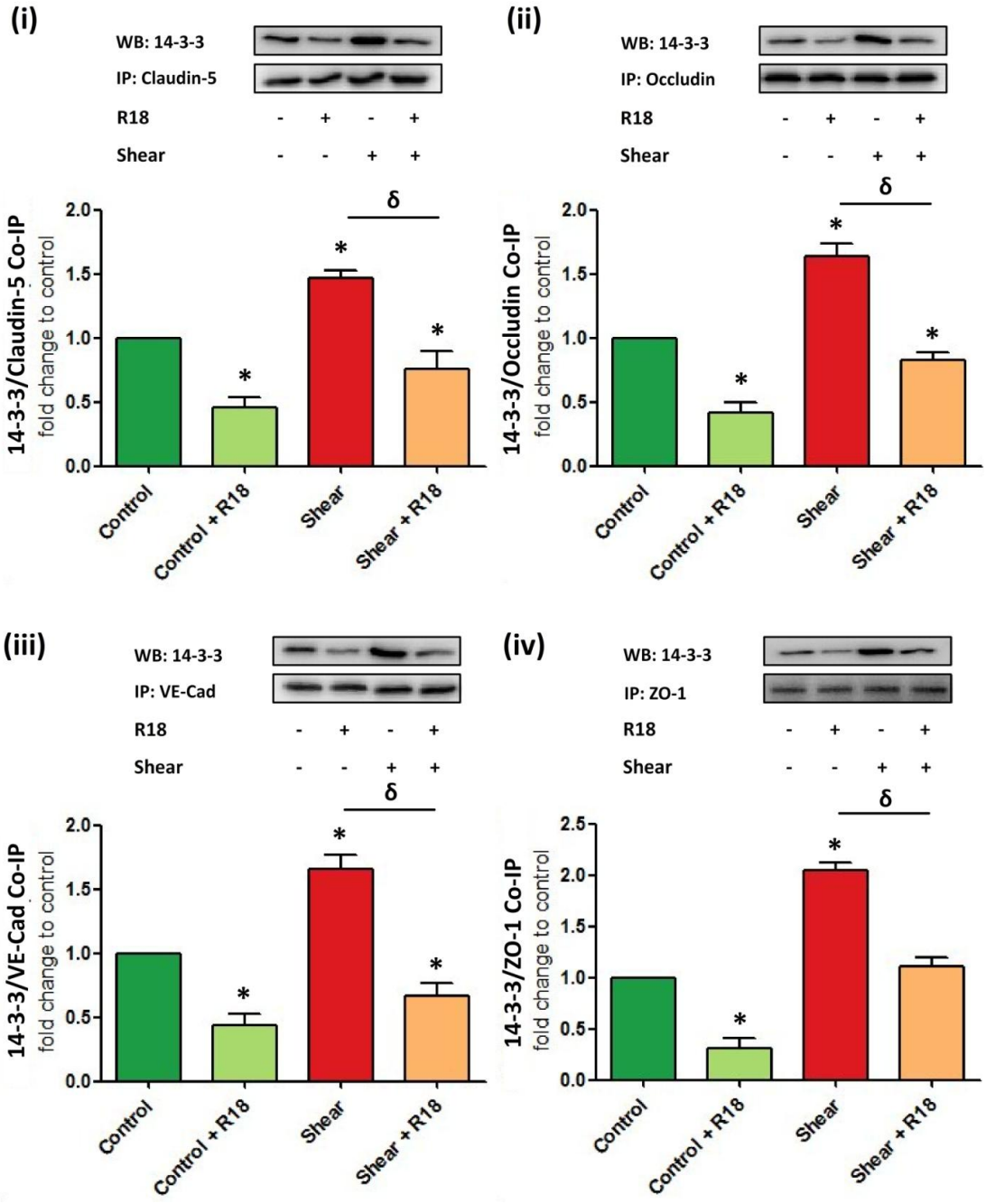

Figure 6.3: The effect of laminar shear stress on 14-3-3/interendothelial junction protein co-association and the subsequent effect of 14-3-3 inhibition. Confluent HBMvECs were either maintained in static cultures or exposed to laminar shear stress (8 dynes cm^{-2}, 24 hr) in the absence and presence of R18 peptide, following which they were harvested for whole cell protein lysate. The lysates were subjected to IP/IB analysis for relative 14-3-3 levels against total target interendothelial junction protein levels. The histograms represent the relative 14-3-3 levels to total Claudin-5 (i), Occludin (ii), VE-Cadherin (iii) and ZO-1 (iv) derived by scanning densitometry from western blots. Results are averaged from three independent experiments ± SD; *P≤0.05 vs. Untreated Control. δP≤0.05. Blots are representative.

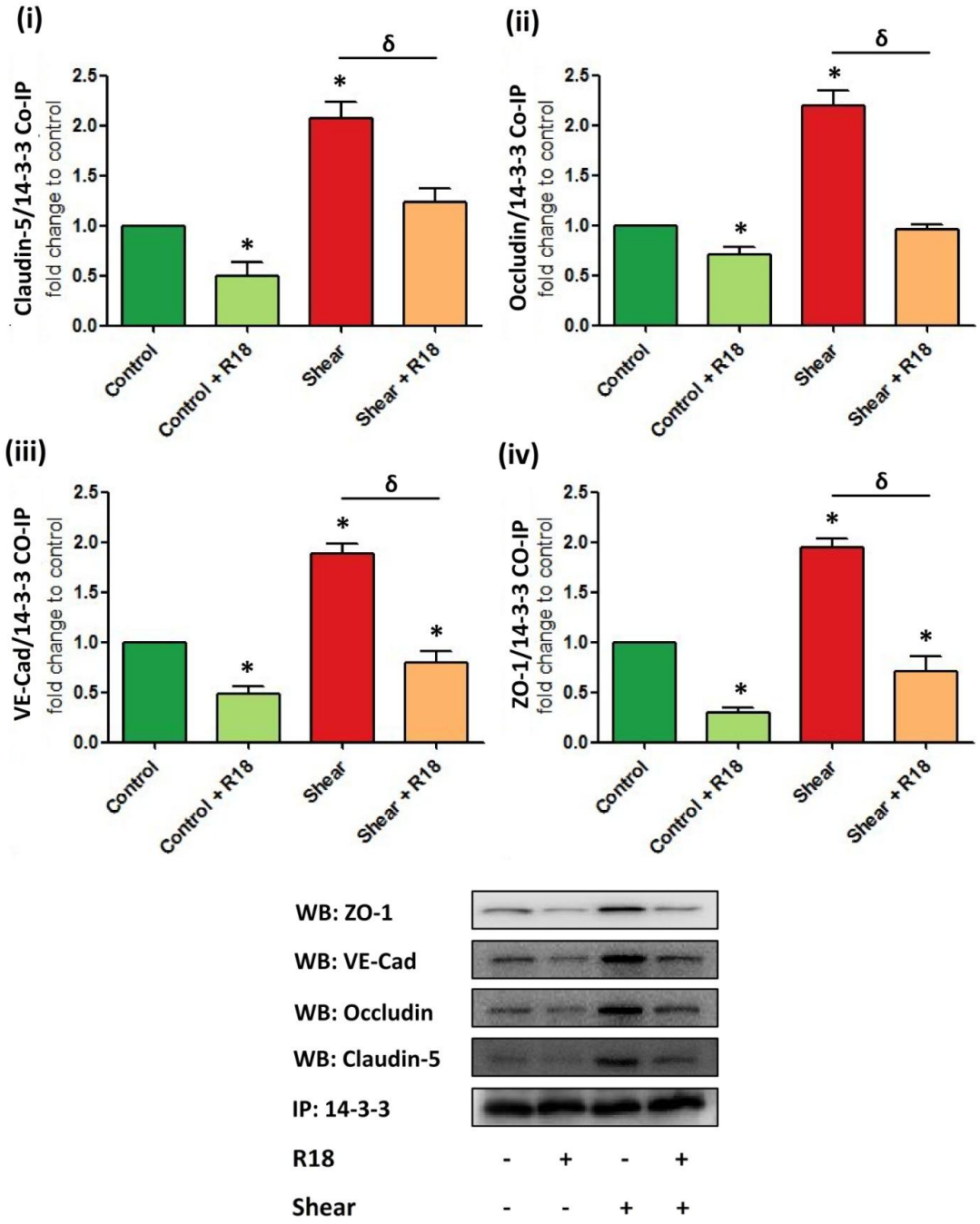

Figure 6.4: The effect of laminar shear stress on interendothelial junction protein/14-3-3 co-association and the subsequent effect of 14-3-3 inhibition. Confluent HBMvECs were either maintained in static cultures or exposed to laminar shear stress (8 dynes cm^{-2}, 24 hr) in the absence and presence of R18 peptide, following which they were harvested for whole cell protein lysate. The lysates were subjected to a reverse IP/IB analysis for relative interendothelial junction protein levels against total target 14-3-3 levels. The histograms represent the relative Claudin-5 (i), Occludin (ii), VE-Cadherin (iii) and ZO-1 (iv) levels to total 14-3-3 derived by scanning densitometry from western blots. Results are averaged from three independent experiments ± SD; *P≤0.05 vs. Untreated Control. δP≤0.05. Blots are representative.

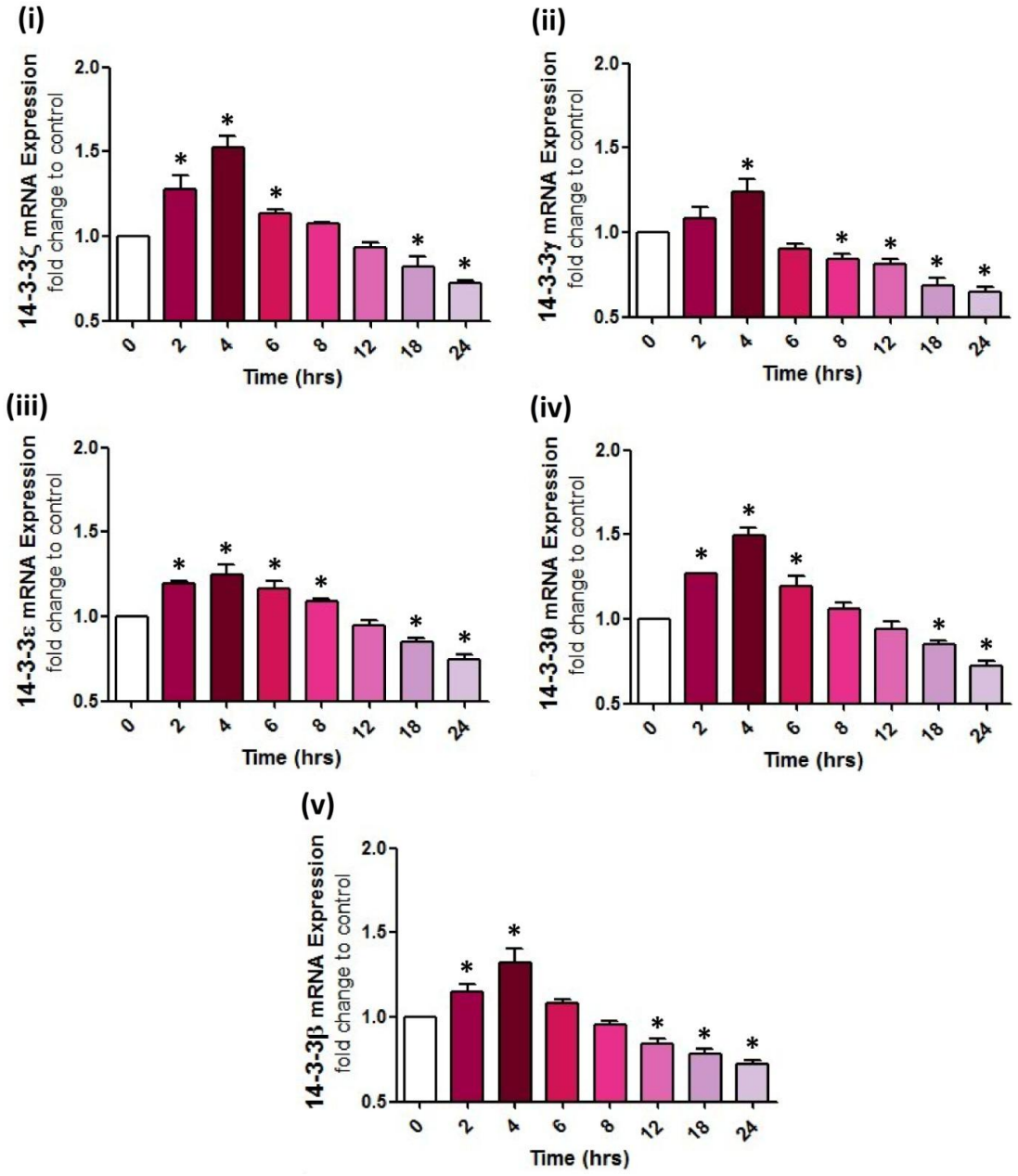

Figure 6.5: The effect of laminar shear stress on specific 14-3-3 isoform expression. Confluent HBMvECs were exposed to laminar shear stress (8 dynes cm^{-2}, 0-24 hr), following which they were harvested for whole cell mRNA. The samples were analysed by qPCR for the transcriptional levels of specific 14-3-3 isoforms that were present in the peptide libraries for each intercellular junction protein; 14-3-3ζ (i), 14-3-3γ (ii), 14-3-3ε (iii) 14-3-3θ (iv) and 14-3-3β (vi). Results are averaged from three independent experiments ± SD; *P≤0.05 vs. 0 hrs.

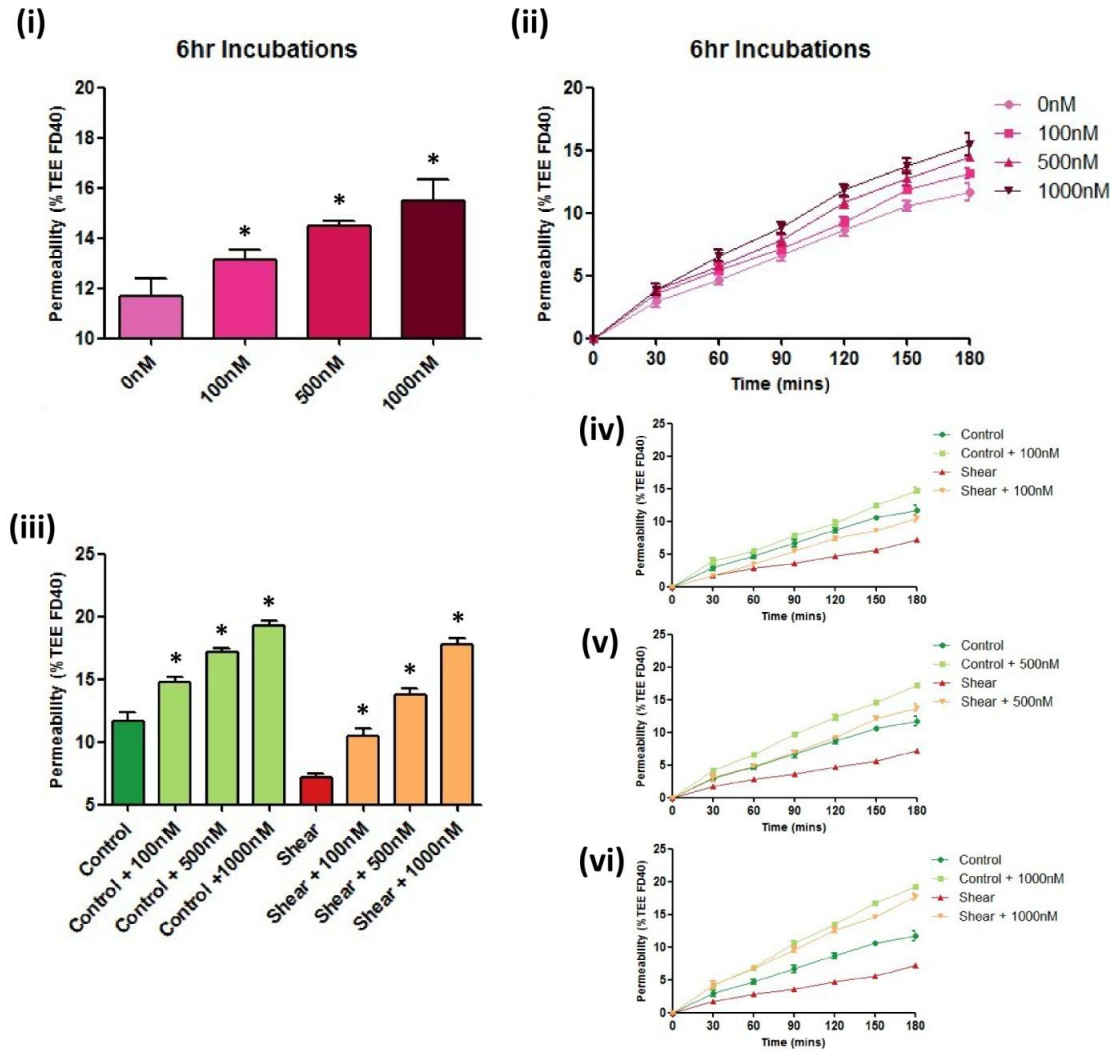

Figure 6.6: The effect of 14-3-3 inhibition on HBMvEC barrier function. HBMvECs were seeded at a known density and allowed to adhere prior to addition of R18 peptide for 6 hrs. Following this the HBMvEC sultures were examined by transendothelial permeability assay. The histogram (i) and line graph (ii) show the change in permeability (% TEE FD40) at a given time point(s) (t) = 180 mins or 0-180 mins, respectively in response to R18 (0-1000 nM). Results are averaged from three independent experiments ± SD; *P≤0.05 vs. 0 nM. In a parallel study, HBMvECs were either maintained under static conditions or exposed to laminar shear stress (8 dynes cm^{-2}, 24 hr) in the absence and presence of R18 peptide and examined by transendothelial permeability assay. The histogram (iii) and line graphs (iv, v, vi) show the change in permeability (% TEE FD40) at a given time point(s) (t) = 180 mins and 0-180 mins, respectively. Results are averaged from three independent experiments ± SD; *P≤0.05 vs. Untreated Control.

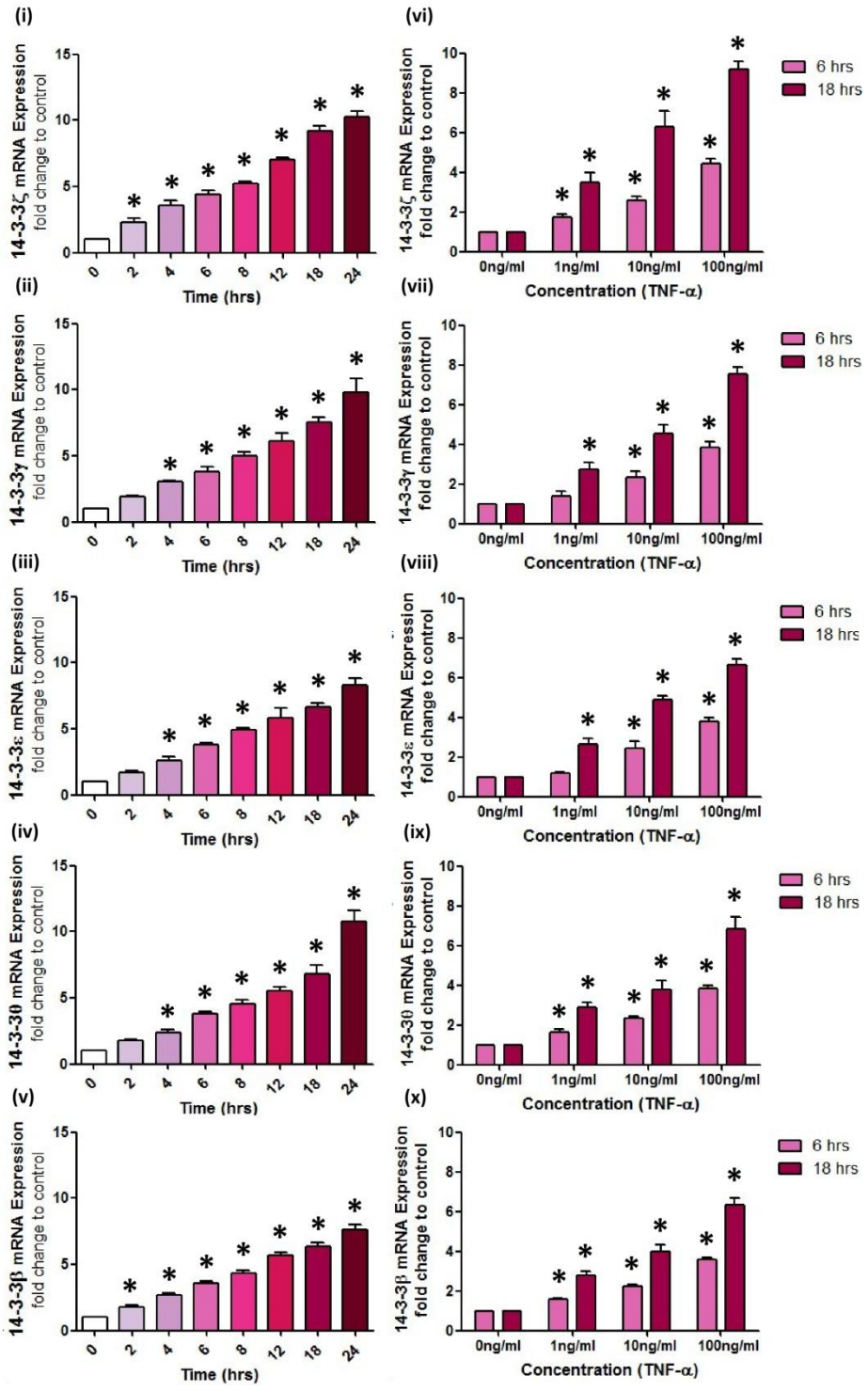

Figure 6.7: The effect of TNF-α on specific 14-3-3 isoform transcription. Confluent HBMvECs were stimulated with TNF-α (0-100 ng/ml) for 0-24 hr, following which they were harvested for whole cell mRNA. The LHS histograms represent the mRNA changes in 14-3-3ζ (i), 14-3-3γ (ii), 14-3-3ε (iii) 14-3-3θ (iv) and 14-3-3β (vi) in response to 100 ng/ml TNF-α. The RHS histograms represent the mRNA changes in 14-3-3ζ (vi), 14-3-3γ (vii), 14-3-3ε (viii) 14-3-3θ (ix) and 14-3-3β (x) in response to TNF-α (0-100 ng/ml) at 6 and 18 hrs. Results are averaged from three independent experiments ± SD; *P≤0.05 vs. 0 hrs (i-v) or 0 ng/ml (vi-x).

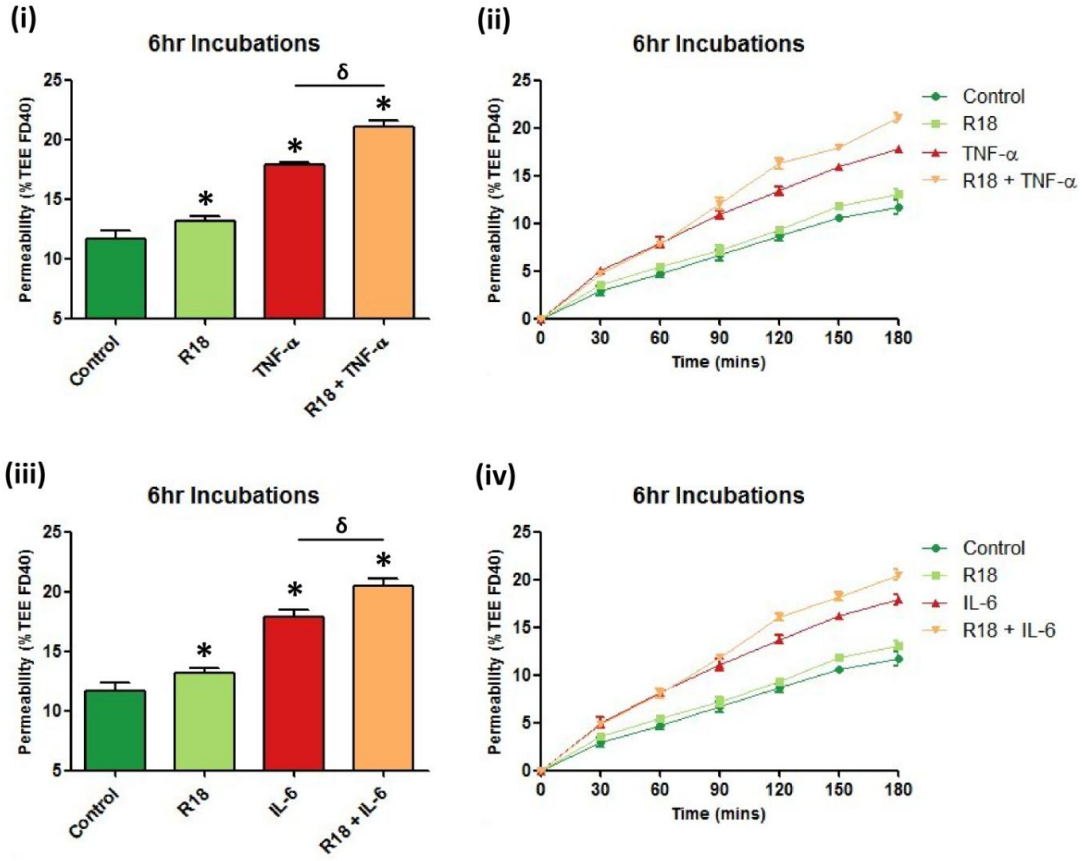

Figure 6.8: The effect of 14-3-3 inhibition on TNF-α- and IL-6-induced HBMvEC damage-Barrier Function. HBMvECs were seeded at a known density and allowed to adhere prior to examination by transendothelial permeability. HBMvECs were then maintained in the presence of TNF-α or IL-6 (100ng/ml) for 6 hrs in the absence and presence of R18 peptide. Post-treatment the HBMvEC cultures were examined by transendothelial permeability assay. The histograms (LHS) and line graphs (RHS) show the change in permeability (% TEE FD40) at a given time point(s) (t) = 180 mins or 0-180 mins, respectively, in response to TNF-α (i, ii) or IL-6 (iii, iv). Results are averaged from three independent experiments ± SD; *P≤0.05 vs. Control. δP≤0.05.

6.3 Discussion

There is now much evidence demonstrating how the endothelium can discriminate among the various fluid mechanical forces acting upon it leading it to transduce these forces into cellular responses (Davies 1995, Gimbrone, Topper et al. 2000). This has been a primary focus within the endothelium biology field and, within our own research group, we have published on the positive effects exerted by both cyclic strain (Collins, Cummins et al. 2006) and laminar shear stress (Colgan, Ferguson et al. 2007, Walsh, Murphy et al. 2011) on endothelial barrier phenotype. One recent publication from our group examined the effects of laminar shear stress on brain endothelium and demonstrated how VE-Cadherin-mediated regulation of Rac1 had subsequent consequences for BBMvEC levels of pTyr-occludin and barrier function (Walsh, Murphy et al. 2011). As such, post-translational modification of the interendothelial junction proteins has been a consistent mechanism and a key interest in our group in recent studies (Colgan, Ferguson et al. 2007, Colgan, Collins et al. 2008, Walsh, Murphy et al. 2011) and we aimed to build on our findings by indentifying novel kinases, phosphatases or other binding partners which interact at the interendothelial junction and mediate the post-translational modification-dependent modulation of endothelial barrier function (Mehta, Malik 2006, Komarova, Malik 2010, Luissint, Artus et al. 2012).

Our strategy for identifying potential binding partners was to employ IP techniques to 'pull down' our proteins of interest in HBMvEC and BBMvEC cultures maintained both in static conditions and under laminar shear stress (8 dynes cm^{-2}). Immunoprecipitation techniques have been utilised to great effect in examining the relationship between novel binding partners and proteins of the interendothelial junctions; for example density enhanced phosphatase-1 (DEP-1) (Chabot, Spring et al. 2009, Spring, Chabot et al. 2012). However, in contrast to our approach, these studies used immunoprecipitation to examine the relationship between two pre-hypothesised binding partners. In our approach, the resulting precipitates would then be analysed by mass spectrometry to generate peptide libraries of proteins directly (and indirectly) binding to each of our proteins of interest. Prior to mass spec analysis, we implemented numerous controls to ensure proper binding specificity. IP's were typically conducted using an antibody-coupled resin immobilised on a centrifugal spin column. To identify any non-specific binding proteins, control resin with antibody and antibody-free resin columns were prepared for each of our IP target proteins (occludin, claudin-5, VE-Cadherin, ZO-1) and used with our generated lysates from both sets of species (bovine and human). Following the standard IP protocol, spun out lysate, wash steps and elutions were separated on SDS-PAGE gels and stained using colloidal coomassie. Typically, we were able to identify our bands of interest based on their size however some proteins required western blot analysis for verification of presence.

Following optimisation of our technique and confirmation of successful immunoprecipitations, elutions of our target protein and excised bands of interest were analysed by LC-MS/MS with subsequent generation of peptide libraries. We then compared our peptide libraries for each condition against one another (i.e. static vs. shear), across protein targets (occludin vs. claudin-5 vs. VE-Cadherin vs. ZO-1) and across species (human vs. bovine). Whilst a number of trends and potentially novel binding partners were present in the mass spec data, a prominent protein which appeared in all sheared samples and was absent in static (or significantly reduced in claudin-5's case) was identified as 14-3-3. The 14-3-3 family is comprised of seven isoforms, five of which appeared in our mass spec profiles depending on the detection limits set. As a result of the variety of isoforms observed across the intercellular junction proteins, we assessed the potential association by western blot using a general 14-3-3 antibody which had the ability to detect all isoforms. Following SDS-PAGE and western blot analysis of IP-treated samples, we confirmed 14-3-3 association with each of the intercellular junction proteins.

The widespread occurrence of 14-3-3 proteins in eukaryotes and their involvement in multiple cellular processes (Darling, Yingling et al. 2005, van Heusden 2005) have prompted researchers to examine them with two perspectives; first and foremost, there remains a lot to be uncovered with regards to the pathways in which the members of the 14-3-3 family are involved; secondly, a clearer understanding of 14-3-3 proteins will reveal their association with cellular homeostasis and pathology of human diseases (Wilker, Yaffe 2004, Foote, Zhou 2012). The complexity of this field, in conjunction with the complexity of 14-3-3's binding capabilities (i.e. dimer formation (Jones, Ley et al. 1995, Chaudhri, Scarabel et al. 2003, Wilker, Grant et al. 2005) and ligand binding (Furukawa, Ikuta et al. 1993, Muslin, Tanner et al. 1996, Aitken, Baxter et al. 2002) made the job of elucidating 14-3-3's interaction with interendothelial junction proteins quite difficult.

Luckily, a large volume of current 14-3-3 information derives from brain models (Baxter, Liu et al. 2002, Baxter, Fraser et al. 2002, Berg, Holzmann et al. 2003, Steinacker, Aitken et al. 2011). Given its initial discovery in the brain and the large percentage of total brain protein that 14-3-3 accounts for (1% (Martin, Rostas et al. 1994)), in conjunction with its initial function indentified to be regulation of neuronal activity, it was of no surprise that the 14-3-3 protein activity would play a critical role in a number of cerebral functions (Moore BW and Perez VJ 1967). As more and more functional roles for 14-3-3 were discovered it was not long before it was implicated in disease pathogenesis. 14-3-3 involvement has been reported for a number of cerebral-based diseases, with 14-3-3 assemblies found in lesions and protein aggregates within the brain (Berg, Holzmann et al. 2003). An elevated presence of 14-3-3 has been reported within the neurofibrillary tangles seen in patients suffering from

Alzheimers disease (Layfield, Fergusson et al. 1996), and a possible link to polymorphisms in certain 14-3-3 isoforms has been suggested for early onset of schizophrenia (Toyooka, Muratake et al. 1999). Other *in vitro, in vivo* and post-mortem analyses have identified 14-3-3 involvement in cerebral disease development (e.g. Parkinson's disease, Amyotrophic Lateral Sclerosis). Elevated levels of 14-3-3 proteins have also been detected in the cerebrospinal fluid of patients suffering from stroke (Boston, Jackson et al. 1982, Collins, Boyd et al. 2000), subarachnoid haemorrhage (Hsich, Kinney et al. 1996) and Multiple Sclerosis (Boston, Jackson et al. 1982, Satoh, Kurohara et al. 1999). This reported elevation in levels, particularly in areas of injury, initially lead to some confusion as we had believed 14-3-3 was a positive benefactor in cell functions. It was therefore critical to establish whether 14-3-3 presence in our HBMvEC cultures was acting as a general marker for brain injury and local tissue destruction or if they are actually involved in the pathogenesis of these debilitating neurological diseases.

We decided to first examine the role of 14-3-3 in our shear model and subsequently the potential effect in our cytokine-injury model. To date little or no information exists on the role of 14-3-3 at the interendothelial junction. The majority of data available examines the relationship between 14-3-3 and the tight junction-associated PAR proteins in maintaining and regulating cell polarity, typically in epithelial models (Hurd, Fan et al. 2003, Suzuki, Hirata et al. 2004, Izaki, Kamakura et al. 2005, Cohen, Fernandez et al. 2011). The trend observed in the mass spectrum data was maintained in our examination of the effect of laminar shear stress on 14-3-3 association with each of the intercellular tight junction proteins. Upon exposure to laminar shear stress (8 dynes cm^{-2}), a significant increase in the association between 14-3-3 family (verified by western) and each of the intercellular tight junction proteins (IP target) was observed. We also further confirmed 14-3-3's association with each of the intercellular junction proteins by 'reverse' IP. Moreover, identical results were obtained when 14-3-3 was used as the IP target, and the junctional protein designated as western blot targets.

In order to assess the impact of 14-3-3 on the interendothelial junction, it was necessary to find a means of interfering with its function and extrapolating the subsequent effect. 14-3-3 has been shown to bind to a wide variety of proteins and a number of characteristics have been identified in the ligands which permit 14-3-3 binding. For many years, successful 14-3-3-ligand association was believed to be dictated by the phosphorylation state of the ligand (Muslin, Tanner et al. 1996). Consequently, research focussed on the phosphorylation-dependency of 14-3-3 binding and subsequent production of inhibitors attempted to capitalise on this mechanism. However, the binding capabilities of 14-3-3 were subsequently discovered to operate independently of the phosphorylation of certain ligands. As a result, a

number of unphosphorylated ligands were developed which can dock to in the binding groove of 14-3-3 proteins and act as an antagonist regardless of their phosphorylation state. R18 is one such antagonist and was identified from a phage display library by virtue of its high affinity for 14-3-3 proteins (Petosa, Masters et al. 1998, Wang, Yang et al. 1999). R18 exhibits a high affinity for all the 14-3-3 isoforms with estimated K_d values of 70-90 nM, which is as effective as some of its phosphopeptide equivalents. Studies which looked at 14-3-3 ζ-R18 binding showed successful association similar to that of phosphorylated peptides, without affecting the overall protein structure (Petosa, Masters et al. 1998). Thus R18 functionally acts as an effective blocking agent to both phosphorylated and unphosphorylated protein ligands associating with 14-3-3 (Masters, Pederson et al. 1999, Wang, Yang et al. 1999, Zhang, Chen et al. 1999). Employment of this peptide in our studies was preferred over siRNA silencing for two reasons; firstly; we wanted to completely eradicate all 14-3-3 activity, which R18 peptide facilitates in one treatment and secondly; while the knockout of individual 14-3-3 isoforms has proven effective, there are no assurances that functional overlap between isoforms may not confound results.

Despite the efficacy of the R18 peptide computationally calculated to work within the nM concentration range, numerous studies have reported effective 14-3-3 inhibition only occurring in the mM range (Petosa, Masters et al. 1998, Du, Khuri et al. 2008, Mu, Andrews et al. 2008, Mancini, Corradi et al. 2011). Therefore we first examined the effect of R18 peptide concentration on HBMvEC viability (as 14-3-3 could potentially regulate hundreds of functions in HBMvECs). We therefore we tested a range of published effective concentrations (10-5000 nM) of R18 peptide on HBMvEC viability by flow cytometry, aiming to assess the limits at which we could administer the peptide without having a significant impact on cell viability. We found we could examine up to nearly 10-times the recommended concentration (70-90 nM) without having a significant impact on cell viability.

We also decided to further confirm our working concentrations (10-1000 nM) by first looking at the effect of R18 on cellular adhesion using an assay based upon the principle of cellular uptake of a crystal violet solution. We looked at the effect of R18 concentration on adhered HBMvEC cell numbers over 24 hrs of incubation, and were surprised to see a ~20% drop in crystal violet retention over this time course. Brightfield microscopy confirmed cellular monolayer compromise however this did not correlate with previous monolayer integrity of HBMvECs in response to R18 when viability was examined by flow cytometry. Assay parameters that may have contributed to this observation include variance in initial cell number, variance between plates, variance in technique etc. To eliminate these potential problems and further clarify the effect of R18 on our cell populations we examined the effect

of R18 on confluent HBMvECs using the xCelligence® system to monitor the monolayers response in real time. According to the xCelligence®, R18 peptide caused a neglible reduction in monolayer integrity (at our highest working concentration of 1000 nM, monolayer integrity did not drop below 98% after 24 hrs). These results not only confirmed our working concentrations were within a suitable range and that monolayer integrity was not lost, but further confirmed the efficacy of the xCelligence® system over cruder established protocols for assessing similar functions.

With the working concentration range firmly established we examined the effect of R18 peptide on the association of 14-3-3 with each of the interendothelial junction proteins. Upon IP of static and sheared HBMvEC for each of the interendothelial targets, a significant reduction in 14-3-3 association was observed in the presence of R18 peptide. In essence, R18 peptide completely ablated the shear-induced co-association of 14-3-3 with each of the target junctional proteins.

To summarise at this point, our data clearly indicated that 14-3-3 family isoforms associate with interendothelial tight junction proteins in response to laminar shear stress. Given that laminar shear stress enhances barrier phenotype, this interaction would suggest a 'pro-barrier' role for these proteins. With this in mind, the effect of laminar shear stress on expression of 14-3-3 isoforms was therefore examined. We observed a significant increase in the transcription levels of each of the five 14-3-3 isoforms (ζ, γ, θ, ε, β) within 4 hrs of laminar shear stress onset. This increase returned to baseline levels within 8 hrs and by 24 hrs each of the five isoforms experienced an overall moderate decrease in their transcription levels. Interestingly, the trend observed in the 14-3-3 isoforms resembled that of the cytokine receptors in response to laminar shear stress (Chapter 3). It is entirely possible that during the early (0-4 hr) endothelial remodelling associated with inflammatory signalling, an initial spike in 14-3-3 levels can regulate the adaptive process before creating a negative feedback to restore 14-3-3 to new baseline levels in chronically sheared cells. We can only claim this based on transcription levels – we have not conducted studies on the overall translational levels of the 14-3-3 proteins to date. However a study by Nakamuta (2008) demonstrated the HIV-induced gp120-mediated disruption of ZO-1 and ZO-2 in HBMvECs. In response to elevated levels of gp120, significant increases in 14-3-3τ were observed and silencing of 14-3-3τ accelerated the gp120-mediated breakdown of the tight junction.

With our current model for laminar shear stress on HBMvEcs potentially expanded to include a role for 14-3-3, we next decided to assess the degree of influence 14-3-3 had on barrier function by inhibiting its binding via R18 peptide and measuring the changes in HBMvEC permeability. Very little data is available on the role of 14-3-3 and barrier

modulation. Wong (2009) demonstrated that 14-3-3θ silencing in a blood-testis barrier model induced the mislocalisation of N-cadherin and ZO-1 from the cell-cell interface to the cytosol leading to disruption of the adhesion profile of Sertoli cells. Moreover, Ngok (2013) demonstrated the regulation of the junction-coordinating protein; Syx, by 14-3-3 dependent binding. We demonstrated in static cultures that R18 could significantly decrease the association of 14-3-3 with the intercellular junction proteins. We further demonstrated that in HBMvEC static cultures, R18 caused a significant increase in permeability in a dose-dependent (0-1000 nM) manner (and in a time-dependent manner). A similar trend was also observed in HBMvECs exposed to laminar shear stress in that R18 exposure appeared to completely reverse the shear-dependent reduction in permeability in parallel with the junction proteins.

Based on these collective observations, we conclude that 14-3-3 family isoforms can modulate HBMvEC barrier phenotype particularly under shear conditions via interaction with junctional proteins. We then decided to investigate whether the 14-3-3 family had a role in modulating cytokine-driven disruption of barrier function. We first examined the effect of TNF-α (100 ng/ml) on the transcription levels of members of the 14-3-3 family that had a confirmed presence in HBMvECs via mass spectroscopy; ζ, γ, ε, θ and β. We found TNF-α (and IL-6) significantly and robustly increased the transcription of each of the five isoforms examined within 4 hours of TNF-α exposure, with 5+ fold change observed across all isoforms by 24 hrs.

Considering the 'barrier-weakening' effect displayed by cytokines, we next considered if the cytokine-induced expression of 14-3-3 protein had a contributory effect to the cytokine-induced damage. We therefore examined the effect of R18 inhibition of 14-3-3 on barrier function in the presence of both inflammatory cytokines. A slight but significant increase in monolayer permeability was observed in HBMvECs exposed to either TNF-α or IL-6 in the presence of R18 in comparison to the absence of R18. We concluded that if 14-3-3 had a damage-exacerbating effect, inhibition of its function would likely result in a decrease in permeability following exposure to TNF-α or IL-6. Instead, a significant increase was observed. We therefore hypothesised that the increase in transcription of 14-3-3 members reflected in-part a cellular defence mechanism to compensate for cytokine exposure. In response to inflammation HBMvECs increase endogenous levels of 14-3-3 in an attempt to restore barrier function (amongst other things), although the expression and increased phosphorylation of interendothelial junction proteins may prevent attempts at barrier restoration. Interestingly, Liu (Liu, Yin et al. 2001) demonstrated 14-3-3 could actively inhibit TNF-α signalling in endothelial cells via binding to ASK1. TNF-α partly mediates its effects through ASK1 dissociation from 14-3-3, a process that could be inhibited following

exposure to laminar shear stress. This adds credence to our hypothesis that increased transcription of these proteins is a pro-homeostatic feature in our model. Future investigation will undoubtedly reveal the mechanistic relationship between AJ/TJ dynamics and 14-3-3 isoforms under barrier-strengthening (shear) and –weakening (cytokines) influences.

In conclusion, we have comprehensively demonstrated how the 14-3-3 family plays a pivotal role in the maintenance of vascular homeostasis and BBB phenotype through association with proteins of the interendothelial junction, with consequences for BBB barrier function. In addition, we also demonstrated how the 14-3-3 family may play a pivotal anti-inflammatory role in response to cytokine injury.

Chapter 7:

Final Summary.

7.1 Final Summary

Global CNS diseases account for approximately US$2 trillion a year (The Neurotechnology Industry Report 2009). This economic burden coincides with the fact that the CNS is currently regarded as one of the most difficult areas in which to achieve clinical success (Kola, Landis 2004). Between 1991 and 2000, only 8% of clinical trial developing drugs for CNS based therapeutics successfully achieved registration (Kola, Landis 2004). More than 90% of developed CNS therapies are abandoned between Clinical Phases I and III incurring extravagant loss of capital and time (CNS drug development exceeds the average time frame for normal drugs of 10-12 years to 12-16 years) (Kola, Landis 2004).

While drug companies strive to formulate a way of crossing the blood brain barrier by targeted drug delivery means, a number of radical therapies are currently in use and have shown a respectable success rate despite their impracticality and flaws. These can range from direct injection into the brain or CSF (Liebert, Wahl et al. 1990, Schroeder, Weinger et al. 1991, Gabathuler 2010) to targeted modulation of the microvasculatures tight junctions by osmotic or chemical means (Saija, Princi et al. 1995, Sanovich, Bartus et al. 1995, Rapoport 2000). Osmotic disruption of the tight junctions remains the favoured and more clinically implemented strategies, particularly in the delivery of anticancer therapeutics to cerebral tumours (Hall, Doolittle et al. 2006, Hall, Sherr 2006). This method is still highly flawed however in that it often results in widespread disruption of the tight junctions in areas that are not identified to require treatment. This results in non-specific delivery of the drug in questions diluting its target dose and opens up healthy areas of the brain to invading blood-present toxic products.

The latter mentioned therapy highlights one of the key problems associated with successful targeted drug delivery to the brain, notably the degree of difficulty maintaining drug accumulation in the injured area of the brain as opposed to other organs. It is estimated that over 98% of currently available drugs are ineffective at achieving the required therapeutic concentrations in the CNS while close to 100% of biological drugs fail (Pardridge 2003). Therefore most drugs actually fail at treating the intended disease and more often invoke secondary effects or even toxicity should higher doses be administered to counteract the problem. While many strategies have been able to overcome this problem they have encountered others such as the compound maintaining stability en route to the area of interest, evading potential disruptive proteins and their binding actions, and perhaps most difficult of all, passing across the membranes of the already well established endothelial barrier. The problem herein lies with developing a strategy that overcomes ALL of these problems at once and it is for this reason that It is for this reason that some of the more radical therapies have been resorted to. There has been moderate success in achieving this in

the form of ‘trojan horse’ drug delivery (Pardridge 2006). Pharmaceutical companies are currently developing non-viral vectors with unique chemical and surface properties which maximise stability and plasma solubility while avoiding eliciting an immune response. Already these therapies have been used to deliver DNA-, peptide- and protein- based therapeutics (Schroeder, Sommerfeld et al. 1998, Schroeder, Sommerfeld et al. 1998, Liu, Huang 2002). These agents have been used to successfully treat chronic pain, insomnia, and epilepsy in addition to several affective disorders such as schizophrenia and depression. However treatment for the damage caused by the more severe injuries such as brain cancer and stroke remains quite limited.

To date, controlling the permeability of the BBB remains a clinically unmet challenge. Since the NVU is comprised of a number of different cell types which contribute by regulating and modulating a number of different cell signalling cascades, BBB dysfunction can arise from many a ways. While much progress has been made in understanding these cell types and the respective pathways that they are involved in, there still remain a lot of unanswered questions or conflict on certain aspects. Whether or not it may be beneficial or contradictory, new avenues are being explored with the miRNA field opening up a fresh perspective on the development and functionality of the NVU. Already several miRNA have redefined some of the ideas that were held for so long with a number shown to influence angiogenesis (Caporali, Meloni et al. 2011) and other vascular functions (Hartmann, Thum 2011).

Despite these difficulties, progress has been made with regards to some pathologic diseases. For example administration of anti-inflammatory medication has been shown to restore BBB function in certain animal models and these studies have been taken forward into humans, successfully controlling seizures associated with drug-refractory epilepsy (Sotgiu, Murrighile et al. 2010, Marchi, Granata et al. 2011). Cases like this demonstrate that there is hope in eventually understanding the BBB and translating this knowledge in to therapeutics.

The homeostasis of the CNS environment is regulated and maintained by the BBB, a complex cellular system comprised of astrocytes, pericytes, neurons and at the forefront, microvascular endothelial cells. The BBB separates the brain from the systemic blood circulation, protecting the brain from blood-borne compounds which may disrupt the strict homeostasis of the neural environment. Therefore it is critical that the barrier remains intact and fully operational in order to preserve neuronal activity and brain function.

The focal point of this thesis is the cerebral endothelium of the microvasculature. These BMvECs display a number of functional and morphological differences in comparison to endothelial cells of the peripheral vasculature; an increase in cytosolic mitochondria, the absence of fenestrae of the membrane, and a reduction in pinocytotic vesicular activity.

Perhaps the most well known trait of the BMvECs is their enhanced barrier properties. BMvECs present restrictive intercellular junction complexes often collectively referred to as the 'tight junction'. These tight junctions, in partnership with the adherens junction, form a continuum of intercellular junction complexes between adjacent endothelial cells to generate a uniform monolayer of substantially higher barrier function. The enhanced junctions restrict the passage of charged particles, proteins, ions, hydrophilic molecules and hormones, all of which may act as neurotransmitters and thus destabilise the neural environment. However the brain has a high metabolism rate and requires a constant source of nutrition and waste removal, which in turn requires passage across this seemingly impermeable barrier. The phenotypic barrier of BMvECs can dynamically defend the brain from blood-born antigens, enable the passage of essential nutrients and filter waste products or harmful substances from the cerebral tissue into the blood stream, whilst maintaining the impedance of paracellular transport of aforementioned agents.

It is said the BBB was born from the selective evolutionary process, giving those species an evolutionary advantage. However its highly effective barrier properties make it a major obstacle in the development and delivery of CNS drugs. Overcoming the barrier-impeded delivery and subsequent enzymatic degradation of targeted therapeutics represents a major rate-limiting step in translating potential drug candidates into an effective neurotherapeutic. Conversely, BBB disruption has been associated with the pathophysiology of a number of neurological disorders, including ischemia, tumours, HIV-encephalitis, multiple sclerosis and neurodegenerative diseases such as Parkinson's and Alzheimer's disease (Persidsky, Heilman et al. 2006, Abbott 2002, Abbott 2013). Therefore, progression of targeted therapeutics for the treatment of these disorders hinges on the delineation of the mechanisms behind the brain microvascular endothelium maintenance and regulation of junctions, as well as the environmental factors which impact this.

This thesis aimed to explore both physiological and pathophysiological factors impacting on the microvascular endothelium's intercellular junctions at both a molecular and functional level via employment of an *in vitro* HBMvEC culture model. In this regard, the apical location of the cerebral endothelium places it in immediate contact with frictional shear stress imparted by blood and its constituents. A host of factors can mediate the fluctuation in levels of the various blood-borne components; diet, exercise, injury and infection to name but a few. These components can exact their effect via the appropriate cellular receptor, which in turn can initiate one or more signalling cascades and ultimately yield a cellular response. For better or worse, the independent effect of each component depends on its cumulative interaction with other agents in the cellular vicinity. In the instance where inflammatory agents may exceed that of anti-inflammatory defences, the imbalance can

disrupt vascular homeostasis and lead to the onset and progression of CVD. Sites where the level of force exerted by the blood is subject to inconsistencies and fluctuation can generate areas of low or 'disturbed' shear stress. These areas are subject to dysfunctional tendencies i.e. a reduction in barrier, promotion of coagulant activity and the release of inflammatory mediators (Fig. 7.1). ***Thus we hypothesised that a physiological level of laminar shear stress and pathophysiological levels of inflammatory mediators impact on BBB function by directly (and indirectly) modulating the expression and biochemical properties of the intercellular junctions which comprise the BBB.***

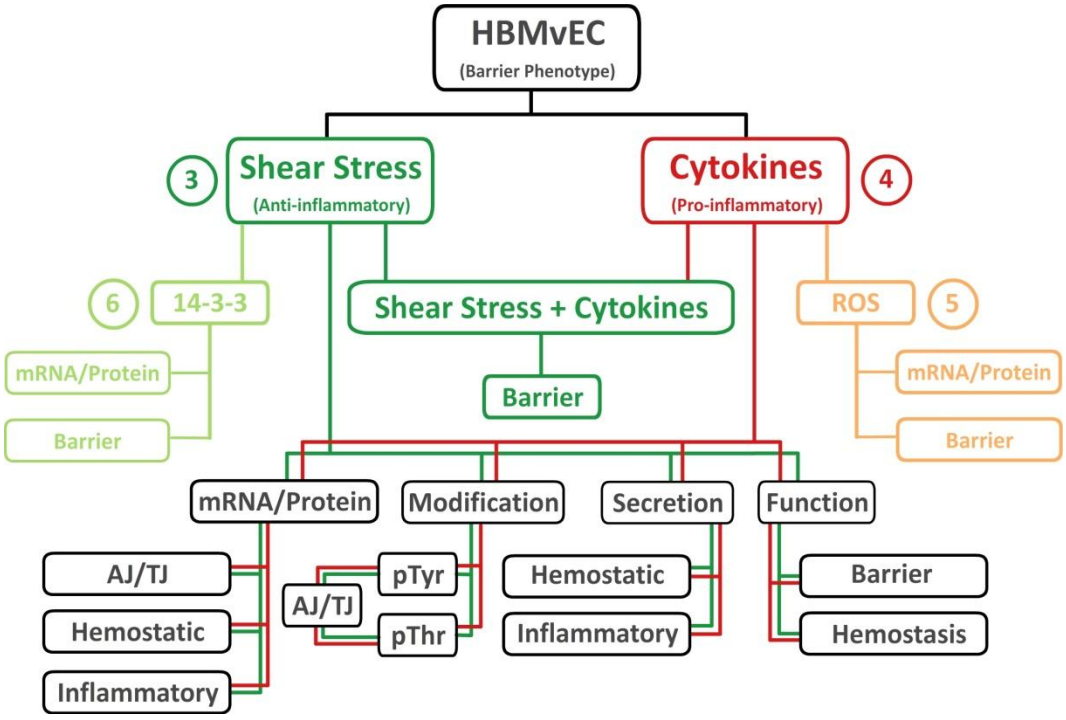

Figure 7.1: Schematic depiction of experimental approach. Primary human brain microvascular endothelial cells (HBMvECs) were subjected to different experimental paradigms; physiological shear conditions (dark green, chapter 3) and pathophysiological inflammatory cytokines (red, chapter 4) and monitored for genetic, molecular, structural and functional changes in BBB phenotype, particularly pertaining to the interendothelial junction. The effect of co-exposing the HBMvECs to both stimuli was then investigated on barrier function, in parallel with further mechanistic studies related to each stimulus's experimental outcomes; the influence of ROS of cytokine-induced damage (orange, chapter 5) and the role of 14-3-3 in shear-mediated barrier enhanced (light green, chapter 6).

Hemodynamic forces are a fundamental stimulus of the entire vascular system. Varying in magnitude, frequency and direction, these fluid-driven mechanical forces have been demonstrated to significantly impact on vessels at several levels; molecular, genetic,

structural and functional (Davies 1995, Chiu, Wang et al. 1998, Chiu, Chen et al. 2003, Chiu, Usami et al. 2009). Thus haemodynamic forces are regarded as critical mediators of BBB induction and regulation (Krizanac-Bengez, Kapural et al. 2003, Krizanac-Bengez, Mayberg et al. 2004, Krizanac-Bengez, Hossain et al. 2006, Krizanac-Bengez, Mayberg et al. 2006). In this regard, previous work in our laboratory has demonstrated that simulation of physiological levels of *in vivo* haemodynamic forces act as a positive stimulus to bovine endothelial cultures, mediating the putative mechanisms involved in endothelial junction assembly/enhancement and thus barrier function (Collins, Cummins et al. 2006, Colgan, Ferguson et al. 2007, Walsh, Murphy et al. 2011). We decided to expand on these studies. By employing human cultures in place of bovine, we were taking a step closer towards translational relevance. As this was the first time our laboratory had employed human cerebral tissue in our studies, an extensive characterisation of biomarkers typically found in the same cultures *in vivo* was carried out. Of particular importance was the expression of the proteins integral in the formation of intercellular junctions; occludin, claudin-5, VE-Cadherin and ZO-1 (Weksler, Subileau et al. 2005). The expression of the aforementioned proteins was subsequently investigated and confirmed for our primary derived HBMvECs.

In chapter 3, our initial studies focussed on the trends observed in our laboratory's previous bovine endothelial cell model and whether they translated into a comparative human endothelial cell model. Exposure to physiological levels of laminar shear stress demonstrated a similar induced pattern of cellular realignment in the direction of the flow. Each protein; occludin, claudin-5, VE-Cadherin and ZO-1 was also observed to be significantly increased at the mRNA and protein levels in response to laminar shear stress (Schnittler 1998, Cucullo, Hossain et al. 2011). This increase in expression/localisation in response to shear stress suggested a correlative increase in barrier function (Colgan, Ferguson et al. 2007, Siddharthan, Kim et al. 2007, Colgan, Collins et al. 2008). This theory was substantiated when cultures exposed to laminar shear stress exhibited a significant reduction in permeability in comparison to control static cultures.

At this point, the bulk of this preliminary data corroborated a number of characteristics attributed to BMvECs previously observed in similar models by our laboratory and others. We next decided to focus our efforts on novel mechanisms and pathways previously explored in our laboratory, in particular post-translational modifications of the proteins at the cell-cell junction. Previous work in our laboratory demonstrated haemodynamic modulation of phosporylation of tyrosine, threonine and serine residues in occludin and ZO-1 in bovine endothelial cells of macro and microvascular origin (Collins, Cummins et al. 2006, Walsh, Murphy et al. 2011). We demonstrated in HBMvECs a significant reduction in tyrosine and threonine phosphorylation of all four junctional proteins in response to laminar shear stress.

The impact of such an event was partially explored via the inhibition of tyrosine phosphatase activity, in which laminar shear-induced enhancement of HBMvEC barrier was partially attenuated, corroborating previous studies (Collins, Cummins et al. 2006, Walsh, Murphy et al. 2011). In summation, a wealth of data currently exists regarding the effect of hemodynamic forces on the endothelium, (though the majority of studies focus on the macrovasculature (Davies 1995, Chiu, Wang et al. 1998, Chiu, Chen et al. 2003, Chiu, Usami et al. 2009)). Regarding the microvasculature, studies have primarily focussed on inductive effect of the surrounding cell types that along with the endothelium comprise the NVU (Bauer, Bauer 2000, Abbott 2002). However the inductive influence of hemodynamic forces, in particular, shear stress, on the microvasculature is increasingly becoming an area of interest with several studies replicating and/or corroborating several findings presented in this thesis (Krizanac-Bengez, Mayberg et al. 2004, Krizanac-Bengez, Hossain et al. 2006, Krizanac-Bengez, Mayberg et al. 2006, Cucullo, Hossain et al. 2011). However, the data presented here represents one of the first extensive characterisations conducted on the influence of laminar shear stress on HBMvEC barrier modulation, detailing consequences for the proteins that form the crucial interendothelial junctions on genetic, molecular, structural and functional levels.

Having characterised our HBMvEC barrier phenotype model with respect to an anti-inflammatory stimulus (shear), we next turned our attention ***in chapter 4*** to a pro-inflammatory stimulus, namely cytokines. Having conducted an extensive literature search on the inflammatory mediators which are locally produced in the neural environment, we selected cytokines based on a number of criteria; the source of the mediator, the established role of the mediator in disease progression, and whether it had a proven effect on endothelial cells. Based on these criteria, we chose TNF-α, IL-6 and MCP-1 (Fabry, Fitzsimmons et al. 1993, Shohami, Novikov et al. 1994, Fassbender, Rossol et al. 1994, Simpson, Newcombe et al. 1998, Reyes, Fabry et al. 1999, Lee, Hennig et al. 2001, Hallenbeck 2002, Weber, Blumenthal et al. 2003, Verma, Nakaoke et al. 2006). Our overall aim was to expose our cultures to varying concentrations of these cytokines and monitor barrier phenotype (as for shear stress). As this was previously unexplored in our laboratory, the incubation times and cytokine concentrations were subject to much scrutiny and were run through a battery of viability and functional assays to assess to overall impact of the aforementioned variables on whole cell well-being. Membrane integrity, metabolism and adhesion were all deemed stable in our set conditions (1-100ng/ml, 6 or 18 hrs incubations) allowing for the assessment of an intact monolayer in response to each mediator. In addition to exploring the molecular and functional aspects affecting the intercellular junctions, we also conducted a screen of the secretory profile of the HBMvEC cultures to identify what additional, if any, mediators may

play a part in the overall consequential effect of our primary cytokines. TNF-α, IL-6, IFNγ and IL-1β secretory levels were screened in tandem using a novel Multiplex ELISA platform with each cytokine levels observed to increase in a time- and dose-dependent manner following exposure to either TNF-α, IL-6 or MCP-1. Interesting trends observed from this data bank were subsequently investigated using standard single-plex ELISA, the strong release of IL-6 in response to TNF-α being particularly noteworthy. We subsequently decided to investigate the individual effects of TNF-α and IL-6 on the molecular and functional aspects of endothelial junction expression and function.

Overall, HBMvEc barrier function decreased as cytokine concentration and incubation time increased, an inverse to the relationship established in our laminar shear model (Brett, Mizisin et al. 1995, Mark, Miller 1999). We therefore decided to advance our study, using three different concentrations to investigate the impact on the previously studied proteins comprising intercellular junction assembly. We found mRNA and protein expression of occludin, claudin-5, VE-Cadherin and ZO-1 was reduced following exposure to our inflammatory cytokines, TNF-α and IL-6, in a dose- and time-dependent manner, correlating with the previously demonstrated reduction in barrier function (i.e. increase in permeability (Duchini, Govindarajan et al. 1996, Aveleira, Lin et al. 2010). Moreover, given the impact of laminar shear on tyrosine and threonine phosphorylation levels of some of the proteins of interest, we decided to investigate the impact of cytokines in the context. Once again, in contrast to the effect seen with laminar shear, cytokines robustly increased the phosphorylation of both tyrosine and threonine residues of occludin, claudin-5 and VE-Cadherin, functional modifications which could impact barrier integrity/permeability as dictated by use of the tyrosine kinase inhibitor genistein (Soma, Chiba et al. 2004, Persidsky, Heilman et al. 2006, Willis, Meske et al. 2010, Yukitatsu, Hata et al. 2013). Overall, the inflammatory mediated opening of HBMvEC barriers may present an ideal opportunity to explore the size restrictiveness of the cytokine-induced opening of the paracellular pathway. Utilisation of dextran tracers that vary in size may allow the degree of barrier failure to be calibrated. This may present a potential opportunity to explore the effect of these barrier disrupting mediators on diapedesis mechanisms via employment of whole blood primary derived immune cells or immune cell cell lines. In summation, inflammatory cytokines are a well characterised promoter of injury within the CNS (Kim, Wass et al. 1992, Megyeri, Abraham et al. 1992, Deli, Descamps et al. 1995, DeVries, BlomRoosemalen et al. 1996). Whilst a wealth of data currently exists detailing their pathophysiological (and physiological) effects within the NVU, much like our reasons for laminar shear stress, the data presented here represents one of the first extensive characterisations conducted on the influence of TNF-α, and in particular, IL-6, on HBMvEC barrier modulation, again detailing

the consequences for the proteins that form the crucial interendothelial junctions on genetic, molecular, structural and functional levels.

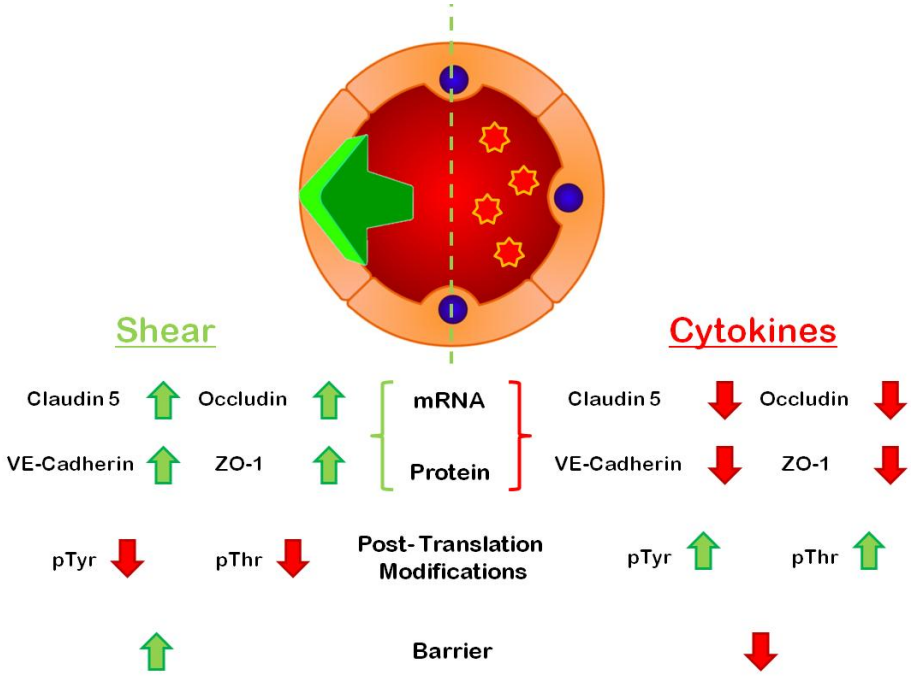

Figure 7.2: The polarising effects of an anti-inflammatory (shear stress, LHS) and pro-inflammatory (TNF-α/IL-6, RHS) on HBMvEC BBB phenotype-barrier.

To summarise at this point, our work corroborated (and expanded) a number of observations in a human model which had been previously observed in bovine endothelial models (Colgan, Ferguson et al. 2007, Walsh, Murphy et al. 2011). Vascular homeostasis encompasses a multitude of functionalities aside from maintenance of barrier function (Ryan, Ryan 1984, Hunt, Jurd 1998). Recently, concurrent work to this thesis has focussed on the release of the anti-coagulant molecule thrombomodulin from endothelial cells of aortic origin in response to varying levels of cyclic strain. We decided to test aspects of this model in our cerebral model to further elucidate the pro-homeostasis effects of laminar shear stress on our HBMvEC cultures. We found that in response to physiological levels of shear stress, a surge in thrombomodulin release occurred, a response which correlated with an increase in intracellular levels suggesting that laminar shear stress was perhaps promoting anti-coagulant activity (Takada, Shinkai et al. 1994, Kawai, Matsumoto et al. 1997, Ishibazawa, Nagaoka et al. 2011, Giwa, Williams et al. 2012). In examining this paradigm, we tested the activity of the shear-induced medium levels of soluble thrombomodulin by introducing pro-inflammatory/pro-coagulant thrombin into our barrier function assays and observed a significant reduction in thrombin-induced disruption of HBMvEC barrier function. In parallel with this, another factor involved in the coagulation cascade; vWF was

investigated with a significant reduction in the mRNA levels of this pro-coagulant molecule following exposure to shear stress (Rand, Badimon et al. 1987, Wu, Drouet et al. 1987, Badimon, Badimon et al. 1993). These trends offered another dimension in assessing vascular homeostasis independently of barrier function. Parallel studies demonstrated that inflammatory cytokines increased the release of soluble thrombomodulin (Nawroth, Stern 1986, Bauer, Rosenberg 1987) (although not to the degree seen following exposure to laminar shear stress). Conversely, intracellular levels were reduced following cytokine exposure suggesting that production of the anti-coagulant molecule ceases, leaving it prone to coagulative activity over chronic periods of time. Concurrently, the pro-coagulant molecule vWF is seen to increase at both a transcriptional and translational level following exposure to our cytokine regime, further intensifying our coagulation paradigm in cerebral cultures (Tsuchida, Salem et al. 1992, Faust, Levin et al. 2001, Isermann, Hendrickson et al. 2001).

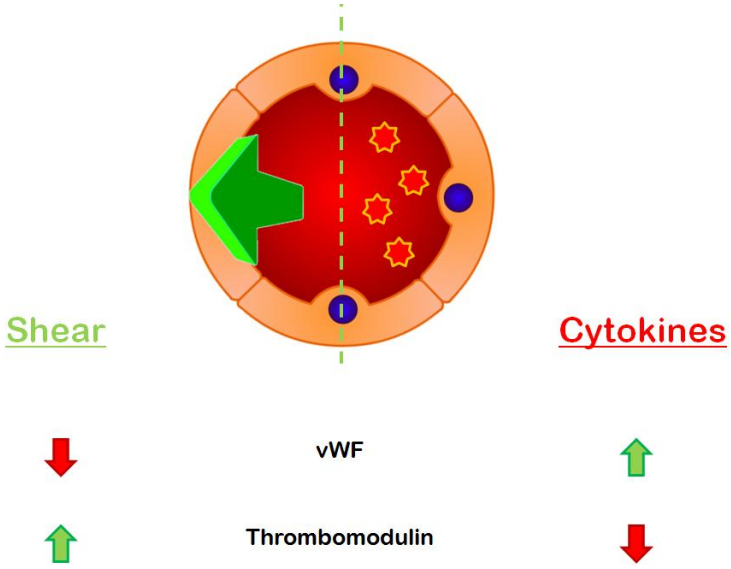

Figure 7.3: The polarising effects of an anti-inflammatory (shear stress, LHS) and pro-inflammatory (TNF-α/IL-6, RHS) on HBMvEC BBB phenotype-hemostasis.

Based on our efforts thus far revolving around the exposure of our HBMvEC cultures to laminar shear and inflammatory cytokines we decided to combine the two stimuli in one model and investigate if shear can ameliorate cytokine injury *in vitro*. We explored this from two approaches; the concurrent effect of inflammatory cytokines and laminar shear stress on pre-sheared HBMvEC cultures and the effect of inflammatory cytokines on pre-sheared cultures. In both instances, a significant reduction in cytokine-mediated barrier dysfunction was observed, suggesting the protective influence of laminar shear stress towards inflammatory mediators (Surapisitchat, Hoefen et al. 2001, Berk, Abe et al. 2001, Berk, Min

et al. 2002, Yamawaki, Lehoux et al. 2003, Ni, Hsieh et al. 2004). We subsequently investigated the effects of each stimulus on the expression of the respective signal transducing cytokine receptors to explore whether that might have any potential bearing on these events. Interestingly, on a transcriptional level, laminar shear stress and inflammatory cytokines drove the expression of certain receptors in opposite directions. gp130 and TNFR1 were significantly unregulated in cultures exposed to inflammatory cytokines, whilst TNFR2 displayed a significant reduction. Laminar shear stress by contrast invoked an inverse response. These findings may offer an interesting aspect for further exploration. For example, TNFR1 facilitates the induction of apoptotic pathways – reduction or increase of such would therefore have an enormous bearing on the overall induced immune response (Pradillo, Romera et al. 2005, Cook, Stahl et al. 2008, Wang, Young et al. 2011).

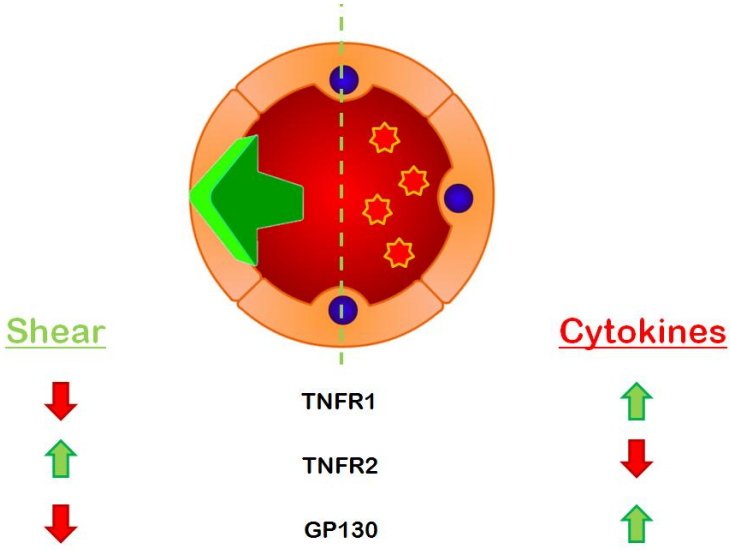

Figure 7.4: The polarising effects of an anti-inflammatory (shear stress, LHS) and pro-inflammatory (TNF-α/IL-6, RHS) on HBMvEC BBB phenotype-cytokine receptors.

In summary, these studies not only expanded on the impact imparted by a healthy (shear) and injurious (cytokines) stimuli on BBB homeostasis, but highlighted in one of the few *in vitro* studies available, the protective effect that shear exudes in an inflammatory BBB model. For example, much of the existing knowledge on hemostasis in the vasculature was based on data derived from the macrovasculature. Whilst much of the knowledge has translated quite well to the microvasculature, the extreme difference in phenotype between the endothelium of the brain and the peripheral vasculature has lead for some of these hemostatic aspects to be revaluated (Abbott 2005). While not extensively investigated, the data presented offers a fresh perspective on the influence of both a healthy (shear) and injurious (cytokines) stimuli on regulation of hemostasis by HBMvECs. The observed anti-inflammatory effects of shear were further investigated in one of the few *in vitro* studies

existing that examines the overall effect of laminar shear stress on cytokine-induced modulation of HBMvEC barrier function. In addition, preliminary work on the effects of each stimulus on each cytokine-signalling receptor offers encouraging data that with further work may unearth novel signalling processes involved in HBMvECs immune response. Together, these effects, in conjunction with the characterisation of each stimulus on HBMvEC barrier function, comprise an extensive profiling of the behaviour of HBMvECs in response to environmental stimuli encountered at the BBB with the crux that shear stress can ameliorate the disruptive effects induced by CNS-produced cytokines.

In chapter 5, we set out to explore potential mechanisms mediating the injurious effects of cytokines on HBMvEC barrier characteristics. As noted earlier, we used a Multiplex ELISA to investigate a focal group of inflammatory mediators previously identified as being involved in the onset and progression of CVD. A key inflammatory mediator not present on this panel however, so not considered until now were ROS. The acute phase of vascular injury is the point at which surges in cytokines and chemokines occur. ROS are integral players in the acute phase of injury and thus could not be ignored in our attempts to further understand inflammatory pathways in our model. Via employment of ROS-tracking dyes, we observed a significant increase in the fold-change of levels of intracellular ROS following exposure to our cytokine regime. This increase was later deemed injury-progressive as inhibition/catabolism of ROS in the presence of inflammatory cytokines demonstrated a reduction in the cytokine-induced injury imparted on both barrier function and intercellular junction protein expression. Once again, this work was undertaken in order to add another dimension to our inflammatory study. It is worth noting that previous work in our laboratory explored the influence of laminar shear stress on the role of NADPH oxidase in ROS-dependent endothelial dysfunction (Fitzpatrick, Guinan et al. 2009, Guinan, Rochfort et al. 2013) yet this pertained to endothelial cultures of a macrovascular origin. For the first time in our lab, the effect of naturally occurring, injurious stimuli on ROS production in the microvasculature was comprehensively covered. Several studies corroborate certain aspects of the data presented in this thesis (Haorah, Knipe et al. 2005, Haorah, Ramirez et al. 2007, Schreibelt, Kooij et al. 2007, Basuroy, Bhattacharya et al. 2009) yet for the first time, a detailed examination of the role of cytokine-induced ROS on human BBB phenotype, particularly with regards to barrier modulation, is covered here.

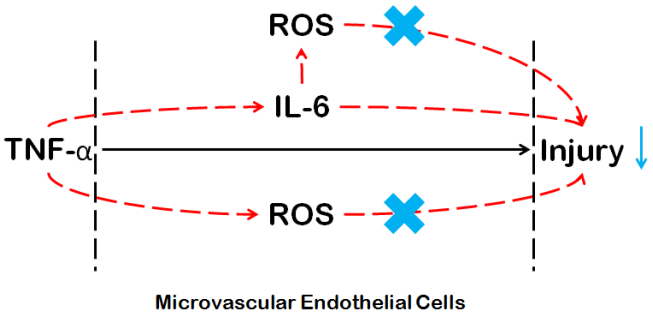

Figure 7.5: The contributory effect of ROS release in pro-inflammatory (TNF-α/IL-6) induced injury to HBMvECs.

As addressed earlier, a trend of particular interest was the TNF-α-induced expression and release of IL-6. Having extensively characterised the effect of IL-6 on HBMvEC barrier properties we shifted our focus to explore the hypothesis that the effects of TNF-α are mediated in-part through IL-6 production. In addressing this hypothesis we took the approach of neutralising any TNF-α-induced release of IL-6. Following IL-6 neutralisation, a significant reduction in the TNF-α-induced generation of intracellular ROS was observed. In addition, each of the examined proteins at the intercellular junctions demonstrated a significant recovery in expression following TNF-α treatment in the presence of the IL-6 NtAb, an effect which also imparted a correlative recovery in barrier function. IL-6 has a detailed complex role in the CNS (Barkhudaryan, Dunn 1999, Erta, Quintana et al. 2012). Whilst several studies have outlined its beneficial effects in coordinating the CNS immune response (Woodroofe, Sarna et al. 1991, Taupin, Toulmond et al. 1993, Klein, Moller et al. 1997, Hans, Kossmann et al. 1999, Penkowa, Moos et al. 1999, Penkowa, Giralt et al. 2000, Galiano, Liu et al. 2001, Swartz, Liu et al. 2001) very few have examined the effects of endothelial IL-6 release on the endothelium itself in the acute phase of BBB injury. Some *in vitro* studies have demonstrated the direct disruptive effect of IL-6 on BMvEC barrier function (Brett, Mizisin et al. 1995, Saija, Princi et al. 1995), whilst some *in vivo* studies have explored similar barrier-disruptive effects following injury in IL-6 knockout models (Paul, Koedel et al. 2003). Our data shows for the first time that TNF-α-induced IL-6 release not only has a direct negative impact on BBB phenotype, particularly pertaining to barrier function (~30% of overall impact), but it does so through the release of inflammatory mediators such as ROS. This adds a fresh dimension to the already existing data, in that while IL-6 might have an overall beneficial impact on the NVU, its acute release sustains negative consequences for the endothelium, and potentially neighbouring cell types via its subsequent secretory events.

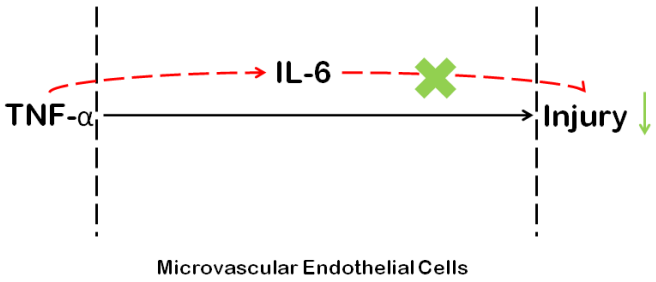

Figure 7.6: The contributory effect of IL-6 release in TNF-α-induced injury to HBMvECs.

In the final chapter of this thesis (chapter 6), our objective was to identify novel binding partners of the junctional proteins that maintain BBB phenotype (such binding partners potentially facilitating the post-translational modification observed in response to shear and cytokine treatments). Samples from shear and control cultures were prepared and subjected to optimised IP protocols for each of the junction proteins of interest. IP eluates and protein bands of interest isolated from SDS-PAGE gels run for IP eluates were subject to digestion and subsequent analysis by LC-M/MS. The peptide libraries generated yielded a substantial amount of potential targets. We therefore extrapolated targets from the bulk of the data based on cross relativity between species (bovine cultures were also prepared to investigate any overlap), trends observed between static and shear samples, and trends across the four proteins of interest. Numerous isoforms of the 14-3-3 family met each of these criteria, in particular an increase in 14-3-3 association with each of the junctional targets was observed following exposure to laminar shear stress. This relationship was clarified by repeat immunoprecipitation and reverse-immunprecipitation (pull-down of 14-3-3) with subsequent analysis of eluates by immunoblot techniques. Based on these screening studies, we concluded that 14-3-3 plays a role in the upregulation of barrier function through interaction with TJ/AJ proteins within the interendothelial complex.

In order to fully conceptualise the role of 14-3-3 at the intercellular junction plaque, we optimised an established inhibitor of 14-3-3 interaction; R18 peptide (Petosa, Masters et al. 1998, Wang, Yang et al. 1999), and simulated laminar shear stress in the presence of inhibitor. As validated by immunoblot analysis, R18 inhibited the laminar-shear induced association with each of the intercellular junction proteins of interest, a mechanism which could now be utilised in establishing 14-3-3's role in junction formation/enhancement. Based on the efficacy of R18, initial studies focussed on whether R18 inhibition of 14-3-3 could induce barrier dysfunction. Indeed, R18 could increase permeability of HBMvEC monolayers in both a dose- and time-dependent manner and completely reverse the barrier-strengthening effects of shear stress, adding credence to a pro-barrier role of 14-3-3.

Our studies with 14-3-3 up to this point utilised an antibody capable of detecting all seven isoforms. We therefore referred to our mass spectrometry data bank and noted that five of the seven isoforms surpassed the threshold as valid binding partners for each of the intercellular junction proteins of interest. We shifted our focus to examining the transcriptional levels of each isoform in response to laminar shear stress. Each isoform demonstrated an overall increase in mRNA levels in the acute stages of laminar shear onset prior to an overall moderate reduction following sustained shear exposure. The impact of this on respective proteins levels has yet to be investigated but it should be noted that 14-3-3 plays a role in numerous functions within the cell and while global levels of 14-3-3 may fluctuate, this may have no bearing on the increased association observed at the junction complex. This theory could be applied to the preliminary studies in effect in our laboratory in which 14-3-3 association at the junction complex following exposure to our inflammatory mediators; TNF-α and IL-6, is being investigated. Early work has demonstrated a surge in 14-3-3 transcription levels in both a dose- and time-dependent manner following exposure to these cytokines. Subsequent assessments of barrier function following exposure to TNF-α and IL-6 in the presence of R18 has demonstrated a slight but significant increase in permeability of the HBMvEC cultures. As inhibition of 14-3-3 binding in the presence of cytokines exacerbates barrier injury, this may suggest that increased transcription of these five isoforms following cytokine treatment is perhaps a defensive mechanism to reduce injury. Overall, studies have identified 14-3-3 as having a critical role in maintaining cell polarity in epithelial models (Hurd, Fan et al. 2003, Suzuki, Hirata et al. 2004, Izaki, Kamakura et al. 2005, Cohen, Fernandez et al. 2011), some studies of which have identified consequences for some of the intercellular proteins of interest in this thesis (i.e. ZO-1 (Wong, Sun et al. 2009)). One of the few studies in endothelial cells pertaining to 14-3-3 identified it as having a protective role in response to inflammatory injury (Liu, Yin et al. 2001), a process that could be interestingly enhanced following exposure to shear stress. Apart from the aforementioned studies, evidence of 14-3-3 participation in intercellular junction modulation is scarce and the work conducted in our laboratory to date, and presented in this thesis, suggests for the first time such association is plausible. Given its substantial presence in the brain (Martin, Rostas et al. 1994), in conjunction with evidence that elevated levels coincide with the onset of CNS pathologies (Boston, Jackson et al. 1982, Collins, Boyd et al. 2000), newly identified functions of 14-3-3 in the BBB may be detailed in this thesis, functions that may lead to better understanding of the physiology and pathophysiology of the BBB.

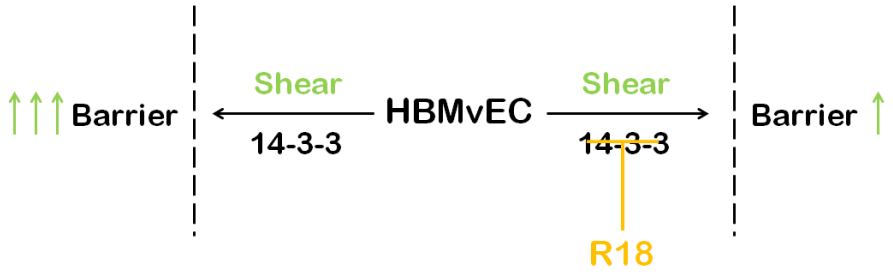

Figure 7.7: The contributory effect of 14-3-3 in shear-mediated stabilisation of HBMvECs barrier.

For future considerations, our laminar shear model is a well-published and validated means of examining the effect of said haemodynamic forces on our cerebral cultures (Pearce, McIntyre et al. 1996, Hendrickson, Cappadona et al. 1999, Colgan, Ferguson et al. 2007, Fitzpatrick, Guinan et al. 2009), however it presents some limitations. With regard to the real-time assessment of barrier function, pre-sheared cultures required replating into transwell inserts in which they were evaluated for transendothelial permeability. Exposure of the HBMvEC cultures in transwell inserts to orbital shear stress was not option due to the introduction of basolateral turbulence. Whilst not 100% ideal, previous studies have demonstrated that endothelial cultures retain 'mechanical memory' (Collins, Cummins et al. 2006) and indeed a consistent and significant improvement in barrier function is observed in our basic assessment of the effect of laminar shear on cerebral cultures despite the requirement for replating the cells post-shearing. A cone and plate viscometer offers a means of navigating this problem facilitating the in situ application of uniform shear stress profiles to cultures prepared for barrier assessment by the transwell permeability assay (Dewey, Bussolari et al. 1981, Blackman, Barbee et al. 2000, Orr, Stockton et al. 2007).

An additional criterion not explored in this thesis is the influence of the other cell populations which comprise the NVU on the MvECs. The influence of these diverse cell types on the MvECs in establishing the BBB is well documented, ranging from the impact of their released soluble factors to their physical contact. Colgan (2007) noted an improvement in paracellular permeability and TEER levels of BBMvECs following co-culture with astrocytes cultures or astrocyte-conditioned medium. *In vivo* levels of TEER with regards to the BBB are estimated to exceed 1000 Ω/cm^2. Colgan (2008) however observed a maximum electrical resistance of 80 Ω/cm^2 with BBMvECs *in vitro*. The presence of these factors, and indeed as we have shown, the hemodynamic forces associated with the blood flow of the microvasculature, are thus imperative in recreating the BBB microenvironment. Several apparatuses acknowledge this in that they are designed to facilitate both stimuli in experimental paradigms.

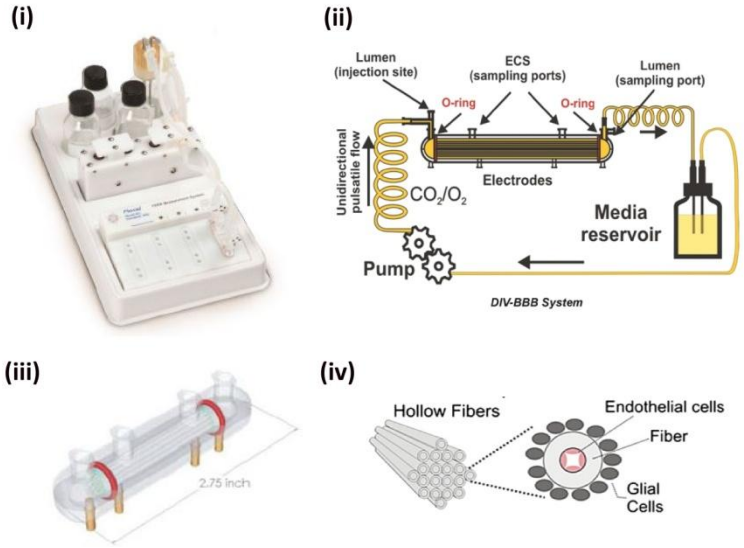

Figure 7.8: The DIV-BBB perfusion system. (i) The DIV-BBB is a small scale system that facilitates the (ii) simulation of hemodynamic forces found at the BBB. (iii) The cartridges allow for TEER measurements to be made whilst allowing for the (iv) 3D replication of anatomical aspects found at the BBB, (http://flocel.com/).

The CellMax artificial capillary system is a closed perfusion system currently employed in our lab for assessment of macrovascular environments. It facilitates not only the 3D co-culturing of cell populations, but allows the application of haemodynamic forces to the cultures. While we have achieved success with this system to date (Collins, Cummins et al. 2006, Colgan, Ferguson et al. 2007, Colgan, Collins et al. 2008), the DIV-BBB (Flocel Inc. Cleveland, Ohio) offers a similar setup, on a smaller, more anatomically correct scale, with the added feature of real-time measurement of TEER (Fig. 7.1). This system has been utilised in studies that corroborate some of the data in this thesis (Santaguida, Janigro et al. 2006, Krizanac-Bengez, Hossain et al. 2006, Krizanac-Bengez, Mayberg et al. 2006, Desai, Marroni et al. 2002, Cucullo, Hossain et al. 2011).

In conclusion, we have attempted to generate a detailed model, *in vitro*, of how the brain microvascular endothelium responds to positive and negative regulators of barrier phenotype. Our main findings can be summarised as follows:

- Laminar shear stress plays a pivotal role in the maintenance of vascular homeostasis and BBB phenotype through modulation and post-translational modification of interendothelial protein expression.
- Inflammatory cytokines, such as TNF-α and IL-6, play a pivotal role in the disruption of vascular homeostasis and BBB phenotype by directly (and indirectly via the release of pro-inflammatory mediators) promoting an injured BBB

phenotype through the modulation and post-translational modification of interendothelial protein expression.

- Laminar shear stress is also involved in the modulation of endothelial anti-inflammatory mechanisms and responsiveness to cytokine injury. TNF-α and IL-6 exert an opposite effect on the aspects examined promoting pro-inflammatory mechanisms and responsiveness to cytokine injury. Together, laminar shear stress had a protective effect against the influence of inflammatory cytokines as observed via the interendothelial junction.
- TNF-α and IL-6 are capable of elevating ROS production of HBMvECs. Using antioxidant strategies, the elevated levels of ROS induced by TNF-α and IL-6 were verified to sufficiently cause a reduction in tight junction protein levels and subsequently cause a reduction in barrier function. In addition, the levels of TNF-α-induced IL-6 on HBMvECs impacts significantly across a number of BBB molecular and functional aspects. We feel this data presents a comprehensive outlook on the cytokine-induced mechanisms in the acute and chronic stages of microvascular injury and underlines the importance of developing antioxidant treatments which are capable of effectively treating oxidative stress in the cerebral tissue
- The 14-3-3 family plays a pivotal role in the maintenance of vascular homeostasis and BBB phenotype through association with proteins of the interendothelial junction, with consequences for BBB barrier function. In addition, the 14-3-3 family may play a pivotal anti-inflammatory role in response to cytokine injury.

We find the effect of laminar shear stress on several aspects of cerebral endothelium homeostasis was explored comprehensively with physiological levels proven to be a dynamic regulator of intercellular junction assembly and consequently barrier function, in addition to anti-inflammatory and anti-coagulative mechanisms. Conversely, at an injury-induced level, locally produced inflammatory mediators induce adverse regulation of these mechanisms, promoting endothelial barrier dysfunction and at the molecular and functional level.

Bibliography.

ABBOTT, N.J., 2005. Dynamics of CNS barriers: Evolution, differentiation, and modulation. *Cellular and molecular neurobiology,* **25**(1), pp. 5-23.

ABBOTT, N.J., 2000. Inflammatory mediators and modulation of blood-brain barrier permeability. *Cellular and molecular neurobiology,* **20**(2), pp. 131-147.

ABBOTT, N.J., 1987. Glia and the Blood-Brain-Barrier. *Nature,* **325**(6101), pp. 195-195.

ABBOTT, N.J., LANE, N.J. and BUNDGAARD, M., 1986. The Blood-Brain Interface in Invertebrates. *Annals of the New York Academy of Sciences,* **481**, pp. 20-42.

ABBOTT, N.J. and REVEST, P.A., 1991. Control of Brain Endothelial Permeability. *Cerebrovascular and brain metabolism reviews,* **3**(1), pp. 39-72.

ABBOTT, N.J., REVEST, P.A. and ROMERO, I.A., 1992. Astrocyte Endothelial Interaction - Physiology and Pathology. *Neuropathology and applied neurobiology,* **18**(5), pp. 424-433.

ABBOTT, N.J. and ROMERO, I.A., 1996. Transporting therapeutics across the blood-brain barrier. *Molecular medicine today,* **2**(3), pp. 106-113.

ABBOTT, N.J., RONNBACK, L. and HANSSON, E., 2006. Astrocyte-endothelial interactions at the blood-brain barrier. *Nature Reviews Neuroscience,* **7**(1), pp. 41-53.

ABBOTT, N.J., 2013. Blood-brain barrier structure and function and the challenges for CNS drug delivery. *Journal of inherited metabolic disease,* **36**(3), pp. 437-449.

ABBOTT, N.J. and FRIEDMAN, A., 2012. Overview and introduction: The blood-brain barrier in health and disease. *Epilepsia,* **53**, pp. 1-6.

ABBOTT, N.J., PATABENDIGE, A.A.K., DOLMAN, D.E.M., YUSOF, S.R. and BEGLEY, D.J., 2010. Structure and function of the blood-brain barrier. *Neurobiology of disease,* **37**(1), pp. 13-25.

ABBOTT, N., 2002. Astrocyte-endothelial interactions and blood-brain barrier permeability. *Journal of anatomy,* **200**(6), pp. 629-638.

ABBRUSCATO, T.J., LOPEZ, S.P., MARK, K.S., HAWKINS, B.T. and DAVIS, T.P., 2002. Nicotine and cotinine modulate cerebral microvascular permeability and protein expression of ZO-1 through nicotinic acetylcholine receptors expressed on brain endothelial cells. *Journal of pharmaceutical sciences,* **91**(12), pp. 2525-2538.

ABRAHAM, C.S., DELI, M.A., JOO, F., MEGYERI, P. and TORPIER, G., 1996. Intracarotid tumor necrosis factor-alpha administration increases the blood-brain barrier permeability in cerebral cortex of the newborn pig: Quantitative aspects of double-labelling studies and confocal laser scanning analysis. *Neuroscience letters,* **208**(2), pp. 85-88.

ADAMSON, P., WILBOURN, B., ETIENNE-MANNEVILLE, S., CALDER, V., BERAUD, E., MILLIGAN, G., COURAUD, P.O. and GREENWOOD, J., 2002. Lymphocyte trafficking through the blood-brain barrier is dependent on endothelial cell heterotrimeric G-protein signaling. *Faseb Journal,* **16**(10), pp. UNSP 0892-6638/02/0016-1185.

AFONSO, P.V., OZDEN, S., PREVOST, M., SCHMITT, C., SEILHEAN, D., WEKSLER, B., COURAUD, P., GESSAIN, A., ROMERO, I.A. and CECCALDI, P., 2007. Human blood-brain barrier disruption by retroviral-infected lymphocytes: Role of myosin light chain kinase in endothelial tight-junction disorganization. *Journal of Immunology,* **179**(4), pp. 2576-2583.

AGGARWAL, B.B., 2003. Signalling pathways of the TNF superfamily: A double-edged sword. *Nature Reviews Immunology,* **3**(9), pp. 745-756.

AGGARWAL, B.B., EESSALU, T.E. and HASS, P.E., 1985. Characterization of Receptors for Human-Tumor Necrosis Factor and their Regulation by Gamma-Interferon. *Nature,* **318**(6047), pp. 665-667.

AIRD, W.C., 2006. Mechanisms of endothelial cell heterogeneity in health and disease. *Circulation research,* **98**(2), pp. 159-162.

AIRD, W.C., 2007. Phenotypic heterogeneity of the endothelium II. Representative vascular beds. *Circulation research,* **100**(2), pp. 174-190.

AITKEN, A., BAXTER, H., DUBOIS, T., CLOKIE, S., MACKIE, S., MITCHELL, K., PEDEN, A. and ZEMLICKOVA, E., 2002. Specificity of 14-3-3 isoform dimer interactions and phosphorylation. *Biochemical Society transactions,* **30**, pp. 351-360.

AITKEN, A., HOWELL, S., JONES, D., MADRAZO, J. and PATEL, Y., 1995. 14-3-3-Alpha and 14-3-3-Delta are the Phosphorylated Forms of Raf-Activating 14-3-3-Beta and 14-3-3-Zeta - In-Vivo Stoichiometric Phosphorylation in Brain at a Ser-Pro-Glu-Lys Motif. *Journal of Biological Chemistry,* **270**(11), pp. 5706-5709.

AKASSOGLOU, K., DOUNI, E., BAUER, J., LASSMANN, H., KOLLIAS, G. and PROBERT, L., 2003. Exclusive tumor necrosis factor (TNF) signaling by the p75TNF receptor triggers inflammatory ischemia in the CNS of transgenic mice. *Proceedings of the National Academy of Sciences of the United States of America,* **100**(2), pp. 709-714.

AKIRA, S., TAGA, T. and KISHIMOTO, T., 1993. Interleukin-6 in Biology and Medicine. *Advances in Immunology, Vol 54,* **54**, pp. 1-78.

ALEJANDRO LOPEZ-RAMIREZ, M., FISCHER, R., TORRES-BADILLO, C.C., DAVIES, H.A., LOGAN, K., PFIZENMAIER, K., MALE, D.K., SHARRACK, B. and ROMERO, I.A., 2012. Role of Caspases in Cytokine-Induced Barrier Breakdown in Human Brain Endothelial Cells. *Journal of Immunology,* **189**(6), pp. 3130-3139.

ALI, F.E.A., BARNHAM, K.J., BARROW, C.J. and SEPAROVIC, F., 2004. Metal-catalyzed oxidative damage and oligomerization of the amyloid-peptide of Alzheimer's disease. *Australian Journal of Chemistry,* **57**(6), pp. 511-518.

ALI, M.H., SCHLIDT, S.A., CHANDEL, N.S., HYNES, K.L., SCHUMACKER, P.T. and GEWERTZ, B.L., 1999. Endothelial permeability and IL-6 production during hypoxia: role of ROS in signal transduction. *American Journal of Physiology-Lung Cellular and Molecular Physiology,* **277**(5), pp. L1057-L1065.

ALI, M.H. and SCHUMACKER, P.T., 2002. Endothelial responses to mechanical stress: Where is the mechanosensor? *Critical Care Medicine,* **30**(5), pp. S198-S206.

ALLAN, S.M. and ROTHWELL, N.J., 2001. Cytokines and acute neurodegeneration. *Nature Reviews Neuroscience,* **2**(10), pp. 734-744.

ALON, R., KASSNER, P.D., CARR, M.W., FINGER, E.B., HEMLER, M.E. and SPRINGER, T.A., 1995. The Integrin Vla-4 Supports Tethering and Rolling in Flow on Vcam-1. *Journal of Cell Biology,* **128**(6), pp. 1243-1253.

ALVAREZ, J.I., DODELET-DEVILLERS, A., KEBIR, H., IFERGAN, I., FABRE, P.J., TEROUZ, S., SABBAGH, M., WOSIK, K., BOURBONNIERE, L., BERNARD, M., VAN HORSSEN, J., DE VRIES, H.E., CHARRON, F. and PRAT, A., 2011. The Hedgehog Pathway Promotes Blood-Brain Barrier Integrity and CNS Immune Quiescence. *Science*, **334**(6063), pp. 1727-1731.

ANDA, T., YAMASHITA, H., KHALID, H., TSUTSUMI, K., FUJITA, H., TOKUNAGA, Y. and SHIBATA, S., 1997. Effect of tumor necrosis factor-alpha on the permeability of bovine brain microvessel endothelial cell monolayers. *Neurological research,* **19**(4), pp. 369-376.

ANDO, J., TSUBOI, H., KORENAGA, R., TAKADA, Y., TOYAMASORIMACHI, N., MIYASAKA, M. and KAMIYA, A., 1994. Shear-Stress Inhibits Adhesion of Cultured Mouse Endothelial-Cells to Lymphocytes by Down-Regulating Vcam-1 Expression. *American Journal of Physiology,* **267**(3), pp. C679-C687.

ANDO-AKATSUKA, Y., SAITOU, M., HIRASE, T., KISHI, M., SAKAKIBARA, A., ITOH, M., YONEMURA, S., FURUSE, M. and TSUKITA, S., 1996. Interspecies diversity of the occludin sequence: cDNA cloning of human mouse, dog, and rat-kangaroo homologues. *Molecular biology of the cell,* **7**(SUPPL.), pp. 606A-606A.

ANDRAS, I.E., PU, H., TIAN, J., DELI, M.A., NATH, A., HENNIG, B. and TOBOREK, M., 2005. Signaling mechanisms of HIV-1 Tat-induced alterations of claudin-5 expression in brain endothelial cells. *Journal of Cerebral Blood Flow and Metabolism,* **25**(9), pp. 1159-1170.

ANDREEVA, A.Y., KRAUSE, E., MULLER, E.C., BLASIG, I.E. and UTEPBERGENOV, D.I., 2001. Protein kinase C regulates the phosphorylation and cellular localization of occludin. *Journal of Biological Chemistry,* **276**(42), pp. 38480-38486.

ANDRIOPOULOU, P., NAVARRO, P., ZANETTI, A., LAMPUGNANI, M.G. and DEJANA, E., 1999. Histamine induces tyrosine phosphorylation of endothelial cell-to-cell adherens junctions. *Arteriosclerosis Thrombosis and Vascular Biology,* **19**(10), pp. 2286-2297.

ANTONELLIORLIDGE, A., SAUNDERS, K.B., SMITH, S.R. and DAMORE, P.A., 1989. An Activated Form of Transforming Growth Factor-Beta is Produced by Cocultures of Endothelial-Cells and Pericytes. *Proceedings of the National Academy of Sciences of the United States of America,* **86**(12), pp. 4544-4548.

ANTONETTI, D.A., BARBER, A.J., HOLLINGER, L.A., WOLPERT, E.B. and GARDNER, T.W., 1999. Vascular endothelial growth factor induces rapid phosphorylation of tight junction proteins occludin and zonula occluden 1 - A potential mechanism for vascular permeability in diabetic retinopathy and tumors. *Journal of Biological Chemistry,* **274**(33), pp. 23463-23467.

ARGAW, A.T., GURFEIN, B., ZHANG, Y., ZAMEER, A. and JOHN, G., 2009. VEGF-mediated disruption of endothelial CLN-5 promotes blood-brain barrier breakdown. *Multiple Sclerosis,* **15**(9), pp. S91-S91.

ARMULIK, A., ABRAMSSON, A. and BETSHOLTZ, C., 2005. Endothelial/pericyte interactions. *Circulation research,* **97**(6), pp. 512-523.

ARMULIK, A., GENOVE, G., MAE, M., NISANCIOGLU, M.H., WALLGARD, E., NIAUDET, C., HE, L., NORLIN, J., LINDBLOM, P., STRITTMATTER, K., JOHANSSON, B.R. and BETSHOLTZ, C., 2010. Pericytes regulate the blood-brain barrier. *Nature,* **468**(7323), pp. 557-U231.

ARSENIJEVIC, D., GIRARDIER, L., SEYDOUX, J., PECHERE, J., GARCIA, I., LUCAS, R., CHANG, H. and DULLOO, A., 1998. Metabolic-cytokine responses to a second immunological challenge with LPS in mice with T-gondii infection. *American Journal of Physiology-Endocrinology and Metabolism,* **274**(3), pp. E439-E445.

ASANUMA, K., MAGID, R., JOHNSON, C., NEREM, R.M. and GALIS, Z.S., 2003. Uniaxial strain upregulates matrix-degrading enzymes produced by human vascular smooth muscle cells. *American Journal of Physiology-Heart and Circulatory Physiology,* **284**(5), pp. H1778-H1784.

ATAIE-KACHOIE, P., POURGHOLAMI, M.H. and MORRIS, D.L., 2013. Inhibition of the IL-6 signaling pathway: A strategy to combat chronic inflammatory diseases and cancer. *Cytokine & growth factor reviews,* **24**(2), pp. 163-173.

ATTWELL, D., BUCHAN, A.M., CHARPAK, S., LAURITZEN, M., MACVICAR, B.A. and NEWMAN, E.A., 2010. Glial and neuronal control of brain blood flow. *Nature,* **468**(7321), pp. 232-243.

AUGUSTIN, H.G., KOZIAN, D.H. and JOHNSON, R.C., 1994. Differentiation of Endothelial-Cells - Analysis of the Constitutive and Activated Endothelial-Cell Phenotypes. *Bioessays,* **16**(12), pp. 901-906.

AURRAND-LIONS, M., DUNCAN, L., BALLESTREM, C. and IMHOF, B.A., 2001. JAM-2, a novel immunoglobulin superfamily molecule, expressed by endothelial and lymphatic cells. *Journal of Biological Chemistry,* **276**(4), pp. 2733-2741.

AVELEIRA, C.A., LIN, C., ABCOUWER, S.F., AMBROSIO, A.F. and ANTONETTI, D.A., 2010. TNF-alpha Signals Through PKC zeta/NF-kappa B to Alter the Tight Junction Complex and Increase Retinal Endothelial Cell Permeability. *Diabetes,* **59**(11), pp. 2872-2882.

AZUMI, H., INOUE, N., TAKESHITA, S., RIKITAKE, Y., KAWASHIMA, S., HAYASHI, Y., ITOH, H. and YOKOYAMA, M., 1999. Expression of NADH/NADPH oxidase p22(phox) in human coronary arteries. *Circulation,* **100**(14), pp. 1494-1498.

BABIOR, B.M., 2000. Phagocytes and oxidative stress. *American Journal of Medicine,* **109**(1), pp. 33-44.

BADIMON, L., BADIMON, J.J., CHESEBRO, J.H. and FUSTER, V., 1993. Von-Willebrand-Factor and Cardiovascular-Disease. *Thrombosis and haemostasis,* **70**(1), pp. 111-118.

BALAMI, J.S., CHEN, R., GRUNWALD, I.Q. and BUCHAN, A.M., 2011. Neurological complications of acute ischaemic stroke. *Lancet Neurology,* **10**(4), pp. 357-371.

BALDA, M.S., GONZALEZ-MARISCAL, L., MATTER, K., CEREIHJIDO, M. and ANDERSON, J.M., 1993. Assembly of the Tight Junction - the Role of Diacylglycerol. *Journal of Cell Biology,* **123**(2), pp. 293-302.

BALDA, M.S. and MATTER, K., 2000. The tight junction protein ZO-1 and an interacting transcription factor regulate ErbB-2 expression. *Embo Journal,* **19**(9), pp. 2024-2033.

BALDA, M.S. and MATTER, K., 2000. Transmembrane proteins of tight junctions. *Seminars in cell & developmental biology,* **11**(4), pp. 281-289.

BALDA, M.S., WHITNEY, J.A., FLORES, C., GONZALEZ, S., CEREIJIDO, M. and MATTER, K., 1996. Functional dissociation of paracellular permeability and transepithelial electrical resistance and disruption of the apical-basolateral intramembrane diffusion barrier by expression of a mutant tight junction membrane protein. *Journal of Cell Biology,* **134**(4), pp. 1031-1049.

BALDA, M., FLORES-MALDONADO, C., CEREIJIDO, M. and MATTER, K., 2000. Multiple domains of occludin are involved in the regulation of paracellular permeability. *Journal of cellular biochemistry,* **78**(1), pp. 85-96.

BALLABH, P., BRAUN, A. and NEDERGAARD, M., 2004. The blood-brain barrier: an overview - Structure, regulation, and clinical implications. *Neurobiology of disease,* **16**(1), pp. 1-13.

BALLERMANN, B.J. and OTT, M.J., 1995. Adhesion and Differentiation of Endothelial-Cells by Exposure to Chronic Shear-Stress - a Vascular Graft Model. *Blood purification,* **13**(3-4), pp. 125-134.

BAMFORTH, S.D., LIGHTMAN, S. and GREENWOOD, J., 1996. The effect of TNF-alpha and IL-6 on the permeability of the rat blood-retinal barrier in vivo. *Acta Neuropathologica,* **91**(6), pp. 624-632.

BANDOPADHYAY, R., ORTE, C., LAWRENSON, J.G., REID, A.R., DE SILVA, S. and ALLT, G., 2001. Contractile proteins in pericytes at the blood-brain and blood-retinal barriers. *Journal of neurocytology,* **30**(1), pp. 35-44.

BANERJEE, S. and BHAT, M.A., 2007. Neuron-glial interactions in blood-brain barrier formation. *Annual Review of Neuroscience,* **30**, pp. 235-258.

BANKS, W.A., 2005. Blood-brain barrier transport of cytokines: A mechanism for neuropathology. *Current pharmaceutical design,* **11**(8), pp. 973-984.

BARBEE, K.A., DAVIES, P.F. and LAL, R., 1994. Shear Stress-Induced Reorganization of the Surface-Topography of Living Endothelial-Cells Imaged by Atomic-Force Microscopy. *Circulation research,* **74**(1), pp. 163-171.

BARBEE, K.A., DAVIES, P.F. and LAL, R., 1994. Shear Stress-Induced Reorganization of the Surface-Topography of Living Endothelial-Cells Imaged by Atomic-Force Microscopy. *Circulation research,* **74**(1), pp. 163-171.

BARBEE, K.A., MUNDEL, T., LAL, R. and DAVIES, P.F., 1995. Subcellular-Distribution of Shear-Stress at the Surface of Flow-Aligned and Nonaligned Endothelial Monolayers. *American Journal of Physiology-Heart and Circulatory Physiology,* **268**(4), pp. H1765-H1772.

BARGER, S.W., HORSTER, D., FURUKAWA, K., GOODMAN, Y., KRIEGLSTEIN, J. and MATTSON, M.P., 1995. Tumor-Necrosis-Factor-Alpha and Tumor-Necrosis-Factor-Beta Protect Neurons Against Amyloid Beta-Peptide Toxicity - Evidence for Involvement of a Kappa-B-Binding Factor and Attenuation of Peroxide and Ca2+ Accumulation. *Proceedings of the National Academy of Sciences of the United States of America,* **92**(20), pp. 9328-9332.

BARKHUDARYAN, N. and DUNN, A.J., 1999. Molecular mechanisms of actions of interleukin-6 on the brain, with special reference to serotonin and the hypothalamo-pituitary-adrenocortical axis. *Neurochemical research,* **24**(9), pp. 1169-1180.

BARNES, T.C., SPILLER, D.G., ANDERSON, M.E., EDWARDS, S.W. and MOOTS, R.J., 2011. Endothelial activation and apoptosis mediated by neutrophil-dependent interleukin 6 trans-signalling: a novel target for systemic sclerosis? *Annals of the Rheumatic Diseases,* **70**(2), pp. 366-372.

BARONE, F.C., ARVIN, B., WHITE, R.F., MILLER, A., WEBB, C.L., WILLETTE, R.N., LYSKO, P.G. and FEUERSTEIN, G.Z., 1997. Tumor necrosis factor-alpha - A mediator of focal ischemic brain injury. *Stroke,* **28**(6), pp. 1233-1244.

BARONE, F.C. and PARSONS, A.A., 2000. Therapeutic potential of anti-inflammatory drugs in focal stroke. *Expert opinion on investigational drugs,* **9**(10), pp. 2281-2306.

BASUROY, S., BHATTACHARYA, S., LEFFLER, C.W. and PARFENOVA, H., 2009. Nox4 NADPH oxidase mediates oxidative stress and apoptosis caused by TNF-alpha in cerebral vascular endothelial cells. *American Journal of Physiology-Cell Physiology,* **296**(3), pp. C422-C432.

BAUER, H.C., TRAWEGER, A. and BAUER, H., 2004. Proteins of the tight junction in the blood-brain barrier. In: H.S. SHARMA and J. WESTMAN, eds, *Blood-Spinal Cord and Brain Barriers in Health and Disease.* San Diego: Elsevier, pp. 1.

BAUER, H.C. and BAUER, H., 2000. Neural induction of the blood-brain barrier: Still an enigma. *Cellular and molecular neurobiology,* **20**(1), pp. 13-28.

BAUER, H.C., BAUER, H., LAMETSCHWANDTNER, A., AMBERGER, A., RUIZ, P. and STEINER, M., 1993. Neovascularization and the Appearance of Morphological-Characteristics of the Blood-Brain-Barrier in the Embryonic Mouse Central-Nervous-System. *Developmental Brain Research,* **75**(2), pp. 269-278.

BAUER, K.A. and ROSENBERG, R.D., 1987. The Pathophysiology of the Prethrombotic State in Humans - Insights Gained from Studies using Markers of Hemostatic System Activation. *Blood,* **70**(2), pp. 343-350.

BAXTER, H.C., FRASER, J.R., LIU, W.G., FORSTER, J.L., CLOKIE, S., STEINACKER, P., OTTO, M., BAHN, E., WILTFANG, J. and AITKEN, A., 2002. Specific 14-3-3 isoform detection and immunolocalization in prion diseases. *Biochemical Society transactions,* **30**, pp. 387-391.

BAXTER, H.C., LIU, W.G., FORSTER, J.L., AITKEN, A. and FRASER, J.R., 2002. Immunolocalisation of 14-3-3 isoforms in normal and scrapie-infected murine brain. *Neuroscience*, **109**(1), pp. 5-14.

BAZAN, J.F., 1990. Hematopoietic Receptors and Helical Cytokines. *Immunology today*, **11**(10), pp. 350-354.

BAZAN, J.F., 1990. Structural Design and Molecular Evolution of a Cytokine Receptor Superfamily. *Proceedings of the National Academy of Sciences of the United States of America*, **87**(18), pp. 6934-6938.

BAZZONI, G., 2006. Endothelial tight junctions: permeable barriers of the vessel wall. *Thrombosis and haemostasis*, **95**(1), pp. 36-42.

BAZZONI, G., MARTINEZ-ESTRADA, O.M., MUELLER, F., NELBOECK, P., SCHMID, G., BARTFAI, T., DEJANA, E. and BROCKHAUS, M., 2000. Hemophilic interaction of junctional adhesion molecule. *Journal of Biological Chemistry*, **275**(40), pp. 30970-30976.

BEAMER, N.B., COULL, B.M., CLARK, W.M., HAZEL, J.S. and SILBERGER, J.R., 1995. Interleukin-6 and Interleukin-1 Receptor Antagonist in Acute Stroke. *Annals of Neurology*, **37**(6), pp. 800-805.

BEATTIE, E.C., STELLWAGEN, D., MORISHITA, W., BRESNAHAN, J.C., HA, B.K., VON ZASTROW, M., BEATTIE, M.S. and MALENKA, R.C., 2002. Control of synaptic strength by glial TNF alpha. *Science*, **295**(5563), pp. 2282-2285.

BEEVERS, G., LIP, G.Y.H. and O'BRIEN, E., 2001. ABC of hypertension - The pathophysiology of hypertension. *British medical journal*, **322**(7291), pp. 912-916.

BEHRENDT, D. and GANZ, P., 2007. Oxidative Stress and Vascular Disease. In: R. DE CATERINA and P. LIBBY, eds, *Endothelial Dysfunctions and Vascular Disease.* Oxford: Blackwell Futura, pp. 148.

BEHRENDT, I. and KRAWINKEL, M., 2007. Antioxidants in oncotogy - benefit or risk? *Ernahrungs-Umschau*, **54**(6), pp. 314-+.

BENSON, T.J., NEREM, R.M. and PEDLEY, T.J., 1980. Assessment of Wall Shear-Stress in Arteries, Applied to the Coronary Circulation. *Cardiovascular research*, **14**(10), pp. 568-576.

BENZINGER, A., POPOWICZ, G., JOY, J., MAJUMDAR, S., HOLAK, T. and HERMEKING, H., 2005. The crystal structure of the non-liganded 14-3-3 sigma protein: insights into determinants of isoform specific ligand binding and dimerization. *Cell research*, **15**(4), pp. 219-227.

BERG, D., HOLZMANN, C. and RIESS, O., 2003. 14-3-3 Proteins in the Nervous System. *Nature Reviews Neuroscience*, **4**(9), pp. 752-762.

BERGERS, G. and SONG, S., 2005. The role of pericytes in blood-vessel formation and maintenance. *Neuro-oncology*, **7**(4), pp. 452-464.

BERK, B.C., ABE, J., MIN, W., SURAPISITCHAT, J. and YAN, C., 2001. Endothelial atheroprotective and anti-inflammatory mechanisms. *Atherosclerosis Vi,* **947**, pp. 93-111.

BERK, B.C., MIN, W., YAN, C., SURAPISITCHAT, J., LIU, Y.M. and HOEFEN, R., 2002. Atheroprotective mechanisms activated by fluid shear stress in endothelial cells. *Drug News & Perspectives,* **15**(3), pp. 133-139.

BERNATCHEZ, P.N., BAUER, P.M., YU, J., PRENDERGAST, J.S., HE, P.N. and SESSA, W.C., 2005. Dissecting the molecular control of endothelial NO synthase by caveolin-1 using cell-permeable peptides. *Proceedings of the National Academy of Sciences of the United States of America,* **102**(3), pp. 761-766.

BERTI, R., WILLIAMS, A.J., MOFFETT, J.R., HALE, S.L., VELARDE, L.C., ELLIOTT, P.J., YAO, C.P., DAVE, J.R. and TORTELLA, F.C., 2002. Quantitative real-time RT-PCR analysis of inflammatory gene expression associated with ischemia-reperfusion brain injury. *Journal of Cerebral Blood Flow and Metabolism,* **22**(9), pp. 1068-1079.

BETANZOS, A., HUERTA, M., LOPEZ-BAYGHEN, E., AZUARA, E., AMERENA, J. and GONZALEZ-MARISCAL, L., 2004. The tight junction protein ZO-2 associates with Jun, Fos and C/EBP transcription factors in epithelial cells. *Experimental cell research,* **292**(1), pp. 51-66.

BETZ, A.L., FIRTH, J.A. and GOLDSTEIN, G.W., 1980. Polarity of the Blood-Brain-Barrier - Distribution of Enzymes between the Luminal and Antiluminal Membranes of Brain Capillary Endothelial-Cells. *Brain research,* **192**(1), pp. 17-28.

BHULLAR, I.S., LI, Y.S., MIAO, H., ZANDI, E., KIM, M., SHYY, J.Y.J. and CHIEN, S., 1998. Fluid shear stress activation of I kappa B kinase is integrin-dependent. *Journal of Biological Chemistry,* **273**(46), pp. 30544-30549.

BIRUKOVA, A.A., TIAN, Y., MELITON, A., LEFF, A., WU, T. and BIRUKOV, K.G., 2012. Stimulation of Rho signaling by pathologic mechanical stretch is a "second hit" to Rho-independent lung injury induced by IL-6. *American Journal of Physiology-Lung Cellular and Molecular Physiology,* **302**(9), pp. L965-L975.

BLACK, R.A., RAUCH, C.T., KOZLOSKY, C.J., PESCHON, J.J., SLACK, J.L., WOLFSON, M.F., CASTNER, B.J., STOCKING, K.L., REDDY, P., SRINIVASAN, S., NELSON, N., BOIANI, N., SCHOOLEY, K.A., GERHART, M., DAVIS, R., FITZNER, J.N., JOHNSON, R.S., PAXTON, R.J., MARCH, C.J. and CERRETTI, D.P., 1997. A metalloproteinase disintegrin that releases tumour-necrosis factor-alpha from cells. *Nature,* **385**(6618), pp. 729-733.

BLACKMAN, B., BARBEE, K. and THIBAULT, L., 2000. In vitro cell shearing device to investigate the dynamic response of cells in a controlled hydrodynamic environment. *Annals of Biomedical Engineering,* **28**(4), pp. 363-372.

BLENNOW, K., DE LEON, M.J. and ZETTERBERG, H., 2006. Alzheimer's disease. *Lancet,* **368**(9533), pp. 387-403.

BOEHME, M.W.J., DENG, Y., RAETH, U., BIERHAUS, A., ZIEGLER, R., STREMMEL, W. and NAWROTH, P.P., 1996. Release of thrombomodulin from endothelial cells by concerted action of TNF-alpha and neutrophils: In vivo and in vitro studies. *Immunology,* **87**(1), pp. 134-140.

BOEKHOLDT, S.M. and STROES, E.S.G., 2012. The interleukin-6 pathway and atherosclerosis. *Lancet,* **379**(9822), pp. 1176-1178.

BOERMA, T., ABOU-ZAHR, C. and YOHANNES, K., 2008. *World Health Statistics 2008.* Geneva: WHO Publications.

BOGATCHEVA, N.V., GARCIA, J.G.N. and VERIN, A.D., 2002. Molecular mechanisms of thrombin-induced endothelial cell permeability. *Biochemistry-Moscow,* **67**(1), pp. 75-84.

BOLTON, S.J., ANTHONY, D.C. and PERRY, V.H., 1998. Loss of the tight junction proteins occludin and zonula occludens-1 from cerebral vascular endothelium during neutrophil-induced blood-brain barrier breakdown in vivo. *Neuroscience,* **86**(4), pp. 1245-1257.

BONEU, B., ABBAL, M., PLANTE, J. and BIERME, R., 1975. Factor-Viii Complex and Endothelial Damage. *Lancet,* **1**(7922), pp. 1430-1430.

BOSTON, P.F., JACKSON, P., KYNOCH, P.A.M. and THOMPSON, R.J., 1982. Purification, Properties, and Immunohistochemical Localization of Human-Brain 14-3-3 Protein. *Journal of neurochemistry,* **38**(5), pp. 1466-1474.

BOSTON, P.F., JACKSON, P. and THOMPSON, R.J., 1982. Human 14-3-3 Protein - Radioimmunoassay, Tissue Distribution, and Cerebrospinal-Fluid Levels in Patients with Neurological Disorders. *Journal of neurochemistry,* **38**(5), pp. 1475-1482.

BOULANGER, M.J., CHOW, D.C., BREVNOVA, E.E. and GARCIA, K.C., 2003. Hexameric structure and assembly of the interleukin-6/IL-6 alpha-receptor/gp130 complex. *Science,* **300**(5628), pp. 2101-2104.

BRAAK, H. and BRAAK, E., 1991. Demonstration of Amyloid Deposits and Neurofibrillary Changes in Whole Brain Sections. *Brain Pathology,* **1**(3), pp. 213-216.

BRADBURY, M.W.B., 1979. *The Concept of a Blood-Brain Barrier*. Chichester: John Wiley.

BRETT, F.M., MIZISIN, A.P., POWELL, H.C. and CAMPBELL, I.L., 1995. Evolution of Neuropathologic Abnormalities Associated with Blood-Brain-Barrier Breakdown in Transgenic Mice Expressing Interleukin-6 in Astrocytes. *Journal of neuropathology and experimental neurology,* **54**(6), pp. 766-775.

BRIGHTMAN, M. and REESE, T., 1969. Junctions between Intimately Apposed Cell Membranes in Vertebrate Brain. *Journal of Cell Biology,* **40**(3), pp. 648-&.

BROADWELL, R.D., 1989. Transcytosis of Macromolecules through the Blood-Brain-Barrier - a Cell Biological Perspective and Critical-Appraisal. *Acta Neuropathologica,* **79**(2), pp. 117-128.

BROADWELL, R.D., BALIN, B.J. and SALCMAN, M., 1988. Transcytotic Pathway for Blood-Borne Protein through the Blood-Brain Barrier. *Proceedings of the National Academy of Sciences of the United States of America,* **85**(2), pp. 632-636.

BROOKS, A.R., LELKES, P.I. and RUBANYI, G.M., 2002. Gene expression profiling of human aortic endothelial cells exposed to disturbed flow and steady laminar flow. *Physiological Genomics,* **9**(1), pp. 27-41.

BROWN, R.C. and DAVIS, T.P., 2005. Hypoxia/aglycemia alters expression of occludin and actin in brain endothelial cells. *Biochemical and biophysical research communications,* **327**(4), pp. 1114-1123.

BROWN, R.C. and DAVIS, T.P., 2002. Calcium modulation of adherens and tight junction function - A potential mechanism for blood-brain barrier disruption after stroke. *Stroke,* **33**(6), pp. 1706-1711.

BROWNSON, E.A., ABBRUSCATO, T.J., GILLESPIE, T.J., HRUBY, V.J. and DAVIS, T.P., 1994. Effect of Peptidases at the Blood-Brain-Barrier on the Permeability of Enkephalin. *Journal of Pharmacology and Experimental Therapeutics,* **270**(2), pp. 675-680.

BRUCE, A.J., BOLING, W., KINDY, M.S., PESCHON, J., KRAEMER, P.J., CARPENTER, M.K., HOLTSBERG, F.W. and MATTSON, M.P., 1996. Altered neuronal and microglial responses to excitotoxic and ischemic brain injury in mice lacking TNF receptors. *Nature medicine,* **2**(7), pp. 788-794.

BRUNS, T.J. and HAUSER, W.A., 2003. The epidemiology of traumatic brain injury: A review. *Epilepsia,* **44**, pp. 2-10.

BUSIK, J.V., MOHR, S. and GRANT, M.B., 2008. Hyperglycemia-induced reactive oxygen species toxicity to endothelial cells is dependent on paracrine mediators. *Diabetes,* **57**(7), pp. 1952-1965.

BUSTIN, S.A., BENES, V., GARSON, J.A., HELLEMANS, J., HUGGETT, J., KUBISTA, M., MUELLER, R., NOLAN, T., PFAFFL, M.W., SHIPLEY, G.L., VANDESOMPELE, J. and WITTWER, C.T., 2009. The MIQE guidelines: minimum information for publication of quantitative real-time PCR experiments. *Clinical chemistry,* **55**(4), pp. 611-622.

BUTLER, P.J., NORWICH, G., WEINBAUM, S. and CHIEN, S., 2001. Shear stress induces a time- and position-dependent increase in endothelial cell membrane fluidity. *American Journal of Physiology-Cell Physiology,* **280**(4), pp. C962-C969.

BUTT, A.M., JONES, H.C. and ABBOTT, N.J., 1990. Electrical-Resistance Across the Blood-Brain-Barrier in Anesthetized Rats - a Developmental-Study. *Journal of Physiology-London,* **429**, pp. 47-62.

BUTT, A., 1995. Effect of Inflammatory Agents on Electrical-Resistance Across the Blood-Brain-Barrier in Pial Microvessels of Anesthetized Rats. *Brain research,* **696**(1-2), pp. 145-150.

BUTTINI, M., APPEL, K., SAUTER, A., GEBICKEHAERTER, P.J. and BODDEKE, H.W.G.M., 1996. Expression of tumor necrosis factor alpha after focal cerebral ischaemia in the rat. *Neuroscience,* **71**(1), pp. 1-16.

CANDELA, P., GOSSELET, F., SAINT-POL, J., SEVIN, E., BOUCAU, M., BOULANGER, E., CECCHELLI, R. and FENART, L., 2010. Apical-to-Basolateral Transport of Amyloid-beta Peptides through Blood-Brain Barrier Cells is Mediated by the

Receptor for Advanced Glycation End-Products and is Restricted by P-Glycoprotein. *Journal of Alzheimers Disease,* **22**(3), pp. 849-859.

CANNON, R.O., 1998. Potential mechanisms for the effect of angiotensin-converting enzyme inhibitors on endothelial dysfunction: The role of nitric oxide. *American Journal of Cardiology,* **82**(10A), pp. 8S-10S.

CANNON, R.O., 1998. Role of nitric oxide in cardiovascular disease: focus on the endothelium. *Clinical chemistry,* **44**(8), pp. 1809-1819.

CAPORALI, A., MELONI, M., VOELLENKLE, C., BONCI, D., SALA-NEWBY, G.B., ADDIS, R., SPINETTI, G., LOSA, S., MASSON, R., BAKER, A.H., AGAMI, R., LE SAGE, C., CONDORELLI, G., MADEDDU, P., MARTELLI, F. and EMANUELI, C., 2011. Deregulation of microRNA-503 Contributes to Diabetes Mellitus-Induced Impairment of Endothelial Function and Reparative Angiogenesis After Limb Ischemia. *Circulation,* **123**(3), pp. 282-U117.

CARLIER, S.G., VAN DAMME, L.C.A., BLOMMERDE, C.P., WENTZEL, J.J., VAN LANGEHOVE, G., VERHEYE, S., KOCKX, M.M., KNAAPEN, M.W.M., CHENG, C., GIJSEN, F., DUNCKER, D.J., STERGIOPULOS, N., SLAGER, C.J., SERRUYS, P.W. and KRAMS, R., 2003. Augmentation of wall shear stress inhibits neointimal hyperplasia after stent implantation - Inhibition through reduction of inflammation? *Circulation,* **107**(21), pp. 2741-2746.

CARMELIET, P., LAMPUGNANI, M.G., MOONS, L., BREVIARIO, F., COMPERNOLLE, V., BONO, F., BALCONI, G., SPAGNUOLO, R., OOSTHUYSE, B., DEWERCHIN, M., ZANETTI, A., ANGELLILO, A., MATTOT, V., NUYENS, D., LUTGENS, E., CLOTMAN, F., DE RUITER, M.C., GITTENBERGER-DE GROOT, A., POELMANN, R., LUPU, F., HERBERT, J.M., COLLEN, D. and DEJANA, E., 1999. Targeted deficiency or cytosolic truncation of the VE-cadherin gene in mice impairs VEGF-mediated endothelial survival and angiogenesis. *Cell,* **98**(2), pp. 147-157.

CARMELIET, P., NG, Y.S., NUYENS, D., THEILMEIER, G., BRUSSELMANS, K., CORNELISSEN, I., EHLER, E., KAKKAR, V.V., STALMANS, I., MATTOT, V., PERRIARD, J.C., DEWERCHIN, M., FLAMENG, W., NAGY, A., LUPU, F., MOONS, L., COLLEN, D., D'AMORE, P.A. and SHIMA, D.T., 1999. Impaired myocardial angiogenesis and ischemic cardiomyopathy in mice lacking the vascular endothelial growth factor isoforms VEGF(164) and VEGF(188). *Nature medicine,* **5**(5), pp. 495-502.

CARO, C.G., FITZGERALD, J.M. and SCHROTER, R.C., 1971. Atheroma and Arterial Wall Shear - Observation, Correlation and Proposal of a Shear Dependent Mass Transfer Mechanism for Altherogenesis. *Proceedings of the Royal Society Series B-Biological Sciences,* **177**(1046), pp. 109-+.

CARRANO, A., HOOZEMANS, J.J.M., VAN DER VIES, S.M., ROZEMULLER, A.J.M., VAN HORSSEN, J. and DE VRIES, H.E., 2011. Amyloid Beta Induces Oxidative Stress-Mediated Blood-Brain Barrier Changes in Capillary Amyloid Angiopathy. *Antioxidants & Redox Signaling,* **15**(5), pp. 1167-1178.

CARSWELL, E.A., OLD, L.J., KASSEL, R.L., GREEN, S., FIORE, N. and WILLIAMSON, B., 1975. Endotoxin-Induced Serum Factor that Causes Necrosis of Tumors. *Proceedings of the National Academy of Sciences of the United States of America,* **72**(9), pp. 3666-3670.

CARTER, W.O., NARAYANAN, P.K. and ROBINSON, J.P., 1994. Intracellular Hydrogen-Peroxide and Superoxide Anion Detection in Endothelial-Cells. *Journal of leukocyte biology,* **55**(2), pp. 253-258.

CATTANEO, E., CONTI, L. and DE-FRAJA, C., 1999. Signalling through the JAK-STAT pathway in the developing brain. *Trends in neurosciences,* **22**(8), pp. 365-369.

CECCHELLI, R., BEREZOWSKI, V., LUNDQUIST, S., CULOT, M., RENFTEL, M., DEHOUCK, M. and FENART, L., 2007. Modelling of the blood-brain barrier in drug discovery and development. *Nature Reviews Drug Discovery,* **6**(8), pp. 650-661.

CECCHELLI, R., BEREZOWSKI, V., LUNDQUIST, S., CULOT, M., RENFTEL, M., DEHOUCK, M. and FENART, L., 2007. Modelling of the blood-brain barrier in drug discovery and development. *Nature Reviews Drug Discovery,* **6**(8), pp. 650-661.

CELIS, J.E., GESSER, B., RASMUSSEN, H.H., MADSEN, P., LEFFERS, H., DEJGAARD, K., HONORE, B., OLSEN, E., RATZ, G., LAURIDSEN, J.B., BASSE, B., MOURITZEN, S., HELLERUP, M., ANDERSEN, A., WALBUM, E., CELIS, A., BAUW, G., PUYPE, M., VANDAMME, J. and VANDEKERCKHOVE, J., 1990. Comprehensive 2-Dimensional Gel Protein Databases Offer a Global Approach to the Analysis of Human-Cells - the Transformed Amnion Cells (Ama) Master Database and its Link to Genome Dna-Sequence Data. *Electrophoresis,* **11**(12), pp. 989-1071.

CHABOT, C., SPRING, K., GRATTON, J., ELCHEBLY, M. and ROYAL, I., 2009. New Role for the Protein Tyrosine Phosphatase DEP-1 in Akt Activation and Endothelial Cell Survival. *Molecular and cellular biology,* **29**(1), pp. 241-253.

CHAO, C.C., HU, S.X., EHRLICH, L. and PETERSON, P.K., 1995. Interleukin-1 and tumor necrosis factor-alpha synergistically mediate neurotoxicity: Involvement of nitric oxide and of N-methyl-D-aspartate receptors. *Brain Behavior and Immunity,* **9**(4), pp. 355-365.

CHARO, I. and RANSOHOFF, R., 2006. Mechanisms of disease - The many roles of chemokines and chemokine receptors in inflammation. *New England Journal of Medicine,* **354**(6), pp. 610-621.

CHATZIZISIS, Y.S., COSKUN, A.U., JONAS, M., EDELMAN, E.R., FELDMAN, C.L. and STONE, P.H., 2007. Role of endothelial shear stress in the natural history of coronary atherosclerosis and vascular remodeling - Molecular, cellular, and vascular behavior. *Journal of the American College of Cardiology,* **49**(25), pp. 2379-2393.

CHAUDHRI, M., SCARABEL, M. and AITKEN, A., 2003. Mammalian and yeast 14-3-3 isoforms form distinct patterns of dimers in vivo. *Biochemical and biophysical research communications,* **300**(3), pp. 679-685.

CHEN, B.P.C., LI, Y.S., ZHAO, Y.H., CHEN, K.D., LI, S., LAO, J.M., YUAN, S.L., SHYY, J.Y.J. and CHIEN, S., 2001. DNA microarray analysis of gene expression in endothelial cells in response to 24-h shear stress. *Physiological Genomics,* **7**(1), pp. 55-63.

CHEN, K.D., LI, Y.S., KIM, M., LI, S., YUAN, S., CHIEN, S. and SHYY, J.Y.J., 1999. Mechanotransduction in response to shear stress - Roles of receptor tyrosine kinases, integrins, and Shc. *Journal of Biological Chemistry,* **274**(26), pp. 18393-18400.

CHEN, X.L., NAM, J., JEAN, C., LAWSON, C., WALSH, C.T., GOKA, E., LIM, S., TOMAR, A., TANCIONI, I., URYU, S., GUAN, J., ACEVEDO, L.M., WEIS, S.M., CHERESH, D.A. and SCHLAEPFER, D.D., 2012. VEGF-Induced Vascular Permeability Is Mediated by FAK. *Developmental Cell,* **22**(1), pp. 146-157.

CHENG, C., VAN HAPEREN, R., DE WAARD, M., VAN DAMME, L.C.A., TEMPEL, D., HANEMAAIJER, L., VAN CAPPELLEN, G.W.A., BOS, J., SLAGER, C.J., DUNCKER, D.J., VAN DER STEEN, A.F.W., DE CROM, R. and KRAMS, R., 2005. Shear stress affects the intracellular distribution of eNOS: direct demonstration by a novel in vivo technique. *Blood,* **106**(12), pp. 3691-3698.

CHIEN, S., LI, S. and SHYY, J.Y.J., 1998. Effects of mechanical forces on signal transduction and gene expression in endothelial cells. *Hypertension,* **31**(1), pp. 162-169.

CHIU, J.J., CHEN, C.N., LEE, P.L., YANG, C.T., CHUANG, H.S., CHIEN, S. and USAMI, S., 2003. Analysis of the effect of disturbed flow on monocytic adhesion to endothelial cells. *Journal of Biomechanics,* **36**(12), pp. 1883-1895.

CHIU, J.J., WANG, D.L., CHIEN, S., SKALAK, R. and USAMI, S., 1998. Effects of disturbed flow on endothelial cells. *Journal of Biomechanical Engineering-Transactions of the Asme,* **120**(1), pp. 2-8.

CHIU, J., USAMI, S. and CHIEN, S., 2009. Vascular endothelial responses to altered shear stress: Pathologic implications for atherosclerosis. *Annals of Medicine,* **41**(1), pp. 19-28.

CHO, A., COURTMAN, D.W. and LANGILLE, B.L., 1995. Apoptosis (Programmed Cell-Death) in Arteries of the Neonatal Lamb. *Circulation research,* **76**(2), pp. 168-175.

CHO, A., MITCHELL, L., KOOPMANS, D. and LANGILLE, B.L., 1997. Effects of changes in blood flow rate on cell death and cell proliferation in carotid arteries of immature rabbits. *Circulation research,* **81**(3), pp. 328-337.

CHOBANIAN, A.V. and ALEXANDER, R.W., 1996. Exacerbation of atherosclerosis by hypertension - Potential mechanisms and clinical implications. *Archives of Internal Medicine,* **156**(17), pp. 1952-1956.

CHODOBSKI, A., ZINK, B.J. and SZMYDYNGER-CHODOBSKA, J., 2011. Blood-Brain Barrier Pathophysiology in Traumatic Brain Injury. *Translational Stroke Research,* **2**(4), pp. 492-516.

CHOI, Y.K. and KIM, K., 2008. Blood-neural barrier: its diversity and coordinated cell-to-cell communication. *Bmb Reports,* **41**(5), pp. 345-352.

CHOMCZYNSKI, P. and SACCHI, N., 2006. The single-step method of RNA isolation by acid guanidinium thiocyanate-phenol-chloroform extraction: twenty-something years on. *Nature protocols,* **1**(2), pp. 581-585.

CHOMCZYNSKI, P. and SACCHI, N., 1987. Single-Step Method of Rna Isolation by Acid Guanidinium Thiocyanate Phenol Chloroform Extraction. *Analytical Biochemistry,* **162**(1), pp. 156-159.

CHRISTOV, A., OTTMAN, J.T. and GRAMMAS, P., 2004. Vascular inflammatory, oxidative and protease-based processes: implications for neuronal cell death in Alzheimer's disease. *Neurological research,* **26(**5), pp. 540-546.

CINES, D., POLLAK, E., BUCK, C., LOSCALZO, J., ZIMMERMAN, G., MCEVER, R., POBER, J., WICK, T., KONKLE, B., SCHWARTZ, B., BARNATHAN, E., MCCRAE, K., HUG, B., SCHMIDT, A. and STERN, D., 1998. Endothelial cells in physiology and in the pathophysiology of vascular disorders. *Blood,* **91**(10), pp. 3527-3561.

CLARK, W.M., RINKER, L.G., LESSOV, N.S., HAZEL, K., HILL, J.K., STENZEL-POORE, M. and ECKENSTEIN, F., 2000. Lack of interleukin-6 expression is not protective against focal central nervous system ischemia. *Stroke,* **31**(7), pp. 1715-1720.

COHEN, D., FERNANDEZ, D., LAZARO-DIEGUEZ, F. and MUESCH, A., 2011. The serine/threonine kinase Par1 b regulates epithelial lumen polarity via IRSp53-mediated cell-ECM signaling. *Journal of Cell Biology,* **192**(3), pp. 525-540.

COHEN, Z., MOLINATTI, G. and HAMEL, E., 1997. Astroglial and vascular interactions of noradrenaline terminals in the rat cerebral cortex. *Journal of Cerebral Blood Flow and Metabolism,* **17**(8), pp. 894-904.

COLGAN, O.C., COLLINS, N.T., FETGUSON, G., MURPHY, R.P., BITNEY, Y.A., CAHILL, P.A. and CUMMINS, P.M., 2008. Influence of basolateral condition on the regulation of brain microvascular endothelial tight junction properties and barrier function. *Brain research,* **1193**, pp. 84-92.

COLGAN, O.C., FERGUSON, G., COLLINS, N.T., MURPHY, R.P., MEADE, G., CAHILL, P.A. and CUMMINS, P.M., 2007. Regulation of bovine brain microvascular endothelial tight junction assembly and barrier function by laminar shear stress. *American Journal of Physiology-Heart and Circulatory Physiology,* **292**(6), pp. H3190-H3197.

COLLINS, N.T., CUMMINS, P.M., COLGAN, O.C., FERGUSON, G., BIRNEY, Y.A., MURPHY, R.P., MEADE, G. and CAHILL, P.A., 2006. Cyclic strain-mediated regulation of vascular endothelial occludin and ZO-1: influence on intercellular tight junction assembly and function. *Arteriosclerosis, Thrombosis, and Vascular Biology,* **26**(1), pp. 62-68.

COLLINS, S., BOYD, A., FLETCHER, A., GONZALES, M., MCLEAN, C.A., BYRON, K. and MASTERS, C.L., 2000. Creutzfeldt-Jakob disease: diagnostic utility of 14-3-3 protein immunodetection in cerebrospinal fluid. *Journal of Clinical Neuroscience,* **7**(3), pp. 203-208.

COLLINS, T., 1993. Biology of Disease - Endothelial Nuclear Factor-Kappa-B and the Initiation of the Atherosclerotic Lesion. *Laboratory Investigation,* **68**(5), pp. 499-508.

COLLINS, T., LAPIERRE, L.A., FIERS, W., STROMINGER, J.L. and POBER, J.S., 1986. Recombinant Human-Tumor Necrosis Factor Increases Messenger-Rna Levels and Surface Expression of Hla-A,b Antigens in Vascular Endothelial-Cells and Dermal Fibroblasts Invitro. *Proceedings of the National Academy of Sciences of the United States of America,* **83(**2), pp. 446-450.

COLLINS-UNDERWOOD, J.R., ZHAO, W., SHARPE, J.G. and ROBBINS, M.E., 2008. NADPH oxidase mediates radiation-induced oxidative stress in rat brain microvascular endothelial cells. *Free Radical Biology and Medicine,* **45**(6), pp. 929-938.

COOK, E.B., STAHL, J.L., GRAZIANO, F.M. and BARNEY, N.P., 2008. Regulation of the receptor for TNF alpha, TNFR1, in human conjunctival epithelial cells. *Investigative ophthalmology & visual science,* **49**(9), pp. 3992-3998.

CORDON-CARDO, C., O' BRIEN, J.P., CASALS, D., RITTMANGRAUER, L., BIEDLER, J.L., MELAMED, M.R. and BERTINO, J.R., 1989. Multidrug-Resistance Gene (P-Glycoprotein) is Expressed by Endothelial-Cells at Blood-Brain Barrier Sites. *Proceedings of the National Academy of Sciences of the United States of America,* **86**(2), pp. 695-698.

CROCKER, D.J., MURAD, T.M. and GEER, J.C., 1970. Role of Pericyte in Wound Healing - an Ultrastructural Study. *Experimental and molecular pathology,* **13**(1), pp. 51-&.

CUCULLO, L., HOSSAIN, M., PUVENNA, V., MARCHI, N. and JANIGRO, D., 2011. The role of shear stress in Blood-Brain Barrier endothelial physiology. *Bmc Neuroscience,* **12**, pp. 40.

CUNNINGHAM, K.S. and GOTLIEB, A.I., 2005. The role of shear stress in the pathogenesis of atherosclerosis. *Laboratory Investigation,* **85**(1), pp. 9-23.

DALLASTA, L.M., PISAROV, L.A., ESPLEN, J.E., WERLEY, J.V., MOSES, A.V., NELSON, J.A. and ACHIM, C.L., 1999. Blood-brain barrier tight junction disruption in human immunodeficiency virus-1 encephalitis. *American Journal of Pathology,* **155**(6), pp. 1915-1927.

DANEMAN, R., ZHOU, L., KEBEDE, A.A. and BARRES, B.A., 2010. Pericytes are required for blood-brain barrier integrity during embryogenesis. *Nature,* **468**(7323), pp. 562-U238.

DARLING, D.L., YINGLING, J. and WYNSHAW-BORIS, A., 2005. Role of 14-3-3 proteins in eukaryotic signaling and development. *Current Topics in Developmental Biology, Volume 68,* **68**, pp. 281-+.

DARNELL, J.E., KERR, I.M. and STARK, G.R., 1994. Jak-Stat Pathways and Transcriptional Activation in Response to Ifns and Other Extracellular Signaling Proteins. *Science,* **264**(5164), pp. 1415-1421.

DAUGHERTY, B.L., WARD, C., SMITH, T., RITZENTHALER, J.D. and KOVAL, M., 2007. Regulation of heterotypic claudin compatibility. *Journal of Biological Chemistry,* **282**(41), pp. 30005-30013.

DAVIES, P.F., 1995. Flow-Mediated Endothelial Mechanotransduction. *Physiological Reviews,* **75**(3), pp. 519-560.

DAVIES, P.F., REMUZZI, A., GORDON, E.J., DEWEY, C.F. and GIMBRONE, M.A., 1986. Turbulent Fluid Shear-Stress Induces Vascular Endothelial-Cell Turnover Invitro. *Proceedings of the National Academy of Sciences of the United States of America,* **83**(7), pp. 2114-2117.

DAVIS, M.J., WU, X., NURKIEWICZ, T.R., KAWASAKI, J., DAVIS, G.E., HILL, M.A. and MEININGER, G.A., 2001. Integrins and mechanotransduction of the vascular myogenic response. *American Journal of Physiology-Heart and Circulatory Physiology,* **280**(4), pp. H1427-H1433.

DAVSON, H. and OLDENDORF, W.H., 1967. Transport in the central nervous system. *Proceedings of the Royal Society of Medicine*, **60**, pp. 326.

DE KEULENAER, G.W., ALEXANDER, R.W., USHIO-FUKAI, M., ISHIZAKA, N. and GRIENDLING, K.K., 1998. Tumour necrosis factor alpha activates a p22(phox)-based NADH oxidase in vascular smooth muscle. *Biochemical Journal*, **329**, pp. 653-657.

DEANE, R. and ZLOKOVIC, B.V., 2007. Role of the blood-brain barrier in the pathogenesis of Alzheimer's disease. *Current Alzheimer Research*, **4**(2), pp. 191-197.

DECLERCQ, W., DENECKER, G., FIERS, W. and VANDENABEELE, P., 1998. Cooperation of both TNF receptors in inducing apoptosis: Involvement of the TNF receptor-associated factor binding domain of the TNF receptor 75. *Journal of Immunology*, **161**(1), pp. 390-399.

DEHOUCK, M.P., MERESSE, S., DELORME, P., FRUCHART, J.C. and CECCHELLI, R., 1990. An Easier, Reproducible, and Mass-Production Method to Study the Blood-Brain-Barrier Invitro. *Journal of neurochemistry*, **54**(5), pp. 1798-1801.

DEHOUCK, M.P., VIGNE, P., TORPIER, G., BREITTMAYER, J.P., CECCHELLI, R. and FRELIN, C., 1997. Endothelin-1 as a mediator of endothelial cell-pericyte interactions in bovine brain capillaries. *Journal of Cerebral Blood Flow and Metabolism*, **17**(4), pp. 464-469.

DEJANA, E., CORADA, M. and LAMPUGNANI, M.G., 1995. Endothelial Cell-To-Cell Junctions. *Faseb Journal*, **9**(10), pp. 910-918.

DEJANA, E., LAMPUGNANI, M.G., MARTINEZ-ESTRADA, O. and BAZZONI, G., 2000. The molecular organization of endothelial junctions and their functional role in vascular morphogenesis and permeability. *International Journal of Developmental Biology*, **44**(6), pp. 743-748.

DEJANA, E., ORSENIGO, F. and LAMPUGNANI, M.G., 2008. The role of adherens junctions and VE-cadherin in the control of vascular permeability. *Journal of cell science*, **121**(13), pp. 2115-2122.

DEL MASCHIO, A., DE LUIGI, A., MARTIN-PADURA, I., BROCKHAUS, M., BARTFAI, T., FRUSCELLA, P., ADORINI, L., MARTINO, G.V., FURLAN, R., DE SIMONI, M.G. and DEJANA, E., 1999. Leukocyte recruitment in the cerebrospinal fluid of mice with experimental meningitis is inhibited by an antibody to junctional adhesion molecule (JAM). *Journal of Experimental Medicine*, **190**(9), pp. 1351-1356.

DEL ZOPPO, G.J., 2008. Virchow's triad: the vascular basis of cerebral injury. *Reviews in neurological diseases*, **5 Suppl 1**, pp. S12-21.

DELI, M.A., ABRAHAM, C.S., KATAOKA, Y. and NIWA, M., 2005. Permeability studies on in vitro blood-brain barrier models: Physiology, pathology, and pharmacology. *Cellular and molecular neurobiology*, **25**(1), pp. 59-127.

DELI, M.A., DESCAMPS, L., DEHOUCK, M.P., CECCHELLI, R., JOO, F., ABRAHAM, C. and TORPIER, G., 1995. Exposure of Tumor-Necrosis-Factor-Alpha to Luminal Membrane of Bovine Brain Capillary Endothelial-Cells Cocultured with Astrocytes Induces

a Delayed Increase of Permeability and Cytoplasmic Stress Fiber Formation of Actin. *Journal of neuroscience research,* **41**(6), pp. 717-726.

DELI, M.A. and JOO, F., 1996. Cultured vascular endothelial cells of the brain. *Keio Journal of Medicine,* **45**(3), pp. 183-199.

DEMAIO, L., CHANG, Y.S., GARDNER, T.W., TARBELL, J.M. and ANTONETTI, D.A., 2001. Shear stress regulates occludin content and phosphorylation. *American Journal of Physiology-Heart and Circulatory Physiology,* **281**(1), pp. H105-H113.

DEMEULE, M., REGINA, A., JODOIN, J., LAPLANTE, A., DAGENAIS, C., BERTHELET, F., MOGHRABI, A. and BELIVEAU, R., 2002. Drug transport to the brain: Key roles for the efflux pump P-glycoprotein in the blood-brain barrier. *Vascular Pharmacology,* **38**(6), pp. 339-348.

DENDORFER, U., OETTGEN, P. and LIBERMANN, T.A., 1994. Multiple Regulatory Elements in the Interleukin-6 Gene Mediate Induction by Prostaglandins, Cyclic-Amp, and Lipopolysaccharide. *Molecular and cellular biology,* **14**(7), pp. 4443-4454.

DESAI, S.Y., MARRONI, M., CUCULLO, L., KRIZANAC-BENGEZ, L., MAYBERG, M.R., HOSSAIN, M.T., GRANT, G.G. and JANIGRO, D., 2002. Mechanisms of endothelial survival under shear stress. *Endothelium-New York,* **9**(2), pp. 89-102.

DESAI, T.R., LEEPER, N.J., HYNES, K.L. and GEWERTZ, B.L., 2002. Interleukin-6 causes endothelial barrier dysfunction via the protein kinase C pathway. *Journal of Surgical Research,* **104**(2), pp. 118-123.

DEVRIES, H.E., BLOMROOSEMALEN, M.C.M., DEBOER, A.G., VANBERKEL, T.J.C., BREIMER, D.D. and KUIPER, J., 1996. Effect of endotoxin on permeability of bovine cerebral endothelial cell layers in vitro. *Journal of Pharmacology and Experimental Therapeutics,* **277**(3), pp. 1418-1423.

DEVRIES, H.E., BLOMROOSEMALEN, M.C.M., VANOOSTEN, M., DEBOER, A.G., VANBERKEL, T.J.C., BREIMER, D.D. and KUIPER, J., 1996. The influence of cytokines on the integrity of the blood-brain barrier in vitro. *Journal of neuroimmunology,* **64**(1), pp. 37-43.

DEVRIES, H.E., KUIPER, J., DEBOER, A.G., VANBERKEL, T.J.C. and BREIMER, D.D., 1997. The blood-brain barrier in neuroinflammatory diseases. *Pharmacological reviews,* **49**(2), pp. 143-155.

DEWEY, C.F., BUSSOLARI, S.R., GIMBRONE, M.A. and DAVIES, P.F., 1981. The Dynamic-Response of Vascular Endothelial-Cells to Fluid Shear-Stress. *Journal of Biomechanical Engineering-Transactions of the Asme,* **103**(3), pp. 177-185.

DIAZ-FLORES, L., GUTIERREZ, R., VARELA, H., RANCEL, N. and VALLADARES, F., 1991. Microvascular Pericytes - a Review of their Morphological and Functional-Characteristics. *Histology and histopathology,* **6**(2), pp. 269-286.

DICKSTEIN, D.L., BIRON, K.E., UJIIE, M., PFEIFER, C.G., JEFFRIES, A.R. and JEFFERIES, W.A., 2006. A beta peptide immunization restores blood-brain barrier integrity in Alzheimer disease. *Faseb Journal,* **20**(3), pp. 426-433.

DIMMELER, S., HAENDELER, J., RIPPMANN, V., NEHLS, M. and ZEIHER, A.M., 1996. Shear stress inhibits apoptosis of human endothelial cells. *FEBS letters,* **399**(1-2), pp. 71-74.

DIMMELER, S., HERMANN, C. and ZEIHER, A.M., 1998. Apoptosis of endothelial cells. Contribution to the pathophysiology of atherosclerosis? *European cytokine network,* **9**(4), pp. 697-698.

DITTMAN, W.A. and MAJERUS, P.W., 1990. Structure and Function of Thrombomodulin - a Natural Anticoagulant. *Blood,* **75**(2), pp. 329-336.

DONNAN, G.A., FISHER, M., MACLEOD, M. and DAVIS, S.M., 2008. Stroke. *Lancet,* **371**(9624), pp. 1612-1623.

DOPP, J.M., MACKENZIEGRAHAM, A., OTERO, G.C. and MERRILL, J.E., 1997. Differential expression, cytokine modulation, and specific functions of type-1 and type-2 tumor necrosis factor receptors in rat glia. *Journal of neuroimmunology,* **75**(1-2), pp. 104-112.

DORE-DUFFY, P., OWEN, C., BALABANOV, R., MURPHY, S., BEAUMONT, T. and RAFOLS, J.A., 2000. Pericyte migration from the vascular wall in response to traumatic brain injury. *Microvascular research,* **60**(1), pp. 55-69.

DU, Y., KHURI, F.R. and FU, H., 2008. A homogenous luminescent proximity assay for 14-3-3 interactions with both phosphorylated and nonphosphorylated client peptides. *Current chemical genomics,* **2**, pp. 40-7.

DUCHINI, A., GOVINDARAJAN, S., SANTUCCI, M., ZAMPI, G. and HOFMAN, F.M., 1996. Effects of tumor necrosis factor-alpha and interleukin-6 on fluid-phase permeability and ammonia diffusion in CNS-derived endothelial cells. *Journal of Investigative Medicine,* **44**(8), pp. 474-482.

EASTON, A.S. and ABBOTT, N.J., 2002. Bradykinin increases permeability by calcium and 5-lipoxygenase in the ECV304/C6 cell culture model of the blood-brain barrier. *Brain research,* **953**(1-2), pp. 157-169.

EBNET, K., SCHULZ, C.U., BRICKWEDDE, M.K.M.Z., PENDL, G.G. and VESTWEBER, D., 2000. Junctional adhesion molecule interacts with the PDZ domain-containing proteins AF-6 and ZO-1. *Journal of Biological Chemistry,* **275**(36), pp. 27979-27988.

EHRLICH, P., 1904. Ueber die beziehungen von chemischer constitution, verteilung und pharmakologischer wirkung. *Gesammelte Arbeiten zur Immunitaetsforschung,* , pp. 574.

EHRLICH, P., 1885. Das sauerstufbudurfnis des organismus. *Eine Farbenanalytische Studie,* .

EISSNER, G., KIRCHNER, S., LINDNER, H., KOLCH, W., JANOSCH, P., GRELL, M., SCHEURICH, P., ANDREESEN, R. and HOLLER, E., 2000. Reverse signaling through transmembrane TNF confers resistance to lipopolysaccharide in human monocytes and macrophages. *Journal of Immunology,* **164**(12), pp. 6193-6198.

EISSNER, G., KOLCH, W. and SCHEURICH, P., 2004. Ligands working as receptors: reverse signaling by members of the TNF superfamily enhance the plasticity of the immune system. *Cytokine & growth factor reviews*, **15**(5), pp. 353-366.

ELHAFNY, B., BOURRE, J.M. and ROUX, F., 1996. Synergistic stimulation of gamma-glutamyl transpeptidase and alkaline phosphatase activities by retinoic acid and astroglial factors in immortalized rat brain microvessel endothelial cells. *Journal of cellular physiology*, **167**(3), pp. 451-460.

ELHAFNY, B., CHAPPEY, O., PICIOTTI, M., DEBRAY, M., BOVAL, B. and ROUX, F., 1997. Modulation of P-glycoprotein activity by glial factors and retinoic acid in an immortalized rat brain microvessel endothelial cell line. *Neuroscience letters*, **236**(2), pp. 107-111.

ENDEMANN, D.H. and SCHIFFRIN, E.L., 2004. Endothelial dysfunction. *Journal of the American Society of Nephrology*, **15**(8), pp. 1983-1992.

ERTA, M., QUINTANA, A. and HIDALGO, J., 2012. Interleukin-6, a Major Cytokine in the Central Nervous System. *International Journal of Biological Sciences*, **8**(9), pp. 1254-1266.

ESSER, S., LAMPUGNANI, M.G., CORADA, M., DEJANA, E. and RISAU, W., 1998. Vascular endothelial growth factor induces VE-cadherin tyrosine phosphorylation in endothelial cells. *Journal of cell science*, **111**, pp. 1853-1865.

FABRY, Z., FITZSIMMONS, K.M., HERLEIN, J.A., MONINGER, T.O., DOBBS, M.B. and HART, M.N., 1993. Product Ion of the Cytokines Interleukin-1 and Interleukin-6 by Murine Brain Microvessel Endothelium and Smooth-Muscle Pericytes. *Journal of neuroimmunology*, **47**(1), pp. 23-34.

FALK, E., 1996. Plaque vulnerability and disruption. *Revista clinica espanola*, **196**, pp. 6-12.

FANGER, G.R., WIDMANN, C., PORTER, A.C., SATHER, S., JOHNSON, G.L. and VAILLANCOURT, R.R., 1998. 14-3-3 proteins interact with specific MEK kinases. *Journal of Biological Chemistry*, **273**(6), pp. 3476-3483.

FARKAS, E. and LUITEN, P.G.M., 2001. Cerebral microvascular pathology in aging and Alzheimer's disease. *Progress in neurobiology*, **64**(6), pp. 575-611.

FARSHORI, P. and KACHAR, B., 1999. Redistribution and phosphorylation of occludin during opening and resealing of tight junctions in cultured epithelial cells. *Journal of Membrane Biology*, **170**(2), pp. 147-156.

FASSBENDER, K., ROSSOL, S., KAMMER, T., DAFFERTSHOFER, M., WIRTH, S., DOLLMAN, M. and HENNERICI, M., 1994. Proinflammatory Cytokines in Serum of Patients with Acute Cerebral-Ischemia - Kinetics of Secretion and Relation to the Extent of Brain-Damage and Outcome of Disease. *Journal of the neurological sciences*, **122**(2), pp. 135-139.

FAUST, S., LEVIN, M., HARRISON, O., GOLDIN, R., LOCKHART, M., KONDAVEETI, S., LASZIK, Z., ESMON, C. and HEYDERMAN, R., 2001. Dysfunction

of endothelial protein C activation in severe meningococcal sepsis. *New England Journal of Medicine,* **345**(6), pp. 408-416.

FELDMAN, C.L., ILEGBUSI, O.J., HU, Z.J., NESTO, R., WAXMAN, S. and STONE, P.H., 2002. Determination of in vivo velocity and endothelial shear stress patterns with phasic flow in human coronary arteries: A methodology to predict progression of coronary atherosclerosis. *American Heart Journal,* **143**(6), pp. 931-939.

FENSTERMACHER, J.D., TAVAREKERE, N. and DAVIES, K.R., 2001. Overview of the Structure and Function of the Blood-Brain Barrier*in vivo*. *Blood-Brain Barrier*. New York: Springer US, pp. 1.

FENSTERMACHER, J., GROSS, P., SPOSITO, N., ACUFF, V., PETTERSEN, S. and GRUBER, K., 1988. Structural and functional variations in capillary systems within the brain. *Annals of the New York Academy of Sciences,* **529**, pp. 21-30.

FERRARESE, C., MASCARUCCI, P., ZOIA, C., CAVARRETTA, G., FRIGO, M., BEGNI, B., SARINELLA, F., FRATTOLA, L. and DE SIMONI, M.G., 1999. Increased cytokine release from peripheral blood cells after acute stroke. *Journal of Cerebral Blood Flow and Metabolism,* **19**(9), pp. 1004-1009.

FERRARIDILEO, G., DAVIS, E.B. and ANDERSON, D.R., 1996. Glaucoma, capillaries and pericytes .3. Peptide hormone binding and influence on pericytes. *Ophthalmologica,* **210**(5), pp. 269-275.

FERRERO, E., ZOCCHI, M.R., MAGNI, E., PANZERI, M.C., CURNIS, F., RUGARLI, C., FERRERO, M.E. and CORTI, A., 2001. Roles of tumor necrosis factor p55 and p75 receptors in TNF-alpha-induced vascular permeability. *American Journal of Physiology-Cell Physiology,* **281**(4), pp. C1173-C1179.

FIALA, M., LIU, Q.N., SAYRE, J., POP, V., BRAHMANDAM, V., GRAVES, M.C. and VINTERS, H.V., 2002. Cyclooxygenase-2-positive macrophages infiltrate the Alzheimer's disease brain and damage the blood-brain barrier. *European journal of clinical investigation,* **32**(5), pp. 360-371.

FISCHER, S., WIESNET, M., MARTI, H.H., RENZ, D. and SCHAPER, W., 2004. Simultaneous activation of several second messengers in hypoxia-induced hyperpermeability of brain derived endothelial cells. *Journal of cellular physiology,* **198**(3), pp. 359-369.

FISCHER, S., WOBBEN, M., MARTI, H.H., RENZ, D. and SCHAPER, W., 2002. Hypoxia-induced hyperpermeability in brain microvessel endothelial cells involves VEGF-mediated changes in the expression of zonula occludens-1. *Microvascular research,* **63**(1), pp. 70-80.

FISHMAN, A.P., 1982. Endothelium - a Distributed Organ of Diverse Capabilities. *Annals of the New York Academy of Sciences,* **401**(December), pp. 1-8.

FITZPATRICK, P.A., GUINAN, A.F., WALSH, T.G., MURPHY, R.P., KILLEEN, M.T., TOBIN, N.P., PIEROTTI, A.R. and CUMMINS, P.M., 2009. Down-regulation of neprilysin (EC3.4.24.11) expression in vascular endothelial cells by laminar shear stress involves NADPH oxidase-dependent ROS production. *International Journal of Biochemistry & Cell Biology,* **41**(11), pp. 2287-2294.

FLORIAN, J.A., KOSKY, J.R., AINSLIE, K., PANG, Z.Y., DULL, R.O. and TARBELL, J.M., 2003. Heparan sulfate proteoglycan is a mechanosensor on endothelial cells. *Circulation research,* **93**(10), pp. E136-E142.

FONTAINE, V., MOHAND-SAID, S., HANOTEAU, N., FUCHS, L., PFIZENMAIER, K. and EISEL, U., 2002. Neurodegenerative and neuroprotective effects of tumor necrosis factor (TNF) in retinal ischemia: Opposite roles of TNF receptor 1 and TNF receptor 2. *Journal of Neuroscience,* **22**(7), pp. RC216.

FOOTE, M. and ZHOU, Y., 2012. 14-3-3 Proteins in Neurological Disorders. *International journal of biochemistry and molecular biology,* **3**(2), pp. 152-64.

FRANCIS, K., VAN BEEK, J., CANOVA, C., NEAL, J.W. and GASQUE, P., 2003. Innate immunity and brain inflammation: The key role of complement. *Expert Reviews in Molecular Medicine,* **5**(03006252 Cited December 12, 2003), pp. 1-19.

FRANGOS, J.A., ESKIN, S.G., MCINTIRE, L.V. and IVES, C.L., 1985. Flow Effects on Prostacyclin Production by Cultured Human-Endothelial Cells. *Science,* **227**(4693), pp. 1477-1479.

FRANGOS, S.G., GAHTAN, V. and SUMPIO, B., 1999. Localization of atherosclerosis - Role of hemodynamics. *Archives of Surgery,* **134**(10), pp. 1142-1149.

FREED, E., SYMONS, M., MACDONALD, S.G., MCCORMICK, F. and RUGGIERI, R., 1994. Binding of 14-3-3-Proteins to the Protein-Kinase Raf and Effects on its Activation. *Science,* **265**(5179), pp. 1713-1716.

FREI, B., ENGLAND, L. and AMES, B.N., 1989. Ascorbate is an Outstanding Antioxidant in Human-Blood Plasma. *Proceedings of the National Academy of Sciences of the United States of America,* **86**(16), pp. 6377-6381.

FREI, K., SIEPL, C., GROSCURTH, P., BODMER, S., SCHWERDEL, C. and FONTANA, A., 1987. Antigen Presentation and Tumor-Cytotoxicity by Interferon-Gamma-Treated Microglial Cells. *European journal of immunology,* **17**(9), pp. 1271-1278.

FU, H.A., SUBRAMANIAN, R.R. and MASTERS, S.C., 2000. 14-3-3 proteins: Structure, function, and regulation. *Annual Review of Pharmacology and Toxicology,* **40**, pp. 617-647.

FUJIWARA, K., MASUDA, M., OSAWA, M., KANO, Y. and KATOH, K., 2001. A PECAM-1 a mechanoresponsive molecule? *Cell structure and function,* **26**(1), pp. 11-17.

FURCHGOTT, R.F. and ZAWADZKI, J.V., 1980. The Obligatory Role of Endothelial-Cells in the Relaxation of Arterial Smooth-Muscle by Acetylcholine. *Nature,* **288**(5789), pp. 373-376.

FURUKAWA, Y., IKUTA, N., OMATA, S., YAMAUCHI, T., ISOBE, T. and ICHIMURA, T., 1993. Demonstration of the Phosphorylation-Dependent Interaction of Tryptophan-Hydroxylase with the 14-3-3-Protein. *Biochemical and biophysical research communications,* **194**(1), pp. 144-149.

FURUSE, M., FUJITA, K., HIIRAGI, T., FUJIMOTO, K. and TSUKITA, S., 1998. Claudin-1 and -2: Novel integral membrane proteins localizing at tight junctions with no sequence similarity to occludin. *Journal of Cell Biology,* **141**(7), pp. 1539-1550.

FURUSE, M., HATA, M. and TSUKITA, S., 2001. Mice lacking claudin-1, a constituent of tight junction strands. *Molecular biology of the cell*, **12**, pp. 133A-134A.

FURUSE, M., HIRASE, T., ITOH, M., NAGAFUCHI, A., YONEMURA, S., TSUKITA, S. and TSUKITA, S., 1993. Occludin - a Novel Integral Membrane-Protein Localizing at Tight Junctions. *Journal of Cell Biology*, **123**(6), pp. 1777-1788.

FURUSE, M., SASAKI, H. and TSUKITA, S., 1999. Manner of interaction of heterogeneous claudin species within and between tight junction strands. *Journal of Cell Biology*, **147**(4), pp. 891-903.

GABATHULER, R., 2010. Approaches to transport therapeutic drugs across the blood-brain barrier to treat brain diseases. *Neurobiology of disease*, **37**(1), pp. 48-57.

GALBRAITH, C.G. and SHEETZ, M.P., 1998. Forces on adhesive contacts affect cell function. *Current opinion in cell biology*, **10**(5), pp. 566-571.

GALBRAITH, C.G., SKALAK, R. and CHIEN, S., 1998. Shear stress induces spatial reorganization of the endothelial cell cytoskeleton. *Cell motility and the cytoskeleton*, **40**(4), pp. 317-330.

GALBUSERA, M., ZOJA, C., DONADELLI, R., PARIS, S., MORIGI, M., BENIGNI, A., FIGLIUZZI, M., REMUZZI, G. and REMUZZI, A., 1997. Fluid shear stress modulates von Willebrand factor release from human vascular endothelium. *Blood*, **90**(4), pp. 1558-1564.

GALIANO, M., LIU, Z.Q., KALLA, R., BOHATSCHEK, M., KOPPIUS, A., GSCHWENDTNER, A., XU, S.L., WERNER, A., KLOSS, C.U.A., JONES, L.L., BLUETHMANN, H. and RAIVICH, G., 2001. Interleukin-6 (IL-6) and cellular response to facial nerve injury: effects on lymphocyte recruitment, early microglial activation and axonal outgrowth in IL6-deficient mice. *European Journal of Neuroscience*, **14**(2), pp. 327-341.

GAMBILLARA, V., CHAMBAZ, C., MONTORZI, G., ROY, S., STERGIOPULOS, N. and SILACCI, P., 2006. Plaque-prone hemodynamics impair endothelial function in pig carotid arteries. *American Journal of Physiology-Heart and Circulatory Physiology*, **290**(6), pp. H2320-H2328.

GARCIA, J.G.N., DAVIS, H.W. and PATTERSON, C.E., 1995. Regulation of Endothelial-Cell Gap Formation and Barrier Dysfunction - Role of Myosin Light-Chain Phosphorylation. *Journal of cellular physiology*, **163**(3), pp. 510-522.

GARCIA-CARDENA, G., COMANDER, J., ANDERSON, K.R., BLACKMAN, B.R. and GIMBRONE, M.A., 2001. Biomechanical activation of vascular endothelium as a determinant of its functional phenotype. *Proceedings of the National Academy of Sciences of the United States of America*, **98**(8), pp. 4478-4485.

GARCIA-GUZMAN, M., DOLFI, F., RUSSELLO, M. and VUORI, K., 1999. Cell adhesion regulates the interaction between the docking protein p130(Cas) and the 14-3-3 proteins. *Journal of Biological Chemistry*, **274**(9), pp. 5762-5768.

GARY, D.S., BRUCE-KELLER, A.J., KINDY, M.S. and MATTSON, M.P., 1998. Ischemic and excitotoxic brain injury is enhanced in mice lacking the p55 tumor necrosis factor receptor. *Journal of Cerebral Blood Flow and Metabolism*, **18**(12), pp. 1283-1287.

GERTZBERG, N., NEUMANN, P., RIZZO, V. and JOHNSON, A., 2004. NAD(P)H oxidase mediates the endothelial barrier dysfunction induced by TNF-alpha. *American Journal of Physiology-Lung Cellular and Molecular Physiology,* **286**(1), pp. L37-L48.

GIANNOGLOU, G.D., ANTONIADIS, A.P., KOSKINAS, K.C. and CHATZIZISIS, Y.S., 2010. Flow and atherosclerosis in coronary bifurcations. *Eurointervention,* **6**, pp. J16-J23.

GIMBRONE, M.A., 1995. Vascular endothelium in health and disease. *Molecular Cardiovascular Medicine.* Haber E edn. New York: Scientific American Medicine, pp. 67B.

GIMBRONE, M.A.,Jr., KUME, N. and CYBULSKY, M.I., 1993. Vascular endothelial dysfunction and the pathogenesis of atherosclerosis. *Atherosclerosis Reviews; Atherosclerosis: Cellular interactions, growth factors, and lipids,* **25**, pp. 1-9.

GIMBRONE, M., TOPPER, J., NAGEL, T., ANDERSON, K. and GARCIA-CARDENA, G., 2000. Endothelial dysfunction, hemodynamic forces, and atherogenesis. *Atherosclerosis V: the Fifth Saratoga Conference,* **902**, pp. 230-240.

GIULIAN, D., HAVERKAMP, L.J., LI, J., KARSHIN, W.L., YU, J., TOM, D., LI, X. and KIRKPATRICK, J.B., 1995. Senile Plaques Stimulate Microglia to Release a Neurotoxin found in Alzheimer Brain. *Neurochemistry international,* **27**(1), pp. 119-137.

GIULIAN, D., 1995. *Microglia and neuronal dysfunction.*

GIWA, M.O., WILLIAMS, J., ELDERFIELD, K., JIWA, N.S., BRIDGES, L.R., KALARIA, R.N., MARKUS, H.S., ESIRI, M.M. and HAINSWORTH, A.H., 2012. Neuropathologic evidence of endothelial changes in cerebral small vessel disease. *Neurology,* **78**(3), pp. 167-174.

GO, Y.M., BOO, Y.C., PARK, H., MALAND, M.C., PATEL, R., PRITCHARD, K.A., FUJIO, Y., WALSH, K., DARLEY-USMAR, V. and JO, H., 2001. Protein kinase B/Akt activates c-Jun NH2-terminal kinase by increasing NO production in response to shear stress. *Journal of applied physiology,* **91**(4), pp. 1574-1581.

GOLDMANN, E.E., 1913. Vitalfarbung am zentralnervensystem. *Abhandl Konigl preuss Akad Wiss,* **1**, pp. 1.

GONUL, E., DUZ, B., KAHRAMAN, S., KAYALI, H., KUBAR, A. and TIMURKAYNAK, E., 2002. Early pericyte response to brain hypoxia in cats: An ultrastructural study. *Microvascular research,* **64**(1), pp. 116-119.

GONZALEZ-MARISCAL, L., BETANZOS, A. and AVILA-FLORES, A., 2000. MAGUK proteins: structure and role in the tight junction. *Seminars in cell & developmental biology,* **11**(4), pp. 315-324.

GOODE, T.B., DAVIES, P.F., REIDY, M.A. and BOWYER, D.E., 1977. Aortic Endothelial Cell Morphology Observed Insitu by Scanning Electron-Microscopy during Atherogenesis in Rabbit. *Atherosclerosis,* **27**(2), pp. 235-251.

GOODMAN, Y. and MATTSON, M.P., 1996. Ceramide protects hippocampal neurons against excitotoxic and oxidative insults, and amyloid beta-peptide toxicity. *Journal of neurochemistry,* **66**(2), pp. 869-872.

GORELICK, P.B., SCUTERI, A., BLACK, S.E., DECARLI, C., GREENBERG, S.M., IADECOLA, C., LAUNER, L.J., LAURENT, S., LOPEZ, O.L., NYENHUIS, D., PETERSEN, R.C., SCHNEIDER, J.A., TZOURIO, C., ARNETT, D.K., BENNETT, D.A., CHUI, H.C., HIGASHIDA, R.T., LINDQUIST, R., NILSSON, P.M., ROMAN, G.C., SELLKE, F.W., SESHADRI, S., AMER HEART ASSOC STROKE COUNCIL, COUNCIL EPIDEMIOLOGY PREVENTION, COUNCIL CARDIOVASC NURSING, COUNCIL CARDIOVASC RADIOLOGY INTER and COUNCIL CARDIOVASC SURG ANESTHESIA, 2011. Vascular Contributions to Cognitive Impairment and Dementia A Statement for Healthcare Professionals From the American Heart Association/American Stroke Association. *Stroke,* **42**(9), pp. 2672-2713.

GOTTARDI, C.J., ARPIN, M., FANNING, A.S. and LOUVARD, D., 1996. The junction-associated protein, zonula occludens-1, localizes to the nucleus before the maturation and during the remodeling of cell-cell contacts. *Proceedings of the National Academy of Sciences of the United States of America,* **93**(20), pp. 10779-10784.

GRELL, M., DOUNI, E., WAJANT, H., LOHDEN, M., CLAUSS, M., MAXEINER, B., GEORGOPOULOS, S., LESSLAUER, W., KOLLIAS, G., PFIZENMAIER, K. and SCHEURICH, P., 1995. The Transmembrane Form of Tumor-Necrosis-Factor is the Prime Activating Ligand of the 80 Kda Tumor-Necrosis-Factor Receptor. *Cell,* **83**(5), pp. 793-802.

GRIEB, P., FORSTER, R.E., STROME, D., GOODWIN, C.W. and PAPE, P.C., 1985. O-2 Exchange between Blood and Brain-Tissues Studies with O-18(2) Indicator-Dilution Technique. *Journal of applied physiology,* **58**(6), pp. 1929-1941.

GRIENDLING, K.K. and HARRISON, D.G., 1999. Dual role of reactive oxygen species in vascular growth. *Circulation research,* **85**(6), pp. 562-563.

GRIENDLING, K.K., SORESCU, D., LASSEGUE, B. and USHIO-FUKAI, M., 2000. Modulation of protein kinase activity and gene expression by reactive oxygen species and their role in vascular physiology and pathophysiology. *Arteriosclerosis Thrombosis and Vascular Biology,* **20**(10), pp. 2175-2183.

GRIENDLING, K.K., SORESCU, D. and USHIO-FUKAI, M., 2000. NAD(P)H oxidase - Role in cardiovascular biology and disease. *Circulation research,* **86**(5), pp. 494-501.

GRILLI, M., CHENTRAN, A. and LENARDO, M.J., 1993. Tumor-Necrosis-Factor-Alpha Mediates a T-Cell Receptor-Independent Induction of the Gene Regulatory Factor Nf-Kappa-B in T-Lymphocytes. *Molecular immunology,* **30**(14), pp. 1287-1294.

GROTE, K., FLACH, I., LUCHTEFELD, M., AKIN, E., HOLLAND, S.M., DREXLER, H. and SCHIEFFER, B., 2003. Mechanical stretch enhances mRNA expression and proenzyme release of matrix metalloproteinase-2 (MMP-2) via NAD(P)H oxidase-derived reactive oxygen species. *Circulation research,* **92**(11), pp. E80-E86.

GRYGLEWSKI, R.J., 1995. Interactions between Endothelial Mediators. *Pharmacology & toxicology,* **77**(1), pp. 1-9.

GRYGLEWSKI, R.J., CHLOPICKI, S., SWIES, J. and NIEZABITOWSKI, P., 1995. Prostacyclin, Nitric-Oxide, and Atherosclerosis. *Atherosclerosis Iii: Recent Advances in Atherosclerosis Research: the Third Saratoga International Conference on Atherosclerosis in Nekoma,* **748**, pp. 194-207.

GRYGLEWSKI, R.J., PALMER, R.M.J. and MONCADA, S., 1986. Superoxide Anion is Involved in the Breakdown of Endothelium-Derived Vascular Relaxing Factor. *Nature,* **320**(6061), pp. 454-456.

GUAN, J.X., SUN, S.G., CAO, X.B., CHEN, Z.B. and TONG, E.T., 2004. Effect of thrombin on blood brain barrier permeability and its mechanism. *Chinese medical journal,* **117**(11), pp. 1677-1681.

GUDI, S., HUVAR, I., WHITE, C.R., MCKNIGHT, N.L., DUSSERRE, N., BOSS, G.R. and FRANGOS, J.A., 2003. Rapid activation of Ras by fluid flow is mediated by G alpha(q) and G beta gamma subunits of heterotrimeric G proteins in human endothelial cells. *Arteriosclerosis Thrombosis and Vascular Biology,* **23**(6), pp. 994-1000.

GUDI, S., NOLAN, J. and FRANGOS, J., 1998. Modulation of GTPase activity of G proteins by fluid shear stress and phospholipid composition. *Proceedings of the National Academy of Sciences of the United States of America,* **95**(5), pp. 2515-2519.

GUDI, S.R.P., CLARK, C.B. and FRANGOS, J.A., 1996. Fluid flow rapidly activates G proteins in human endothelial cells - Involvement of G proteins in mechanochemical signal transduction. *Circulation research,* **79**(4), pp. 834-839.

GUINAN, A.F., ROCHFORT, K.D., FITZPATRICK, P.A., WALSH, T.G., PIEROTTI, A.R., PHELAN, S., MURPHY, R.P. and CUMMINS, P.M., 2013. Shear stress is a positive regulator for thimet oligopeptidase (EC3.4.24.15) in vascular endothelial cells: consequences for MHC1 levels. *Cardiovascular Research,* **99**(3), pp. 545.

GUMBINER, B., LOWENKOPF, T. and APATIRA, D., 1991. Identification of a 160-Kda Polypeptide that Binds to the Tight Junction Protein-Zo-1. *Proceedings of the National Academy of Sciences of the United States of America,* **88**(8), pp. 3460-3464.

GURSOY-OZDEMIR, Y., QIU, J.H., MATSUOKA, N., BOLAY, H., BERMPOHL, D., JIN, H.W., WANG, X.Y., ROSENBERG, G.A., LO, E.H. and MOSKOWITZ, M.A., 2004. Cortical spreading depression activates and upregulates MMP-9. *Journal of Clinical Investigation,* **113**(10), pp. 1447-1455.

HAHN, C. and SCHWARTZ, M.A., 2009. Mechanotransduction in vascular physiology and atherogenesis. *Nature Reviews Molecular Cell Biology,* **10**(1), pp. 53-62.

HAIDEKKER, M.A., L'HEUREUX, N. and FRANGOS, J.A., 2000. Fluid shear stress increases membrane fluidity in endothelial cells: a study with DCVJ fluorescence. *American Journal of Physiology-Heart and Circulatory Physiology,* **278**(4), pp. H1401-H1406.

HALL, W.A., DOOLITTLE, N.D., DAMAN, M., BRUNS, P.K., MULDOON, L., FORTIN, D. and NEUWELT, E.A., 2006. Osmotic blood-brain barrier disruption chemotherapy for diffuse pontine gliomas. *Journal of neuro-oncology,* **77**(3), pp. 279-284.

HALL, W.A. and SHERR, G.T., 2006. Convection-enhanced delivery: targeted toxin treatment of malignant glioma. *Neurosurgical focus,* **20**(4), pp. E10-E10.

HALLENBECK, J.M., 2002. The many faces of tumor necrosis factor in stroke. *Nature medicine,* **8**(12), pp. 1363-1368.

HALLENBECK, J.M., 2002. The many faces of tumor necrosis factor in stroke. *Nature medicine,* **8**(12), pp. 1363-1368.

HANS, V.H.J., KOSSMANN, T., LENZLINGER, P.M., PROBSTMEIER, R., IMHOF, H.G., TRENTZ, O. and MORGANTI-KOSSMANN, M.C., 1999. Experimental axonal injury triggers interleukin-6 mRNA, protein synthesis and release into cerebrospinal fluid. *Journal of Cerebral Blood Flow and Metabolism,* **19**(2), pp. 184-194.

HANSSON, G., 2005. Mechanisms of disease - Inflammation, atherosclerosis, and coronary artery disease. *New England Journal of Medicine,* **352**(16), pp. 1685-1695.

HAORAH, J., HEILMAN, D., KNIPE, B., CHRASTIL, J., LEIBHART, J., GHORPADE, A., MILLER, D.W. and PERSIDSKY, Y., 2005. Ethanol-induced activation of myosin light chain kinase leads to dysfunction of tight junctions and blood-brain barrier compromise. *Alcoholism-Clinical and Experimental Research,* **29**(6), pp. 999-1009.

HAORAH, J., HEILMAN, D., KNIPE, B., CHRASTIL, J., LEIBHART, J., GHORPADE, A., MILLER, D.W. and PERSIDSKY, Y., 2005. Ethanol-induced activation of myosin light chain kinase leads to dysfunction of tight junctions and blood-brain barrier compromise. *Alcoholism-Clinical and Experimental Research,* **29**(6), pp. 999-1009.

HAORAH, J., KNIPE, B., LEIBHART, J., GHORPADE, A. and PERSIDSKY, Y., 2005. Alcohol-induced oxidative stress in brain endothelial cells causes blood-brain barrier dysfunction. *Journal of leukocyte biology,* **78**(6), pp. 1223-1232.

HAORAH, J., RAMIREZ, S.H., SCHALL, K., SMITH, D., PANDYA, R. and PERSIDSKY, Y., 2007. Oxidative stress activates protein tyrosine kinase and matrix metalloproteinases leading to blood-brain barrier dysfunction. *Journal of neurochemistry,* **101**(2), pp. 566-576.

HARASHIMA, S., HORIUCHI, T., HATTA, N., MORITA, C., HIGUCHI, M., SAWABE, T., TSUKAMOTO, H., TAHIRA, T., HAYASHI, K., FUJITA, S. and NIHO, Y., 2001. Outside-to-inside signal through the membrane TNF-alpha induces E-selectin (CD62E) expression on activated human CD4(+) T cells. *Journal of Immunology,* **166**(1), pp. 130-136.

HARDY, J. and SELKOE, D.J., 2002. Medicine - The amyloid hypothesis of Alzheimer's disease: Progress and problems on the road to therapeutics. *Science,* **297**(5580), pp. 353-356.

HARHAJ, N.S., FELINSKI, E.A., WOLPERT, E.B., SUNDSTROM, J.M., GARDNER, T.W. and ANTONETTI, D.A., 2006. VEGF activation of protein kinase C stimulates occludin phosphorylation and contributes to endothelial permeability. *Investigative ophthalmology & visual science,* **47**(11), pp. 5106-5115.

HARRISON, D., GRIENDLING, K.K., LANDMESSER, U., HORNIG, B. and DREXLER, H., 2003. Role of oxidative stress in atherosclerosis. *American Journal of Cardiology,* **91**(3), pp. 7A-11A.

HARRISON, D.G., 1997. Cellular and molecular mechanisms of endothelial cell dysfunction. *Journal of Clinical Investigation,* **100**(9), pp. 2153-2157.

HARRISON, D.G., WIDDER, J., GRUMBACH, I., CHEN, W., WEBER, M. and SEARLES, C., 2006. Endothelial mechanotransduction, nitric oxide and vascular inflammation. *Journal of internal medicine,* **259**(4), pp. 351-363.

HARTMANN, D. and THUM, T., 2011. MicroRNAs and vascular (dys)function. *Vascular Pharmacology,* **55**(4), pp. 92-105.

HASELOFF, R.F., BLASIG, I.E., BAUER, H.C. and BAUER, H., 2005. In search of the astrocytic factor(s) modulating blood-brain barrier functions in brain capillary endothelial cells in vitro. *Cellular and molecular neurobiology,* **25**(1), pp. 25-39.

HATASHITA, S. and HOFF, J.T., 1990. Brain Edema and Cerebrovascular Permeability during Cerebral-Ischemia in Rats. *Stroke,* **21**(4), pp. 582-588.

HAWKINS, B.T., ABBRUSCATO, T.J., EGLETON, R.D., BROWN, R.C., HUBER, J.D., CAMPOS, C.R. and DAVIS, T.P., 2004. Nicotine increases in vivo blood-brain barrier permeability and alters cerebral microvascular tight junction protein distribution. *Brain research,* **1027**(1-2), pp. 48-58.

HAWKINS, B.T. and DAVIS, T.P., 2005. The blood-brain barrier/neurovascular unit in health and disease. *Pharmacological reviews,* **57**(2), pp. 173-185.

HEALY, D.P. and WILK, S., 1993. Localization of Immunoreactive Glutamyl Aminopeptidase in Rat-Brain .2. Distribution and Correlation with Angiotensin-Ii. *Brain research,* **606**(2), pp. 295-303.

HEINRICH, P.C., BEHRMANN, I., HAAN, S., HERMANNS, H.M., MULLER-NEWEN, G. and SCHAPER, F., 2003. Principles of interleukin (IL)-6-type cytokine signalling and its regulation. *Biochemical Journal,* **374**, pp. 1-20.

HEISKALA, M., PETERSON, P.A. and YANG, Y., 2001. The roles of claudin superfamily proteins in paracellular transport. *Traffic (Copenhagen, Denmark),* **2**(2), pp. 93-8.

HELMKE, B.P. and DAVIES, P.F., 2002. The cytoskeleton under external fluid mechanical forces: Hemodynamic forces acting on the endothelium. *Annals of Biomedical Engineering,* **30**(3), pp. 284-296.

HELMKE, B.P., GOLDMAN, R.D. and DAVIES, P.F., 2000. Rapid displacement of vimentin intermediate filaments in living endothelial cells exposed to flow. *Circulation research,* **86**(7), pp. 745-752.

HELMKE, B.P., THAKKER, D.B., GOLDMAN, R.D. and DAVIES, P.F., 2001. Spatiotemporal analysis of flow-induced intermediate filament displacement in living endothelial cells. *Biophysical journal,* **80**(1), pp. 184-194.

HENDRICKSON, R., CAPPADONA, C., YANKAH, E., SITZMANN, J., CAHILL, P. and REDMOND, E., 1999. Sustained pulsatile flow regulates endothelial nitric oxide synthase and cyclooxygenase expression in co-cultured vascular endothelial and smooth muscle cells. *Journal of Molecular and Cellular Cardiology,* **31**(3), pp. 619-629.

HERMAN, S.T., 2002. Epilepsy after brain insult - Targeting epileptogenesis. *Neurology,* **59**(9), pp. S21-S26.

HERVE, F., GHINEA, N. and SCHERRMANN, J., 2008. CNS Delivery Via Adsorptive Transcytosis. *Aaps Journal,* **10**(3), pp. 455-472.

HIBI, M., MURAKAMI, M., SAITO, M., HIRANO, T., TAGA, T. and KISHIMOTO, T., 1990. Molecular-Cloning and Expression of an Il-6 Signal Transducer, Gp130. *Cell,* **63**(6), pp. 1149-1157.

HICKEY, W.F., 2001. Basic principles of immunological surveillance of the normal central nervous system. *Glia,* **36**(2), pp. 118-124.

HIRANO, T., AKIRA, S., TAGA, T. and KISHIMOTO, T., 1990. Biological and Clinical Aspects of Interleukin-6. *Immunology today,* **11**(12), pp. 443-449.

HIRANO, T., TAGA, T., NAKANO, N., YASUKAWA, K., KASHIWAMURA, S., SHIMIZU, K., NAKAJIMA, K., PYUN, K.H. and KISHIMOTO, T., 1985. Purification to Homogeneity and Characterization of Human B-Cell Differentiation Factor (Bcdf Or Bsfp-2). *Proceedings of the National Academy of Sciences of the United States of America,* **82**(16), pp. 5490-5494.

HIRAO, M., NAMPEI, A., SHI, K., YOSHIKAWA, H., NISHIMOTO, N. and HASHIMOTO, J., 2011. Diagnostic features of mild cellulitis phlegmon in patients with rheumatoid arthritis treated with tocilizumab: a report of two cases. *Modern Rheumatology,* **21**(6), pp. 673-677.

HIRASE, T., KAWASHIMA, S., WONG, E.Y.M., UEYAMA, T., RIKITAKE, Y., TSUKITA, S., YOKOYAMA, M. and STADDON, J.M., 2001. Regulation of tight junction permeability and occludin phosphorylation by RhoA-p160ROCK-dependent and -independent mechanisms. *Journal of Biological Chemistry,* **276**(13), pp. 10423-10431.

HIRASE, T., STADDON, J.M., SAITOU, M., ANDOAKATSUKA, Y., ITOH, M., FURUSE, M., FUJIMOTO, K., TSUKITA, S. and RUBIN, L.L., 1997. Occludin as a possible determinant of tight junction permeability in endothelial cells. *Journal of cell science,* **110**, pp. 1603-1613.

HIROTA, H., IZUMI, M., HAMAGUCHI, T., SUGIYAMA, S., MURAKAMI, E., KUNISADA, K., FUJIO, Y., OSHIMA, Y., NAKAOKA, Y. and YAMAUCHI-TAKIHARA, K., 2004. Circulating interleukin-6 family cytokines and their receptors in patients with congestive heart failure. *Heart and vessels,* **19**(5), pp. 237-241.

HOFFMAN, W.H., STAMATOVIC, S.M. and ANDJELKOVIC, A.V., 2009. Inflammatory mediators and blood brain barrier disruption in fatal brain edema of diabetic ketoacidosis. *Brain research,* **1254**, pp. 138-148.

HOFMAN, A., SCHULTE, W., TANJA, T.A., VANJUIJN, C.M., HAAXMA, R., LAMERIS, A.J., OTTEN, V.M. and SAAN, R.J., 1989. History of Dementia and Parkinsons-Disease in 1st-Degree Relatives of Patients with Alzheimers-Disease. *Neurology,* **39**(12), pp. 1589-1592.

HOFMANN, S., GRASBERGER, H., JUNG, P., BIDLINGMAIER, M., VLOTIDES, J., JANSSEN, O.E. and LANDGRAF, R., 2002. The tumour necrosis FACTOR-U induced vascular permeability is associated with a reduction of VE-cadherin expression. *European journal of medical research,* **7**(4), pp. 171-176.

HOHEISEL, D., NITZ, T., FRANKE, H., WEGENER, J., HAKVOORT, A., TILLING, T. and GALLA, H.J., 1998. Hydrocortisone reinforces the blood-brain barrier properties in a serum free cell culture system. *Biochemical and biophysical research communications,* **244**(1), pp. 312-316.

HOLASH, J.A., NODEN, D.M. and STEWART, P.A., 1993. Reevaluating the Role of Astrocytes in Blood-Brain-Barrier Induction. *Developmental Dynamics,* **197**(1), pp. 14-25.

HONDA, M., YAMAMOTO, S., CHENG, M., YASUKAWA, K., SUZUKI, H., SAITO, T., OSUGI, Y., TOKUNAGA, T. and KISHIMOTO, T., 1992. Human Soluble Il-6 Receptor - its Detection and Enhanced Release by Hiv-Infection. *Journal of Immunology,* **148**(7), pp. 2175-2180.

HONG, Y.M., 2010. Atherosclerotic cardiovascular disease beginning in childhood. *Korean circulation journal,* **40**(1), pp. 1-9.

HOWARTH, A.G., HUGHES, M.R. and STEVENSON, B.R., 1992. Detection of the Tight Junction-Associated Protein Zo-1 in Astrocytes and Other Nonepithelial Cell-Types. *American Journal of Physiology,* **262**(2), pp. C461-C469.

HSICH, G., KINNEY, K., GIBBS, C.J., LEE, K.H. and HARRINGTON, M.G., 1996. The 14-3-3 brain protein in cerebrospinal fluid as a marker for transmissible spongiform encephalopathies. *New England Journal of Medicine,* **335**(13), pp. 924-930.

HSU, H.L., SHU, H.B., PAN, M.G. and GOEDDEL, D.V., 1996. TRADD-TRAF2 and TRADD-FADD interactions define two distinct TNF receptor 1 signal transduction pathways. *Cell,* **84**(2), pp. 299-308.

HSU, H.L., SHU, H.B., PAN, M.G. and GOEDDEL, D.V., 1996. TRADD-TRAF2 and TRADD-FADD interactions define two distinct TNF receptor 1 signal transduction pathways. *Cell,* **84**(2), pp. 299-308.

HSU, H.L., XIONG, J. and GOEDDEL, D.V., 1995. The Tnf Receptor 1-Associated Protein Tradd Signals Cell-Death and Nf-Kappa-B Activation. *Cell,* **81**(4), pp. 495-504.

HUANG, J., UPADHYAY, U.A. and TAMARGO, R.J., 2006. Inflammation in stroke and focal cerebral ischemia. *Surgical neurology,* **66**(3), pp. 232-245.

HUANG, Y., POTTER, R., SIGURDSON, W., SANTACRUZ, A., SHIH, S., JU, Y., KASTEN, T., MORRIS, J.C., MINTUN, M., DUNTLEY, S. and BATEMAN, R.J., 2012. Effects of Age and Amyloid Deposition on A beta Dynamics in the Human Central Nervous System. *Archives of Neurology,* **69**(1), pp. 51-58.

HUBER, J.D., HAU, V.S., BORG, L., CAMPOS, C.R., EGLETON, R.D. and DAVIS, T.P., 2002. Blood-brain barrier tight junctions are altered during a 72-h exposure to lambda-carrageenan-induced inflammatory pain. *American Journal of Physiology-Heart and Circulatory Physiology,* **283**(4), pp. H1531-H1537.

HUBER, J.D., HAU, V.S., BORG, L., CAMPOS, C.R., EGLETON, R.D. and DAVIS, T.P., 2002. Blood-brain barrier tight junctions are altered during a 72-h exposure to lambda-carrageenan-induced inflammatory pain. *American Journal of Physiology-Heart and Circulatory Physiology,* **283**(4), pp. H1531-H1537.

HUBER, J.D., HAU, V.S., MARK, K.S., BROWN, R.C., CAMPOS, C.R. and DAVIS, T.P., 2002. Viability of microvascular endothelial cells to direct exposure of formalin, lambda-carrageenan, and complete Freund's adjuvant. *European journal of pharmacology,* **450**(3), pp. 297-304.

HUBER, J.D., WITT, K.A., HOM, S., EGLETON, R.D., MARK, K.S. and DAVIS, T.P., 2001. Inflammatory pain alters blood-brain barrier permeability and tight junctional protein expression. *American Journal of Physiology-Heart and Circulatory Physiology,* **280**(3), pp. H1241-H1248.

HUNT, B.J. and JURD, K.M., 1998. Endothelial cell activation - A central pathophysiological process. *British medical journal,* **316**(7141), pp. 1328-1329.

HUPPERT, J., CLOSHEN, D., CROXFORD, A., WHITE, R., KULIG, P., PIETROWSKI, E., BECHMANN, I., BECHER, B., LUHMANN, H.J., WAISMAN, A. and KUHLMANN, C.R.W., 2010. Cellular mechanisms of IL-17-induced blood-brain barrier disruption. *Faseb Journal,* **24**(4), pp. 1023-1034.

HURD, T.W., FAN, S.L., LIU, C.J., KWEON, H.K., HAKANSSON, K. and MARGOLIS, B., 2003. Phosphorylation-dependent binding of 14-3-3 to the polarity protein Par3 regulates cell polarity in mammalian epithelia. *Current Biology*, **13**(23), pp. 2082-2090.

HURST, R.D. and FRITZ, I.B., 1996. Properties of an immortalised vascular endothelial glioma cell co-culture model of the blood-brain barrier. *Journal of cellular physiology,* **167**(1), pp. 81-88.

HURTADO, O., CARDENAS, A., LIZASOAIN, I., BOSCA, L., LEZA, J.C., LORENZO, P. and MORO, M.A., 2001. Up-regulation of TNF-alpha convertase (TACE/ADAM17) after oxygen-glucose deprivation in rat forebrain slices. *Neuropharmacology,* **40**(8), pp. 1094-1102.

HURTADO, O., LIZASOAIN, I., FERNANDEZ-TOME, P., ALVAREZ-BARRIENTOS, A., LEZA, J.C., LORENZO, P. and MORO, M.A., 2002. TACE/ADAM17-TNF-alpha pathway in rat cortical cultures after exposure to oxygen-glucose deprivation or glutamate. *Journal of Cerebral Blood Flow and Metabolism,* **22**(5), pp. 576-585.

HWANG, J., ING, M.H., SALAZAR, A., LASSEGUE, B., GRIENDLING, K., NAVAB, M., SEVANIAN, A. and HSIAI, T.K., 2003. Pulsatile versus oscillatory shear stress regulates NADPH oxidase subunit expression - Implication for native LDL oxidation. *Circulation research,* **93**(12), pp. 1225-1232.

HWANG, J., SAHA, A., BOO, Y.C., SORESCU, G.P., MCNALLY, J.S., HOLLAND, S.M., DIKALOV, S., GIDDENS, D.P., GRIENDLING, K.K., HARRISON, D.G. and JO, H., 2003. Oscillatory shear stress stimulates endothelial production of O2- from p47(phox)-dependent NAD(P)H oxidases, leading to monocyte adhesion. *Journal of Biological Chemistry,* **278**(47), pp. 47291-47298.

HYNES, R.O., 1992. Integrins - Versatility, Modulation, and Signaling in Cell-Adhesion. *Cell,* **69**(1), pp. 11-25.

IADECOLA, C. and NEDERGAARD, M., 2007. Glial regulation of the cerebral microvasculature. *Nature neuroscience,* **10**(11), pp. 1369-1376.

ICHIMURA, T., ISOBE, T., OKUYAMA, T., TAKAHASHI, N., ARAKI, K., KUWANO, R. and TAKAHASHI, Y., 1988. Molecular-Cloning of Cdna Coding for Brain-Specific 14-3-3 Protein, a Protein Kinase-Dependent Activator of Tyrosine and Tryptophan Hydroxylases. *Proceedings of the National Academy of Sciences of the United States of America,* **85**(19), pp. 7084-7088.

IMBERTI, B., MORIGI, M., ZOJA, C., ANGIOLETTI, S., ABBATE, M., REMUZZI, A. and REMUZZI, G., 2000. Shear stress-induced cytoskeleton rearrangement mediates NF-kappa B-dependent endothelial expression of ICAM-1. *Microvascular research,* **60**(2), pp. 182-188.

INAI, T., KOBAYASHI, J. and SHIBATA, Y., 1999. Claudin-1 contributes to the epithelial barrier function in MDCK cells. *European journal of cell biology,* **78**(12), pp. 849-855.

INGBER, D.E., 1998. The architecture of life. *Scientific American,* **278**(1), pp. 48-57.

INOKO, A., ITOH, M., TAMURA, A., MATSUDA, M., FURUSE, M. and TSUKITA, S., 2003. Expression and distribution of ZO-3, a tight junction MAGUK protein, in mouse tissues. *Genes to Cells,* **8**(11), pp. 837-845.

INTA, I., WEBER, D., GRUNDT, C., VELTKAMP, R., WINTEROLL, S., AUFFARTH, G.U., BETTENDORF, M., LEMMER, B. and SCHWANINGER, M., 2009. Correlation of soluble gp130 serum concentrations with arterial blood pressure. *Journal of hypertension,* **27**(3), pp. 527-534.

INTEGAN, H.D. and SCHIFFRIN, E.L., 2000. Structure and mechanical properties of resistence arteries in hypertension. Role of adhesion molecules and extracellular matrix determinants. *Hypertension,* **36**, pp. 312.

ISERMANN, B., HENDRICKSON, S.B., ZOGG, M., WING, M., CUMMISKEY, M., KISANUKI, Y.Y., YANAGISAWA, M. and WEILER, H., 2001. Endothelium-specific loss of murine thrombomodulin disrupts the protein C anticoagulant pathway and causes juvenile-onset thrombosis. *Journal of Clinical Investigation,* **108**(4), pp. 537-546.

ISHIBAZAWA, A., NAGAOKA, T., TAKAHASHI, T., YAMAMOTO, K., KAMIYA, A., ANDO, J. and YOSHIDA, A., 2011. Effects of Shear Stress on the Gene Expressions of Endothelial Nitric Oxide Synthase, Endothelin-1, and Thrombomodulin in Human Retinal Microvascular Endothelial Cells. *Investigative ophthalmology & visual science,* **52**(11), pp. 8496-8504.

ISHIKAWA, M., STOKES, K.Y., ZHANG, J.H., NANDA, A. and GRANGER, D.N., 2004. Cerebral microvascular responses to hypercholesterolemia roles of NADPH oxidase and P-selectin. *Circulation research,* **94**(2), pp. 239-244.

ITOH, M., MORITA, K. and TSUKITA, S., 1999. Characterization of ZO-2 as a MAGUK family member associated with tight as well as adherens junctions with a binding affinity to occludin and alpha catenin. *Journal of Biological Chemistry,* **274**(9), pp. 5981-5986.

IVENS, S., KAUFER, D., FLORES, L.P., BECHMANN, I., ZUMSTEG, D., TOMKINS, O., SEIFFERT, E., HEINEMANN, U. and FRIEDMAN, A., 2007. TGF-beta receptor-mediated albumin uptake into astrocytes is involved in neocortical epileptogenesis. *Brain,* **130**, pp. 535-547.

IZAKI, T., KAMAKURA, S., KOHJIMA, M. and SUMIMOTO, H., 2005. Phosphorylation-dependent binding of 14-3-3 to Par3 beta, a human Par3-related cell polarity protein. *Biochemical and biophysical research communications,* **329**(1), pp. 211-218.

JACKSON, C., 2002. Matrix metalloproteinases and angiogenesis. *Current opinion in nephrology and hypertension,* **11**(3), pp. 295-299.

JAFFE, E.A., HOYER, L.W. and NACHMAN, R.L., 1973. Synthesis of Antihemophilic Factor Antigen by Cultured Human Endothelial Cells. *Journal of Clinical Investigation,* **52**(11), pp. 2757-2764.

JAFFE, E.A., NACHMAN, R.L., BECKER, C.G. and MINICK, C.R., 1973. Culture of Human Endothelial Cells Derived from Umbilical Veins - Identification by Morphologic and Immunological Criteria. *Journal of Clinical Investigation,* **52**(11), pp. 2745-2756.

JALALI, S., DEL POZO, M.A., CHEN, K.D., MIAO, H., LI, Y.S., SCHWARTZ, M.A., SHYY, J.Y.J. and CHIEN, S., 2001. Integrin-mediated mechanotransduction requires its dynamic interaction with specific extracellular matrix (ECM) ligands. *Proceedings of the National Academy of Sciences of the United States of America,* **98**(3), pp. 1042-1046.

JANEWAY, C. and MEDZHITOV, R., 2002. Innate immune recognition. *Annual Review of Immunology,* **20**, pp. 197-216.

JANZER, R.C. and RAFF, M.C., 1987. Astrocytes Induce Blood-Brain-Barrier Properties in Endothelial-Cells. *Nature,* **325**(6101), pp. 253-257.

JELINEK, D.F. and LIPSKY, P.E., 1987. Enhancement of Human B-Cell Proliferation and Differentiation by Tumor-Necrosis-Factor-Alpha and Interleukin-1. *Journal of Immunology,* **139**(9), pp. 2970-2976.

JESAITIS, L.A. and GOODENOUGH, D.A., 1994. Molecular Characterization and Tissue Distribution of Zo-2, a Tight Junction Protein Homologous to Zo-1 and the Drosophila Disks-Large Tumor-Suppressor Protein. *Journal of Cell Biology,* **124**(6), pp. 949-961.

JIANG, Y.P., WORONICZ, J.D., LIU, W. and GOEDDEL, D.V., 1999. Prevention of constitutive TNF receptor 1 signaling by silencer of death domains. *Science,* **283**(5401), pp. 543-546.

JIAO, H., WANG, Z., LIU, Y., WANG, P. and XUE, Y., 2011. Specific Role of Tight Junction Proteins Claudin-5, Occludin, and ZO-1 of the Blood-Brain Barrier in a Focal Cerebral Ischemic Insult. *Journal of Molecular Neuroscience,* **44**(2), pp. 130-139.

JIN, J., SMITH, F.D., STARK, C., WELLS, C.D., FAWCETT, J.P., KULKARNI, S., METALNIKOV, P., O'DONNELL, P., TAYLOR, P., TAYLOR, L., ZOUGMAN, A., WOODGETT, J.R., LANGEBERG, L.K., SCOTT, J.D. and PAWSON, T., 2004. Proteomic, functional, and domain-based analysis of in vivo 14-3-3 binding proteins involved in cytoskeletal regulation and cellular organization. *Current Biology,* **14**(16), pp. 1436-1450.

JIN, Z.G., UEBA, H., TANIMOTO, T., LUNGU, A.O., FRAME, M.D. and BERK, B.C., 2003. Ligand-independent activation of vascular endothelial growth factor receptor 2 by fluid shear stress regulates activation of endothelial nitric oxide synthase. *Circulation research,* **93**(4), pp. 354-363.

JONES, D.H., LEY, S. and AITKEN, A., 1995. Isoforms of 14-3-3-Protein can Form Homodimers and Heterodimers In-Vivo and In-Vitro - Implications for Function as Adapter Proteins. *FEBS letters,* **368**(1), pp. 55-58.

JONES, D., LEY, S. and AITKEN, A., 1995. Isoforms of 14-3-3-Protein can Form Homodimers and Heterodimers In-Vivo and In-Vitro - Implications for Function as Adapter Proteins. *FEBS letters,* **368**(1), pp. 55-58.

JONES, S.A., SCHELLER, J. and ROSE-JOHN, S., 2011. Therapeutic strategies for the clinical blockade of IL-6/gp130 signaling. *Journal of Clinical Investigation,* **121**(9), pp. 3375-3383.

JOO, F. and KARNUSHI, I., 1973. Procedure for Isolation of Capillaries from Rat-Brain. *Cytobios,* **8**(29-3), pp. 41-48.

KACEM, K., LACOMBE, P., SEYLAZ, J. and BONVENTO, G., 1998. Structural organization of the perivascular astrocyte endfeet and their relationship with the endothelial glucose transporter: A confocal microscopy study. *Glia,* **23**(1), pp. 1-10.

KAHALEH, M.B., OSBORN, I. and LEROY, E.C., 1981. Increased Factor-Viii-Vonwillebrand Factor Antigen and Vonwillebrand-Factor Activity in Scleroderma and in Raynaud Phenomenon. *Annals of Internal Medicine,* **94**(4), pp. 482-484.

KAISER, D., FREYBERG, M.A. and FRIEDL, P., 1997. Lack of hemodynamic forces triggers apoptosis in vascular endothelial cells. *Biochemical and biophysical research communications,* **231**(3), pp. 586-590.

KALARIA, R.N., 1992. The Blood-Brain-Barrier and Cerebral Microcirculation in Alzheimer-Disease. *Cerebrovascular and brain metabolism reviews,* **4**(3), pp. 226-260.

KANO, Y., KATOH, K. and FUJIWARA, K., 2000. Lateral zone of cell-cell adhesion as the major fluid shear stress-related signal transduction site. *Circulation research,* **86**(4), pp. 425-433.

KAWAI, Y., MATSUMOTO, Y., IKEDA, Y. and WATANABE, K., 1997. [Regulation of antithrombogenicity in endothelium by hemodynamic forces]. *Rinsho byori.The Japanese journal of clinical pathology,* **45**(4), pp. 315-20.

KIM, D.W., GOTLIEB, A.I. and LANGILLE, B.L., 1989. Invivo Modulation of Endothelial-F-Actin Microfilaments by Experimental Alterations in Shear-Stress. *Arteriosclerosis,* **9**(4), pp. 439-445.

KIM, D.W., LANGILLE, B.L., WONG, M.K.K. and GOTLIEB, A.I., 1989. Patterns of Endothelial Microfilament Distribution in the Rabbit Aorta Insitu. *Circulation research,* **64**(1), pp. 21-31.

KIM, J.A., CHO, K., SHIN, M.S., LEE, W.G., JUNG, N., CHUNG, C. and CHANG, J.K., 2008. A novel electroporation method using a capillary and wire-type electrode. *Biosensors & bioelectronics,* **23**(9), pp. 1353-1360.

KIM, K.S., WASS, C.A., CROSS, A.S. and OPAL, S.M., 1992. Modulation of Blood-Brain-Barrier Permeability by Tumor-Necrosis-Factor and Antibody to Tumor-Necrosis-Factor in the Rat. *Lymphokine and cytokine research,* **11**(6), pp. 293-298.

KIM, K.S., WASS, C.A., CROSS, A.S. and OPAL, S.M., 1992. Modulation of Blood-Brain-Barrier Permeability by Tumor-Necrosis-Factor and Antibody to Tumor-Necrosis-Factor in the Rat. *Lymphokine and cytokine research,* **11**(6), pp. 293-298.

KIM, S.Y., BUCKWALTER, M., SOREQ, H., VEZZANI, A. and KAUFER, D., 2012. Blood-brain barrier dysfunction-induced inflammatory signaling in brain pathology and epileptogenesis. *Epilepsia,* **53**, pp. 37-44.

KIMELBERG, H.K., 2004. Water homeostasis in the brain: Basic concepts. *Neuroscience,* **129**(4), pp. 851-860.

KIRK, J., PLUMB, J., MIRAKHUR, M. and MCQUAID, S., 2003. Tight junctional abnormality in multiple sclerosis white matter affects all calibres of vessel and is associated with blood-brain barrier leakage and active demyelination. *Journal of Pathology,* **201**(2), pp. 319-327.

KIS, B., ABRAHAM, C.S., DELI, M.A., KOBAYASHI, H., NIWA, M., YAMASHITA, H., BUSIJA, D.W. and UETA, Y., 2003. Adrenomedullin, an autocrine mediator of blood-brain barrier function. *Hypertension Research,* **26**, pp. S61-S70.

KISHIMOTO, T., 2005. Interleukin-6: From basic science to medicine - 40 years in immunology. *Annual Review of Immunology,* **23**, pp. 1-21.

KISHIMOTO, T., AKIRA, S., NARAZAKI, M. and TAGA, T., 1995. Interleukin-6 Family of Cytokines and Gp130. *Blood,* **86**(4), pp. 1243-1254.

KISHIMOTO, T., AKIRA, S. and TAGA, T., 1992. Interleukin-6 and its Receptor - a Paradigm for Cytokines. *Science,* **258**(5082), pp. 593-597.

KLEGERIS, A. and MCGEER, P.L., 1997. Beta-Amyloid Protein Enhances Macrophage Production of Oxygen Free Radicals and Glutamate. *Journal of neuroscience research,* **49**(2), pp. 229-235.

KLEGERIS, A., WALKER, D.G. and MCGEER, P.L., 1997. Interaction of Alzheimer beta-amyloid peptide with the human monocytic cell line THP-1 results in a protein kinase C-dependent secretion of tumor necrosis factor-alpha. *Brain research,* **747**(1), pp. 114-121.

KLEIN, M.A., MOLLER, J.C., JONES, L.L., BLUETHMANN, H., KREUTZBERG, G.W. and RAIVICH, G., 1997. Impaired neuroglial activation in interleukin-6 deficient mice. *Glia,* **19**(3), pp. 227-233.

KLINGLER, C., KNIESEL, U., BAMFORTH, S.D., WOLBURG, H., ENGELHARDT, B. and RISAU, W., 2000. Disruption of epithelial tight junctions is prevented by cyclic nucleotide-dependent protein kinase inhibitors. *Histochemistry and cell biology,* **113**(5), pp. 349-361.

KLYACHKO, N.L., MANICKAM, D.S., BRYNSKIKH, A.M., UGLANOVA, S.V., LI, S., HIGGINBOTHAM, S.M., BRONICH, T.K., BATRAKOVA, E.V. and KABANOV, A.V., 2012. Cross-linked antioxidant nanozymes for improved delivery to CNS. *Nanomedicine-Nanotechnology Biology and Medicine,* **8**(1), pp. 119-129.

KNIESEL, U., RISAU, W. and WOLBURG, H., 1996. Development of blood-brain barrier tight junctions in the rat cortex. *Developmental Brain Research,* **96**(1-2), pp. 229-240.

KNIESEL, U. and WOLBURG, H., 2000. Tight junctions of the blood-brain barrier. *Cellular and molecular neurobiology,* **20**(1), pp. 57-76.

KNUDSEN, H.L. and FRANGOS, J.A., 1997. Role of cytoskeleton in shear stress-induced endothelial nitric oxide production. *American Journal of Physiology-Heart and Circulatory Physiology,* **273**(1), pp. H347-H355.

KNUDSEN, K.A., SOLER, A.P., JOHNSON, K.R. and WHEELOCK, M.J., 1995. Interaction of Alpha-Actinin with the Cadherin/catenin Cell-Cell Adhesion Complex Via Alpha-Catenin. *Journal of Cell Biology,* **130**(1), pp. 67-77.

KOBAYASHI, H., MAGNONI, M.S., GOVONI, S., IZUMI, F., WADA, A. and TRABUCCHI, M., 1985. Neuronal Control of Brain Microvessel Function. *Experientia,* **41**(4), pp. 427-434.

KOBAYASHI, K., TSUBOSAKA, Y., HORI, M., NARUMIYA, S., OZAKI, H. and MURATA, T., 2013. Prostaglandin D-2-DP Signaling Promotes Endothelial Barrier Function via the cAMP/PKA/Tiam1/Rac1 Pathway. *Arteriosclerosis Thrombosis and Vascular Biology,* **33**(3), pp. 565-+.

KOBILER, D., SHLOMO, L. and SHLOMO, S., 2012. *Blood-Brain Barrier: Drug Delivery and Brain Pathology.* 2001 edn. New York: Springer.

KOCHANEK, K.D., XU, J., MURPHY, S.L. and MININO, A.M., 2011. Deaths: Final Data for 2009. *National Vital Statistics Report,* **60**(3), pp. 1.

KOGO, J., TAKEBA, Y., KUMAI, T., KITAOKA, Y., MATSUMOTO, N., UENO, S. and KOBAYASHI, S., 2006. Involvement of TNF-alpha in glutamate-induced apoptosis in a differentiated neuronal cell line. *Brain research,* **1122**, pp. 201-208.

KOLA, I. and LANDIS, J., 2004. Can the pharmaceutical industry reduce attrition rates? *Nature Reviews Drug Discovery,* **3**(8), pp. 711-715.

KOMAROVA, Y. and MALIK, A.B., 2010. Regulation of Endothelial Permeability via Paracellular and Transcellular Transport Pathways. *Annual Review of Physiology,* **72**, pp. 463-493.

KORENAGA, R., ANDO, J., TSUBOI, H., YANG, W.D., SAKUMA, I., TOYOOKA, T. and KAMIYA, A., 1994. Laminar-Flow Stimulates Atp- and Shear Stress-Dependent Nitric-Oxide Production in Cultured Bovine Endothelial-Cells. *Biochemical and biophysical research communications,* **198**(1), pp. 213-219.

KOTO, T., TAKUBO, K., ISHIDA, S., SHINODA, H., INOUE, M., TSUBOTA, K., OKADA, Y. and IKEDA, E., 2007. Hypoxia disrupts the barrier function of neural blood vessels through changes in the expression of claudin-5 in endothelial cells. *American Journal of Pathology,* **170**(4), pp. 1389-1397.

KOWALSKY, G.B., BYFIELD, F.J. and LEVITAN, I., 2008. oxLDL facilitates flow-induced realignment of aortic endothelial cells. *American Journal of Physiology-Cell Physiology,* **295**(2), pp. C332-C340.

KRAMER, S.D., ABBOTT, N.J. and BEGLEY, D.J., 2001. Biological models to study blood-brain barrier permeation. In: H. VAN DE WATERBEEMD, G. FOLKERS and R. GUY, eds, *Pharmacokinetic Strategies.* Weinham: Wiley-VCH, pp. 127.

KRIZANAC-BENGEZ, L., KAPURAL, M., PARKINSON, F., CUCULLO, L., HOSSAIN, M., MAYBERG, M.R. and JANIGRO, D., 2003. Effects of transient loss of shear stress on blood-brain barrier endothelium: role of nitric oxide and IL-6. *Brain research,* **977**(2), pp. 239-246.

KRIZANAC-BENGEZ, L., MAYBERG, M.R., CUNNINGHAM, E., HOSSAIN, M., PONNAMPALAM, S., PARKINSON, F.E. and JANIGRO, D., 2006. Loss of shear stress induces leukocyte-mediated cytokine release and blood-brain barrier failure in dynamic in vitro blood-brain barrier model. *Journal of cellular physiology,* **206**(1), pp. 68-77.

KRIZANAC-BENGEZ, L., MAYBERG, M.R. and JANIGRO, D., 2004. The cerebral vasculature as a therapeutic target for neurological disorders and the role of shear stress in vascular homeostatis and pathophysiology. *Neurological research,* **26**(8), pp. 846-853.

KRIZANAC-BENGEZ, L., HOSSAIN, M., FAZIO, V., MAYBERG, M. and JANIGRO, D., 2006. Loss of flow induces leukocyte-mediated MMP/TIMP imbalance in dynamic in vitro blood-brain barrier model: role of pro-inflammatory cytokines. *American Journal of Physiology-Cell Physiology,* **291**(4), pp. C740-C749.

KRUM, J.M., KENYON, K.L. and ROSENSTEIN, J.M., 1997. Expression of blood-brain barrier characteristics following neuronal loss and astroglial damage after administration of anti-Thy-1 immunotoxin. *Experimental neurology,* **146**(1), pp. 33-45.

KUBOTA, K., FURUSE, M., SASAKI, H., SONODA, N., FUJITA, K., NAGAFUCHI, A. and TSUKITA, S., 1999. Ca2+-independent cell-adhesion activity of claudins, a family of integral membrane proteins localized at tight junctions. *Current Biology,* **9**(18), pp. 1035-1038.

KUMAR, S., SELIM, M.H. and CAPLAN, L.R., 2010. Medical complications after stroke. *Lancet Neurology,* **9**(1), pp. 105-118.

KUNSCH, C. and MEDFORD, R.M., 1999. Oxidative stress as a regulator of gene expression in the vasculature. *Circulation research,* **85**(8), pp. 753-766.

KURIHARA, H., ANDERSON, J.M. and FARQUHAR, M.G., 1995. Increased Tyr Phosphorylation of Zo-1 during Modification of Tight Junctions between Glomerular Foot Processes. *American Journal of Physiology-Renal Fluid and Electrolyte Physiology,* **268**(3), pp. F514-F524.

KURZCHALIA, T.V. and PARTON, R.G., 1999. Membrane microdomains and caveolae. *Current opinion in cell biology,* **11**(4), pp. 424-431.

LAEMMLI, U.K., 1970. Cleavage of Structural Proteins during Assembly of Head of Bacteriophage-T4. *Nature,* **227**(5259), pp. 680-&.

LAM, C.F., PETERSON, T.E., RICHARDSON, D.M., CROATT, A.J., D'USCIO, L.V., NATH, K.A. and KATUSIC, Z.S., 2006. Increased blood flow causes coordinated upregulation of arterial eNOS and biosynthesis of tetrahydrobiopterin. *American Journal of Physiology-Heart and Circulatory Physiology,* **290**(2), pp. H786-H793.

LAMPUGNANI, M.G., CORADA, M., ANDRIOPOULOU, P., ESSER, S., RISAU, W. and DEJANA, E., 1997. Cell confluence regulates tyrosine phosphorylation of adherens junction components in endothelial cells. *Journal of cell science,* **110**, pp. 2065-2077.

LAMPUGNANI, M.G., CORADA, M., CAVEDA, L., BREVIARIO, F., AYALON, O., GEIGER, B. and DEJANA, E., 1995. The Molecular-Organization of Endothelial-Cell to Cell-Junctions - Differential Association of Plakoglobin, Beta-Catenin, and Alpha-Catenin with Vascular Endothelial Cadherin (Ve-Cadherin). *Journal of Cell Biology,* **129**(1), pp. 203-217.

LAMPUGNANI, M.G., 2010. Endothelial adherens junctions and the actin cytoskeleton: an 'infinity net'? *Journal of biology,* **9**(3), pp. 16-16.

LAMPUGNANI, M.G. and DEJANA, E., 2007. Adherens junctions in endothelial cells regulate vessel maintenance and angiogenesis. *Thrombosis research,* **120**, pp. S1-S6.

LAMPUGNANI, M. and DEJANA, E., 1997. Interendothelial junctions: structure, signalling and functional roles. *Current opinion in cell biology,* **9**(5), pp. 674-682.

LANDMESSER, U., MERTEN, R., SPIEKERMANN, S., BUTTNER, K., DREXLER, H. and HORNIG, B., 2000. Vascular extracellular superoxide dismutase activity in patients with coronary artery disease - Relation to endothelium-dependent vasodilation. *Circulation,* **101**(19), pp. 2264-2270.

LANG, H., JACOBSEN, H., IKEMIZU, S., ANDERSSON, C., HARLOS, K., MADSEN, L., HJORTH, P., SONDERGAARD, L., SVEJGAARD, A., WUCHERPFENNIG, K., STUART, D., BELL, J., JONES, E. and FUGGER, L., 2002. A functional and structural basis for TCR cross-reactivity in multiple sclerosis. *Nature immunology,* **3**(10), pp. 940-943.

LANGILLE, B.L., BENDECK, M.P. and KEELEY, F.W., 1989. Adaptations of Carotid Arteries of Young and Mature Rabbits to Reduced Carotid Blood-Flow. *American Journal of Physiology,* **256**(4), pp. H931-H939.

LANGILLE, B.L. and O' DONNELL, F., 1986. Reductions in Arterial Diameter Produced by Chronic Decreases in Blood-Flow are Endothelium-Dependent. *Science,* **231**(4736), pp. 405-407.

LAYFIELD, R., FERGUSSON, J., AITKEN, A., LOWE, J., LANDON, M. and MAYER, R.J., 1996. Neurofibrillary tangles of Alzheimer's disease brains contain 14-3-3 proteins. *Neuroscience letters,* **209**(1), pp. 57-60.

LEE, E.J., HUNG, Y.C. and LEE, M.Y., 1999. Early alterations in cerebral hemodynamics, brain metabolism, and blood-brain barrier permeability in experimental intracerebral hemorrhage. *Journal of neurosurgery,* **91**(6), pp. 1013-1019.

LEE, H.S., NAMKOONG, K., KIM, D.H., KIM, K.J., CHEONG, Y.H., KIM, S.S., LEE, W.B. and KIM, K.Y., 2004. Hydrogen peroxide-induced alterations of tight junction proteins in bovine brain microvascular endothelial cells. *Microvascular research,* **68**(3), pp. 231-238.

LEE, J., ZENG, Q., OZAKI, H., WANG, L., HAND, A.R., HLA, T., WANG, E. and LEE, M., 2006. Dual roles of tight junction-associated protein, Zonula Occludens-1, in

sphingosine 1-phosphate-mediated endothelial chemotaxis and barrier integrity. *Journal of Biological Chemistry,* **281**(39), pp. 29190-29200.

LEE, Y.W., HENNIG, B., FIALA, M., KIM, K.S. and TOBOREK, M., 2001. Cocaine activates redox-regulated transcription factors and induces TNF-alpha expression in human brain endothelial cells. *Brain research,* **920**(1-2), pp. 125-133.

LEE, Y.W., HENNIG, B., YAO, J. and TOBOREK, M., 2001. Methamphetamine induces AP-1 and NF-kappa B binding and transactivation in human brain endothelial cells. *Journal of neuroscience research,* **66**(4), pp. 583-591.

LEE, Y.W., LEE, W.H. and KIM, P.H., 2010. Oxidative mechanisms of IL-4-induced IL-6 expression in vascular endothelium. *Cytokine,* **49**(1), pp. 73-79.

LEHOUX, S., CASTIER, Y. and TEDGUI, A., 2006. Molecular mechanisms of the vascular responses to haemodynamic forces. *Journal of internal medicine,* **259**(4), pp. 381-392.

LEHOUX, S., LEMARIE, C.A., ESPOSITO, B., LIJNEN, H.R. and TEDGUI, A., 2004. Pressure-induced matrix metalloproteinase-9 contributes to early hypertensive remodeling. *Circulation,* **109**(8), pp. 1041-1047.

LELKES, P.I., 1999. *Mechanical Forces and the Endothelium.* VI edn. Informa Healthcare.

LENTZ, S.R., TSIANG, M. and SADLER, J.E., 1991. Regulation of Thrombomodulin by Tumor-Necrosis-Factor-Alpha - Comparison of Transcriptional and Posttranscriptional Mechanisms. *Blood,* **77**(3), pp. 542-550.

LENZLINGER, P.M., MARX, A., TRENTZ, O., KOSSMANN, T. and MORGANTI-KOSSMANN, M.C., 2002. Prolonged intrathecal release of soluble Fas following severe traumatic brain injury in humans. *Journal of neuroimmunology,* **122**(1-2), pp. 167-174.

LEON, L.R., 2002. Molecular biology of thermoregulation - Invited review: Cytokine regulation of fever: studies using gene knockout mice. *Journal of applied physiology,* **92**(6), pp. 2648-2655.

LEOPOLD, J.A. and LOSCALZO, J., 2005. Oxidative enzymopathies and vascular disease. *Arteriosclerosis Thrombosis and Vascular Biology,* **25**(7), pp. 1332-1340.

LEUNG, D.Y.M., GLAGOV, S. and MATHEWS, M.B., 1977. New Invitro System for Studying Cell Response to Mechanical Stimulation - Different Effects of Cyclic Stretching and Agitation on Smooth-Muscle Cell Biosynthesis. *Experimental cell research,* **109**(2), pp. 285-298.

LEVESQUE, M.J., NEREM, R.M. and SPRAGUE, E.A., 1990. Vascular Endothelial-Cell Proliferation in Culture and the Influence of Flow. *Biomaterials,* **11**(9), pp. 702-707.

LEVIN, E.G. and SANTELL, L., 1987. Association of a Plasminogen-Activator Inhibitor (Pai-1) with the Growth Substratum and Membrane of Human-Endothelial Cells. *Journal of Cell Biology,* **105**(6), pp. 2543-2549.

LEVIN, E., 1996. Endothelins as cardiovascular peptides. *American Journal of Nephrology,* **16**(3), pp. 246-251.

LEWANDOWSKY, M., 1900. Zur lehre von der cerebrospinalflussigkeit. *Zeitschrift fur Klinische Psychologie Psychiatrie Und Psychotherapie,* **40**, pp. 480.

LI, J.Y., BOADO, R.J. and PARDRIDGE, W.M., 2001. Blood-brain barrier genomics. *Journal of Cerebral Blood Flow and Metabolism,* **21**(1), pp. 61-68.

LIBBY, P., 2002. Inflammation in atherosclerosis. *Nature,* **420**(6917), pp. 868-874.

LIBBY, P. and GALIS, Z.S., 1995. Cytokines Regulate Genes Involved in Atherogenesis. *Atherosclerosis Iii: Recent Advances in Atherosclerosis Research: the Third Saratoga International Conference on Atherosclerosis in Nekoma,* **748**, pp. 158-170.

LIBBY, P., SUKHOVA, G., LEE, R.T. and LIAO, J.K., 1997. Molecular biology of atherosclerosis. *International journal of cardiology,* **62**, pp. S23-S29.

LIBBY, P., RIDKER, P.M. and HANSSON, G.K., 2011. Progress and challenges in translating the biology of atherosclerosis. *Nature,* **473**(7347), pp. 317-325.

LIEBERMAN, A.P., PITHA, P.M., SHIN, H.S. and SHIN, M.L., 1989. Production of Tumor Necrosis Factor and Other Cytokines by Astrocytes Stimulated with Lipopolysaccharide Or a Neurotropic Virus. *Proceedings of the National Academy of Sciences of the United States of America,* **86**(16), pp. 6348-6352.

LIEBERT, M., WAHL, R.L., LAWLESS, G., MCKEEVER, P.E., TAREN, J.A., BEIERWALTES, W.H. and BRASSWELL, R., 1990. Direct Stereotactic Intracerebral Injection of Monoclonal Antibodies and their Fragments a Potential Approach to Brain Tumor Immunotherapy. *American Journal of Physiologic Imaging,* **5**(2), pp. 55-59.

LIEBNER, S., FISCHMANN, A., RASCHER, G., DUFFNER, F., GROTE, E.H., KALBACHER, H. and WOLBURG, H., 2000. Claudin-1 and claudin-5 expression and tight junction morphology are altered in blood vessels of human glioblastoma multiforme. *Acta Neuropathologica,* **100**(3), pp. 323-331.

LIEBNER, S., KNIESEL, U., KALBACHER, H. and WOLBURG, H., 2000. Correlation of tight junction morphology with the expression of tight junction proteins in blood-brain barrier endothelial cells. *European journal of cell biology,* **79**(10), pp. 707-717.

LIMAYE, V. and VADAS, M., 2006. The vascular endothelium: structure and function. In: R. FITZRIDGE and M. THOMPSON, eds, *Mechanisms of Vascular Disease.* New York: Cambridge University Press, pp. 1.

LIN, S., HSIEH, F., CHEN, Y., LIN, C., KUAN, I., WANG, S., WU, C., CHIEN, H., LIN, F. and CHEN, Y., 2009. Atorvastatin induces thrombomodulin expression in the aorta of cholesterol-fed rabbits and in TNF alpha-treated human aortic endothelial cells. *Histology and histopathology,* **24**(9), pp. 1147-1159.

LINDAHL, P., JOHANSSON, B.R., LEVEEN, P. and BETSHOLTZ, C., 1997. Pericyte loss and microaneurysm formation in PDGF-B-deficient mice. *Science,* **277**(5323), pp. 242-245.

LIP, G.Y.H., BLANN, A.D., FAROOQI, I.S., ZARIFIS, J., SAGAR, G. and BEEVERS, D.G., 2002. Sequential alterations in haemorheology, endothelial dysfunction, platelet

activation and thrombogenesis in relation to prognosis following acute stroke: The West Birmingham Stroke Project. *Blood Coagulation & Fibrinolysis,* **13**(4), pp. 339-347.

LIPPOLDT, A., KNIESEL, U., LIEBNER, S., KALBACHER, H., KIRSCH, T., WOLBURG, H. and HALLER, H., 2000. Structural alterations of tight junctions are associated with loss of polarity in stroke-prone spontaneously hypertensive rat blood-brain barrier endothelial cells. *Brain research,* **885**(2), pp. 251-261.

LIU, D., BIENKOWSKA, J., PETOSA, C., COLLIER, R.J., FU, H. and LIDDINGTON, R., 1995. Crystal-Structure of the Zeta-Isoform of the 14-3-3 Protein. *Nature,* **376**(6536), pp. 191-194.

LIU, F. and HUANG, L., 2002. Development of non-viral vectors for systemic gene delivery. *Journal of Controlled Release,* **78**(1-3), pp. 259-266.

LIU, Y. and HU, M., 2000. P-glycoprotein and bioavailability-implication of polymorphism. *Clinical Chemistry and Laboratory Medicine,* **38**(9), pp. 877-881.

LIU, Y.M., YIN, G.Y., SURAPISITCHAT, J., BERK, B.C. and MIN, W., 2001. Laminar flow inhibits TNF-induced ASK1 activation by preventing dissociation of ASK1 from its inhibitor 14-3-3. *Journal of Clinical Investigation,* **107**(7), pp. 917-923.

LODDICK, S.A., TURNBULL, A.V. and ROTHWELL, N.J., 1998. Cerebral interleukin-6 is neuroprotective during permanent focal cerebral ischemia in the rat. *Journal of Cerebral Blood Flow and Metabolism,* **18**(2), pp. 176-179.

LOHMANN, C., KRISCHKE, M., WEGENER, J. and GALLA, H.J., 2004. Tyrosine phosphatase inhibition induces loss of blood-brain barrier integrity by matrix metalloproteinase-dependent and -independent pathways. *Brain research,* **995**(2), pp. 184-196.

LOPEZ, A.D. and MATHERS, C.D., 2006. Measuring the global burden of disease and epidemiological transitions: 2002-2030. *Annals of Tropical Medicine and Parasitology,* **100**(5-6), pp. 481-499.

LOSSINSKY, A.S. and SHIVERS, R.R., 2004. Structural pathways for macromolecular and cellular transport across the blood-brain barrier during inflammatory conditions. Review. *Histology and histopathology,* **19**(2), pp. 535-564.

LOSY, J. and ZAREMBA, J., 2001. Monocyte chemoattractant protein-1 is increased in the cerebrospinal fluid of patients with ischemic stroke. *Stroke,* **32**(11), pp. 2695-2696.

LUCAS, R., JUILLARD, P., DECOSTER, E., REDARD, M., BURGER, D., DONATI, Y., GIROUD, C., MONSOHINARD, C., DEKESEL, T., BUURMAN, W.A., MOORE, M.W., DAYER, J.M., FIERS, W., BLUETHMANN, H. and GRAU, G.E., 1997. Crucial role of tumor necrosis factor (TNF) receptor 2 and membrane-bound TNF in experimental cerebral malaria. *European journal of immunology,* **27**(7), pp. 1719-1725.

LUCAS, R., LOU, J.N., JUILLARD, P., MOORE, M., BLUETHMANN, H. and GRAU, G.E., 1997a. Respective role of TNF receptors in the development of experimental cerebral malaria. *Journal of neuroimmunology,* **72**(2), pp. 143-148.

LUCAS, R., LOU, J.N., MOREL, D.R., RICOU, B., SUTER, P.M. and GRAU, G.E., 1997b. TNF receptors in the microvascular pathology of acute respiratory distress syndrome and cerebral malaria. *Journal of leukocyte biology,* **61**(5), pp. 551-558.

LUFT, F.C., MERVAALA, E., MULLER, D.N., GROSS, V., SCHMIDT, F., PARK, J.K., SCHMITZ, C., LIPPOLDT, A., BREU, V., DECHEND, R., DRAGUN, D., SCHNEIDER, W., GANTEN, D. and HALLER, H., 1999. Hypertension-induced end-organ damage - A new transgenic approach to an old problem. *Hypertension,* **33**(1), pp. 212-218.

LUISSINT, A., ARTUS, C., GLACIAL, F., GANESHAMOORTHY, K. and COURAUD, P., 2012. Tight junctions at the blood brain barrier: physiological architecture and disease-associated dysregulation. *Fluids and barriers of the CNS,* **9**(1), pp. 23-23.

LUISSINT, A., FEDERICI, C., GUILLONNEAU, F., CHRETIEN, F., CAMOIN, L., GLACIAL, F., GANESHAMOORTHY, K. and COURAUD, P., 2012. Guanine nucleotide-binding protein G alpha i2: a new partner of claudin-5 that regulates tight junction integrity in human brain endothelial cells. *Journal of Cerebral Blood Flow and Metabolism,* **32**(5), pp. 860-873.

LUST, J.A., DONOVAN, K.A., KLINE, M.P., GREIPP, P.R., KYLE, R.A. and MAIHLE, N.J., 1992. Isolation of an Messenger-Rna Encoding a Soluble Form of the Human Interleukin-6 Receptor. *Cytokine,* **4**(2), pp. 96-100.

LUTTICKEN, C., WEGENKA, U.M., YUAN, J.P., BUSCHMANN, J., SCHINDLER, C., ZIEMIECKI, A., HARPUR, A.G., WILKS, A.F., YASUKAWA, K., TAGA, T., KISHIMOTO, T., BARBIERI, G., PELLEGRINI, S., SENDTNER, M., HEINRICH, P.C. and HORN, F., 1994. Association of Transcription Factor Aprf and Protein-Kinase Jak1 with the Interleukin-6 Signal Transducer Gp130. *Science,* **263**(5143), pp. 89-92.

LV, S., SONG, H., ZHOU, Y., LI, L., CUI, W., WANG, W. and LIU, P., 2010. Tumour necrosis factor-alpha affects blood-brain barrier permeability and tight junction-associated occludin in acute liver failure. *Liver International,* **30**(8), pp. 1198-1210.

MACKO, R.F., KILLEWICH, L.A., FERNANDEZ, J.A., COX, D.K., GRUBER, A. and GRIFFIN, J.H., 1999. Brain-specific protein C activation during carotid artery occlusion in humans. *Stroke,* **30**(3), pp. 542-545.

MAHER, P.A. and PASQUALE, E.B., 1988. Tyrosine Phosphorylated Proteins in Different Tissues during Chick-Embryo Development. *Journal of Cell Biology,* **106**(5), pp. 1747-1755.

MAJNO, G., 1992. The Capillary then and Now - an Overview of Capillary Pathology. *Modern Pathology,* **5**(1), pp. 9-22.

MALEK, A.M., ALPER, S.L. and IZUMO, S., 1999. Hemodynamic shear stress and its role in atherosclerosis. *Jama-Journal of the American Medical Association,* **282**(21), pp. 2035-2042.

MANCINI, M., CORRADI, V., PETTA, S., BARBIERI, E., MANETTI, F., BOTTA, M. and SANTUCCI, M.A., 2011. A New Nonpeptidic Inhibitor of 14-3-3 Induces Apoptotic Cell Death in Chronic Myeloid Leukemia Sensitive or Resistant to Imatinib. *Journal of Pharmacology and Experimental Therapeutics,* **336**(3), pp. 596-604.

MANICKAM, D.S., BRYNSKIKH, A.M., KOPANIC, J.L., SORGEN, P.L., KLYACHKO, N.L., BATRAKOVA, E.V., BRONICH, T.K. and KABANOV, A.V., 2012. Well-defined cross-linked antioxidant nanozymes for treatment of ischemic brain injury. *Journal of Controlled Release,* **162**(3), pp. 636-645.

MANIOTIS, A.J., CHEN, C.S. and INGBER, D.E., 1997. Demonstration of mechanical connections between integrins cytoskeletal filaments, and nucleoplasm that stabilize nuclear structure. *Proceedings of the National Academy of Sciences of the United States of America,* **94**(3), pp. 849-854.

MANN, K.G., GOLDEN, N.J. and VANTVEER, C., 1997. Tissue factor pathway to thrombin: Analyses of normal concentration variations in procoagulant and anticoagulant factors. *Thrombosis and haemostasis,* , pp. P1653-P1653.

MARCHI, N., GRANATA, T., FRERI, E., CIUSANI, E., RAGONA, F., PUVENNA, V., TENG, Q., ALEXOPOLOUS, A. and JANIGRO, D., 2011. Efficacy of Anti-Inflammatory Therapy in a Model of Acute Seizures and in a Population of Pediatric Drug Resistant Epileptics. *Plos One,* **6**(3), pp. e18200.

MARCUM, J.A., MCKENNEY, J.B. and ROSENBERG, R.D., 1984. Acceleration of Thrombin-Antithrombin Complex-Formation in Rat Hindquarters Via Heparinlike Molecules Bound to the Endothelium. *Journal of Clinical Investigation,* **74**(2), pp. 341-350.

MARCUM, J.A. and ROSENBERG, R.D., 1984. Anticoagulantly Active Heparin-Like Molecules from Vascular Tissue. *Biochemistry,* **23**(8), pp. 1730-1737.

MARK, K.S. and DAVIS, T.P., 2002. Cerebral microvascular changes in permeability and tight junctions induced by hypoxia-reoxygenation. *American Journal of Physiology-Heart and Circulatory Physiology,* **282**(4), pp. H1485-H1494.

MARK, K.S. and DAVIS, T.P., 2002. Cerebral microvascular changes in permeability and tight junctions induced by hypoxia-reoxygenation. *American Journal of Physiology-Heart and Circulatory Physiology,* **282**(4), pp. H1485-H1494.

MARK, K.S. and MILLER, D.W., 1999. Increased permeability of primary cultured brain microvessel endothelial cell monolayers following TNF-alpha exposure. *Life Sciences,* **64**(21), pp. 1941-1953.

MARTIN, H., PATEL, Y., JONES, D., HOWELL, S., ROBINSON, K. and AITKEN, A., 1993. Antibodies Against the Major Brain Isoforms of 14-3-3-Protein - an Antibody Specific for the N-Acetylated Amino-Terminus of a Protein. *FEBS letters,* **331**(3), pp. 296-303.

MARTIN, H., ROSTAS, J., PATEL, Y. and AITKEN, A., 1994. Subcellular-Localization of 14-3-3-Isoforms in Rat-Brain using Specific Antibodies. *Journal of neurochemistry,* **63**(6), pp. 2259-2265.

MARTIN-PADURA, I., LOSTAGLIO, S., SCHNEEMANN, M., WILLIAMS, L., ROMANO, M., FRUSCELLA, P., PANZERI, C., STOPPACCIARO, A., RUCO, L., VILLA, A., SIMMONS, D. and DEJANA, E., 1998. Junctional adhesion molecule, a novel member of the immunoglobulin superfamily that distributes at intercellular junctions and modulates monocyte transmigration. *Journal of Cell Biology,* **142**(1), pp. 117-127.

MARUI, N., OFFERMANN, M.K., SWERLICK, R., KUNSCH, C., ROSEN, C.A., AHMAD, M., ALEXANDER, R.W. and MEDFORD, R.M., 1993. Vascular Cell-Adhesion Molecule-1 (Vcam-1) Gene-Transcription and Expression are Regulated through an Antioxidant Sensitive Mechanism in Human Vascular Endothelial-Cells. *Journal of Clinical Investigation,* **92**(4), pp. 1866-1874.

MARUMO, T., SCHINI-KERTH, V.B., FISS-LTHALER, B. and BUSSE, R., 1997. Platelet-derived growth factor-stimulated superoxide anion production modulates activation of transcription factor NF-kappa B and expression of monocyte chemoattractant protein 1 in human aortic smooth muscle cells. *Circulation,* **96**(7), pp. 2361-2367.

MARUO, N., MORITA, I., SHIRAO, M. and MUROTA, S.I., 1992. Il-6 Increases Endothelial Permeability Invitro. *Endocrinology,* **131**(2), pp. 710-714.

MARUYAMA, I., 1992. Thrombomodulin, an Endothelial Anticoagulant - its Structure, Function and Expression. *Japanese Circulation Journal-English Edition,* **56**(2), pp. 187-191.

MARUYAMA, I. and MAJERUS, P.W., 1985. The Turnover of Thrombin-Thrombomodulin Complex in Cultured Human Umbilical Vein Endothelial-Cells and A549 Lung-Cancer Cells - Endocytosis and Degradation of Thrombin. *Journal of Biological Chemistry,* **260**(29), pp. 5432-5438.

MARZ, P., OTTEN, U. and ROSE-JOHN, S., 1999. Neural activities of IL-6-type cytokines often depend on soluble cytokine receptors. *European Journal of Neuroscience,* **11**(9), pp. 2995-3004.

MASTERS, S.C., PEDERSON, K.J., ZHANG, L.X., BARBIERI, J.T. and FU, H.A., 1999. Interaction of 14-3-3 with a nonphosphorylated protein ligand, exoenzyme S of Pseudomonas aeruginosa. *Biochemistry,* **38**(16), pp. 5216-5221.

MATSUGI, T., CHEN, Q. and ANDERSON, D.R., 1997. Contractile responses of cultured bovine retinal pericytes to angiotensin II. *Archives of Ophthalmology,* **115**(10), pp. 1281-1285.

MATSUGI, T., CHEN, Q. and ANDERSON, D.R., 1997. Suppression of CO2-induced relaxation of bovine retinal pericytes by angiotensin II. *Investigative ophthalmology & visual science,* **38**(3), pp. 652-657.

MATTER, K. and BALDA, M.S., 2003. Holey barrier: claudins and the regulation of brain endothelial permeability. *Journal of Cell Biology,* **161**(3), pp. 459-460.

MATTER, K. and BALDA, M.S., 2003. Signalling to and from tight junctions. *Nature Reviews Molecular Cell Biology,* **4**(3), pp. 225-236.

MATZINGER, P., 2002. An innate sense of danger. *Reparative Medicine: Growing Tissues and Organs,* **961**, pp. 341-342.

MAWUENYEGA, K.G., SIGURDSON, W., OVOD, V., MUNSELL, L., KASTEN, T., MORRIS, J.C., YARASHESKI, K.E. and BATEMAN, R.J., 2010. Decreased Clearance of CNS beta-Amyloid in Alzheimer's Disease. *Science,* **330**(6012), pp. 1774-1774.

MAXWELL, K., BERLINER, J.A. and CANCILLA, P.A., 1987. Induction of Gamma-Glutamyl-Transferase Transpeptidase in Cultured Cerebral Endothelial-Cells by a Product Released by Astrocytes. *Brain research,* **410**(2), pp. 309-314.

MCALLISTER, M.S., KRIZANAC-BENGEZ, L., MACCHIA, F., NAFTALIN, R.J., PEDLEY, K.C., MAYBERG, M.R., MARRONI, M., LEAMAN, S., STANNESS, K.A. and JANIGRO, D., 2001. Mechanisms of glucose transport at the blood-brain barrier: an in vitro study. *Brain research,* **904**(1), pp. 20-30.

MCCARTHY, K.M., SKARE, I.B., STANKEWICH, M.C., FURUSE, M., TSUKITA, S., ROGERS, R.A., LYNCH, R.D. and SCHNEEBERGER, E.E., 1996. Occludin is a functional component of the tight junction. *Journal of cell science,* **109**, pp. 2287-2298.

MCCORMICK, S.M., ESKIN, S.G., MCINTIRE, L.V., TENG, C.L., LU, C.M., RUSSELL, C.G. and CHITTUR, K.K., 2001. DNA microarray reveals changes in gene expression of shear stressed human umbilical vein endothelial cells. *Proceedings of the National Academy of Sciences of the United States of America,* **98**(16), pp. 8955-8960.

MCNALLY, J.S., DAVIS, M.E., GIDDENS, D.P., SAHA, A., HWANG, J.N., DIKALOV, S., JO, H. and HARRISON, D.G., 2003. Role of xanthine oxidoreductase and NAD(P)H oxidase in endothelial superoxide production in response to oscillatory shear stress. *American Journal of Physiology-Heart and Circulatory Physiology,* **285**(6), pp. H2290-H2297.

MEEK, S.E.M., LANE, W.S. and PIWNICA-WORMS, H., 2004. Comprehensive proteomic analysis of interphase and mitotic 14-3-3-binding proteins. *Journal of Biological Chemistry,* **279**(31), pp. 32046-32054.

MEGYERI, P., ABRAHAM, C.S., TEMESVARI, P., KOVACS, J., VAS, T. and SPEER, C.P., 1992. Recombinant Human Tumor-Necrosis-Factor-Alpha Constricts Pial Arterioles and Increases Blood-Brain-Barrier Permeability in Newborn Piglets. *Neuroscience letters,* **148**(1-2), pp. 137-140.

MEHTA, D. and MALIK, A.B., 2006. Signaling mechanisms regulating endothelial permeability. *Physiological Reviews,* **86**(1), pp. 279-367.

MEISTRELL, M.E., BOTCHKINA, G.I., WANG, H.C., DISANTO, E., COCKROFT, K.M., BLOOM, O., VISHNUBHAKAT, J.M., GHEZZI, P. and TRACEY, K.J., 1997. Tumor necrosis factor is a brain damaging cytokine in cerebral ischemia. *Shock,* **8**(5), pp. 341-348.

MERRILL, J.E., 1991. Effects of Interleukin-1 and Tumor-Necrosis-Factor-Alpha on Astrocytes, Microglia, Oligodendrocytes, and Glial Precursors Invitro. *Developmental neuroscience,* **13**(3), pp. 130-&.

MERRILL, J.E. and CHEN, I.S.Y., 1991. Hiv-1, Macrophages, Glial-Cells, and Cytokines in Aids Nervous-System Disease. *Faseb Journal,* **5**(10), pp. 2391-2397.

MERRILL, J.E., IGNARRO, L.J., SHERMAN, M.P., MELINEK, J. and LANE, T.E., 1993. Microglial Cell Cytotoxicity of Oligodendrocytes is Mediated through Nitric-Oxide. *Journal of Immunology,* **151**(4), pp. 2132-2141.

METTINGER, K.L., 1982. A Study of Hemostasis in Ischemic Cerebrovascular-Disease .1. Abnormalities in Factor-Viii and Antithrombin. *Thrombosis research,* **26**(3), pp. 183-192.

MILLER, D.M., BUETTNER, G.R. and AUST, S.D., 1990. Transition-Metals as Catalysts of Autoxidation Reactions. *Free Radical Biology and Medicine,* **8**(1), pp. 95-108.

MILLER, D.M., BUETTNER, G.R. and AUST, S.D., 1990. Transition-Metals as Catalysts of Autoxidation Reactions. *Free Radical Biology and Medicine,* **8**(1), pp. 95-108.

MINAGAR, A. and ALEXANDER, J.S., 2003. Blood-brain barrier disruption in multiple sclerosis. *Multiple Sclerosis,* **9**(6), pp. 540-549.

MINAKAWA, T., BREADY, J., BERLINER, J., FISHER, M. and CANCILLA, P.A., 1991. Invitro Interaction of Astrocytes and Pericytes with Capillary-Like Structures of Brain Microvessel Endothelium. *Laboratory Investigation,* **65**(1), pp. 32-40.

MINN, A., GHERSIEGEA, J.F., PERRIN, R., LEININGER, B. and SIEST, G., 1991. Drug-Metabolizing-Enzymes in the Brain and Cerebral Microvessels. *Brain Research Reviews,* **16**(1), pp. 65-82.

MISRA, A., GANESH, S., SHAHIWALA, A. and SHAH, S.P., 2003. Drug delivery to the central nervous system: a review. *Journal of Pharmacy and Pharmaceutical Sciences,* **6**(2), pp. 252-273.

MITIC, L.L., VAN ITALLIE, C.M. and ANDERSON, J.M., 2000. Molecular Physiology and Pathophysiology of Tight Junctions - I. Tight junction structure and function: lessons from mutant animals and proteins. *American Journal of Physiology-Gastrointestinal and Liver Physiology,* **279**(2), pp. G250-G254.

MOCHIZUKI, S., VINK, H., HIRAMATSU, O., KAJITA, T., SHIGETO, F., SPAAN, J.A.E. and KAJIYA, F., 2003. Role of hyaluronic acid glycosaminoglycans in shear-induced endothelium-derived nitric oxide release. *American Journal of Physiology-Heart and Circulatory Physiology,* **285**(2), pp. H722-H726.

MODUR, V., LI, Y.J., ZIMMERMAN, G.A., PRESCOTT, S.M. and MCINTYRE, T.M., 1997. Retrograde inflammatory signaling from neutrophils to endothelial cells by soluble interleukin-6 receptor alpha. *Journal of Clinical Investigation,* **100**(11), pp. 2752-2756.

MODUR, V., ZIMMERMAN, G.A., PRESCOTT, S.M. and MCINTYRE, T.M., 1996. Endothelial cell inflammatory responses to tumor necrosis factor alpha - Ceramide-dependent and -independent mitogen-activated protein kinase cascades. *Journal of Biological Chemistry,* **271**(22), pp. 13094-13102.

MOHAN, S., KOYOMA, K., THANGASAMY, A., NAKANO, H., GLICKMAN, R.D. and MOHAN, N., 2007. Low shear stress preferentially enhances IKK activity through selective sources of ROS for persistent activation of NF-kappa B in endothelial cells. *American Journal of Physiology-Cell Physiology,* **292**(1), pp. C362-C371.

MOHAZZAB-H, K.M., KAMINSKI, P.M. and WOLIN, M.S., 1994. NADH oxidoreductase is a major source of superoxide anion in bovine coronary artery endothelium. *American Journal of Physiology,* **266**(6 PART 2), pp. H2568-H2572.

MONTIEL-DAVALOS, A., DE JESUS IBARRA-SANCHEZ, M., LUIS VENTURA-GALLEGOS, J., ALFARO-MORENO, E. and LOPEZ-MARURE, R., 2010. Oxidative stress and apoptosis are induced in human endothelial cells exposed to urban particulate matter. *Toxicology in Vitro,* **24**(1), pp. 135-141.

MOORE BW AND PEREZ VJ, 1967. Specific acidic proteins of the nervous system. In: FD CARLSON, ENGLEWOOD CLIFFS, NJ: PRENTICE- HALL, ed, *Physiological and Biochemical Aspects of Nervous Integration.* pp. 343.

MOORE, B.W. and PEREZ, V.J., 1967. Specific acidic proteins of the nervous system. In: FD CARLSON, ed, *Physiological and Biochemical Aspects of Nervous Integration.* Englewood Cliffs, NJ: Prentice- Hall;: pp. 343.

MORCOS, Y., HOSIE, M.J., BAUER, H.C. and CHAN-LING, T., 2001. Immunolocalization of occludin and claudin-1 to tight junctions in intact CNS vessels of mammalian retina. *Journal of neurocytology,* **30**(2), pp. 107-123.

MORITA, K., FURUSE, M., FUJIMOTO, K. and TSUKITA, S., 1999. Claudin multigene family encoding four-transmembrane domain protein components of tight junction strands. *Proceedings of the National Academy of Sciences of the United States of America,* **96**(2), pp. 511-516.

MORRISSEY, S.P., STODAL, H., ZETTL, U., SIMONIS, C., JUNG, S., KIEFER, R., LASSMANN, H., HARTUNG, H.P., HAASE, A. and TOYKA, K.V., 1996. In vivo MRI and its histological correlates in acute adoptive transfer experimental allergic encephalomyelitis - Quantification of inflammation and oedema. *Brain,* **119**, pp. 239-248.

MORROW, C.M.K., TYAGI, G., SIMON, L., CARNES, K., MURPHY, K.M., COOKE, P.S., HOFMANN, M.C. and HESS, R.A., 2009. Claudin 5 Expression in Mouse Seminiferous Epithelium Is Dependent upon the Transcription Factor Ets Variant 5 and Contributes to Blood-Testis Barrier Function. *Biology of reproduction,* **81**(5), pp. 871-879.

MOZO, J., FERRY, G., STUDENY, A., PECQUEUR, C., RODRIGUEZ, M., BOUTIN, J.A. and BOUILLAUD, F., 2006. Expression of UCP3 in CHO cells does not cause uncoupling, but controls mitochondrial activity in the presence of glucose. *Biochemical Journal,* **393**, pp. 431-439.

MU, F., ANDREWS, R.K., ARTHUR, J.F., MUNDAY, A.D., CRANMER, S.L., JACKSON, S.P., STOMSKI, F.C., LOPEZ, A.F. and BERNDT, M.C., 2008. A functional 14-3-3 zeta-independent association of PI3-kinase with glycoprotein Ib alpha, the major ligand-binding subunit of the platelet glycoprotein Ib-IX-V complex. *Blood,* **111**(9), pp. 4580-4587.

MUELLER, C., WIDDER, J., MCNALLY, J., MCCANN, L., JONES, D. and HARRISON, D., 2005. The role of the multidrug resistance protein-1 in modulation of endothelial cell oxidative stress. *Circulation research,* **97**(7), pp. 637-644.

MUGGE, A., ELWELL, J.H., PETERSON, T.E., HOFMEYER, T.G., HEISTAD, D.D. and HARRISON, D.G., 1991. Chronic Treatment with Polyethylene-Glycolated Superoxide-Dismutase Partially Restores Endothelium-Dependent Vascular Relaxations in Cholesterol-Fed Rabbits. *Circulation research,* **69**(5), pp. 1293-1300.

MULLBERG, J., SCHOOLTINK, H., STOYAN, T., GUNTHER, M., GRAEVE, L., BUSE, G., MACKIEWICZ, A., HEINRICH, P.C. and ROSEJOHN, S., 1993. The Soluble Interleukin-6 Receptor is Generated by Shedding. *European journal of immunology,* **23**(2), pp. 473-480.

MULLER, C., ENDLICH, K., BARTHELMEBS, M. and HELWIG, J.J., 1997. AT(2)-antagonist sensitive potentiation of angiotensin II-induced vasoconstrictions by blockade of nitric oxide synthesis in rat renal vasculature. *British journal of pharmacology,* **122**(7), pp. 1495-1501.

MULLER, C., ENDLICH, K. and HELWIG, J.J., 1998. AT(2) antagonist-sensitive potentiation of angiotensin II-induced constriction by NO blockade and its dependence on endothelium and P450 eicosanoids in rat renal vasculature. *British journal of pharmacology,* **124**(5), pp. 946-952.

MURPHY, M., PERUSSIA, B. and TRINCHIERI, G., 1988. Effects of Recombinant Tumor Necrosis Factor, Lymphotoxin, and Immune Interferon on Proliferation and Differentiation of Enriched Hematopoietic Precursor Cells. *Experimental hematology,* **16**(2), pp. 131-138.

MUSLIN, A.J., TANNER, J.W., ALLEN, P.M. and SHAW, A.S., 1996. Interaction of 14-3-3 with signaling proteins is mediated by the recognition of phosphoserine. *Cell,* **84**(6), pp. 889-897.

NADEAU, S. and RIVEST, S., 1999. Effects of circulating tumor necrosis factor on the neuronal activity and expression of the genes encoding the tumor necrosis factor receptors (p55 and p75) in the rat brain: A view from the blood-brain barrier. *Neuroscience,* **93**(4), pp. 1449-1464.

NAGATSU, T., MOGI, M., ICHINOSE, H. and TOGARI, A., 2000. Changes in cytokines and neurotrophins in Parkinson's disease. *Journal of Neural Transmission Supplement,* **60**, pp. 277-290.

NAGEL, T., RESNICK, N., DEWEY, C.F. and GIMBRONE, M.A., 1999. Vascular endothelial cells respond to spatial gradients in fluid shear stress by enhanced activation of transcription factors. *Arteriosclerosis Thrombosis and Vascular Biology,* **19**(8), pp. 1825-1834.

NAGY, Z., GOEHLERT, U.G., WOLFE, L.S. and HUTTNER, I., 1985. Ca-2+ Depletion-Induced Disconnection of Tight Junctions in Isolated Rat-Brain Microvessels. *Acta Neuropathologica,* **68**(1), pp. 48-52.

NAGYOSZI, P., WILHELM, I., FARKAS, A.E., FAZAKAS, C., DUNG, N.T.K., HASKO, J. and KRIZBAI, I.A., 2010. Expression and regulation of toll-like receptors in cerebral endothelial cells. *Neurochemistry international,* **57**(5), pp. 556-564.

NAKA, T., NISHIMOTO, N. and KISHIMOTO, T., 2002. The paradigm of IL-6: from basic science to medicine. *Arthritis research,* **4 Suppl 3**, pp. S233-42.

NAKAHARA, H., SONG, H., SUGIMOTO, M., HAGIHARA, K., KISHIMOTO, T., YOSHIZAKI, K. and NISHIMOTO, N., 2003. Anti-interleukin-6 receptor antibody therapy reduces vascular endothelial growth factor production in rheumatoid arthritis. *Arthritis and Rheumatism,* **48**(6), pp. 1521-1529.

NAKAMUTA, S., ENDO, H., HIGASHI, Y., KOUSAKA, A., YAMADA, H., YANO, M. and KIDO, H., 2008. Human immunodeficiency virus type 1 gp120-mediated disruption of tight junction proteins by induction of proteasome-mediated degradation of zonula occludens-1 and-2 in human brain microvascular endothelial cells. *Journal of neurovirology,* **14**(3), pp. 186-195.

NAPOLI, C., D'ARMIENTO, F.P., MANCINI, F.P., POSTIGLIONE, A., WITZTUM, J.L., PALUMBO, G. and PALINSKI, W., 1997. Fatty streak formation occurs in human fetal aortas and is greatly enhanced by maternal hypercholesterolemia - Intimal accumulation of low density lipoprotein and its oxidation precede monocyte recruitment into early atherosclerotic lesions. *Journal of Clinical Investigation,* **100**(11), pp. 2680-2690.

NARAZAKI, M., YASUKAWA, K., SAITO, T., OHSUGI, Y., FUKUI, H., KOISHIHARA, Y., YANCOPOULOS, G.D., TAGA, T. and KISHIMOTO, T., 1993. Soluble Forms of the Interleukin-6 Signal-Transducing Receptor Component Gp130 in Human Serum Possessing a Potential to Inhibit Signals through Membrane-Anchored Gp130. *Blood,* **82**(4), pp. 1120-1126.

NAWASHIRO, H., MARTIN, D. and HALLENBECK, J.M., 1997. Inhibition of tumor necrosis factor and amelioration of brain infarction in mice. *Journal of Cerebral Blood Flow and Metabolism,* **17**(2), pp. 229-232.

NAWASHIRO, H., MARTIN, D. and HALLENBECK, J.M., 1997. Neuroprotective effects of TNF binding protein in focal cerebral ischemia. *Brain research,* **778**(2), pp. 265-271.

NAWASHIRO, H., TASAKI, K., RUETZLER, C.A. and HALLENBECK, J.M., 1997. TNF-alpha pretreatment induces protective effects against focal cerebral ischemia in mice. *Journal of Cerebral Blood Flow and Metabolism,* **17**(5), pp. 483-490.

NAWROTH, P.P. and STERN, D.M., 1986. Modulation of Endothelial-Cell Hemostatic Properties by Tumor-Necrosis-Factor. *Journal of Experimental Medicine,* **163**(3), pp. 740-745.

NEREM, R.M., LEVESQUE, M.J. and CORNHILL, J.F., 1981. Vascular Endothelial Morphology as an Indicator of the Pattern of Blood-Flow. *Journal of Biomechanical Engineering-Transactions of the Asme,* **103**(3), pp. 172-176.

NEUHAUS, J., RISAU, W. and WOLBURG, H., 1991. Induction of blood-brain barrier characteristics in bovine brain endothelial cells by rat astroglial cells in transfilter coculture. *Annals of the New York Academy of Sciences,* **633**, pp. 578-80.

NGOK, S.P., GEYER, R., KOURTIDIS, A., STORZ, P. and ANASTASIADIS, P.Z., 2013. Phosphorylation-mediated 14-3-3 Protein Binding Regulates the Function of the Rho-specific Guanine Nucleotide Exchange Factor (RhoGEF) Syx. *Journal of Biological Chemistry,* **288**(9), pp. 6640-6650.

NI, C.W., HSIEH, H.J., CHAO, Y.J. and WANG, D.L., 2004. Interleukin-6-induced JAK2/STAT3 signaling pathway in endothelial cells is suppressed by hemodynamic flow. *American Journal of Physiology-Cell Physiology,* **287**(3), pp. C771-C780.

NICHOLS, M., TOWNSEND, N., LUENGO-FERNANDEZ, R., LEAL, J., GRAY, A., SCARBOROUGH, P. and RAYNER, M., 2012. *European Cardiovascular Disease Statistics 2012*. Brussels: Sophia Antipolis.

NICHOLS, W., 2005. Clinical measurement of arterial stiffness obtained from noninvasive pressure waveforms. *American Journal of Hypertension,* **18**(1), pp. 3S-10S.

NICKENIG, G. and HARRISON, D.G., 2002. The AT(1)-type angiotensin receptor in oxidative stress and atherogenesis part I: Oxidative stress and atherogenesis. *Circulation,* **105**(3), pp. 393-396.

NICOLA, N.A., 1994. Cytokine Pleiotropy and Redundancy - a View from the Receptor. *Stem cells,* **12**, pp. 3-14.

NISHIMOTO, N., MIYASAKA, N., YAMAMOTO, K., KAWAI, S., TAKEUCHI, T. and AZUMA, J., 2009. Long-term safety and efficacy of tocilizumab, an anti-IL-6 receptor monoclonal antibody, in monotherapy, in patients with rheumatoid arthritis (the STREAM study): evidence of safety and efficacy in a 5-year extension study. *Annals of the Rheumatic Diseases,* **68**(10), pp. 1580-1584.

NISHIMOTO, N., MIYASAKA, N., YAMAMOTO, K., KAWAI, S., TAKEUCHI, T., AZUMA, J. and KISHIMOTO, T., 2009. Study of active controlled tocilizumab monotherapy for rheumatoid arthritis patients with an inadequate response to methotrexate (SATORI): significant reduction in disease activity and serum vascular endothelial growth factor by IL-6 receptor inhibition therapy. *Modern Rheumatology,* **19**(1), pp. 12-19.

NITTA, T., HATA, M., GOTOH, S., SEO, Y., SASAKI, H., HASHIMOTO, N., FURUSE, M. and TSUKITA, S., 2003. Size-selective loosening of the blood-brain barrier in claudin-5-deficient mice. *Journal of Cell Biology,* **161**(3), pp. 653-660.

NOBLES, M. and ABBOTT, N.J., 1998. Modulation of the effects of extracellular ATP on [Ca2+](i) in rat brain microvascular endothelial cells. *European journal of pharmacology,* **361**(1), pp. 119-127.

NOBLES, M., REVEST, P.A., COURAUD, P.O. and ABBOTT, N.J., 1995. Characteristics of Nucleotide Receptors that Cause Elevation of Cytoplasmic Calcium in Immortalized Rat-Brain Endothelial-Cells (Rbe4) and in Primary Cultures. *British journal of pharmacology,* **115**(7), pp. 1245-1252.

NORIA, S., COWAN, D.B., GOTLIEB, A.I. and LANGILLE, B.L., 1999. Transient and steady-state effects of shear stress on endothelial cell adherens junctions. *Circulation research,* **85**(6), pp. 504-514.

NOVICK, D., ENGELMANN, H., WALLACH, D. and RUBINSTEIN, M., 1989. Soluble Cytokine Receptors are Present in Normal Human-Urine. *Journal of Experimental Medicine,* **170**(4), pp. 1409-1414.

OGATA, A., MORISHIMA, A., HIRANO, T., HISHITANI, Y., HAGIHARA, K., SHIMA, Y., NARAZAKI, M. and TANAKA, T., 2011. Improvement of HbA1c during treatment with humanised anti-interleukin 6 receptor antibody, tocilizumab. *Annals of the Rheumatic Diseases,* **70**(6), pp. 1164-1165.

OGUNSHOLA, O.O., 2011. In Vitro Modeling of the Blood-Brain Barrier: Simplicity Versus Complexity. *Current pharmaceutical design,* **17**(26), pp. 2755-2761.

OLDENDORF, W.H., CORNFORD, M.E. and BROWN, W.J., 1977. Large Apparent Work Capability of Blood-Brain-Barrier - Study of Mitochondrial Content of Capillary Endothelial Cells in Brain and Other Tissues of Rat. *Annals of Neurology*, **1**(5), pp. 409-417.

O'LEARY, D.H., POLAK, J.F., KRONMAL, R.A., MANOLIO, T.A., BURKE, G.L., WOLFSON, S.K. and CARDIOVASCULAR HLTH STUDY COLLABORATIVE RES GRP, 1999. Carotid-artery intima and media thickness as a risk factor for myocardial infarction and stroke in older adults. *New England Journal of Medicine*, **340**(1), pp. 14-22.

ORR, A.W., SANDERS, J.M., BEVARD, M., COLEMAN, E., SAREMBOCK, I.J. and SCHWARTZ, M.A., 2005. The subendothelial extracellular matrix modulates NF-kappa B activation by flow: a potential role in atherosclerosis. *Journal of Cell Biology*, **169**(1), pp. 191-202.

ORR, A.W., STOCKTON, R., SIMMERS, M.B., SANDERS, J.M., SAREMBOCK, I.J., BLACKMAN, B.R. and SCHWARTZ, M.A., 2007. Matrix-specific p21-activated kinase activation regulates vascular permeability in atherogenesis. *Journal of Cell Biology*, **176**(5), pp. 719-727.

ORZYLOWSKA, O., ODERFELD-NOWAK, B., ZAREMBA, M., JANUSZEWSKI, S. and MOSSAKOWSKI, M., 1999. Prolonged and concomitant induction of astroglial immunoreactivity of interleukin-1beta and interleukin-6 in the rat hippocampus after transient global ischemia. *Neuroscience letters*, **263**(1), pp. 72-76.

OSAWA, M., MASUDA, M., HARADA, N., LOPES, R.B. and FUJIWARA, K., 1997. Tyrosine phosphorylation of platelet endothelial cell adhesion molecule-1 (PECAM-1, CD31) in mechanically stimulated vascular endothelial cells. *European journal of cell biology*, **72**(3), pp. 229-237.

OSAWA, M., MASUDA, M., KUSANO, K. and FUJIWARA, K., 2002. Evidence for a role of platelet endothelial cell adhesion molecule-1 in endothelial cell mechanosignal transduction: is it a mechanoresponsive molecule? *Journal of Cell Biology*, **158**(4), pp. 773-785.

OSAWA, M., MASUDA, M., KUSANO, K. and FUJIWARA, K., 2002. Evidence for a role of platelet endothelial cell adhesion molecule-1 in endothelial cell mechanosignal transduction: is it a mechanoresponsive molecule? *Journal of Cell Biology*, **158**(4), pp. 773-785.

OTT, M.J. and BALLERMANN, B.J., 1995. Shear Stress-Conditioned, Endothelial Cell-Seeded Vascular Grafts - Improved Cell Adherence in Response to In-Vitro Shear-Stress. *Surgery*, **117**(3), pp. 334-339.

PACKER, L. and VALACCHI, G., 2002. Antioxidants and the response of skin to oxidative stress: Vitamin E as a key indicator. *Skin pharmacology and applied skin physiology*, **15**(5), pp. 282-290.

PAHAKIS, M.Y., KOSKY, J.R., DULL, R.O. and TARBELL, J.M., 2007. The role of endothelial glycocalyx components in mechanotransduction of fluid shear stress. *Biochemical and biophysical research communications*, **355**(1), pp. 228-233.

PALMERI, D., VAN ZANTE, A., HUANG, C.C., HEMMERICH, S. and ROSEN, S.D., 2000. Vascular endothelial junction-associated molecule, a novel member of the

immunoglobulin superfamily, is localized to intercellular boundaries of endothelial cells. *Journal of Biological Chemistry,* **275**(25), pp. 19139-19145.

PANULA, P., JOO, F. and RECHARDT, L., 1978. Evidence for Presence of Viable Endothelial Cells in Cultures Derived from Dissociated Rat-Brain. *Experientia,* **34**(1), pp. 95-97.

PARDRIDGE, W.M., 2006. *An introduction to the blood-brain barrier: methodology, biology and pathology.* New York: Cambridge University Press.

PARDRIDGE, W.M., EISENBERG, J. and YANG, J., 1985. Human Blood-Brain-Barrier Insulin-Receptor. *Journal of neurochemistry,* **44**(6), pp. 1771-1778.

PARDRIDGE, W.M., 2003. Blood-brain barrier drug targeting: the future of brain drug development. *Molecular interventions,* **3**(2), pp. 90-51.

PARK, H., GO, Y.M., DARJI, R., CHOI, J.W., LISANTI, M.P., MALAND, M.C. and JO, H., 2000. Caveolin-1 regulates sheer stress-dependent activation of extracellular signal-regulated kinase. *American Journal of Physiology-Heart and Circulatory Physiology,* **278**(4), pp. H1285-H1293.

PARK, H., GO, Y.M., JOHN, P.L.S., MALAND, M.C., LISANTI, M.P., ABRAHAMSON, D.R. and JO, H., 1998. Plasma membrane cholesterol is a key molecule in shear stress-dependent activation of extracellular signal-regulated kinase. *Journal of Biological Chemistry,* **273**(48), pp. 32304-32311.

PASSERINI, A.G., POLACEK, D.C., SHI, C.Z., FRANCESCO, N.M., MANDUCHI, E., GRANT, G.R., PRITCHARD, W.F., POWELL, S., CHANG, G.Y., STOECKERT, C.J. and DAVIES, P.F., 2004. Coexisting proinflammatory and antioxidative endothelial transcription profiles in a disturbed flow region of the adult porcine aorta. *Proceedings of the National Academy of Sciences of the United States of America,* **101**(8), pp. 2482-2487.

PATRICK, C.W. and MCINTIRE, L.V., 1995. Shear-Stress and Cyclic Strain Modulation of Gene-Expression in Vascular Endothelial-Cells. *Blood purification,* **13**(3-4), pp. 112-124.

PAUL, R., KOEDEL, U., WINKLER, F., KIESEIER, B.C., FONTANA, A., KOPF, M., HARTUNG, H.P. and PFISTER, H.W., 2003. Lack of IL-6 augments inflammatory response but decreases vascular permeability in bacterial meningitis. *Brain,* **126**, pp. 1873-1882.

PAWSON, T. and SCOTT, J.D., 1997. Signaling through scaffold, anchoring, and adaptor proteins. *Science,* **278**(5346), pp. 2075-2080.

PEARCE, M.J., MCINTYRE, T.M., PRESCOTT, S.M., ZIMMERMAN, G.A. and WHATLEY, R.E., 1996. Shear stress activates cytosolic phospholipase A(2) (cPLA(2)) and MAP kinase in human endothelial cells. *Biochemical and biophysical research communications,* **218**(2), pp. 500-504.

PEDRINELLI, R., GIAMPIETRO, O., CARMASSI, F., MELILLO, E., DELLOMO, G., CATAPANO, G., MATTEUCCI, E., TALARICO, L., MORALE, M., DENEGRI, F. and DIBELLO, V., 1994. Microalbuminuria and Endothelial Dysfunction in Essential-Hypertension. *Lancet,* **344**(8914), pp. 14-18.

PENKOWA, M., GIRALT, M., CARRASCO, J., HADBERG, H. and HIDALGO, J., 2000. Impaired inflammatory response and increased oxidative stress and neurodegeneration after brain injury in interleukin-6-deficient mice. *Glia,* **32**(3), pp. 271-285.

PENKOWA, M., MOOS, T., CARRASCO, J., HADBERG, H., MOLINERO, A., BLUETHMANN, H. and HIDALGO, J., 1999. Strongly compromised inflammatory response to brain injury in interleukin-6-deficient mice. *Glia,* **25**(4), pp. 343-357.

PENKOWA, M., MOOS, T., CARRASCO, J., HADBERG, H., MOLINERO, A., BLUETHMANN, H. and HIDALGO, J., 1999. Strongly compromised inflammatory response to brain injury in interleukin-6-deficient mice. *Glia,* **25**(4), pp. 343-357.

PERRY, S.W., DEWHURST, S., BELLIZZI, M.J. and GELBARD, H.A., 2002. Tumor necrosis factor-alpha in normal and diseased brain: Conflicting effects via intraneuronal receptor crosstalk? *Journal of neurovirology,* **8**(6), pp. 611-624.

PERRY, V.H., ANTHONY, D.C., BOLTON, S.J. and BROWN, H.C., 1997. The blood-brain barrier and the inflammatory response. *Molecular medicine today,* **3**(8), pp. 335-341.

PERSIDSKY, Y., HEILMAN, D., HAORAH, J., ZELIVYANSKAYA, M., PERSIDSKY, R., WEBER, G.A., SHIMOKAWA, H., KAIBUCHI, K. and IKEZU, T., 2006. Rho-mediated regulation of tight junctions during monocyte migration across the blood-brain barrier in HIV-1 encephalitis (HIVE). *Blood,* **107**(12), pp. 4770-4780.

PETOSA, C., MASTERS, S.C., BANKSTON, L.A., POHL, J., WANG, B.C., FU, H.I. and LIDDINGTON, R.C., 1998. 14-3-3 zeta binds a phosphorylated Raf peptide and an unphosphorylated peptide via its conserved amphipathic groove. *Journal of Biological Chemistry,* **273**(26), pp. 16305-16310.

PETOSA, C., MASTERS, S.C., BANKSTON, L.A., POHL, J., WANG, B.C., FU, H.I. and LIDDINGTON, R.C., 1998. 14-3-3 zeta binds a phosphorylated Raf peptide and an unphosphorylated peptide via its conserved amphipathic groove. *Journal of Biological Chemistry,* **273**(26), pp. 16305-16310.

PETTY, M.A. and LO, E.H., 2002. Junctional complexes of the blood-brain barrier: permeability changes in neuroinflammation. *Progress in neurobiology,* **68**(5), pp. 311-323.

PETTY, M.A. and WETTSTEIN, J.G., 2001. Elements of cerebral microvascular ischaemia. *Brain Research Reviews,* **36**(1), pp. 23-34.

PHAN, S.H., GANNON, D.E., VARANI, J., RYAN, U.S. and WARD, P.A., 1989. Xanthine-Oxidase Activity in Rat Pulmonary-Artery Endothelial-Cells and its Alteration by Activated Neutrophils. *American Journal of Pathology,* **134**(6), pp. 1201-1211.

PICKERING, M., CUMISKEY, D. and O'CONNOR, J.J., 2005. Actions of TNF-alpha on glutamatergic synaptic transmission in the central nervous system. *Experimental physiology,* **90**(5), pp. 663-670.

PITMAN, W., OSGOOD, D., SMITH, D., SCHAEFER, E. and ORDOVAS, J., 1998. The effects of diet and lovastatin on regression of fatty streak lesions and on hepatic and intestinal mRNA levels for the LDL receptor and HMG CoA reductase in F1B hamsters. *Atherosclerosis,* **138**(1), pp. 43-52.

PLANT, S.R., ARNETT, H.A. and TING, J.P.Y., 2005. Astroglial-derived lymphotoxin-alpha exacerbates inflammation and demyelination, but not remyelination. *Glia,* **49**(1), pp. 1-14.

PLUMB, J., MCQUAID, S., MIRAKHUR, M. and KIRK, J., 2002. Abnormal endothelial tight junctions in active lesions and normal-appearing white matter in multiple sclerosis. *Brain Pathology,* **12**(2), pp. 154-169.

PODREZ, E., ABU-SOUD, H. and HAZEN, S., 2000. Myeloperoxidase-generated oxidants and atherosclerosis. *Free Radical Biology and Medicine,* **28**(12), pp. 1717-1725.

POURATI, J., MANIOTIS, A., SPIEGEL, D., SCHAFFER, J.L., BUTLER, J.P., FREDBERG, J.J., INGBER, D.E., STAMENOVIC, D. and WANG, N., 1998. Is cytoskeletal tension a major determinant of cell deformability in adherent endothelial cells? *American Journal of Physiology-Cell Physiology,* **274**(5), pp. C1283-C1289.

POZUELO RUBIO, M., GERAGHTY, K.M., WONG, B.H.C., WOOD, N.T., CAMPBELL, D.G., MORRICE, N. and MACKINTOSH, C., 2004. 14-3-3-Affinity Purification of Over 200 Human Phosphoproteins Reveals New Links to Regulation of Cellular Metabolism, Proliferation and Trafficking. *The Biochemical journal,* **379**(Pt 2), pp. 395-408.

PRADILLO, J.M., ROMERA, C., HURTADO, O., CARDENAS, A., MORO, M.A., LEZA, J.C., DAVALOS, A., CASTILLO, J., LORENZO, P. and LIZASOAIN, I., 2005. TNFR1 upregulation mediates tolerance after brain ischemic preconditioning. *Journal of Cerebral Blood Flow and Metabolism,* **25**(2), pp. 193-203.

PRIES, A.R. and KUEBLER, W.M., 2006. Normal endothelium. *Handbook of Experimental Pharmacology,* **176**, pp. 1-40.

PRIES, A.R., SECOMB, T.W. and GAEHTGENS, P., 2000. The endothelial surface layer. *Pflugers Archiv-European Journal of Physiology,* **440**(5), pp. 653-666.

PRITCHARD, K.A., GROSZEK, L., SMALLEY, D.M., SESSA, W.C., WU, M.D., VILLALON, P., WOLIN, M.S. and STEMERMAN, M.B., 1995. Native Low-Density-Lipoprotein Increases Endothelial-Cell Nitric-Oxide Synthase Generation of Superoxide Anion. *Circulation research,* **77**(3), pp. 510-518.

PRUDHOMME, J., SHERMAN, I., LAND, K., MOSES, A., STENGLEIN, S. and NELSON, J., 1996. Studies of Plasmodium falciparum cytoadherence using immortalized human brain capillary endothelial cells. *International journal for parasitology,* **26**(6), pp. 647-655.

PUEYO, M.E., GONZALEZ, W., NICOLETTI, A., SAVOIE, F., ARNAL, J.F. and MICHEL, J.B., 2000. Angiotensin II stimulates endothelial vascular cell adhesion molecule-1 via nuclear factor-kappa B activation induced by intracellular oxidative stress. *Arteriosclerosis Thrombosis and Vascular Biology,* **20**(3), pp. 645-651.

PUN, P.B.L., LU, J. and MOOCHHALA, S., 2009. Involvement of ROS in BBB dysfunction. *Free radical research,* **43**(4), pp. 348-364.

QIN, Y. and SATO, T.N., 1995. Mouse Multidrug-Resistance 1a/3 Gene is the Earliest Known Endothelial-Cell Differentiation Marker during Blood-Brain-Barrier Development. *Developmental Dynamics,* **202**(2), pp. 172-180.

QIU, Y.C. and TARBELL, J.M., 2000. Interaction between wall shear stress and circumferential strain affects endothelial cell biochemical production. *Journal of vascular research,* **37**(3), pp. 147-157.

QUINTANA, A., GIRALT, M., ROJAS, S., PENKOWA, M., CAMPBELL, I.L., HIDALGO, J. and MOLINERO, A., 2005. Differential role of tumor necrosis factor receptors in mouse brain inflammatory responses in cryolesion brain injury. *Journal of neuroscience research,* **82**(5), pp. 701-716.

RAINES, E.W. and ROSS, R., 1996. Multiple growth factors are associated with lesions of atherosclerosis: Specificity or redundancy? *Bioessays,* **18**(4), pp. 271-282.

RAMSAUER, M., KRAUSE, D. and DERMIETZEL, R., 2002. Angiogenesis of the blood-brain barrier in vitro and the function of cerebral pericytes. *Faseb Journal,* **16**(8), pp. 1274-+.

RAND, J.H., BADIMON, L., GORDON, R.E., USON, R.R. and FUSTER, V., 1987. Distribution of Vonwillebrand-Factor in Porcine Intima Varies with Blood-Vessel Type and Location. *Arteriosclerosis,* **7**(3), pp. 287-291.

RAPOPORT, S.I., 2000. Osmotic opening of the blood-brain barrier: Principles, mechanism, and therapeutic applications. *Cellular and molecular neurobiology,* **20**(2), pp. 217-230.

RASCHER, G., FISCHMANN, A., KROGER, S., DUFFNER, F., GROTE, E.H. and WOLBURG, H., 2002. Extracellular matrix and the blood-brain barrier in glioblastoma multiforme: spatial segregation of tenascin and agrin. *Acta Neuropathologica,* **104**(1), pp. 85-91.

RAUB, T.J., 1996. Signal transduction and glial cell modulation of cultured brain microvessel endothelial cell tight junctions. *American Journal of Physiology-Cell Physiology,* **271**(2), pp. C495-C503.

REESE, T. and KARNOVSK, M., 1967. Fine Structural Localization of a Blood-Brain Barrier to Exogenous Peroxidase. *Journal of Cell Biology,* **34**(1), pp. 207-&.

REICHEL, A., BEGLEY, D.J. and ABBOTT, N.J., 2003. An overview of in vitro techniques for blood-brain barrier studies. *Methods in Molecular Medicine,* **89**, pp. 307-24.

REICHENBACH, A., DEROUICHE, A., GROSCHE, J. and HANANI, M., 2004. Structural association of glia with the various compartments of neurons. In: G.I. HATTON and V. PARPURA, eds, *Glial Neuronal Signaling.* Boston; London: Kluwer Academic Publishers, pp. 53.

REINHARDT, C.A. and GLOOR, S.M., 1997. Co-culture blood-brain barrier models and their use for pharmatoxicological screening. *Toxicology in Vitro,* **11**(5), pp. 513-518.

RENEMAN, R.S., ARTS, T. and HOEKS, A.P.G., 2006. Wall shear stress - an important determinant of endothelial cell function and structure - in the arterial system in vivo. *Journal of vascular research,* **43**(3), pp. 251-269.

RESNICK, N., YAHAV, H., SCHUBERT, S., WOLFOVITZ, E. and SHAY, A., 2000. Signalling pathways in vascular endothelium activated by shear stress: relevance to atherosclerosis. *Current opinion in lipidology,* **11**(2), pp. 167-177.

REVEST, P.A., ABBOTT, N.J. and GILLESPIE, J.I., 1991. Receptor-Mediated Changes in Intracellular [Ca2+] in Cultured Rat-Brain Capillary Endothelial-Cells. *Brain research,* **549**(1), pp. 159-161.

REYES, T.M., FABRY, Z. and COE, C.L., 1999. Brain endothelial cell production of a neuroprotective cytokine, interleukin-6, in response to noxious stimuli. *Brain research,* **851**(1-2), pp. 215-220.

RIDKER, P.M., RIFAI, N., STAMPFER, M.J. and HENNEKENS, C.H., 2000. Plasma concentration of interleukin-6 and the risk of future myocardial infarction among apparently healthy men. *Circulation,* **101**(15), pp. 1767-1772.

RIECKMANN, P., ALBRECHT, M., KITZE, B., WEBER, T., TUMANI, H., BROOCKS, A., LUER, W., HELWIG, A. and POSER, S., 1995. Tumor-Necrosis-Factor-Alpha Messenger-Rna Expression in Patients with Relapsing-Remitting Multiple-Sclerosis is Associated with Disease-Activity. *Annals of Neurology,* **37**(1), pp. 82-88.

RIESEN, F.K., ROTHEN-RUTISHAUSER, B. and WUNDERLI-ALLENSPACH, H., 2002. A ZO1-GFP fusion protein to study the dynamics of tight junctions in living cells. *Histochemistry and cell biology,* **117**(4), pp. 307-315.

RISAU, W., 1995. Differentiation of Endothelium. *Faseb Journal,* **9**(10), pp. 926-933.

RIST, R.J., ROMERO, I.A., CHAN, M.W.K., COURAUD, P.O., ROUX, F. and ABBOTT, N.J., 1997. F-actin cytoskeleton and sucrose permeability of immortalised rat brain microvascular endothelial cell monolayers: effects of cyclic AMP and astrocytic factors. *Brain research,* **768**(1-2), pp. 10-18.

RIZZO, V., MCINTOSH, D.P., OH, P. and SCHNITZER, J.E., 1998. In situ flow activates endothelial nitric oxide synthase in luminal caveolae of endothelium with rapid caveolin dissociation and calmodulin association. *Journal of Biological Chemistry,* **273**(52), pp. 34724-34729.

RODRIGUEZ-BAEZA, A., LA TORRE, F.R.D., POCA, A., MARTI, M. and GARNACHO, A., 2003. Morphological features in human cortical brain microvessels after head injury: A three-dimensional and immunocytochemical study. *Anatomical Record Part A-Discoveries in Molecular Cellular and Evolutionary Biology,* **273A**(1), pp. 583-593.

ROGER, V.L., GO, A.S., LLOYD-JONES, D.M., BENJAMIN, E.J., BERRY, J.D., BORDEN, W.B., BRAVATA, D.M., DAI, S., FORD, E.S., FOX, C.S., FULLERTON, H.J., GILLESPIE, C., HAILPERN, S.M., HEIT, J.A., HOWARD, V.J., KISSELA, B.M., KITTNER, S.J., LACKLAND, D.T., LICHTMAN, J.H., LISABETH, L.D., MAKUC, D.M., MARCUS, G.M., MARELLI, A., MATCHAR, D.B., MOY, C.S., MOZAFFARIAN, D., MUSSOLINO, M.E., NICHOL, G., PAYNTER, N.P., SOLIMAN, E.Z., SORLIE, P.D., SOTOODEHNIA, N., TURAN, T.N., VIRANI, S.S., WONG, N.D., WOO, D., TURNER, M.B., AMER HEART ASSOC STAT COMM and STROKE STAT SUBCOMM, 2012. Heart Disease and Stroke Statistics-2012 Update A Report From the American Heart Association. *Circulation,* **125**(1), pp. E2-E220.

ROLFE, D.F.S. and BROWN, G.C., 1997. Cellular energy utilization and molecular origin of standard metabolic rate in mammals. *Physiological Reviews,* **77**(3), pp. 731-758.

ROMERO, I.A., RADEWICZ, K., JUBIN, E., MICHEL, C.C., GREENWOOD, J., COURAUD, P.O. and ADAMSON, P., 2003. Changes in cytoskeletal and tight junctional proteins correlate with decreased permeability induced by dexamethasone in cultured rat brain endothelial cells. *Neuroscience letters,* **344**(2), pp. 112-116.

ROSE-JOHN, S., SCHELLER, J., ELSON, G. and JONES, S.A., 2006. Interleukin-6 biology is coordinated by membrane-bound and soluble receptors: role in inflammation and cancer. *Journal of leukocyte biology,* **80**(2), pp. 227-236.

ROSENBERG, G.A., ESTRADA, E., KELLEY, R.O. and KORNFELD, M., 1993. Bacterial Collagenase Disrupts Extracellular-Matrix and Opens Blood-Brain-Barrier in Rat. *Neuroscience letters,* **160**(1), pp. 117-119.

ROSS, R., 1999. Mechanisms of disease - Atherosclerosis - An inflammatory disease. *New England Journal of Medicine,* **340**(2), pp. 115-126.

ROTHE, M., SARMA, V., DIXIT, V.W. and GOEDDEL, D.V., 1995. Traf2-Mediated Activation of Nf-Kappa-B by Tnf Receptor-2 and Cd40. *Science,* **269**(5229), pp. 1424-1427.

ROTHE, M., WONG, S.C., HENZEL, W.J. and GOEDDEL, D.V., 1994. A Novel Family of Putative Signal Transducers Associated with the Cytoplasmic Domain of the 75 Kda Tumor-Necrosis-Factor Receptor. *Cell,* **78**(4), pp. 681-692.

RUBANYI, G.M., ROMERO, J.C. and VANHOUTTE, P.M., 1986. Flow-Induced Release of Endothelium-Derived Relaxing Factor. *American Journal of Physiology,* **250**(6), pp. 1145-1149.

RUBANYI, G.M. and VANHOUTTE, P.M., 1986. Superoxide Anions and Hyperoxia Inactivate Endothelium-Derived Relaxing Factor. *American Journal of Physiology,* **250**(5), pp. H822-H827.

RUBIN, L.L., HALL, D.E., PORTER, S., BARBU, K., CANNON, C., HORNER, H.C., JANATPOUR, M., LIAW, C.W., MANNING, K., MORALES, J., TANNER, L.I., TOMASELLI, K.J. and BARD, F., 1991. A Cell-Culture Model of the Blood-Brain-Barrier. *Journal of Cell Biology,* **115**(6), pp. 1725-1735.

RUBIN, L.L. and STADDON, J.M., 1999. The cell biology of the blood-brain barrier. *Annual Review of Neuroscience,* **22**, pp. 11-28.

RUBIO-PEREZ, J.M. and MORILLAS-RUIZ, J.M., 2012. A review: inflammatory process in Alzheimer's disease, role of cytokines. *TheScientificWorldJournal,* **2012**, pp. 756357-756357.

RYAN, U.S. and RYAN, J.W., 1984. Cell biology of pulmonary endothelium. *Circulation,* **70**(5 Pt 2), pp. III46-62.

SADLER, J., 1997. Thrombomodulin structure and function. *Thrombosis and haemostasis,* **78**(1), pp. 392-395.

SAIJA, A., PRINCI, P., LANZA, M., SCALESE, M., ARAMNEJAD, E. and DESARRO, A., 1995. Systemic Cytokine Administration can Affect Blood-Brain-Barrier Permeability in the Rat. *Life Sciences,* **56**(10), pp. 775-784.

SAIRANEN, T., CARPEN, O., KARJALAINEN-LINDSBERG, M.L., PAETAU, A., TURPEINEN, U., KASTE, M. and LINDSBERG, P.J., 2001. Evolution of cerebral tumor necrosis factor-alpha production during human ischemic stroke. *Stroke,* **32**(8), pp. 1750-1757.

SAIRANEN, T.R., LINDSBERG, P.J., BRENNER, M., CARPEN, O. and SIREN, A.L., 2001. Differential cellular expression of tumor necrosis factor-alpha and Type I tumor necrosis factor receptor after transient global forebrain ischemia. *Journal of the neurological sciences,* **186**(1-2), pp. 87-99.

SAITO, M., YOSHIDA, K., HIBI, M., TAGA, T. and KISHIMOTO, T., 1992. Molecular-Cloning of a Murine Il-6 Receptor-Associated Signal Transducer, Gp130, and its Regulated Expression Invivo. *Journal of Immunology,* **148**(12), pp. 4066-4071.

SAITOU, M., FURUSE, M., SASAKI, H., SCHULZKE, J.D., FROMM, M., TAKANO, H., NODA, T. and TSUKITA, S., 2000. Complex phenotype of mice lacking occludin, a component of tight junction strands. *Molecular biology of the cell,* **11**(12), pp. 4131-4142.

SAKAKIBARA, A., FURUSE, M., SAITOU, M., ANDOAKATSUKA, Y. and TSUKITA, S., 1997. Possible involvement of phosphorylation of occludin in tight junction formation. *Journal of Cell Biology,* **137**(6), pp. 1393-1401.

SANCHEZ DEL PINO, M.M., HAWKINS, R.A. and PETERSON, D.R., 1995. Biochemical Discrimination between Luminal and Abluminal Enzyme and Transport Activities of the Blood-Brain Barrier. *Journal of Biological Chemistry,* **270**(25), pp. 14907-14912.

SANCHEZ-DEL-RIO, M. and REUTER, U., 2004. Migraine aura: new information on underlying mechanisms. *Current opinion in neurology,* **17**(3), pp. 289-293.

SANDER, J.W., 2003. The epidemiology of epilepsy revisited. *Current opinion in neurology,* **16**(2), pp. 165-170.

SANOVICH, E., BARTUS, R.T., FRIDEN, P.M., DEAN, R.L., LE, H.Q. and BRIGHTMAN, M.W., 1995. Pathway across blood-brain barrier opened by the bradykinin agonist, RMP-7. *Brain research,* **705**(1-2), pp. 125-135.

SANTAGUIDA, S., JANIGRO, D., HOSSAIN, M., OBY, E., RAPP, E. and CUCULLO, L., 2006. Side by side comparison between dynamic versus static models of blood-brain barrier in vitro: A permeability study. *Brain research,* **1109**, pp. 1-13.

SARWAR, N., BUTTERWORTH, A.S., FREITAG, D.F., GREGSON, J., WILLEIT, P., GORMAN, D.N., GAO, P., SALEHEEN, D., RENDON, A., NELSON, C.P., BRAUND, P.S., HALL, A.S., CHASMAN, D.I., TYBJAERG-HANSEN, A., CHAMBERS, J.C., BENJAMIN, E.J., FRANKS, P.W., CLARKE, R., WILDE, A.A.M., TRIP, M.D., STERI, M., WITTEMAN, J.C.M., QI, L., VAN DER SCHOOT, C.E., DE FAIRE, U., ERDMANN, J., STRINGHAM, H.M., KOENIG, W., RADER, D.J., MELZER, D., REICH, D., PSATY, B.M., KLEBER, M.E., PANAGIOTAKOS, D.B., WILLEIT, J., WENNBERG, P., WOODWARD, M., ADAMOVIC, S., RIMM, E.B., MEADE, T.W., GILLUM, R.F., SHAFFER, J.A., HOFMAN, A., ONAT, A., SUNDSTROM, J., WASSERTHEIL-SMOLLER, S., MELLSTROM, D., GALLACHER, J., CUSHMAN, M., TRACY, R.P., KAUHANEN, J., KARLSSON, M., SALONEN, J.T., WILHELMSEN, L., AMOUYEL, P., CANTIN, B., BEST, L.G., BEN-SHLOMO, Y., MANSON, J.E., DAVEY-SMITH, G., DE BAKKER, P.I.W., O'DONNELL, C.J., WILSON, J.F., WILSON, A.G., ASSIMES, T.L., JANSSON, J., OHLSSON, C., TIVESTEN, A., LJUNGGREN, O., REILLY, M.P.,

HAMSTEN, A., INGELSSON, E., CAMBIEN, F., HUNG, J., THOMAS, G.N., BOEHNKE, M., SCHUNKERT, H., ASSELBERGS, F.W., KASTELEIN, J.J.P., GUDNASON, V., SALOMAA, V., HARRIS, T.B., KOONER, J.S., ALLIN, K.H., NORDESTGAARD, B.G., HOPEWELL, J.C., GOODALL, A.H., RIDKER, P.M., HOLM, H., WATKINS, H., OUWEHAND, W.H., SAMANI, N.J., KAPTOGE, S., DI ANGELANTONIO, E., HARARI, O., DANESH, J. and IL6R GENETICS CONSORTIUM EMERGING, 2012. Interleukin-6 receptor pathways in coronary heart disease: a collaborative meta-analysis of 82 studies. *Lancet,* **379**(9822), pp. 1205-1213.

SATOH, J., KUROHARA, K., YUKITAKE, M. and KURODA, Y., 1999. The 14-3-3 protein detectable in the cerebrospinal fluid of patients with prion-unrelated neurological diseases is expressed constitutively in neurons and glial cells in culture. *European neurology,* **41**(4), pp. 216-225.

SATRIANO, J.A., SHULDINER, M., HORA, K., XING, Y., SHAN, Z. and SCHLONDORFF, D., 1993. Oxygen Radicals as 2nd Messengers for Expression of the Monocyte Chemoattractant Protein, Je/mcp-1, and the Monocyte Colony-Stimulating Factor, Csf-1, in Response to Tumor-Necrosis-Factor-Alpha and Immunoglobulin-G - Evidence for Involvement of Reduced Nicotinamide Adenine-Dinucleotide Phosphate (Nadph)-Dependent Oxidase. *Journal of Clinical Investigation,* **92**(3), pp. 1564-1571.

SAUNDERS, N.R., DZIEGIELEWSKA, K.M. and MOLLGARD, K., 1991. The Importance of the Blood-Brain-Barrier in Fetuses and Embryos. *Trends in neurosciences,* **14**(1), pp. 14-14.

SAUNDERS, N.R., EK, C.J., HABGOOD, M.D. and DZIEGIELEWSKA, K.M., 2008. Barriers in the brain: a renaissance? *Trends in neurosciences,* **31**(6), pp. 279-286.

SAVETTIERI, G., DI LIEGRO, I., CATANIA, C., LICATA, L., PITARRESI, G.L., D'AGOSTINO, S., SCHIERA, G., DE CARO, V., GIANDALIA, G., GIANNOLA, L.I. and CESTELLI, A., 2000. Neurons and ECM regulate occludin localization in brain endothelial cells. *Neuroreport,* **11**(5), pp. 1081-1084.

SAWDEY, M.S. and LOSKUTOFF, D.J., 1991. Regulation of Murine Type-1 Plasminogen-Activator Inhibitor Gene-Expression Invivo - Tissue-Specificity and Induction by Lipopolysaccharide, Tumor-Necrosis-Factor-Alpha, and Transforming Growth-Factor-Beta. *Journal of Clinical Investigation,* **88**(4), pp. 1346-1353.

SCHIEFFER, B., SCHIEFFER, E., HILFIKER-KLEINER, D., HILFIKER, A., KOVANEN, P.T., KAARTINEN, M., NUSSBERGER, J., HARRINGER, W. and DREXLER, H., 2000. Expression of angiotensin II and interleukin 6 in human coronary atherosclerotic plaques - Potential implications for inflammation and plaque instability. *Circulation,* **101**(12), pp. 1372-1378.

SCHIEVELLA, A.R., CHEN, J.H., GRAHAM, J.R. and LIN, L.L., 1997. MADD, a novel death domain protein that interacts with the type 1 tumor necrosis factor receptor and activates mitogen-activated protein kinase. *Journal of Biological Chemistry,* **272**(18), pp. 12069-12075.

SCHNITTLER, H.J., 1998. Structural and functional aspects of intercellular junctions in vascular endothelium. *Basic research in cardiology,* **93**, pp. 30-39.

SCHOBITZ, B., PEZESHKI, G., POHL, T., HEMMANN, U., HEINRICH, P.C., HOLSBOER, F. and REUL, J.M.H.M., 1995. Soluble Interleukin-6 (Il-6) Receptor Augments Central Effects of Il-6 In-Vivo. *Faseb Journal*, **9**(8), pp. 659-664.

SCHOKNECHT, K. and SHALEV, H., 2012. Blood-brain barrier dysfunction in brain diseases: Clinical experience. *Epilepsia*, **53**, pp. 7-13.

SCHREIBELT, G., KOOIJ, G., REIJERKERK, A., VAN DOORN, R., GRINGHUIS, S.I., VAN DER POL, S., WEKSLER, B.B., ROMERO, I.A., COURAUD, P., PIONTEK, J., BLASIG, I.E., DIJKSTRA, C.D., RONKEN, E. and DE VRIES, H.E., 2007. Reactive oxygen species alter brain endothelial tight junction dynamics via RhoA, PI3 kinase, and PKB signaling. *Faseb Journal*, **21**(13), pp. 3666-3676.

SCHROEDER, R.L., WEINGER, M.B., VAKASSIAN, L. and KOOB, G.F., 1991. Methylnaloxonium Diffuses Out of the Rat-Brain More Slowly than Naloxone After Direct Intracerebral Injection. *Neuroscience letters*, **121**(1-2), pp. 173-177.

SCHROEDER, U., SOMMERFELD, P. and SABEL, B.A., 1998. Efficacy of oral dalargin-loaded nanoparticle delivery across the blood-brain barrier. *Peptides*, **19**(4), pp. 777-780.

SCHROEDER, U., SOMMERFELD, P., ULRICH, S. and SABEL, B.A., 1998. Nanoparticle technology for delivery of drugs across the blood-brain barrier. *Journal of pharmaceutical sciences*, **87**(11), pp. 1305-1307.

SCHUBERT-UNKMEIR, A., KONRAD, C., SLANINA, H., CZAPEK, F., HEBLING, S. and FROSCH, M., 2010. Neisseria meningitidis Induces Brain Microvascular Endothelial Cell Detachment from the Matrix and Cleavage of Occludin: A Role for MMP-8. *Plos Pathogens*, **6**(4), pp. e1000874.

SCHULZE, C. and FIRTH, J.A., 1993. Immunohistochemical Localization of Adherens Junction Components in Blood-Brain-Barrier Microvessels of the Rat. *Journal of cell science*, **104**, pp. 773-782.

SCHULZE, C., SMALES, C., RUBIN, L.L. and STADDON, J.M., 1997. Lysophosphatidic acid increases tight junction permeability in cultured brain endothelial cells. *Journal of neurochemistry*, **68**(3), pp. 991-1000.

SCHWARTZ, M.A. and GINSBERG, M.H., 2002. Networks and crosstalk: integrin signalling spreads. *Nature cell biology*, **4**(4), pp. E65-E68.

SEDGWICK, J.D., RIMINTON, D.S., CYSTER, J.G. and KORNER, H., 2000. Tumor necrosis factor: a master-regulator of leukocyte movement. *Immunology today*, **21**(3), pp. 110-113.

SEDLAKOVA, R., SHIVERS, R.R. and DEL MAESTRO, R.F., 1999. Ultrastructure of the blood-brain barrier in the rabbit. *Journal of submicroscopic cytology and pathology*, **31**(1), pp. 149-161.

SEELDRAYERS, P.A., SYHA, J., MORRISSEY, S.P., STODAL, H., VASS, K., JUNG, S., GNEITING, T., LASSMANN, H., HAASE, A., HARTUNG, H.P. and TOYKA, K.V., 1993. Magnetic-Resonance-Imaging Investigation of Blood-Brain-Barrier Damage in Adoptive Transfer Experimental Autoimmune Encephalomyelitis. *Journal of neuroimmunology*, **46**(1-2), pp. 199-206.

SEHNKE, P.C., DELILLE, J.M. and FERL, R.J., 2002. Consummating signal transduction: The role of 14-3-3 proteins in the completion of signal-induced transitions in protein activity. *Plant Cell,* **14**, pp. S339-S354.

SEIFFERT, E., DREIER, J.P., IVENS, S., BECHMANN, I., TOMKINS, O., HEINEMANN, U. and FRIEDMAN, A., 2004. Lasting blood-brain barrier disruption induces epileptic focus in the rat somatosensory cortex. *Journal of Neuroscience,* **24**(36), pp. 7829-7836.

SELKOE, D.J., 2000. Toward a comprehensive theory for Alzheimer's disease - Hypothesis: Alzheimer's disease is caused by the cerebral accumulation and cytotoxicity of amyloid beta-protein. *Alzeheimer's Disease: a Compendium of Current Theories,* **924**, pp. 17-25.

SELMAJ, K.W., FAROOQ, M., NORTON, W.T., RAINE, C.S. and BROSNAN, C.F., 1990. Proliferation of Astrocytes Invitro in Response to Cytokines - a Primary Role for Tumor Necrosis Factor. *Journal of Immunology,* **144**(1), pp. 129-135.

SEMMLER, A., OKULLA, T., SASTRE, M., DUMITRESCU-OZIMEK, L. and HENEKA, M.T., 2005. Systemic inflammation induces apoptosis with variable vulnerability of different brain regions. *Journal of chemical neuroanatomy,* **30**(2-3), pp. 144-157.

SHAYAN, G., SHULER, M.L. and LEE, K.H., 2011. The Effect of Astrocytes on the Induction of Barrier Properties in Aortic Endothelial Cells. *Biotechnology progress,* **27**(4), pp. 1137-1145.

SHAY-SALIT, A., SHUSHY, M., WOLFOVITZ, E., YAHAV, H., BREVIARIO, F., DEJANA, E. and RESNICK, N., 2002. VEGF receptor 2 and the adherens junction as a mechanical transducer in vascular endothelial cells. *Proceedings of the National Academy of Sciences of the United States of America,* **99**(14), pp. 9462-9467.

SHEN, H. and PERVAIZ, S., 2006. TNF receptor superfamily-induced cell death: redox-dependent execution. *Faseb Journal,* **20**(10), pp. 1589-1598.

SHEN, W., LI, S., CHUNG, S.H., ZHU, L., STAYT, J., SU, T., COURAUD, P., ROMERO, I.A., WEKSLER, B. and GILLIES, M.C., 2011. Tyrosine phosphorylation of VE-cadherin and claudin-5 is associated with TGF-beta 1-induced permeability of centrally derived vascular endothelium. *European journal of cell biology,* **90**(4), pp. 323-332.

SHIN, H.W., HSUEH, Y.P., YANG, F.C., KIM, E. and SHENG, M., 2000. An intramolecular interaction between Src homology 3 domain and guanylate kinase-like domain required for channel clustering by postsynaptic density-95/SAP90. *Journal of Neuroscience,* **20**(10), pp. 3580-3587.

SHLOSBERG, D., BENIFLA, M., KAUFER, D. and FRIEDMAN, A., 2010. Blood-brain barrier breakdown as a therapeutic target in traumatic brain injury. *Nature Reviews Neurology,* **6**(7), pp. 393-403.

SHOHAMI, E., NOVIKOV, M., BASS, R., YAMIN, A. and GALLILY, R., 1994. Closed-Head Injury Triggers Early Production of Tnf-Alpha and Il-6 by Brain-Tissue. *Journal of Cerebral Blood Flow and Metabolism,* **14**(4), pp. 615-619.

SHU, H.B., TAKEUCHI, M. and GOEDDEL, D.V., 1996. The tumor necrosis factor receptor 2 signal transducers TRAF2 and c-IAP1 are components of the tumor necrosis

factor receptor 1 signaling complex. *Proceedings of the National Academy of Sciences of the United States of America,* **93**(24), pp. 13973-13978.

SHYY, J.Y. and CHIEN, S., 2002. Role of integrins in endothelial mechanosensing of shear stress. *Circulation research,* **91**(9), pp. 769-775.

SIDDHARTHAN, V., KIM, Y.V., LIU, S. and KIM, K.S., 2007. Human astrocytes/astrocyte-conditioned medium and shear stress enhance the barrier properties of human brain microvascular endothelial cells. *Brain research,* **1147**, pp. 39-50.

SIMIONESCU, M., GHINEA, N., FIXMAN, A., LASSER, M., KUKES, L., SIMIONESCU, N. and PALADE, G.E., 1988. The Cerebral Microvasculature of the Rat - Structure and Luminal Surface-Properties during Early Development. *Journal of submicroscopic cytology and pathology,* **20**(2), pp. 243-261.

SIMPSON, J.E., NEWCOMBE, J., CUZNER, M.L. and WOODROOFE, M.N., 1998. Expression of monocyte chemoattractant protein-1 and other beta-chemokines by resident glia and inflammatory cells in multiple sclerosis lesions. *Journal of neuroimmunology,* **84**(2), pp. 238-249.

SINGER, C., ed, 1957. *A short history of anatomy and physiology from Greeks to Harvey.* New York: Dover Publications.

SLOT, K.B., BERGE, E., SANDERCOCK, P., LEWIS, S.C., DORMAN, P., DENNIS, M., OXFORDSHIRE COMMUNITY STROKE PROJE and INT STROKE TRIAL UK, 2009. Causes of Death by Level of Dependency at 6 Months After Ischemic Stroke in 3 Large Cohorts. *Stroke,* **40**(5), pp. 1585-1589.

SLOWIK, M.R., DELUCA, L.G., FIERS, W. and POBER, J.S., 1993. Tumor-Necrosis-Factor Activates Human Endothelial-Cells through the P55-Tumor Necrosis Factor-Receptor but the P75-Receptor Contributes to Activation at Low Tumor-Necrosis-Factor Concentration. *American Journal of Pathology,* **143**(6), pp. 1724-1730.

SMITH, M.L., LONG, D.S., DAMIANO, E.R. and LEY, K., 2003. Near-wall mu-PIV reveals a hydrodynamically relevant endothelial surface layer in venules in vivo. *Biophysical journal,* **85**(1), pp. 637-645.

SMITH, P.K., KROHN, R.I., HERMANSON, G.T., MALLIA, A.K., GARTNER, F.H., PROVENZANO, M.D., FUJIMOTO, E.K., GOEKE, N.M., OLSON, B.J. and KLENK, D.C., 1985. Measurement of Protein using Bicinchoninic Acid. *Analytical Biochemistry,* **150**(1), pp. 76-85.

SOBUE, K., YAMAMOTO, N., YONEDA, K., HODGSON, M.E., YAMASHIRO, K., TSURUOKA, N., TSUDA, T., KATSUYA, H., MIURA, Y., ASAI, K. and KATO, T., 1999. Induction of blood-brain barrier properties in immortalized bovine brain endothelial cells by astrocytic factors. *Neuroscience research,* **35**(2), pp. 155-164.

SOMA, T., CHIBA, H., KATO-MORI, Y., WADA, T., YAMASHITA, T., KOJIMA, T. and SAWADA, N., 2004. Thr(207) of claudin-5 is involved in size-selective loosening of the endothelial barrier by cyclic AMP. *Experimental cell research,* **300**(1), pp. 202-212.

SONG, L. and PACHTER, J.S., 2004. Monocyte chemoattractant protein-1 alters expression of tight junction-associated proteins in brain microvascular endothelial cells. *Microvascular research,* **67**(1), pp. 78-89.

SONG, X., ZENG, Y., YU, H., HU, J. and HAO, Y., 2001. The effect of fluid shear stress on ICAM-1 expression of rat brain microvascular endothelial cells. *Technology and health care : official journal of the European Society for Engineering and Medicine,* **9**(3), pp. 287-93.

SOTGIU, S., MURRIGHILE, M.R. and CONSTANTIN, G., 2010. Treatment of refractory epilepsy with natalizumab in a patient with multiple sclerosis. Case report. *Bmc Neurology,* **10**, pp. 84.

SPRING, K., CHABOT, C., LANGLOIS, S., LAPOINTE, L., NGUYEN THU NGAN TRINH, CARON, C., HEBDA, J.K., GAVARD, J., ELCHEBLY, M. and ROYAL, I., 2012. Tyrosine phosphorylation of DEP-1/CD148 as a mechanism controlling Src kinase activation, endothelial cell permeability, invasion, and capillary formation. *Blood,* **120**(13), pp. 2745-2756.

STADDON, J.M., HERRENKNECHT, K., SMALES, C. and RUBIN, L.L., 1995. Evidence that Tyrosine Phosphorylation may Increase Tight Junction Permeability. *Journal of cell science,* **108**, pp. 609-619.

STAHL, N., BOULTON, T.G., FARRUGGELLA, T., IP, N.Y., DAVIS, S., WITTHUHN, B.A., QUELLE, F.W., SILVENNOINEN, O., BARBIERI, G., PELLEGRINI, S., IHLE, J.N. and YANCOPOULOS, G.D., 1994. Association and Activation of Jak-Tyk Kinases by Cntf-Lif-Osm-Il-6 Beta-Receptor Components. *Science,* **263**(5143), pp. 92-95.

STAHL, N., FARRUGGELLA, T.J., BOULTON, T.G., ZHONG, Z., DARNELL, J.E. and YANCOPOULOS, G.D., 1995. Choice of Stats and Other Substrates Specified by Modular Tyrosine-Based Motifs in Cytokine Receptors. *Science,* **267**(5202), pp. 1349-1353.

STAMATOVIC, S.M., DIMITRIJEVIC, O.B., KEEP, R.F. and ANDJELKOVIC, A.V., 2006. Protein kinase C alpha-RhoA cross-talk in CCL2-induced alterations in brain endothelial permeability. *Journal of Biological Chemistry,* **281**(13), pp. 8379-8388.

STAMATOVIC, S.M., SHAKUI, P., KEEP, R.F., MOORE, B.B., KUNKEL, S.L., VAN ROOIJEN, N. and ANDJELKOVIC, A.V., 2005. Monocyte chemoattractant protein-1 regulation of blood-brain barrier permeability. *Journal of Cerebral Blood Flow and Metabolism,* **25**(5), pp. 593-606.

STAMATOVIC, S.M., KEEP, R.F. and ANDJELKOVIC, A.V., 2008. Brain endothelial cell-cell junctions: How to "Open" the blood brain barrier. *Current Neuropharmacology,* **6**(3), pp. 179-192.

STAMATOVIC, S.M., KEEP, R.F., WANG, M.M., JANKOVIC, I. and ANDJELKOVIC, A.V., 2009. Caveolae-mediated Internalization of Occludin and Claudin-5 during CCL2-induced Tight Junction Remodeling in Brain Endothelial Cells. *Journal of Biological Chemistry,* **284**(28), pp. 19053-19066.

STANNESS, K.A., WESTRUM, L.E., FORNACIARI, E., MASCAGNI, P., NELSON, J.A., STENGLEIN, S.G., MYERS, T. and JANIGRO, D., 1997. Morphological and functional

characterization of an in vitro blood-brain barrier model. *Brain research,* **771**(2), pp. 329-342.

STARLING, E., 1896. On the absorption of fluids from the connective tissue space. *The Journal of Physiology,* **19**, pp. 312.

STEINACKER, P., AITKEN, A. and OTTO, M., 2011. 14-3-3 Proteins in Neurodegeneration. *Seminars in cell & developmental biology,* **22**(7), pp. 696-704.

STEINBERG, D., 1997. Low density lipoprotein oxidation and its pathobiological significance. *Journal of Biological Chemistry,* **272**(34), pp. 20963-20966.

STEINHUBL, S.R., 2008. Why have antioxidants failed in clinical trials? *American Journal of Cardiology,* **101**(10A), pp. 14D-19D.

STERN, D.M., ESPOSITO, C., GERLACH, H., GERLACH, M., RYAN, J., HANDLEY, D. and NAWROTH, P., 1991. Endothelium and Regulation of Coagulation. *Diabetes care,* **14**(2), pp. 160-166.

STERPETTI, A.V., CUCINA, A., MORENA, A.R., DIDONNA, S., DANGELO, L.S., CAVALLARO, A. and STIPA, S., 1993. Shear-Stress Increases the Release of Interleukin-1 and Interleukin-6 by Aortic Endothelial-Cells. *Surgery,* **114**(5), pp. 911-914.

STEVENSON, B.R., ANDERSON, J.M., BRAUN, I.D. and MOOSEKER, M.S., 1989. Phosphorylation of the Tight-Junction Protein Zo-1 in 2 Strains of Madin-Darby Canine Kidney-Cells which Differ in Trans-Epithelial Resistance. *Biochemical Journal,* **263**(2), pp. 597-599.

STEVENSON, B.R. and BEGG, D.A., 1994. Concentration-Dependent Effects of Cytochalasin-D on Tight Junctions and Actin-Filaments in Mdck Epithelial-Cells. *Journal of cell science,* **107**, pp. 367-375.

STEVENSON, B.R., SILICIANO, J.D., MOOSEKER, M.S. and GOODENOUGH, D.A., 1986. Identification of Zo-i - a High-Molecular-Weight Polypeptide Associated with the Tight Junction (Zonula Occludens) in a Variety of Epithelia. *Journal of Cell Biology,* **103**(3), pp. 755-766.

STEWART, P.A. and WILEY, M.J., 1981. Developing Nervous-Tissue Induces Formation of Blood-Brain-Barrier Characteristics in Invading Endothelial-Cells - a Study using Quail-Chick Transplantation Chimeras. *Developmental biology,* **84**(1), pp. 183-192.

STONE, P.H., COSKUN, A.U., KINLAY, S., CLARK, M.E., SONKA, M., WAHLE, A., ILEGBUSI, O.J., YEGHIAZARIANS, Y., POPMA, J.J., ORAV, J., KUNTZ, R.E. and FELDMAN, C.L., 2003. Effect of endothelial shear stress on the progression of coronary artery disease, vascular remodeling, and in-stent restenosis in humans - In vivo 6-month follow-up study. *Circulation,* **108**(4), pp. 438-444.

STONE, P.H., COSKUN, A.U., YEGHIAZARIANS, Y., KINLAY, S., POPMA, J.J., KUNTZ, R.E. and FELDMAN, C.L., 2003. Prediction of sites of coronary atherosclerosis progression: In vivo profiling of endothelial shear stress, lumen, and outer vessel wall characteristics to predict vascular behavior. *Current opinion in cardiology,* **18**(6), pp. 458-470.

STUART, R.O., SUN, A., BUSH, K.T. and NIGAM, S.K., 1996. Dependence of epithelial intercellular junction biogenesis on thapsigargin-sensitive intracellular calcium stores. *Journal of Biological Chemistry,* **271**(23), pp. 13636-13641.

SUN, Y. and OBERLEY, L.W., 1996. Redox regulation of transcriptional activators. *Free Radical Biology and Medicine,* **21**(3), pp. 335-348.

SURAPISITCHAT, J., HOEFEN, R.J., PI, X.C., YOSHIZUMI, M., YAN, C. and BERK, B.C., 2001. Fluid shear stress inhibits TNF-alpha activation of JNK but not ERK1/2 or p38 in human umbilical vein endothelial cells: Inhibitory crosstalk among MAPK family members. *Proceedings of the National Academy of Sciences of the United States of America,* **98**(11), pp. 6476-6481.

SUZUKI, A., HIRATA, M., KAMIMURA, K., MANIWA, R., YAMANAKA, T., MIZUNO, K., KISHIKAWA, M., HIROSE, H., AMANO, Y., IZUMI, N., MIWA, Y. and OHNO, S., 2004. aPKC acts upstream of PAR-1b in both the establishment and maintenance of mammalian epithelial polarity. *Current Biology,* **14**(16), pp. 1425-1435.

SUZUKI, S., TANAKA, K., NOGAWA, S., NAGATA, E., ITO, D., DEMBO, T. and FUKUUCHI, Y., 1999. Temporal profile and cellular localization of interleukin-6 protein after focal cerebral ischemia in rats. *Journal of Cerebral Blood Flow and Metabolism,* **19**(11), pp. 1256-1262.

SUZUKI, S., TANAKA, K. and SUZUKI, N., 2009. Ambivalent aspects of interleukin-6 in cerebral ischemia: inflammatory versus neurotrophic aspects. *Journal of Cerebral Blood Flow and Metabolism,* **29**(3), pp. 464-479.

SWARTZ, K.R., LIU, F., SEWELL, D., SCHOCHET, T., CAMPBELL, I., SANDOR, M. and FABRY, Z., 2001. Interleukin-6 promotes post-traumatic healing in the central nervous system. *Brain research,* **896**(1-2), pp. 86-95.

SWEENEY, C., MORROW, D., BIRNEY, Y.A., COYLE, S., HENNESSY, C., SCHELLER, A., CUMMINS, P.M., WALLS, D., REDMOND, E.M. and CAHILL, P.A., 2004. Notch 1 and 3 receptors modulate vascular smooth muscle cell growth, apoptosis and migration via a CBF-1/RBP-Jk dependent pathway. *Faseb Journal,* **18**(10), pp. 1421-+.

TADDEI, A., GIAMPIETRO, C., CONTI, A., ORSENIGO, F., BREVIARIO, F., PIRAZZOLI, V., POTENTE, M., DALY, C., DIMMELER, S. and DEJANA, E., 2008. Endothelial adherens junctions control tight junctions by VE-cadherin-mediated upregulation of claudin-5. *Nature cell biology,* **10**(8), pp. 923-934.

TAGAMI, M., NARA, Y., KUBOTA, A., FUJINO, H. and YAMORI, Y., 1990. Ultrastructural-Changes in Cerebral Pericytes and Astrocytes of Stroke-Prone Spontaneously Hypertensive Rats. *Stroke,* **21**(7), pp. 1064-1071.

TAI, L.M., HOLLOWAY, K.A., MALE, D.K., LOUGHLIN, A.J. and ROMERO, I.A., 2010. Amyloid-beta-induced occludin down-regulation and increased permeability in human brain endothelial cells is mediated by MAPK activation. *Journal of Cellular and Molecular Medicine,* **14**(5), pp. 1101-1112.

TAKADA, Y., SHINKAI, F., KONDO, S., YAMAMOTO, S., TSUBOI, H., KORENAGA, R. and ANDO, J., 1994. Fluid Shear-Stress Increases the Expression of Thrombomodulin by

Cultured Human Endothelial-Cells. *Biochemical and biophysical research communications*, **205**(2), pp. 1345-1352.

TAKAHASHI, H., ITO, S., HANANO, M., WADA, K., NIWANO, H., SEKI, Y. and SHIBATA, A., 1992. Circulating Thrombomodulin as a Novel Endothelial-Cell Marker - Comparison of its Behavior with Vonwillebrand-Factor and Tissue-Type Plasminogen-Activator. *American Journal of Hematology*, **41**(1), pp. 32-39.

TAKAHASHI, M., ISHIDA, T., TRAUB, O., CORSON, M.A. and BERK, B.C., 1997. Mechanotransduction in endothelial cells: Temporal signaling events in response to shear stress. *Journal of vascular research*, **34**(3), pp. 212-219.

TAKASATO, Y., RAPOPORT, S.I. and SMITH, Q.R., 1984. An Insitu Brain Perfusion Technique to Study Cerebrovascular Transport in the Rat. *American Journal of Physiology*, **247**(3), pp. H484-H493.

TAKEICHI, M., 1995. Morphogenetic Roles of Classic Cadherins. *Current opinion in cell biology*, **7**(5), pp. 619-627.

TAKENAGA, Y., TAKAGI, N., MUROTOMI, K., TANONAKA, K. and TAKEO, S., 2009. Inhibition of Src activity decreases tyrosine phosphorylation of occludin in brain capillaries and attenuates increase in permeability of the blood-brain barrier after transient focal cerebral ischemia. *Journal of Cerebral Blood Flow and Metabolism*, **29**(6), pp. 1099-1108.

TAKENAGA, Y., TAKAGI, N., MUROTOMI, K., TANONAKA, K. and TAKEO, S., 2009. Inhibition of Src activity decreases tyrosine phosphorylation of occludin in brain capillaries and attenuates increase in permeability of the blood-brain barrier after transient focal cerebral ischemia. *Journal of Cerebral Blood Flow and Metabolism*, **29**(6), pp. 1099-1108.

TANAKA, T., NARAZAKI, M. and KISHIMOTO, T., 2012. Therapeutic Targeting of the Interleukin-6 Receptor. *Annual Review of Pharmacology and Toxicology, Vol 52*, **52**, pp. 199-219.

TANAKA, T., NARAZAKI, M. and KISHIMOTO, T., 2011. Anti-interleukin-6 receptor antibody, tocilizumab, for the treatment of autoimmune diseases. *FEBS letters*, **585**(23), pp. 3699-3709.

TANDON, V., BANO, G., KHAJURIA, V., PARIHAR, A. and GUPTA, S., 2005. Pleiotropic effects of statins. *Indian Journal of Pharmacology*, **37**(2), pp. 77-85.

TANG, S.J., SUEN, T.C., MCINNES, R.R. and BUCHWALD, M., 1998. Association of the TLX-2 homeodomain and 14-3-3 eta signaling proteins. *Journal of Biological Chemistry*, **273**(39), pp. 25356-25363.

TANSEY, M.G. and WYSS-CORAY, T., 2008. *Cytokines in CNS inflammation and disease.*

TAOCHENG, J.H., NAGY, Z. and BRIGHTMAN, M.W., 1987. Tight Junctions of Brain Endothelium in Vitro are Enhanced by Astroglia. *Journal of Neuroscience*, **7**(10), pp. 3293-3299.

TARDY, Y., RESNICK, N., NAGEL, T., GIMBRONE, M.A. and DEWEY, C.F., 1997. Shear stress gradients remodel endothelial monolayers in vitro via a cell proliferation-migration-loss cycle. *Arteriosclerosis Thrombosis and Vascular Biology,* **17**(11), pp. 3102-3106.

TARKOWSKI, E., BLENNOW, K., WALLIN, A. and TARKOWSKI, A., 1999. Intracerebral production of tumor necrosis factor-alpha, a local neuroprotective agent, in Alzheimer disease and vascular dementia. *Journal of clinical immunology,* **19**(4), pp. 223-230.

TARKOWSKI, E., ROSENGREN, L., BLOMSTRAND, C., WIKKELSO, C., JENSEN, C., EKHOLM, S. and TARKOWSKI, A., 1995. Early Intrathecal Production of Interleukin-6 Predicts the Size of Brain Lesion in Stroke. *Stroke,* **26**(8), pp. 1393-1398.

TARTAGLIA, L.A., AYRES, T.M., WONG, G.H.W. and GOEDDEL, D.V., 1993. A Novel Domain within the 55 Kd Tnf Receptor Signals Cell-Death. *Cell,* **74**(5), pp. 845-853.

TARTAGLIA, L.A., PENNICA, D. and GOEDDEL, D.V., 1993. Ligand Passing - the 75-Kda Tumor-Necrosis-Factor (Tnf) Receptor Recruits Tnf for Signaling by the 55-Kda Tnf Receptor. *Journal of Biological Chemistry,* **268**(25), pp. 18542-18548.

TARTAGLIA, L.A., ROTHE, M., HU, Y.F. and GOEDDEL, D.V., 1993. Tumor Necrosis Factors Cytotoxic Activity is Signaled by the P55 Tnf Receptor. *Cell,* **73**(2), pp. 213-216.

TATSUTA, T., NAITO, M., OHHARA, T., SUGAWARA, I. and TSURUO, T., 1992. Functional Involvement of P-Glycoprotein in Blood-Brain-Barrier. *Journal of Biological Chemistry,* **267**(28), pp. 20383-20391.

TAUPIN, V., TOULMOND, S., SERRANO, A., BENAVIDES, J. and ZAVALA, F., 1993. Increase in Il-6, Il-1 and Tnf Levels in Rat-Brain Following Traumatic Lesion - Influence of Pre-Traumatic and Posttraumatic Treatment with Ro5 4864, a Peripheral-Type (P-Site) Benzodiazepine Ligand. *Journal of neuroimmunology,* **42**(2), pp. 177-185.

TAYLOR, C.W., 1990. The Role of G-Proteins in Transmembrane Signaling. *Biochemical Journal,* **272**(1), pp. 1-13.

TCHELINGERIAN, J.L., LESAUX, F. and JACQUE, C., 1996. Identification and topography of neuronal cell populations expressing TNF alpha and IL-1 alpha in response to hippocampal lesion. *Journal of neuroscience research,* **43**(1), pp. 99-106.

THE NEUROTECHNOLOGY INDUSTRY REPORT, 2009. *The Neurotechnology Industry Report 2009: Drugs, Devices and Diagnostics for the Brain and Nervous System, Market Analysis and Strategic Investment Guide of the Global Neurological Disease and Psychiatric Illness Markets.* 2009. NeuroInsights.

THOMA, R., 1893. *Untersuchungen uber die Histogenese und Histomechanikdes Gefasssytems.* Stuttgart: Ferdinand Enke.

THORIN, E. and THORIN-TRESCASES, N., 2009. Vascular endothelial ageing, heartbeat after heartbeat. *Cardiovascular research,* **84**(1), pp. 24-32.

TIAN, S., BAI, Y., YANG, L., WANG, X., WU, Y., JIA, J., ZHU, Y., CHENG, Y., ZHANG, P., WU, J., WANG, N., XIA, G., LIAO, H., ZHANG, Y., SHEN, X., YU, H. and

HU, Y., 2013. Shear Stress Inhibits Apoptosis of Ischemic Brain Microvascular Endothelial Cells. *International Journal of Molecular Sciences,* **14**(1), pp. 1412-1427.

TILLING, T., KORTE, D., HOHEISEL, D. and GALLA, H.J., 1998. Basement membrane proteins influence brain capillary endothelial barrier function in vitro. *Journal of neurochemistry,* **71**(3), pp. 1151-1157.

TOBIUME, K., MATSUZAWA, A., TAKAHASHI, T., NISHITOH, H., MORITA, K., TAKEDA, K., MINOWA, O., MIYAZONO, K., NODA, T. and ICHIJO, H., 2001. ASK1 is required for sustained activations of JNK/p38 MAP kinases and apoptosis. *EMBO reports,* **2**(3), pp. 222-228.

TONG, X.K. and HAMEL, E., 1999. Regional cholinergic denervation of cortical microvessels and nitric oxide synthase-containing neurons in Alzheimer's disease. *Neuroscience,* **92**(1), pp. 163-175.

TORTORA, G.J. and DERRICKSON, B., 2007. *Principles of Anatomy and Physiology, Atlas and Registration Card.* 11 edn. New York: John Wiley & Sons.

TOWBIN, H., STAEHELIN, T. and GORDON, J., 1979. Electrophoretic Transfer of Proteins from Polyacrylamide Gels to Nitrocellulose Sheets - Procedure and some Applications. *Proceedings of the National Academy of Sciences of the United States of America,* **76**(9), pp. 4350-4354.

TOWNSLEY, M.I., 2012. Structure and Composition of Pulmonary Arteries, Capillaries, and Veins. *Comprehensive Physiology,* **2**(1), pp. 675-709.

TOYOOKA, K., MURATAKE, T., TANAKA, T., IGARASHI, S., WATANABE, H., TAKEUCHI, H., HAYASHI, S., MAEDA, M., TAKAHASHI, M., TSUJI, S., KUMANISHI, T. and TAKAHASHI, Y., 1999. 14-3-3 protein eta chain gene (YWHAH) polymorphism and its genetic association with schizophrenia. *American Journal of Medical Genetics,* **88**(2), pp. 164-167.

TRAUB, O. and BERK, B.C., 1998. Laminar shear stress - Mechanisms by which endothelial cells transduce an atheroprotective force. *Arteriosclerosis Thrombosis and Vascular Biology,* **18**(5), pp. 677-685.

TRONC, F., WASSEF, M., ESPOSITO, B., HENRION, D., GLAGOV, S. and TEDGUI, A., 1996. Role of NO in flow-induced remodeling of the rabbit common carotid artery. *Arteriosclerosis Thrombosis and Vascular Biology,* **16**(10), pp. 1256-1262.

TSAO, N., HSU, H.P., WU, C.M., LIU, C.C. and LEI, H.Y., 2001. Tumour necrosis factor-alpha causes an increase in blood-brain barrier permeability during sepsis. *Journal of medical microbiology,* **50**(9), pp. 812-821.

TSAO, P.S., BUITRAGO, R., CHAN, J.R. and COOKE, J.P., 1996. Fluid flow inhibits endothelial adhesiveness - Nitric oxide and transcriptional regulation of VCAM-1. *Circulation,* **94**(7), pp. 1682-1689.

TSUCHIDA, A., SALEM, H., THOMSON, N. and HANCOCK, W.W., 1992. Tumor-Necrosis-Factor Production during Human Renal-Allograft Rejection is Associated with Depression of Plasma Protein-C and Free Protein-S Levels and Decreased Intragraft Thrombomodulin Expression. *Journal of Experimental Medicine,* **175**(1), pp. 81-90.

TSUKAMOTO, T. and NIGAM, S.K., 1999. Role of tyrosine phosphorylation in the reassembly of occludin and other tight junction proteins. *American Journal of Physiology-Renal Physiology,* **276**(5), pp. F737-F750.

TSUKITA, S. and FURUSE, M., 2000. The structure and function of claudins, cell adhesion molecules at tight junctions. *Epithelial Transport and Barrier Function: Pathomechanisms in Gastrointestinal Disorders,* **915**, pp. 129-135.

TSUKITA, S. and FURUSE, M., 1999. Occludin and claudins in tight-junction strands: leading or supporting players? *Trends in cell biology,* **9**(7), pp. 268-273.

TSUKITA, S., OISHI, K., AKIYAMA, T., YAMANASHI, Y., YAMAMOTO, T. and TSUKITA, S., 1991. Specific Protooncogenic Tyrosine Kinases of Src Family are Enriched in Cell-To-Cell Adherens Junctions Where the Level of Tyrosine Phosphorylation is Elevated. *Journal of Cell Biology,* **113**(4), pp. 867-879.

TUCKER, I.G., YANG, L. and MUJOO, H., 2012. Delivery of drugs to the brain via the blood brain barrier using colloidal carriers. *Journal of microencapsulation,* **29**(5), pp. 475-486.

TZIMA, E., DEL POZO, M.A., KIOSSES, W.B., MOHAMED, S.A., LI, S., CHIEN, S. and SCHWARTZ, M.A., 2002. Activation of Rac1 by shear stress in endothelial cells mediates both cytoskeletal reorganization and effects on gene expression. *Embo Journal,* **21**(24), pp. 6791-6800.

TZIMA, E., IRANI-TEHRANI, M., KIOSSES, W.B., DEJANA, E., SCHULTZ, D.A., ENGELHARDT, B., CAO, G.Y., DELISSER, H. and SCHWARTZ, M.A., 2005. A mechanosensory complex that mediates the endothelial cell response to fluid shear stress. *Nature,* **437**(7057), pp. 426-431.

TZIMA, E., KIOSSES, W.B., DEL POZO, M.A. and SCHWARTZ, M.A., 2003. Localized Cdc42 activation, detected using a novel assay, mediates microtubule organizing center positioning in endothelial cells in response to fluid shear stress. *Journal of Biological Chemistry,* **278**(33), pp. 31020-31023.

TZIMA, E., READER, J.S., IRANI-TEHRANI, M., EWALT, K.L., SCHWARTZ, M.A. and SCHIMMEL, P., 2003. Biologically active fragment of a human tRNA synthetase inhibits fluid shear stress-activated responses of endothelial cells. *Proceedings of the National Academy of Sciences of the United States of America,* **100**(25), pp. 14903-14907.

ULICH, T.R., YIN, S.M., GUO, K.Z., YI, E.H.S., REMICK, D. and DELCASTILLO, J., 1991. Intratracheal Injection of Endotoxin and Cytokines .2. Interleukin-6 and Transforming Growth-Factor-Beta Inhibit Acute-Inflammation. *American Journal of Pathology,* **138**(5), pp. 1097-1101.

USUI, M., EGASHIRA, K., TOMITA, H., KOYANAGI, M., KATOH, M., SHIMOKAWA, H., TAKEYA, M., YOSHIMURA, T., MATSUSHIMA, K. and TAKESHITA, A., 2000. Important role of local angiotensin II activity mediated via type 1 receptor in the pathogenesis of cardiovascular inflammatory changes induced by chronic blockade of nitric oxide synthesis in rats. *Circulation,* **101**(3), pp. 305-310.

VALERIA PEREZ, C., MARCELO SOBARZO, C., VERONICA JACOBO, P., HERMINIA PELLIZZARI, E., BEATRIZ CIGORRAGA, S., DENDUCHIS, B. and

LUSTIG, L., 2012. Loss of Occludin Expression and Impairment of Blood-Testis Barrier Permeability in Rats with Autoimmune Orchitis: Effect of Interleukin 6 on Sertoli Cell Tight Junctions. *Biology of reproduction,* **87**(5), pp. 122.

VALKO, M., LEIBFRITZ, D., MONCOL, J., CRONIN, M.T.D., MAZUR, M. and TELSER, J., 2007. Free radicals and antioxidants in normal physiological functions and human disease. *International Journal of Biochemistry & Cell Biology,* **39**(1), pp. 44-84.

VALLANCE, P., COLLIER, J. and MONCADA, S., 1989. Effects of Endothelium-Derived Nitric-Oxide on Peripheral Arteriolar Tone in Man. *Lancet,* **2**(8670), pp. 997-1000.

VAN ASSEMA, D.M.E., LUBBERINK, M., BAUER, M., VAN DER FLIER, W.M., SCHUIT, R.C., WINDHORST, A.D., COMANS, E.F.I., HOETJES, N.J., TOLBOOM, N., LANGER, O., MULLER, M., SCHELTENS, P., LAMMERTSMA, A.A. and VAN BERCKEL, B.N.M., 2012. Blood-brain barrier P-glycoprotein function in Alzheimer's disease. *Brain,* **135**(1), pp. 181.

VAN BROECK, B., VAN BROECKHOVEN, C. and KUMAR-SINGH, S., 2007. Current insights into molecular mechanisms of Alzheimer disease and their implications for therapeutic approaches. *Neurodegenerative Diseases,* **4**(5), pp. 349-365.

VAN DEN BERGHE, W., VERMEULEN, L., DE WILDE, G., DE BOSSCHER, K., BOONE, E. and HAEGEMAN, G., 2000. Signal transduction by tumor necrosis factor and gene regulation of the inflammatory cytokine interleukin-6. *Biochemical pharmacology,* **60**(8), pp. 1185-1195.

VAN DER WAL, A.C. and BECKER, A.E., 1999. Atherosclerotic plaque rupture - pathologic basis of plaque stability and instability. *Cardiovascular research,* **41**(2), pp. 334-344.

VAN HEMERT, M.J., DE STEENSMA, H.Y. and VAN HEUSDEN, G.P.H., 2001. 14-3-3 Proteins: Key Regulators of Cell Division, Signalling and Apoptosis. *Bioessays,* **23**(10), pp. 936-946.

VAN HEUSDEN, G.P.H., 2005. 14-3-3 proteins: Regulators of numerous eukaryotic proteins. *IUBMB life,* **57**(9), pp. 623-629.

VAN HINSBERGH, V. and AMERONGEN, G., 2002. Intracellular signalling involved in modulating human endothelial barrier function. *Journal of anatomy,* **200**(6), pp. 549-560.

VAN VLIET, E.A., ARAUJO, S.D.C., REDEKER, S., VAN SCHAIK, R., ARONICA, E. and GORTER, J.A., 2007. Blood-brain barrier leakage may lead to progression of temporal lobe epilepsy. *Brain,* **130**, pp. 521-534.

VAN WAGONER, N.J. and BENVENISTE, E.N., 1999. Interleukin-6 expression and regulation in astrocytes. *Journal of neuroimmunology,* **100**(1-2), pp. 124-139.

VANDEURS, B. and AMTORP, O., 1978. Blood-Brain-Barrier in Rats to Hemepeptide Microperoxidase. *Neuroscience,* **3**(8), pp. 737-748.

VANZWIETEN, E.J., RAVID, R., SWAAB, D.F. and VANDERWOUDE, T., 1988. Immunocytochemically Stained Vasopressin Binding-Sites on Blood-Vessels in the Rat-Brain. *Brain research,* **474**(2), pp. 369-373.

VAUCHER, E. and HAMEL, E., 1995. Cholinergic Basal Forebrain Neurons Project to Cortical Microvessels in the Rat - Electron-Microscopic Study with Anterogradely Transported Phaseolus-Vulgaris-Leukoagglutinin and Choline-Acetyltransferase Immunocytochemistry. *Journal of Neuroscience,* **15**(11), pp. 7427-7441.

VEERHUIS, R., HOOZEMANS, J., JANSSEN, I., BOSHUIZEN, R., LANGEVELD, J. and EIKELENBOOM, P., 2002. Adult human microglia secrete cytokines when exposed to neurotoxic prion protein peptide: no intermediary role for prostaglandin E-2. *Brain research,* **925**(2), pp. 195-203.

VERMA, S., NAKAOKE, R., DOHGU, S. and BANKS, W.A., 2006. Release of cytokines by brain endothelial cells: A polarized response to lipopolysaccharide. *Brain Behavior and Immunity,* **20**(5), pp. 449-455.

VEZZANI, A., BALOSSO, S. and RAVIZZA, T., 2008. The role of cytokines in the pathophysiology of epilepsy. *Brain Behavior and Immunity,* **22**(6), pp. 797-803.

VILA, N., CASTILLO, J., DAVALOS, A. and CHAMORRO, A., 2000. Proinflammatory cytokines and early neurological worsening in ischemic stroke. *Stroke,* **31**(10), pp. 2325-2329.

VINCENT, P.A., XIAO, K.Y., BUCKLEY, K.M. and KOWALCZYK, A.P., 2004. VE-cadherin: adhesion at arm's length. *American Journal of Physiology-Cell Physiology,* **286**(5), pp. C987-C997.

VINCENZ, C. and DIXIT, V.M., 1996. 14-3-3 proteins associate with A20 in an isoform-specific manner and function both as chaperone and adapter molecules. *Journal of Biological Chemistry,* **271**(33), pp. 20029-20034.

VINK, H. and DULING, B.R., 2000. Capillary endothelial surface layer selectively reduces plasma solute distribution volume. *American Journal of Physiology-Heart and Circulatory Physiology,* **278**(1), pp. H285-H289.

VIVIANI, B., BARTESAGHI, S., CORSINI, E., GALLI, C.L. and MARINOVICH, M., 2004. Cytokines role in neurodegenerative events. *Toxicology letters,* **149**(1-3), pp. 85-89.

VON ROCKLINGHAUSEN, F., 1860. Eine method, mikroskopische hohle und solide gebilde voneinander zu unterscheiden. *Virckow Arch,* **19**(451),.

WAJANT, H., PFIZENMAIER, K. and SCHEURICH, P., 2003. Tumor necrosis factor signaling. *Cell death and differentiation,* **10**(1), pp. 45-65.

WALLACH, D., VARFOLOMEEV, E.E., MALININ, N.L., GOLTSEV, Y.V., KOVALENKO, A.V. and BOLDIN, M.P., 1999. Tumor necrosis factor receptor and Fas signaling mechanisms. *Annual Review of Immunology,* **17**, pp. 331-367.

WALSH, T.G., MURPHY, R.P., FITZPATRICK, P., ROCHFORT, K.D., GUINAN, A.F., MURPHY, A. and CUMMINS, P.M., 2011. Stabilization of Brain Microvascular Endothelial Barrier Function by Shear Stress Involves VE-Cadherin Signaling Leading to Modulation of pTyr-Occludin Levels. *Journal of cellular physiology,* **226**(11), pp. 3053-3063.

WALSH, T.G., MURPHY, R.P., FITZPATRICK, P., ROCHFORT, K.D., GUINAN, A.F., MURPHY, A. and CUMMINS, P.M., 2011. Stabilization of Brain Microvascular Endothelial Barrier Function by Shear Stress Involves VE-Cadherin Signaling Leading to Modulation of pTyr-Occludin Levels. *Journal of cellular physiology,* **226**(11), pp. 3053-3063.

WANG, B.C., YANG, H.Z., LIU, Y.C., JELINEK, T., ZHANG, L.X., RUOSLAHTI, E. and FU, H., 1999. Isolation of high-affinity peptide antagonists of 14-3-3 proteins by phage display. *Biochemistry,* **38**(38), pp. 12499-12504.

WANG, H., NAWATA, J., KAKUDO, N., SUGIMURA, K., SUZUKI, J., SAKUMA, M., IKEDA, J. and SHIRATO, K., 2004. The upregulation of ICAM-1 and P-selectin requires high blood pressure but not circulating renin-angiotensin system in vivo. *Journal of hypertension,* **22**(7), pp. 1323-1332.

WANG, H., YOUNG, S.R., GERARD-O'RILEY, R., HUM, J.M., YANG, Z., BIDWELL, J.P. and PAVALKO, F.M., 2011. Blockade of TNFR1 Signaling: A Role of Oscillatory Fluid Shear Stress in Osteoblasts. *Journal of cellular physiology,* **226**(4), pp. 1044-1051.

WANG, H.D., PAGANO, P.J., DU, Y., CAYATTE, A.J., QUINN, M.T., BRECHER, P. and COHEN, R.A., 1998. Superoxide anion from the adventitia of the rat thoracic aorta inactivates nitric oxide. *Circulation research,* **82**(7), pp. 810-818.

WANG, J., SUN, L., SI, Y. and LI, B., 2012. Overexpression of actin-depolymerizing factor blocks oxidized low-density lipoprotein-induced mouse brain microvascular endothelial cell barrier dysfunction. *Molecular and cellular biochemistry,* **371**(1-2), pp. 1-8.

WANG, L., TRAN, N.D., KITTAKA, M., FISHER, M.J., SCHREIBER, S.S. and ZLOKOVIC, B.V., 1997. Thrombomodulin expression in bovine brain capillaries - Anticoagulant function of the blood-brain barrier, regional differences, and regulatory mechanisms. *Arteriosclerosis Thrombosis and Vascular Biology,* **17**(11), pp. 3139-3146.

WANG, W., LV, S., ZHOU, Y., FU, J., LI, C. and LIU, P., 2011. Tumor necrosis factor-alpha affects blood-brain barrier permeability in acetaminophen-induced acute liver failure. *European journal of gastroenterology & hepatology,* **23**(7), pp. 552-558.

WANG, W. and SHAKES, D., 1996. Molecular evolution of the 14-3-3 protein family. *Journal of Molecular Evolution,* **43**(4), pp. 384-398.

WARE, C.F., VANARSDALE, S. and VANARSDALE, T.L., 1996. Apoptosis mediated by the TNF-related cytokine and receptor families. *Journal of cellular biochemistry,* **60**(1), pp. 47-55.

WARE, C., 2005. Network communications: Lymphotoxins, LIGHT, and TNF. *Annual Review of Immunology,* **23**, pp. 787-819.

WASSERMAN, S.M. and TOPPER, J.N., 2004. Adaptation of the endothelium to fluid flow: in vitro analyses of gene expression and in vivo implications. *Vascular Medicine,* **9**(1), pp. 35-45.

WATABE-UCHIDA, M., UCHIDA, N., IMAMURA, Y., NAGAFUCHI, A., FUJIMOTO, K., UEMURA, T., VERMEULEN, S., VAN ROY, F., ADAMSON, E.D. and TAKEICHI,

M., 1998. Alpha-Catenin-Vinculin Interaction Functions to Organize the Apical Junctional Complex in Epithelial Cells. *Journal of Cell Biology,* **142**(3), pp. 847-857.

WEBER, C., ERL, W., PIETSCH, A., STROBEL, M., ZIEGLERHEITBROCK, H.W.L. and WEBER, P.C., 1994. Antioxidants Inhibit Monocyte Adhesion by Suppressing Nuclear Factor-Kappa-B Mobilization and Induction of Vascular Cell-Adhesion Molecule-1 in Endothelial-Cells Stimulated to Generate Radicals. *Arteriosclerosis and Thrombosis,* **14**(10), pp. 1665-1673.

WEBER, N., BLUMENTHAL, S., HARTUNG, T., VOLLMAR, A. and KIEMER, A., 2003. ANP inhibits TNF-alpha-induced endothelial MCP-1 expression - involvement of p38 MAPK and MKP-1. *Journal of leukocyte biology,* **74**(5), pp. 932-941.

WEBERSINKE, G., BAUER, H., AMBERGER, A., ZACH, O. and BAUER, H.C., 1992. Comparison of Gene-Expression of Extracellular-Matrix Molecules in Brain Microvascular Endothelial-Cells and Astrocytes. *Biochemical and biophysical research communications,* **189**(2), pp. 877-884.

WECHEZAK, A.R., WIGHT, T.N., VIGGERS, R.F. and SAUVAGE, L.R., 1989. Endothelial Adherence Under Shear-Stress is Dependent upon Microfilament Reorganization. *Journal of cellular physiology,* **139**(1), pp. 136-146.

WEINBAUM, S., ZHANG, X.B., HAN, Y.F., VINK, H. and COWIN, S.C., 2003. Mechanotransduction and flow across the endothelial glycocalyx. *Proceedings of the National Academy of Sciences of the United States of America,* **100**(13), pp. 7988-7995.

WEINBAUM, S., TARBELL, J.M. and DAMIANO, E.R., 2007. The structure and function of the endothelial glycocalyx layer. *Annual Review of Biomedical Engineering,* **9**, pp. 121-167.

WEKERLE, H. and HOHLFELD, R., 2003. Molecular mimicry in multiple sclerosis. *New England Journal of Medicine,* **349**(2), pp. 185-186.

WEKSLER, B.B., SUBILEAU, E.A., PERRIERE, N., CHARNEAU, P., HOLLOWAY, K., LEVEQUE, M., TRICOIRE-LEIGNEL, H., NICOTRA, A., BOURDOULOUS, S., TUROWSKI, P., MALE, D.K., ROUX, F., GREENWOOD, J., ROMERO, I.A. and COURAUD, P.O., 2005. Blood-brain barrier-specific properties of a human adult brain endothelial cell line. *Faseb Journal,* **19**(11), pp. 1872-+.

WESTERGAARD, E. and BRIGHTMAN, M.W., 1973. Transport of Proteins Across Normal Cerebral Arterioles. *Journal of Comparative Neurology,* **152**(1), pp. 17-44.

WHITE, C.R., HAIDEKKER, M., BAO, X.P. and FRANGOS, J.A., 2001. Temporal gradients in shear, but not spatial gradients, stimulate endothelial cell proliferation. *Circulation,* **103**(20), pp. 2508-2513.

WIELAND, T. and MITTMANN, C., 2003. Regulators of G-protein signalling: multifunctional proteins with impact on signalling in the cardiovascular system. *Pharmacology & therapeutics,* **97**(2), pp. 95-115.

WILKER, E. and YAFFE, M.B., 2004. 14-3-3 Proteins - a focus on cancer and human disease. *Journal of Molecular and Cellular Cardiology,* **37**(3), pp. 633-642.

WILKER, E.W., GRANT, R.A., ARTIM, S.C. and YAFFE, M.B., 2005. A structural basis for 14-3-3 sigma functional specificity. *Journal of Biological Chemistry,* **280**(19), pp. 18891-18898.

WILLIS, C.L., NOLAN, C.C., REITH, S.N., LISTER, T., PRIOR, M.J.W., GUERIN, C.J., MAVROUDIS, G. and RAY, D.E., 2004. Focal astrocyte loss is followed by microvascular damage, with subsequent repair of the blood-brain barrier in the apparent absence of direct astrocytic contact. *Glia,* **45**(4), pp. 325-337.

WILLIS, C.L., MESKE, D.S. and DAVIS, T.P., 2010. Protein kinase C activation modulates reversible increase in cortical blood-brain barrier permeability and tight junction protein expression during hypoxia and posthypoxic reoxygenation. *Journal of Cerebral Blood Flow and Metabolism,* **30**(11), pp. 1847-1859.

WINSTON, B.W., LANGECARTER, C.A., GARDNER, A.M., JOHNSON, G.L. and RICHES, D.W.H., 1995. Tumor-Necrosis-Factor-Alpha Rapidly Activates the Mitogen-Activated Protein-Kinase (Mapk) Cascade in a Mapk Kinase Kinase-Dependent, C-Raf-1-Independent Fashion in Mouse Macrophages. *Proceedings of the National Academy of Sciences of the United States of America,* **92**(5), pp. 1614-1618.

WINYARD, P.G. and BLAKE, D.R., 1997. Antioxidants, redox-regulated transcription factors, and inflammation. *Advances in Pharmacology (San Diego, Calif.),* **38**, pp. 403-421.

WITT, K.A., MARK, K.S., HOM, S. and DAVIS, T.P., 2003. Effects of hypoxia-reoxygenation on rat blood-brain barrier permeability and tight junctional protein expression. *American Journal of Physiology-Heart and Circulatory Physiology,* **285**(6), pp. H2820-H2831.

WITT, K.A., MARK, K.S., HOM, S. and DAVIS, T.P., 2003. Effects of hypoxia-reoxygenation on rat blood-brain barrier permeability and tight junctional protein expression. *American Journal of Physiology-Heart and Circulatory Physiology,* **285**(6), pp. H2820-H2831.

WITT, K.A., MARK, K.S., SANDOVAL, K.E. and DAVIS, T.P., 2008. Reoxygenation stress on blood-brain barrier paracellular permeability and edema in the rat. *Microvascular research,* **75**(1), pp. 91-96.

WOLBURG, H., NEUHAUS, J., KNIESEL, U., KRAUSS, B., SCHMID, E.M., OCALAN, M., FARRELL, C. and RISAU, W., 1994. Modulation of Tight Junction Structure in Blood-Brain-Barrier Endothelial-Cells - Effects of Tissue-Culture, 2nd Messengers and Cocultured Astrocytes. *Journal of cell science,* **107**, pp. 1347-1357.

WOLBURG, H., WOLBURG-BUCHHOLZ, K., KRAUS, J., RASCHER-EGGSTEIN, G., LIEBNER, S., HAMM, S., DUFFNER, F., GROTE, E.H., RISAU, W. and ENGELHARDT, B., 2003. Localization of claudin-3 in tight junctions of the blood-brain barrier is selectively lost during experimental autoimmune encephalomyelitis and human glioblastoma multiforme. *Acta Neuropathologica,* **105**(6), pp. 586-592.

WONG, E.W.P., SUN, S., LI, M.W.M., LEE, W.M. and CHENG, C.Y., 2009. 14-3-3 Protein Regulates Cell Adhesion in the Seminiferous Epithelium of Rat Testes. *Endocrinology,* **150**(10), pp. 4713-4723.

WOOD, K.C., HEBBEL, R.P. and GRANGER, D.N., 2005. Endothelial cell NADPH oxidase mediates the cerebral microvascular dysfunction in sickle cell transgenic mice. *Faseb Journal,* **19**(3), pp. 989-+.

WOODROOFE, M.N., SARNA, G.S., WADHWA, M., HAYES, G.M., LOUGHLIN, A.J., TINKER, A. and CUZNER, M.L., 1991. Detection of Interleukin-1 and Interleukin-6 in Adult-Rat Brain, Following Mechanical Injury, by Invivo Microdialysis - Evidence of a Role for Microglia in Cytokine Production. *Journal of neuroimmunology,* **33**(3), pp. 227-236.

WOSIK, K., BIERNACKI, K., KHOUZAM, M. and PRAT, A., 2007. Death receptor expression and function at the human blood brain barrier. *Journal of the neurological sciences,* **259**(1-2), pp. 53-60.

WOSIK, K., CAYROL, R., DODELET-DEVILLERS, A., BERTHELET, F., BERNARD, M., MOUMDJIAN, R., BOUTHILLIER, A., REUDELHUBER, T.L. and PRAT, A., 2007. Angiotensin II controls occludin function and is required for blood-brain barrier maintenance: Relevance to multiple sclerosis. *Journal of Neuroscience,* **27**(34), pp. 9032-9042.

WOYWODT, A., BAHLMANN, F.H., DE GROOT, K., HALLER, H. and HAUBITZ, M., 2002. Circulating endothelial cells: life, death, detachment and repair of the endothelial cell layer. *Nephrology Dialysis Transplantation,* **17**(10), pp. 1728-1730.

WU, J.H., HAGAMAN, J., KIM, S., REDDICK, R.L. and MAEDA, N., 2002. Aortic constriction exacerbates atherosclerosis and induces cardiac dysfunction in mice lacking apolipoprotein E. *Arteriosclerosis Thrombosis and Vascular Biology,* **22**(3), pp. 469-475.

WU, Q.Y., DROUET, L., CARRIER, J.L., ROTHSCHILD, C., BERARD, M., ROUAULT, C., CAEN, J.P. and MEYER, D., 1987. Differential Distribution of Vonwillebrand-Factor in Endothelial-Cells - Comparison between Normal Pigs and Pigs with Vonwillebrand Disease. *Arteriosclerosis,* **7**(1), pp. 47-54.

WUNG, B.S., CHENG, J.J., HSIEH, H.J., SHYY, Y.J. and WANG, D.L., 1997. Cyclic strain-induced monocyte chemotactic protein-1 gene expression in endothelial cells involves reactive oxygen species activation of activator protein 1. *Circulation research,* **81**(1), pp. 1-7.

XAIO, H.P., BANKS, W.A., NIEHOFF, M.L. and MORLEY, J.E., 2001. Effect of LPS on the permeability of the blood-brain barrier to insulin. *Brain research,* **896**(1-2), pp. 36-42.

XANTHOS, D.N., PUENGEL, I., WUNDERBALDINGER, G. and SANDKUEHLER, J., 2012. Effects of peripheral inflammation on the blood-spinal cord barrier. *Molecular Pain,* **8**, pp. 44.

XIAO, B., SMERDON, S.J., JONES, D.H., DODSON, G.G., SONEJI, Y., AITKEN, A. and GAMBLIN, S.J., 1995. Structure of a 14-3-3 Protein and Implications for Coordination of Multiple Signaling Pathways. *Nature,* **376**(6536), pp. 188-191.

XING, Z., GAULDIE, J., COX, G., BAUMANN, H., JORDANA, M., LEI, X.F. and ACHONG, M.K., 1998. IL-6 is an antiinflammatory cytokine required for controlling local or systemic acute inflammatory responses. *Journal of Clinical Investigation,* **101**(2), pp. 311-320.

XU, M., WATERS, C.L., HU, C., WYSOLMERSKI, R.B., VINCENT, P.A. and MINNEAR, F.L., 2007. Sphingosine 1-phosphate rapidly increases endothelial barrier function independently of VE-cadherin but requires cell spreading and Rho kinase. *American Journal of Physiology-Cell Physiology*, **293**(4), pp. C1309-C1318.

YAFFE, M., 2002. How do 14-3-3 proteins work? - Gatekeeper phosphorylation and the molecular anvil hypothesis. *FEBS letters*, **513**(1), pp. 53-57.

YAMAGAMI, H., KITAGAWA, K., NAGAI, Y., HOUGAKU, H., SAKAGUCHI, M., KUWABARA, K., KONDO, K., MASUYAMA, T., MATSUMOTO, M. and HORI, M., 2004. Higher levels of interleukin-6 are associated with lower echogenicity of carotid artery plaques. *Stroke*, **35**(3), pp. 677-681.

YAMAGISHI, S.I., INAGAKI, Y., NAKAMURA, K., ABE, R., SHIMIZU, T., YOSHIMURA, A. and IMAIZUMI, T., 2004. Pigment epithelium-derived factor inhibits TNF-alpha-induced interleukin-6 expression in endothelial cells by suppressing NADPH oxidase-mediated reactive oxygen species generation. *Journal of Molecular and Cellular Cardiology*, **37**(2), pp. 497-506.

YAMAMOTO, M., RAMIREZ, S.H., SATO, S., KIYOTA, T., CERNY, R.L., KAIBUCHI, K., PERSIDSKY, Y. and IKEZU, T., 2008. Phosphorylation of claudin-5 and occludin by Rho kinase in brain endothelial cells. *American Journal of Pathology*, **172**(2), pp. 521-533.

YAMASAKI, K., TAGA, T., HIRATA, Y., YAWATA, H., KAWANISHI, Y., SEED, B., TANIGUCHI, T., HIRANO, T. and KISHIMOTO, T., 1988. Cloning and Expression of the Human Interleukin-6 (Bsf-2/ifn-Beta-2) Receptor. *Science*, **241**(4867), pp. 825-828.

YAMAWAKI, H., LEHOUX, S. and BERK, B.C., 2003. Chronic physiological shear stress inhibits tumor necrosis factor-induced proinflammatory responses in rabbit aorta perfused ex vivo. *Circulation*, **108**(13), pp. 1619-1625.

YAN, Q. and SAGE, E.H., 1998. Transforming growth factor-beta 1 induces apoptotic cell death in cultured retinal endothelial cells but not pericytes: Association with decreased expression of p2l(waf1/cip1). *Journal of cellular biochemistry*, **70**(1), pp. 70-83.

YANG, G.Y., GONG, C., QIN, Z., LIU, X.H. and BETZ, A.L., 1999. Tumor necrosis factor alpha expression produces increased blood-brain barrier permeability following temporary focal cerebral ischemia in mice. *Molecular Brain Research*, **69**(1), pp. 135-143.

YE, J.M., TSUKAMOTO, T., SUN, A. and NIGAM, S.K., 1999. A role for intracellular calcium in tight junction reassembly after ATP depletion-repletion. *American Journal of Physiology-Renal Physiology*, **277**(4), pp. F524-F532.

YOKOTA, S., MIYAMAE, T., IMAGAWA, T., IWATA, N., KATAKURA, S., MORI, M., WOO, P., NISHIMOTO, N., YOSHIZAKI, K. and KISHIMOTO, T., 2005. Therapeutic Efficacy of Humanized Recombinant Anti-Interleukin-6 Receptor Antibody in Children With Systemic-Onset Juvenile Idiopathic Arthritis. *Arthritis and Rheumatism*, **52**(3), pp. 818-825.

YOSHIDA, Y., OKANO, M., WANG, S., KOBAYASHI, M., KAWASUMI, M., HAGIWARA, H. and MITSUMATA, M., 1995. Hemodynamic-Force-Induced Difference of Interendothelial Junctional Complexes. *Atherosclerosis Iii: Recent Advances in*

Atherosclerosis Research: the Third Saratoga International Conference on Atherosclerosis in Nekoma, **748**, pp. 104-121.

YOSHIZUMI, M., ABE, J., TSUCHIYA, K., BERK, B.C. and TAMAKI, T., 2003. Stress and vascular responses: Atheroprotective effect of laminar fluid shear stress in endothelial cells: Possible role of mitogen-activated protein kinases. *Journal of Pharmacological Sciences,* **91**(3), pp. 172-176.

YOUNG, B.A., SUI, X.F., KISER, T.D., HYUN, S.W., WANG, P., SAKARYA, S., ANGELINI, D.J., SCHAPHORST, K.L., HASDAY, J.D., CROSS, A.S., ROMER, L.H., PASSANITI, A. and GOLDBLUM, S.E., 2003. Protein tyrosine phosphatase activity regulates endothelial cell-cell interactions, the paracellular pathway, and capillary tube stability. *American Journal of Physiology-Lung Cellular and Molecular Physiology,* **285**(1), pp. L63-L75.

YU, C., KASTIN, A.J. and PAN, W., 2007. TNF reduces LIF endocytosis despite increasing NF kappa B-mediated gp130 expression. *Journal of cellular physiology,* **213**(1), pp. 161-166.

YUKITATSU, Y., HATA, M., YAMANEGI, K., YAMADA, N., OHYAMA, H., NAKASHO, K., KOJIMA, Y., OKA, H., TSUZUKI, K., SAKAGAMI, M. and TERADA, N., 2013. Decreased expression of VE-cadherin and claudin-5 and increased phosphorylation of VE-cadherin in vascular endothelium in nasal polyps. *Cell and tissue research,* **352**(3), pp. 647-657.

YUSUF, S., REDDY, S., OUNPUU, S. and ANAND, S., 2001. Global burden of cardiovascular diseases - Part II: Variations in cardiovascular disease by specific ethnic groups and geographic regions and prevention strategies. *Circulation,* **104**(23), pp. 2855-2864.

ZAHLER, S., KUPATT, C. and BECKER, B.F., 2000. Endothelial preconditioning by transient oxidative stress reduces inflammatory responses of cultured endothelial cells to TNF-alpha. *Faseb Journal,* **14**(3), pp. 555-564.

ZAIDI, S.M.K.R. and BANU, N., 2004. Antioxidant potential of vitamins A, E and C in modulating oxidative stress in rat brain. *Clinica Chimica Acta,* **340**(1-2), pp. 229-233.

ZALBA, G., BEAUMONT, F.J., SAN JOSE, G., FORTUNO, A., FORTUNO, M.A., ETAYO, J.C. and DIEZ, J., 2000. Vascular NADH/NADPH oxidase is involved in enhanced superoxide production in spontaneously hypertensive rats. *Hypertension,* **35**(5), pp. 1055-1061.

ZARIFIS, J., BLANN, A.D., FAROOQI, I.S., SAGAR, G., BEEVERS, D.G. and LIP, G.Y.H., 1996. Increased soluble adhesion molecule P-selectin, von Willebrand factor and fibrinogen in acute stroke: Evidence for early endothelial and haemorheological dysfunction. *Clinical Science (London),* **90**(2), pp. 27P-27P.

ZEISSIG, S., BUERGEL, N., GUENZEL, D., RICHTER, J., MANKERTZ, J., WAHNSCHAFFE, U., KROESEN, A.J., ZEITZ, M., FROMM, M. and SCHULZKE, J.-., 2007. Changes in expression and distribution of claudin 2, 5 and 8 lead to discontinuous tight junctions and barrier dysfunction in active Crohn's disease. *Gut,* **56**(1), pp. 61-72.

ZHANG, C., 2008. The role of inflammatory cytokines in endothelial dysfunction. *Basic research in cardiology*, **103**(5), pp. 398-406.

ZHANG, L.X., CHEN, J. and FU, H.A., 1999. Suppression of apoptosis signal-regulating kinase 1-induced cell death by 14-3-3 proteins. *Proceedings of the National Academy of Sciences of the United States of America*, **96**(15), pp. 8511-8515.

ZHANG, X., BANERJEE, A., BANKS, W.A. and ERCAL, N., 2009. N-Acetylcysteine amide protects against methamphetamine-induced oxidative stress and neurotoxicity in immortalized human brain endothelial cells. *Brain research*, **1275**, pp. 87-95.

ZHANG, Y. and PARDRIDGE, W.M., 2001. Rapid transferrin efflux from brain to blood across the blood-brain barrier. *Journal of neurochemistry*, **76**(5), pp. 1597-1600.

ZHANG, Y. and BARRES, B.A., 2010. Astrocyte heterogeneity: an underappreciated topic in neurobiology. *Current opinion in neurobiology*, **20**(5), pp. 588-594.

ZIEGLER, T., BOUZOURENE, K., HARRISON, V.J., BRUNNER, H.R. and HAYOZ, D., 1998. Influence of oscillatory and unidirectional flow environments on the expression of endothelin and nitric oxide synthase in cultured endothelial cells. *Arteriosclerosis Thrombosis and Vascular Biology*, **18**(5), pp. 686-692.

ZIEGLER, T., SILACCI, P., HARRISON, V.J. and HAYOZ, D., 1998. Nitric oxide synthase expression in endothelial cells exposed to mechanical forces. *Hypertension*, **32**(2), pp. 351-355.

ZLOKOVIC, B.V., YAMADA, S., HOLTZMAN, D., GHISO, J. and FRANGIONE, B., 2000. Clearance of amyloid beta-peptide from brain: transport or metabolism? *Nature Medicine*, **6**(7), pp. 718.

ZLOKOVIC, B.V., 2008. The blood-brain barrier in health and chronic neurodegenerative disorders. *Neuron*, **57**(2), pp. 178-201.

ZLOKOVIC, B., DEANE, R., SALLSTROM, J., CHOW, N. and MIANO, J., 2005. Neurovascular pathways and Alzheimer amyloid beta-peptide. *Brain Pathology*, **15**(1), pp. 78-83.

Appendix.

Table of Contents

Chapter 3

Chapter 4

Chapter 5

Chapter 6

Miscellaneous

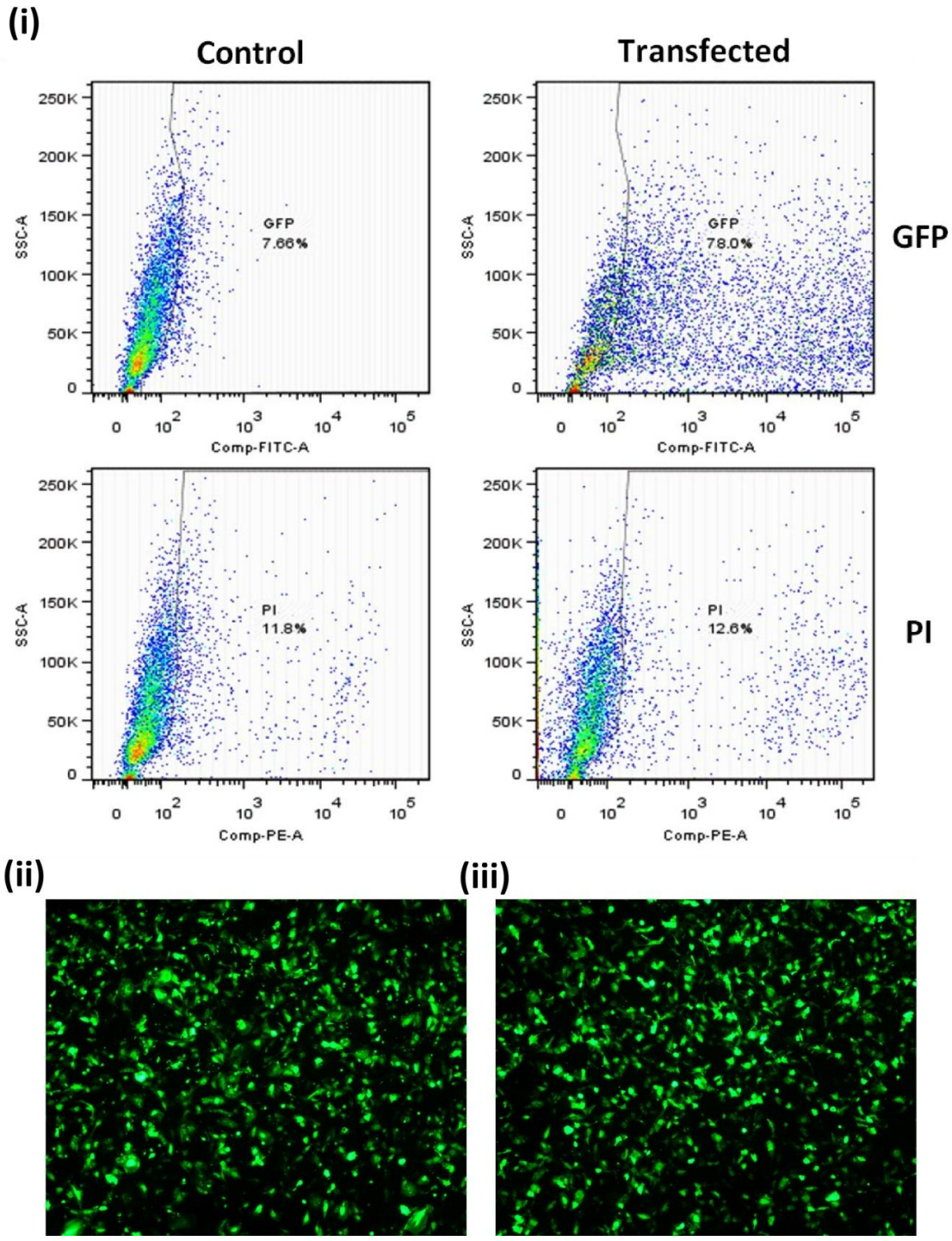

Figure A.1: Assessment of transfection viability and efficiency. HBMvECs were grown to 70-80% confluency and subjected to electroporation for recombinant GFP protein and pEGFPN1 plasmid as described in section XXX. The following day cells were harvested and prepared for flow cytometry analysis using PI stain to measure cytotoxicity. The dot plots represent the spread of the cell populations as a result of successful expression of GFP and PI staining, which reflect the degree of transfection efficiency and the viability, respectively. Moreover, GFP expression was also verified by immunofluorescence microscopy for both recombinant GFP protein (ii) and pEGFPN1 plasmid (ii).

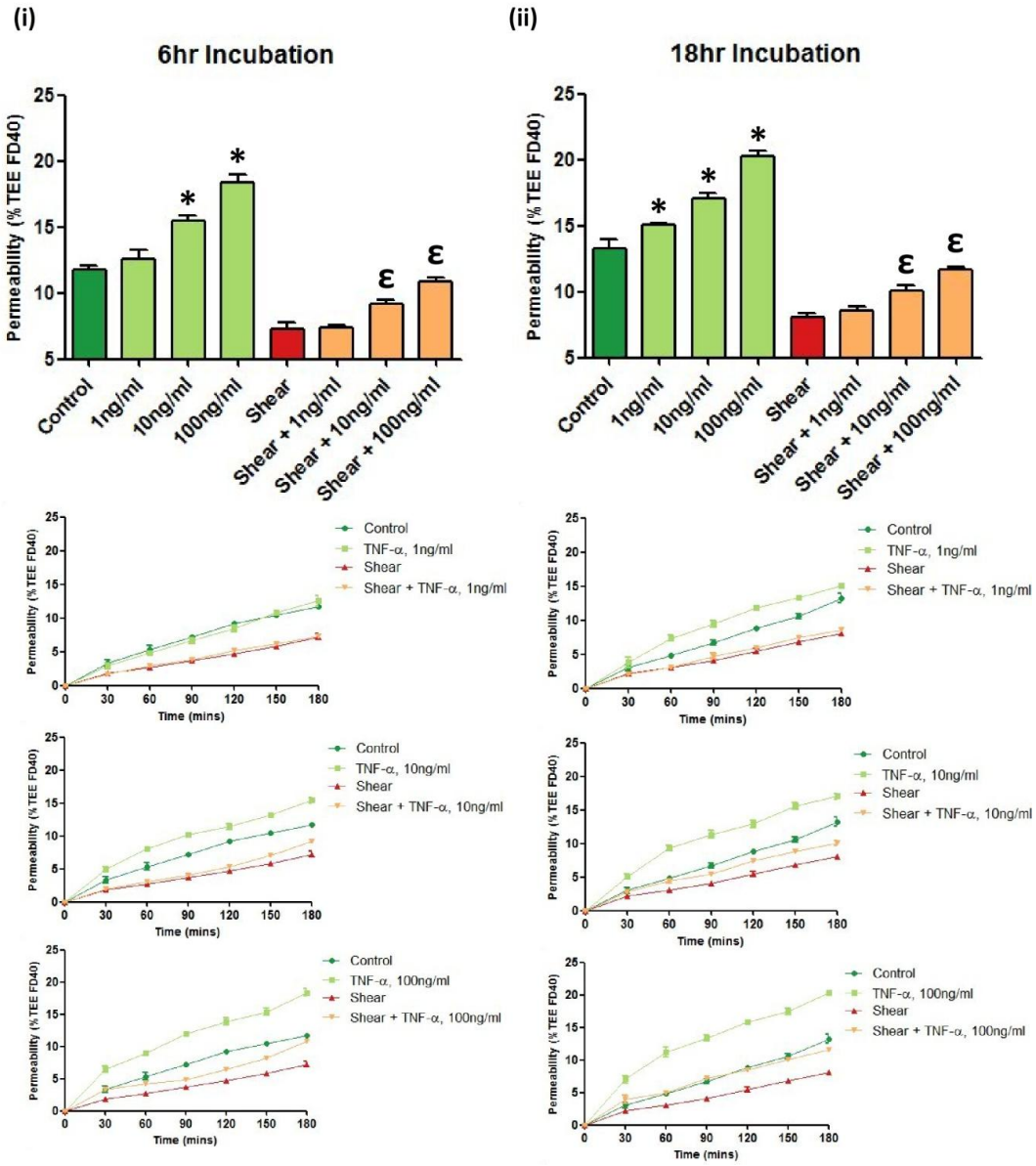

Figure A.2: The effect of laminar shear stress on TNF-α-induced injury of HBMvECs. Confluent HBMvECs were pre-conditioned by laminar shear stress (8 dynes cm^{-2}, 24 hr), following which the cultures were replated into transwell inserts and left to adhere overnight. TNF-α (0-100 ng/ml) was then added to the cultures for an additional 6 or 18 hr before they were examined by transendothelial permeability assay. The histograms and line graphs show the change in permeability (%TEE FD40) at a given time point(s) (t) = 180 mins and 0-180 mins after 6 hr (i) and 18 hr (ii) exposure to TNF-α (0-100 ng/ml). Results are averaged from three independent experiments ± SD; *P≤0.05 vs. Unsheared Control. εP≤0.05 vs. Sheared Control.

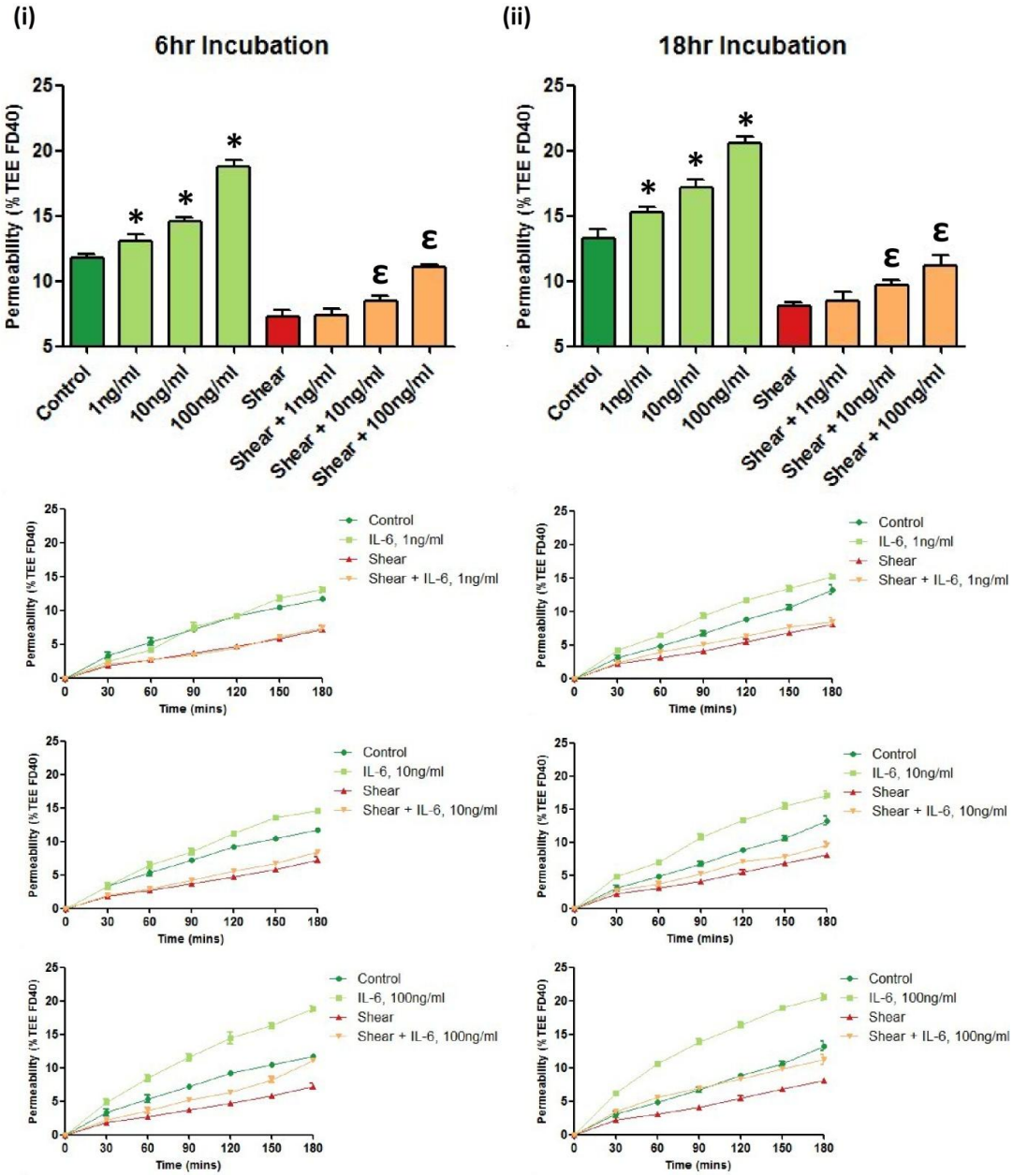

Figure A.3: The effect of laminar shear stress on IL-6-induced injury of HBMvECs. Confluent HBMvECs were pre-conditioned by laminar shear stress (8 dynes cm^{-2}, 24 hr), following which the cultures were replated into transwell inserts and left to adhere overnight. IL-6 (0-100 ng/ml) was then added to the cultures for an additional 6 or 18 hr before they were examined by transendothelial permeability assay. The histograms and line graphs show the change in permeability (%TEE FD40) at a given time point(s) (t) = 180 mins and 0-180 mins after 6 hr (i) and 18 hr (ii) exposure to IL-6 (0-100 ng/ml). Results are averaged from three independent experiments ± SD; *P≤0.05 vs. Unsheared Control. εP≤0.05 vs. Sheared Control.

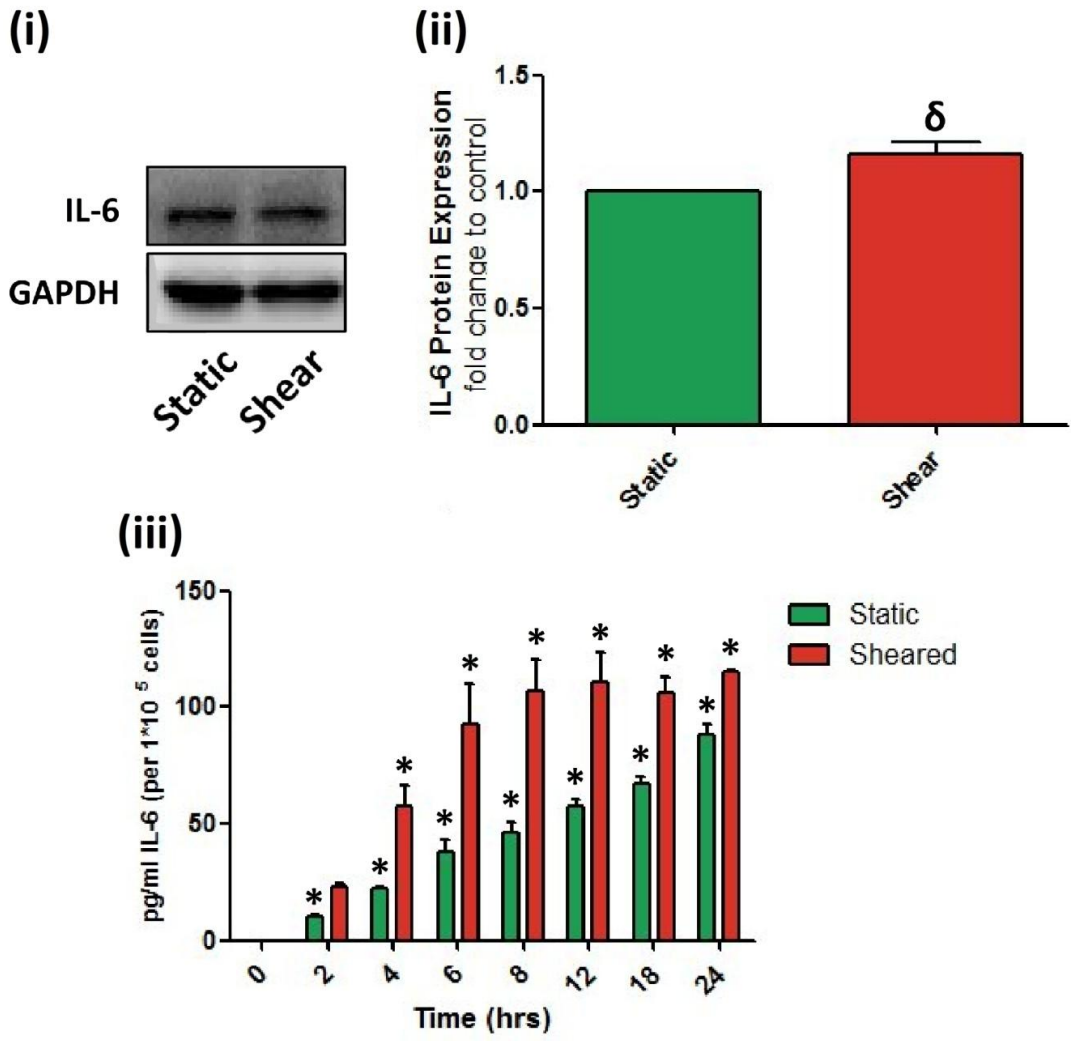

Figure A.4: The effect of laminar shear stress on IL-6 expression and secretion. Confluent HBMvECs were maintained under static conditions or exposed to laminar shear stress (8 dynes cm^{-2}, 0-24 hr) following which they were harvested for whole cell protein lysate and conditioned medium. The samples were analysed by western blot for the translational levels of IL-6. The conditioned medium was examined by ELISA to monitor the effect on IL-6 release in the absence or presence of shear forces (iii) Results are averaged from three independent experiments ± SD; $\delta P \leq 0.05$ vs. Unsheared Control. $^{*}P \leq 0.05$ vs. 0 hrs. Blot is representative.

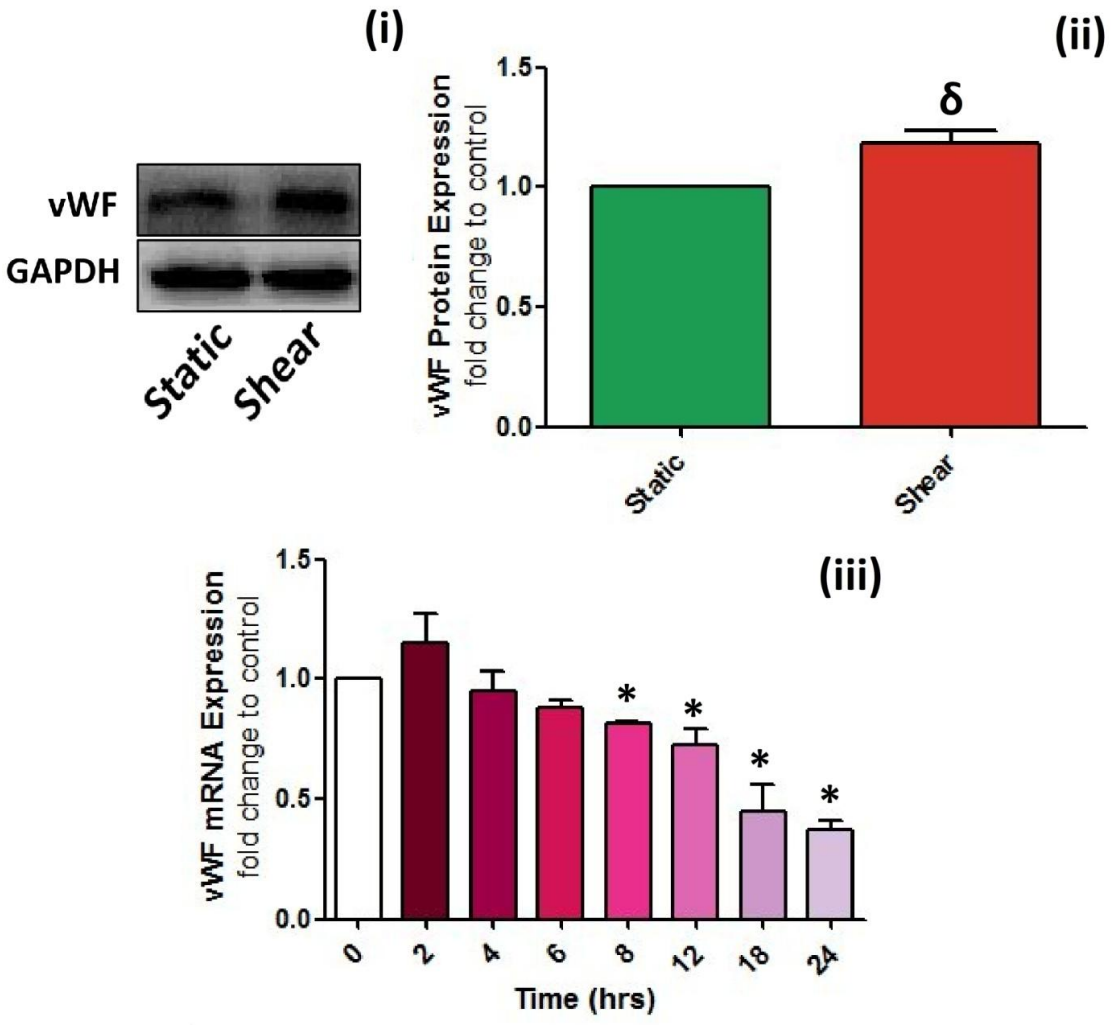

Figure A.5: The effect of laminar shear stress on vWF expression. Confluent HBMvECs were maintained under static conditions or exposed to laminar shear stress (8 dynes cm^{-2}, 0-24 hr) following which they were harvested for whole cell mRNA and protein lysate. The samples were analysed by western blot for the translational levels (i, ii) and qPCR for the transcriptional levels (iii) of vWF. Results are averaged from three independent experiments ± SD; δP≤0.05 vs. Unsheared Control. *P≤0.05 vs. 0 hrs. Blot is representative.

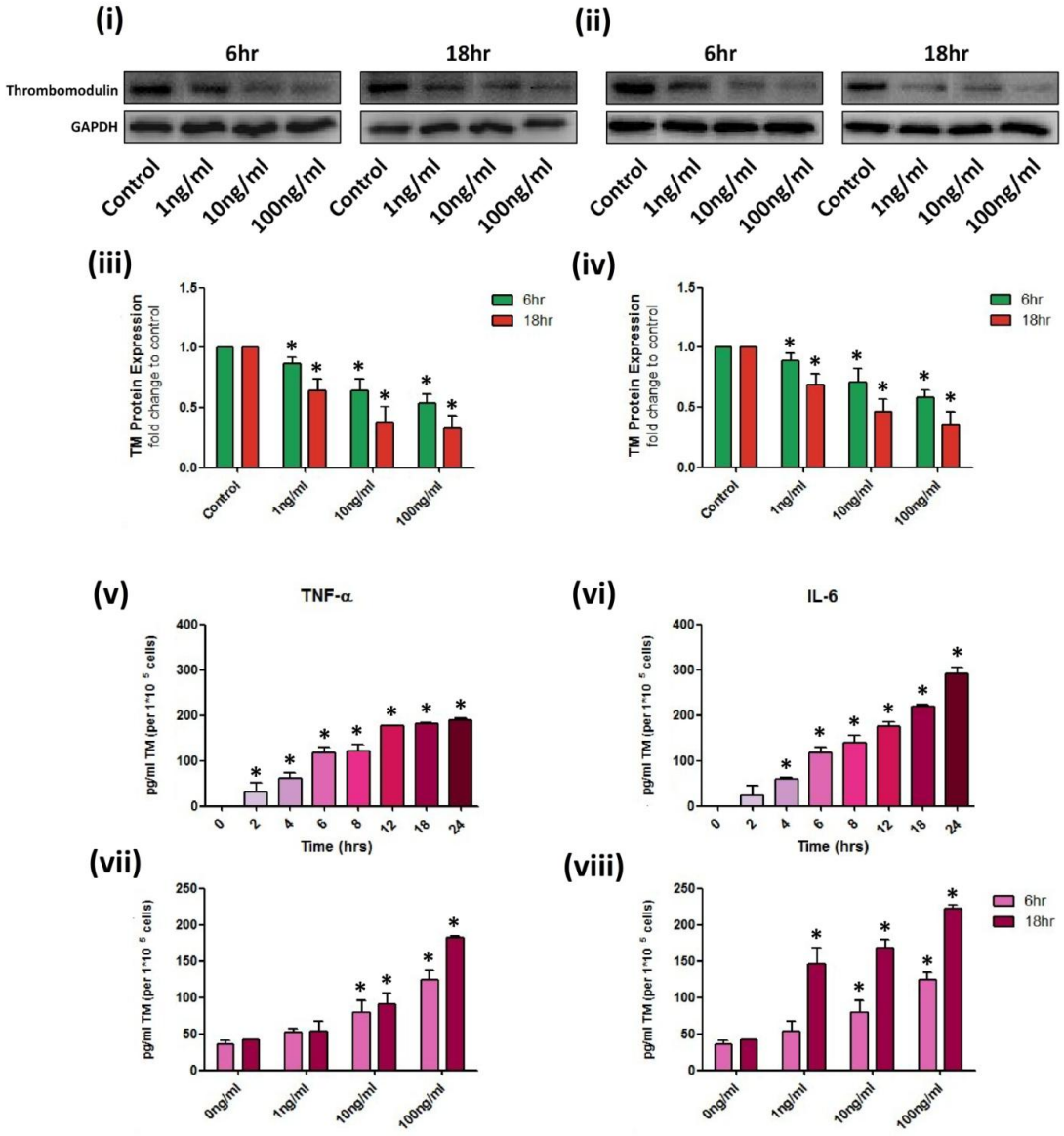

Figure A.6: The effect of TNF-α and IL-6 on thrombomodulin expression and secretion. Confluent HBMvECs were stimulated with TNF-α (LHS) or IL-6 (RHS) (0-100 ng/ml) for 0-24 hrs following which they were harvested for whole cell protein lysate and conditioned medium. Post-treatment, the samples were analysed by western blot for the translational levels of thrombomodulin. The conditioned medium was examined by ELISA to monitor the effect on thrombomodulin release in response to both cytokines (100 ng/ml) over 24 hrs (v, vi) or in response to both cytokines (0-100 ng/ml) at 6 and 18 hrs (vii, viii), respectively. Results are averaged from three independent experiments ± SD. *P≤0.05 vs. Untreated Control (iii, iv) and 0 hrs (v-viii) respectively. Blots are representative.

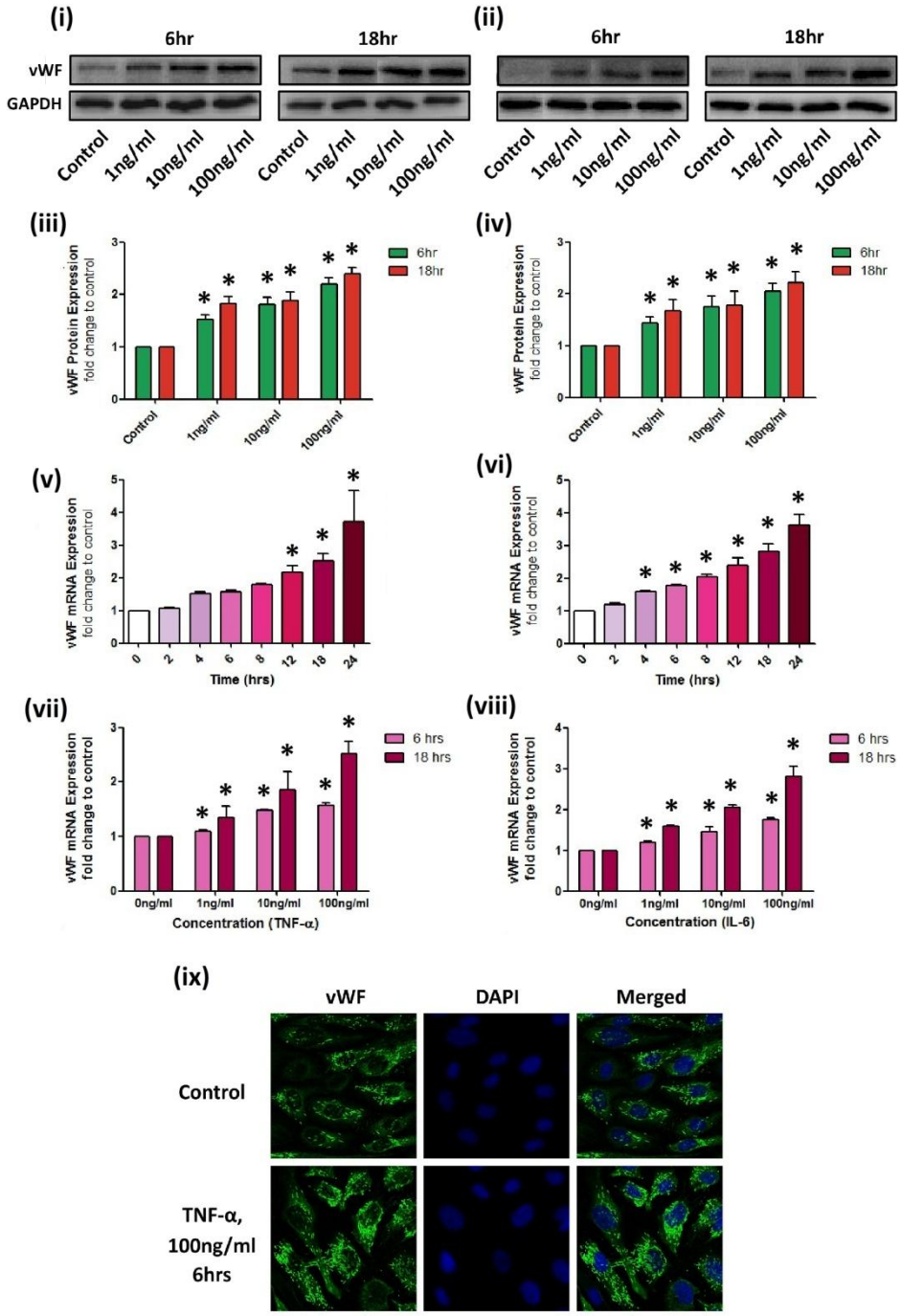

Figure A.7: The effect of TNF-α and IL-6 on vWF expression and secretion. Confluent HBMvECs were stimulated with TNF-α (LHS) or IL-6 (RHS) (0-100 ng/ml) for 0-24 hrs following which they were harvested for whole cell protein lysate and mRNA. Post-treatment, the samples were analysed by western blot for the translational levels (i-iv) and by qPCR for the transcriptional levels (v-viii) of vWF. Results are averaged from three independent experiments ± SD. *P≤0.05 vs. Untreated Control (iii, iv) and 0 hrs (v-viii), respectively. Blots are representative. In addition, confluent HBMvECs were stimulated with TNF-α or IL-6 (0-100 ng/ml) for 6 or 18 hrs following which they were examined for changes in the expression and localisation patterns of vWF (green). Untreated control cultures were employed as a control (ix). All cultures were counterstained for nuclei (blue). Images are representative.

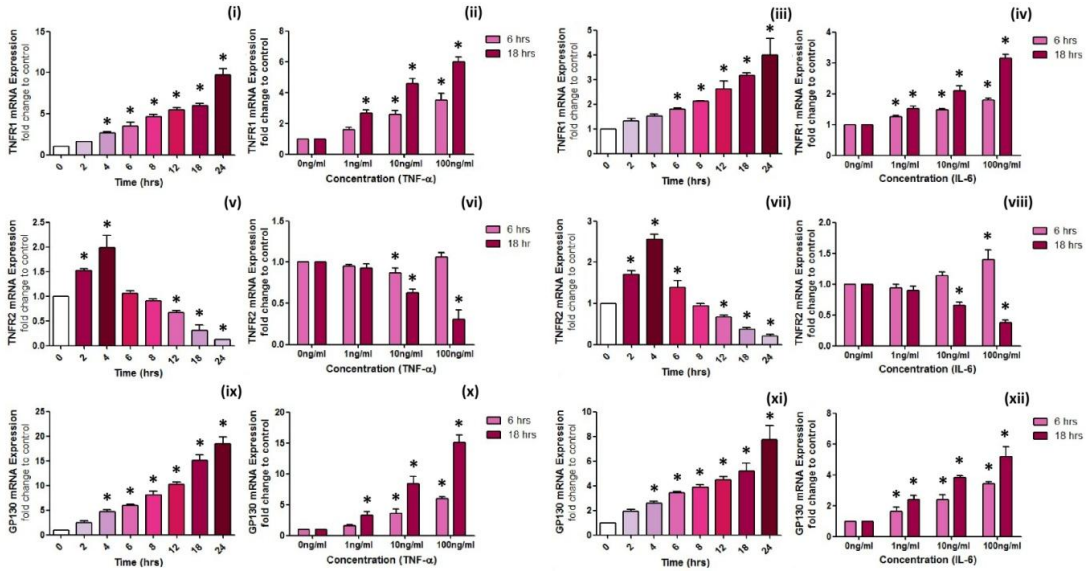

Figure A.8: The effect of TNF-α and IL-6 on cytokine signal-transducing receptors. Confluent HBMvECs were stimulated with TNF-α (LHS) or IL-6 (RHS) (0-100 ng/ml) for 0-24 hrs following which they were harvested for whole cell mRNA. The samples were analysed by qPCR for the transcriptional levels of TNFR1 (i-iv), TNFR2 (v-viii) and GP130 (ix-xii). The histograms represent the changes in the respective signal-transducing receptors on a transcriptional level over time (i, iii, v, vii, ix, xi) and with respect to dose at 6 and 18 hrs (ii, iv, vi, viii, x). Results are averaged from three independent experiments ± SD; *P≤0.05 vs. 0 hrs (i, iii, v, vii, ix, xi) or 0ng/ml (ii, iv, vi, viii, x, xii) respectively.

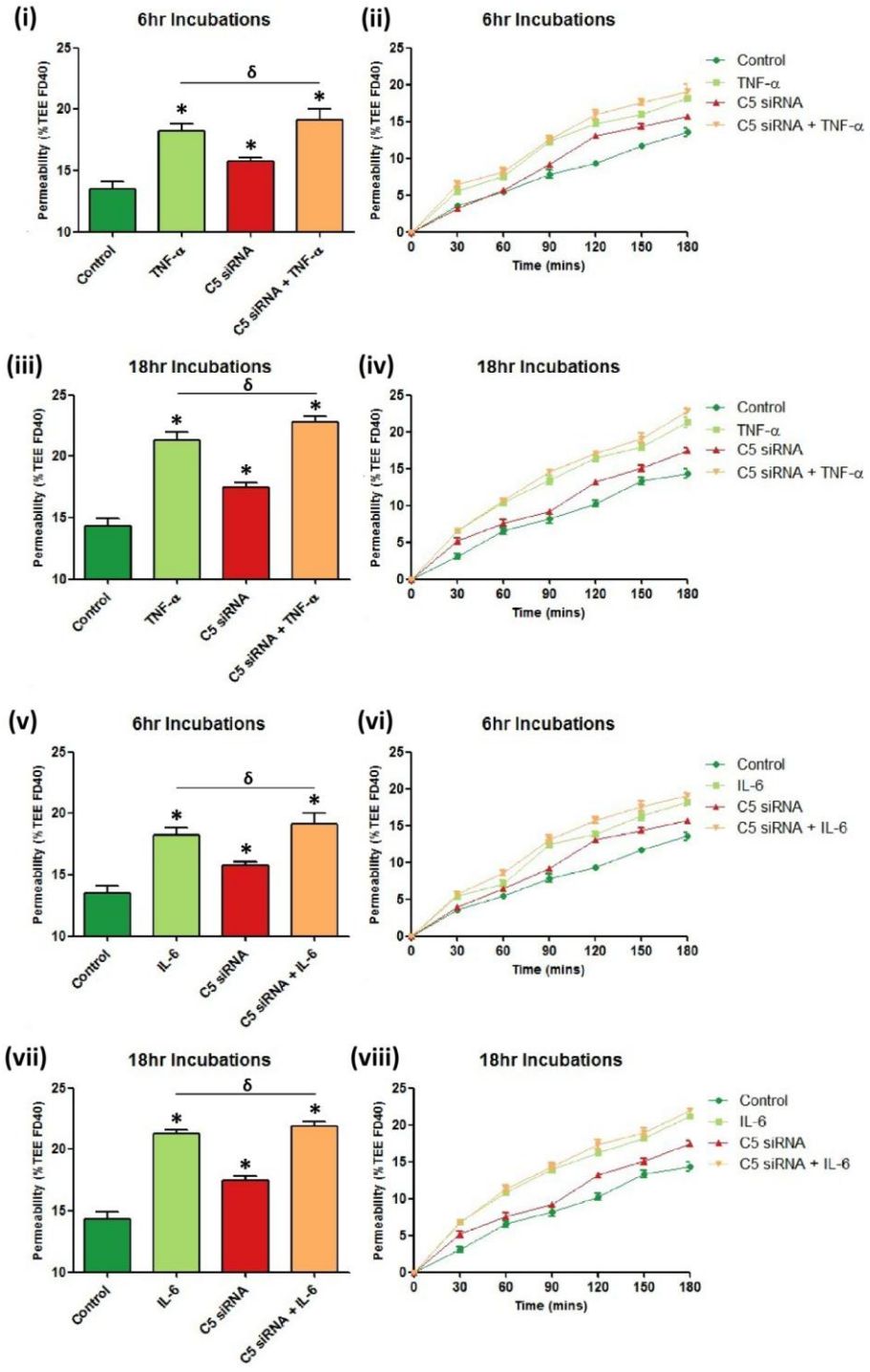

Figure A.9: The effect cytokines and claudin-5 knockout on HBMvEC Barrier Function. HBMvECs were grown to 70-80% confluency and subjected to electroporation for claudin-5 siRNA as described in section XXX. The following day the transfected cultures were replated into transwell inserts and left to adhere overnight. The following day, the cultures were treated with TNF-α or IL-6 (100 ng/ml) for 6 or 18 hrs before being examined by transendothelial permeability assay. The histograms (LHS) and line graphs (RHS) show the change in permeability (%TEE FD40) at a given time point(s) (t) = 180 mins and 0-180 mins, respectively. Results are averaged from three independent experiments ± SD; *P≤0.05 vs. Untreated Control, δP≤0.05.

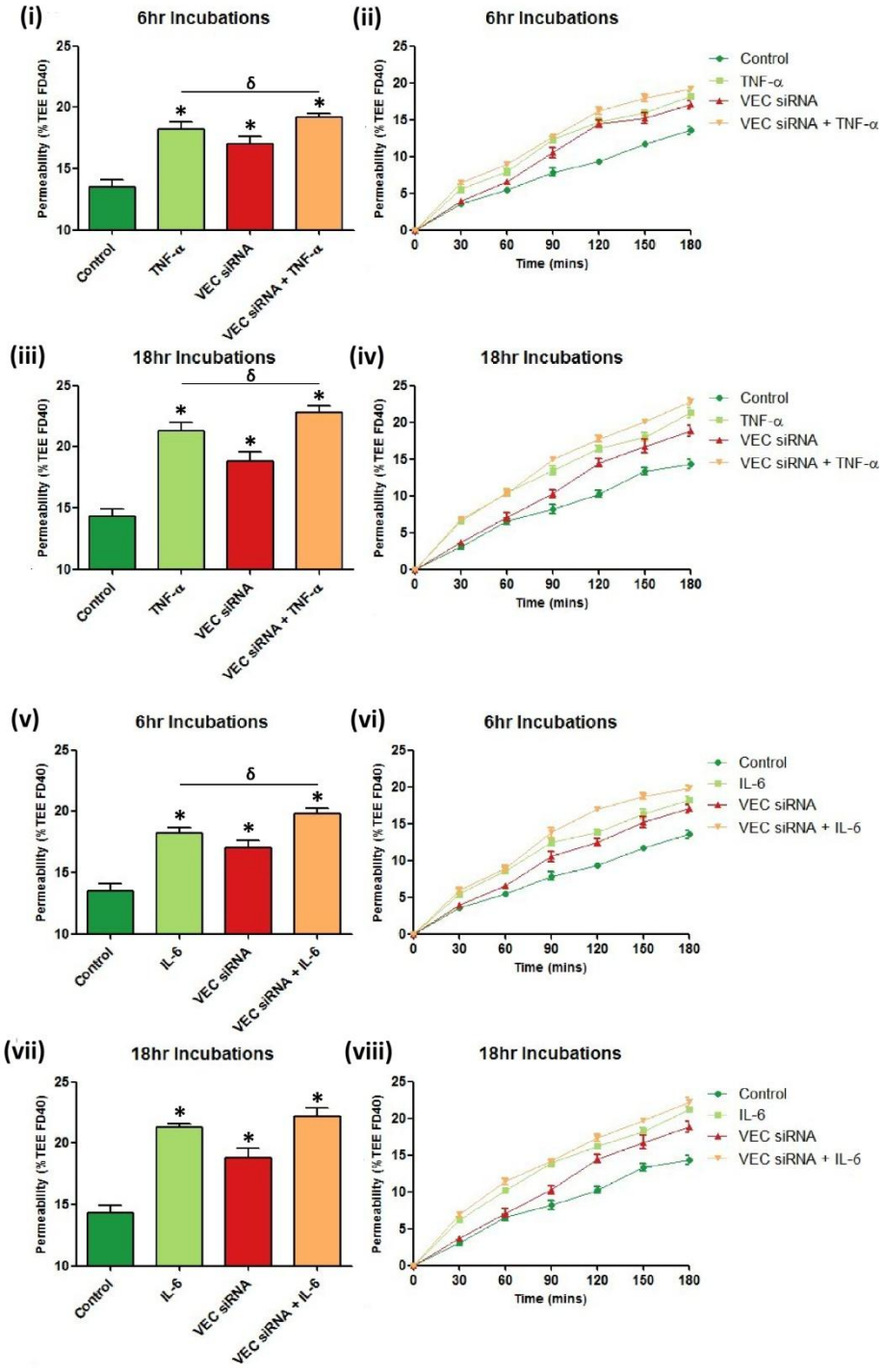

Figure A.10: The effect cytokines and VE-Cadherin knockout on HBMvEC Barrier Function. HBMvECs were grown to 70-80% confluency and subjected to electroporation for VE-Cadherin siRNA as described in section XXX. The following day the transfected cultures were replated into transwell inserts and left to adhere overnight. The following day, the cultures were treated with TNF-α or IL-6 (100 ng/ml) for 6 or 18 hrs before being examined by transendothelial permeability assay. The histograms (LHS) and line graphs (RHS) show the change in permeability (%TEE FD40) at a given time point(s) (t) = 180 mins and 0-180 mins, respectively. Results are averaged from three independent experiments ± SD; *P≤0.05 vs. Untreated Control, δP≤0.05.

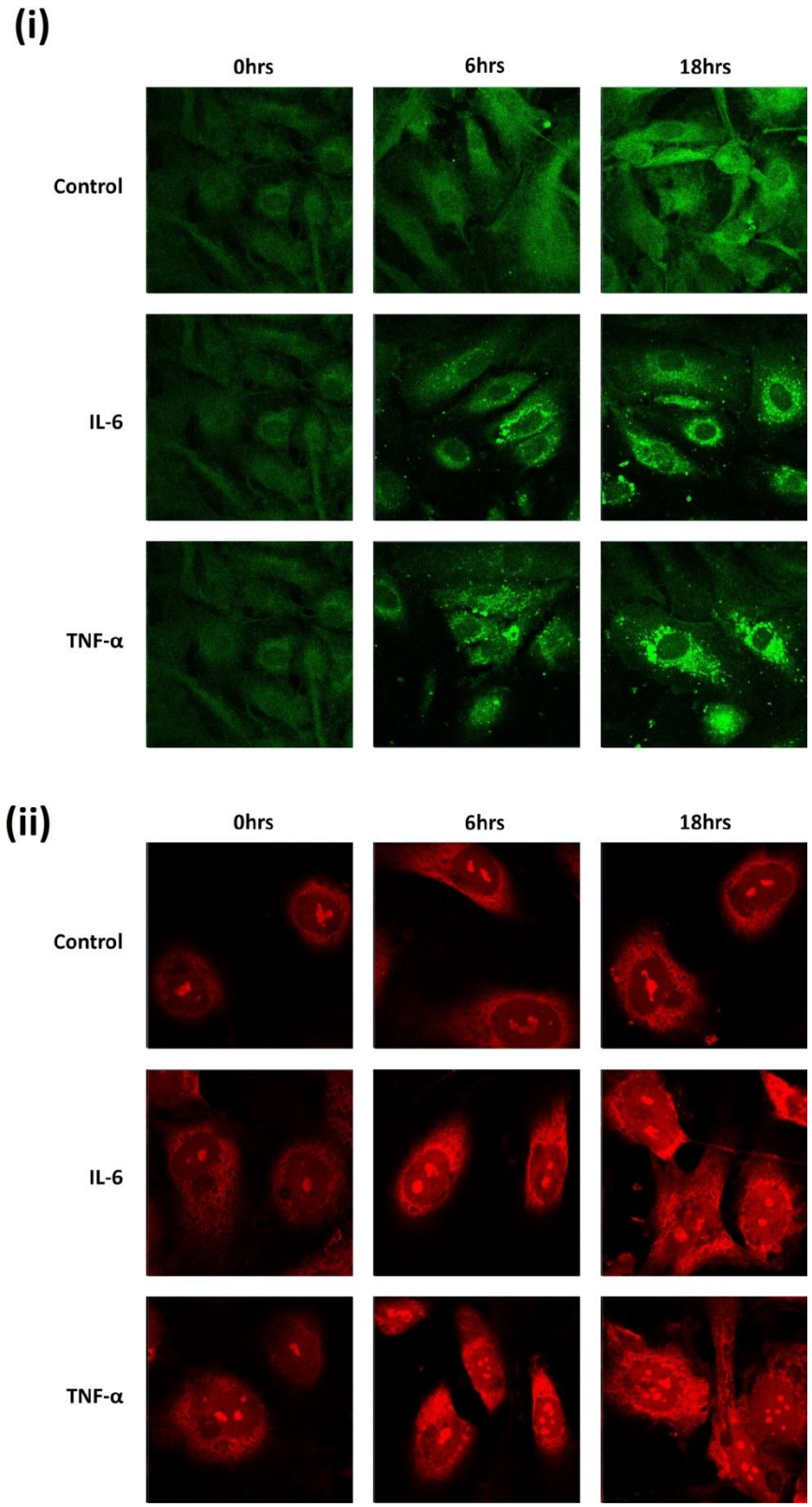

Figure A.11: The effect of TNF-α and IL-6 on ROS production-Time Response, Immunofluorescence. Confluent HBMvECs were treated with TNF-α or IL-6 (100 ng/ml) for 6 or 18 hrs in the presence of CFDA (i) or DHE (ii). Images are representative.

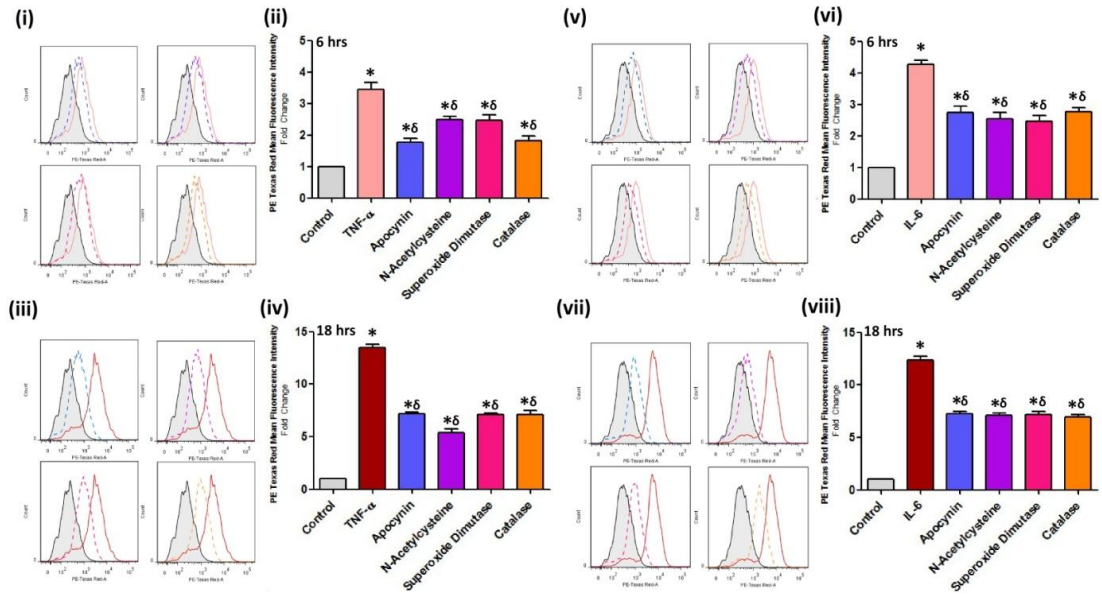

Figure A.12: The effect of antioxidants on TNF-α- and IL-6-induced ROS production-DHE. Confluent HBMvECs were stimulated with TNF-α or IL-6 (100 ng/ml) for 6 or 18 hrs in the presence of DHE and a range of antioxidant compounds. Post-treatment, cells were harvested and subsequently prepared for flow cytometry. The histograms represent the intensity of the DHE dye prepared from the corresponding representative FACS scans. The cytokine-treated samples were analysed using FlowJo Flow Cytometry Analysis Software to quantify the respective signal from DHE-stained cell populations in response to TNF-α (ii, iv) and IL-6 (v, vii) at 6 (upper) and 18 (lower) hrs. Results are averaged from three independent experiments ± SD. *P≤0.05 vs. Untreated Control. δP≤0.05 vs. TNF-α or IL-6 treatment.

Legend: PE-Texas Red-A = DHE

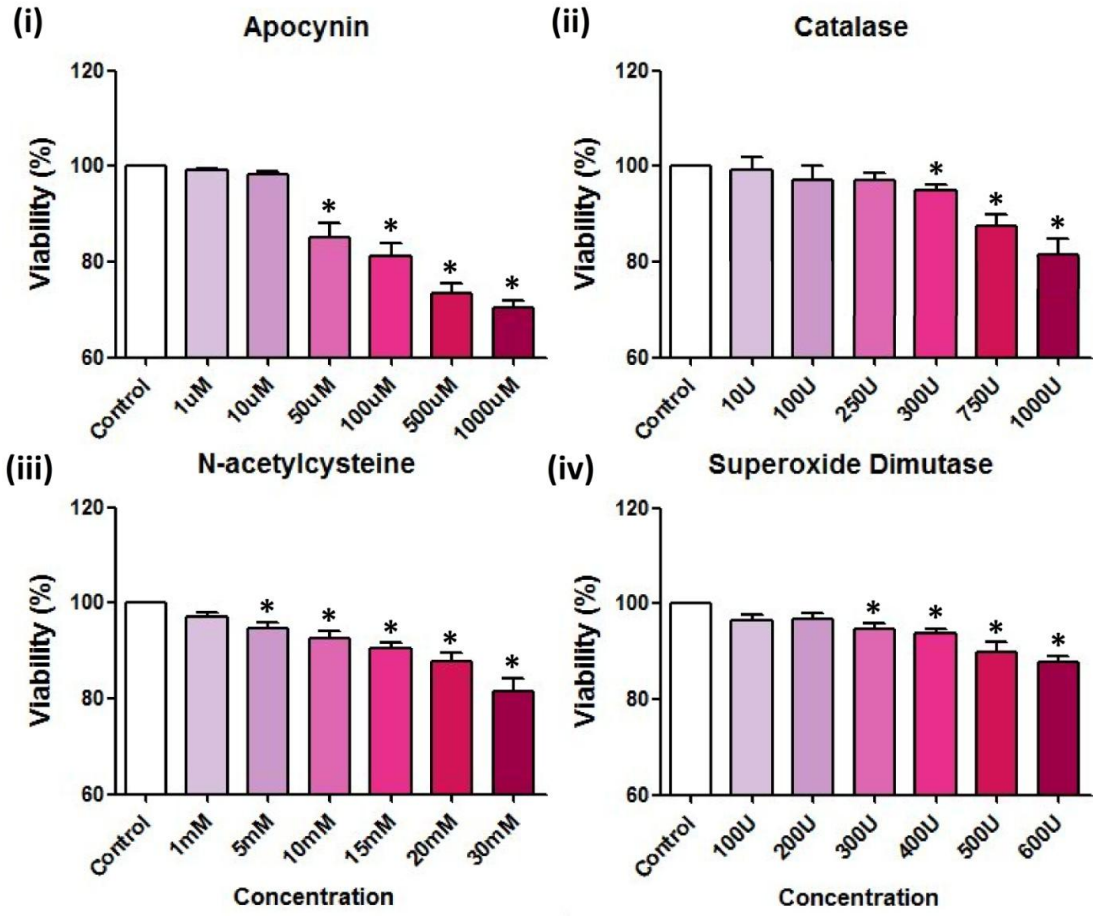

Figure A.13: The effect of antioxidants on HBMvEC viability-Flow Cytometry Analysis. Confluent HBMvECs were stimulated with antioxidants for 18 hr. Post-treatment cells were harvested and subsequently prepared for flow cytometry analysis using PI stain. Samples were analysed using FlowJo Flow Cytometry Analysis Software to identify the viable and cytotoxic cell populations in response to a range of concentrations of apocynin (i), catalase(ii), N-acetylcysteine (iii) and superoxide dismutase (iv). Results are averaged from three independent experiments ± SD; *P≤0.05 vs. Untreated Control.

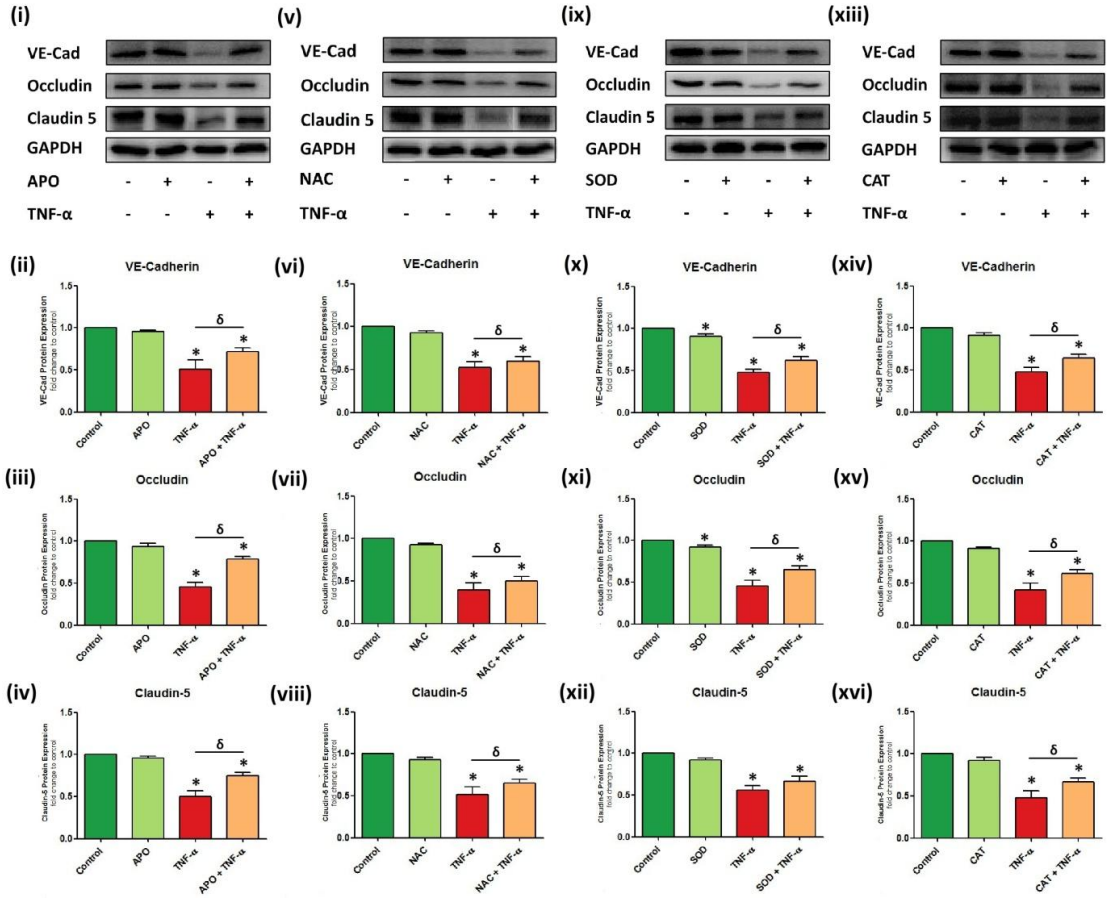

Figure A.14: The effect of antioxidants on TNF-α-induced downregulation of TJ/AJ proteins. Confluent HBMvECs were treated with TNF-α (100 ng/ml) for 6 hrs in the presence of a number of antioxidant compounds. Post-treatment, cells were harvested for whole cell protein lysate. The translational effect on particular intercellular junction proteins was investigated by western blot. The histograms represent the changes in relative protein expression for VE-Cadherin (ii, vi, x, xiv), occludin (iii, vii, xi, xv) and claudin-5 (iv, viii, xii, xvi). Results are averaged from three independent experiments ± SD; *P≤0.05 vs. Untreated Control. δP≤0.05. Blots are representative.

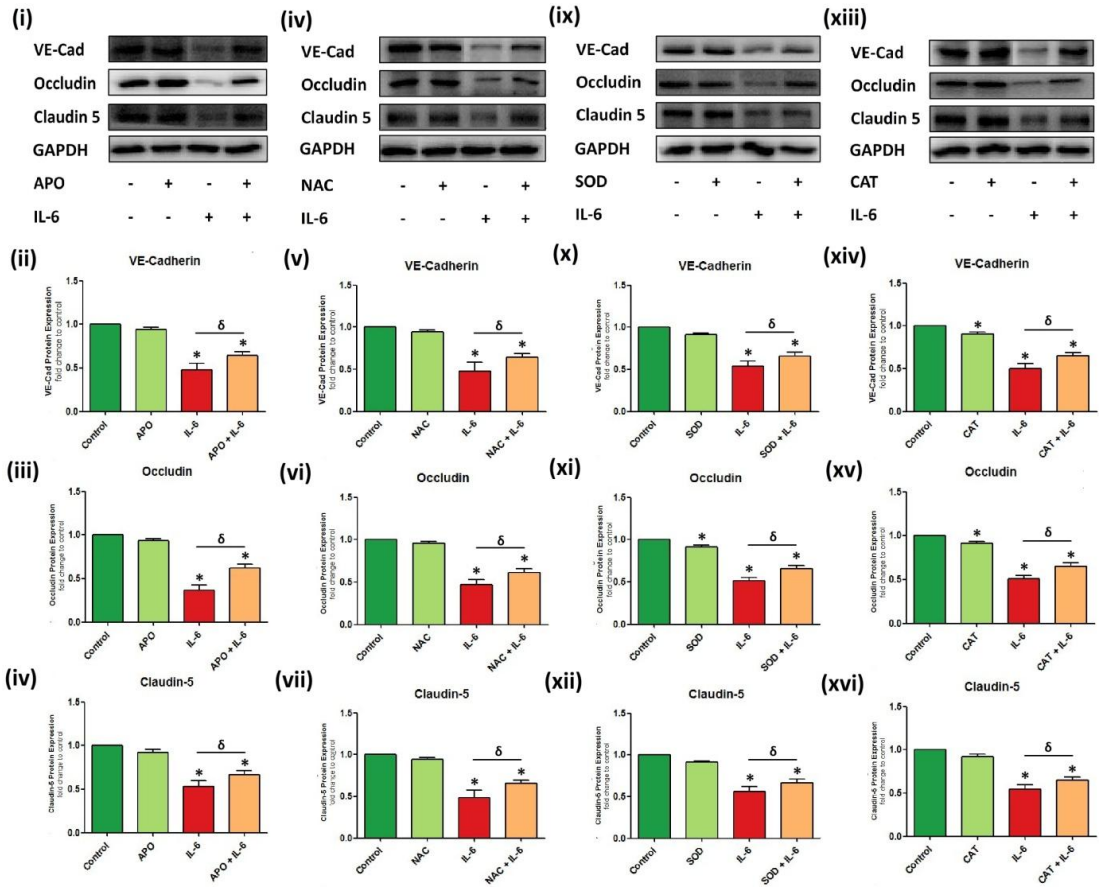

Figure A.15: The effect of antioxidants on IL-6-induced downregulation of TJ/AJ proteins. Confluent HBMvECs were treated with IL-6 (100 ng/ml) for 6 hrs in the presence of a number of antioxidant compounds. Post-treatment, cells were harvested for whole cell protein lysate. The translational effect on particular intercellular junction proteins was investigated by western blot. The histograms represent the changes in relative protein expression for VE-Cadherin (ii, vi, x, xiv), occludin (iii, vii, xi, xv) and claudin-5 (iv, viii, xii, xvi). Results are averaged from three independent experiments ± SD; *P≤0.05 vs. Untreated Control. δP≤0.05. Blots are representative.

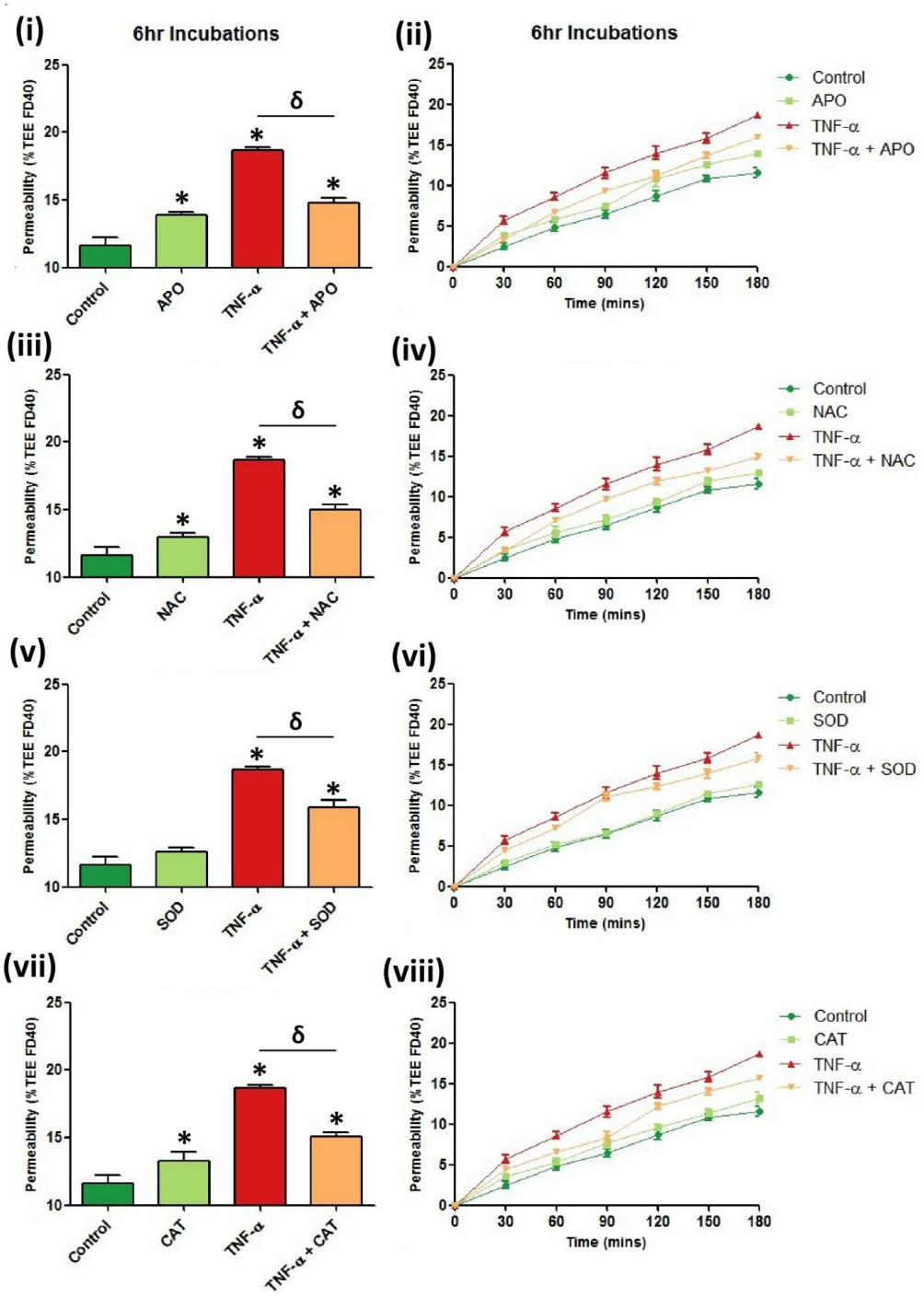

Figure A.16: The effect of antioxidants on TNF-α-induced disruption of HBMvEC barrier function. HBMvECs were seeded at a known density and allowed to adhere prior to examination by transendothelial permeability. HBMvECs were then pre-treated with TNF-α (100 ng/ml) for 6 hrs in the presence of a number of antioxidant compounds. Post-treatment, monolayers were examined by transendothelial permeability assay. The histograms (LHS) and line graphs (RHS) show the change in permeability (% TEE FD40) at a given time point(s) (t) = 180 mins or 0-180 mins, respectively. Results are averaged from three independent experiments ± SD; *P≤0.05 vs. Untreated Control. δP≤0.05.

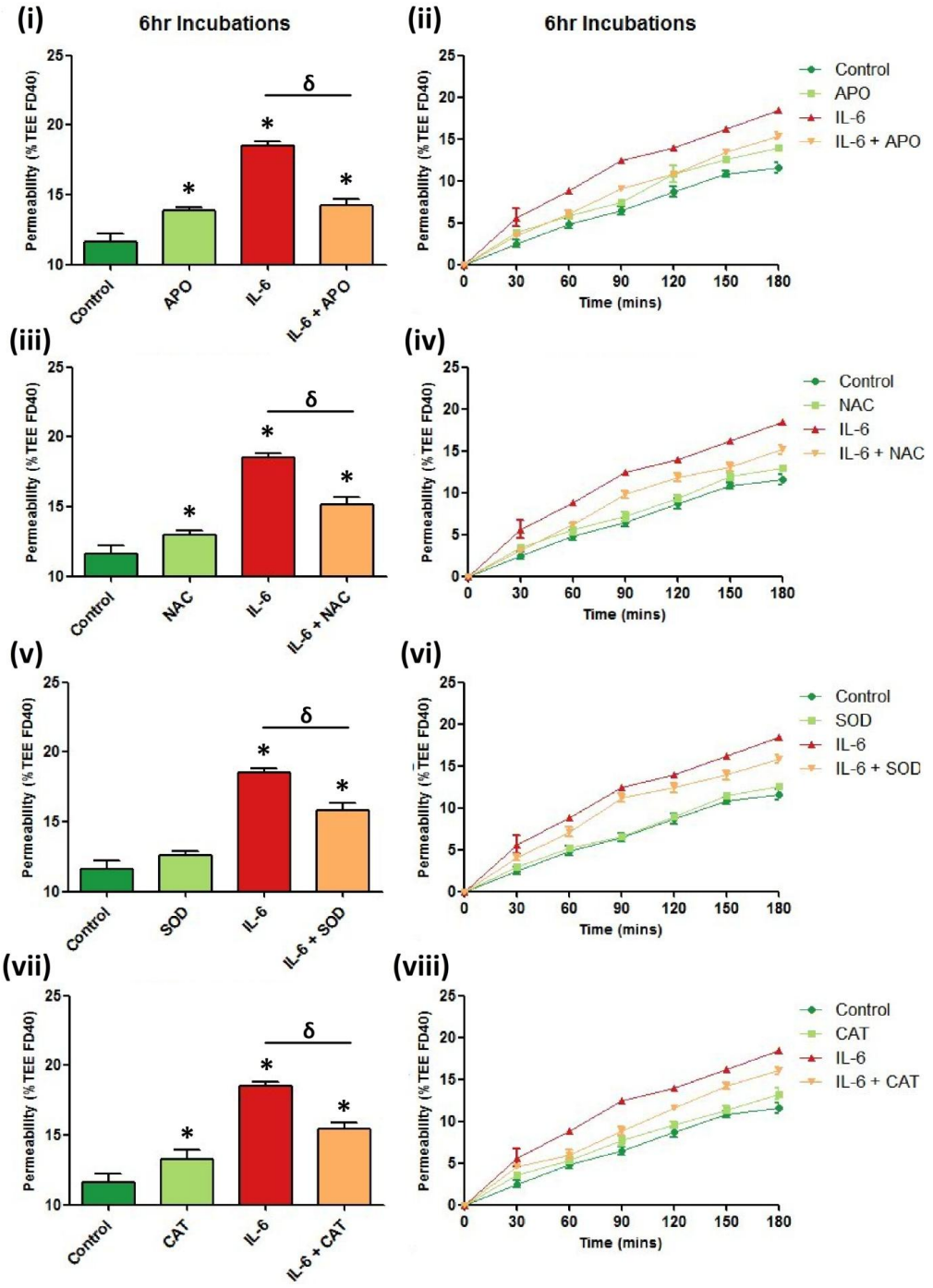

Figure A.17: The effect of antioxidants on IL-6-induced disruption of HBMvEC barrier function. HBMvECs were seeded at a known density and allowed to adhere prior to examination by transendothelial permeability. HBMvECs were pre-treated with IL-6 (100 ng/ml) for 6 hrs in the presence of a number of antioxidant compounds. Post-treatment, monolayers were examined by transendothelial permeability assay. The histograms (LHS) and line graphs (RHS) show the change in permeability (% TEE FD40) at a given time point(s) (t) = 180 mins or 0-180 mins, respectively. Results are averaged from three independent experiments ± SD; *P≤0.05 vs. Untreated Control. δP≤0.05.

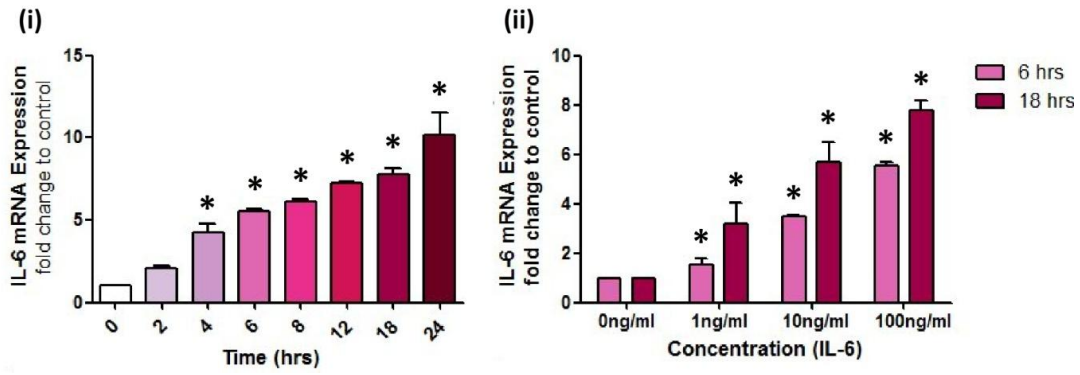

Figure A.18: The effect of IL-6 on IL-6 expression. Confluent HBMvECs were stimulated with IL-6 (0-100 ng/ml) for 0-24 hrs following which they were harvested for whole cell mRNA. The histograms represent the changes in IL-6 on a transcriptional level over time (i) and with respect to dose at 6 and 18 hrs (ii). Results are averaged from three independent experiments ± SD; *P≤0.05 vs. 0 hrs (i), 0 ng/ml (ii) respectively.

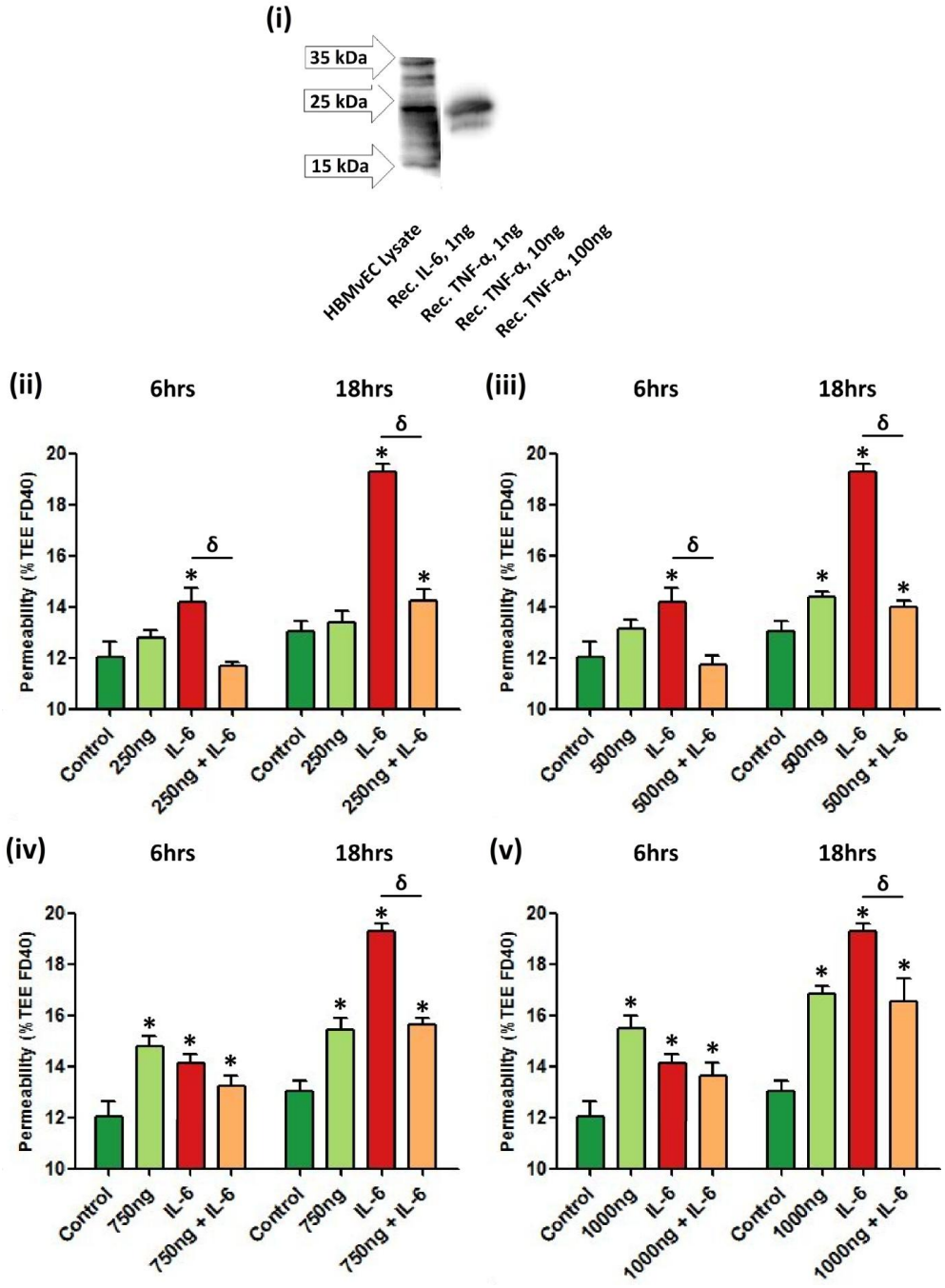

Figure A.19: The optimisation of an IL-6 NtAb on IL-6-Induced disruption of HBMvEC barrier function. The efficacy of the particular IL-6 NtAb was investigated by western blot. HBMvEC lysate, recombinant IL-6 and recombinant TNF-α were run out on an SDS-PAGE gel and subjected to immunoblot analysis. In a parallel study, HBMvECs were seeded at a known density and allowed to adhere overnight. HBMvECs were then treated with IL-6 (20ng/ml) for 6 hrs and 18 hrs in the presence of a range of IL-6 NtAb concentrations. Post-treatment, the HBMvEC cultures were examined by transendothelial permeability assay. The histograms (ii, iii, iv, v) show the change in permeability (% TEE FD40) at a given time point (t) = 180 mins. Results are averaged from three independent experiments ± SD; *P≤0.05 vs. Untreated Control. δP≤0.05.

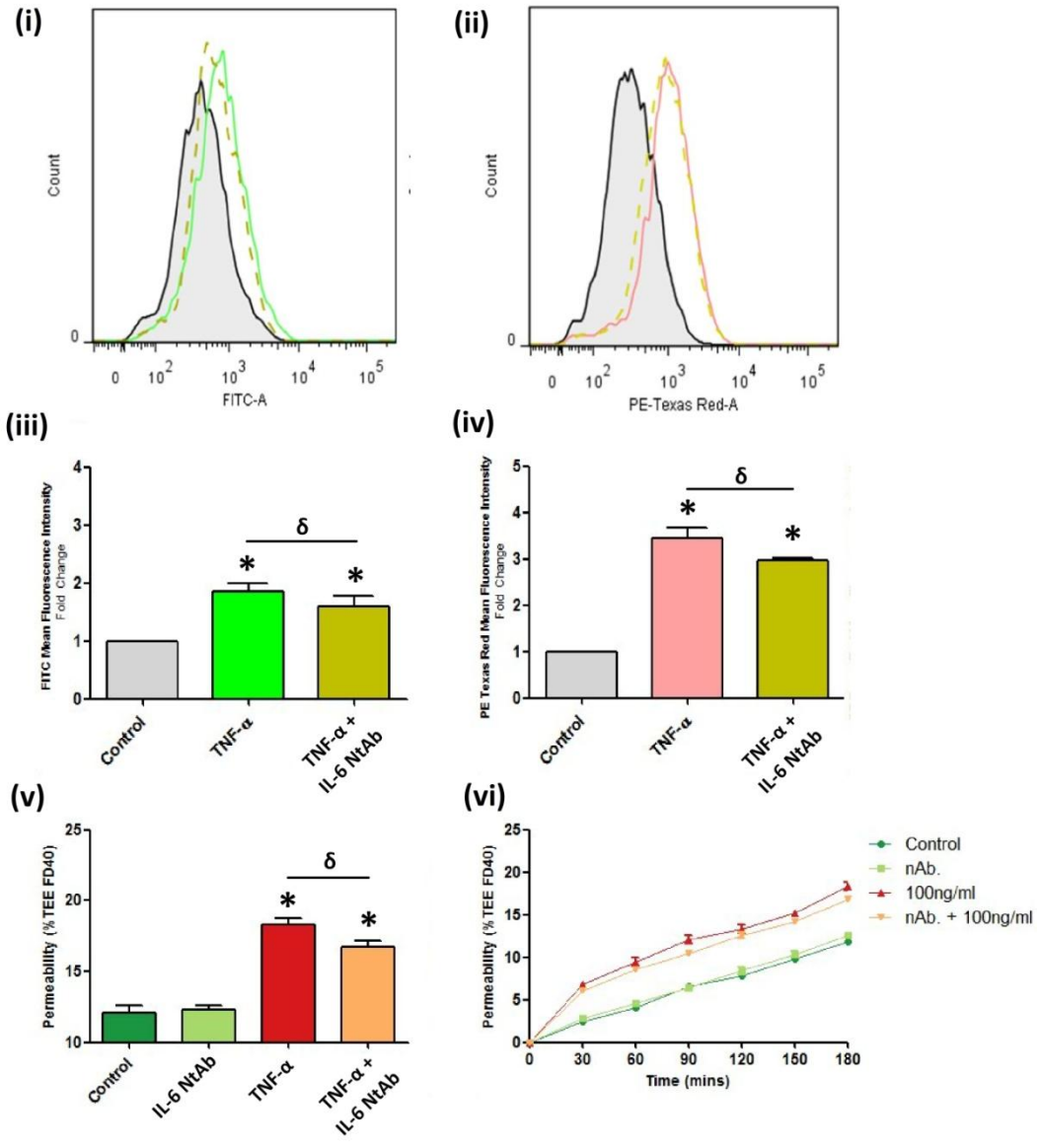

Figure A.20: The effects of an IL-6 NtAb on TNF-α-induced disruption of HBMvEC barrier properties. Confluent HBMvECs were stimulated with TNF-α (100 ng/ml) for 6 hrs in the presence of CFDA or DHE, and in the absence and presence of an IL-6 NtAb. Post-treatment, cells were harvested and subsequently prepared for flow cytometry. The histograms represent the intensity of the CFDA (iii) and DHE (iv) ROS signals prepared from the corresponding FACS scans. The TNF-α-treated samples were analysed using FlowJo Flow Cytometry Analysis Software. Results are averaged from three independent experiments ± SD. *P≤0.05 vs. Untreated Control. In a parallel study, HBMvECs were seeded into transwell inserts at a known density and allowed to adhere prior to examination by transendothelial permeability assay. HBMvECs were then treated with TNF-α (100 ng/ml) for 6 hrs in the presence of the IL-6 NtAb. The histogram (v) and line graph (vi) show the change in permeability (% TEE FD40) at a given time point(s) (t) = 180 mins or 0-180, respectively. Results are averaged from three independent experiments ± SD; *P≤0.05 vs. Untreated Control. δP≤0.05.

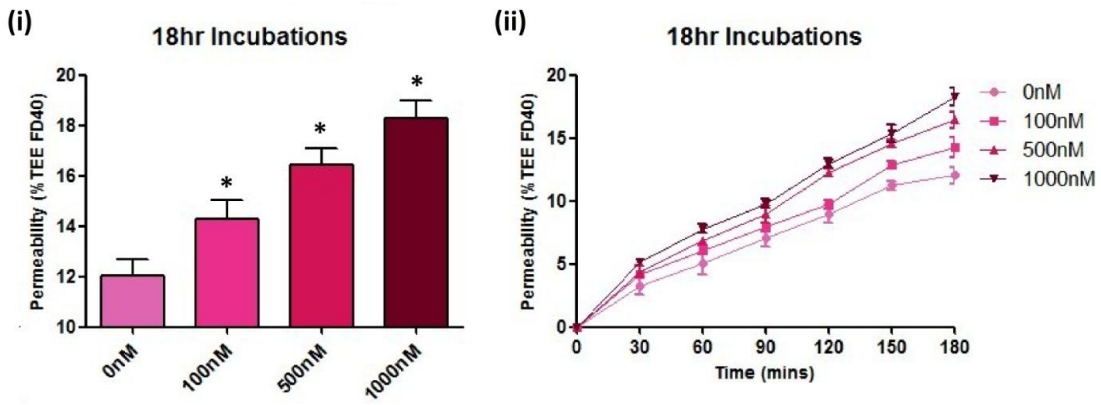

Figure A.21: The effect of 14-3-3 inhibition on HBMvEC barrier function. HBMvECs were seeded at a known density and allowed to adhere prior to addition of R18 peptide for 18 hrs. Following this the HBMvEC sultures were examined by transendothelial permeability assay. The histogram (i) and line graph (ii) show the change in permeability (% TEE FD40) at a given time point(s) (t) = 180 mins or 0-180 mins, respectively, in response to R18 (0-1000 nM). Results are averaged from three independent experiments ± SD; *P≤0.05 vs. 0 nM.

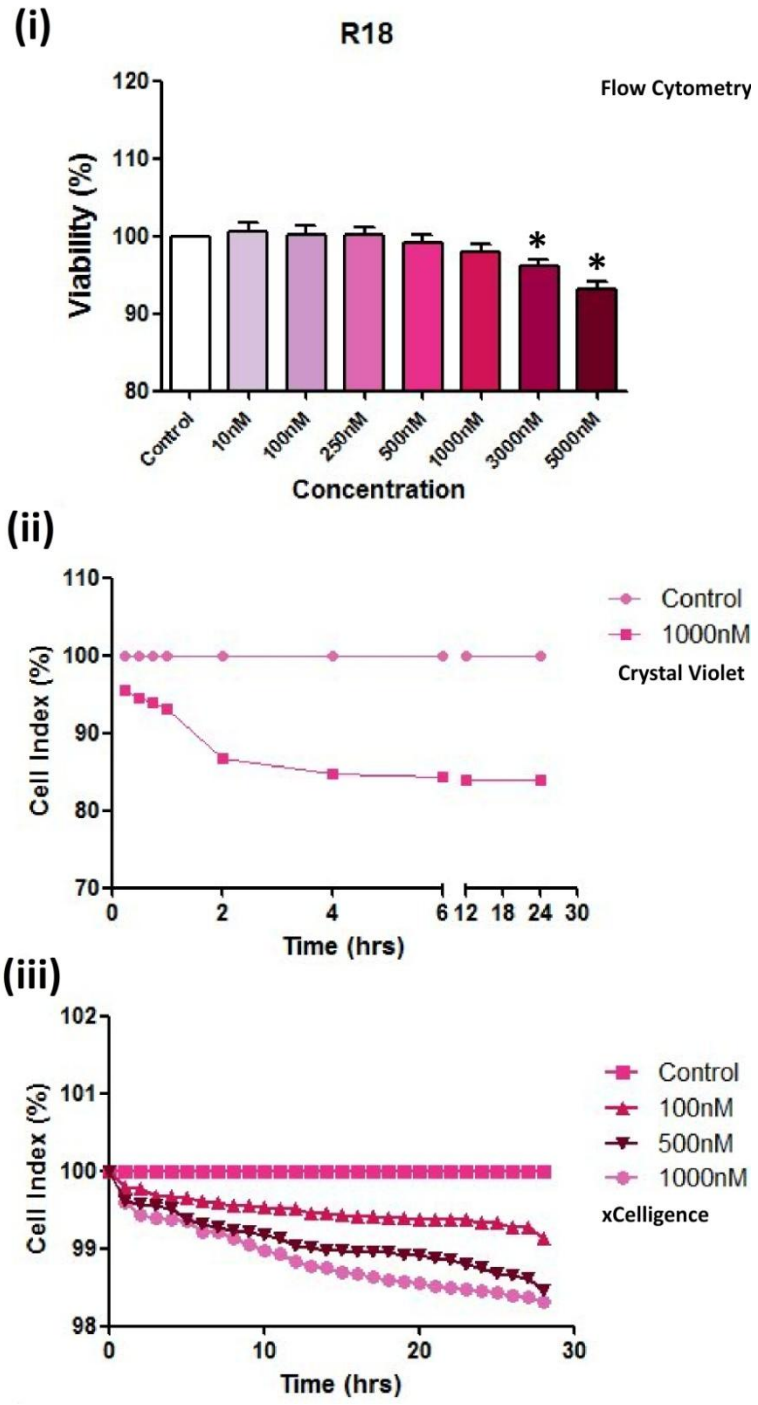

Figure A.22: The effect of R18 peptide on HBMvEC viability-Flow Cytometry and Adhesion Analysis. Confluent HBMvECs were treated with R18 for 18 hr. Post-treatment cells were harvested and subsequently prepared for flow cytometry analysis using PI stain. The cytokine treated samples were analysed using FlowJo Flow Cytometry Analysis Software to identify the viable and cytotoxic cell populations in response to R18 (i). In a parallel experiment HBMvECs were seeded at a known density on 96-well plates and treated with R18 at different concentrations over 24 hrs. Post-treatment, the plates were stained with a crystal violet solution to assess cell number. HBMvECs were also seeded at a known density on xCelligence® plates and had their Cell Index (%) monitored in real-time in response to a range of R18 peptide concentrations. Results are averaged from three independent experiments ± SD; *P≤0.05 vs. Untreated Control.

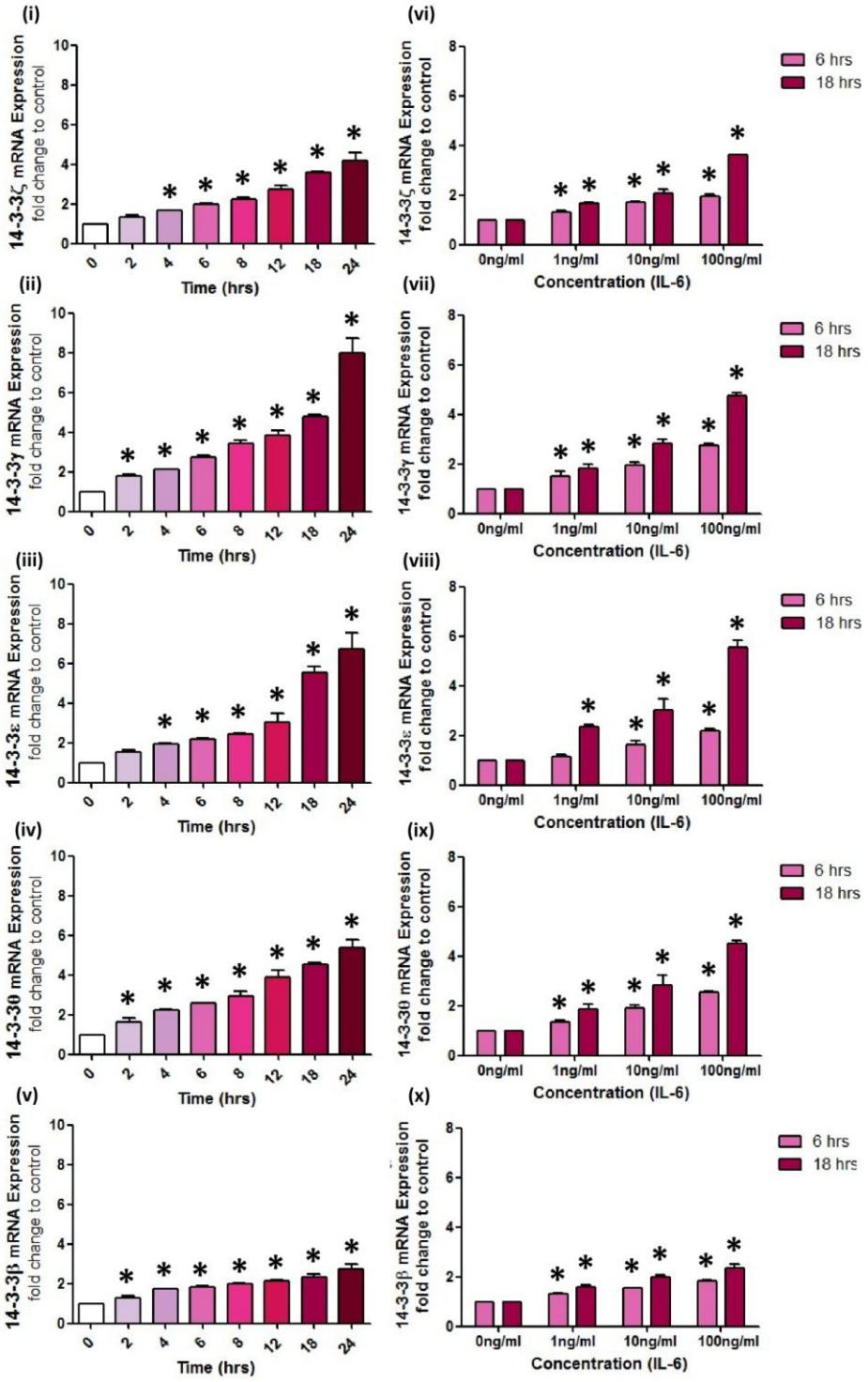

Figure A.23: The effect of IL-6 on specific 14-3-3 isoform transcription. Confluent HBMvECs were stimulated with IL-6 (0-100ng/ml) for 0-24 hrs, following which they were harvested for whole cell mRNA. The LHS histograms represent the mRNA changes in 14-3-3ζ (i), 14-3-3γ (ii), 14-3-3ε (iii) 14-3-3θ (iv) and 14-3-3β (vi) in response to 100 ng/ml TNF-α. The RHS histograms represent the mRNA changes in 14-3-3ζ (vi), 14-3-3γ (vii), 14-3-3ε (viii) 14-3-3θ (ix) and 14-3-3β (x) in response to IL-6 (0-100 ng/ml) at 6 and 18 hrs. Results are averaged from three independent experiments ± SD; *P≤0.05 vs. 0 hrs (i-v) or 0 ng/ml (vi-x).

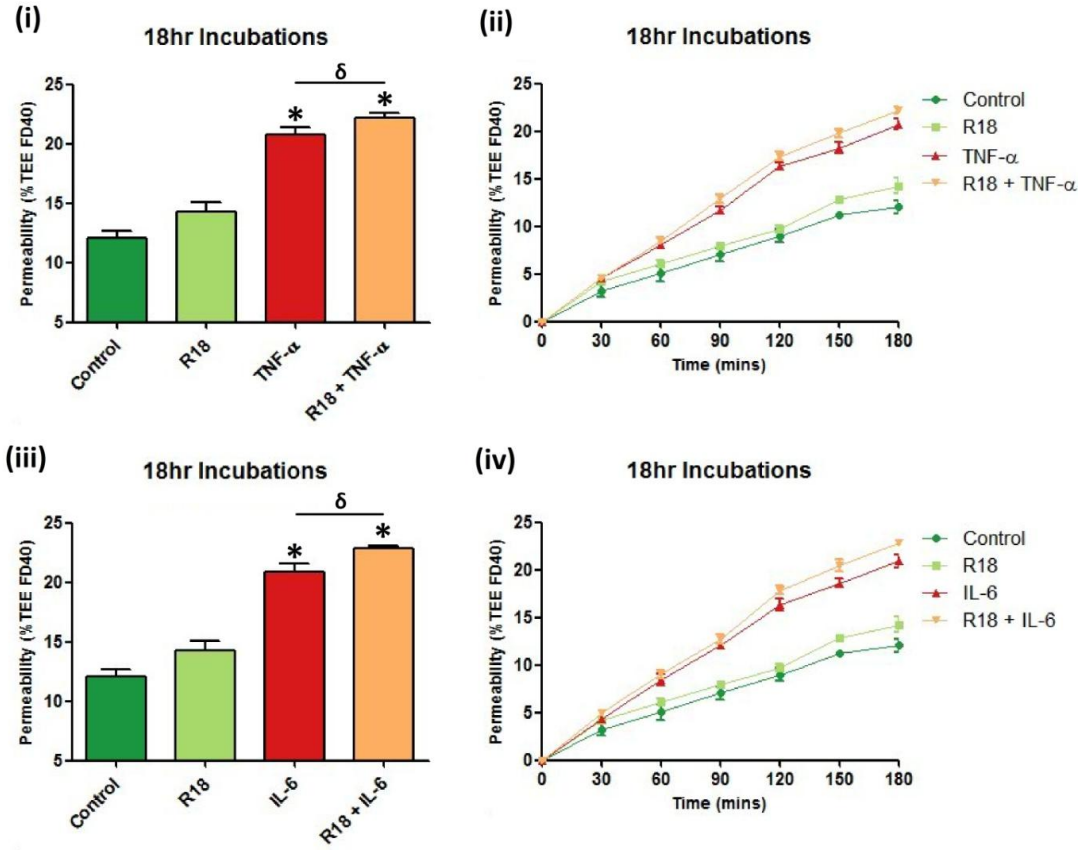

Figure A.24: The effect of 14-3-3 inhibition on TNF-α- and IL-6-induced HBMvEC damage-Barrier Function. HBMvECs were seeded at a known density and allowed to adhere prior to examination by transendothelial permeability. HBMvECs were then maintained in the presence of TNF-α or IL-6 (100ng/ml) for 18 hrs in the absence and presence of R18 peptide. Post-treatment the HBMvEC cultures were examined by transendothelial permeability assay. The histograms (LHS) and line graphs (RHS) show the change in permeability (% TEE FD40) at a given time point(s) (t) = 180 mins or 0-180 mins, respectively, in response to TNF-α (i, ii) or IL-6 (iii, iv). Results are averaged from three independent experiments ± SD; *P≤0.05 vs. Control. δP≤0.05.

Target	Primer Set Efficiency
Human GAPDH	97%
Human Occludin	94%
Human Claudin 5	94%
Human VE-Cad	95%
Human ZO-1	94%
Human vWF	93%
Human TNF-α	91%
Human IL-6	95%
Human TNFR1	95%
Human TNFR2	94%
Human GP130	94%
Human sIL-6R	93%
Human 14-3-3β	95%
Human 14-3-3γ	95%
Human 14-3-3ζ	96%
Human 14-3-3θ	94%
Human 14-3-3ε	95%
Bovine GAPDH	95%
Bovine Occludin	94%
Bovine Claudin 5	95%
Bovine VE-Cad	94%
Bovine ZO-1	93%

Figure A.25: Primer Efficiencies. To conduct primer efficiency curves the same reaction mixture used for qPCR is utilised with the exception that the template cDNA is omitted. Instead, a dilution of a PCR product which had been run previously using the same primer set is substituted. Briefly, the PCR product was excised from the reaction plate and a 1/1000 dilution was made in RNase-free water. From here a 7-fold 1/10 serial dilution of this 1/1000 dilution was made with 6.5 µl of each dilution substituting for the raw cDNA in each reaction mixture. An additional reaction mixture was made substituting the PCR product for RNase-free water. This acted as a non-template control. The temperature profile run for standard qPCR was utilised and the software was programmed to recognise the serial dilutions and plot their Threshold Cycle (C_T Value) versus the immunofluorescent signal (number of copies of the target gene). Ideally primer sets should have an efficiency of between 90 and 105%.